# WOOD POLYMER NANOCOMPOSITE BASED ON NON CONVENTIONAL PLANT MATERIAL AND NANOFILLERS

**A thesis submitted**
**in partial fulfillment of the requirements for the degree of**
**Doctor of Philosophy**

**By**

**BIPLAB KR DEKA**

Registration No. 008 of 2010


**School of Science and Technology**
***Department of Chemical Sciences***
**Tezpur University, Napaam**
**Assam-784028, India**
**January, 2012**

*Dedicated to my beloved mother*

तेजपुर विश्वविद्यालय
(केंद्रीय विश्वविद्यालय)
नपाम, तेजपुर - 784 028, असम, भारत

TEZPUR UNIVERSITY
( A Central University)
Napaam, Tezpur - 784 028, Assam, India

# CERTIFICATE

This is to certify that the thesis entitled "**WOOD POLYMER NANOCOMPOSITE BASED ON NON CONVENTIONAL PLANT MATERIAL AND NANOFILLERS**" submitted by Biplab Kr Deka, Research Scholar of Department of Chemical Sciences, Tezpur University, Assam for the award of degree of Doctor of Philosophy in Science, is a record of bonafide research work done under my supervision and guidance at Department of Chemical Sciences, Tezpur University, Assam-784028. He has successfully completed the work.

He has fulfilled all the requirements for submitting the thesis for award of the degree of Doctor of Philosophy in Science.

The results embodied in the thesis have not been submitted to any other University or Institution for award of any degree or diploma.

Place: Tezpur
Date: 17.01.12

Tarun K. Maji
(Prof. Tarun K. Maji)

फोन / Phone : 03712-267007 - 9 (3 lines) • फेक्स / Fax : 03712-267005, 267006 • ई-मेल / e-mail : admn@tezu.ernet.in

# DECLARATION

I hereby declare that the thesis entitled "WOOD POLYMER NANOCOMPOSITE BASED ON NON CONVENTIONAL PLANT MATERIAL AND NANOFILLERS" is an authentic work carried out by me under the supervision of Prof. Tarun K. Maji, Department of Chemical Sciences, Tezpur University, Assam. No part of this work had been presented for any other degree or diploma earlier.

Place: Tezpur

Date: 17.01.12

Biplab Kr Deka

(Biplab Kr Deka)

# ACKNOWLEDGEMENTS

*I express my deep gratitude and sincere thanks to my research guide, Prof. Tarun K. Maji for his invaluable guidance and constant encouragement. I am grateful for his advice, ideas and criticisms throughout my research, which has made me richer both in experience as well as in understanding what scientific research is all about.*

*I am thankful to my doctoral research committee member, Prof. N. Karak, HOD and Dr. A. J. Thakur for their valuable help and suggestion in my research work.*

*I am very grateful to Prof. N. S. Islam, Dean, Science & Technology, Prof. S. K. Dolui, Prof. R. C. Deka, Dr. R. Dutta, Dr. R. Borah, Dr. A. Phukan, Dr. P. Pujari, Mr. K. K. Bania, Dr. P. Bharali and Dr. N. Gogoi for their invaluable help, guidance and encouragement throughout my work.*

*A special thanks goes to Dr. M. Mandal, Department of Molecular Biology & Biotechnology and Dr. S. D. Baruah, North East Institute of Science & Technology, Jorhat for their valuable help, support and suggestion in my research work.*

*I am also greatly indebted to all my senior lab mated Rashmiba, Rabiulda, Nirmalaba and present lab mates Rashmi, Nibedita, Rasna, Murshid, Ankita, Chinmayee, Prasanta and Pankaj for their constant help and support in carrying my entire research work. It gives me great pleasure to thank all my near and dear friends, well wishers, who shared all kinds of moments with me. I am thankful to Dr. Biren Gohain, Dr. Binoy Saikia, Mr. Rajen Bora, Mr. Juwesh Binong, Nipuda, Ratanda, Rajuda, Sankur, Biraj, Manuranjan, Hemantada, Babita, Durlavda and Champak for helping me in different ways in my work.*

*I would like to thanks Mr. Jorze of SAIF, North East Hill Univeristy, Shillong for TEM analysis. A special thanks goes to Dr. D. K. Setua, DMSRDE, Kanpur for DMA analysis.*

*Heartful acknowledge goes to my mother for giving me this beautiful life and all efforts that gives in my entire life. A special thanks to all my uncles, aunties and cousins for their enormous support and encouragement. Mere words cannot express my thanks to Ankita, who inspired me and co-operated with me in my research work.*

*Finally, I am thankful to Prof. M. K. Choudhury, Vice-Chancellor, Tezpur University for permitting me to present this work in the form of thesis. I would also like to acknowledge the financial support received from Tezpur University in the form of Institutional Fellowship, without which this research would not have been possible.*

*January, 2012* *Biplab Kr Deka*

# ABSTRACT

# ABSTRACT

Wood polymer composite (WPC) covers a wide range of area in the field of polymer composite. Due to different advantages of WPC over conventional composite, it has been gaining special support to the industrial market. Its use ranges from different indoor and outdoor applications like windows, doors, railing, decking, fencing etc. to different parts of automobiles. Because of its advantages like low cost of production, light weight, corrosion protection, biodegradability etc. they are potentially used over metallic composites.

The North Eastern region, like any other tropical part of the country, is rich in forest based cellulosic resources to a lucrative extent. Out of various species available in this region, only a few of them have been explored for economic development of this region. Some of the non conventional plants like Nal (*Phragmites karka*), Khagra (*Neyraudia reynaudiana*), Kohua (*Saccharum spontaneum*), Kolomou (*Ipomoea carniva*) etc. are abundantly available in the forests of Assam. These plants are not suitable for structural applications due to their poor mechanical, dimensional and other properties. They remain as bio wastes in the forest and or at the most utilized for making temporary shades, domestic fuels etc. There is a great prospect of utilizing these materials for producing composites to be used for various constructional purposes.

Varieties of waste plastic materials in the form of carry bags, packaging film, container, etc. cause environmental pollution. The majority of waste plastic materials consist of a substantial amount of polyethylene (PE), polypropylene (PP), poly(vinly chloride) (PVC) and less amount of poly ethylene terephthalate (PET), polystyrene (PS) etc. Recycling is one of the processes to reduce the pollution. But the mechanical and other properties of the recycled materials are poor due to poor compatibility among different plastics. These waste plastic materials can be made value added by forming composites with non conventional plant materials.

For composites, the improvements in bond formation among plastic materials themselves as well as with wood fibers are very much important. The bond formation can be improved by the use of a suitable compatibilizer. The compatibilizer will be such that it can able to react with the hydrophilic wood fibers and hydrophobic polymers and at the same time will improve the interfacial adhesion among different thermoplastic materials.

Solution blending is one of the processes used for blending of different kind of plastics. The effectivity of the blending process can be improved by the use of a mixture of solvents. The optimum ratio of solvents can be judged properly if the percentage of individual polymer along with their physical characteristics in waste plastics is known.

This can be overcome if a mixture of known percentage of virgin HDPE, LDPE, PP, PVC, etc. is used as starting waste plastic material.

Now days, nanotechnology covers a wide range of area in science and technology. Nanotechnology deals with the material in sub micron level. Nanoscale materials have large surface area for a given volume. Since many important physical and chemical interactions are governed by surface and surface properties, a nano structured material will have substantially different properties from a larger dimensional material (conventional composite) of same composition. The properties of nanocomposites are greatly influenced by the size scale of its component phases and degree of mixing between the two phases. Without proper dispersion, nano material will not offer improved properties over that of conventional composites.

In this part of work, wood polymer nanocomposite was developed by using high density polyethylene, low density polyethylene, polypropylene, poly(vinyl chloride) and wood flour. Two types of non conventional wood, Nal (*Phragmites karka*) and Kolomou (*Ipomoea carniva*) were used in the work. A Comparison among different types of compatibilizer was done. Nanofillers like nanoclay, ZnO, $SiO_2$ and $TiO_2$ nanopowder were used to improve the properties of the composite. Different properties like mechanical, thermal, flame retardancy, UV resistance, water uptake etc. were studied and reported.

***Chapter I:*** This chapter includes introduction and literature review part. In this chapter, the concept of polymer composite and development of wood polymer nanocomposite have been elaborated. Different types of polymers used in the development process have also been discussed. The origin of non conventional plant, its chemical structure and property have been incorporated in the chapter. The properties of different nanofiller like clay, ZnO, $SiO_2$ and $TiO_2$ have been included in the chapter. All the properties of wood polymer composite viz. mechanical, thermal, flame retardancy, UV resistance, water uptake etc. have been discussed. Thorough literature search pertaining to wood polymer composite has been done and reported in this chapter.

***Chapter II:*** This chapter covers the materials and methods used in the investigation. It includes the raw materials used, modification of the nanofillers and preparation of composite. It also includes the characterization procedures of the composite.

***Chapter III:*** This chapter includes results and discussion part. This chapter has been further sub divided into the following four sections.

***Section A*: Study on the properties of nanocomposite based on high density polyethylene, polypropylene, polyvinyl chloride, wood and clay.**

In this part of work, a mixture of high density polyethylene (HDPE), polypropylene (PP), polyvinyl chloride (PVC) and glycidyl methacrylate (GMA) have been used as polymer matrix and compatibilizer respectively. The aim of this study is to prepare and evaluate the various properties of the nanocomposite. The nanocomposites have been prepared by solution blending method using polymer matrix, GMA as stated, wood flour and organically modified MMT (CTAB-modified).

Montmorillonite (MMT) was modified by cetyl trimethyl ammonium bromide (CTAB) and verified by X-ray diffractometer. The interlayer spacing for modified clay was found to increase. The interlayer spacing was further increased in WPC reinforced with modified clay as studied by X-ray diffractometer. FTIR study indicated an interaction between wood, GMA treated polymer blend and nanoclay. Glycidyl methacrylate (GMA) improved the compatibility among the polymers as revealed by SEM study. SEM study also showed more roughness on the surface of unmodified clay treated WPC compared to modified clay treated WPC. TEM study showed an increase in interlayer spacing in WPC treated with CTAB modified clay compared to WPC treated with unmodified clay. Significant improvements in mechanical properties, thermal properties and flammability were obtained in WPC treated with CTAB modified clay. Modified clay based WPC exhibited lower water absorption and highest hardness compared to WPC or unmodified clay treated WPC.

***Section B*: Effect of different compatibilizer and nanoclay on the physical properties of wood (*Phragmites karka*) polymer composite.**

The present investigation has been carried out to study and compare the effect of different compatibilizer on the various properties of WPC prepared by using nonconventional plant materials and mixture of plastics. The effect of nanoclay alongwith the compatibilizer on the final properties of WPC has also been investigated.

WPC was prepared by using three different compatibilizers namely glycidyl methacrylate (GMA), polyethylene-*graft*-maleic anhydride (PE-*g*-MA) and polyethylene-*co*-glycidyl methacrylate (PE-*co*-GMA). It was observed that WPC having mixture of all the three compatibilizer showed maximum improvement in miscibility compared to WPC containing glycidyl methacrylate, polyethylene-*graft*-maleic anhydride and polyethylene-*co*-glycidyl methacrylate alone as compatibilizer. The miscibility was judged by the appearance of smoothness of the fractured surface. FTIR study showed that the shifting and reduction in intensity of the hydroxyl group were more in PE-*co*-GMA and PE-*g*-

MA compatibilized WPC compared to GMA compatibilized WPC. The shifting was further decreased in WPC compatibilized with (1:1:1) molar ratio of blended compatibilizer and nanoclay. WPC reinforced with nanoclay and compatibilized with (1:1:1) molar ratio of GMA, PE-*g*-MA and PE-*co*-GMA showed maximum improvement in tensile, flexural and hardness properties. Thermal stabilities of the WPC enhanced over virgin wood due to incorporation of compatibilizer. Maximum thermal stability and flame resistance property were noticed for nanoclay based WPC compatibilized with (GMA+PE-*g*-MA+PE-*co*-GMA) followed by WPC compatibilized with PE-*co*-GMA, PE-*g*-MA and GMA. Nanoclay reinforced mixed compatibilizer based WPC showed least water absorption in comparison with polymer blend and other compatibilizer based WPC.

***Section C*: Effect of coupling agent and nanoclay on the properties of HDPE, LDPE, PP, PVC blend and *Phragmites karka* nanocomposite.**

The objective of the present study was to prepare the nanocomposites using wood flour, PE-*co*-GMA compatibilizer, nanoclay and polymer mixture of (HDPE + LDPE + PP + PVC) by solution blending. Efforts have also been made to study the various properties like mechanical, thermal, flame retardancy, water resistance, biodegradation etc. of the nanocomposite.

The distribution of silicate layers of nanoclay in wood polymer matrix was investigated by XRD and TEM studies. X-ray diffraction studies of WPC treated with 1 and 3 phr nanoclay showed higher exfoliation compared to WPC treated with 5 phr nanoclay. TEM study also supported the above findings. FTIR studies indicated an interaction between wood, PE-*co*-GMA treated polymer blend and clay. It was found that the intensity of the hydroxyl peak decreased as well as shifted to lower wave number in the wood polymer composite. Furthermore, the intensity of peaks corresponding to –CH stretching was more in wood composites compared to pure wood which indicated the formation of bond between polymers, PE-*co*-GMA and wood. The increase in miscibility among polymers due to addition of PE-*co*-GMA as compatibilizer was studied by SEM study. In WPC, there was no significant difference in the surface characteristics on increasing the amount of nanoclay from 1.0 to 3.0 phr. However, the surface appeared little bit rough on addition of 5 phr of clay. It was observed that both flexural and tensile properties of polymer blends increased on addition of PE-*co*-GMA and wood flour. The incorporation of nanoclay with wood, polymer blend and PE-*co*-GMA further enhanced the flexural and tensile properties. Both flexural and tensile values increased with clay loading up to 3 phr, beyond that the values decreased. Hardness values also increased as

PE-*co*-GMA and clay was added to the polymer blend. The storage and loss modulus were found to enhance on incorporation of clay to WPC. The damping peak was found to be lowered by the addition of clay to WPC. $T_l$ and $T_m$ value of polymer blend improved on addition of PE-*co*-GMA and wood flour. The values were found to enhance further when nanoclay was added. The values increased upto addition of 3 phr clay beyond that it decreased. Nanoclay showed highest RW values while the polymer blend showed lowest RW values. The trend of RW values of clay treated WPC was similar to those of $T_l$ values. Further, it was observed that polymer blend decomposed at higher temperature compared to wood flour. Temperature of decomposition ($T_D$) values increased on addition of wood flour and PE-*co*-GMA to the polymer blend. $T_D$ value increased initially upto addition of 3 phr clay after that it decreased with the increase in the amount of clay (5 phr). The LOI values of the nanoclay treated wood polymer composites were found more compared to nanoclay untreated wood polymer composite. The higher the percentage of nanoclay, the higher was the LOI. Composites samples were exposed for microbial degradation for eight weeks and wood polymer composites had shown high rate of degradation. It was observed that with increasing bacterial exposure time, the growth of bacterial stains increased. With the increase in the clay content, the rate of bacterial growth enhanced. From the study, it was observed that WPC loaded with 5 phr clay showed maximum bacterial growth. It was found that with efficient degradation of WPCs, flexural and tensile properties of the WPCs decreased. In all the cases, the water uptake was found to increase with the increase of time of immersion. The water absorption of the neat polymer decreased on addition of PE-*co*-GMA. It decreased further on addition of nanoclay to the PE-*co*-GMA treated polymer blend. The water absorption was found to enhance when wood flour was added. The water absorption of wood flour/polymer blend composite decreased with the incorporation the clay. The higher the amount of clay, the lower was the water absorption.

***Section D*: Wood flour (*Ipomoea carniva*) reinforced polymer/clay nanocomposite.**

The aim of the present study is to prepare the nanocomposite via solution blending by using a different type of wood flour (*Ipomoea carniva*), PE-*co*-GMA, nanoclay, polymer mixture of high density of polyethylene (HDPE), low density polyethylene (LDPE), polypropylene (PP) and polyvinyl chloride (PVC) and to evaluate the various properties of composites.

The optimum ratio of solvent xylene and THF for solution blending of HDPE, LDPE, PP and PVC (1:1:1:0.5) was 70:30. The compatibility among the polymers and WF was improved as revealed by SEM study. XRD and TEM study showed that WPC

loaded with 3 phr nanoclay exhibited better exfoliation compared to those of WPC loaded with 1 and 5 phr clay. Decrease in intensity of –OH stretching and shifting of hydroxyl group peak to lower wavenumber as judged by the FTIR studies showed a strong interaction among wood, PE-*co*-GMA treated polymer blend and nanoclay. Moreover, the increased in intensity of –CH stretching also confirmed the interaction between polymer, wood flour (*Ipomoea carniva*) and clay. WPC treated with 3 phr nanoclay showed highest mechanical, thermal, UV resistance and flame retarding properties. Incorporation of nanoclay had improved biodegradability of the composite. It has been observed that with increasing clay content the rate of biodegradation improved. Water uptake resistance, chemical resistance and hardness were found to improve in nanoclay loaded WPC.

***Chapter IV***: This chapter embodies the results of addition of multiple nanofiller. This chapter has been subdivided into the following five sections.

***Section A*: Effect of silica nanopowder on the properties of wood flour/polymer composite.**

In polymer composites, $SiO_2$ nanopowder is one of the widely used fillers. $SiO_2$ can enhance the mechanical as well as thermal properties of the composite. In this communication, we report the modification of $SiO_2$ by treatment with cetyl trimethyl ammonium bromide and study the effect of $SiO_2$ on various properties of composites based on wood, PE-*co*-GMA and polymer mixture of HDPE/LDPE/PP/PVC.

The ratio of xylene and THF for solution blending of HDPE, LDPE, PP and PVC (1:1:1:0.5) was optimized as 70:30. Nanosilica was modified and mixed with the solution blended polymer and wood flour. The influence of nanosilica on the mechanical and thermal properties, flame retardancy and water absorbancy were investigated. X-ray studies showed that $SiO_2$ nanoparticles were infused into the WPC. At lower loading of $SiO_2$ (1-3 phr), the dispersion was found to improve as revealed by TEM study. SEM study showed that the surface of the composite became smooth upto the addition of 3 phr $SiO_2$ nanoparticles. FTIR study indicated the interaction between $SiO_2$, polymer, PE-*co*-GMA and wood. Tensile, flexural and hardness properties of the WPC increased with the increase in $SiO_2$ content upto 3 phr, beyond that it decreased. The incorporation of nanosilica in wood flour/polymer composite significantly improved the thermal stability. Flame retardancy of WPC nanocomposite enhanced due to formation of silica char on the surface of composite. Water absorption of the composite decreased with the incorporation of $SiO_2$ in the composite.

***Section B*: Effect of nanoclay and $SiO_2$ on the properties of wood polymer nanocomposite.**

Mechanical property improvement is an important parameter in wood polymer composite. Most of the fillers are used to improve some particular property of composite. In polymer composite, $SiO_2$ nanopowder is one of the widely used filler. $SiO_2$ can enhance the mechanical as well as thermal properties of the composite. In this part, we report the modification of $SiO_2$ by treatment with cetyl trimethyl ammonium bromide and study the effect of modified $SiO_2$ nanopowder along with nanoclay on various properties of composites based on wood, PE-*co*-GMA and polymer mixture of HDPE, LDPE, PP and PVC.

The distribution of silicate layers of nanoclay and $SiO_2$ in the composite was examined by XRD and TEM study. The improvement in compatibility among the polymers and WF by using polyethylene-*co*-glycidyl methacrylate (PE-*co*-GMA) as compatibilizer was improved as studied by SEM. Surface modification of $SiO_2$ nanoparticles by cationic surfactant CTAB and the interactions among wood, PE-*co*-GMA, $SiO_2$ and nanoclay were examined by FTIR study. WPC loaded with nanoclay and $SiO_2$ showed a remarkable improvement in mechanical properties. Thermal and flame retardance properties were also increased in nanoclay/$SiO_2$ loaded WPC. Water uptake of composite decreased after the incorporation of nanoclay and $SiO_2$ nanoparticles. WPC loaded with 3 phr each of clay and $SiO_2$ exhibited maximum improvement in properties.

***Section C*: Effect of nanoclay and $TiO_2$ on the properties of wood polymer nanocomposite.**

Among many nanocomposite precursors, $TiO_2$ nanopowder is increasingly being investigated because it is non-toxic, chemically inert, low cost, corrosion resistant and has a high refractive index, UV filtration capacity and high hardness. In the present study, wood polymer nanocomposite has been prepared by using polymer blend (HDPE, LDPE, PP, PVC), wood flour, PE-co-GMA and clay/$TiO_2$ combined nanopowder. Effect of inclusion of clay/$TiO_2$ on different properties of the composite has also been highlighted in the present study.

Surface modification of $TiO_2$ by cationic surfactant CTAB was done and confirmed by FTIR study. The exfoliation of silicate layers in the wood polymer matrix and appearance of crystalline peak of $TiO_2$ was examined by X-ray diffraction study. TEM study revealed the distribution of nanoclay and $TiO_2$ nanoparticles in the wood polymer matrix. The compatibilizer improved the miscibility by enhancing the interfacial adhesion among the polymers. The smoothness of fractured surface of composites was

improved due to the incorporation of wood, clay and $TiO_2$ into the composites as observed by SEM study. At constant clay loading (3 phr), the fractured surface of WPC loaded with 5 phr $TiO_2$ appeared less smoother compared to WPC loaded with 3 phr $TiO_2$. Strong interaction between polymer blend, wood, nanoclay and organically modified $TiO_2$ was confirmed by FTIR study. The shifting of hydroxyl peak to lower wavenumber and increase in $-CH_2$ peak intensity were observed maximum in the case of WPC loaded with 3 phr each of clay and $TiO_2$. The mechanical properties were found to increase after the incorporation of clay and $TiO_2$. Flexural, tensile and hardness were found maximum in WPC loaded with 3 phr clay and $TiO_2$. WPC loaded with nanoclay and $TiO_2$ showed an improvement in thermal properties. UV stability of the composite was found to increase by incorporation of $TiO_2$. After 60 days of exposure to UV irradiation, WPC loaded with 3 phr $TiO_2$ showed lowest weight loss. The incorporation of $TiO_2$ improved the UV resistance as evident from carbonyl index measurement and SEM study. Nanoclay/$TiO_2$ treated WPC further improved the flame retardancy and decreased the water absorption capacity.

***Section D*: Effect of nanoclay and ZnO on the physical and chemical properties of wood polymer nanocomposite.**

Thermal stability is one of the important properties of wood polymer composite (WPC). It has been established that thermostability along with the other properties of the composite can be improved by using clay particles. The present study is aimed to discuss the effect of ZnO nanopowder along with nanoclay to the thermal and mechanical properties of HDPE/LDPE/PP/PVC blend/wood composite. The aim is also to study the effect of ZnO to other properties like UV resistance, flame retardancy and water uptake of the composites.

The distribution of silicate layers of nanoclay and ZnO in WPCs were examined by XRD and TEM study. The compatibility among the polymers and wood flour was improved by using polyethylene-*co*-glycidyl methacrylate (PE-*co*-GMA) compatibilizer as revealed by SEM study. The fractured surface of composite having 3 phr each of nanoclay and ZnO appeared to be smoother compared to those of composite prepared with either 1 or 5 phr ZnO and 3 phr nanoclay. Surface modification of ZnO nanoparticles by cationic surfactant cetyl trimethyl ammonium bromide (CTAB) was examined by FTIR studies. The interactions among wood, PE-*co*-GMA, ZnO and nanoclay were studied by FTIR. Both flexural and tensile properties of the polymer blend increased after incorporation of compatibilizer and wood flour. At a fixed clay loading (3 phr), both the flexural and tensile properties improved upto addition of 3 phr of ZnO. The

properties decreased on addition of higher amount of ZnO (5 phr). Hardness value was found maximum at 3 phr clay/ZnO loading, after that it decreased. WPC treated with clay and ZnO showed an improvement in thermal stability. Both initial decomposition temperature ($T_i$) and maximum pyrolysis temperature ($T_m$) value were found maximum when the concentration of ZnO was 3 phr. At that concentration, RW value was also found maximum. The incorporation of ZnO improved the UV resistance of the composites as judged from the weight loss, carbonyl index value and SEM study. Nanoclay/ZnO treated WPC further improved the flame retardancy and decreased the water absorption capacity.

***Section E*: Synergistic effect of $SiO_2$, ZnO and nanoclay on the physical and chemical properties of wood polymer nanocomposite.**

Nanocomposite technology with layered silicate as reinforcing filler has been the subject matter of many discussions in recent years. In this part, efforts have been done to improve all the properties i.e. thermal, mechanical, UV resistance, flame retardancy etc. at a time. We discussed the effect of $SiO_2$ and ZnO nanopowder alongwith nanoclay on the improvement of thermal, mechanical, UV resistance and other relevant properties of HDPE/LDPE/PP/PVC blend/wood/nanoclay composite.

The compatibility among the polymers and WF was improved by using polyethylene-*co*-glycidyl methacrylate (PE-*co*-GMA) compatibilizer as revealed by SEM study. The distribution of silicate layers of nanoclay, $SiO_2$ and ZnO in WPCs were examined by XRD and TEM study. Surface modification of $SiO_2$ and ZnO nanoparticles by cationic surfactant CTAB was examined by FTIR study. The interactions among wood, PE-*co*-GMA, $SiO_2$, ZnO and nanoclay were also studied by FTIR. WPC loaded with nanoclay, $SiO_2$ and ZnO showed an improvement in mechanical, thermal, chemical resistance and UV resistance properties. Nanoclay/$SiO_2$/ZnO treated WPC further improved the flame retardancy and decreased the water absorption capacity. WPC loaded with 3 phr clay and 3 phr each of $SiO_2$/ZnO exhibited maximum improvement in overall properties. Biodegradability of the composite increased linearly with the incorporation of nanofillers.

***Chapter V*:** This chapter includes the summary and conclusions of the present investigation. Salient outcomes of the thesis have been summarized.

Wood polymer composite (WPC) was developed by using solution blended high density polyethylene (HDPE), low density polyethylene (LDPE), polypropylene (PP), poly(vinyl chloride) (1:1:1:0.5) and wood flour from non conventional plant materials.

The ratio of xylene and tetrahydrofuran used for the blending process was optimized as 70:30. The miscibility among the polymers and with wood flour was studied by using compatibilizer viz. glycidyl methacrylate (GMA), polyethylene-*co*-glycidyl methacrylate (PE-*co*-GMA) and polyethylene-*graft*-maleic anhydride (PE-*g*-MA). Polyethylene-*co*-glycidyl methacrylate was the most efficient compatibilizer among the studied three compatibilizers. The properties of the composite were improved by the use of clay. WPC developed with organically modified clay showed superior properties compared to the composite developed with unmodified clay. Maximum improvement in properties was obtained by the addition of 3 phr clay. At higher percentage of clay (5 phr), the properties of the composite decreased due to agglomeration of clay. Both the two types of wood viz. nal (*Phragmities karka*) and Kalmou (*Ipomoea carniva*) showed significant improvement in the properties. Incorporation of $SiO_2$ nanoparticles to the composite increased the mechanical, thermal and other properties. The properties were improved upto 3 phr $SiO_2$ loading, beyond that it decreased. The mechanical properties of the composite were further enhanced by using $SiO_2$ nanoparticles in combination with clay. The incorporation of $SiO_2$ along with clay (3 phr each) improved thermal, flame retardancy, mechanical and water resistance properties. $TiO_2$ nanoparticles in combination with clay were used particularly to improve UV resistance. The combination of 3 phr each of clay and $TiO_2$ improved UV stability, thermal stability etc. compared to 3 phr clay/1 phr $TiO_2$ and 3 phr clay/5 phr $TiO_2$ loading. The addition of ZnO nanoparticles with clay further enhanced the thermal, UV resistance and flame retardancy. The addition of 3 phr each of clay and ZnO to the composite improved UV resistance, thermal resistance, flame retardant property etc. At 3 phr clay and 5 phr ZnO loading, the occurrence of surface interaction among the nanoparticles resulted in the decrease of properties. A significant improvement in mechanical, thermal, UV resistance, flame retardancy and other allied properties was achieved by the incorporation of 3 phr each of nanoclay, ZnO and $SiO_2$. The overall improvement in properties of WPNC could be obtained by the use of combined fillers.

***Future scope*:** The non conventional plant materials and mixture of different plastics along with varieties of nanofillers were successfully used for the preparation of composites. Laboratory study indicated a remarkable improvement in various properties of composites. But still a thorough investigation is necessary. The ratio of different fillers used has to be tuned further in order to obtain better properties. However, this investigation is restricted to laboratory scale only. Further work on a large scale has to be done for commercial utilization of the product. Besides this, melt blending can be

employed for the preparation of composites as it is environmentally safe since no solvents are required. Melt blending can also be tried by using waste plastic materials from municipal garbages as polymer matrix. The information from these above study may further be extended to explore the possibility of making hybrid constructions which consists of waste plastics, wood fibers, waste steel, concrete etc. together. This could open up a new avenue for obtaining value added products and may be take the wood industries to a new direction in future.

## CONTENTS PAGE NO.

# LIST OF ABBREVIATIONS & SYMBOLS

**Chapter I:**

PNC : Polymer nanocomposite

WPC : Wood polymer composite

WPNC : Wood polymer nanocomposite

HDPE : High density polyethylene

LDPE : Low density polyethylene

PP : Polypropylene

PVC : Poly(vinyl chloride)

PMMA : Polymethyl methacrylate

GMA : Glycidyl methacrylate

PE-*co*-GMA : Polyethylene-*co*-glycidyl methacrylate

PE-*g*-MA : Polyethylene-*graft*-maleic anhydride

MMT : Montmorillonite

CTAB : N-cetyl-N,N,N-trimethyl ammonium bromide

WF : Wood flour

MFI : Melt flow index

$T_g$ : Glass transition temperature

$T_m$ : Melting temperature

MPa : Mega Pascal

BPO : Benzoperoxide

AIBN : Azobisisobutyronitrile

UV : Ultra violet

MOE : Modulus of elasticity

MOR : Modulus of rupture

CEC : Cation exchange capacity

phr : Parts per 100 parts of materials

meq : Mili equivalent

ppm : Parts per million

DSC : Differential scanning calorimetry

FR : Flame retardant

**Chapter II:**

h : Hour

g : Gram

mg : Milligram

ml : Millilitre

$lb_f$ : Pound force

µl : Microlitre

mm : Millimetre

nm : Nanometer

kV : Kilovolt

cc : Cubic centimeter

XRD : X-ray diffraction

TG : Thermogravimetric

TEM : Transmission electron microscopy

SEM : Scanning electron microscopy

FTIR : Fourier transform infrared spectroscopy

TGA : Thermogravimetric analyzer

DMA : Dynamic mechanical analyzer

LOI : Limiting oxygen index

**Chapter III:**

*Section A:*

PB : Polymer blend (HDPE+PP+PVC)

PB/G5 : Polymer blend/5 phr GMA

PB/G10 : Polymer blend/10 phr GMA

PB/G15 : Polymer blend/15 phr GMA

PB/G10/W40 : Polymer blend/10 phr GMA/40 phr wood flour

PB/G10/W40/C3*: Polymer blend/10 phr GMA/40 phr wood flour/3 phr MMT (unmodified)

PB/G10/W40/C3 : Polymer blend/10 phr GMA/40 phr wood flour/3 phr MMT (modified)

*Section B:*

PB : Polymer blend (HDPE+LDPE+PP+PVC)

PB/G7/W40 : Polymer blend/7 phr GMA/40 phr wood flour

PB/PM7/W40 : Polymer blend/7 phr PE-*g*-MA/40 phr wood flour

PB/PG7/W40 : Polymer blend/7 phr PE-*co*-GMA/40 phr wood flour

PB/(G+PM+PG)7/W40 : Polymer blend/7 phr (GMA+PE-*g*-MA+PE-*co*-GMA)/ 40 phr wood Flour

PB/(G+PM+PG)7/W20/N3 : Polymer blend/7 phr (GMA+PE-*g*-MA+PE-*co*-GMA)/ 20 phr wood flour/3 phr nanoclay

PB/(G+PM+PG)7/W40/N3 : Polymer blend/7 phr (GMA+PE-*g*-MA+PE-*co*-GMA)/ 40 phr wood flour/3 phr nanoclay

PB/(G+PM+PG)7/W20/N3 : Polymer blend/7 phr (GMA+PE-*g*-MA+PE-*co*-GMA)/ 60 phr wood flour/3 phr nanoclay

*Section C:*

PB : Polymer blend (HDPE+LDPE+PP+PVC)

PB/G5 : Polymer blend/5 phr PE-*co*-GMA

PB/G5/N3 : Polymer blend/5 phr PE-*co*-GMA/3 phr nanoclay

PB/G5/W40 : Polymer blend/5 phr PE-*co*-GMA/40 phr wood flour

PB/G5/W40/N1 : Polymer blend/5 phr PE-*co*-GMA/40 phr wood flour/1 phr nanoclay

PB/G5/W40/N3 : Polymer blend/5 phr PE-*co*-GMA/40 phr wood flour/3 phr nanoclay

PB/G5/W40/N5 : Polymer blend/5 phr PE-*co*-GMA/40 phr wood flour/5 phr nanoclay

*Section D:*

PB : Polymer blend (HDPE+LDPE+PP+PVC)

PB/G5 : Polymer blend/5 phr PE-*co*-GMA

PB/G5/N3 : Polymer blend/5 phr PE-*co*-GMA/3 phr nanoclay

PB/G5/W40 : Polymer blend/5 phr PE-*co*-GMA/40 phr wood flour

PB/G5/W40/N1 : Polymer blend/5 phr PE-*co*-GMA/40 phr wood flour/1 phr nanoclay

PB/G5/W40/N3 : Polymer blend/5 phr PE-*co*-GMA/40 phr wood flour/3 phr nanoclay

PB/G5/W40/N5 : Polymer blend/5 phr PE-*co*-GMA/40 phr wood flour/5 phr nanoclay

**Chapter IV:**

*Section A:*

PB : Polymer blend (HDPE+LDPE+PP+PVC)

PB/G5 : Polymer blend/5 phr PE-*co*-GMA

PB/G5/W40 : Polymer blend/5 phr PE-*co*-GMA/40 phr wood flour

PB/G5/W40/S1 : Polymer blend/5 phr PE-*co*-GMA/40 phr wood flour/1 phr $SiO_2$

PB/G5/W40/S3 : Polymer blend/5 phr PE-*co*-GMA/40 phr wood flour/3 phr $SiO_2$

PB/G5/W40/S5 : Polymer blend/5 phr PE-*co*-GMA/40 phr wood flour/5 phr $SiO_2$

*Section B:*

PB : Polymer blend (HDPE+LDPE+PP+PVC)

PB/G5 : Polymer blend/5 phr PE-*co*-GMA

PB/G5/W40 : Polymer blend/5 phr PE-*co*-GMA/40 phr wood flour

PB/G5/W40/N3/S1 : Polymer blend/5 phr PE-*co*-GMA/40 phr wood flour/ 3 phr nanoclay/1 phr $SiO_2$

PB/G5/W40/N3/S3 : Polymer blend/5 phr PE-*co*-GMA/40 phr wood flour/ 3 phr nanoclay/3 phr $SiO_2$

PB/G5/W40/N3/S5 : Polymer blend/5 phr PE-*co*-GMA/40 phr wood flour/ 3 phr nanoclay/5 phr $SiO_2$

*Section C:*

PB : Polymer blend (HDPE+LDPE+PP+PVC)

PB/G5 : Polymer blend/5 phr PE-*co*-GMA

PB/G5/W40 : Polymer blend/5 phr PE-*co*-GMA/40 phr wood flour

PB/G5/W40/N3/T1 : Polymer blend/5 phr PE-*co*-GMA/40 phr wood flour/ 3 phr nanoclay/1 phr $TiO_2$

PB/G5/W40/N3/T3 : Polymer blend/5 phr PE-*co*-GMA/40 phr wood flour/ 3 phr nanoclay/3 phr $TiO_2$

PB/G5/W40/N3/T5 : Polymer blend/5 phr PE-*co*-GMA/40 phr wood flour/ 3 phr nanoclay/5 phr $TiO_2$

*Section D:*

PB : Polymer blend (HDPE+LDPE+PP+PVC)

PB/G5 : Polymer blend/5 phr PE-*co*-GMA

PB/G5/W40 : Polymer blend/5 phr PE-*co*-GMA/40 phr wood flour

PB/G5/W40/N3/Z1 : Polymer blend/5 phr PE-*co*-GMA/40 phr wood flour/ 3 phr nanoclay/1 phr ZnO

PB/G5/W40/N3/Z3 : Polymer blend/5 phr PE-*co*-GMA/40 phr wood flour/ 3 phr nanoclay/3 phr ZnO

PB/G5/W40/N3/Z5 : Polymer blend/5 phr PE-*co*-GMA/40 phr wood flour/ 3 phr nanoclay/5 phr ZnO

*Section E:*

PB : Polymer blend (HDPE+LDPE+PP+PVC)

PB/G5 : Polymer blend/5 phr PE-*co*-GMA

PB/G5/W40 : Polymer blend/5 phr PE-*co*-GMA/40 phr wood flour

PB/G5/W40/N3/S1/Z1 : Polymer blend/5 phr PE-*co*-GMA/40 phr wood flour/ 3 phr nanoclay/1 phr $SiO_2$/1 phr ZnO

PB/G5/W40/N3/S3/Z3 : Polymer blend/5 phr PE-*co*-GMA/40 phr wood flour/ 3 phr nanoclay/3 phr $SiO_2$/3 phr ZnO

PB/G5/W40/N3/S5/Z5 : Polymer blend/5 phr PE-*co*-GMA/40 phr wood flour/ 3 phr nanoclay/5 phr $SiO_2$/5 phr ZnO

# LIST OF TABLES

# LIST OF FIGURES

# CHAPTER I

# INTRODUCTION
# &
# LITERATURE REVIEW

# CHAPTER I

# INTRODUCTION & LITERATURE REVIEW

## 1.1. Introduction to composite materials

In recent years, the interest in composite materials is increasing due to its advantages as compared to monolithic metal alloys. Composite materials can be defined as engineered materials which exist as a combination of two or more materials that result in better properties compared to individual components when used alone. Composites consist of a discontinuous phase known as reinforcement and a continuous phase known as matrix. In practice, most composites consist of a bulk material (the "matrix"), and a reinforcement of some kind, added primarily to increase the strength and stiffness of the matrix.

***Matrix Phase***: The matrix phase generally comprises the bulk part of a composite. Matrix may consist of any of the three basic material types mainly polymer, ceramics or metals.

***Reinforcement***: The reinforcement is generally responsible for strengthening the composite and improves its various physical properties. All of the different fibers used in composites have different properties and thus affect the properties of the composite in different ways. It also provides stiffness to the composites.

### 1.1.1. Classification of Composites

Composite materials can be classified into many categories depending on the type of reinforcing material, matrix etc. They are namely:

- ***On the basis of the type of matrix material:***

***(a) Metal matrix composite***: It consists of a metallic matrix (Al, Mg, Cu, Fe, etc.). There are several reasons for the re-emergence of interest in metal matrix composites, the most important one being their engineering properties. They are of light weight, exhibit good stiffness and low specific weight as compared to other metals and metal alloys. It is generally considered that these materials offer savings in weights, at the same time maintain their properties. Although it has many advantages, cost remains a major point of interest for many applications.

***(b) Polymer matrix composite***: Polymer matrix composites are considered to be a more prominent class of composites in commercial applications. It comprises of a matrix from thermosetting (unsaturated polyester, epoxy etc.) or thermoplastic (polyethylene, polypropylene, poly(vinyl chloride), nylon, polystyrene etc.) and embedded glass carbon, steel or Kevlar fibers (dispersed phase).

*(c) Ceramic matrix composite*: It comprises of a material consisting of a ceramic combined with a ceramic dispersed phase. The availability of new technologies, processing methods and the demand for high performance products, have together promoted the growth of advanced ceramic products, but the brittleness of ceramics still remains a major disadvantage.

➢ ***On the basis of reinforcing material:***

*(a) Particulate composites*: In this case, the reinforcement is of particle nature (platelets are also included in this class). It may be spherical, cubic, tetragonal, platelet, or of other regular or irregular shape, but it is approximately equiaxed. In general, particles are not very effective in improving fracture resistance but they enhance the stiffness of the composite to a limited extent. Particle fillers are widely used to improve the various properties of matrix materials such as modification of thermal and electrical conductivities, improvement in performance at elevated temperatures, reduction in friction, enhancement in wear and abrasion resistance, improvement in machinability, surface hardness and reduction in shrinkage. Some of the useful properties of ceramics and glasses include high melting temperature, low density, high strength, stiffness, wear resistance, and corrosion resistance. Many ceramics are good electrical and thermal insulators. Some ceramics have special properties; some ceramics are magnetic materials; some are piezoelectric materials; and a few special ceramics are even superconductors at very low temperatures. Ceramics and glasses have one major drawback: they are brittle. An example of particle reinforced composites is an automobile tyre, which has carbon black particles in a matrix of poly-isobutylene or styrene-butadiene elastomeric polymer.

*(b) Fibrous composites*: Fibers, because of their small cross-sectional dimensions, are not directly usable in engineering applications. They are, therefore, embedded in matrix materials to form fibrous composites. The matrix serves to bind the fibers together, transfer loads to the fibers, and protect them against environmental attack and damage due to handling. In discontinuous fiber reinforced composites, the load transfer function of the matrix is more critical than in continuous fiber composites. Fibers are of two types, namely synthetic and natural.

## 1.2. What is Nanocomposite ?

Nanotechnology is now recognized as one of the most promising areas for technological development in the 21st century. In materials research, the development of

polymer nanocomposites is rapidly emerging as a multidisciplinary research activity whose results could broaden the applications of polymers to the great benefit of many different industries. Most of the existing commercial polymers do not have desirable level of properties for many advanced applications, where high mechanical strength, high thermo-stability, low gas permeability, high chemical resistance, light weight, good transparency, etc. are the requirements. Development of a new high performance polymer is time consuming, laborious and involves a huge amount of cost. So, the modification of commercial polymers by addition of other additives and or materials is well known techniques to produce filled polymer and conventional polymer composite systems. But both the techniques have some demerits like causing processing difficulties and increasing density, as a number of different additives and/or materials have to be added to achieve the desired level of properties. Further in both the cases, the improvements in combined properties are not up to the mark and thus limit their applications in different fields. Thus recently, a new technique for development of polymer nanocomposite (PNC) has attracted considerable attention to the material scientists as a way to enhance the properties of polymer or to get a material with intrinsically new set of properties and hence, extends their utility in different fields of applications. This is the main aim of development of polymer nanocomposites. They have been envisaged to have potential applications ranging from automobile to electronics.

The term 'nano' is derived from the Greek word nanos meaning 'dwarf', though in nanoscience and nanotechnology, it is used to indicate the size of the used material ($10^{-9}$ metre). Polymer nanocomposites (PNC) are polymers (thermoplastics, thermosets or elastomers) that have been reinforced with small quantities (less than 5% by weight) of nano-sized particles having high aspect ratios (l/h > 300) [1]. Thus, one component of nanocomposite has at least one dimension (length or width or thickness) in the nanometer range. The advantages of nanocomposites over macrocomposites include reduced filler amount and better properties than obtained for the conventional composites. Different types of thermoplastic and thermosetting polymer nanocomposites, viz. clay/polymer nanocomposites, carbon nanotube/polymer nanocomposites, metal/polymer nanocomposites (metals like Au, Ag, Cu, Cd, Zn, Fe, etc. and their oxides, sulphides, etc.) are good demonstration of nanotechnology. The main significance of polymer nanocomposites are:

- Enhanced physical properties; modulus, dimensional stability, etc.
- Improved barrier properties; reduced gas permeability to oxygen and carbon dioxide
- Improved chemical resistance, weatherability and biodegradation

- Improved flame retardance and slow smoke emission
- Increased heat distortion temperature
- Increased optical clarity over that of conventional filler

As for example, in case of wood/polymer-clay nanocomposites, the clay particles have high aspect ratios and are composed of layered structures, so that the degrees of enhancement in properties obtained can be varied according to the types of nanocomposite structures. There are three types [2-4] of wood/polymer-clay nanocomposites.

*(a) Tactoid structures*: These are obtained when the interlayer space of the clay doesn't expand, due to its poor affinity with the polymer. As a consequence, clay in this form plays little role in property enhancement and is used only for cost reduction. Property improvement in which tactoid structures are present requires a loss of other properties as in the case of conventional fillers.

*(b) Intercalated structures*: It is obtained due to little interlayer expansion of clay. In this case, there is a well-ordered stacked multilayer structure as a result of some affinity between the polymer and the clay. The interlayer spaces of the clay are expanded as few polymer chains penetrate into the basal spacing of clay, but the shape of layered stack remains unchanged.

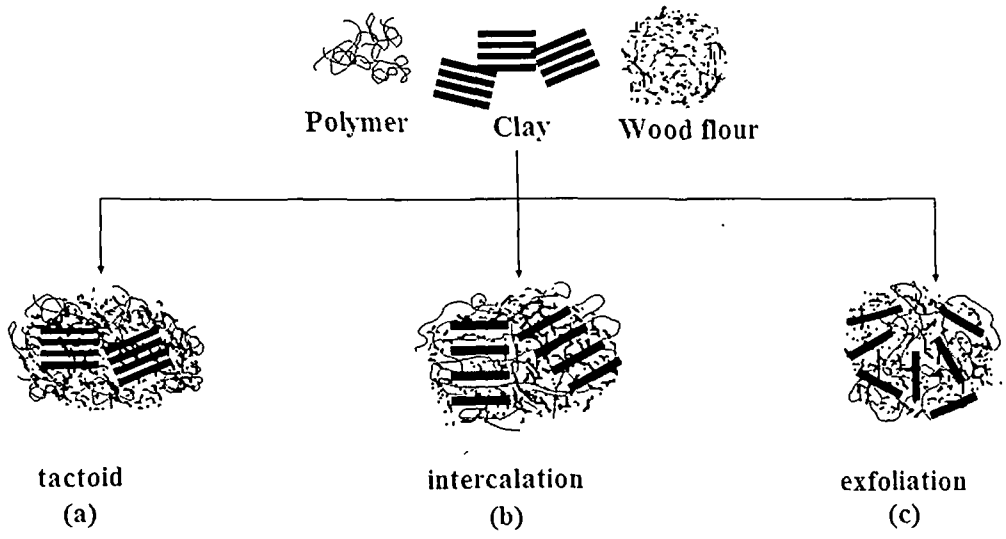


**Figure 1.1.** Different types of wood/polymer-clay nanocomposite.

*c) Exfoliated structures*: In this case, the host clay layers have lost their registry and are well separated into single layers within a continuous polymer matrix. This is due to very

high affinity between the polymer and clay. The three nanocomposites structures are shown in Figure 1.1 and could be observed separately or jointly in one sample.

To get maximum improvement in properties in a clay based nanocomposite, an exfoliated structure is required. The maximum dispersity of clay and interfacial interaction of clay platelets with polymer can be obtained in exfoliated structure. The proper hydrophobicity of clay and compatibility between organically modified clay and polymer are critical factors in nanocomposite formation [5]. Additionally, large interlayer spacing in clay and interaction ability between clay and polymer are the other factors which are considered to develop exfoliated nanostructures.

## 1.3. Concept of polymer nanocomposite (PNC)

Thermoplastic composites play an important role in our society [6]. They are widely used because of their versatile properties, light weight, resistance to breakage, low cost, ease of manufacture, fabrication and shaping, etc. The use of these composites ranges from different houseware products to components of the space shuttle. These materials are used as rigid containers, flexible film, trays, drums, caps, plastic cans, cushions, etc. Moreover, they can be used by combining with other materials or laminating or blending with other polymers to gain the benefit of their various attributes [7,8]. But due to their non biodegradable, low thermal and photo degradation nature, these are becoming a serious threat to the environment. Once their application is over, the polymer materials are thrown in the form of garbage which is a major environmental concern in the present decades [9]. Recycling and reusing is one of the methods to minimize the bio-waste. Pracella et al. [10] has blended polyethylene terephthalate (PET) and polyolefins (HDPE, PP) obtained from post consumer packaging materials.

The field of nanotechnology is one of the most popular areas for current research and development in basically all technical disciplines. This obviously includes polymer science and technology and even in this field the investigations cover a broad range of topics. The areas include nanoelectronics, polymer-based biomaterials, nanoparticle drug delivery, miniemulsion particles, fuel cell electrode polymer bound catalysts, layer-by-layer self-assembled polymer films, electrospun nanofibers, imprint lithography, polymer blends and nanocomposites. Even in the field of nanocomposites, many diverse topics exist including composite reinforcement, barrier properties, flame resistance, electro-optical properties, cosmetic applications, bactericidal properties etc. Researchers at Toyota have developed the

method for preparation of composites made from olefin and inorganic fillers such as clay and calcium carbonate. Use of clay as reinforcing agent has tremendously improved the properties of the composite. It has been observed that the mechanical properties of isotactic polypropylene nanocomposite have increased due to reinforcement by organoclay [11]. Streky et al. [12] has studied the thermal properties of poly(vinyl chloride) nanocomposites reinforced with montmorillonite clay and found an improvement in thermal stability of the composite. Lagaly [13] has described the nature of fillers that are currently in use and also has reported the difference between conventional fillers and nanofillers.

## 1.4. Why wood polymer nanocomposite (WPNC) ?

Synthetic composite materials have different disadvantages like high cost, low mechanical properties, low thermal stability and the most important things is that these are derived from non-renewable materials. These are not biodegradable and remains as bio waste in the environment for long time. Therefore, the importance of some new composites have emerged which are nature friendly and at the same time can enhance properties. With the increase in population, consumption and environmental awareness, renewable materials like natural fibers, wood etc. are gaining importance over the materials derived from non-renewable sources.

Natural fiber reinforced composites is an emerging area in polymer science. These natural fibers are low cost fibers with low density and high specific properties. These are biodegradable and nonabrasive. They offer specific properties comparable to those of conventional fiber composites. In the early 1990's, researchers began to focus on wood fibers as potential filler for organic-inorganic composites. The advantages of using wood fibers are: low cost (or flour), low density, light weight, corrosion protective, resistance to breakage and the most important is it's biodegradability [14]. The main disadvantage of using wood fiber/or flour as filler is the thermal instability of wood above 200 °C. The majority of the thermoplastic exhibits melting point between 160 and 220 °C, which is the range of thermal decomposition of wood. So, the thermoplastics which have their processing temperature below 200 °C can only be used for development of wood polymer composite. Wambua et al. [15] and Bismarck et al. [16] have reported that plant fibers are in general suitable to reinforce plastics due to their relative high strength, stiffness and low density. The characteristic values for flax and softwood reach levels close to the values for glass fibers, types E. The cost of glass fibers is comparatively high and the most important thing is that

these are nonbiodegradable. Therefore the natural fibers can be used in the composites in lieu of glass fibers. Tasdemir et al. [17] has developed wood-LDPE composite and found the increase in mechanical and thermal properties of the composite due to the reinforcement of wood flour. Bledzki et al. [18] has developed polypropylene composite based on wheat husk, rice husk and soft wood. They have studied the physical, chemical and surface properties of the composite and found an improvement in all the properties. Islam et al. [19] has investigated the physico-mechanical properties of coir reinforced polypropylene (PP) composites. The mechanical properties of the composites prepared from chemically treated coir are found to be much better compared to those of untreated ones. It has been observed that though conventional composites have higher mechanical and other properties still there is some limitations. So, the concept of nanocomposite has come.

Nanodimensional $TiO_2$, ZnO, clay etc. are reported to improve moisture barrier, fire retardancy, UV protection etc. UV protection, dimensional stability and weather resistance are very important for wood based materials used in exterior applications. Nanomaterial based wood polymer composites will have superior properties compared to conventional composites.

## 1.5. Basic components of wood polymer nanocomposite

There are three main basic components of wood polymer nanocomposite viz. wood, polymer and nanofiller. Wood fibers are used for the reinforcement of the polymer. This reinforcement leads to increase in the properties of the composite. The third component nanofillers, also have significant effect in increasing the desired properties of the composite. In case of clay, it depends on the orientation of the silicate layers. Exfoliated arrangement of silicate layers leads to maximum increase in properties compared to intercalate one as mentioned earlier. In case of nanoparticles, it depends on the distribution of the nanoparticles. Higher the distribution, better is the properties of the desired composite. The main ingredients of the wood polymer nanocomposites are discussed below:

### 1.5.1. Polymers

Polymers are widely used as a bonding agent for wood fibers in production of different wood based composite panels (e.g. particle board, MDF), but combinations of wood fibers and thermoplastics are virtually unknown to the industry. The thermoplastics

used for WPCs should have a melting or softening temperature less than the thermal degradation temperature of wood (around 210 °C) [20]. Commonly used thermoplastics for WPCs include high density polyethylene (HDPE), low density polyethylene (LDPE), polypropylene (PP), poly(vinyl chloride) (PVC), polyethylene terephthalate (PET) and polystyrene (PS). Both virgin and recycled plastics can be used for the development of composite [21]. Use of thermoplastic resins as a matrix in wood fiber-plastic composites has two main advantages: the resulting composite is thermoformable (i.e. it can be formed into various shapes when heated), and recyclable (i.e. the same batch of material can be used all over again). Liu et al. has [22] investigated the mechanical properties and morphologies of HDPE/bamboo flour (BF) composites modified with maleated ethylene/propylene elastomers (EPR-*g*-MA) and maleated polyethylene (PE-*g*-MA). Sui et al. [23] has developed polypropylene (PP) composites reinforced with a novel plant fiber, sunflower hull sanding dust (SHSD), and observed the increase in mechanical and thermal properties of the composite. Some of polymers which are commonly used for the composite development are as follows-

### 1.5.1.1. High density polyethylene (HDPE)

High density polyethylene is one of the most widely used commodity plastics. It is synthesized by using coordination catalysts or supported metal oxide catalysts that allow polymerization of ethylene at a much lower pressure as well as at a relatively low temperature. The low pressure polymers, HDPE, are by and large linear, having only 2-5 short branches or side chains per 1000 carbon atoms in the main chain, thus having a higher density range (0.945-0.96 g/cm$^3$) and higher melting temperature (125-130°C). MFI and Izod impact strength are in the range of 0.02-2.5 and 1.5-5 ft lb per inch of notch. The tensile strength of HDPE is in the range of 3000-5000 psi. HDPE has high crystallinity of 65-90%, good moisture-barrier properties and chemical resistance. It is the second most used packaging plastics. Products made of HDPE include containers for milk, detergent, juice, and water; industrial chemical drums; pharmaceutical bottles; shampoo and deodorant containers, etc. [24]. Ali Gungor [25] has developed HDPE composite by incorporating 5, 10 and 15 vol.% of Fe powder and observed an increase in modulus of elasticity and hardness compared to virgin HDPE. It has been reported that the addition of calcium carbonate to polyethylene increases the impact strength in the temperature range of −40 to +70 °C [26].

Natural fiber-reinforced thermoplastic composites have recently gained importance in various applications. Rice straw fiber can be considered as important potential reinforcing filler for thermoplastic composite because of its lignocellulosic characteristics. The HDPE based composite reinforced with rice straw fiber has been prepared and investigated by Yao et al. [27]. Nanoclay and wood flour reinforced HDPE composite has been prepared and studied by Faruk and Matuana [28]. The experimental results indicate that the mechanical properties of HDPE/wood-flour composites can be significantly improved with an appropriate combination of the coupling agent and types of nanoclay in the composites.

### 1.5.1.2. Low density polyethylene (LDPE)

LDPE is one of the leading plastics in the field of polymer. It is produced by free radical polymerization of ethylene under very high pressure (1500-3000 atm), using oxygen, peroxides or azo-compounds as initiator. LDPE has nearly 25-50 branches per 1000 linear carbon atoms in the chain molecules. The loss of molecular symmetry due to high degree of branching results in low density (0.915-0.94 g/cm$^3$), low softening and melting temperature (110-117 $^{o}$C). Due to lower molecular weight, it has a wide MFI range (0.3-70). The tensile strength range of LDPE is quite low (1500-2500 psi) but Izod impact strength value is as high as 10 ft lb per inch of notch. Its chemical resistance is low but its gas permeability is comparatively better compared to HDPE. Being adequately flexible, it is extensively used as an insulator in wires and cables.

The properties of LDPE can be improved by incorporation of clay. Zhao et al. [29] has developed low density polyethylene-clay nanocomposites by using chlorosilane modified clay. The results demonstrate that nanocomposites are more effective than conventional composites in reinforcement and addition of organoclay results in the increase of glass transition temperature ($T_g$) of the composite. Giannakas et al. [30] has prepared LDPE/clay nanocomposites and observed a gradual increase in crystallization temperatures ($T_c$) as clay content increases. Thermogravimetric analysis and tensile measurements results indicate that thermal stability and elastic modulus increment are more prevalent for nanocomposites prepared using organomontmorillonite as filler. Rusu and Tudurachi [31] have blended LDPE with acrylamide grafted wood flour. The tensile strength for LDPE–wood flour composite has been found to improve via peroxide crosslinking due to improved interfacial adhesion. Sailaja [32] has prepared LDPE-wood pulp composite grafted with

PMMA and reported an increase in mechanical, thermal properties and decrease in crystallinity of the composite.

### 1.5.1.3. Polypropylene (PP)

Poly(propylene) is the most widely used low density (0.9 g/cc) polymer in the automotive industry and in commodity products. This is mainly used in moulding articles like boxes, cages, automobile parts, hospital sterilize equipments, luggage, stacking chairs, parts of washing machine, toiletries, textile cover, goods packaging, etc. These applications are mainly based on its good mechanical strength, sterilizability, flexibility and overall low cost [33]. While it is less expensive, but it's mechanical and thermal properties are inferior to the engineering plastics. It has linear hydrocarbon structure with methyl group in each repeating unit. As the structure possesses only C-C single bonds in the main chain, thus it is sufficiently flexible and soluble in many hydrocarbon solvents. Its electric insulation property is almost similar to PE. Due to the presence of methyl groups, its flexibility is very less and thus $T_g$ (0 °C) and $T_m$ (150-165 °C) are comparatively higher than the other commodity plastics. Its mechanical properties like tensile strength (30-35 MPa), elongation at break (75-100%), hardness (90-95 Rockwell), and impact strength (180-250 kg/m) are very good.

Now days, to overcome the disadvantages of PP, such as low toughness and low service temperature, researchers have tried to improve the properties with the addition of nanoparticles that contain polar functional groups. Yuan and Misra [34] have used nanoclay to improve the impact strength of polypropylene composites. The incorporation of silicate layers gives rise to a considerable increase in storage modulus (stiffness) and a decrease in tanδ value, demonstrating the reinforcing effect of clay on the PP matrix [35]. Polypropylene (PP) has also been widely used for production of natural fiber/polymer composites because of its low density, high water and chemical resistance, good processability, and high cost–performance ratio [36-38]. Suppakarn and Jarukumjorn [39] have studied the mechanical and flammability properties of sisal/PP composite by using magnesium hydroxide [$Mg(OH)_2$] and zinc borate, as flame retardants and observed an increase in mechanical and thermal properties of the composite compared to neat PP. The storage modulus and thermal stability of PP/PALF nanocomposites have enhanced after the incorporation of clay. The $T_g$ of the matrix has shifted to high temperature regions with the incorporation of clays and fibers [40].

### 1.5.1.4. Poly(vinyl chloride) (PVC)

Poly(vinyl chloride), commonly named as PVC, is the most important of the vinyl thermoplastics in terms of production and application. The commercial products range from very rigid to very flexible items. The polymer is highly unstable when thermally treated at the processing temperatures and it is due to the discovery of a variety of heat stabilizers that the prospect of PVC technology becomes very bright and technology has reached its present height of success [41]. By varying the amount of plasticizer and other ingredients, it can be used for a wide range of applications from hard building materials to soft baby pants. It is also used as electrical insulation material for cable application especially sheathing (cover over the insulator of electrical wire) material. The unplasticized PVC is used in chemical plants and equipments, storage tank, building items like pipes, sheets, door, frame, containers, roof sheet, floor tiles, wall lining, etc. Semirigid and flexible application includes packaging, tubes, flexible pipes, hoses, sheets, films, footwear, belting, cables, baby pants, toys, etc.

PVC has linear structure but some short branches are formed sometimes in the structure, chlorine atom in each repeating unit. Because of the presence of chlorine atoms, the intermolecular attraction among the chain is very high, which makes the polymer horny rigid, stiff and hard. However, because of random polymerization the polymer is amorphous in nature with all possible tacticity in the structure with 55% syndiotactic (5% crystalline) and hence $T_g$ is approximately 80 °C. Mechanically it is good and properties vary with plasticizer content. It is soluble (solubility parameter 19.4 $MPa^{1/2}$) in THF, cyclohexanone, methyl ethyl ketone (MEK), etc. It exhibits self extinguishing characteristic due to presence of large amount of chlorine atom (56.8%) in its structure. PVC has low thermal stability which causes discolouration due to elimination of HCl and formation of conjugated polyene sequences. PVC–LDH composite is reported to exhibit better thermal stability than does PVC [42]. Awad et al. [43] has developed PVC nanocomposites based on organically modified clay and observed an increase in mechanical as well as thermal stability of the composites.

PVC based wood composites are widely used in building construction applications, such as window/door profiles, decking, railing and siding because they offer good mechanical properties, chemical and water resistance, rot-proof ability, stain and paint-ability, as well as a long lifetime (UV resistance, free from maintenance). Furthermore, PVC/wood composites can be cut, sawed, nailed, screwed, and processed by the

conventional wood working equipment [44]. It has been reported that increasing the addition of wood flour (sapwood and heartwood) to PVC has caused a small but progressive improvement of the decomposition temperature of the composites, whereas the glass transition temperature remains practically unchanged [45]. Augier et al. [46] has investigated the recycling of internal waste of poly(vinyl chloride) (PVC) and wood fiber-reinforced PVC composite and compared. Vegetable fibers accelerate the degradation of the polymer matrix leading to dehydrochlorination, formation of unsaturation and then crosslinking. As a consequence, the polymer chain length increases and the matrix show better mechanical properties, which enhance the entire mechanical properties of the composite.

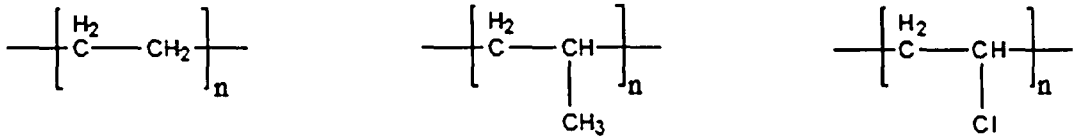


**Polyethylene** **Polypropylene** **Poly(vinyl chloride)**

**Figure 1.2.** Chemical structure of the polymers used in the formation of WPC.

## 1.5.2. Wood

Wood, a renewable resource, is the most abundant naturally occurring polymeric composite material. Wood was the multi-use structural material for the early beginning of industrial development.

The chemical and anatomic structure of wood affects strength properties; appearance; resistance to penetration by water, chemicals, and decay; pulp quality; and chemical reactivity [47,48]. The knowledge of the amounts and distribution of constitutive substances in the wood cell is required in order to use it effectively.

Woods are divided into hardwoods and softwoods. Hardwood trees are deciduous (angiosperms), generally have broad leaves, found in the temperate regions of the world, and contain a special cell called a vessel element. Softwood trees (conifers or gymnosperm) are cone-bearing, generally have scalelike or needlelike leaves, are not deciduous, and do not contain vessel elements. The terms hardwood and softwood have no direct application to the hardness or softness of the wood. In fact, hardwood trees such as cottonwood, aspen, and balsa have softer wood than the western white pines and true firs. Certain softwoods, such as

longleaf pine and Douglas fir, produce wood that is much harder than that of basswood or yellow poplar.

Because of the extreme structural variations in wood, species can be selected for a specific purpose. Some species, like spruce, combine light weight with relatively high stiffness and bending strength. Very heavy woods, like lignum vitae, are extremely hard and resistant to abrasion. Moreover, many mechanical properties of wood, such as bending strength, crushing strength, and hardness, depend on its density; the heavier woods are generally stronger [49]. Wood density is determined largely by the relative thickness of the cell wall and by the proportion of thick walled to thin-walled cells.

Nal (*Phragmites karka*) and kalmou (*Ipomea carniva*) which are the types of nonconventional plant, are widely available in the forests of Assam and on both the banks of The Brahmaputra river. These plants are not considered for structural applications due to their poor mechanical, dimensional and other properties. They are mostly used for making temporary shades and domestic fuels.

### 1.5.2.1. Hard wood

Figure 1.3 illustrates the cellular structure of a yellow poplar, an example of a hardwood [50]. The horizontal plane (TT) of the block corresponds to a minute portion of the top surface of a stump or end surface of a log, called the transverse surface. The vertical plane (RR) corresponds to a surface cut parallel to the radius and parallel to the wood rays (WR), called the radial surface. The vertical plane (TG) corresponds to a surface cut at right angles to the radius and the wood rays (WR) and is called the tangential surface. In temperate climates, trees often produce distinct growth layers called growth rings or annual rings (AR). These rings vary in width according to environmental conditions. Where there is visible contrast within a single growth ring, the first formed layer is called earlywood (S) and the remainder latewood (SM). Hardwoods have specialized structures called vessels for conducting sap upward. Vessels are a series of relatively large cells with open ends set one on top of the other and continuing as open passages for long distances. In most hardwoods the ends of the individual cells are entirely open, whereas in others they are separated by a grating, as indicated at SC. On the end grain, vessels appear as holes and are termed pores (P). The size, shape, and arrangement of pores vary considerably between species but are fairly constant within a species. Most of the smaller cells on the end grain are wood fibers (F), which are the strength-giving elements of hardwoods. They usually have small cavities

and relatively thick walls. Thin places or pits (K) in the walls of the wood fibers and vessels allow sap to pass from one cavity to another. Wood rays (WR) are strips of short, horizontal cells that extend in a radial direction. Their function is food storage and lateral conduction. In Figure 1.3, most of the rays in surface TG are two cells wide, but their width and height vary in different species of hardwoods, from 1 to more than 50 cells in width and from less than 100 μm to more than 100 mm in height.

All the cells in wood, including vessel cells, fibers, and ray cells, are cemented together by a thin layer, the middle lamella. This thin, intercellular layer is composed of lignin and carbohydrate.

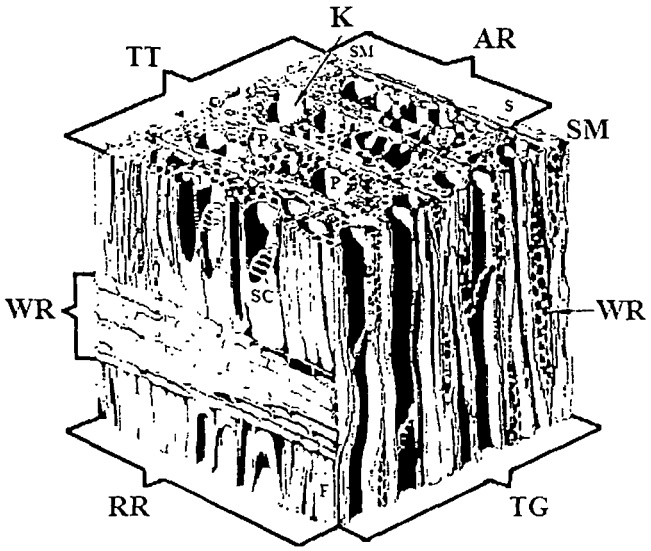


**Figure 1.3.** Cellular structure of hardwood (yellow poplar), enlargement of a block of 1 mm high. AR, annual rings; F, fiber; K, pits; P, pores; RR, edge grain; S, earlywood; SC, grating separating vessels; SM, latewood; TG, flat grain; TT, end grain; WR, wood rays.

### 1.5.2.2. Soft wood

Figure 1.4 illustrates the cell structure of white pine, an example of softwood. The three planes, TT, RR, and TG, represent the same three planes described for hardwoods. The rectangular units that make up the transverse surface (TT) are sections through long vertical cells called tracheids (TR). Because softwoods do not contain vessel cells, the tracheids serve the dual function of transporting sap vertically and giving strength to the wood. The wood rays (WR) store and distribute sap horizontally. Fusiform wood rays (FWR) are rays

with horizontal resin ducts (HRD) at their centers. The large hole in the center of the end grain is a vertical resin duct (VRD). Some softwood, such as cedar and true fir, do not have resin ducts. The annual ring (AR) is often divided into an earlywood zone (S) composed of thin-walled cells and a latewood zone (SM) composed of thicker walled cells. The symbol SP indicates a simple pit, an unthickened portion of the cell wall through which sap passes from ray parenchyma cells to tracheids or vice versa. Bordered pits (BP) have their margins overhung by the surrounding cell walls but still function as a passageway for sap to move from one cell to another.

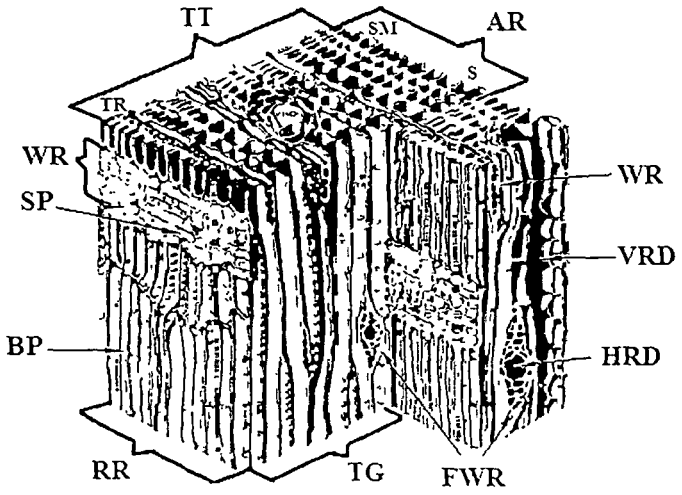


**Figure 1.4.** Cellular structure of softwood (white pine), enlargement of a block of 1mm high. AR, annual rings; BP, border pit; FWR, fusiform wood rays; HRD, horizontal resin duct; RR, edge grain; S, earlywood; SM, latewood; SP, simple pits; TG, flat grain; TR, tracheid; TT, end grain; VRD, vertical resin duct; WR, wood rays.

### 1.5.2.3. Chemical composition of wood

The principal chemical components of wood are carbohydrates (70–80%), lignin (20–30%), and extraneous materials (5–10%). Because the chemical composition varies between and among species, it is impossible to define absolute compositions. The average lignin content of softwood is slightly higher than that of hardwood. The carbohydrate consists primarily of cellulose, a linear polymer of anhydroglucose units, and lesser amounts of hemicelluloses, branch-chained polymers of several different compositions that include

five or six anhydro-sugars plus uronic anhydride.and acetyl substituents. The chain length of wood cellulose polymers is between 7,000 and 10,000 glucose units, whereas the hemicelluloses have chain lengths of 200 or less sugar units. Lignins are complex phenolic polymers of irregular structure. Molecular weights of isolated lignins have been measured up to 16,000. The extraneous materials are of much lower molecular weight (<1000) and can be removed from the wood with organic or aqueous solvents. They are not an integral part of the wood structure and include a wide variety of organic compounds and a small amount of inorganic salts.

***Carbohydrates.*** The carbohydrate portion of wood can be isolated as a white, fluffy material, called holocellulose, by dissolving the lignin. (The holocellulose consists of cellulose and hemicellulose.) The lignin is dissolved by treating wood meal alternately with chlorine gas and 2-aminoethanol. Alpha-cellulose, which is largely pure cellulose, is obtained from holocellulose by extracting the hemicellulose with 17.5% NaOH [51]. The carbohydrate wood polymers are built up from five sugars: glucose, xylose, mannose, galactose, and arabinose.

Cellulose is the principal component of wood carbohydrate (40–50% of the total wood). A cellulose molecule is a linear, straight-chain polymer of up to 10,000 anhydroglucose units [52]. X-ray diffraction studies have shown that much of wood cellulose is crystalline and resists attack from mild chemicals such as dilute acid. The length of a cellulose polymer chain (degree of polymerization) in wood is between 7,000 and 10,000 glucose units [53]. The degree of polymerization of cellulose and other wood polymers can be determined by light scattering, gel permeation chromatography, viscometry, osmometry, or sedimentation equilibrium.

Hemicelluloses are sugar polymers with a degree of polymerization of 200 or less. They have normally monomeric substituents or, in some cases, branch oligomer chains, and vary in composition and structure. A dozen or more different wood hemicelluloses have been isolated and characterized [54,55]. None of these is known to be a homopolymer, even though names such as xylans, mannans, and galactans are used. These hemicelluloses are soluble in NaOH and easily hydrolyzed by dilute acid [51]. Some, such as the galactans found in larch, are soluble in water [56]. The two most abundant wood hemicelluloses are xylans and glucomannans. The xylans occur in relatively large amounts in hardwoods (12–20%) and lesser amounts in softwoods (3–8%). Glucomannans are heteropolymers consisting of glucose and mannose units in slightly branched chains. The ratio of mannose to glucose units in hardwood glucomannans ranges from 1.5 to 2.0:1. The average degree of

polymerization is 60–70, and hardwood glucomannans comprise about 2–5% of the total wood. Softwoods contain 20–25% glucomannans, with an average degree of polymerization of 100. The glucomannans are substituted with acetyl and galactose groups. The average molar ratio of each group is approximately 3:1:0.1:1 for mannose, glucose, galactose, and acetyl, respectively. In both hardwood and softwood glucomannans, the glucose and mannose units are randomly distributed in the linear polymer chain.

Pectin substances are carbohydrates, which consist of low molecular weight galacturonans, galactans, and arabinans. Some also contain sugar units. They are present in less than 1% of most woods and occur in the middle lamellae and bordered pit membranes. The pectins are usually considered part of the extraneous materials in wood.

***Lignin.*** Wood lignin is an irregular, complex polymer consisting of methoxy- and hydroxy-substituted phenylpropane units. The lignin building blocks in the biosynthetic pathway are *p*- cournaryl alcohol (I), coniferyl alcohol (II), and syringyl alcohol (III) [57]. Softwood lignins result from the polymerization of H with very minor amounts of I and III. Hardwood lignins contain large amounts of II and III and traces of I. The most frequent bond types between monomers are ether bonds and carbon–carbon single bonds.

Lignins are difficult to isolate from wood and are chemically modified or degraded in the process. Lignin is present in both the cell wall and the middle lamella between fibers. It imparts such strength to the wood that trees are able to grow to enormous heights (up to 100m). Such heights are not possible in plants lacking lignin. Indirect evidence indicates that lignin is chemically bonded to the carbohydrate material in wood; such bonds are referred to as L-C bonds. Lignin samples are obtained by removing most of the carbohydrate material by milling and solvent extraction [58,59] or milling and enzymatic hydrolysis [60].

The existence and distribution of different lignins within a given wood are controversial. Some evidence (UV microscopy) indicates that cell-wall lignin of hardwoods is enriched in syringyl lignin (units derived from syringyl alcohol, III) and middle lamella lignin is enriched in guaiacyl lignin (units derived from coniferyl alcohol, II) [61]. However, conflicting evidence from methoxyl analysis of isolated morphological parts of white-oak wood *(Quercus alba* L.) indicates a uniform distribution of guaiacyl and syringyl components [62]. Pyrolysis–gas chromatography-mass spectrometry is another method to determine lignin type by identification of pyrolysis products [63]. The pyrolysis products from the vessels of white oak, white birch, and American elm show that the vessel lignin is of the syringyl-guaiacyl type, in contrast to the guaiacyl type found by UV microscopy.

***Extraneous Materials.*** Extraneous materials in wood are nonpolymeric, low molecular weight substances that can be removed by a solvent without being chemically modified. They include organic materials such as gums, mucilages, sugars, tannins, fats, waxes, pectins, resin acids, terpenes, lignins, flavonoids, stilbenes, phenolics, alcohols, steroids, and inorganic salts. The organic materials are usually referred to as extractives; they are present in varying amounts, depending on tree part, species, location, and time of year. Organic materials constitute 5–10% of most wood in temperate climates; they are usually soluble in neutral or slightly polar solvents, such as diethyl ether or a 2:1 mixture of ethanol–toluene. The inorganic component of the extraneous material, commonly referred to as ash, is the residue remaining after the wood has been heated to a high temperature. Most woods generally comprises of 0.3–0.5% of ash in temperate climates. Calcium is usually the most abundant constituent (500–1200 ppm), followed by potassium (200–1000 ppm) and magnesium (100–300 ppm); manganese, sodium, chlorine, phosphorus, aluminum, and zinc are present in amounts less than 100 ppm. Tropical woods generally have higher ash content (0.5–1.5%) [64].

## 1.5.3. Compatibilizer

One of the major disadvantages of WPC is the poor compatibility between the fibers and the polymeric matrices, which results in non-uniform dispersion of fibers within the matrix and poor mechanical properties. Most polymers, especially thermoplastics, are nonpolar (hydrophobic) substances, which are not compatible with polar (hydrophilic) wood fibers and, therefore, poor adhesion occurs between polymer and fiber in WPC [65].

In order to improve the affinity and adhesion between fibers and thermoplastic matrices, chemical "coupling" or "compatibilizing" agents have been employed [66]. Chemical coupling agents are substances, typically polymers that are used in small quantities to treat a surface so that bonding occurs between it and other surfaces, e.g. wood and thermoplastics. The coupling agent forms bond chemically with hydrophilic fiber and the polymer chain [67]. The coupling forms include covalent bonds, secondary bonding (such as hydrogen bonding and van der Waals forces), polymer molecular entanglement and mechanical interblocking [68]. Therefore, chemical treatments can be considered in modifying the properties of plant fibers. The mechanism of compatibilizing agent is shown in Figure 1.5.

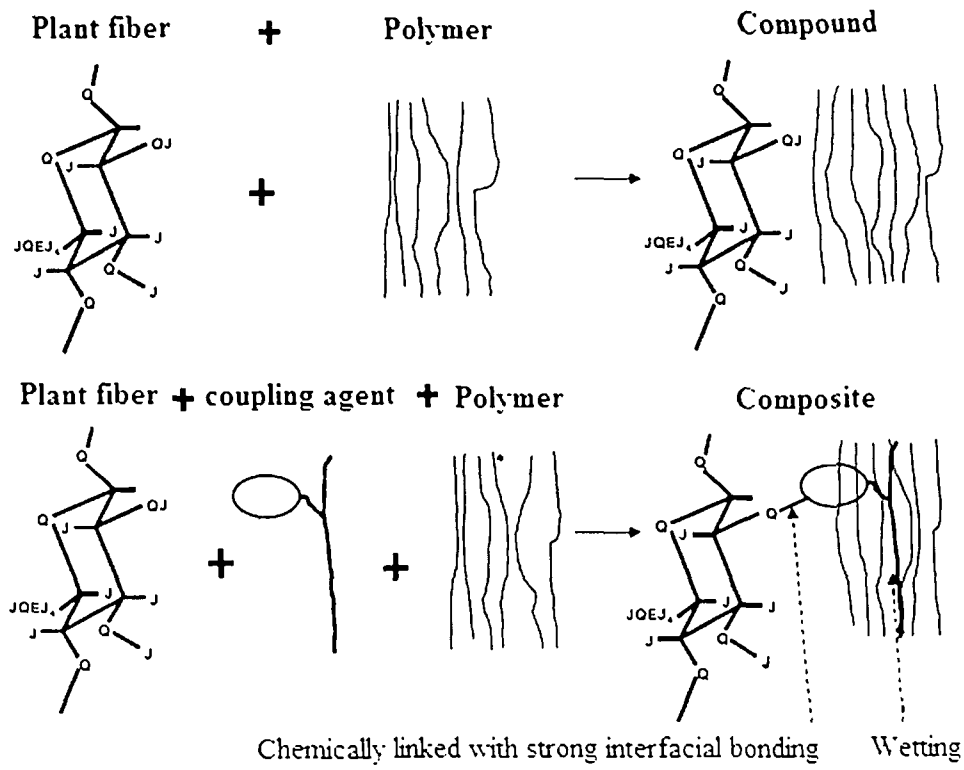


**Figure 1.5.** Mechanism of coupling agent between hydrophilic fiber and hydrophobic polymer matrix.

The various compatibilizers used in composites are shown as below:

### 1.5.3.1. Glycidyl methacrylate (GMA)

Crosslinking of material in wood provides better dimensional stability and other properties to the wood polymer composite [69]. Glycidyl methacrylate is one of the commonly used compatibilizer in wood polymer composite. The homopolymer and copolymers based on glycidyl methacrylate (GMA) belong to the class of potential functional polymers. The high reactivity of the epoxy group to a large variety of reagents provides novel routes to prepare numerous multifunctional polymers through chemical modification of these polymers [70]. It is a water insoluble clear liquid having molecular formula $C_7H_{10}O_3$. Its molar mass and density is 142.2 g/mol and 1.07 g/cm$^3$ with boiling point 189.0 °C. In GMA, both double bond and epoxy group are present. The glycidyl group is capable of reacting with groups containing active hydrogen such as amino, hydroxyl, and carbonyl group [71]. The glycidyl group and terminal double bond in GMA can be exploited

for reaction with hydroxyl group of cellulose present in wood and for co-polymerization with vinyl or acrylic type monomers, respectively. Research has demonstrated that chemical modification enhances a number of wood properties including its resistance to fungal decay, colonization by moulded fungi, and attack by marine wood borers and insects [72-74]. Rubber wood treated with styrene and GMA as the crosslinking monomer improves various physical and chemical properties [75-77]. Devi and Maji [78] have used glycidyl methacrylate (GMA) with styrene to improve the dimensional stability, mechanical properties and biodegradation property of pine wood. Rozman et al. [79] has developed rubber wood-polymer composite based on glycidyl methacrylate and diallyl phthalate (DAP). The results have shown that WPC based on GMA exhibits about five times more dimensional stability than those based on DAP alone. Modulus of elasticity (MOE), modulus of rupture (MOR), compressive and impact properties for all the samples tested have improved, especially for those having higher chemical loading. GMA-grafted nylon-6 type membrane has been developed by Teke and Baysal [80] for immobilization of urease which is a useful system in kidney machine to maintain the urea level in the blood of patients suffering alterations in kidney function.

### 1.5.3.2. Polyethylene-*co*-glycidyl methacrylate (PE-*co*-GMA)

Polyethylene-*co*-glycidyl methacrylate is one of the efficient compatibilizer. It is a copolymer of polyethylene and glycidyl methacrylate. It is solid having melting point around 115-120 °C. In the molecular structure, the long chain of polyethylene is grafted to the double bond of glycidyl methacrylate group. In wood polymer composite, due to the presence of olefinic long chain, it can be worked in a better way as compatibilizer compared to glycidyl methacrylate. The long olefinic chain and the glycidyl group can interact with the polymers and the hydroxyl group of wood resulting in better compatibility between polymers and wood. Dikobe and Luyt [81] have developed ethylene vinyl acetate (EVA)–wood fiber (WF) composite with and without the addition of compatibilizer, and investigated their morphology, mechanical, thermal, $O_2$ permeability, and water absorption properties. A weak interaction exists between EVA and WF in absence of compatibilizer and as a result the composites show poor properties. The presence of PE-*co*-GMA in the composite improves almost all of the investigated properties. The addition of polyethylene-*co*-glycidyl methacrylate to increase the Izod impact strength and toughness of recycled polyethylene terephthalate has been reported by Kunimune et al. [82]. They have observed that the impact

strength increases in a regular manner upto a certain level of loading, but beyond that level it drastically improves the toughness of the blend. The increase in the mechanical and thermal properties of wood polymer composite is due to the presence of polyethylene-*co*-glycidyl methacrylate as reported by Sailaja [32].

### 1.5.3.3. Polyethylene-*graft*-maleic anhydride (PE-*g*-MA)

A possible solution to overcome the problem of incompatibility among the wood polymer composite (WPC) is the introduction of additives like polyethylene-*graft*-maleic anhydride (PE-*g*-MA). The anhydride and the polyethylene groups can react with the hydroxyl groups of wood flour and long chain of polymer. The incorporation of an optimum amount of PP-*g*-MA to polypropylene based WPC improves various properties [83]. The effect of polyethylene-*g*-maleic anhydride (PE-*g*-MA) as a compatibilizer on tensile properties and morphology of low density polyethylene/thermoplastic sago starch (TPSS) kenaf fiber composites has studied by Ismail et al. [84]. Results indicate that at higher fiber loading, PE-*g*-MA added LDPE/TPSS-kenaf fiber composites exhibit higher tensile strength and Young's modulus than the composites without having PE-*g*-MA. The interfacial properties between LDPE, TPSS and fiber have been improved after the addition of PE-*g*-MA as evident from the morphology study of fractured tensile surface. The incorporation of maleic anhydride grafted polyethylene to the wood/HDPE composites has reduced linear thermal expansion coefficients and improved mechanical properties [85]. With the increase in the amount of MAPP to the PP/bagasse flour/clay nanocomposites, the physical and mechanical properties of the composite increase [86].

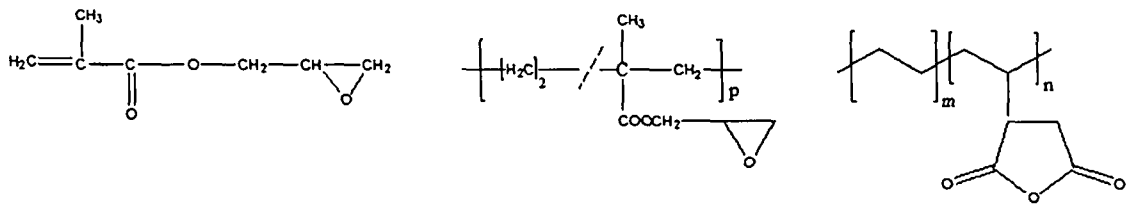

**GMA** **PE-*co*-GMA** **PE-*g*-MA**

**Figure 1.6.** The chemical structure of different compatibilizers.

## 1.6. Different types of additives

The chemicals or substrate or materials, which are necessary to incorporate into the virgin polymers to obtain the desired level of properties for their different applications are known as additives for polymers. All the chemicals or materials cannot be an additive for polymers. They should fulfill some criteria to act as an additive for polymers. They should be efficient in their function, i.e. the purpose for which they are being incorporated into the polymer, should efficiently work for that. They should be stable under processing as well as service conditions. The additive should not degrade or decompose or alter its nature during processing and under service conditions. They should not bleed or bloom. They should be non-toxic and should not impart any taste, odour or colour to the polymer matrix. The additives should be inert other than their own functions. They should be available in sufficient quantity as required and should have low cost. The physical state of additive may be solid, liquid or even gaseous. The semi-liquid like rubbery and gel are also used in some cases. However, gaseous additives are only used in case of foam products.

### 1.6.1. Clay

The layered silicates commonly used in nanocomposites belong to the structural family known as the 2:1 phyllosilicates. Their crystal lattice consists of two-dimensional layers where a central octahedral sheet of alumina or magnesia is fused to two external silica tetrahedron by the tip so that the oxygen ions of the octahedral sheet do also belong to the tetrahedral sheets. The layer thickness is around 1 nm and the lateral dimensions of these layers may vary from 300 Å to several microns and even larger depending on the particular silicate. These layers organize themselves to form stacks with a regular van der Waals gap in between them called the interlayer or the gallery. Isomorphic substitution within the layers (for example, $Al^{3+}$. replaced by $Mg^{2+}$ or by $Fe^{2+}$, or $Mg^{2+}$ replaced by $Li^{+}$) generates negative charges that are counterbalanced by alkali or alkaline earth cations situated in the interlayer. As the forces that hold the stacks together are relatively weak, the intercalation of small molecules between the layers is easy [87]. In order to render these hydrophilic phyllosilicates more organophilic, the hydrated cations of the interlayer can be exchanged with cationic surfactants such as alkylammonium or alkylphosphonium (onium). The modified clay (or organoclay) being organophilic, its surface energy is lowered and is more

compatible with organic polymers. These polymers may be able to intercalate within the galleries, under well defined experimental conditions.

Montmorillonite, hectorite and saponite are the most commonly used layered silicates. Their structure is given in Figure 1.7 [88] and their chemical formula are shown in Table 1.1.

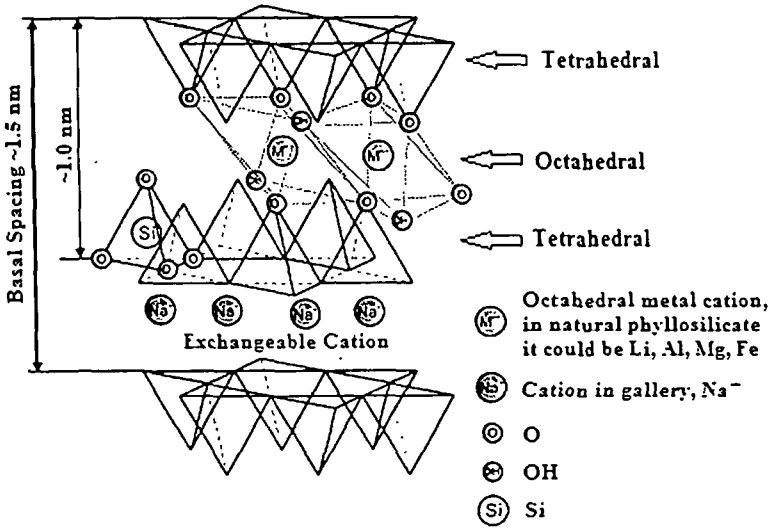


**Figure 1.7.** Structure of 2:1 phyllosilicates.

This type of clay is characterized by a moderate negative surface charge (known as the cation exchange capacity, CEC and expressed in meq/100 g). The charge of the layer is not locally constant as it varies from layer to layer and must rather be considered as an average value over the whole crystal. Proportionally, even if a small part of the charge balancing cations is located on the external crystallite surface, the majority of these exchangeable cations are located inside the galleries. When the hydrated cations are ion-exchanged with organic cations such as more bulky alkyammoniums, it usually results in a larger interlayer spacing.

In order to describe the structure of the interlayer in organoclays, one has to know that, as the negative charge originates in the silicate layer, the cationic head group of the alkylammonium molecule preferentially resides at the layer surface, leaving the organic tail radiating away from the surface. In a given temperature range, two parameters then define the equilibrium layer spacing: the cation exchange capacity of the layered silicate, driving the packing of the chains, and the chain length of organic tail (s). According to X-ray diffraction (XRD) data, the organic chains have been long thought to lie either parallel to the

silicate layer, forming mono or bilayers or, depending on the packing density and the chain length, to radiate away from the surface, forming mono or even bimolecular tilted 'paraffinic' arrangement [89] as shown in Figure 1.8.

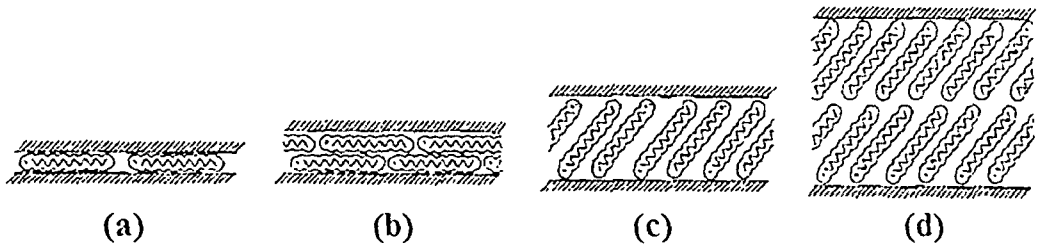


**Figure 1.8.** Alkyl chain aggregation in layered silicates (a) lateral monolayer (b) lateral bilayer (c) paraffin-type monolayer (d) paraffin-type bilayer.

**Table 1.1.** Chemical structure of commonly used 2:1 phyllosilicates[a].

| 2:1 Phyllosilicate | General formula |
|---|---|
| Montmorillonite | $M_x(Al_{4-x}Mg_x)Si_8O_{20}(OH)_4$ |
| Hectorite | $M_x(Mg_{6-x}Li_x)Si_8O_{20}(OH)_4$ |
| Saponite | $M_xMg_6(Si_{8-x}Al_x)O_{20}(OH)_4$ |

[a]M=monovalent cation; x=degree of isomorphous substitution (between 0.5 and 1.3).

### 1.6.2. Silicon dioxide ($SiO_2$)

Nanopowders are the three dimensional uni-axial nanosized objects at a level intermediate between atom/molecule and bulk. Although nanopowders involving metals (Au, Pt, Pd, Cu, etc.), semiconductors (ZnS, CdS, CdSe, etc.), metal oxides ($SiO_2$, $Al_2O_3$, $TiO_2$, ZnO, $Fe_2O_3$, etc.) are everywhere in nature, they grow into micro-powders or macroscopic materials instantaneously and then lose their specific features. Therefore, how to produce a nanopowder with controlled size and degree of aggregation is a key issue. Generally, nanopowders do not exhibit classical bulk properties. They differ from the molecules or atoms that in some way represent pieces of matter related to the bulk material they originate from.

Silica nanoparticles occupy a prominent position in scientific research, because of their easy preparation and their wide uses in various industrial applications, such as catalysis,

pigments, pharmacy, electronic and thin film substrates, thermal insulators, and humidity sensors [90]. The quality of some of these products is highly dependent on the size and size distribution of these particles. Silica ($SiO_2$) has a structure in which all oxygen atoms of $SiO_4$ units are shared. Pure silica occurs in two forms: quartz and cristobalite. In cristobalite the silicon atoms are placed as the carbon atoms in diamond (cubic close-packed (ccp) with half of the tetrahedral holes occupied), with the oxygen atoms midway between each pair of silicon atoms. Quartz is built up of $SiO_4$ tetrahedra as in silicates with each oxygen atom shared by two silicon atoms so that the empirical formula is $SiO_2$. Quartz and cristobalite can be interconverted when heated. The interconversion process is slow. However, the rates of conversion are profoundly affected by the presence of impurities, or by the introduction of alkali-metal oxides.

The synthesis of monodisperse and uni-sized silica nanoparticles has been carried out using ultrasonication by sol-gel process [91]. The silica particles are obtained by hydrolysis of tetraethyl orthosilicate (TEOS) in ethanol medium and a detailed study relating to the effect of different reagents on particle sizes has been carried out. One of the important properties of $SiO_2$ is its high ability to improve thermal and mechanical property of the polymers.

### 1.6.3. Zinc oxide (ZnO)

With a wide direct bandgap, strong excitonic binding energy and controllable morphology, zinc oxide (ZnO) nanostructures have attracted much interest recently, for promising application in nano-optoelectronic devices. So far, various nanostructures of ZnO, such as nanowires, nanorods, nanobelts, nanotubes and nanocables, have been fabricated by means of various methods, including vapour phase transport, metal organic vapour-phase epitaxy, aqueous thermal decomposition and electrochemical deposition. Significant advances in realizing ZnO nanostructure devices, for instance, ultraviolet (UV) nanolaser action and field emission have been demonstrated [92].

Besides uniform one-dimensional structural ZnO, some three-dimensional (with branches) nanostructures have been prepared by combining ZnO with other oxides. For example, Lao et al. [93] has fabricated the ZnO–$In_2O_3$ hierarchical structures with mutli-facets, and Gao and Wang [94] have synthesized nanowire–nanoribbon junction array of ZnO by introducing $SnO_2$ into source material. Some researchers [95-97] have grown ZnO

whiskers with tetrapod or multipod structure, however, the diameter of the legs was often too large in diameter (more than several micrometers or even several tens micrometers).

In polymer composite, nano ZnO is widely used as anti photodegradant. On the contrary to $TiO_2$, with the incorporation of nano-ZnO into the PP, the extent of photodegradation was significantly reduced. This is due to the superior UV light screening effects offered by the ZnO nanoparticles. UV irradiation induced degradation causes a significant drop in the ductility for unfilled PP whereas, its nanocomposites with nano-ZnO, the ductility, and hence the tensile strength are recovered to some extent. The higher the ZnO particle content, the higher the elongation at break value in the UV irradiation treated nanocomposites. It is also reported that surface cracks are induced by photodegradation, and the *Talysurf* surface profile measurements indicate that the severity of the surface cracks is significantly reduced in the ZnO/PP nanocomposites [98]. Besides anti photodegradant effect, ZnO nanopowder can also improve thermal stability of polymer. Laachachi and co workers [99] have studied the thermal properties of PMMA by incorporation of ZnO and organo-modified MMT and found an increase in thermal stability.

### 1.6.4. Titanium dioxide ($TiO_2$)

Titanium dioxide adopts at least 8 structures. Besides its four polymorphs found in nature (i.e. rutile, anatase, brookite, $TiO_2$ (B)), additional high-pressure forms have been synthesized: $TiO_2$ (II) with the $\alpha$-$PbO_2$ structure, $TiO_2$ (H) with hollandite, baddelleyite with $ZrO_2$, Cotunnite with $PdCl_2$ [100]. Among them, rutile, anatase are mostly manufactured in chemical industry as microcrystalline materials. The two polymorphs are based on interconnected $TiO_6$ octahedra, but their linkages and degree of edge and face sharing differ. Anatase can be regarded to be built-up from octahedrals that are connected by their vertices; in rutile, the edges are connected. $TiO_{2-x}$ with x=0.0001 to 0.0004 is found in bulk materials. Principally the surface contains several atoms, ions and molecules via ionic, covalent or coordinated bonding such as basic terminal and acidic bridged hydroxyl groups; labile Ti-O-Ti bonds; water molecules adsorbed at Lewis acid sites or bound to surface hydroxyl groups; adsorbed anions such as sulphate or chloride process residues; potential electron donor and acceptor sites; possibly adsorbed oxidants such as hydroxyl or hydroperoxyl radicals; or activated oxygen species generated by photocatalytic processes [101].

Thermodynamic calculations show that rutile is the most stable phase at all temperatures and pressures below 60 kbar, when $TiO_2$ (II) becomes the favourable phase [100]. Reverse phase stability is described by particle size experiments due to size effect on surface energy. Anatase is most stable at sizes less than 11 nm, brookite at sizes between 11-35 nm, rutile at sizes greater than 35 nm [102].

$TiO_2$ has received a great amount of applications due to its strong oxidizing power of the photogenerated holes, chemical inertness, non toxicity, low cost, high refractive index and other advantageous surface properties. Half of all $TiO_2$ pigment produced is consumed in decorative and architectural paints widely serving to house buildings, wood or furniture, industrial coating, and automobile finishes. $TiO_2$ is non-toxic, safe, and corrosion protective and can be dispersed easily as well as absorbs incident UV and protects the paint from direct photochemical degradation of organic binder, making it ideally suited for the paint industry [103]. $TiO_2$ is also added to provide opacity to the plastic materials and improve photodurability. In the paper industry, $TiO_2$ is used in conjunction with clay, $CaCO_3$, and other pigments to impart brightness and opacity. Even the marking on gelatin capsule can contain $TiO_2$. In addition, pure $TiO_2$ is highly effective as a new sun screener, applied to many cosmetic products; as an anticorrosive additive, applied to food industry [104].

$TiO_2$ photocatalysis has its origins in early research effort into photoelectrochemical systems for solar to chemical energy conversion. Fujishima and Honda have found that $TiO_2$ can be used as catalytic electrode in photoelectrolysis cell to decompose water into $H_2$ and $O_2$, without the application of an external voltage [105]. After a few years, it is realized that this micro-cells, consisting of $TiO_2$ particles with deposit of Pt on them, is also able to work as photocatalysis for splitting $H_2O$. The importance of $TiO_2$ in heterogeneous catalysis is also profound and the performances of many metals or metal oxides on high-surface-area $TiO_2$ support have been studied. These metal oxide/$TiO_2$ systems often serve as a model for other metal/oxide surfaces. It is well known that the role of $TiO_2$ on catalytic activity is more complex than simple to increase catalyst surface area. The interactions between the catalyst and $TiO_2$ may occur that lead to changes in reactivity and selectivity [106]. Another successfully existing utilization of $TiO_2$ is as gas sensor because it may change its electrical conductivity upon gas adsorption like $SnO_2$ and ZnO semiconductors. $TiO_2$ is used as an oxygen gas sensor, e.g. to evaluate the combustion process of fuel in car engines for controlling fuel consumption and environmental pollution [107].

## 1.7. Different techniques of composite preparation

Regardless of the type of nanoparticles, there are generally three methods to fabricate polymer nanocomposites: melt blending, solution blending and in-situ polymerization.

### 1.7.1. Melt blending process

It is environmental friendly since it does not require any solvent. Melt blending is the most widely used technique to synthesize polymer composites. Due to its compatibility to the current polymer extrusion process, melt blending offers a promising route to produce polymer composites on a large scale. In this process, the nanoparticles (nanoclay, ZnO, $SiO_2$, $TiO_2$ etc.) are mixed directly with the molten polymers. Mixing may occur either statically or under high shear.

Twin-screw extrusion is the most common method to blend the polymers with the particles. It has been found that both the screw design and the residence time affect the dispersion of nanoparticles. Generally, increasing the mean residence time and the use of back mixing will improve the particle dispersion. However, excessive shear intensity or back mixing will lead to a poor mixing. The reason for this phenomenon is yet not clear. Additionally, owing to the complexity of the process itself, the studies on how the process conditions affect the formation of nanocomposites is inadequate. Another important disadvantage of melt blending process is that it suffers from stress development and generates high temperature [108]. High temperature sometime leads to degrade the raw materials which have lower processing temperature.

To date, a wide variety of nanocomposites has been prepared via melt blending. For nanoclay-filled systems, examples include nylon 6 [109-111], PS [112,113], polypropylene (PP) [114-116], PEO [117,118], ethylene-vinyl acetate copolymer (EVA) [118]. Different polymer based wood composite has also been extensively developed by using melt blending process [18,119-121].

Lattice-based mean field theory has been applied to explain the thermodynamics that is driving the intercalation of polymers into the spacing among nanoparticles. Generally, a mixing process is controlled by both entropic and enthalpic factors. While an unfavourable entropy loss may occur during mixing, the enthalpy can be rendered favourable by maximizing the magnitude and number of polymer-particle interactions [122].

Although melt blending offers a simple way to synthesize nanocomposites, it is not a feasible method to achieve a nano-scaled particle dispersion for composite systems composed of a large volume of nanoelements and high molecular weight polymers. Moreover, in the case of CNTs/CNFs, a high temperature (to lower the melt viscosity) and a high shear force (for mixing) will result in the degradation of CNTs/CNFs.

### 1.7.2. Solution blending process

In solution blending, the polymer is first dissolved in a common solvent or a solvent mixture. Subsequently, nanoparticles are mixed into the polymer solution, usually with the aid of ultrasonication. Depending on the interactions between the nanoparticles and the solvent, the van der Waals force among nanoparticles (stacks for nanoclay, ropes or bundles for CNTs/CNFs) can be reduced, thus facilitating the polymer chains to diffuse into the spaces among nanoparticles. The unique advantage of this method is that it is capable of dispersing nanoparticles in the polymer matrices while maintaining the large aspect ratio of the original nanoparticles. Moreover, with the aid of an electric or a magnetic field, solution blending can provide a novel way to orient those anisotropic nanoparticles (e.g. nanoclay and CNTs/CNFs). The major disadvantages of this method are its toxicity and the large amount of solvent needed, resulting in higher purification costs. In addition, its applicability will be greatly limited by the selection of proper solvents. Nevertheless, this method is especially attractive in preparing water soluble polymer-clay nanocomposites, e.g. polyvinyl alcohol (PVA) [123], poly ethylene oxide (PEO) [114,117,124], poly acrylic acid (PAA) [125].

Some non polar polymer composite can also be developed by using solution blending method. PP-clay nanocomposite using xylene as solvent has been prepared by Sarkar et al. [126]. They have found an improvement in mechanical properties of the final composite. Several other literatures are available regarding the solution blending of polymers using different non polar solvent [11,127,128].

### 1.7.3. In-*situ* polymerization

The idea of in-situ polymerization was first proposed in the 1960s and it has been widely applied to the polymer-clay systems. Unlike solution blending or melt blending where nanoparticles interact with the polymer molecules, in-situ polymerization offers a

route where the dispersion of the nanoparticles takes place simultaneously with the growth of the polymer chains, from low-molecular-weight monomers to high-molecular-weight polymers. In this method, the nanoparticles are first mixed with the monomer. Subsequently, polymerization takes place. Due to the lower viscosity of the monomer (as compared to that of polymer melt or polymer solution), it is much easier to break the aggregated particles using either sonication or high shear mixing. In addition, once the monomer diffuses into the clay interlayer, the interlayer can be further expanded due to the growth of the polymer chains. Furthermore, combined with the use of surface modifications, this technique provides a practical way to grow the polymer chains directly from the particle surfaces. Therefore, both the particle dispersion and the interfacial bonding between the particles and the polymers can be significantly improved.

For thermosets, such as epoxy composites, in-*situ* polymerization is the only viable method to incorporate nanoparticles into the polymer domain [129-131]. For thermoplastics such as poly(methyl methacrylate)(PMMA) [132,133], polyimide [134], PS [135,136], *in-situ* polymerization also exhibits unique advantages to facilitate the particle dispersion and to improve the wettability between the particles and the polymers. To summarize, in-situ polymerization can be used to produce polymer nanocomposites with molecular-level particle dispersion. In particular, functionalized nanoparticles become an integral, chemically bonded part of the polymer matrix, leading to a significant improvement in both mechanical and physical properties.

### 1.7.4. Template synthesis

This technique, where the silicates are formed in situ in an aqueous solution containing the polymer and the silicate building blocks, has been widely used for the synthesis of double-layer hydroxide-based nanocomposites [137,138] but is far less developed for layered silicates. In this technique, based on self-assembly forces, the polymer aids the nucleation and growth of the inorganic host crystals and gets trapped within the layers as they grow.

### 1.7.5. Other techniques

Wood polymer composites are processed by other simple processing techniques such as hand layup and spraying, compression, transfer, resin transfer, injection, compression

injection, and pressure bag molding operations etc. A few other methods such as centrifugal casting, cold press molding, continuous laminating, encapsulation, filament winding, pultrusion, reinforced reaction injection molding, rotational molding, and vacuum forming are being used for composites but use of these methods for natural fiber composites is hardly reported. In thermoset polymers, the fibers are used as unidirectional tapes or mats. These are impregnated with the thermosetting resins and then exposed to high temperature for curing.

## 1.8. Properties evaluation of wood polymer nanocomposite

### 1.8.1. X-ray diffraction (XRD)

X-ray diffraction is a widely used technique to characterize the wood polymer nanocomposite. Due to easy availability and simple analysis method, it is frequently used to analyze the nanocomposite structure, and sometimes to study the kinetics of polymer melt intercalation. XRD technique offers a convenient way to determine the interlayer spacing of the silicate layers in the original layered silicates and in the intercalated nanocomposites in the range of 1-4 nm. In case of polymer/nanolayer nanocomposite the shape, size, position and intensity of XRD pattern indicate the intercalated or exfoliated structure of the nanocomposite. Faruk and Matuana [28] have used X-ray diffraction method to characterize the degree of intercalation of nanoclay in HDPE based wood polymer composite. The increase in the interlayer spacing of nanoclay layers in wood flour loaded PP composite has been studied by Ghasemi and Kord [139]. Again appearance of new desired peaks confirms the formation of polymer/metal nanoparticles nanocomposite. The appearance of crystalline peaks of $TiO_2$ nanoparticles in PP matrix has been investigated by Mina et al. [140]. Typical XRD pattern of silicon powder in HDPE/$SiO_2$ composite has also been cited in the literature [141]. The shifting and disappearance of the peaks may suggest the formation of intercalated or exfoliated structure but it is not conclusive, as several factors affect the accuracy of this analysis. If the sensitivity and scanning time is low, concentration of the nanolayers are beyond the detection capacity and the presence of strong absorbing atom may result in loss of diffraction peaks. Thus the analysis may mislead and are not quantitative.

### 1.8.2. Transmission electron microscopy (TEM)

Transmission electron microscopy is a powerful microscopy technique, which provides qualitative understanding on internal structure, spatial distribution of various phases and views the defect structure through direct visualization. The intercalated structure of PE nanocomposites based on clay has been observed by TEM study [142]. Salimi et al. [143] has examined different images taken at different points for evaluation of clay dispersion. In all samples, different degrees of clay intercalation ranging from clay agglomeration to fully exfoliation have been observed. The distribution pattern of nanoclay into the HDPE/wood flour composite has been studied by Guo et al. [144]. However, TEM is time intensive and gives only localized qualitative information of the sample as a whole. In some instances, the organic component of the samples may decompose under electron beam. In such condition, cryogenic microscopy (cryo-TEM) is used where the specimen is measured at liquid nitrogen or liquid helium temperature in a frozen state. In recent time, high resolution TEM (HRTEM) is used to obtain a much closer look at the samples. The application of electron energy loss spectroscopy imaging techniques to TEM (ESI-TEM) can provide information on the composition of polymer surface and proved to be a powerful technique for the characterization of colloidal nanocomposites.

### 1.8.3. Scanning electron microscopy (SEM)

SEM is an electron microscopy technique for analysis and imaging of micro and nanostructures. SEM creates characteristic 3D appearance of images and therefore useful for judging the surface morphology of the samples. The miscibility among different polymers can be well investigated by the SEM analysis. Due to the phase separation among the polymers, there exists always an interfacial phase separation. The increase in compatibility among the polymers after the incorporation of compatibilizer has been investigated by SEM study. Pracella et al. [10] has observed the phase separation between PET and polyolefins (HDPE, PP) by SEM analysis. They have also observed the increase in miscibility among the polymers after the incorporation of compatibilizer. The final morphology and the anisotropic phase formation of layered silicate nanocomposites depend on the clay content. Moreover, SEM analysis also helps in evaluating the existence of microbes in polymer composite after the degradation study. Konwar et al. [145] has prepared polyester/clay nanocomposite and studied the biodegradation property by using *Pseudomonas aeruginosa*

and *Bacillus subtilis* strain and SEM study shows the growth of microbes colony in the composite. The attack of *Xylophagus fungi* on WPC has been studied by Lomeli-Ramirez et al. [146]. The SEM micrograph of the decomposed samples reveals the presence of the fungi on the WPC.

### 1.8.4. Fourier transform infrared (FTIR) spectroscopy

FTIR is a widely used technique to verify the formation of nanocomposites. These spectra are useful to predict existence/disappearances of H-bonding between the nanomaterial and matrix. It has been observed that the intensity of the hydroxyl peak always decreased and shifted to lower wave number after the formation of nanocomposite. A decrease in peak intensity of hydroxyl group and shifting to lower wave number in wood polymer composite has been reported by Dikobe and Luyt [81]. The incorporation of polymer molecules to the wood polymer composite can also well justified by observing the –CH peak intensity. Awal et al. [147] has developed PP/wood composite and they have observed an increase in the –CH peak intensity of PP after the formation of composite. The information about the formation of metal-oxygen bond in nanocomposite can also determined by FTIR study. For example, the appearance of the bands at ~1130 $cm^{-1}$ and ~820 $cm^{-1}$ corresponds to the Si-O-Si and Si-OH bond stretching in the FTIR spectra of polymer/clay nanocomposites.

### 1.8.5. Mechanical properties

The properties of natural fiber reinforced composites depend on a number of parameters such as volume fraction of the fibers, fiber aspect ratio, fiber– matrix adhesion, stress transfer at the interface, and orientation. Most of the studies on natural fiber composites involve study of mechanical properties as a function of fiber content, effect of various treatments of fibers, and the use of external coupling agents [148,149]. Other aspects include the prediction of modulus and strength using some well-established models for two-phase systems and comparison with experimental data.

Both the matrix and fiber properties are important in improving mechanical properties of the composites. The tensile strength is more sensitive to the matrix properties, whereas the modulus is dependent on the fiber properties. To improve the tensile strength, a strong interface, low stress concentration, fiber orientation is required whereas fiber

concentration, fiber wetting in the matrix phase,.and high fiber aspect ratio determine tensile modulus. The aspect ratio is very important for determining the fracture properties. In short-fiber-reinforced composites, there exists a critical fiber length that is required to develop its full stressed condition in the polymer matrix. Fiber lengths shorter than this critical length lead to failure due to debonding at the interface at lower load. On the other hand, for fiber lengths greater than the critical length, the fiber is stressed under applied load and thus results in a higher strength of the composite.

For good impact strength, an optimum bonding level is necessary. The degree of adhesion, fiber pullout, and a mechanism to absorb energy are some of the parameters that can influence the impact strength of a short-fiber-filled composite. The properties mostly vary with composition as per the rule of mixtures and increase linearly with composition. However, it has been observed that this linear dependence on percentage of fiber content does not hold at high percentage (>80%) of the fiber, probably due to lack of wetting of the fiber surface by the polymer.

Clay nanocomposites, especially nanoclay/polymer composites, exhibit dramatic increases in modulus and strength compared with conventional composites [150-152]. Koo et al. [153] has prepared PE/clay hybrids that exhibit higher tensile yield strengths and tensile moduli than those of PE matrices. The mechanical properties of WPC further can be enhanced by the addition of different additives like clay, nano $SiO_2$, nano ZnO etc. The presence of nanoclay has observed increased mechanical and dynamic modulus of wood-PP matrix [40]. The flexural and tensile strength of HDPE/pine composites is increased to about 20 and 24%, respectively, with addition of 1% clay. The tensile modulus and tensile elongation are also increased with the addition of 1% clay [154]. A remarkable improvement in hardness property has been observed by Jinshu et al. [155]. They have developed wood composite by impregnation of urea-formaldehyde resin and nano-$SiO_2$ into wood. It is observed that the specimens treated with urea-formaldehyde resin and the modifiers containing nano-$SiO_2$, have higher hardness compared to those of composites treated with urea-formaldehyde resin only. Etienne et al. [156] have successfully incorporated various sizes silica nanoparticles by melt compounding in a poly(methyl methacrylate) (PMMA) matrix to enhance its mechanical properties. Saeed et al. [157] observed an increase in mechanical properties of electrospun nanofibers after incorporating $TiO_2$ nanopowder. The interaction of ZnO nanoparticles has increased the tensile modulus of polyacrylonitrile [158].

### 1.8.6. Thermal properties

Improving the thermal stability and reducing the thermal expansion of bio-composites are very important research areas for application of bio-composites to final products. For example, bathroom interiors can suffer thermal deformation due to hot water while automotive interiors are affected by high interior temperatures in summer. Improved thermal stability of bio-composites is also an important factor for application as building interior and automotive interior materials with acceptable fire-retardant characteristics [159]. The idea of adding volcanic pozzolan to the bio-composites has been proposed in order to improve the thermal stability and decrease the thermal expansion [160].

The weight loss of wood at different temperatures due to thermal degradation is reported in the literature [49]. A small weight loss prior to 100 °C occurs due to the evaporation of moisture. Pyrolysis takes place between 150 and 200 °C, with the hemicellulose starting to decompose at about 200 °C, followed by lignin at about 200 °C, and subsequently by cellulose at 250 °C. At temperature higher than 250 °C, rapid weight loss due to the volatilization of the wood components occurs. Pyrolysis followed by oxidative combustion occurs at around 360 and 400 °C respectively. Complete decomposition is achieved at around 480 °C.

The decomposition of PVC above 250 °C is due to the dehydrochlorination of PVC [161]. The decomposition of HDPE and PP occurs above 400 °C [162,163]. Awal et al. [147] has observed an increase in thermal stability of polymer after incorporation of compatibilizer and wood flour.

The gas permeability of polymer blend is decreased to 30% when clay is added. It is reported that the peak temperature of crystallization, the crystallinity, and the thermal conductivity of the nanocomposites decrease with an increase of the silicate volume fraction. It is also reported that the dispersed clay layers effectively act as nucleating agent, resulting in the increase of crystallization peak temperature of virgin polymer [154].

Incorporation of clay to wood polymer matrix increases thermal stability of the composite. The increase in decomposition temperature, melting temperature and crystalline peak temperature of PP have been found to increase after the addition of wood flour, clay and compatibilizer as reported by Lee et al. [164]. Tabari et al. [165] has studied the thermal stability of wood flour/PP composite and observed an improvement in thermal stability after the incorporation of nanoclay. The usefulness of sisal fiber as a good reinforcing agent and Surlyn ionomer as an effective coupling agent for composite fabrication with polyethylene

matrix has been investigated by Choudhury [166]. DSC analysis demonstrates that the presence and the concentration of short sisal fibers affect markedly the crystallization behaviour of HDPE matrix. A noticeable decrease in the half time of HDPE crystallization is observed by the incorporation of short sisal fibers to HDPE.

The incorporation of ZnO into PET results in increased of the melting transition temperature ($T_m$) and crystallization temperature ($T_c$) of PET-ZnO nanocomposites [167]. Another important nanomaterial used to increase the thermal stability is $SiO_2$ nanopowder. Incorporation of $SiO_2$ nanopowder along with nanoclay increases the thermal stability of polymethacrylic acid [168]. The crystallization temperature of PET nanocomposite is improved after the incorporation of polystyrene coated $SiO_2$ nanoparticles [169]. Laachachi et al. [170] studied the thermal stability of PMMA by using organoclay and $TiO_2$ and found a significant increase in thermal stability of PMMA due to the synergistic effect of clay/$TiO_2$.

### 1.8.7. Photodegradation properties

All the main polymeric components of wood, such as cellulose, hemicellulose, lignin, and extractives, suffer from photodegradation. Because visible light (400-700 nm) carries energy less than 292.9 kJ/mol, it cannot provide sufficient energy to break the major chemical bonds in the wood components [171]. Thus, the photodegradation of wood results primarily from the ultraviolet aspect of sunlight. The degrees of photodegradation of wood components largely depend on their ability to absorb UV light. The location of most wood chromophores is in lignin. Lignin accounts for 80-95% of light absorption of wood, and hence causing the discoloration of the wood. Generally, wood in outdoor environments initially becomes yellow and brown and then gray due to leaching of the degraded product of lignin. Absorption of UV light initiates the photochemical reactions of wood surfaces leading to the formation of aromatic and other free radicals, which causes the degradation of lignin and photo-oxidation of cellulose and hemicelluloses, eventually causing discoloration. This discoloration and yellowing of wood surfaces result from the loss of methoxyl content of lignin, photo-dissociation of carbon-carbon bonds and formation of carbonyl-based chromophoric groups [172]. Numerous studies report that wood exposed to artificial weathering (only exposure to UV radiation) darkens as the radiation time increases [173].

Similar to the photodegradation of wood, the photodegradation of polyolefins is a radical-based oxidative process. The presence of catalyst residues, hydroperoxide groups,

and carbonyl groups introduced during polymer manufacturing, processing, and storage accounts for this similarity [174]. All of these species absorb UV light above 290 nm and initiate photochemical reactions. Photodegradation causes changes in all scales of polymer dimension, including the monomer unit (oxidation), the chain (crosslinking or chain scission), the morphology (breakdown of tie molecules and crystal), and on the macroscopic scale. Diffusion of oxygen in the polymer controls polyolefin photodegradation. Density gradients due to oxidation gradients cause the stresses, which combined with chain scission, could initiate and propagate cracks. Cracks on the surface result in light diffusion (a whitening effect in appearance) and also lead to the loss of mechanical properties [175].

Photodegradation of WPCs involves several factors including the wood flour content, coupling agents, manufacturing methods, and weathering conditions, among others. Matuana and Kamdem [176] have investigated the influence of accelerated artificial weathering on the colour changes and tensile properties of PVC/wood-flour composites with various wood flour contents. The composites retain original tensile properties, but they experience severe discoloration (darkening) after weathering for 2600 h. PVC/wood-flour composites containing 15 phr wood flour darken more than those containing 30 phr and 45 phr wood flour. Conversely, reports indicate the opposite trend for weathered HDPE/wood-flour composites; the composites containing 50% wood flour lighten more than the counterparts with 25% wood flour [177]. Ndiaye et al. [178] has studied the effects of wood flour content and compatibilizer on the durability of HDPE-based and PP-based WPCs. Their results indicate that the oxidation rate of the composites increases with wood content and decreases with the presence of compatibilizer due to better dispersion of wood flour in polymer matrix.

Current approaches of improving the weathering resistance of WPCs focus on the bulk of WPCs, i.e., incorporation of additives into the entire product or surface treatment of the wood fiber [179,180]. For example, adding photostabilizers and pigments provides protection against discoloration caused by UV radiation. Stark and Matuana [181] have investigated the effects of an ultraviolet light absorber (UVA), a colorant, and two hindered amine light stabilizers (HALS, low molecular weight diester and secondary amine triazine) on the photostabilization of HDPE-based WPCs composites using a factorial design. Because UVA absorbs some UV radiation and the colorant's ability to block the penetration of UV radiation, as well as masking the bleaching of wood fiber, UVA and colorant significantly lowered the lightness upon weathering. Clausen et al. [182] has observed an increase in the leach resistance and UV protection of pine specimen after incorporation of nano ZnO. Cao et al. [183] has studied the UV shielding properties of ZnO nanoparticles

modified with $SiO_2$ and trimethyl siloxane and observed an improvement in UV stability compared to unmodified ZnO. Du et al. [184] has observed an increase in UV stability of WF/HDPE composite after the incorporation of $TiO_2$.

### 1.8.8. Flame retardant properties

The increasing use of flame retardant (FR) materials in industry has put lot of thrust on the scientific community to develop new polymer materials and FR chemicals for wide range of end use applications. During the last two decades, there has been a resurgence of interest in the development of FR systems for railways and aviation industries. Fire hazard is associated with a combination of factors including the material ignitability, the rate at which heat is released, the total amount of heat that is released, flame spread, smoke production, toxicity of the smoke, degradation products of the polymer, the calorific value of the polymer, and ability of the material to char. It has now been established that the property which most critically defines a fire is the heat release [185].

Fiber reinforced polymer matrix composites have become attractive engineering materials to replace conventional metallic materials in many important sectors of industry such as aircraft, naval constructions, ships, building and offshore structures. However, these materials are susceptible to combustion and fire damage due to their chemical structures. But higher amount of lignin present in some types of wood fiber can produce high amount of char. The char is carbon based residue which undergoes slow oxidative degradation [186]. This can form a protective layer and reduce the diffusion of oxygen towards wood polymer composite. Tajvidi and Takemura [187] have reported that the presence of natural fibers delays the decomposition of polyethylene in the composites due to formation of protective layer of char on the surface of composites. The small amount of silicon present in wood fiber may be capable of producing some char. Further, nanoclay produces silicate char on the surface of WPC which decreases the flame propagation property of the composite [188]. In WPC, incorporation of nanoclay has extensively increased flame retardance property [189].

Although the nanoclay, carbon nanotubes and carbon nanofiber have been used to enhance the fire retardancy of polymer nanocomposites, their applications have been limited in fiber reinforced polymer matrix composites. Very few studies have been reported on the fire retardant application of nanopartciles or additives in fiber reinforced polymer matrix composites [190,191]. Nevertheless, some minerals are more specifically used as flame retardants owing to their behaviour at high temperature. The most commonly used mineral

flame retardants are metal hydroxides (especially of aluminium and magnesium), hydroxycarbonates and zinc borates. Besides the afore mentioned general effects, these inorganic fillers have a direct physical flame retardant action. As the temperature rises, these fillers decompose endothermically and therefore absorb energy. Moreover, they release non-flammable molecules ($H_2O$, $CO_2$), which dilute combustible gases, and can also promote the formation of a protective ceramic or vitreous layer [192].

### 1.8.9. Biodegradation properties

The majority of WPC are made by using polyethylene, polypropylene or polyvinyl chloride as the plastic component. The plastic component retards moisture uptake, thereby slowing the initiation of degradation. These plastics are neither biodegradable nor manufactured from renewable raw materials and are therefore not environment friendly. By adding wood particles to the plastic component, the product (WPC) becomes more biodegradable and is considered more environment friendly. The advantages of WPC can be used as a replacement of solid wood in outdoor applications like decking, railing etc. They require low maintenance and have good weather resistance. The major drawback is the non-degradable plastic component present in the composite [193].

Laboratory and field studies have shown the fungal degradation of WPC despite of the plastic surrounding of the wood particles [194-196]. To enhance the fungal deterioration further different additives are to be added. Silva et al. [197] has reported that tests performed on agar or soil are the most effective manner of determining deterioration of WPC under laboratory conditions. They have noticed that the size of the samples is important for the deterioration. The degradation of samples are dependent on the moisture uptake. The thicker samples show lower weight losses than thinner ones due to slower moisture absorption. Another factor for the rate of deterioration is the wood species.

Wood composite as sole carbon source shows higher rate of bacterial growth after 3 weeks of incubation and it continues up to eighth week. This enhancement of bacterial growth may be due to powerful cellulolytic and pectinolytic activity of bacteria [198]. Other than cellulose and pectin, lignin is also a constituent of plant stem and it is reported that *Bacillus sp.* can degrade this [199]. It has been reported that incorporation of nanoclay can enhance the degradation process. With the increase in the clay content, the rate of bacterial growth enhances. The improved biodegradability of nanocomposite is due to the catalytic role played by the clay in the biodegradation mechanism [200]. It is found that with efficient

degradation of WPCs, flexural and tensile properties of the WPCs decrease. This may be due to the loss of physical and chemical interaction in the WPC caused by the degradation effect of bacteria.

### 1.8.10. Chemical resistance properties

Applications and end uses of wood polymer composite for outdoor applications and their exposure to atmosphere or contact with aqueous media (water, acid, alkali, and solvents) has made it necessary to evaluate the chemical resistance of natural fiber thermoplastic composites with the aim of improving the service life and desirable properties for their specific end uses.

Although there are many literatures are present in different work, little information are available regarding the chemical resistance of these composites. Chemicals can decolorize, decrease and degrade the strength of composites. Because of the wide range of natural fillers and fibers (wood and non wood), study of the effect of fiber type on chemical resistance of natural fiber thermoplastic composites seems inevitable. Hemicelluloses are of low acid resistance [201]. Therefore, the considerable weight loss observed for wood fiber composites having higher percentage of hemicellulose. Tajvidi et al. [202] has investigated the effects of selected chemicals on the mechanical properties of various natural fiber polypropylene composites. Devi et al. [75] has studied the chemical resistance of styrene and glycidyl methacrylate (GMA) treated WPC by dipping it in glacial acetic acid and NaOH. They have observed a moderately high chemical resistance of WPC treated with styrene and GMA.

### 1.8.11. Water absorption properties

Instead of the inorganic materials and synthetic fibers which are previously used with plastics as fillers, lignocellulosic materials offer many environmental benefits when used as reinforcing fillers for plastics. These include their capability of making the final product lightweight and decreasing the erosion of the manufacturing machinery. When a composite containing lignocellulosic material is used in moist areas, the composite absorbs water. However, it is believed that no significant change occurs in the microstructure of the composite, because the reinforcing filler is encapsulated in the hydrophobic matrix polymer [203].

In wood polymer composite, water absorption varies depending upon the nanoclay and coupling agent contents. Incorporation of a coupling agent to the composite decreases the water absorption of WPC. It has been observed that the composites containing nanoclay have exhibited lower water absorption as compared to those composites made without nanoclay [165]. According to Das et al. [204], initially, water saturates the cell wall (via porous tubular and lumens) of the fiber, and next water occupies void spaces. As the voids and the lumens of wood fiber in composites are filled with nanoclay, the penetration of water by the capillary action into the deeper parts of composite is prevented. Another reason for less water absorption could be the hydrophilic nature of the clay surface that tends to immobilize some of the moisture, which inhibits the water permeation in the polymer matrix as reported by Ghasemi and Kord [139].

Incorporation of nanoparticles to the composites can also decrease the water transport process through the composites. The composite voids and the lumens of the fibers present in the composite are filled up with nanoparticles and thus reduce the accessible portion for water absorption. Ghasemi and Kord [139] have reported the decrease in water absorption of polypropylene/wood composite due to inclusion of nanoclay.

## 1.9. Merits and demerits of wood polymer nanocomposite

Plant fibers as fillers and reinforcements for polymers are currently the fastest growing type of polymer additives [16]. A major advantage of fiber over wood is the ability of the material to be molded to meet almost any desired spatial conditions. It can also be bent and fixed to form strong arching curves. Research has demonstrated that the use of wood fibers and/or various types of agro-derived fibers for automotive composite applications has many advantages [205,206]. From a technical point of view, the bio-based composites will enhance mechanical strength and acoustic performance, reduce material weight, energy/fuel consumption and processing time, lower production cost, improve passenger safety and shatterproof performance under extreme temperature changes, corrosion protective and improve biodegradability for the auto interior parts [207]. As an example, the Mercedes-Benz E-Class was achieved a remarkable weight reduction of about 20%, and the mechanical properties, important for passenger protection in the event of an accident, were improved. From a viewpoint of the national interest, the plant fibers are renewable (harvesting annually), biodegradable and green. The incorporation of nanomaterials like metal oxides, clay etc. may enhance interaction among the components

due to their large surface area and results in a dramatic improvement of various properties of the composites.

The use of natural fibers as reinforcement for polymer composites has also some drawbacks. The restrictions for successful exploitation is their low thermal stability, microbial and fungi resistance, susceptibility to rotting and their hydrophilic character resulting in high moisture uptake, affecting the properties of their composites [208-210]. The major obstacle against a massive use of natural fibers for composite applications is their non-uniformity, the variability of their dimensions and mechanical properties (even for fibers harvested from plants in the same cultivation). A precondition for increased use of such fibers in technically challenging applications is the availability of constant fiber qualities with a standardized performance profile. The major task to be solved, in order to boost the acceptance of natural fibers as quality alternative to conventional reinforcing fibers in modern production processes, is to build a quality insurance and assurance system for the raw fiber material. Some overarching questions about the conditions of cultivation and harvesting of fiber crops from which natural fibers are extracted on the fiber quality remain largely unanswered [211].

## 1.10. Applications of wood polymer nanocomposite

Wood polymer nanocomposites can be used in those areas where wood polymer composites are already being used. They will have superior properties compared to conventional composites. Despite their current limitations as mentioned earlier, new and more applications for wood polymer composite are being explored. They are extensively used in inner lining of bathtub, structural components include window/window profiles, decking, railing, table tops, partition walls, trim parts in dashboards, door panels, parcel shelves, seat cushions, backrests and cabin linings. Other applications for composites materials can be found in freight containers, the ocean engineering industry, chemical plants, appliances, sport equipment, etc. WPC are increasingly used for thermo-acoustic insulation purposes. So far, there are only very few exterior parts made from natural fiber composites. However, the potential for WPC for automotive components is rapidly growing. Natural fibers as fillers and reinforcements for polymers are currently the fastest-growing type of polymer additives. Other significant markets are emerging in building products, railroad ties, flowerpots, furniture, and marine piers.

## 1.11. Objectives and plan of work

The North Eastern region, like any other tropical part of the country, is rich in forest based cellulosic resources to a lucrative extent. Out of various species available in this region, only a few of them have been explored for economic development of this region. Some of the non conventional plants like Nal (*Phragmites karka*), Khagra (*Neyraudia reynaudiana*), Kohua (*Saccharum spontaneum*), Kolomou (*Ipomoea carniva*) etc. are abundantly available in the forests of Assam. These plants are not suitable for structural components due to their poor mechanical, dimensional and other properties. They remain as bio wastes in the forest and or at the most utilized for making temporary shades, domestic fuels etc. There is a great prospect of utilizing these materials for producing composites to be used for various constructional purposes.

Now-a-days, the use of plastic materials has increased enormously due to their various advantages. After use, the throwing of plastic materials here and there in the form of carry bags, packaging films, boxes etc. has become a serious threat to the environment because of their non-biodegradable behavior. The majority of waste plastic materials consist of a substantial amount of polyethylene (PE), polypropylene (PP), poly(vinly chloride) (PVC) and less amount of poly ethylene terephthalate (PET), polystyrene (PS) etc.

One of the ways to reduce the environmental pollution by the post consumer plastic materials is recycling and reusing. But owing to the problems like separation and purification of different plastic materials from waste, labels in the container, adhesives in the packaging films, different additives, the mechanical and other properties of the recycled materials are poor. These non-conventional plant materials can be made value added material suitable for preparation of structural components by treating with the waste plastic materials. Structural components include window/window profiles, decking, railing, table tops, partition walls etc. Various properties like mechanical properties, thermal properties, dimensional stability, moisture resistance, fire resistance etc. can be improved over virgin plant materials. These composites will not only be cheaper compared to conventional composites but also will help to reduce the waste disposal problem.

Solution blending is one of the processes to mix varieties of plastic materials. In order to chose a solvent/or mixture of solvent, the ratio of different plastic materials in the waste plastic has to be known. But as segregation of different plastic materials in the waste plastic materials is difficult, it is suggested/or proposed to use virgin plastics instead of waste plastics.

Several issues like durability, strength, fire resistance etc. restrict the use of wood in different areas. For composites, the improvements in bond formation among plastic materials themselves as well as with wood fibers are very much important. The bond formation can be improved by the use of a suitable compatibilizer. The compatibilizer will be such that it can able to react with the hydrophilic wood fibers and hydrophobic polymers and at the same time can improve the interfacial adhesion among different thermoplastic materials.

Besides this, majority of the reports addressing the modification of woods emphasized only improvement on the part of the properties of wood rather than all of them. Some treatment even impaired some good performance of wood. The properties will be better understood if the studies are done at sub micron scale or below that.

Wood can be viewed as a complex natural biomaterial that is subjected to variation in quality and engineering performance as a function of species, growth conditions, harvesting, preparation and so on. The study of sub micron structure of wood is essential in order to better exploit and maintain wood resources in future.

Nanotechnology deals with the material in sub micron level. It has been successfully applied in many fields. Nanoscale materials have large surface area for a given volume. Since many important physical and chemical interactions are governed by surface and surface properties, a nano structured material will have substantially different properties from a larger dimensional material (conventional composite) of same composition. The properties of nanocomposites are greatly influenced by the size scale of its component phases and degree of mixing between the two phases. Without proper dispersion, nano material will not offer improved mechanical properties over that of conventional composites.

Among all the potential nanocomposite precursors, those based on clay and layered silicates have particularly montmorillonite is most commonly employed. It contains octahedral metal oxide lamina sandwiched between two tetrahedral sheets of silica lamina with metal atoms. The layered silicate is generally made organophilic by exchanging the inorganic cation with an organic ammonium cation. The organic ammonium ion can lower the surface energy of clay particles and thereby help the polymers with different polarities to get intercalated between layers and cause further separation and dispersion of silicate layers.

As already mentioned the use of non-conventional plant materials is restricted mainly for fuel applications. Modification through formation of nanocomposites using clay, polymers additives, crosslinker etc. may widen the area of applications. Nano dimensional $SiO_2$, $TiO_2$, ZnO etc. may improve mechanical, thermal, moisture barrier, fire retardancy,

UV protection, biodegradation etc. UV protection and weathering resistance are very important for wood based materials used in exterior applications.

Reports on a large no. of polymer nanocomposites are available in literatures. However, far less is known regarding wood polymer nanocomposite. It is envisaged that a systematic and thorough study of wood polymer nanocomposite may provide some valuable and important basis for the development of wood products in future.

With all these in view, it is proposed to develop a nanocomposite using non-conventional wood, polymer, clay and other additives. Efforts will also be made to develop a treatment/process which can confer properties like mechanical, thermal, fire retardation, UV resistance, durability etc. all at the same time.

***The plan of work has been segregated as follows-***

i) To study the adhesion properties of the mixed thermoplastics.

ii) To develop a suitable compatibilizer with improved compatibility towards plastics and wood components.

iii) To prepare wood polymer nanocomposite using modified clay, polymers, and other additives.

iv) To study the effect of various parameters like percentage of clay (either alone or in combination with ZnO/ $SiO_2$ or $TiO_2$ ), modifier, polymers etc. on different properties like mechanical, thermal stability, UV resistance, hardness, morphology, weight percent gain, water absorption etc.

v) To characterize the composites using FTIR, tensile tester, thermogravimetric analyzer, X-ray diffractometer (XRD), dynamic mechanical analyzer (DMA), scanning electron microscope (SEM), transmission electron microscope (TEM) etc.

vi) To study the biodegradability of the nanocomposites.

## REFERENCE

1. Paul, D.R. & Robeson, L.M. Polymer nanotechnology: Nanocomposites, *Polymer* **49**(15), 3187-3204, 2008.

2. Carrado, K.A. In *Advanced Polymeric Materials: Structure-Property Relationships*, G.O. Shonaike & S.G. Advani, eds., CRC Press: Boca Raton, FL, 2003, 349-396.

3. Ray, S.S. & Okamoto, M. Polymer/layered silicate nanocomposites: a review from preparation to processing, *Prog. Polym. Sci.* **28**(11), 1539-1641, 2003.

4. Wang, Z., Massam, J. & Pinnavaia, T.J. In *Polymer-Clay Nanocomposites*, T.J. Pinnavaia & G.W. Beall, eds., John Wiley & Sons, New York, 2000, 127-149.

5. Li, X., et al. Preparation and characterization of poly(butyleneterephthalate)/organoclay nanocomposites, *Macromol. Rapid Commun.* **22**(16), 1306-1312, 2001.

6. Xiaohui, L. & Qiuju, W. PP/clay nanocomposites prepared by grafting-melt intercalation, *Polymer* **42**(25), 10013-10019, 2001.

7. Hernandez, R.J., Selke, S.E.M. & Culter, J.D. *Plastic Packaging Properties, Processing, Application and Regulations*, Hanser Gardner Publications, Inc., Cincinnati, Ohio, 2000.

8. Hanlon, J.F. & Kelsey, R.J. *Handbook of Package Engineering*, 3rd ed., Technomic Publishing Co., Inc., Lancaster, Pennsylvania, 1998.

9. Selke, S.E. & Wichman, I. Wood fiber/polyolefin composites, *Composites Part A* **35**(3), 321-326, 2004.

10. Pracella, M., et al. Recycling of PET and polyolefin based packaging materials by reactive blending, *Polym. Plast. Technol. Eng.* **43**(6), 1711-1722, 2004.

11. Avella, M., et al. Preparation of isotactic polypropylene/organoclay nanocomposites by solution mixing methodology: Structure and properties relationships, *Macromol. Symp.* **228**(1), 147-154, 2005.

12. Sterky, K., et al. Effect of montmorillonite treatment on the thermal stability of poly(vinyl chloride) nanocomposites, *Polym. Degrad. Stab.* **94**(9), 1564-1570, 2009.

13. Lagaly, G. Introduction: from clay mineral-polymer interactions to clay mineral-polymer nanocomposites, *Appl. Clay. Sci.* **15**(1-2), 1-9, 1999.

14. Raj, R.G., et al. Use of wood fibers in thermoplastics. VII. The effect of coupling agents in polyethylene-wood fiber composites, *J. Appl. Polym. Sci.* **37**(4), 1089-1103, 1989.

15. Wambua, P., et al. Natural fibers: can they replace glass in fiber reinforced plastics?, *Compos. Sci. Technol.* **63**(9), 1259-1264, 2003.

16. Bismarck, A., et al. Green composites as Panacea? Socio-economic aspects of green material, *Environ. Dev. Sustain.* **8**(3), 445-463, 2006.

17. Tasdemır, M., et al. Preparation and characterization of LDPE and PP-wood fiber composites, *J. Appl. Polym. Sci.* **112**(5), 3095-3102, 2009.

18. Bledzki, A.K., et al. Physical, chemical and surface properties of wheat husk, rye husk and soft wood and their polypropylene composites, *Composites Part A* **41**(4), 480-488, 2010.

19. Islam, M.N., et al. Physico-mechanical properties of chemically treated coir reinforced polypropylene composites, *Composites Part A* **41**(2), 192-198, 2010.

20. Walcott, M.P. & Englund, K. A technology review of wood-plastic composites, Proceeding of the 33rd Washington State University International Particleboard/Composites Materials Symposium, 1999.

21. Bledzki, A.K., et al. Thermoplastics reinforced with wood fillers: A literature review, *Polym. Plast. Technol. Eng.* **37**(4), 451-468, 1998.

22. Liu, H., et al. Compatibilizing and toughening bamboo flour-filled HDPE composites: Mechanical properties and morphologies, *Composites Part A* **39**(12), 1891-1900, 2008.

23. Sui, G., et al. A plant fiber reinforced polymer composite prepared by a twin-screw extruder, *Bioresour. Technol.* **100**(3), 1246-1251, 2009.

24. Hernandez, R.J. Selke, S.E.M. & Culter, J.D. Plastic Packaging Properties, Processing, Application and Regulation, Hanser Gardner Publications, Inc., Cincinnati, Ohio, 2000.

25. Gungor, A. Mechanical properties of iron powder filled high density polyethylene composites, *Mater. Des.* **28**(3), 1027-1030, 2007.

26. Tanniru, M. & Misra, R.D.K. On enhanced impact strength of calcium carbonate-reinforced high-density polyethylene composites, *Mater. Sci. Eng. A* **405**(1-2), 178-193, 2005.

27. Yao, F., et al. Rice straw fiber-reinforced high-density polyethylene composite: Effect of fiber type and loading, *Ind. crops Prod.* **28**(1), 63-72, 2008.

28. Faruk, O. & Matuana, L.M. Nanoclay reinforced HDPE as a matrix for wood-plastic composites, *Compos. Sci. Technol.* **68**(9), 2073-2077, 2008.

29. Zhao, C., et al. Preparation and characterization of polyethylene–clay nanocomposites by using chlorosilane-modified clay, *J. Appl. Polym. Sci.* **93**(2), 676-680, 2004.

30. Giannakas, A., et al. Preparation and characterization of polymer/organosilicate nanocomposites based on unmodified LDPE, *J. Appl. Polym. Sci.* **114**(1), 83-89, 2009.

31. Rusu, M. & Tudorachi, N. Biodegradable composite materials based on polyethylene and natural polymers. I. Mechanical and thermal properties, *J. Polym. Eng.* **19**(5), 355-369,1999.

32. Sailaja, R.R.N. Mechanical and thermal properties of bleached kraft pulp–LDPE composites: Effect of epoxy functionalized compatibilizer, *Compos. Sci. Technol.* **66**(13), 2039-2048, 2006.

33. Karak, N. *Fundamentals of Polymers: Raw Materials to Finish Products,* PHI Learning Private Limited, New Delhi, 2009.

34. Yuan, Q. & Misra, R.D.K. Impact fracture behavior of clay–reinforced polypropylene nanocomposites, *Polymer* **47**(12), 4421-4433, 2006.

35. Liu, X. & Wu, Q. PP/clay nanocomposites prepared by grafting-melt intercalation, *Polymer* **42**(25), 10013-10019, 2001.

36. Ruksakulpiwat, Y., et al. Vetiver–polypropylene composites: Physical and mechanical properties, *Composites Part A* **38**(2), 590-601, 2007.

37. Rana, A.K., et al. Effect of MAPP as a coupling agent on the performance of jute–PP composites, *J. Appl. Polym. Sci.* **69**(2), 329-338, 1998.

38. Feng, D., et al. Effect of compatibilizer on the structure–property relationships of kenaf-fiber/polypropylene composites, *Polym. Compos.* **22**(4), 506-517, 2001.

39. Suppakarn, N. & Jarukumjorn, K. Mechanical properties and flammability of sisal/PP composites: Effect of flame retardant type and content, *Composites Part B* **40**(7), 613-618, 2009.

40. Biswal, M., et al. Influence of organically modified nanoclay on the performance of pineapple leaf fiber-reinforced polypropylene nanocomposites, *J. Appl. Polym. Sci.* **114**(6), 4091-4103, 2009.

41. Ghosh, P. *Polymer Science and Technology: Plastics, Rubbers, Blends and Composites,* 2nd ed., Tata McGraw-Hill Publishing Company Limited, New Delhi, 2005.

42. Bao, Y.Z., et al. Preparation and characterization of poly(vinyl chloride)/layered double hydroxides nanocomposite via *in situ* suspension polymerization, *J. Appl. Polym. Sci.* **102**(2), 1471-1477, 2006.

43. Awad, W.H., et al. Material properties of nanoclay PVC composites, *Polymer* **50**(8), 1857-1867, 2009.

44. Jiang, H. & Kamdem, D.P. Effects of copper amine treatment on mechanical properties of PVC/wood-flour composites, *J. Vinyl Add. Tech.* **10**(2), 70-78, 2004.

45. Valle, G.C.X., et al. Effect of wood content on the thermal behavior and on the molecular dynamics of wood/plastic composites, *Macromol. Symp.* **258**(1), 113-118, 2007.

46. Augier, L., et al. Influence of the wood fiber filler on the internal recycling of poly(vinyl chloride)-based composites, *Polym. Degrad. Stab.* **92**(7), 1169-1176, 2007.

47. Panshin, A.J. & de Zeeuw, C. *Textbook of Wood Technology: Structure, Identification, Uses, and Properties of the Commercial Woods of the United States*, 4th ed., McGraw Hill Inc., New York, 1980.

48. Haygreen, J.G. & Bowyer, J.L. *Forest Products and Wood Science: An Introduction,* 1st ed., Iowa State University Press, Ames, Iowa, 1982.

49. Forest products Laboratory, *Wood Handbook: Wood as an Engineering Material*, Agriculture Handbook 72, U.S. Department of Agriculture, Washington, D.C., 1987 rev. pp 466.

50. *Research Note FPL 04*, USDA Forest Service Forest Products Laboratory, Madison, Wis., 1980.

51. Browning, B.L. *The Chemistry of Wood*, Vol. 2, Wiley Interscience, New York, 1967.

52. Esau, K. *Anatomy of Seed Plants,* 2nd ed., John Wiley & Sons, Inc., New York, 1967.

53. Goring, D.A.I. & Timell, T.E. Molecular weight of native celluloses, *Tappi* **45**(6), 454-460, 1962.

54. Timell, T.E. Wood hemicellulose. Part I., *Adv. Carbohydr. Chem. Biochem.* **19**, 247-302, 1964.

55. Timell, T.E. Recent progress in the chemistry of wood hemicelluloses, *Wood. Sci. Technol.* **1**(1), 45-70, 1967.

56. Simson, B.W., et al. Studies on larch arabinogalactan, IV. Molecular properties, *Sven. Papperstidn.* **71**, 699-710, 1968.

57. Adler, E. Lignin chemistry-past, present and future, *Wood Sci. Technol.* **11**(3), 169-218, 1977.

58. Bjorkman, A. Studies on finely divided wood. Part 3. Extraction of lignin-carbohydrate complexes with neutral solvents, *Sven. papperstidn.* **60**(7), 243-251, 1957.

59. Lundquist, K., et al. Studies on lignin carbohydrate linkages in milled wood lignin preparations, *Sven. Papperstidn.* **83**(16), 452-454, 1980.

60. Obst, J.R. Frequency and alkali resistance of lignin-carbohydrate bonds in wood, *Tappi* **65**(4), 109-112, 1982.

61. Fergus, B.J. & Goring, D.A.I. The distribution of lignin in birch wood as determined by ultraviolet microscopy, *Holzforschung* **24**(4), 118-124, 1970.

62. Obst, J.R. Guaiacyl and syringyl lignin composition in hardwood cell components, *Holzforschung* **36**(3), 143-152, 1982.

63. Obst, J.R. Analytical pyrolysis of hardwood and softwood lignins and its use in lignin-type determination of hardwood vessel elements, *J. Wood Chem. Technol.* **3**(4), 377-397, 1983.

64. Pettersen, R.C. The chemical composition of wood, Chapter 2, in *The Chemistry of Solid Wood,* R.M. Rowell ed., American Chemical Society, Washington, D.C., 1984, 76-81.

65. Ashori, A. Wood–plastic composites as promising green-composites for automotive industries, *Bioresour. Technol.* **99**(11), 4661-4667, 2008.

66. Kim, J.P., et al. Wood–polyethylene composites using ethylene–vinyl alcohol copolymer as adhesion promoter, *Bioresour. Technol.* **97**(3), 494-499, 2006.

67. Yang, H.S., et al. Effect of compatibilizing agents on rice-husk flour reinforced polypropylene composites, *Compos. Struct.* **77**(1), 45-55, 2007.

68. Lu, J.Z., et al. Chemical coupling in wood fiber and polymer composites: a review of coupling agents and treatments, *Wood Fiber Sci.* **32**(1), 88-104, 2000.

69. Mathias, L.J., et al. Improvement of wood properties by impregnation with multifunctional monomers, *J. Appl. Polym. Sci.* **42**(1), 55-57, 1991.

70. Nishikubo, T., et al. New thermo-crosslinking reactions of polymers containing pendant epoxide groups with various polyfunctional active esters, *J. Polym. Sci., Part A: Polym. Chem.* **25**(5), 1339-1351, 1987.

71. Kakiuchi, H. *Manufacture and Application of Epoxy Resins,* Macromolecule Chemistry Publication Society, Kyoto, 1964, 54-58.

72. Forster, S.C., Hale, M.D. & Williams, W.G. *Efficacy of anhydrides as wood protecting chemicals,* International Research Group on Wood Preservation Document No. IRG/WP 97–30162, 1997.

73. Takahashi, M. "Biological Properties of Chemically Modified Wood", in *Chemical Modification of Lignocellulosic Materials,* S. Hon ed., Marcell Dekker Inc, New York, 1996, 331-359.

74. Militz, H., Beekers, E.P.J. & Homan, W.J. *Modification of solid wood: research and practical potential,* International Research Group on wood preservation Document No. IRG/ WP/ 97–40098, 1997.

75. Devi, R.R., et al. Chemical modification of rubber wood with styrene in combination with a crosslinker: Effect on dimensional stability and strength property, *Bioresour. Technol.* **88**(3), 185-188, 2003.

76. Devi, R.R. & Maji, T.K. Studies of properties of rubber wood with impregnation of polymer, *Bull. Mater. Sci.* **25**(6), 527-531, 2002.

77. Devi, R.R., et al. Studies on dimensional stability and thermal properties of rubber wood chemically modified with styrene and glycidyl methacrylate, *J. Appl. Polym. Sci.* **93**(4), 1938-1945, 2004.

78. Devi, R.R. & Maji, T.K. Effect of glycidyl methacrylate on the physical properties of wood–polymer composites, *Polym. Compos.* **28**(1), 1-5, 2007.

79. Rozman, H.D., et al. Rubber wood–polymer composites based on glycidyl methacrylate and diallyl phthalate, *J. Appl. Polym. Sci.* **67**(7), 1221-1226, 1998.

80. Teke, A.B. & Baysal, S.H. Immobilization of urease using glycidyl methacrylate grafted nylon-6-membranes, *Process Biochem.* **42**(3), 439-443, 2007.

81. Dikobe, D.G. & Luyt, A.S. Effect of poly(ethylene-co-glycidyl methacrylate) compatibilizer content on the morphology and physical properties of ethylene vinyl acetate–wood fiber composites, *J. Appl. Polym. Sci.* **104**(5), 3206-3213, 2007.

82. Kunimune, N., et al. Influence of the reactive processing of recycled poly(ethylene terephthalate)/poly(ethylene-co-glycidyl methacrylate) blends, *J. Appl. Polym. Sci.* **120**(1), 50-55, 2011.

83. Yeh, S.K. & Gupta, R.K. Improved wood–plastic composites through better processing, *Composites Part A* **39**(11), 1694-1699, 2008.

84. Ismail, H., et al. Effects of polyethylene-*g*-maleic anhydride on properties of low density polyethylene/thermoplastic sago starch reinforced kenaf fiber composites, *Iran. Polym. J.* **19**(7), 501-510, 2010.

85. Zhong, Y., et al. Enhancement of wood/polyethylene composites via compatibilization and incorporation of organoclay particles, *Polym. Eng. Sci.* **47**(6), 797-803, 2007.

86. Nourbakhsh, A. & Ashori, A. Influence of nanoclay and coupling agent on the physical and mechanical properties of polypropylene/bagasse nanocomposite, *J. Appl. Polym. Sci.* **112**(3), 1386-1390, 2009.

87. Theng, B.K.G. *The Chemistry of Clay-Organic Reactions,* John Wiley & Sons, New York, 1974, 343 pp.

88. Kiliaris, P. & Papaspyrides, C.D. Polymer/layered silicate (clay) nanocomposites: An overview of flame retardancy, *Prog. Polym. Sci.* **35**(7), 902–958, 2010.

89. Lagaly, G. Interaction of alkylamines with different types of layered compounds, *Solid State Ionics* **22**(1), 43-51, 1986.

90. Herbert, G. Synthesis of monodispersed silica powders II. Controlled growth reaction and continuous production process, *J. Eur. Ceram. Soc.* **14**(3), 205-214, 1994.

91. Rao, K.S., et al. A novel method for synthesis of silica nanoparticles, *J. Colloid Interface Sci.*, **289**(1), 125-131, 2005.

92. Xu, C.X. & Sun, X.W. Multipod zinc oxide nanowhiskers, *J. Cryst. Growth* **277**(1-4), 330-334, 2005.

93. Lao, J.Y., et al. Hierarchical ZnO Nanostructures, *Nano Lett.* **2**(11), 1287-1291, 2002.

94. Gao, P. & Wang, Z.L. Self-Assembled Nanowire-Nanoribbon Junction Arrays of ZnO, *J. Phys. Chem. B* **106**(49), 12653-12658, 2002.

95. Sun, X., et al. Evapouration growth of multipod ZnO whiskers assisted by a $Cu^{2+}$ etching technique, *J. Cryst. Growth* **244**(2), 218-223, 2002.

96. Kiatano, M., et al. Morphology and growth mechanism of new-shaped ZnO crystals, *J. Cryst. Growth* **128**(1-4), 1099-1103, 1993.

97. Zhou, Z., et al. Tetrapod-shaped ZnO whisker and its composites, *J. Mater. Process. Technol.* **89–90**, 415-418, 1999.

98. Zao, H. & Li, R.K.Y. A study on the photo-degradation of zinc oxide (ZnO) filled polypropylene nanocomposites, *Polymer* **47**(9), 3207-3217, 2006.

99. Laachachi, A., et al. Effect of ZnO and organo-modified montmorillonite on thermal degradation of poly(methyl methacrylate) nanocomposites, *Polym. Degrad. Stab.* **94**(4), 670-678, 2009.

100. Banfield, J.F. & Navrotsky, A. (ed.). *Nanoparticles and the Environment*, Mineralogical Society of America, Washington, D.C., 2001, 350 pp.

101. Solomon, D.H. & Hawthorne, D.G. In *Chemistry of Pigments and Fillers*, John Wiley & Sons, Inc., New York, 1983, 1-50.

102. Zhang, H. & Banfield, J.F. Understanding polymorphic phase transformation behavior during growth of nanocrystalline aggregates: Insights from $TiO_2$, *J. Phys. Chem. B* **104**(15), 3481-3487, 2000.

103. Preuss, H.P. *Pigments in Paint*, Noyes Data Corp., Park Ridge, N.J., 1974, 134 pp.

104. Phillips, L.G. & Barbano, D.M. The influence of fat substitutes based on protein and titanium dioxide on the sensory properties of lowfat milks, *J. Dairy Sci.* **80**(11), 2726-2731, 1997.

105. Fujishima, A. & Honda, K. Electrochemical photolysis of water at a semiconductor electrode, *Nature* **238**, 37-38, 1972.

106. Martin, C., et al. Surface reactivity and morphology of vanadia-titania catalysts, *Surf. Sci.* **251-252**, 825-830, 1991.

107. Xu, Y., et al. Platinum-titania oxygen sensors and their sensing mechanisms, *Sens. Actuators, B* **14**(1-3), 492-494, 1993.

108. Filippi, S., et al. Structure and morphology of HDPE-g-MA/organoclays nanocomposites: effects of the preparation procedures, *Eur. Polym. J.* **44**(4), 987-1002, 2008.

109. Liu, L., et al. Studies on nylon 6/clay nanocomposites by melt-intercalation process, *J. Appl. Polym. Sci.* **71**(7), 1133-1138, 1999.

110. Lincóln, D.M., et al. Secondary structure and elevated temperature crystallite morphology of nylon-6/layered silicate nanocomposites, *Polymer* **42**(4), 1621-1631, 2001.

111. Dennis, H.R., et al. Effect of melt processing conditions on the extent of exfoliation in organoclay-based nanocomposites, *Polymer* **42**(23), 9513-9522, 2001.

112. Vaia, R.A. & Giannelis, E.P. Polymer melt intercalation in organically-modified layered silicates: Model predictions and experiment, *Macromolecules* **30**(25), 8000-8009, 1997.

113. Manias, E., et al. Intercalation kinetics of long polymers in 2 nm confinements, *Macromolecules* **33**(21), 7955-7966, 2000.

114. Svoboda, P., et al. Morphology and mechanical properties of polypropylene/organoclay nanocomposites, *J. Appl. Polym. Sci.* **85**(7), 1562-1570, 2002.

115. Nam, P.H., et al. A hierarchical structure and properties of intercalated polypropylene/ clay nanocomposites, *Polymer* **42**(23), 9633-9640, 2001.

116. Galgali, G., et al. A rheological study on the kinetics of hybrid formation in polypropylene nanocomposites, *Macromolecules* **34**(4), 852-858, 2001.

117. Vaia, R.A., et al. Relaxations of confined chains in polymer nanocomposites: Glass transition properties of poly(ethylene oxide) intercalated in montmorillonite, *J. Polym. Sci., Part B: Polym. Phys.* **35**(1), 59-67, 1997.

118. Vaia, R.A., et al. New polymer electrolyte nanocomposites: Melt intercalation of poly(ethylene oxide) in mica-type silicates, *Adv. Mater.* **7**(2), 154-156, 1995.

119. Yao, F., et al. Rice straw fiber reinforced high density polyethylene composite: Effect of coupled compatibilizating and toughening treatment, *J. Appl. Polym. Sci.* **119**(4), 2214-2222, 2011.

120. Li, B. & He, J. Investigation of mechanical property, flame retardancy and thermal degradation of LLDPE–wood-fiber composites, *Polym. Degrad. Stab.* **83**(2), 241-246, 2004.

121. Ge, X.C., et al. Tensile properties, morphology, and thermal behavior of PVC composites containing pine flour and bamboo flour, *J. Appl. Polym. Sci.* **93**(4), 1804-1811, 2004.

122. Alexandre, M. & Dubois, P. Polymer-layered silicate nanocomposites: Preparation, properties and uses of a new class of materials, *Mater. Sci. Eng., R* **28**(1-2), 1-63, 2000.

123. Ogata, N., et al. Poly(vinyl alcohol)-clay and poly(ethylene oxide)-clay blends prepared using water as solvent, *J. Appl. Polym. Sci.* **66**(3), 573-581, 1997.

124. Hyun, Y.H., et al. Rheology of poly(ethylene oxide)/organoclay nanocomposites, *Macromolecules* **34**(23), 8084-8093, 2001.

125. Billingham, J., et al. Adsorption of polyamine, polyacrylic acid and polyethylene glycol on montmorillonite: An in situ study using ATR-FTIR, *Vib. Spectrosc* **14**(1), 19-34, 1997.

126. Sarkar, M., et al. Polypropylene–clay composite prepared from Indian bentonite, *Bull. Mater. Sci.* **3**(1), 23-28, 2008.

127. Chiu, F.C. & Chu, P.H. Characterization of solution-mixed polypropylene/clay nanocomposites without compatibilizers, *J. Polym. Res.* **13**(1), 73-78, 2006.

128. Jeon, H.G., et al. Morphology of polymer/silicate nanocomposites: High density polyethylene and a nitrile copolymer, *Polym. Bull.* **41**(1), 107-113, 1998.

129. Ying, Z., et al. Mechanical properties of surfactant-coating carbon nanofiber/epoxy composite, *Int. J. Nanosci.* **1**(5-6), 425-430, 2002.

130. Sandler, J., et al. Development of a dispersion process for carbon nanotubes in an epoxy matrix and the resulting electrical properties, *Polymer* **40**(21), 5967-5971, 1999.

131. Gong, X., et al. Surfactant-assisted processing of carbon nanotube/polymer composites, *Chem. Mater.* **12**(4), 1049-1052, 2000.

132. Jia, Z., et al. Study on poly(methyl methacrylate)/carbon nanotube composites, *Mater. Sci. Eng., A* **271**(1-2), 395-400, 1999.

133. Velasco-Santos, C., et al. Improvement of thermal and mechanical properties of carbon nanotube composites through chemical functionalization, *Chem. Mater.* **15**(23), 4470-4475, 2003.

134. Park, C., et al. Dispersion of single wall carbon nanotubes by in situ polymerization under sonication, *Chem. Phys. Lett.* **364**(3-4), 303-308, 2002.

135. Shaffer, M.S.P. & Koziol, K. Polystyrene grafted multi-walled carbon nanotubes, *Chem. Commun.* (18), 2074-2075, 2002.

136. Zeng, C. & Lee, L.J. Poly(methyl methacrylate) and polystyrene/clay nanocomposites prepared by in-situ polymerization, *Macromolecules* **34**(12), 4098-4103, 2001.

137. Wilson Jr., O.C., et al. Surface and interfacial properties of polymer-intercalated layered double hydroxide nanocomposites, *Appl. Clay Sci.* **15**(1-2), 265-279, 1999.

138. Oriakhi, C.O., et al. Thermal characterization of poly(styrene sulfonate)/layered double hydroxide nanocomposites, *Clays Clay Miner.* **45**(2), 194-202, 1997.

139. Ghasemi, I. & Kord, B. Long-term water absorption behaviour of polypropylene/ wood flour/organoclay hybrid nanocomposite, *Iran. Polym. J.* **18**(9), 683-691, 2009.

140. Mina F, et al. Improved performance of isotactic polypropylene/titanium dioxide composites: effect of processing conditions and filler content, *Polym. Degrad. Stab.* **94**(2), 183–188, 2009.

141. Dey, T.K. & Tripathi, M. Thermal properties of silicon powder filled high-density polyethylene composites, *Thermochimica Acta* **502**(1-2), 35–42, 2010.

142. Zhang, J., et al. Controlled silylation of montmorillonite and its polyethylene nanocomposites, *Polymer* **47**(13) 4537–4543, 2006.

143. Salimi, A., et al. Oxidized polypropylene wax in polypropylene nanocomposites: A comparative study on clay intercalation, *Iran. Polym. J.* **20**(5), 377-387, 2011.

144. Guo, G., et al. Flame retarding effects of nanoclay on wood–fiber composites, *Polym. Eng. Sci.* **47**(3), 330–336, 2007.

145. Konwar, U., et al. *Mesua ferrea* L. seed oil based highly thermostable and biodegradable polyester/clay nanocomposites, *Polym. Degrad. Stab.* **94**(12), 2221–2230, 2009.

146. Lomeli-Ramirez, M.G., et al. Evaluation of accelerated decay of wood plastic composites by *Xylophagus* fungi, *Int. Biodeterior. Biodegrad.* **63**(8), 1030–1035, 2009.

147. Awal, A., et al. Thermal properties and spectral characterization of wood pulp reinforced bio-composite fibers, *J. Them. Anal. Calorim.* **99**(2), 695–701, 2010.

148. Garcia, Z.F., et al. Numerical analysis of the experimental mechanical properties in polyester resins reinforced with natural fibers, *J. Reinf. Plast. Compos.* **14**(6), 641-649, 1995.

149. Vollenberg, P.H.T. & Heiken, D. Particle size dependence of the Young's modulus of filled polymers: 1. Preliminary experiments, *Polymer* **30**(9), 1656-1662, 1989.

150. Gilman, J.W. Flammability and thermal stability studies of polymer layered-silicate (clay) nanocomposites, *Appl. Clay Sci.* **15**(1-2), 31-49, 1999.

151. Messersmith, P.B. & Giannelis, E.P. Synthesis and barrier properties of poly(ε-caprolactone)-layered silicate nanocomposites, *J. Polym. Sci., Part A: Polym. Chem.* **33**(7), 1047-1057, 1995.

152. Bharadwaj, R.K. Modeling the barrier properties of polymer-layered silicate nanocomposites, *Macromolecules* **34**(26), 9189-9192, 2001.

153. Koo, C.M., et al. Morphology evolution and anisotropic phase formation of the maleated polyethylene-layered silicate nanocomposites, *Macromolecules* **35**(13), 5116-5122, 2002.

154. Lei, Y., et al. Influence of nanoclay on properties of HDPE/Wood composites, *J. Appl. Polym. Sci.* **106**(6), 3958-3966, 2007.

155. Jinshu, S., et al. Improvement of wood properties by urea-formaldehyde resin and nano-$SiO_2$, *Front. For. China* **2**(1), 104-109, 2007.

156. Etienne, S., et al. Effects of incorporation of modified silica nanoparticles on the mechanical and thermal properties of PMMA, *J. Therm. Anal. Calorim.* **87**(1), 101-104, 2007.

157. Saeed, K., et al. Characterization of poly(butylene terephthalate) electrspun nanofibers containing titanium oxide, *Iran. Polym. J.* **18**(8), 671-677, 2009.

158. Chae, D.W. & Kim, B.C. Effects of zinc oxide nanoparticles on the physical properties of polyacrylonitrile, *J. Appl. Polym. Sci.* **99**(4), 1854-1858, 2006.

159. Yang, H.S., et al. Thermal properties of lignocellulosic filler-thermoplastic polymer bio-composites, *J. Therm. Anal. Calorim.* **82**(1), 157-160, 2005.

160. Kim, H.S., et al. Thermal properties of bio flour-filled polypropylene bio-composites with different pozzolan contents, *J. Therm. Anal. Calorim.* **89**(3), 821-827, 2007.

161. Meng, Y.Z. & Tjong, S.C. Preparation and properties of injection-moulded blends of poly(vinyl chloride) and liquid crystal copolyester, *Polymer* **40**(10), 2711-2718, 1999.

162. Yemele, M.C.N., et al. Effect of bark fiber content and size on the mechanical properties of bark/HDPE composites, *Composites Part A* **41**(1), 131-137, 2010.

163. Bouza, R., et al. Design of new polypropylene–wood flour composites: Processing and physical characterization, *Polym. Compos.* **30**(7), 880-886, 2009.

164. Lee, S.Y., et al. Thermal, mechanical and morphological properties of polypropylene/ clay/wood flour nanocomposites, *eXPRESS Polym. Lett.* **2**(2), 78–87, 2008.

165. Tabari, H.Z., et al. Effects of nanoclay and coupling agent on the physico-mechanical, morphological, and thermal properties of wood flour/polypropylene composites, *Polym. Eng. Sci.* **51**(2), 272-277, 2011.

166. Choudhury, A. Isothermal crystallization and mechanical behavior of ionomer treated sisal/HDPE composites, *Mater. Sci. Eng., A* **491**(1-2), 492-500, 2008.

167. He, J., et al. Crystallization behavior and uv-protection property of PET-ZnO nanocomposites prepared by *in situ* polymerization, *J. Appl. Polym. Sci.* **114**(2), 1303-1311, 2009.

168. Bao, Y. & Ma, J.Z. Polymethacrylic acid/Na-montmorillonite/$SiO_2$ nanoparticle composites structures and thermal properties, *Polym. Bull.* **66**(4), 541-549, 2011.

169. Wu, T. & Ke, Y. Melting, crystallization and optical behaviors of poly (ethylene terephthalate)-silica/polystyrene nanocomposite films, *Thin Solid Films* **515**(13), 5220-5226, 2007.

170. Laachachi, A., et al. Use of oxide nanoparticles and organoclays to improve thermal stability and fire retardancy of poly(methyl methacrylate), *Polym. Degrad. Stab.* **89**(2), 344-352, 2005.

171. Feist, W.C. & Hon. D.N.S. *Chemistry of weathering and protection,* In: Rowell R ed., The chemistry of solid wood, Washington, DC, American Chemical Society, 1984, 401-451.

172. Pandey, K.K. Study of the effect of photo-irradiation on the surface chemistry of wood, *Polym. Degrad. Stab.* **90**(1), 9-20, 2005.

173. Matuana, L.M., et al. Ultraviolet weathering of HDPE/wood-flour composites coextruded with a clear HDPE cap layer, *Polym. Degrad. Stab.* **96**(1), 97-106, 2011.

174. Girois, S., et al. Oxidation thickness profiles during photo oxidation of non-photostabilized polypropylene, *Polym. Degrad. Stab.* **56**(2), 169-177, 1997.

175. Yakimets, I., et al. Effect of photo-oxidation cracks on behaviour of thick polypropylene samples, *Polym. Degrad. Stab.* **86**(1), 59-67, 2004.

176. Matuana, L.M. & Kamdem, D.P. Accelerated ultraviolet weathering of PVC/woodflour composites, *Polym. Eng. Sci.* **42**(8), 1657-1666, 2002.

177. Stark, N.M. & Mueller, S.A. Improving the color stability of wood-plastic composites through fiber pre-treatment, *Wood Fiber Sci.* **40**(2), 271-278, 2008.

178. Ndiaye, D., et al. Durability of wood polymer composites: Part 1. Influence of wood on the photochemical properties, *Compos. Sci. Technol.* **68**(3), 2779-2784, 2008.

179. Matuana, L.M., et al. Photo aging and stabilization of rigid PVC/ wood-fiber composites, *J. Appl. Polym. Sci.* **80**(11), 1943-1950, 2001.

180. Muasher, M. & Sain, M. The efficacy of photostabilizers on the color change of wood filled plastic composites, *Polym. Degrad. Stab.* **91**(5), 1156-1165, 2006.

181. Stark, N.M. & Matuana, L.M. Ultraviolet weathering of photostabilized wood flour-filled high-density polyethylene composites, *J. Appl. Polym. Sci.* **90**(10), 2609-2617, 2003.

182. Clausen, C.A., et al. Weatherability and leach resistance of wood impregnated with nano-zinc oxide, *Nanoscale Res. Lett.* **5**(9), 1464-1467, 2010.

183. Cao, Z., et al. Synthesis and UV shielding properties of zinc oxide ultrafine particles modified with silica and trimethyl siloxane, *Colloids Surf. A* **340**(1-3), 161-167, 2009.

184. Du, H., et al. Effects of pigments on the UV degradation of wood-flour/HDPE composites, *J. Appl. Polym. Sci.* **118**(2), 1068–1076, 2010.

185. Shekar, R.I., et al. Flammability behavior of fiber–fiber hybrid fabrics and composites, *J. Appl. Polym. Sci.* DOI 10.1002/app.34373, 2011.

186. Canetti, M., et al. Thermal degradation behaviour of isotactic polypropylene blended with lignin, *Polym. Degrad. Stab.* **91**(3), 494-498, 2006.

187. Tajvidi, M. & Takemura, A. Effect of fiber content and type, compatibilizer, and heating rate on thermogravimetric properties of natural fiber high density polyethylene composites, *Polym. Compos.* **30**(9), 1226-1233, 2009.

188. Camino, G., et al. Thermal and combustion behaviour of layered silicate–epoxy nanocomposite, *Polym. Degrad. Stab.* **90**(2), 354-362, 2005.

189. Guo, G., et al. Effects of nanoparticles on the density reduction and cell morphology of extruded metallocene polyethylene/wood fiber nanocomposites, *J. Appl. Polym. Sci.* **104**(2), 1058-1063, 2007.

190. Kandola, B.K., et al. Mechanical performance of heat/fire damaged novel flame retardant glass-reinforced epoxy composites, *Composites Part A* **34**(9), 863-873, 2003.

191. Kandola, B.K., et al. Use of high-performance fibers and intumescents as char promoters in glass-reinforced polyester composites, *Polym. Degrad. Stab.* **88**(1), 123-129, 2005.

192. Cross, M.S., et al. Effects of tin additives on the flammability and smoke emission characteristics of halogen-free ethylene-vinyl acetate copolymer, *Polym. Degrad. Stab.* **79**(2), 309-318, 2003.

193. Raberg, U. & Hafren, J. Biodegradation and appearance of plastic treated solid wood, *Int. Biodeterior. Biodegrad.* **62**(2), 210-213, 2008.

194. Schauwecker, C., et al. Degradation of a wood-plastic composite exposed under tropical conditions, *Forest Prod. J.* **56**, 123-129, 2006.

195. Karimi, A.N., et al. Effect of compatibilizer on the natural durability of wood flour/high density polyethylene composites against rainbow fungus (Coriolus versicolor), *Polym. Compos.* **28**(3), 273-277, 2007.

196. Schirp, A. & Wolcott, M.P. Influence of fungal decay and moisture absorption on mechanical properties of extruded wood-plastic composites, *Wood Fiber Sci.* **37**(4), 643-652, 2005.

197. Silva, A., et al. Towards the development of accelerated methods for assessing the durability of wood plastic composites, *J. Test. Eval.* **35**(2), 203-210, 2007.

198. Clausen, C.A. Bacterial associations with decaying wood: a review, *Int. Biodeterior. Biodegrad.* **37**(1-2), 101-107, 1996.

199. El-Hanafy, A.A., et al. Molecular characterization of two native Egyptian ligninolytic bacterial strains, *J. Appl. Sci. Res.* **4**, 1291-1296, 2008.

200. Karak, N. Polymer (epoxy) clay nanocomposites, *J. Polym. Mater.* **23**, 1-20, 2006.

201. Sjostrom, E. *Wood Chemistry: Fundamentals and Applications,* 2nd ed., Academic Press, New York, 1993.

202. Tajvidi, M., et al. Effect of chemical reagents on the mechanical properties of natural fiber polypropylene composites, *Polym. Compos.* **27**(5), 563-569, 2006.

203. Yang, H.S., et al. Water absorption behavior and mechanical properties of lignocellulosic filler–polyolefin bio-composites, *Compos. Struct.* **72**(4), 429-437, 2006.

204. Das, S., et al. Effect of steam pretreatment of jute fiber on dimensional stability of jute composite, *J. Appl. Polym. Sci.* **76**(11), 1652-1661, 2000.

205. Muller, D.H. & Stryjewski, D.D. In: Proceedings of Beltwide Cotton Conferences, National Cotton Council of America, Memphis, TN, 2001, 714–717.

206. Muller, D.H. et al. In: Proceedings of Beltwide Cotton Conferences, National Cotton Council of America, Memphis, TN, 2001, 689–696.

207 . Chen, Y., et al. Kenaf/ramie composite for automotive headliner, *J. Polym. Environ.* **13**(2), 107–114, 2005.

208. Costa, F.H.M.M. & D'Almeida, J.R.M. Effect of water absorption on the mechanical properties of sisal and jute fiber composites, *Polym. Plast. Technol. Eng.* **38**(5), 1081-1094, 1999.

209. Stamboulis, A., et al. Environmental durability of flax fibers and their composites based on polypropylene matrix, *Appl. Compos. Mater.* **7**(5-6), 273-294, 2000.

210. Cantero, G., et al. Effects of fiber treatment on wettability and mechanical behaviour of flax/polypropylene composites, *Compos. Sci. Technol.* **63**(9), 1247-1254, 2003.

211. Bismarck, A., et al. Plant fibers as reinforcement for green composites, In A.K. Mohanty, M. Mirsa and L.T. Drzal (eds), Natural Fibers, Bio-polymers and their Composites. CRC Press, Boca Ryton, 2005.

# CHAPTER II

# EXPERIMENTAL

# CHAPTER II

# EXPERIMENTAL

This chapter covers the materials and methods used, which includes the raw materials and techniques for the preparation of composite followed by their characterization.

## 2.1. Materials used

The chemicals used in this study along with the manufacturers are listed below:

| | Materials | Suppliers |
|---|---|---|
| (i) | Low density polyethylene (LDPE) (Grade: PE/20/TK/CN) | Plast Alloys India Ltd. (Harayana, India) |
| (ii) | High density polyethylene (HDPE) (Grade: PE/20/TK/CN) | Plast Alloys India Ltd. (Harayana, India) |
| (iii) | Polypropylene (PP) (Grade: H110MA) | Reliance Industries Ltd. (Mumbai, India) |
| (iv) | Polyvinyl chloride (PVC) (Grade: SPVC FS: 6701) | Finolex Industries Ltd. (Pune, India) |
| (v) | 2,3-epoxy glycidyl methacrylate (GMA) | E, Merck, India |
| (vi) | Polyethylene-*co*-glycidyl methacrylate (PE-*co*-GMA) | Otto chemicals, Mumbai, India |
| (vii) | Polyethylene-*graft*-maleic anhydride (PE-*g*-MA) | Otto chemicals, Mumbai, India |
| (viii) | N-cetyl-N,N,N-trimethyl ammonium bromide (CTAB) | Central Drug house (P) Ltd., Delhi, India |
| (ix) | Montmorillonite K10 | Sigma–Aldrich, USA |
| (x) | Nanomer (MMT modified by 15–35 wt.% octadecylamine and 0.5–5 wt.% aminopropyltriethoxy silane) | Sigma–Aldrich, USA |
| (xi) | Silicon dioxide ($SiO_2$) | Sigma–Aldrich, USA |
| (xii) | Zinc oxide (ZnO) | Sigma–Aldrich, USA |
| (xiii) | Titanium dioxide ($TiO_2$) | Sigma–Aldrich, USA |
| (xiv) | Sodium hydroxide (pellets) | E, Merck, India |

Besides these, other reagents used for the study were of analytical grade.

## 2.2. Methods

### 2.2.1. Preparation of wood samples

Two types of soft wood namely Nal *(Phragmites karka)* and kalmou (*Ipomoea carniva*) were used for the study. Woods were collected from the local forest. It was chopped into small strips. The chopped wood strips were initially washed with 1% soap solution, followed by washing with 1% NaOH solution and finally with cold water. The washed wood strips were oven dried at 105 ± 5 °C till constant weight was achieved. These dried wood strips were grinded in a mixer and sieved at different sizes (40, 60 and 100 mesh size). The sieved wood flour was kept in a container for further use.

### 2.2.2. Modification of montmorillonite K10

20 g of MMT K10 (CEC = 120 meq/100 g) was dispersed into 400 ml of deionised water and ethanol mixture (1:1) under stirring condition at a temperature of 80 °C for 24 h. 0.05 mol of CTAB was mixed with 4.8 ml of 1.0 N HCl and 100 ml of (1:1) deionised water and ethanol mixture. This solution was poured into MMT dispersed solution and stirred at a temperature of 80 °C for another 24 h. The stirring was discontinued when a white precipitate was formed. The clay slurry was filtered and washed with deionised water until no chloride ions were detected by using $AgNO_3$ solution [1].The filtered clay was dried in vacuum oven at 45 °C for 3 days, grinded and kept in dark colour bottle for subsequent use.

### 2.2.3. Modification of Silicon dioxide ($SiO_2$)/Titanium dioxide ($TiO_2$)/Zinc oxide (ZnO)

10 g of $SiO_2$/or $TiO_2$/or ZnO was taken in a round bottom flask containing 1:1 ethanol-water mixture. It was fitted with spiral condenser and stirred at 80 °C for 12 h. 12 g of CTAB was taken in a beaker containing ethanol-water mixture and stirred at 80 °C for 3 h. This mixture was added slowly to the flask containing $SiO_2$/$TiO_2$/ZnO mixture under stirring condition. The stirring was continued for six hours. The mixture was filtered and washed with deionised water for several times. It was collected, dried in vacuum oven at 45 °C, grinded and stored in desiccator to avoid moisture absorption. CTAB modified $SiO_2$/$TiO_2$/ZnO was dispersed in a flask containing xylene and kept for examination of settling of any particles [2]. The dispersion is said to the stable if there is no settling.

### 2.2.4. Optimization of solvent ratio

For the solution blending of high density polyethylene (HDPE), low density polyethylene (LDPE), polypropylene (PP) and polyvinyl chloride (PVC), a mixture of xylene and tetrahydrofuran (THF) was used. In order to optimize the solvent ratio, HDPE, LDPE, PP and PVC were mixed in the ratio of 1:1:1:0.5. Xylene ($\delta$ = 18.4) is a good solvent for HDPE ($\delta$ = 16.2), LDPE ($\delta$ = 16.2) and PP ($\delta$ = 16.6). On the other hand THF ($\delta$ = 20.3) is a good solvent for PVC (19.4). But neither xylene nor THF alone could solubilize the mixture of HDPE, LDPE, PP and PVC (1:1:1:0.5). The solubility of the polymer mixture was checked by varying the ratio of xylene and THF. The optimum ratio of solvent (xylene:THF) and minimum temperature were judged by the conditions at which a homogenous solution was obtained.

### 2.2.5. Preparation of wood polymer nanocomposites

6 g each of HDPE, LDPE and PP (1:1:1) were added slowly to 105 ml of xylene taken in a flask fitted with a spiral condenser at room temperature. This was followed by the addition of either GMA/or PE-*g*-MA/or PE-*co*-GMA (5-15 phr). The temperature of the flask was increased to 130 °C in order to make a homogenous solution. Now, another solution containing 3 g of PVC in 35 ml of tetrahydrofuran (THF) was prepared. The temperature of the previous polymer solution was decreased to 120 °C. The PVC solution was then mixed with the other polymer solution at 120 °C (approximately) under stirring condition for 1 h. A known quantity of nanoclay (1-5 phr) or CTAB modified MMT (1-5 phr) and CTAB modified nanoparticles ($SiO_2$, $TiO_2$ and ZnO) (1-5 phr) were dispersed in 15 ml of tetrahydrofuran (THF) solution using stirrer and sonication. This dispersed mixture was added gradually to the polymer solution under stirring condition. Oven dried WF (20, 40 or 60 phr) of Nal/or Kolmou were added slowly to this mixture and stirred for another 1 h. It was then transferred in tray, oven dried and grinded.

### 2.2.6. Fabrication of composite sheets

The composite sheets were obtained by the compression molding press (Santec, New Delhi). Initially the temperature of the mold was fixed at 150 °C. The wood polymer nanocomposite in powder form was transferred into the mold. It was compressed by hot

press at 80 MPa pressure for about 30 min. It was then allowed to cool at room temperature. The sheets obtained from that were cut according to the specifications of individual test.

### 2.2.7. Preparation of bacterial media

Mineral salt medium with the following composition was prepared for bacterial growth. 4.75 g $KH_2PO_4$, 2.0 g $Na_2HPO_4$, 2.0 g $(NH_4)_2SO_4$, 1.2 g $MgSO_4.7H_2O$, 100 mg $MnSO_4.5H_2O$, 100 mg $CuSO_4.7H_2O$, 70 mg $ZnSO_4.7H_2O$, 10 mg $H_3BO_3.5H_2O$, 10 mg $MoO_3$, 1 mg $FeSO_4.7H_2O$, and 0.5 mg $CaCl_2.2H_2O$ were dissolved in 1000 ml of demineralised water. Certain amount of this liquid culture medium was poured into conical test tube and were sterilized using autoclave at 121 °C and 15 $lb_f$ pressure for 15 min [3]. The autoclaved media were then allowed to cool down to room temperature and WPC samples were added into the media under sterile condition inside a laminar air flow hood. Media containing only polymer samples were also cultured as negative control.

### 2.2.8. Preparation of bacterial strains

For degradation of wood composite, microbial strains were isolated from garden soil containing woody biomass by enrichment of minimal salt medium using 2 % cellulose [4].

The strain showing highest growth was selected for checking the rate of biodegradation of wood composites. Bacterial cultures was centrifuged at 6000 rpm for 15 minutes at room temperature and the pellets were washed with sterilized 0.85 % NaCl solution and re-suspended in mineral salt medium. An amount of the culture medium containing approximately 1 x $10^8$/ml microbes were inoculated to the test tube containing medium for each test. The wood composite samples were cut in small blocks (5 mm x 20 mm x 40 mm) and were sterilized with 70 % alcohol and exposed to UV for 30 minutes in each side of the composite block. The blocks were immersed in sterilized minimal salt medium in test tubes under sterile condition inside a laminar air hood. Media containing no wood composite were also cultured as negative control. The samples were incubated in a shaker incubator at 37 °C with 20 revolutions per minutes for 90 days for degradation study. The samples were collected for spectrophotometric observation at 600 nm against blank culture media on monthly basis under sterile condition.

### 2.2.9. Biodegradation in soil

The degradation test was used to determine the growth and aerobic biodegradation of wood composite exposed to a controlled environment. The biodegradation studies on wood composites were carried out in "bioreactors" (500 ml glass container). The bioreactor was filled with garden soil. The garden soil was collected from the area where degraded woody biomass is present. Before using the soil, it was sieved to remove all larger particles. A controlled environmental condition in the bioreactor with temperature 30 ± 1 °C, moisture content 40 to 50 % and the pH at 7 ± 0.5 was maintained. The degradation tests for the wood composites were conducted for 90 days. After 90 days, the specimens were removed from the soil, carefully cleansed with deionized water and finally dried. The samples were then checked for their weight loss, mechanical properties, growth of microorganisms and degradation. The growth of microorganisms was studied under scanning electron microscope.

## 2.3. Methods of characterization

### 2.3.1. X-ray diffraction (XRD) study

The degree of exfoliation of clay and dispersion of nanoparticles in the wood polymer nanocomposite were evaluated by X-ray diffraction (XRD) analysis. It was carried out in a Rigaku X-ray diffractometer (Miniflax, UK) using CuKα (λ=0.154 nm) radiation at a scanning rate of 1°/min with an angle ranging from 2° to 70°. The interlayer spacing for clay was calculated according to Bragg's law,

$$n\lambda = 2d \sin\theta \qquad (1)$$

where, n = order of reflection (n=1, for first order; n=2, for second order reflection), $\lambda$ = wave length, d = distance between two plane, $\theta$ = diffraction angle.

### 2.3.2. Fourier transform infrared (FTIR) spectroscopy study

FTIR spectra were recorded in FTIR spectrophotometer (Impact-410, Nicolet, USA) using KBr pellet. Wood powder, nanoclay, $SiO_2$, $TiO_2$, ZnO nanoparticles and wood

polymer nanocomposites samples were finely grounded with KBr and FTIR spectra were recorded in the range of 4000-400 $cm^{-1}$.

### 2.3.3. Scanning electron microscopy (SEM) study

The compatibility among different polymers as well as morphological features of the nanocomposites was studied by using scanning electron microscope (JEOL JSM – 6390LV) at an accelerated voltage of 5-10 kV. Fractured surface of some selected samples, deposited on a brass holder and sputtered with platinum, were used for this study.

### 2.3.4. Transmission electron microscopy (TEM) study

The dispersion of silicate layers and other nanoparticles in the wood polymer nanocomposite was examined in transmission electron microscope (model JEOL JEM 100CXII) at an accelerated voltage of 20-100 kV. The nanoparticles and wood polymer nanocomposites powder were dispersed in tetrahydrofuran or xylene solvent followed by sonication for transmission electron microscopy study. A small drop of the dispersed sample was poured through a micropipette on a copper grid. The copper grid was allowed to dry in an oven. The sample was ready for study by transmission electron microscope.

### 2.3.5. Mechanical property study

The tensile and flexural tests for polymer blend, compatibilizer treated polymer blend, and wood polymer composites (WPC) loaded with different percentage of clay or other nanoparticles were carried out using Universal Testing Machine (Zwick, model Z010) at a crosshead speed of 10 mm/min at room temperature according to ASTM D-638 and D-790 respectively. Five samples of each category were tested and their average values were reported.

### 2.3.6. Dynamic mechanical analysis (DMA)

Dynamic mechanical analysis (DMA) of the wood polymer nanocomposites samples were performed using a Universal 2980 DMA V1.7B TA instrument. The dimensions of specimens were taken as (5 × 1.25 × 0.35) $cm^3$. Specimens were scanned over a temperature

range of 25–200 °C. Frequency of the oscillation was fixed at 1 Hz ramped at 2 °C/min to 200 °C. Storage modulus, loss modulus, and mechanical loss factor (tan δ) were recorded and plotted against temperature.

### 2.3.7. Hardness study

The hardness of the samples were measured according to ASTM D-2240 using a durometer (model RR12) and expressed as shore D hardness.

### 2.3.8. Thermal Property study

Thermal properties of wood powder, nanoparticles and wood polymer nanocomposites samples were evaluated by employing thermogravimetric analyzer (TGA) (model TA 50, Shimadzu) at a heating rate of 10 °C/min up to 600 °C under nitrogen atmosphere.

### 2.3.9. Ultra violet (UV) resistance test

The degradation study of the WPC samples were done in UV chamber (Model: S.L.W, voltage: 230 V; Advanced Research Co., India) utilizing a mercury arc lamp system that produces a collimated and highly uniform UV flux in the 254 nm to 365 nm range. Specimens dimensions of (25 x 25 x 5) $mm^3$ were exposed in the UV chamber at room temperature and characterized at specified time intervals. The weight loss was measured and is expressed as [5]:

$$\% \text{ Weight loss} = (W_t - W_o)/W_o \times 100$$

Where, $W_t$ is the specimen weight at time t, $W_o$ is the specimen weight before exposure. Surface morphology of UV degraded specimen was characterized by scanning electron microscopy (SEM). Chemical degradation was studied by FTIR. The intensity of the carbonyl (C=O) stretching peaks of cellulose at 1715 $cm^{-1}$ in WF was measured. The net peak heights were determined by subtracting the height of the baseline directly from the total peak height. The same base line was taken for each peak before and after exposure to UV [6]. The carbonyl index was calculated by using the following equation:

$$\text{Carbonyl index} = I_{1715}/I_{2912}\ (100)$$

Where, $I$ represent the intensity of the peak. The peak intensities were normalised by using -CH stretching peak of alkane at 2912 $cm^{-1}$. This peak was chosen as reference due to its least change during irradiation.

### 2.3.10. Chemical resistance test

Chemical resistance test was carried out according to ASTM D-543-95 method. It was measured by submerging the samples in NaOH (10%), HCl (10%), $H_2O_2$ (10%) and acetone (99%) for 15 days at room temperature. After 15 days, the samples were dried in oven. The changes in weight of the samples (%) were then measured.

### 2.3.11. Limiting oxygen index (LOI) study

Limiting oxygen index (LOI) is defined as the minimum concentration of oxygen, expressed as percent volume, in a flowing mixture of oxygen and nitrogen that will support flaming combustion of a material initially at room temperature. It was measured by flammability tester (S.C. Dey Co., Kolkata) according to ASTM D-2863 method. The total volume of the gas mixture ($N_2$ + $O_2$) was kept fixed at 18 cc. The volume of nitrogen gas and that of oxygen gas were kept initially at a maximum and minimum level. Now, the volume of nitrogen gas was decreased and that of oxygen gas was increased gradually. However, the total volume of gas mixture was kept fixed at 18 cc during the experiment. The sample was placed vertically in the sample holder of the LOI apparatus. The ratio of nitrogen and oxygen at which the sample continued to burn for at least 30 s was recorded.

$$\text{Limiting oxygen index (LOI)} = \text{Volume of } O_2 / \text{ Volume of } (O_2+N_2) \times 100.$$

### 2.3.12. Biodegradation study

The microbial degradation of the polymer blend and wood polymer nanocomposite samples were studied spectrophotometrically by using UV visible spectrophotometer (CECIL CE7400) at 600 nm against blank culture media under sterile condition.

### 2.3.13. Water uptake study

WPC samples were cut into 2.5 × 0.5 × 2.5 $cm^3$ for water uptake study. Percentage water uptake was measured by submerging the samples in distilled water at room temperature (30 °C) for different time periods after conditioning at 65% relative humidity and 30 °C. Weights of the samples were remeasured after 12, 24, 36, 48, 60 and 72 h. It was expressed as a percentage of water absorbed based on oven dry weight according to the formulae,

$$\text{Water uptake (\%)} = (W_s - W_1)/W_1 \times 100$$

Where, '$W_s$' is the weight of the water saturated sample and '$W_1$' is the weight of the oven dried sample.

### 2.3.14. Water vapour uptake study

WPC samples were cut into (2.5 × 0.5 × 2.5) $cm^3$ for the measurement of water vapour uptake test. The samples were oven dried and conditioned at room temperature (30°C) and 30 % relative humidity prior to the test. The test was carried out by placing the samples at two different relative humidities namely 95 % and 65 % and maintaining a temperature of 30 °C. Weights of the samples were remeasured after 12, 24, 36, 48, 60 and 72 h. The experiment was carried out at different time interval. It is expressed as a percentage of moisture absorbed based on oven dry weight.

$$\text{Water vapour uptake (\%)} = (W_t - W_o)/W_o \times 100$$

Where, '$W_t$' is the weight of the specimen after exposure to humidity and '$W_o$' is the weight of oven dried specimen.

## REFERENCE

1. Zeng, Q.H., et al. Synthesis of polymer–montmorillonite nanocomposites by *in situ* intercalative polymerization, *Nanotechnology* **13**(5), 549–553, 2002.

2. Qu, Y., et al. Surface modification of nanocrystalline anatase with CTAB in the acidic condition and its effects on photocatalytic activity and preferential growth of $TiO_2$, *Appl. Surf. Sci.* **257**(1), 151–156, 2010.

3. Konwar, U., et al. *Mesua ferrea* L. seed oil based highly thermostable and biodegradable polyester/clay nanocomposites, *Polym. Degrad. Stab.* **94**(12), 2221–2230, 2009.

4. di Franco, C.R., et al. Degradation of polycaprolactone/starch blends and composites with sisal·fibre, *Polym. Degrad. Stab.* **86**(1), 95-103, 2004.

5. Fa, W., et al. Enhanced photodegradation efficiency of polyethylene-$TiO_2$ nanocomposite film with oxidized polyethylene wax, *J. Appl. Polym. Sci.* **118**(1), 378–384, 2010.

6. Stark, N.M. & Matuana, L.M. Surface chemistry changes of weathered HDPE/wood-flour composites studied by XPS and FTIR spectroscopy, *Polym. Degrad. Stab.* **86**(1), 1-9, 2004.

# CHAPTER III

# RESULTS & DISCUSSION

# CHAPTER III

# RESULTS & DISCUSSION

## *Section A*: Study on the properties of nanocomposite based on high density polyethylene, polypropylene, polyvinyl chloride, wood and clay.

Plant fiber reinforced polymer composite is a widespread used branch of composite materials [1]. Wood is eco-friendly, biodegradable and renewable, but they have poor mechanical, thermal and dimensional stability. These properties can be enhanced by forming composites using polymeric matrix. But, the main disadvantage of using wood flour (WF) to the polymer matrix is its poor compatibility towards the polymer. In order to improve the compatibility between polymers and wood flour, different materials are used. They act as a bridging agent between the two interfaces.

In this part of work, mixtures of HDPE/PP/PVC and glycidyl methacrylate (GMA) have been used as polymer matrix and compatibilizer respectively. Montmorillonite (MMT) has been modified with cetyl trimethyl ammonium bromide (CTAB) and used. The aim of this study is to prepare the nanocomposite by solution blending method and evaluate their various properties. The optimum ratio of solvent (xylene:THF) and minimum temperature to obtain a homogenous solution was 70:30 and 120 °C respectively.

### 3.1. RESULTS & DISCUSSION

#### 3.1.1. X-ray diffraction study

The XRD patterns of MMT, organically modified MMT, wood polymer composites (WPC) loaded with unmodified and modified clay are shown in the Figure 3.1.1. The interlayer spacing was calculated according to Bragg's law. The interlayer spacing for modified clay was found to increase from 0.99 nm to 1.46 nm. The higher order peak in modified MMT indicated that MMT had retained its layer structure upon cation exchange with alkyl ammonium cation. This increased basal spacing could accommodate the long chains of polymer. Composites with unmodified clay showed a diffraction peak at $2\theta = 5.55^{\circ}$ which corresponds to the interlayer spacing of 1.58 nm. This diffraction peak shifted towards lower angle ($2\theta = 4.11^{\circ}$) with basal spacing of 2.15 nm when modified clay was used in the composite. A shifting of diffraction peak to the lower angle for the clay based HDPE

nanocomposite was reported in the literature [2]. The results indicated that the modified clay induced a greater increase in interlayer spacing and intercalated more with the polymer mixture than unmodified clay.

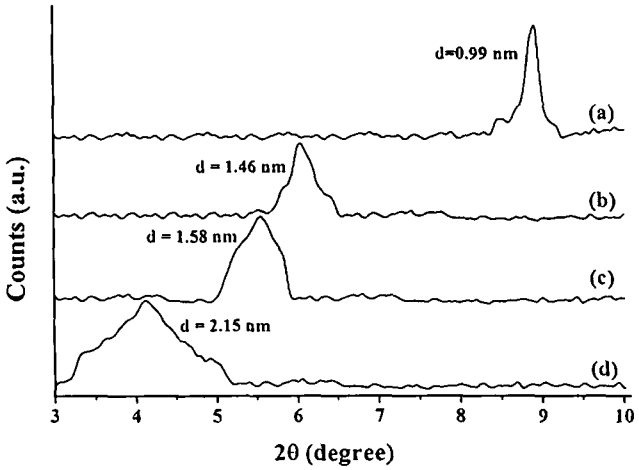


**Figure 3.1.1.** X-ray diffraction of (a) unmodified MMT K10 (b) modified MMT K10 (c) PB/G10/W40/C3* (d) PB/G10/W40/C3.

### 3.1.2. Fourier transform infrared analysis

Modification of MMT was further justified by the FTIR spectra. Figure 3.1.2 shows the FTIR spectra of unmodified and modified clay. Unmodified MMT (curve-3.1.2a) exhibited the peaks at 3473 $cm^{-1}$ (–OH stretching), 1639 $cm^{-1}$ (–OH bending) and 1050–460 $cm^{-1}$ for oxide bands of metals (Si, Al, Mg, etc.). MMT modified with CTAB (curve-3.1.2b) showed two new peaks at 2923 and 2854 $cm^{-1}$ which were due to the presence of –CH stretching of long hydrocarbon chain. Besides this, another peak which was due to –CH bending appeared at 1476 $cm^{-1}$ [3].

Figure 3.1.3 represents the FTIR spectra of MMT, wood flour and wood polymer nanocomposite. The FTIR spectra of wood (curve-3.1.3b) showed the presence of peaks at 3423 $cm^{-1}$ (-OH stretching), 2923 $cm^{-1}$ (-CH stretching), 1734 $cm^{-1}$ (C=O stretching), 1636 $cm^{-1}$ (-OH bending), 1160 and 1046 $cm^{-1}$ (C-O stretching) and 1000-650 $cm^{-1}$ (out of plane C-H bending vibration). PB/G10/W40 (curve-3.1.3c) showed characteristics peaks at 2923 $cm^{-1}$ (–CH stretching), 1734 $cm^{-1}$ (C=O stretching), 1636 $cm^{-1}$ (-OH bending) and 720 $cm^{-1}$ ($–CH_2$ stretching). In the spectrum of PB/G10/W40 (curve-3.1.3c), the intensity of the hydroxyl peak was found to decrease. The intensity of the peak was further decreased and

shifted to a lower wavenumber after the incorporation of modified clay to the WPC (curve-3.1.3d). The decrease in peak intensity in the nanocomposite might be due to the participation of hydroxyl group of clay in the crosslinking reaction with wood and polymer. The shifting of absorption peak, assigned to hydroxyl group, to 3418 $cm^{-1}$ (curve-3.1.3d)

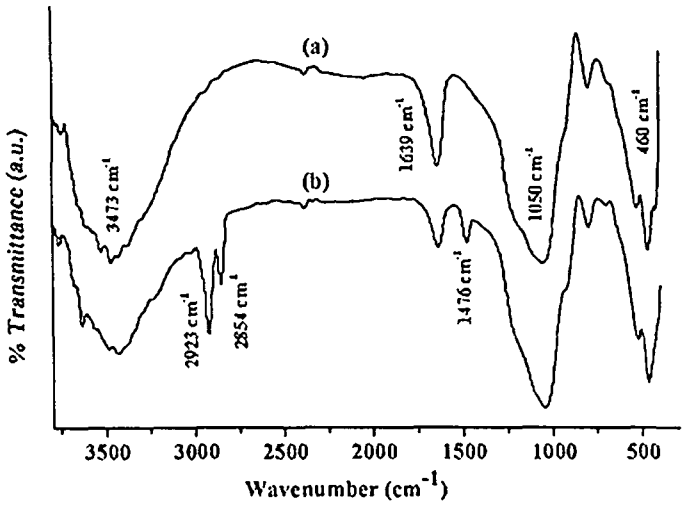


**Figure 3.1.2.** FTIR spectra of (a) unmodified MMT (b) CTAB modified MMT.

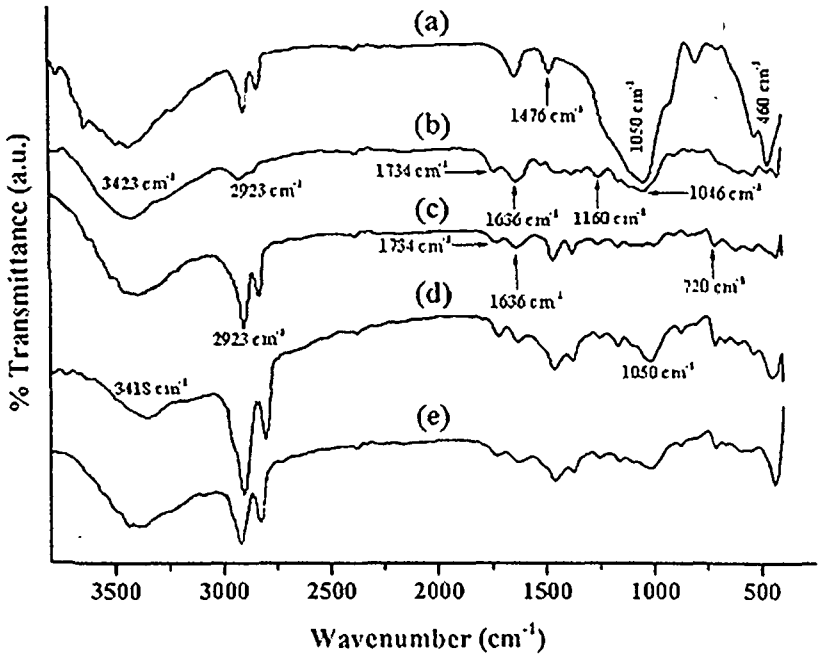


**Figure 3.1.3.** FTIR spectra of (a) modified MMT (b) Wood (c) PB/G10/W40 (d) PB/G10/W40/C3 (e) PB/G10/W40/C3*.

from 3423 $cm^{-1}$ (curve-3.1.3b) indicated the formation of hydrogen bond between wood and polymer blend. In the unmodified MMT based WPC (curve-3.1.3e), the shifting and decrease in intensity of the peak assigned for hydroxyl group was not so much significant like those of modified MMT based WPC. Furthermore, the intensity of peak at 2923 $cm^{-1}$ corresponding to –CH stretching was more in wood composites compared to pure wood which indicated the formation of bond between polymers, GMA and wood. The shifting of peak for hydroxyl group to lower wavenumber and increase in intensity of peak for –CH stretching was reported by Awal et al. [4] while studying the FTIR analysis of wood polymer nanocomposite. The other peaks observed in the spectra of wood polymer composites (curves-3.1.3d and e) at 1050 $cm^{-1}$ and 720 $cm^{-1}$ were due to the C–O stretching of wood, oxide bands of silicon and $-CH_2$ stretching of polymer.

### 3.1.3. Transmission electron microscopy study

Figure 3.1.4 shows the TEM micrographs of WPC loaded with unmodified and modified clay. It was observed that the silicate layers of clay were agglomerated in WPC loaded with unmodified clay. The agglomeration was due to the non compatibility of inorganic silicate layers with organic polymers. The organophilization of MMT with CTAB improved the compatibility of silicate layers with the polymers and as a result no such

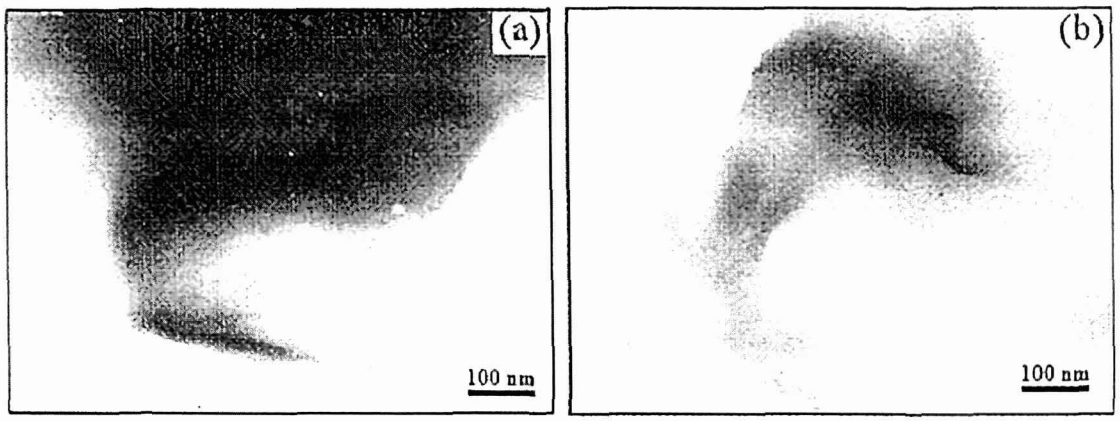


**Figure 3.1.4.** TEM micrographs of (a) PB/G10/W40/C3* (b) PB/G10/W40/C3.

agglomeration was observed in modified clay treated WPC. Rather it was dispersed in the wood polymer matrix which influenced the mechanical, thermal and other properties. Zhao et al. [3] prepared nanocomposite by using organically modified MMT, wood flour and PVC

and found a well dispersion of silicate layers in wood polymer matrix. An improvement in properties of the composite as well as exfoliation of clay layers was observed on addition of organically modified clay to the PP and WF mixture [5].

### 3.1.4. Scanning electron microscopy study

Figure 3.1.5 displays the SEM micrographs of different fractured samples. The fractured surface of untreated polymer sample (Fig. 3.1.5a) exhibited some segregation among different polymers. The segregation decreased when the polymer blend was treated

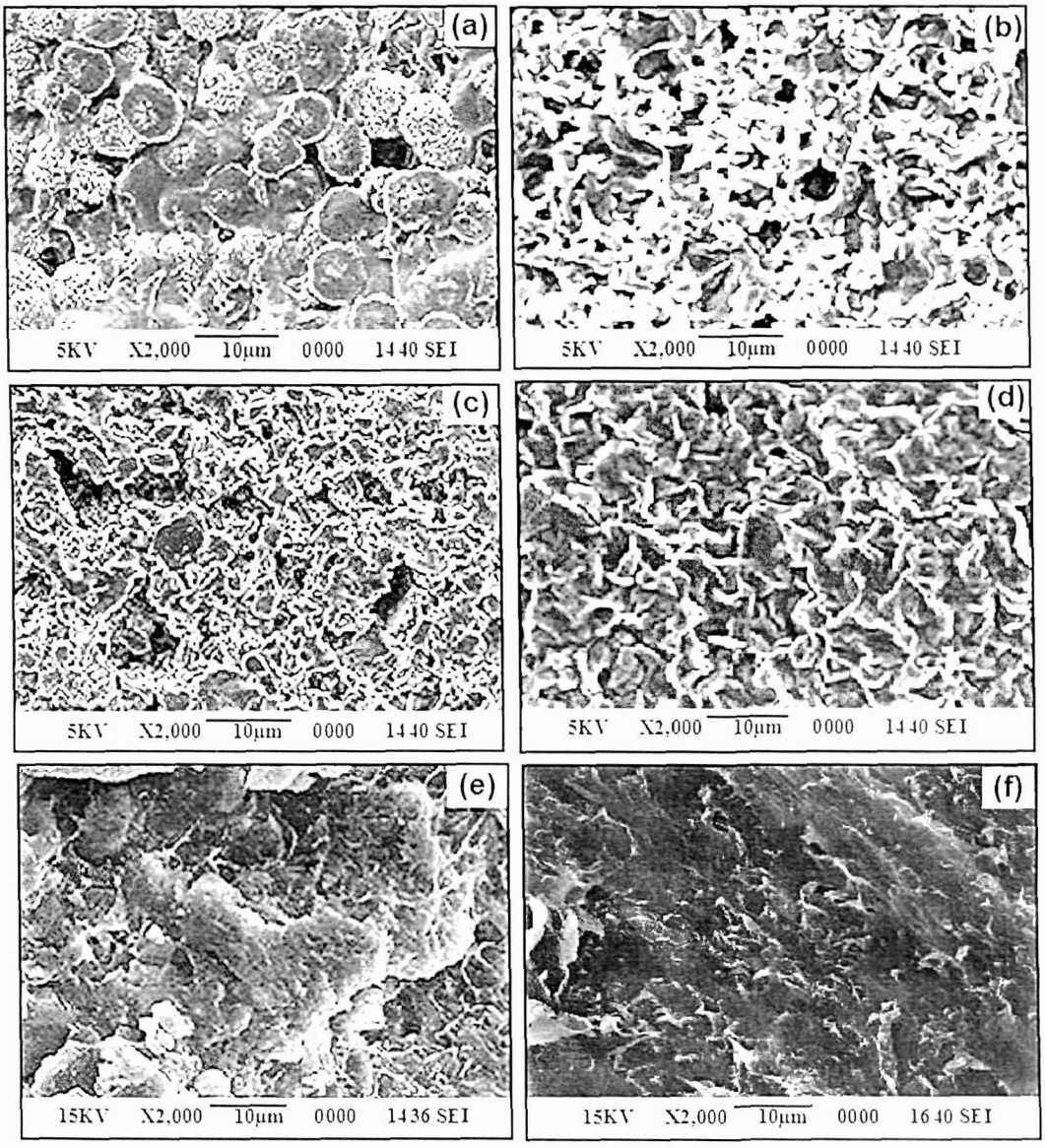


**Figure 3.1.5.** SEM micrographs of (a) PB (b) PB/G5 (c) PB/G10 (d) PB/G15 (e) PB/G10/W40/C3* (f) PB/G10/W40/C3.

with glycidyl methacrylate (Fig. 3.1.5.b-d). Segregation was found to decrease with the increase in the amount of glycidyl methacrylate. This might be due to the improvement in incompatibility among HDPE, PP and PVC. The improvement in adhesion between polyolefins and PET by using ethylene-glycidyl methacrylate copolymer as compatibilizer was cited in the literature [6]. In the formulation with WPC, the addition of clay and wood flour altered the fracture modes. The agglomerates of the clay particles were visible in the case of unmodified clay treated composites (Fig. 3.1.5e). The organic modification of the clay resulted in better dispersion of silicate layers in the WPC matrix as shown in Figure 3.1.5f.

### 3.1.5. Mechanical property study

The flexural and tensile properties of PB, PB/G10, PB/G10/W40, PB/G10/W40/C3* and PB/G10/W40/C3 are shown in Table 3.1.1. The datas presented in the table were the average of five readings. It was observed that both the flexural and tensile properties increased when GMA as compatibilizer was added to the polymer blend. This was due to the improvement in compatibility between HDPE, PP and PVC by GMA as revealed by SEM study. The incorporation of wood flour to the GMA treated polymer blend further improved the mechanical properties because of the increase in rigidity of the composite caused by the wood flour. Moreover, GMA could improve the adhesion between wood and polymer blend through its glycidyl group and double bond. Bouza et al. [7] reported that the mechanical properties of polypropylene modified with maleated polypropylene enhanced with the addition of wood flour.

The addition of unmodified nanoclay had increased the strength and modulus values. A significant increase in the values was observed when organically modified nanoclay was added to the WPC. This enhancement in properties might be attributed to the high stiffness caused by the decreased in mobility of the polymer chains that were intercalated between the nanoclay interlayers. The observed lower values of strength and modulus in unmodified nanoclay loaded composites might be due to the poor dispersion and agglomeration of nanoclay in the system. Similar decrease in flexural properties due to poor dispersion of clay in wood-plastic composites was reported by Faruk and Matuana [2]. The inclusion of organoclay resulted in the improvement in mechanical properties was reported by Lee and Kim [8] while studying the physical properties of wood/PP/clay nanocomposites.

**Table 3.1.1.** Flexural, tensile and hardness properties of polymer blend and WPC loaded with unmodified and modified MMT.

| Sample | Flexural properties | | Tensile properties | | Hardness |
|---|---|---|---|---|---|
| | Strength (MPa) | Modulus (MPa) | Strength (MPa) | Modulus (MPa) | (Shore D) |
| PB | 13 ± 2 | 742 ± 1 | 5 ± 2 | 84 ± 17 | 65.6 ±1.0 |
| PB/G10 | 16 ± 2 | 1084 ± 2 | 9 ± 1 | 172 ± 18 | 68.8 ±0.5 |
| PB/G10/W40 | 18 ± 1 | 3895 ± 1 | 19 ± 1 | 315 ± 17 | 67.0 ±1.0 |
| PB/G10/W40/C3* | 22 ± 2 | 4254 ± 1 | 25 ± 1 | 444 ± 17 | 72.5 ±0.7 |
| PB/G10/W40/C3 | 25 ± 1 | 4682 ± 1 | 30 ± 1 | 513 ± 18 | 76.2 ±0.6 |

### 3.1.6. Hardness study

Table 3.1.1 shows the hardness results of polymer blend and WPCs. The hardness values were found to increase as GMA was added. This was due to the improvement in compatibility between various polymers by GMA which increased the interfacial adhesion among the polymers. However, incorporation of wood flour to the polymer blend decreased the hardness values. Addition of clay further improved the hardness. The improvement was more in the case of modified clay treated composite. The improvement was due to the reduction in the mobility of the intercalated polymer chains. The poor dispersion and agglomeration of clay might be responsible for the observed lower value of hardness exhibited by unmodified clay treated WPC.

### 3.1.7. Thermogravimetric analysis

Table 3.1.2 shows the initial decomposition temperature ($T_i$), maximum pyrolysis temperature ($T_m$), decomposition temperature at different weight loss (%) ($T_D$) and residual weight (RW,%) for wood flour, polymer blend, MMT and WPCs. The respective degradation TG curves were presented in Figure 3.1.6 and Figure 3.1.7. In both wood flour and WPCs, a decrease in weight loss at 45-50 °C was observed (not shown in Table) due to the removal of moisture. Polymer blend showed a higher $T_i$ value than that of wood. The addition of GMA to the polymer blend decreased the $T_i$ value. This might be due to the earlier decomposition of GMA polymer [9]. The $T_i$ value of WPC was higher than those of

either wood flour alone or physical mixture of composite. $T_i$ value of WPC increased after the addition of unmodified and modified MMT. The improvement was more in the case of modified clay treated WPC. The increase in $T_i$ value of clay loaded WPC was due to the intercalated nature of silicate layers which retarded the passage of volatile products. The lower value shown by unmodified clay loaded WPC was due to the agglomeration of silicate layers in the WPC.

**Table 3.1.2.** Thermal analytical data of wood and wood-polymer nanocomposites.

| Sample | $T_i$ | $^aT_m$ | $^bT_m$ | Temperature of decomposition ($T_D$) in °C at different weight loss (%) | | | | RW% at |
|---|---|---|---|---|---|---|---|---|
| | | | | 20% | 40% | 60% | 80% | 600°C |
| Wood flour | 230 | 315 | - | 283 | 319 | 353 | - | 26.6 |
| PB | 242 | 272 | 407 | 297 | 384 | 441 | 470 | 5.2 |
| PB/G10 | 238 | 296 | 470 | 304 | 390 | 447 | 476 | 5.8 |
| PB/G10/W40 | 245 | 292 | 463 | 299 | 375 | 434 | 469 | 6.2 |
| PB/G10/W40 (phy. mix) | 218 | 276 | 455 | 290 | 361 | 422 | 457 | 5.9 |
| MMT K10 | 35 | 50 | - | - | - | - | - | 84.1 |
| PB/G10/W40/C3* | 258 | 302 | 475 | 311 | 394 | 451 | 482 | 12.9 |
| PB/G10/W40/C3 | 265 | 311 | 487 | 321 | 408 | 459 | 490 | 14.9 |

$T_i$ value for initial degradation; $^aT_m$ value for 1st step; $^bT_m$ value for 2nd step.

The observed $T_m$ value for wood flour (shown in Table 3.1.2) might be attributed to the depolymerization of hemicellulose, glycosidic linkages of cellulose and thermal decomposition of cellulose [10]. The first decomposition peak exhibited by the polymer blend was probably due to the dehydrochlorination of PVC [11]. The second decomposition peak was mainly due to the decomposition of HDPE and PP [12,7]. $T_m$ values for the first and second stages of pyrolysis of polymer blend were found to shift when GMA was added. This may be possibly due to the improvement in interaction among the polymers caused by the addition of GMA. $T_m$ values for the first and second stages of pyrolysis of modified

MMT loaded WPC were higher than those of composite without MMT, physical mixture or unmodified MMT based composites.

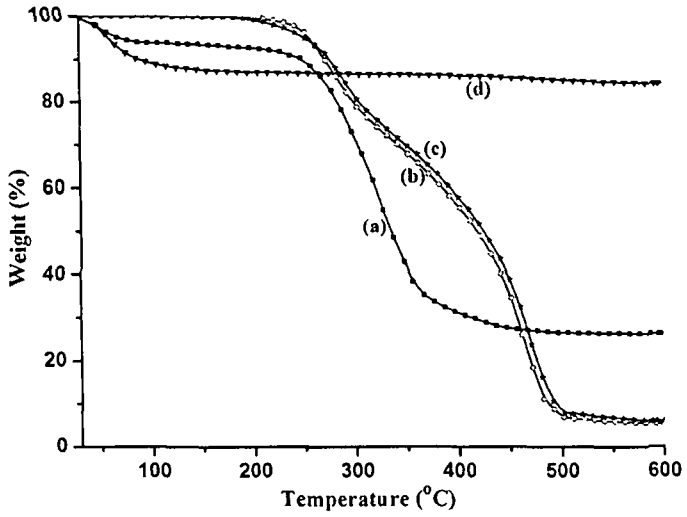


**Figure 3.1.6.** Themogravimetric curves for (a) Wood (b) PB (c) PB/G10 (d) MMT.

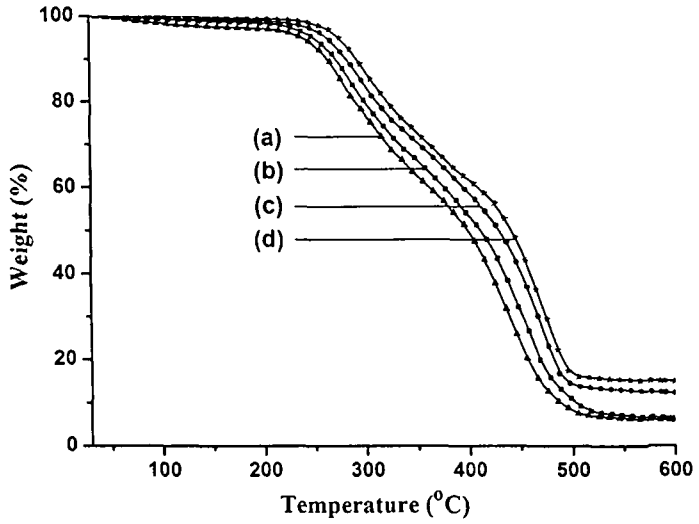


**Figure 3.1.7.** Thermogravimetric curves for (a) PB/G10/W40 (phy. mix) (b) PB/G10/W40 (c) PB/G10/W40/C3* (d) PB/G10/W40/C3.

The weight losses of various samples at different temperature are also listed in the Table 3.1.2. It was observed that wood flour decomposed at lower temperature compared to polymer blend. $T_D$ values increased due to addition of wood flour and GMA to the polymer

blend. This might be due to the increase in interaction between wood flour and polymer blend by GMA through its glycidyl group and double bond respectively. Awal et al. [4] reported that the incorporation of wood pulp and maleated polypropylene into propylene delayed the thermal degradation of WPC. The addition of clay to WPC increased the $T_D$ values. The more improvement in $T_D$ values was observed in the case of modified clay treated WPC.

RW value for the wood fiber was observed maximum. This was due to the carbonization of the wood fiber. RW value of polymer blend increased on addition of GMA. Modified MMT treated WPC showed higher RW value compared to both unmodified MMT treated WPC or MMT free WPC. The maximum improvement in thermal stability was observed by the inclusion of modified clay. This might be attributed to the presence of silicate layers which acted as a barrier and delayed the decomposition of volatile products [13]. The lowered thermal stability exhibited by unmodified clay treated WPC was due to the poor dispersion and agglomeration of the clay.

### 3.1.8. Limiting oxygen index (LOI)

Limiting oxygen index values of polymer blend, unmodified and modified clay loaded WPC are shown in Table 3.1.3. It was observed that polymer blend without compatibilizer showed lowest LOI value while modified clay treated WPC exhibited highest LOI value. LOI value of the polymer blend increased on incorporation of GMA. GMA increased the interfacial adhesion among polymers which resulted in an increase in LOI value. LOI value enhanced after addition of clay to the WPC. Modified clay treated WPC had higher LOI value compared to clay untreated WPC. Wood contains cellulose, hemicellulose, lignin, pectine and wax [14]. Besides these, it contains elements mainly carbon, oxygen and small amount of silicon [15]. The lignin present in the blend could produce a high char. The char was carbon based residue which undergoes slow oxidative degradation [16]. This could form a protective layer which in turn reduces the diffusion of oxygen towards wood polymer composite. Tajvidi and Takemura [17] reported that the presence of natural fibers delayed the decomposition of polyethylene in the composites due to formation of protective layer of char on the surface of composites. The small amount of silicon present in wood might be capable of producing some char. Further, nanoclay produced silicate char on the surface of WPC which decreased the flame propagation

property of the composite [18]. The lower LOI value in unmodified clay treated WPC was due to the poor dispersion and agglomeration of clay in the WPC as discussed earlier.

**Table 3.1.3.** Limiting oxygen index (LOI) values and flaming characteristics of polymer blend and wood/polymer/clay nanocomposites.

| Samples | LOI(%) | Flame description | Smoke & Fumes | Char |
|---|---|---|---|---|
| PB | 23 | Candle like localised | Small and black smoke | little |
| PB/G10 | 38 | Small localized flame | Small and black smoke | little |
| PB/G10/W40 | 42 | Small localized flame | Small and black smoke | medium |
| PB/G10/W40/C3* | 51 | Small localized flame | Small and black smoke | higher |
| PB/G10/W40/C3 | 59 | Small localized flame | Small and black smoke | higher |

### 3.1.9. Water uptake test

The results of water uptake for polymer blends and WPCs are shown in Figure 3.1.8. In all the cases, the water uptake was found to increase with the increase in time of immersion. The water absorption of the polymer blend decreased on addition of GMA. This might be due to the improvement in compatibility among the polymers. GMA increased the interaction between the interfaces of the polymers and thus enhanced water resistance. The water absorption enhanced when wood flour was added. The hydrophilic nature of wood flour was responsible for this. The water absorption of WPC decreased when MMT was added. The decrease in absorption value was more in the case of modified MMT based composite compared to unmodified MMT based composite. The presence of nanoclay in the composite hindered the permeation of water through the composite as reported in the literature [19]. Although the clay on treated with CTAB changed to organophilic in nature, yet it retained its hydrophilic character. The hydrophilic character of unmodified clay surface was more than that of modified clay surface [20]. The surface of modified clay had a tendency to immobilize some of the moisture [8]. Moreover, CTAB modified clay increased the tortuous path for water transport resulting in decrease in water diffusivity [21]. Thus, modified clay treated composite showed lower water absorption compared to unmodified clay.

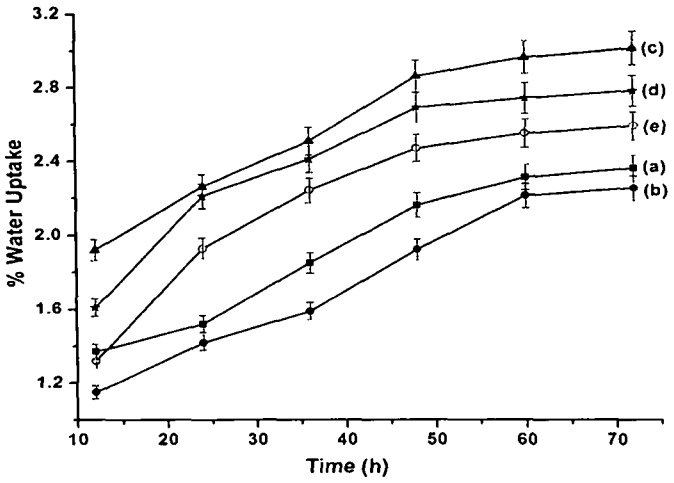


**Figure 3.1.8.** Percent water uptake capacity of (a) PB (b) PB/G10 (c) PB/G10/W40 (d) PB/G10/W40/C3* (e) PB/G10/W40/C3.

### 3.1.10. Water vapour exclusion test

Water vapour exclusion test of the samples was carried out at 30 °C and 65% relative humidity as shown in Figure 3.1.9. From the figure, it was observed that water vapour absorption initially occurred at a rapid rate and finally at a slower rate. In all the samples, water vapour absorption rate increased with the increase in time. It was observed that the polymer blend without compatibilizer had a lower rate of water vapour absorption. This was further decreased after addition of compatibilizer to the polymer blend. Devi et al. [9] reported that WPC treated with GMA, absorbed less water vapour compared to untreated WPC. The absorption of water vapour was found to enhance when wood flour was added. The incorporation of clay in WPC decreased the rate of water vapour absorption. Similar decrease in water vapour absorption was reported by Lei et al. [22]. The decrease in water vapour absorption was less in modified MMT treated WPC compared to unmodified MMT treated composite. The reason for this was explained as earlier. Therefore, it could concluded that organically modified clay treated composite absorbed less water vapour compared to unmodified clay treated composite.

The water vapour exclusion test was also performed at 30 °C and 95% relative humidity. The results followed similar trends with a little higher rate of water vapour absorption compared to those of samples at 65% relative humidity.

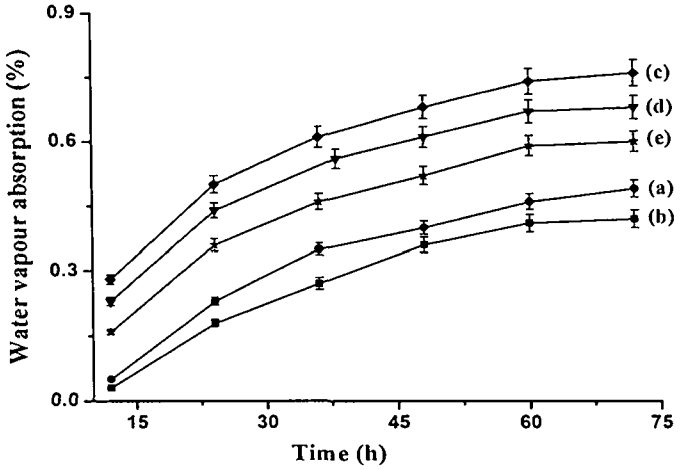


**Figure 3.1.9.** Percent water vapour absorption of (a) PB (b) PB/G10 (c) PB/G10/W40 (d) PB/G10/W40/C3* (e) PB/G10/W40/C3.

## *Section B*: Effect of different compatibilizer and nanoclay on the physical properties of wood (*Phragmites karka*) polymer composite.

One of the major disadvantages of wood polymer composite is the poor compatibility between the fibers and polymeric matrices, which results in non-uniform dispersion of fibers within the matrix and hence poor mechanical properties. Most polymers, especially thermoplastics, are non-polar substances, which are not compatible with polar wood fibers and therefore, poor adhesion results between polymer and fiber in WPC. In order to improve the compatibility between hydrophilic wood and hydrophobic polymer, compatibilizers are used. Compatibilizers are substances, typically polymers that are used in small quantities to treat a surface so that bonding occurs between it and other surfaces, e.g. wood and thermoplastics.

The present investigation has been carried out to study and compare the effect of different compatibilizer on the various properties of WPC prepared by using non conventional plant materials and mixture of plastics. The effect of nanoclay along with the compatibilizer on the final properties of WPC has also been investigated.

## 3.2. RESULTS & DISCUSSION

### 3.2.1. X-ray diffraction study

Figure 3.2.1 shows the X-ray diffraction pattern of nanoclay and WPC loaded with 3 phr nanoclay. Organically modified nanoclay (curve-3.2.1a) shows a sharp diffraction peak (001) at $2\theta = 4.1^{\circ}$ with a basal spacing of 2.14 nm as reported in the literature [22]. The intensity of the peak was decreased almost to baseline after the incorporation of nanoclay to the wood polymer matrix (curve-3.2.1b). The silicate layers were completely exfoliated after the incorporation of nanoclay to the wood polymer matrix. The exfoliated nature of nanoclay was due to the long polymer chains of the polymer matrix that inserted into the gallery space of the nanoclay leading to an increase in interlayer spacing of the silicate layers.

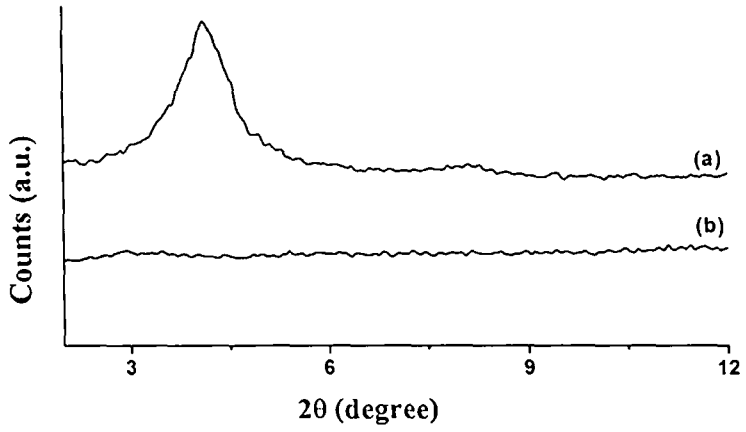


**Figure 3.2.1.** X-ray diffraction of (a) Nanoclay (b) PB/(G+PM+PG)7/W40/N3.

### 3.2.2. Transmission electron microscopy study

Figure 3.2.2 shows the TEM micrographs of mixed compatibilizer based WPC loaded without and with nanoclay. WPC containing mixture of compatibilizer (GMA+PE-*g*-MA+PE-*co*-GMA) is represented by Figure 3.2.2a. The dispersion of nanoclay as shown by dark lines in wood polymer nanocomposite is represented by Fig. 3.2.2b. The silicate layers of nanoclay were found to be distributed well in the wood polymer matrix. Faruk and Matuana [2] prepared nanoclay reinforced wood-HDPE composite and observed a well distribution of silicate layers in the composite. This result supported the observation of XRD studies.

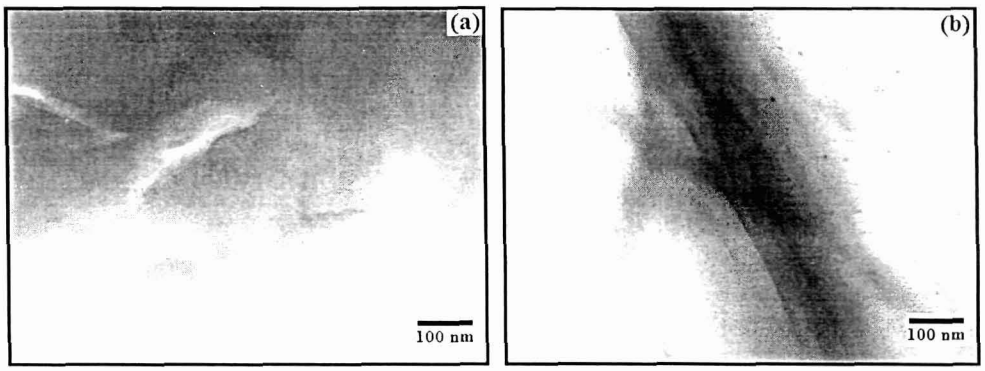


**Figure 3.2.2.** TEM micrographs of (a) PB/(G+PM+PG)7/W40
(b) PB/(G+PM+PG)7/W40/N3.

### 3.2.3. Scanning electron microscopy study

SEM results of fractured surface of polymer blend and WPC samples prepared with different compatibilizer are shown in Figure 3.2.3. The micrographs of polymer blend (Fig. 3.2.3a) shows that the polymers are immiscible. The compatibility of polymer blend was

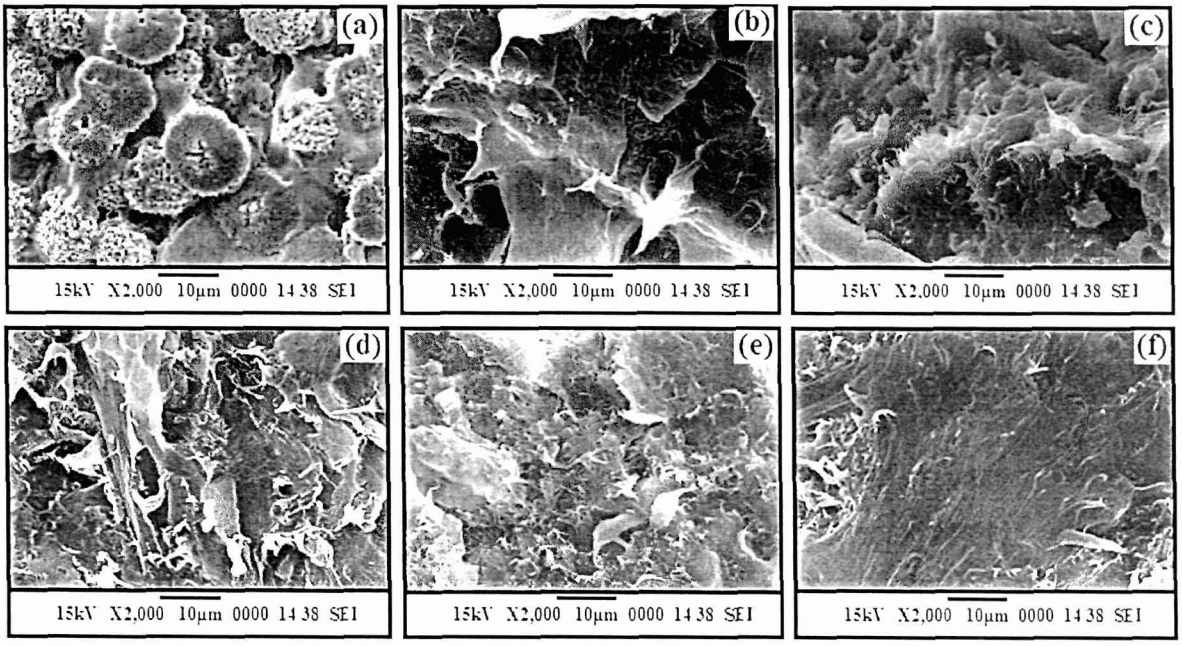


**Figure 3.2.3.** SEM micrographs of (a) PB (b) PB/G7/W40 (c) PB/PM7/W40
(d) PB/PG7/W40 (e) PB/(G+PM+PG)7/W40
(f) PB/(G+PM+PG)7/W40/N3.

improved on addition of compatibilizers (not shown in figure). An improvement in adhesion between polyolefins and PET obtained by the addition of compatibilizer was reported by Pracella et al. [6]. It was observed that WPC having mixture of all the three compatibilizer (Fig. 3.2.3e) showed maximum improvement in miscibility compared to WPC containing either GMA (Fig. 3.2.3b) or PE-*g*-MA (Fig. 3.2.3c) or PE-*co*-GMA (Fig. 3.2.3d) alone as compatibilizer. The miscibility was judged by the appearance of smoothness. The presence of polar groups in GMA, PE-*g*-MA and PE-*co*-GMA enhanced the interaction with the hydroxyl group of wood. On the other hand, the long polyethylene chain present in PE-*g*-MA and PE-*co*-GMA might interact with the polymer blend. As a result, an improvement in smoothness of the surface would occur. Further, better compatibility observed in PE-*co*-GMA added WPC over PE-*g*-MA added WPC. This might be attributed to the higher reactivity of glycidyl group compared to anhydride group towards hydroxyl group of wood [23]. Sailaja [24] used poly(ethylene-*co*-glycidyl methacrylate) as compatibilizer for preparation of wood pulp-LDPE composite and found an improvement in interaction between the wood pulp and LDPE due to the addition of poly(ethylene-*co*-glycidyl methacrylate). The smoothness was further improved after the incorporation of nanoclay (Fig. 3.2.3f). The presence of long hydrocarbon chain, silane and hydroxyl groups of nanoclay improved the interaction between polymer and wood resulting in an increase in compatibility.

### 3.2.4. Fourier transform infrared spectroscopy study

FTIR spectra of wood, nanoclay and wood polymer composite (WPC) are shown in Figure 3.2.4. Curve-3.2.4a representing the spectrum for wood flour shows the presence of bands at 3435 $cm^{-1}$ for –OH stretching, 2932 $cm^{-1}$ and 2848 $cm^{-1}$ for –CH stretching, 1731 $cm^{-1}$ for C=O stretching, 1638 $cm^{-1}$ for –OH bending, 1161 and 1046 $cm^{-1}$ for C–O stretching and 1000-650 $cm^{-1}$ for C-H bending vibration (out of plane). Organically modified nanoclay (curve-3.2.4b) exhibits the peaks at 3471 $cm^{-1}$ (–OH stretching) 2936 and 2851 $cm^{-1}$ (–CH stretching of modified hydrocarbon), 1622 $cm^{-1}$ (–OH bending) and 1031-462 $cm^{-1}$ (oxide bands of metals like Si, Al, Mg etc.). PB/G7/W40 (curve-3.2.4c) exhibits peaks at 3431 $cm^{-1}$ (-OH stretching), 2925 and 2842 $cm^{-1}$ (-CH stretching), 1732 $cm^{-1}$ (C=O stretching), 1633 $cm^{-1}$ (-OH bending), 716 $cm^{-1}$ (-$CH_2$ bending) and the characteristic peak for epoxy group at 995 $cm^{-1}$.

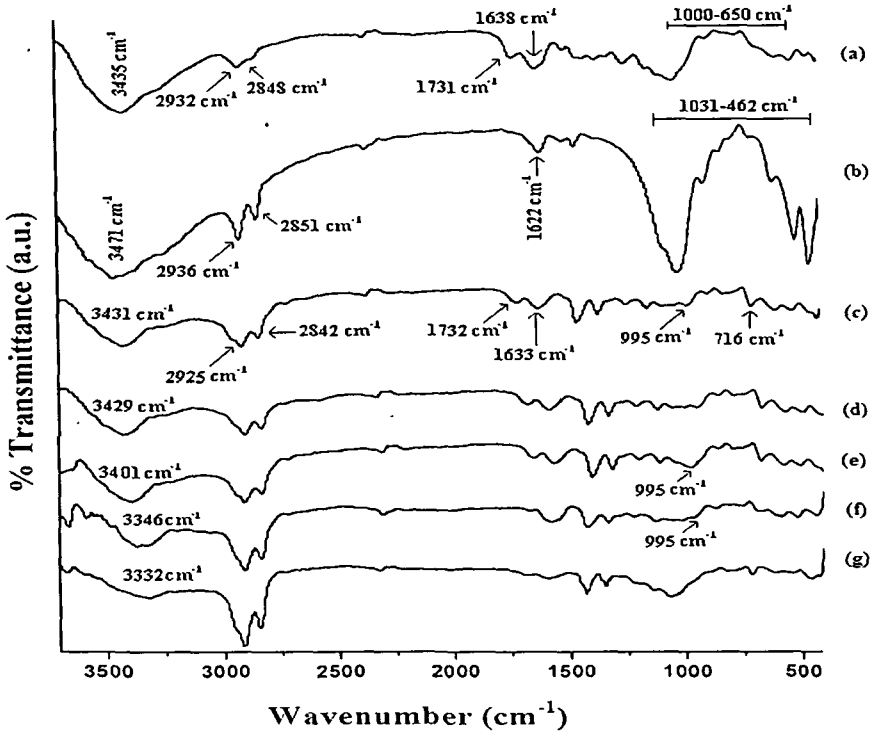


**Figure 3.2.4.** FTIR spectra of (a) Wood flour (b) Nanoclay (c) PB/G7/W40 (d) PB/PM7/W40 (e) PB/PG7/W40 (f) PB/(G+PM+PG)7/W40 (g) PB/(G+PM+PG)7/W40/N3.

Curves-3.2.4d-e show the spectra for WPC compatibilized with PE-*g*-MA and PE-*co*-GMA. The peak at 994 $cm^{-1}$, representing the epoxy group was found to be present in the PE-*co*-GMA compatibilized WPC system (curve-3.2.4e). The intensity of the hydroxyl peak at 3435 $cm^{-1}$ of wood was found to reduce significantly for all the compatibilized WPC. Moreover, the hydroxyl peak was found to shift to lower wavenumber. The reduction in intensity of the hydroxyl group was more in PE-*co*-GMA (curve-3.2.4e) and PE-*g*-MA compatibilized WPC compared to GMA compatibilized WPC. The shifting of hydroxyl peak and decreased in intensity was more in WPC compatibilized with (1:1:1) ratio of blended compatibilizer (curve-3.2.4f). Both the shifting and decrease in intensity of hydroxyl group were further pronounced by the addition of nanoclay (curve-3.2.4g). Furthermore, the intensity of peak at 2925 $cm^{-1}$ corresponding to –CH stretching was more. Dikobe and Luyt [25] reported that the peak intensity of hydroxyl group reduced due to interaction between poly(ethylene-*co*-glycidyl methacrylate) and wood flour. Awal et al. [26] has studied the FTIR spectra of PP/wood pulp/MAPP composite and reported that the hydroxyl peak shifted to lower wavenumber. All these indicated the formation of strong bond between polymer,

compatibilizer, wood and clay. All these indicated the formation of strong bond between polymer, compatibilizer, wood and clay.

### 3.2.5. Mechanical properties study

The flexural and tensile properties of polymer blend and WPC containing different compatibilizer and nanoclay are shown in the Table 3.2.1. The datas are the average of five values. It was observed that WPC containing combined compatibilizer (GMA+PE-*g*-MA+PE-*co*-GMA) showed higher flexural and tensile properties compared to those of either GMA, PE-*g*-MA or PE-*co*-GMA based WPCs. GMA and PE-*co*-GMA facilitated the interfacial adhesion between polymer blend and wood flour through their double bond or polyethylene chain and epoxy group. The polymer chain and anhydride group of PE-*g*-MA also interacted with polymer blend and wood flour. The reactivity of epoxy group towards the hydroxyl group of wood was more in comparison with anhydride group of PE-*g*-MA [23]. As a result, both the flexural and tensile properties of PE-*co*-GMA based WPC were more compared to either GMA or PE-*g*-MA based WPC. The use of poly(ethylene-*co*-glycidyl) methacrylate with wood flour and ethylene vinyl acetate composite had improved the mechanical properties [25]. Liu et al. [27] reported that the mechanical properties of HDPE/bamboo flour enhanced due to addition of PE-*g*-MA. The combined compatibilizer produced better synergism in improving flexural and tensile properties of the WPC compared to individual compatibilizer. The mechanical properties of WPC prepared by using a mixture of compatibilizer were further improved after the incorporation of nanoclay. The improvement in properties was due to the dispersion of nanoclay in the wood polymer matrix and restriction in the movement of the polymer chains inside the silicate layers. Nanoclay had some hydrocarbon as well as silane groups which also favoured the interaction between wood flour and polymer blends. Hence the improvement in properties was observed. Faruk and Matuana [2] reported that the mechanical properties of HDPE/wood-flour composites were improved due to addition of coupling agent and nanoclay in the composites.

The flexural and tensile properties of WPC having clay and different percentage of wood fiber loading are also shown in Table 3.2.1. At a fixed compatibilizer and nanoclay concentration, both flexural and tensile properties increased upto the loading of 40 phr wood flour. Beyond that the values decreased. The increasing trend was probably due to the improved in interaction between wood flour, clay and polymer blend by the mixed

compatibilizer. The compatibilizer would facilitate the transfer of applied load through the interface between polymer matrix and wood flour. The increase in mechanical properties of HDPE/bamboo flour composite with the increase in the bamboo flour loading were reported by Liu et al. [27]. The decrease in the tensile and flexural values at higher loading of wood flour might be due to the reduction in interaction caused by the presence of insufficient amount of compatibilizer to completely react with the hydroxyl group of wood flours, nanoclay and polymers.

**Table 3.2.1.** Mechanical properties of wood polymer composite with various compatibilizers and nanoclay.

| Sample | Flexural properties | | Tensile properties | | Hardness |
|---|---|---|---|---|---|
| | Strength (MPa) | Modulus (MPa) | Strength (MPa) | Modulus (MPa) | (Shore D) |
| PB | 13.43 ± 1.02 | 758.53 ± 1.05 | 8.27 ± 1.09 | 117.37 ± 11.43 | 66 ± 0.2 |
| PB/G7/W40 | 16.19 ± 0.67 | 3221.68 ± 0.93 | 14.56 ± 0.87 | 197.83 ± 17.72 | 65 ± 0.4 |
| PB/PM7/W40 | 17.84 ± 0.58 | 3572.37 ± 0.74 | 16.64 ± 0.71 | 231.45 ± 15.86 | 67 ± 0.7 |
| PB/PG7/W40 | 19.55 ± 0.74 | 3724.28 ± 0.92 | 19.15 ± 0.54 | 274.09 ± 19.37 | 68 ± 0.3 |
| PB/(G+PM+PG)7/W40 | 21.03 ± 0.31 | 4215.64 ± 0.51 | 21.73 ± 0.39 | 325.74 ± 18.68 | 69 ± 0.4 |
| PB/(G+PM+PG)7/W20/N3 | 23.69 ± 0.77 | 4319.25 ± 0.05 | 26.48 ± 0.72 | 391.36 ± 19.65 | 71 ± 0.5 |
| PB/(G+PM+PG)7/W40/N3 | 27.86 ± 0.56 | 4781.22 ± 0.46 | 32.52 ± 0.16 | 572.96 ± 23.62 | 76 ± 0.6 |
| PB/(G+PM+PG)7/W60/N3 | 25.92 ± 0.42 | 4596.79 ± 0.68 | 29.82 ± 0.93 | 458.42 ± 20.27 | 73 ± 0.3 |

### 3.2.6. Hardness results

Table 3.2.1 shows the hardness results of polymer blend and WPC with different compatibilizer and nanoclay. From the table, it was observed that WPC containing mixed compatibilizer exhibited better hardness compared to either polymer blend alone or other compatibilizer based WPC. The increased in hardness in polymer blend was due to the improvement in interfacial adhesion between various polymers and wood by compatibilizer as explained earlier. The hardness values were further increased after the incorporation of nanoclay. Nanoclay improved the interaction between wood flour and polymer blend and reduced the movement of the polymer chains intercalated inside the silicate layers.

### 3.2.7. Thermogravimetric analysis

Table 3.2.2 shows the initial decomposition temperature ($T_i$), maximum pyrolysis temperature ($T_m$), decomposition temperature at different weight loss (%) ($T_D$) and residual weight (RW%) for wood flour, polymer blend and wood polymer composites (WPC). $T_i$ and $T_m$ values of WPC were found higher than those of wood flour and polymer blend. The maximum improvements in $T_i$, $T_m$ and $T_D$ values were observed in the case of nanoclay reinforced (GMA+PE-*g*-MA+PE-*co*-GMA) compatibilized WPC. RW (%) values of the WPCs were found in between those of wood flour and polymer blend.

**Table 3.2.2.** Thermal analysis of wood polymer composite with different compatibilizer and nanoclay.

| Sample | $T_i$ | $T_m{}^a$ | $T_m{}^b$ | Temperature of decomposition ($T_D$) in °C at different weight loss (%) | | | | RW% at 600°C |
|---|---|---|---|---|---|---|---|---|
| | | | | 20% | 40% | 60% | 80% | |
| Wood flour | 232 | 313 | — | 280 | 321 | 349 | — | 26.4 |
| PB | 240 | 271 | 404 | 295 | 386 | 443 | 468 | 5.4 |
| PB/G7/W40 | 247 | 278 | 445 | 302 | 391 | 451 | 474 | 6.3 |
| PB/PM7/W40 | 251 | 285 | 452 | 308 | 397 | 457 | 479 | 6.4 |
| PB/PG7/W40 | 256 | 291 | 460 | 313 | 405 | 463 | 483 | 6.6 |
| PB/(G+PM+PG)7/W40 | 259 | 296 | 465 | 318 | 407 | 468 | 487 | 6.8 |
| PB/(G+PM+PG)7/W40/N3 | 271 | 314 | 477 | 326 | 443 | 480 | 497 | 9.7 |

$T_i$: value for initial degradation; $^aT_m$: value for 1st step; $^bT_m$: value for 2nd step

The thermal stability of WPC was more compared to wood flour. WPC compatibilized with (GMA+PE-*g*-MA+PE-*co*-GMA) was more thermally stable compared to those of composites compatibilized with GMA, PE-*g*-MA or PE-*co*-GMA alone. The increase in thermal stability might be attributed to the increase in interfacial adhesion caused by the reaction between either epoxy group of GMA, PE-*co*-GMA or anhydride group of PE-*co*-GMA with the hydroxyl group of wood flour. The hydrocarbon chains of compatibilizer also enhanced the interaction with the polymer blend. Among the individual compatibilizers, PE-*co*-GMA exhibited maximum interaction. This was due to the higher

reactivity of glycidyl group towards the hydroxyl group of wood. The blend compatibilizer exhibited maximum thermal stability due to synergistic effect. Hetzer et al. [28] reported that the thermal properties of polyethylene/clay composite improved due to the addition of a blend of low and high molecular weight maleic anhydride modified polyethene as mixed compatibilizer. The increase in $T_D$ values of nanoclay reinforced WPC was due to the presence of silicate layers of nanoclay which increased the tortuous path and hence delayed the diffusion of decomposed volatile products throughout the composites [29].

RW value for clay treated WPC was more compared to either polymer blend or WPC. This was due to the formation of char by the inorganic clay.

### 3.2.8. Limiting oxygen index (LOI) study

Table 3.2.3 shows the results of limiting oxygen index (LOI) values of polymer blend and WPC with different compatibilizer and nanoclay. LOI values of WPC were found more in comparison with polymer blend. Highest value was observed for the WPC containing mixed compatibilizer and nanoclay. This was due to the improvement in interfacial adhesion by the various functional groups and long chain hydrocarbon present in different

**Table 3.2.3.** Limiting oxygen index (LOI) values and flaming characteristics of polymer blend and wood polymer composite.

| Samples | LOI (%) | Flame description | Smoke &Fumes | Char |
|---|---|---|---|---|
| PB | 24 | Candlelike localised | — | Little |
| PB/G7/W40 | 40 | Small localized flame | Small and black smoke | Medium |
| PB/PM7/W40 | 43 | Small localized flame | Small and black smoke | Medium |
| PB/PG7/W40 | 45 | Small localized flame | Small and black smoke | Medium |
| PB/(G+PM+PG)7/W40 | 49 | Small localized flame | Small and black smoke | Medium |
| PB/(G+PM+PG)7/W40/N3 | 60 | Small localized flame | Small and black smoke | Higher |

compatibilizer with hydroxyl groups of wood and polymer blend. Zhao et al. [30] studied the flame retardancy of rice hulk-HDPE composite with LLDPE-*g*-MA as a compatibilizer and found that the flame retardancy of WPC improved over neat HDPE. The silicate char that produced by nanoclay on the surface of WPC also increased the flame resistance property of

the composite. Similar observation was reported by Camino et al. [18] while studying the combustion behaviour of silicate-epoxy nanocomposite. The silicate rich surface had better barrier property to heat and oxygen transport due to which ignition of the composite delayed.

### 3.2.9. Water uptake study

The results of water uptake for polymer blend, wood plastic composites without or with nanoclay are shown in the Figure 3.2.5. From the figure, it was observed that water uptake increased with the increase of time of immersion. WPC exhibited higher water absorption compared to the polymer blend. Water absorption was found to follow the order: WPC with GMA system > WPC with PE-*g*-MA system > WPC with PE-*co*-GMA>WPC with (GMA+ PE-*g*-MA + PE-*co*-GMA) system > WPC with (GMA + PE-*g*-MA + PE-*co*-GMA)/ nanoclay system > polymer blend. The higher water absorption shown by WPC

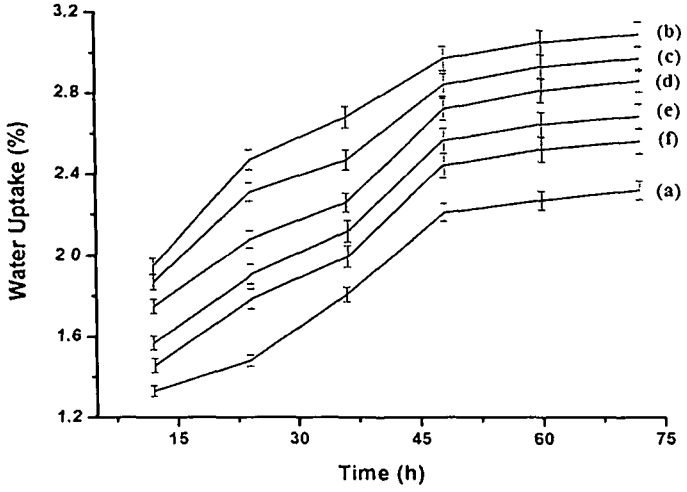


**Figure 3.2.5.** Percent water absorption of (a) PB (b) PB/G7/W40 (c) PB/PM7/W40 (d) PB/PG7/W40 (e) PB/(G+PM+PG)7/W40 (f) PB/(G+PM+PG)7/W40/N3.

compared to polymer blend was due to the hydrophilic nature of wood fibers. The compatibilizer enhanced the interaction between the polymers and wood fibers. The amount of free hydroxyl groups in wood fibers reduced because of the formation of epoxide or ester linkages between the wood fibers and the epoxy part of GMA, PE-*co*-GMA or the anhydride part of PE-*g*-MA. The water absorption of the WPC treated with PE-*g*-MA or PE-*co*-GMA

decreased due to these changes. Avella et al. [31] reported that composites made with fibers and treated with maleated polypropylene showed lower water absorption compared to composites made without maleated polypropylene. The blend compatibilizer further increased the interaction between wood and polymer and decreased the water absorption. The absorption of water vapour decreased further on addition of nanoclay. The silicate layers of clay provided resistance for water transport due to its longer tortuous path and thus decreased the water transportation.

## *Section C*: Effect of coupling agent and nanoclay on the properties of HDPE, LDPE, PP, PVC blend and *Phragmites karka* nanocomposite.

Nal (*Phragmites Karka*), a type of non conventional plant is widely available not only in the forests of Assam but also on both the banks of the Brahmaputra river. These plant material, do not have any economic value and only used for domestic fuel purposes. These plants can be made value added products by producing composites with different polymers. In order to make a good composite, the improvement in adhesion among plastics materials as well as with plant material is very important. The adhesion or compatibility can be improved by using a compatibilizer. The compatibilizer should be such that it can simultaneously react with hydrophilic plant material and hydrophobic plastic materials.

The objective of the present study was to prepare the nanocomposites using wood flour, PE-*co*-GMA compatibilizer, nanoclay and polymer mixture of (HDPE + LDPE + PP + PVC) by solution blending. Efforts have also been made to study the various properties like mechanical, thermal, flame retardancy, water resistance, biodegradation etc. of the nanocomposite.

### 3.3. RESULTS & DISCUSSION

#### 3.3.1. X-ray diffraction study

The XRD patterns of pure nanoclay and wood/polymer/clay nanocomposites (WPC) with different percentage of nanoclay loading are shown in Figure 3.3.1. The interlayer spacing was calculated according to Bragg's law. The organically modified nanoclay (curve-

3.3.1a) shows a sharp peak at $2\theta = 4.1^{\circ}$. The peak (curve-3.3.1e) shifted to a lower diffraction angle ($2\theta = 2.9^{\circ}$) in the case of nanoclay and PE-*co*-GMA containing polymer nanocomposite. The shifting of the peak to lower angle indicated an increase in interlayer spacing of silicate layers. The polymer chains were intercalated into the silicate nanolayers of the polymer composite. A shifting of diffraction peak to the lower angle for the clay based HDPE nanocomposite was reported in the literature [2]. The peak could not be identified in the case of WPC (curve-3.3.1b and c) indicating an exfoliated structure. WPC loaded with 5 phr nanoclay (curve-3.3.1d) showed a small peak at $2\theta = 2.8^{\circ}$. The reduction in peak intensity as well as shifting of peak to lower angle suggested an increased disorder into the nanoclay layers in the nanocomposite. The observed peak at higher loading of nanoclay might be due to agglomeration of some clay. The silicates nanolayers might be partially exfoliated and partially intercalated. The shifting of the peak from higher diffraction angle to lower diffraction angle was reported by Lee and Kim [8] while studying the interaction of organoclay with wood/polypropylene composite.

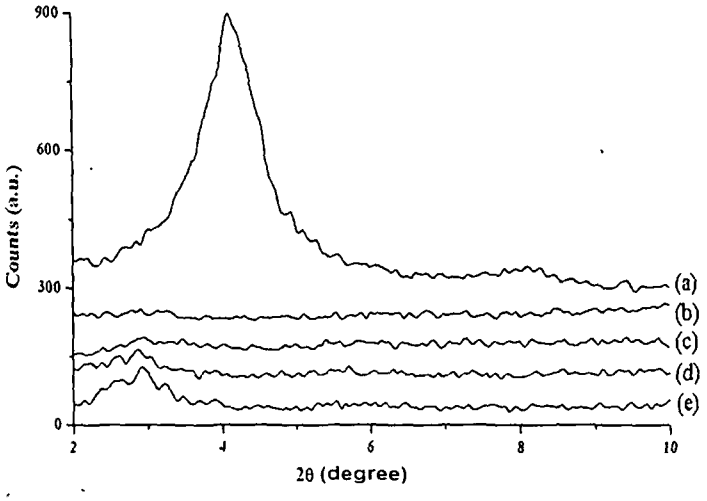


**Figure 3.3.1.** X-ray diffraction of (a) Nanoclay (b) PB/G5/W40/N1 (c) PB/G5/W40/N3 (d) PB/G5/W40/N5 (e) PB/G5/N3.

### 3.3.2. Transmission electron microscopy study

Figure 3.3.2 shows the TEM micrographs of WPC with various percentage of nanoclay content. The dark line represents the intersection of silicate layers. The dispersion of clay layers in the WPC was observed even at lower level of nanoclay (1 phr) loading (Fig. 3.3.2a). The nanoclay exhibited better dispersion of clay layers in WPC when loading of

nanoclay increased to 3 phr (Fig. 3.3.2b). However, with the increase in the level of nanoclay loading to 5 phr (Fig. 3.3.2c), the size of nanoclay became larger or aggregated. Similar observation was reported by Zhao et al. [3] while studying the dispersion of organically modified montmorillonite into wood flour/polyvinyl chloride matrix. TEM results supported the findings of XRD studies.

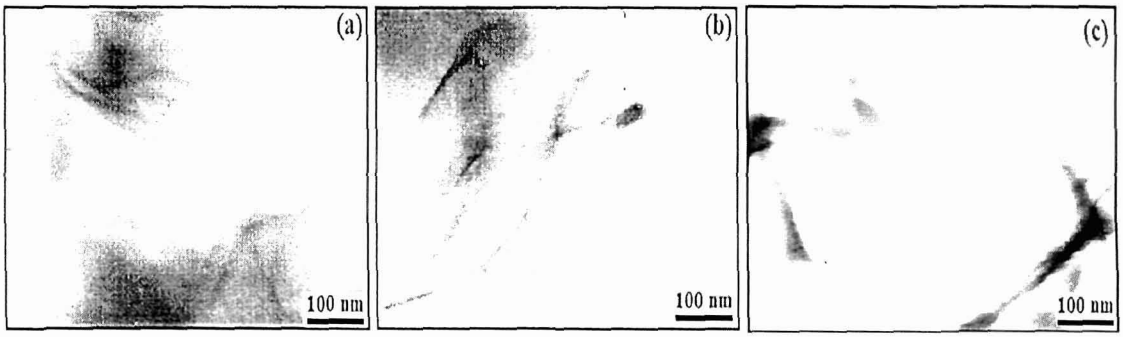


**Figure 3.3.2.** TEM micrographs of (a) PB/G5/W40/N1 (b) PB/G5/W40/N3 (c) PB/G5/W40/N5.

### 3.3.3. Fourier transform infrared spectroscopy study

FTIR spectra of wood, nanoclay, clay added polymer blend and WPCs are shown in Figure 3.3.3. The FTIR spectra of wood (curve-3.3.3a) showed the presence of bands at 3423 $cm^{-1}$ for –OH stretching, 2923 $cm^{-1}$ for –CH stretching, 1734 $cm^{-1}$ for C=O stretching, 1636 $cm^{-1}$ for –OH bending, 1160 and 1046 $cm^{-1}$ for C–O stretching and 1000–650 $cm^{-1}$ for C–H bending vibration (out of plane). Organically modified nanoclay (curve-3.3.3b) exhibited the peaks at 3467 $cm^{-1}$ (–OH stretching) 2927 and 2852 $cm^{-1}$ (–CH stretching of modified hydrocarbon), 1619 $cm^{-1}$ (–OH bending), 1031–460 $cm^{-1}$ (oxide bands of metals like Si, Al, Mg, etc.). PB/G5/N3 (curve-3.3.3c) exhibited characteristic peaks of –CH stretching at 2927 $cm^{-1}$ and 1460 $cm^{-1}$, C–$CH_3$ stretching at 2850 $cm^{-1}$ along with –$CH_2$ stretching at 720 $cm^{-1}$.

Figure 3.3.3d and 3.3.3e represented the FTIR spectra of wood polymer nanocomposite. It was found that the intensity of the hydroxyl peak decreased as well as shifted to lower wavenumber in the wood polymer composite. The decrease in peak intensity in the nanocomposite might be attributed to the participation of hydroxyl group of clay in the crosslinking reaction with wood and polymer. The shifting of absorption peak corresponding to hydroxyl group to 3415 $cm^{-1}$ (curve-3.3.3d) and 3411 $cm^{-1}$ (curve-3.3.3e) confirmed the

formation of hydrogen bond between wood surfaces and matrix. Furthermore, the intensity of peaks at 2923 $cm^{-1}$ corresponding to –CH stretching was more in wood composites compared to pure wood which indicated the formation of bond between polymers, PE-*co*-GMA and wood. Similar type of shifting of hydroxyl group to lower wavenumber and increase in intensity of –C–H stretching was reported by Awal et al. [4] while studying the FTIR analysis of PP/maleated polypropylene/wood composite. The other peaks observed in the spectra of wood polymer composites (curves-3.3.3d and e) at 1050 $cm^{-1}$ and 720 $cm^{-1}$ were due to the C–O stretching of wood, oxide bands of silicon and $-CH_2$ stretching of polymer. The peaks in the range 450-500 $cm^{-1}$ were due to the oxide bands of metals like aluminium and magnesium respectively.

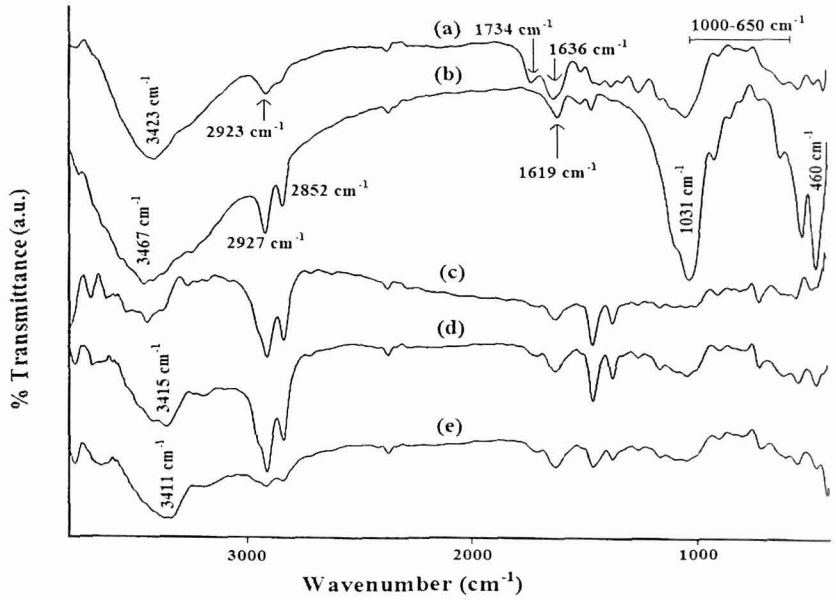


**Figure 3.3.3.** FTIR spectra of (a) Wood flour (b) Nanoclay (c) PB/G5/N3 (d) PB/G5/W40/N3 (e) PB/G5/W40/N5.

### 3.3.4. Scanning electron microscopy study

SEM micrographs of different fractured samples are shown in Figure 3.3.4. The fractured surface of untreated polymer sample is shown in Figure 3.3.4a. The figure showed that different polymers were immiscible. The immiscibility decreased drastically when the polymer blend was treated with PE-*co*-GMA (Fig. 3.3.4b). The miscibility among different polymers was found to increase with the increase in the amount of PE-*co*-GMA (not shown in the figure). This might be due to the improvement in compatibility between HDPE,

LDPE, PP and PVC in which PE-*co*-GMA acted as a compatibilizer among polymers. The improvement in adhesion between polyolefins and PET by using ethylene-glycidyl methacrylate copolymer as compatibilizer was reported in the literature [6]. The surface of the wood/polymer composites became smooth on addition of nanoclay (Fig. 3.3.4c and 3.3.4d). The presence of octadecyl amine and silane groups on nanoclay might have favoured the interaction between polymers and wood. This made both the polymers and wood more compatible with nanoclay. There was no significant difference in the surface characteristics on increasing the amount of nanoclay from 1.0 to 3.0 phr. However, the surface appeared little bit rough on addition of 5 phr of clay (Fig. 3.3.4e). The partial agglomeration of nanoclay might be responsible for this observation.

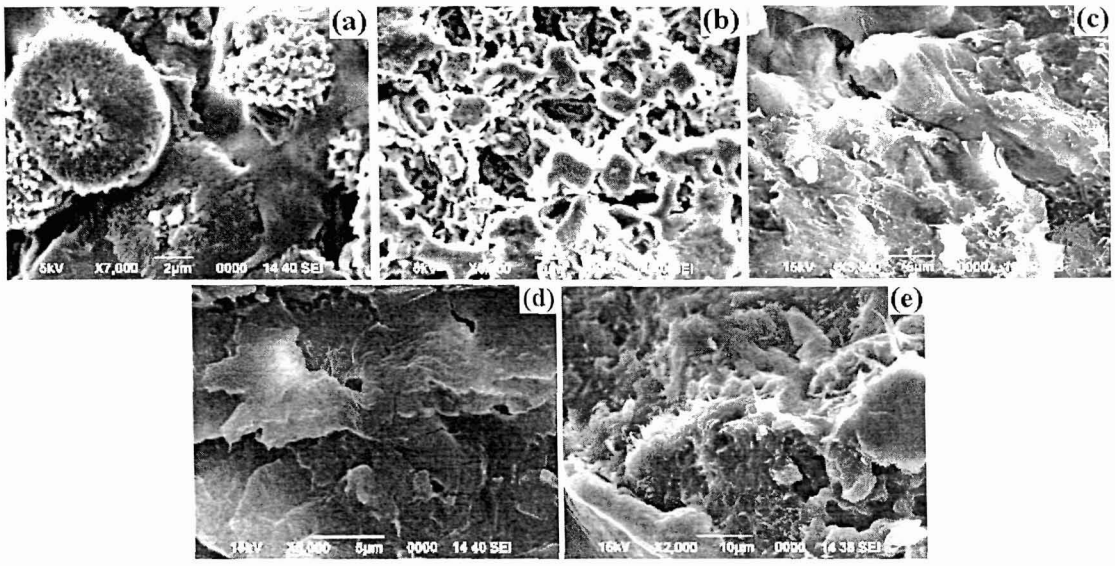


**Figure 3.3.4.** SEM micrographs of (a) PB (b) PB/G5 (c) PB/G5/W40/N1 (d) PB/G5/W40/N3 (e) PB/G5/W40/N5.

### 3.3.5. Mechanical properties study

The flexural and tensile properties of PB, PB/G5, PB/G5/N3 and WPCs with different percentage of clay loading are shown in Table 3.3.1. The datas presented were the average of five readings. It was observed that both flexural and tensile properties of polymer blends increased on addition of PE-*co*-GMA as compatibilizer. PE-*co*-GMA acted as a dispersing agent among different polymers resulting in improved interfacial adhesion due to which flexural and tensile properties increased. This was also supported by XRD and SEM

study. Pracella et al. [6] studied the effect of various compatibilizers on HDPE, PP and PVC blend and found that ethylene glycidyl methacrylate copolymer provided better interfacial adhesions among among different kinds of polymer. Both flexural and tensile properties were increased on addition of wood flour. Since wood flour acted as load carrier, it reinforced the composite and enhanced the flexural and tensile properties. Moreover, PE-*co*-GMA improved the adhesion between wood and polymer blend through its glycidyl group and hydrocarbon backbone respectively. The incorporation of nanoclay with wood, polymer blend and PE-*co*-GMA further enhanced the flexural and tensile properties. Both flexural and tensile values increased with clay loading up to 3 phr, beyond that the values decreased. The observed higher values might be due to the higher dispersion of silicate layers of nanoclay in the wood polymer matrix and the restriction in the mobility of the polymer

**Table 3.3.1.** Flexural, tensile and hardness properties of polymer blend, wood/polymer and wood/polymer/clay nanocomposites.

| Sample | Flexural properties | | Tensile properties | | Hardness |
|---|---|---|---|---|---|
| | Strength (MPa) | Modulus (MPa) | Strength (MPa) | Modulus (MPa) | (Shore D) |
| PB | 13.24 ± 1.09 | 763.28 ± 1.02 | 5.24 ± 1.13 | 84.38 ± 18.19 | 66.0 ± 1.0 |
| PB/G5 | 15.39 ± 1.31 | 1058.36 ± 1.26 | 8.46 ± 1.21 | 113.25 ± 16.19 | 68.5 ± 0.5 |
| PB/G5/N3 | 21.42 ± 0.92 | 4375.61 ± 1.43 | 24.47 ± 1.31 | 356.19 ± 19.07 | 68.0 ± 1.0 |
| PB/G5/W40 | 17.47 ± 1.06 | 3822.13 ± 1.03 | 18.11 ± 1.20 | 261.71 ± 17.34 | 66.0 ± 0.8 |
| PB/G//W40/N1 | 20.32 ± 0.64 | 4215.34 ± 0.58 | 23.34 ± 1.03 | 368.14 ± 16.25 | 72.0 ± 0.9 |
| PB/G//W40/N3 | 26.17 ± 0.85 | 4749.53 ± 0.72 | 31.57 ± 1.01 | 581.40 ± 18.60 | 77.0 ± 0.6 |
| PB/G//W40/N5 | 23.44 ± 1.02 | 4523.82 ± 1.31 | 28.87 ± 1.27 | 547.82 ± 24.09 | 75.0 ± 0.4 |

chains inside the intercalated nanolayers of clay. Besides the nanoclay contained some silane and hydrocarbon portions which facilitated the interaction between wood flour and polymer matrix. All these suggested an improvement in adhesion between polymer blend, wood and clay. The nanocomposites thus exhibited better properties over wood flour/PE-*co*-GMA treated polymer blend composites. The inclusion of organoclay resulted in the improvement in mechanical properties was reported by Lee and Kim [8] while studying the physical properties of wood/PP/clay nanocomposites. The decreased in mechanical properties of

WPC treated with 5 phr clay might be attributed to the migration of clay to the interface between wood flour and polymer blend. The presence of high amount of fiber and its interface with polymer might have reduced the reinforcement effect of clay. Similar observation was reported by Han et al. [32] during the study of nanoclay reinforced HDPE/bamboo fiber composite.

### 3.3.6. Hardness results

Table 3.3.1 also shows the hardness results of PB and WPCs with different percentage of clay loading. From the table, it was observed that hardness increased as PE-*co*-GMA was added to the polymer blend. The increased in hardness in polymer blend was due to the improvement in interfacial adhesion between various polymers by PE-*co*-GMA. The hardness did not improve on addition of clay to the polymer blend. However, on addition of wood flour in the PE-*co*-GMA modified polymer blend, the hardness value decreased. But the hardness was found to increase further as nanoclay was added. The value improved up to an incorporation of certain amount of nanoclay (3 phr) beyond that the value decreased. The improvement was due to the decrease in mobility of the intercalated polymer chains and increase in interaction between wood flour and polymer by the clay as explained earlier. At higher clay loading, migration of clay to the interface of polymer and wood flour surface might decrease the reinforcement effect of clay. As a result the hardness was found to decrease.

### 3.3.7. Dynamic mechanical analysis

Storage modulus and loss modulus of PB, PB/G5/W40 and PB/G5/W40/N3 are presented in the Figure 3.3.5 and 3.3.6. PB/G5/W40 exhibited higher storage and loss modulus compared to PB. This enhancement might be due to the development of strong interaction between wood flour and polymer blend by PE-*co*-GMA. The glycidyl group and long polyethylene chain of PE-*co*-GMA interacted with the hydroxyl group of wood and polymer blend respectively. Storage and loss modulus were found to increase on addition of glycidyl methacrylate as compatibilizer to the WPC [33]. Both the storage and loss modulus were found maximum in the case of PB/G5/W40/N3. The long chain of polymer molecules intercalated into the interlayer space of the silicate layers and restricted the mobility of the polymer chains. As a result, stiffness of the WPC increased and both storage and loss

modulus improved. Matuana et al. [2] studied dynamic mechanical properties of clay/HDPE/wood composite and reported that clay reinforced HDPE/wood composite showed better storage and loss modulus compared to clay free HDPE/wood composite. In both the cases, a reduction in modulus with the increase in temperature was observed. This was due to the softening of the matrix at higher temperature [34].

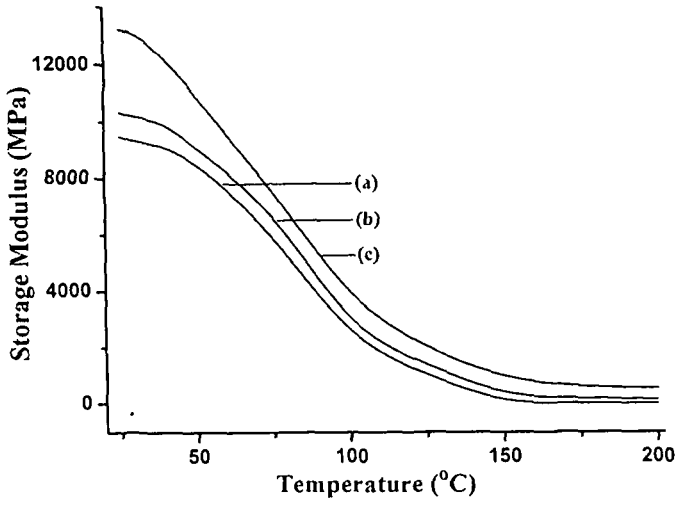


**Figure 3.3.5.** Storage modulus of (a) PB (b) PB/G5/W40 (c) PB/G5/W40/N3.

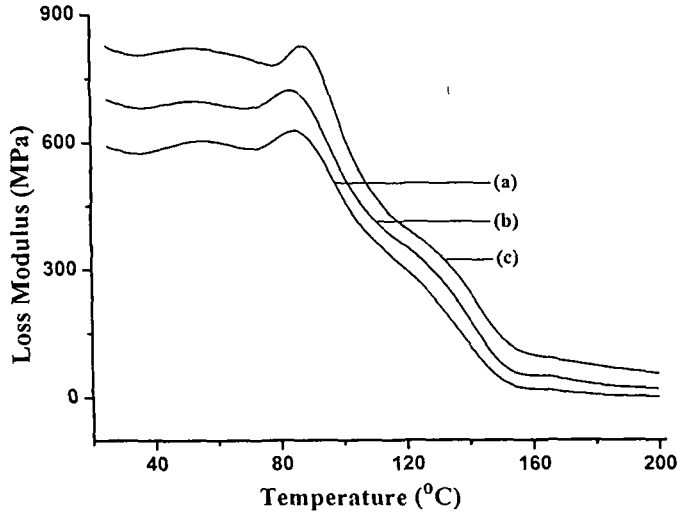


**Figure 3.3.6.** Loss modulus of (a) PB (b) PB/G5/W40 (c) PB/G5/W40/N3.

The damping factor or mechanical loss factor (tan δ) is the ratio of loss modulus to storage modulus and is shown in Figure 3.3.7. PB exhibited a tan δ peak with a peak

temperature of 96.8 °C. There was no significant shifting of tan δ peak in both PB/G5/W40 and PB/G5/W40/N3. However, a lowering of tan δ peak height was observed with the addition of wood flour. This was due to the decrease in the volume fraction of the matrix by the incorporation of wood flour. Similar observation was reported by the literature [35,36]. The reduction of tan δ peak height was more pronounced when clay was added to the composite. This might be due to the restricted movement of the polymer chains caused by the silicate layers of clay and rigid wood flour molecules.

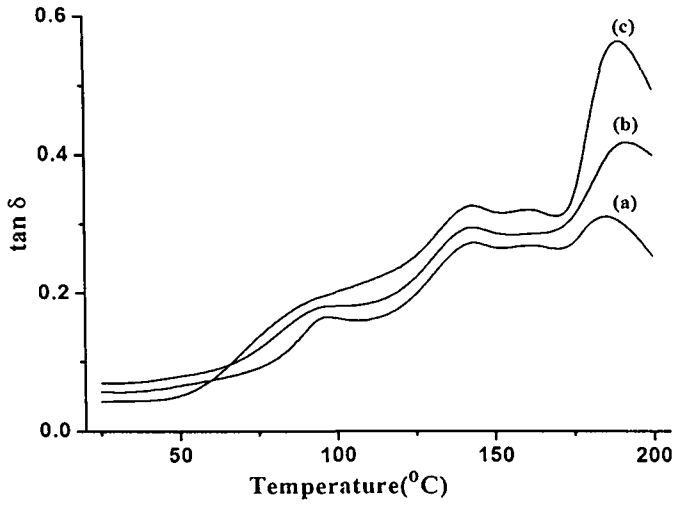


**Figure 3.3.7.** Tan δ of (a) PB (b) PB/G5/W40 (c) PB/G5/W40/N3.

### 3.3.8. Thermogravimetric analysis

Figure 3.3.8 and 3.3.9 show the weight losses for wood flour, nanoclay, polymer blend and WPC. Table 3.3.2 shows the initial decomposition temperature ($T_i$), maximum pyrolysis temperature ($T_m$), weight losses for various samples at different temperature ($T_D$) and residual weight (RW,%) for different samples. $T_i$ value of nanoclay was found maximum. This was followed by polymer blend and wood flour. $T_i$ value of polymer blend improved on addition of PE-*co*-GMA and wood flour. The values were found to enhance further when nanoclay was added. $T_i$ value increased upto addition of 3 wt% clay beyond that it decreased. $T_m$ values observed for wood flour was due to the depolymerization of hemicelluloses, glycidyl linkage and thermal decomposition of cellulose [10]. The first decomposition peak shown by the polymer blend might be due to the dehydrochlorination of PVC [11]. While the second decomposition peak was due to the decomposition of LDPE,

HDPE and PP [12,7]. $T_m$ value of polymer blend enhanced due to incorporation of PE-*co*-GMA and wood flour. $T_m$ value increased further when nanoclay was added. The value increased upto addition of 3 wt% nanoclay beyond that it decreased. Nanoclay showed highest RW values while the polymer blend showed lowest RW values. The trend of RW values of clay treated WPC was similar to those of $T_i$ values. The RW values observed for nanoclay and wood flour were due to the presence of inorganic silicate layer and carbonization of wood respectively.

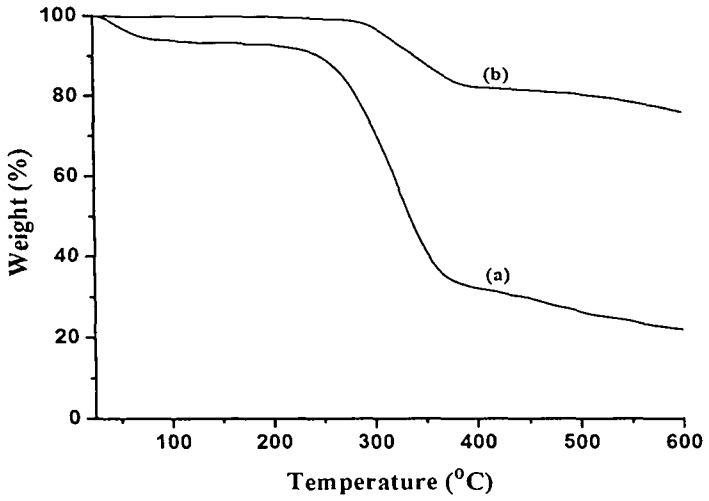


**Figure 3.3.8.** Themogravimetric curves of (a) WF (b) Nanoclay.

Further it was observed from the Table 3.3.2 that polymer blend decomposed at higher temperature compared to wood flour. $T_D$ values increased on addition of wood flour and PE-*co*-GMA to the polymer blend. This might be due to the enhancement of interaction caused by the increase in interfacial adhesion between wood flour and polymer blend by PE-*co*-GMA through its glycidyl group and polyethylene chain. Awal et al. [4] reported that the incorporation of wood pulp, maleated polypropylene into polypropylene delayed the thermal degradation of the composite. $T_D$ value increased initially upto addition of 3 wt% clay after that it decreased with the increase in the amount of clay (5 wt%). Therefore it could be concluded that the inclusion of nanoclay improved the thermal stability of WPC. The improvement in thermal stability may be attributed to the presence of silicate layer which acted as a barrier and delayed the diffusion of decomposed volatile products throughout the composites [29]. At higher clay loading, the silicate layer might become agglomerated and

decreased the barrier resistance. As a result, the diffusion of volatile products would be rapid and thermal stability would be less.

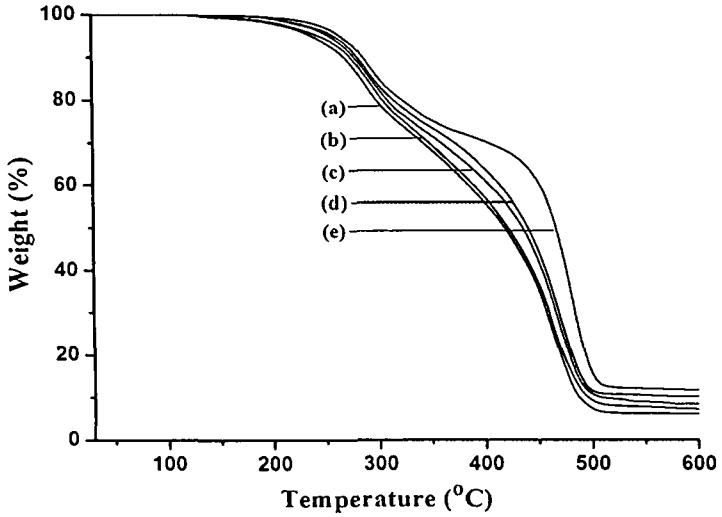


**Figure 3.3.9.** Themogravimetric curves of (a) PB (b) PB/G5/W40 (c) PB/G5/W40/N1 (d) PB/G5/W40/N5 (e) PB/G5/W40/N3.

**Table 3.3.2.** Thermal analysis of wood, polymer blend and wood polymer nanocomposite.

| Sample | $T_i$ | $T_m{}^a$ | $T_m{}^b$ | Temperature of decomposition ($T_D$) in °C at different weight loss (%) | | | | RW% at |
|---|---|---|---|---|---|---|---|---|
| | | | | 20% | 40% | 60% | 80% | 600°C |
| Wood flour | 230 | 315 | - | 282 | 320 | 352 | - | 21.9 |
| Nanoclay | 294 | 352 | - | 514 | - | - | - | 76.0 |
| PB | 251 | 272 | 407 | 297 | 385 | 441 | 470 | 6.1 |
| PB/G5/W40 | 257 | 277 | 455 | 303 | 390 | 444 | 472 | 7.2 |
| PB/G5/W40/N1 | 260 | 281 | 466 | 309 | 404 | 453 | 478 | 8.4 |
| PB/G5/W40/N3 | 270 | 319 | 496 | 322 | 452 | 476 | 493 | 11.7 |
| PB/G5/W40/N5 | 263 | 309 | 480 | 313 | 414 | 456 | 481 | 10.2 |

$T_i$: value for initial degradation; $^aT_m$: value for 1st step; $^bT_m$: value for 2nd step.

### 3.3.9. Limiting oxygen index (LOI) results

Table 3.3.3 shows the results of limiting oxygen index (LOI) values of polymer blend and WPC with varying percentage of nanoclay. It was observed that the value of LOI increased on addition of PE-*co*-GMA to the polymer blend. The increase in interfacial adhesion among polymers by PE-*co*-GMA might be responsible for the observed higher value of LOI. The values were further improved on addition of nanoclay. The LOI values of the nanoclay treated wood polymer composites were found more compared to nanoclay untreated wood polymer composite. The higher the percentage of nanoclay, the higher was the LOI. Wood flour contained cellulose, hemicelluloses, lignin and other low molecular

**Table 3.3.3.** Limiting oxygen index (LOI) values and flaming characteristics of polymer blend and wood/polymer/clay nanocomposites.

| Samples | LOI (%) | Flame description | Smoke & Fumes | Char |
|---|---|---|---|---|
| PB | 22 | Candlelike localised | — | little |
| PB/G5 | 39 | Small localized flame | Small and black smoke | little |
| PB/G5/N3 | 47 | Small localized flame | Small and black smoke | higher |
| PB/G5/W40 | 44 | Small localized flame | Small and black smoke | little |
| PB/G5/W40/N1 | 55 | Small localized flame | Small and black smoke | higher |
| PB/G5/W40/N3 | 61 | Small localized flame | Small and black smoke | higher |
| PB/G5/W40/N5 | 66 | Small localized flame | Small and black smoke | higher |

weight components which required lower concentration of oxygen for the production of flammable volatiles and propagation of flame. As a result, the LOI of nanoclay untreated wood polymer composite was found less. On the other hand, nanoclay produced silicate char on the surface of the clay treated WPC which increased the flame resistance property of the composite [18]. The silicate rich surface had better barrier property to heat and oxygen transport due to which ignition of the composite delayed. Besides this, the nanoclay contains amino propyl triethoxy silane and octadecyl amine groups which could interact and promote adhesion with WF and polymer blend. This adhesion might prevent the flame for

propagation. The higher the percentage of clay, the stronger was the adhesion as well as resistance of flame propagation.

### 3.3.10. Biodegradation study

WPC samples were exposed for microbial degradation and after eight weeks of study, wood polymer composites had shown high rate of degradation. Figure 3.3.10 shows the bacterial growth of the WPC with respect to time. From the figure, it was observed that with increasing bacterial exposure time, the growth of bacterial strains increased. Wood composite as sole carbon source showed higher rate of bacterial growth after three weeks of incubation and it continued up to eighth week. This enhancement of bacterial growth might be due to powerful cellulolytic and pectinolytic activity of bacteria [37]. Other than cellulose and pectin, lignin was also a constituent of *Phragmites karka* plant stem and it was reported that *Bacillus sp.* could degrade this [38]. The growth and degradation property of the wood

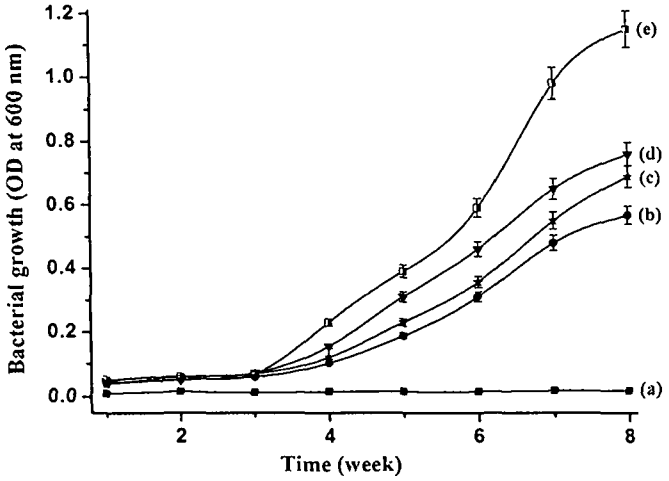


**Figure 3.3.10.** Growth of *Bacillus sp.* on (a) PB (b) PB/G5/W40 (c) PB/G5/W40/N1 (d) PB/G5/W40/N3 (e) PB/G5/W40/N5.

composite by bacteria was also supported by the SEM study (Fig. 3.3.11). With the increase in the clay content, the rate of bacterial growth enhanced. The improved biodegradability of nanocomposite was due to the catalytic role played by the clay in the biodegradation mechanism [39]. From the study, it was observed that WPC loaded with 5 wt% clay showed maximum bacterial growth. The mechanical properties of the degraded WPC samples were checked, compared with undegraded samples and are presented in Table 3.3.4 and 3.3.5. The

higher mechanical properties shown by both degraded and undegraded WPC samples loaded with 3 wt% clay was due to the better dispersion of silicate layers of nanoclay and enhanced

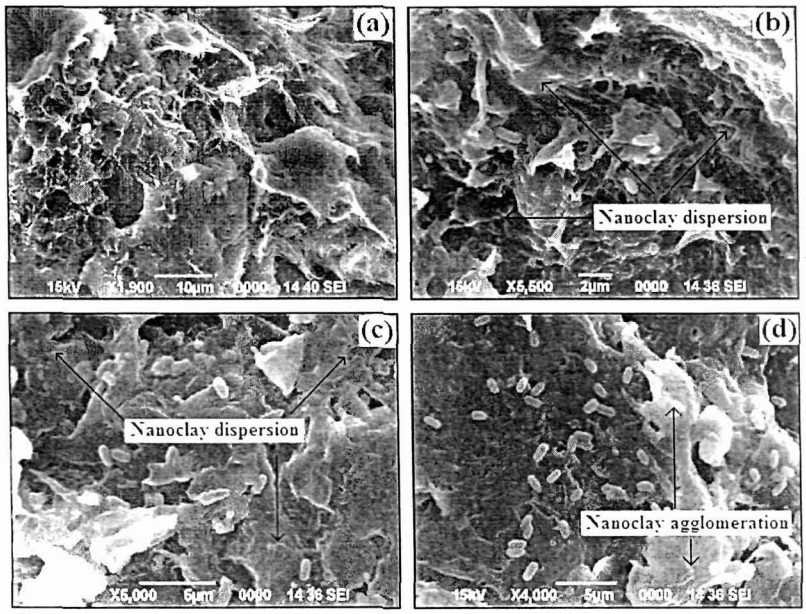


**Figure 3.3.11.** SEM micrographs of (a) PB/G5/W40 (b) PB/G5/W40/N1 (c) PB/G5/W40/N3 (d) PB/G5/W40/N5.

**Table 3.3.4.** Flexural properties of WPC loaded with different percentage of nanoclay after microbial degradation.

| Sample | Before degradation | | After degradation | |
|---|---|---|---|---|
| | Strength (MPa) | Modulus (MPa) | Strength (MPa) | Modulus (MPa) |
| PB/G5/W40 | 18.01 ± 1.12 | 3864.24 ± 1.16 | 16.84 ± 1.09 | 3686.49 ± 1.05 |
| PB/G5/W40/N1 | 20.09 ± 0.81 | 4193.27 ± 0.74 | 17.45 ± 1.53 | 3964.75 ± 0.93 |
| PB/G5/W40/N3 | 25.87 ± 0.93 | 4761.36 ± 0.95 | 20.63 ± 0.87 | 4239.72 ± 1.07 |
| PB/G5/W40/N5 | 22.15 ± 1.66 | 4487.65 ± 1.08 | 17.74 ± 1.04 | 3871.84 ± 1.17 |

restriction in the mobility of the polymer chains intercalated inside the silicate layers. The lower mechanical properties exhibited by 5 wt% clay loaded WPC was due to the reduction in reinforcement effect of clay caused by the migration of the same to the interface between wood flour and polymer blend. It was found that with efficient degradation of WPCs,

flexural and tensile properties of the WPCs decreased. This might be due to the loss of physical and chemical interaction in the WPC caused by the degradation effect of bacteria.

**Table 3.3.5.** Tensile properties of WPC loaded with different percentage of nanoclay after microbial degradation.

| Sample | Before degradation | | After degradation | |
|---|---|---|---|---|
| | Strength (MPa) | Modulus (MPa) | Strength (MPa) | Modulus (MPa) |
| PB/G5/W40 | 17.93 ± 1.05 | 231.63 ± 18.26 | 15.85 ± 1.21 | 194.52 ± 17.74 |
| PB/G5/W40/N1 | 23.01 ± 1.12 | 312.79 ± 17.16 | 20.91 ± 1.06 | 217.83 ± 17.69 |
| PB/G5/W40/N3 | 30.86 ± 0.93 | 605.48 ± 17.49 | 25.14 ± 0.79 | 496.27 ± 18.92 |
| PB/G5/W40/N5 | 28.12 ± 1.06 | 521.54 ± 23.72 | 22.63 ± 1.13 | 415.86 ± 21.63 |

### 3.3.11. Water uptake test

The results of water uptake for PB, PB/G5, PB/G5/N3 and WPCs with different percentage of clay loading are shown in Figure 3.3.12. In all the cases, the water uptake was found to increase with the increase of time of immersion. Water absorption occurred initially at a rapid rate and finally at a slower rate. The water absorption of the neat polymer decreased on addition of PE-*co*-GMA. It was due to the improvement in compatibility among the polymers. PE-*co*-GMA increased the interaction between the interfaces of the polymers and thus enhanced water resistance. Water absorption decreased further on addition of nanoclay to the PE-*co*-GMA treated polymer blend. The water absorption was found to enhance when wood flour was added. The hydrophilic nature of wood flour was responsible for this. The water absorption of wood flour/polymer blend composite decreased with the incorporation the clay. The higher the amount of clay, the lower was the water absorption. Organically modified clay increased the tortuous path for water transport and as a result water diffusivity decreased [21]. Rana et al. [19] has studied the barrier property of nanocomposite where nanoclay hindered the permeation of water through the composite. Moreover, the void spaces in the wood flour were occupied by the polymer and nanoclay. This decreased the available space for water absorption. The higher the nanoclay, the lower was the available space to hold the water. Both the tortuous path and reduction in void space

decreased the water absorption capacity of WPC. Hence nanoclay treated composite showed lower water absorption compared to nanoclay untreated composite.

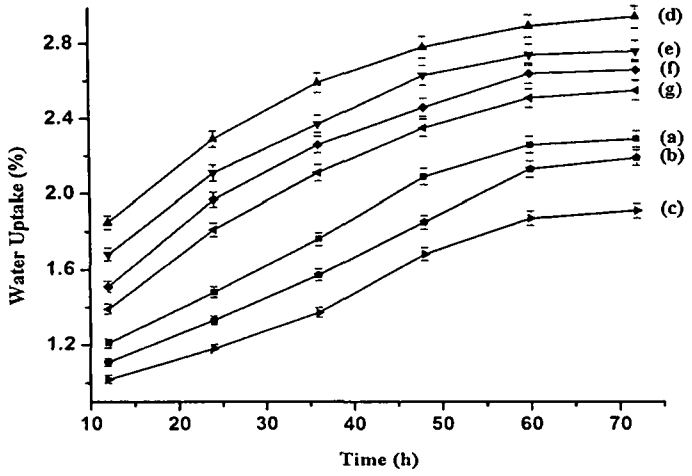


**Figure 3.3.12.** Percent water absorption of (a) PB (b) PB/G5 (c) PB/G5/N3 (d) PB/G5/W40 (e) PB/G5/W40/N1 (f) PB/G5/W40/N3 (g) PB/G5/W40/N5.

### 3.3.12. Water vapour uptake test

Water vapour absorption tests of polymer blend, clay treated and untreated WPC were carried out at 30 °C and two different relative humidities namely 95% and 65% respectively and are shown in Figure 3.3.13 and 3.3.14. As expected, all the samples absorbed less water vapour at 65% R.H. compared to 95% R.H. In all the cases, water vapour absorption occurred initially at a faster rate and finally at a slower rate. The rate of water vapour absorption increased with the increased in time. The water vapour absorption followed the order: PB/G5/W40 > PB/G5/W40/N1 > PB/G5/W40/N5 > PB/G5/W40/N3 > PB > PB/G5 > PB/G5/N3. The water vapour absorption was found to decrease on addition of PE-*co*-GMA to the polymer blend (PB). The compatibilizer, PE-*co*-GMA increased the interfacial adhesion among polymers which led to the decrease in water vapour absorption. Devi et al. [9] reported that GMA treated WPC absorbed less water vapour compared to untreated WPC. The water vapour absorption was further decreased due to inclusion of clay. The silicate layers of clay acted as a barrier for the moisture which resulted in the decrease of the absorption of water vapour. The value was found to enhance when wood flour was added. The hydrophilic nature of the wood flour was responsible for this. Similar results were reported in the literature [40]. The addition of clay to the WPC further decreased the

rate of absorption of water vapour. The value decreased upto addition of 3 wt% clay after that it increased. The overall decrease in the moisture absorption was due to the tortuous path imparted by the organically modified silicate layers which prevented the water vapour from transportation and diffusion through the composite [21].

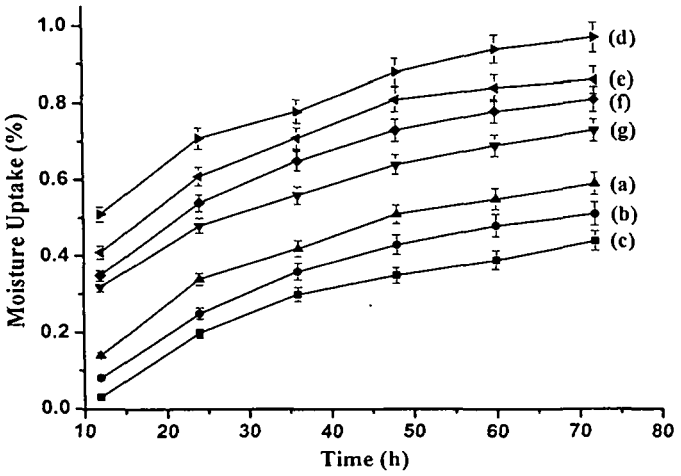


**Figure 3.3.13.** Percent water vapour absorption at room temperature and 95% relative humidity of (a) PB (b) PB/G5 (c) PB/G5/N3 (d) PB/G5/W40 (e) PB/G5/W40/N1 (f) PB/G5/W40/N5 (g) PB/G5/W40/N3.

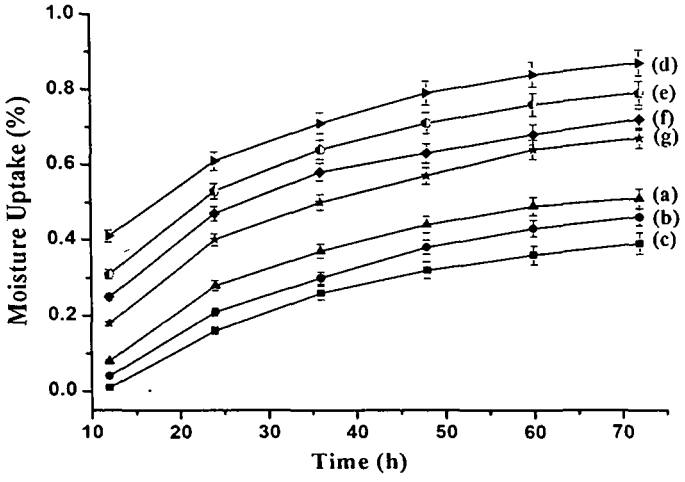


**Figure 3.3.14.** Percent water vapour absorption at room temperature and 65% relative humidity of (a) PB (b) PB/G5 (c) PB/G5/N3 (d) PB/G5/W40 (e) PB/G5/W40/N1 (f) PB/G5/W40/N5 (g) PB/G5/W40/N3.

Moreover, there was less void space available in the wood for the absorption of water vapour due to occupation of the same by nanoclay and polymer. As a result, the water vapour absorption of clay treated WPC would be less due to reduction in void space in wood and the presence of tortuous path imparted by the silicate layers. The higher water vapour absorption exhibited by the WPC containing 5 wt% clay was due to the agglomeration of silicate layers which decreased the tortuous path for transportation and diffusion of water vapour. In general, it can be concluded that nanoclay treated WPC absorbed less water vapour compared to clay free WPC. The trend of water vapour absorption of the samples in the case of 65% R.H. and 30 °C was similar to those of samples tested at 95% R.H. and 30 °C.

## *Section D*: Wood flour (*Ipomoea carniva*) reinforced polymer/clay nanocomposite.

Kalmou (*Ipomoea carniva*), a kind of non-conventional plant, which is also abundantly available in the forest of North-East India. Due to their poor mechanical, dimensional and other properties, these are not used for any constructional purposes. They are mostly used for domestic fuels and sometimes for making temporary shades. These can be made value added by forming a composite with plastic materials.

The aim of the present study is to prepare the nanocomposite via solution blending by using WF, PE-*co*-GMA, nanoclay, polymer mixture of high density of polyethylene (HDPE), low density polyethylene (LDPE), polypropylene (PP) and polyvinyl chloride (PVC) and to evaluate the various properties of composites.

### 3.4. RESULTS AND DISCUSSION

#### 3.4.1. X-ray diffraction results

X-ray diffractograms of pure nanoclay and WPC loaded with different percentage of nanoclay are shown in Figure 3.4.1. The $d_{001}$ spacing between the silicate layers was determined by using Bragg's law. A sharp peak for organically modified nanoclay appeared at 4.1° ($d_{001}$ = 2.15 nm) as shown in Figure 3.4.1a. Figure 3.4.1b shows the diffraction peak

of PE-*co*-GMA treated clay reinforced polymer blend. From the curve, it was observed that the (001) peak of nanoclay shifted to lower angle at $2\theta = 2.9^{\circ}$ ($d_{001} = 3.04$ nm) indicating an increase in gallery space. This was due to the intercalation of long chain of polymers into the silicate layers. The (001) peak of nanoclay in 1phr nanoclay loaded WPC (curve-3.4.1c) was found to shift further to lower angle at $2\theta = 2.6^{\circ}$ ($d_{001} = 3.39$ nm). WPC loaded with 3 phr nanoclay (curve-3.4.1d) did not exhibit any sharp peak indicating an exfoliation of silicate layers in wood polymer matrix. The shifting of diffraction peak to lower angle was reported [2] while studying the properties of clay based HDPE nanocomposite. Further, the glycidyl group of PE-*co*-GMA might interact with the hydroxyl group present in the clay leading to an increase in the gallery space and thus promoting easy insertion of polymer chain into the interlayer space of the clay [41]. The peak (curve-3.4.1e) reappeared with the increase in clay content suggesting an occurrence of agglomeration of clay as evident from TEM study.

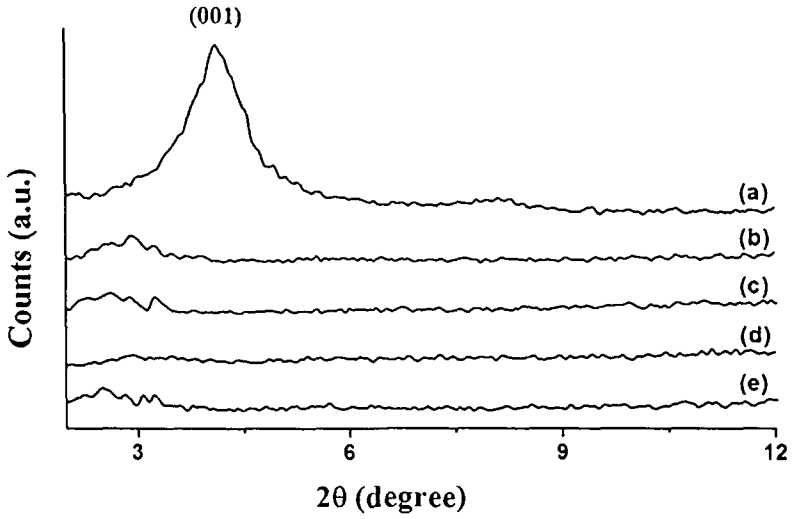


**Figure 3.4.1.** X-ray diffraction of (a) Nanoclay (b) PB/G5/N3 (c) PB/G5/W40/N1 (d) PB/G5/W40/N3 (e) PB/G5/W40/N5.

### 3.4.2. Fourier transform infrared spectroscopy results

Figure 3.4.2 shows the FTIR spectra of wood, nanoclay and WPC loaded with nanoclay. The FTIR spectrum of wood (curve-3.4.2a) showed the presence of bands at 3437 $cm^{-1}$ for –OH stretching, 2931 $cm^{-1}$ and 2851 $cm^{-1}$ for –CH stretching, 1734 $cm^{-1}$ for C=O stretching, 1644 $cm^{-1}$ for –OH bending, 1160 and 1046 $cm^{-1}$ for C–O stretching and 1000–

650 $cm^{-1}$ for -CH bending vibration (out of plane). Nanoclay (curve-3.4.2b) exhibited the peaks at 3480 $cm^{-1}$ (–OH stretching) 2934 and 2853 $cm^{-1}$ (–CH stretching of modified hydrocarbon), 1622 $cm^{-1}$ (–OH bending), 1031-460 $cm^{-1}$ (oxide bands of metals like Si, Al, Mg etc.). The characteristic peaks of –CH stretching at 2921 $cm^{-1}$ and 1467 $cm^{-1}$, C–$CH_3$ stretching at 2845 $cm^{-1}$ along with –$CH_2$ stretching at 721 $cm^{-1}$ for the polymer blend mixed with PE-*co*-GMA and nanoclay was shown in curve-3.4.2c.

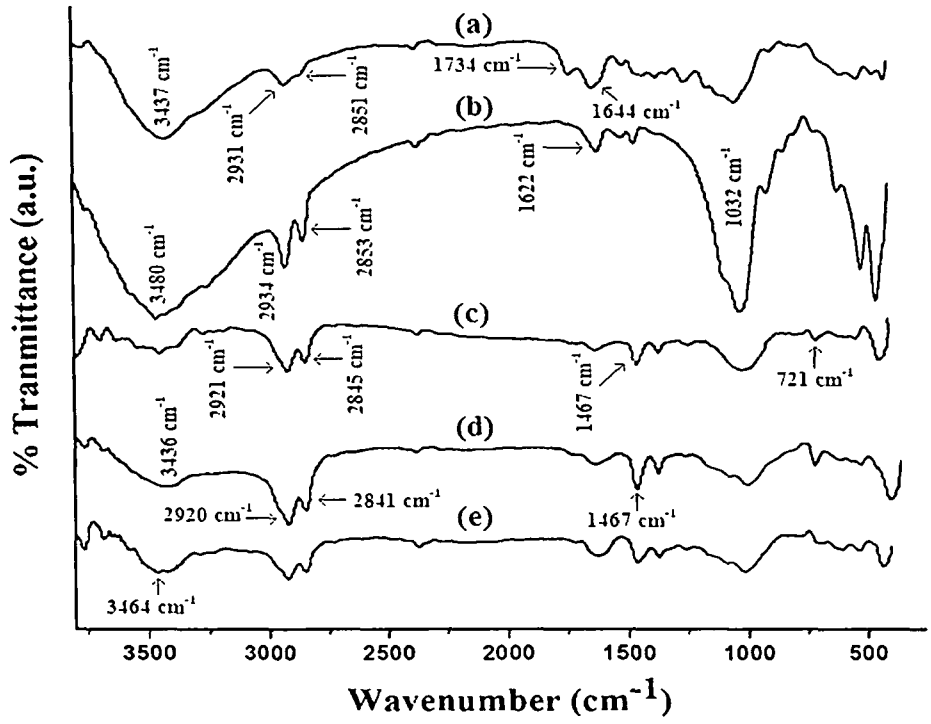


**Figure 3.4.2.** FTIR spectra of (a) Wood (b) Nanoclay (c) PB/G5/N3 (d) PB/G5/W40/N3 (e) PB/G5/W40/N5.

Figure 3.4.2d and e represent the FTIR spectra for WPC loaded with 3 phr and 5 phr nanoclay. From the spectra it was observed that the intensity of –OH peaks decreased and to shifted to lower wave number. The shifting of peak pertaining to –OH group to 3385 $cm^{-1}$ (curve-3.4.2d) and 3497 $cm^{-1}$ (curve-3.4.2e) indicated the formation of hydrogen bond between matrix and wood. The intensity of –CH stretching at 2920 $cm^{-1}$ and 2841 $cm^{-1}$ was more compared to that of wood suggesting formation of the bond formation between polymer, PE-*co*-GMA and wood. Similar shifting of absorption peak of hydroxyl group to lower wave number and increase in intensities of –CH stretching was reported in literature [4]. In the spectra of WPC (curves-3.4.2d-e), the intensity of the metal oxides bands of

nanoclay at 1031-460 $cm^{-1}$ was found to decrease to a desirable extent which also confirmed the formation of bond between wood, clay and polymers.

### 3.4.3. Scanning electron microscopy (SEM) study

Figure 3.4.3 shows SEM micrographs of different fractured samples. Fractured surface of polymer blend without compatibilizer is shown in Figure 3.4.3a. From the figure, it was noticed that different polymers were immiscible without using any kind of compatibilizer. The immiscibility decreased remarkably after adding PE-*co*-GMA compatibilizer (Fig. 3.4.3b). The increase in compatibility among the polymers was due to the increase in interfacial adhesion by the compatibilizer [6]. The addition of nanoclay improved the surface smoothness (Fig. 3.4.3c and d). The change of nanoclay level from 1 phr to 3 phr did not exhibit any significant difference in surface smoothness. The silane

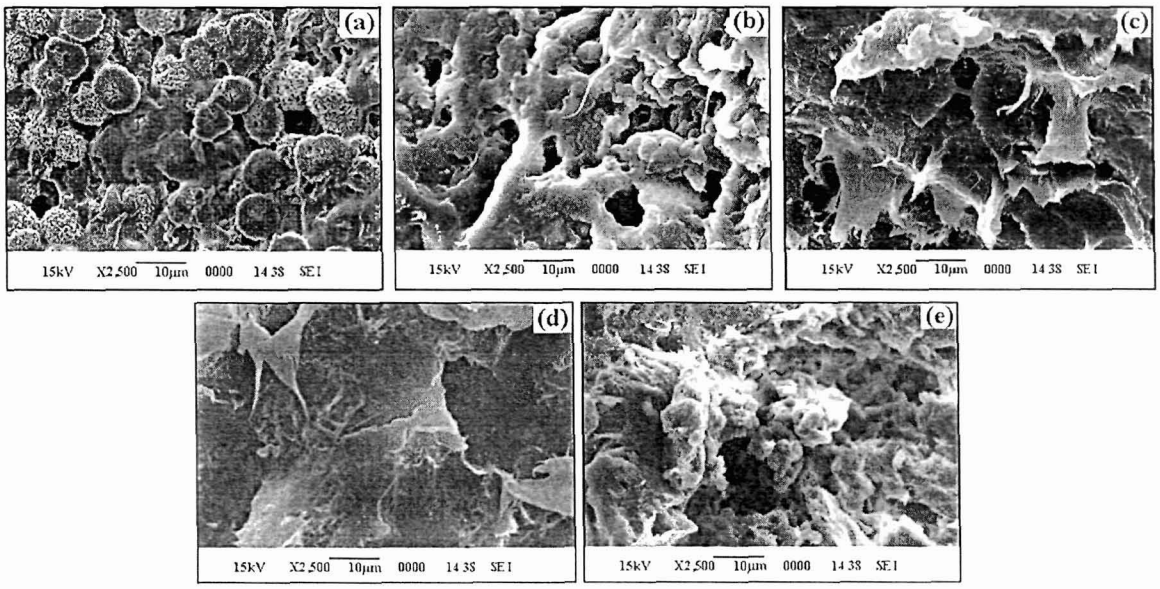


**Figure 3.4.3.** SEM micrographs of (a) PB (b) PB/G5 (c) PB/G5/W40/N1 (d) PB/G5/W40/N3 (e) PB/G5/W40/N5.

group and octadecyl amine present in nanoclay enhanced the interaction with the hydroxyl group of wood and hydrocarbon chain of polymer respectively. The addition of nanoclay was reported to improve the interfacial adhesion in WPC [41]. At 5 phr nanoclay loaded WPC (Fig. 3.4.3e), the agglomeration was observed which might be due to the surface interaction of the clay particles.

### 3.4.4. Transmission electron microscopy study

Figure 3.4.4 shows the TEM micrographs of WPC loaded with different percentage of nanoclay. The silicate layers are shown as dark lines or spot areas. The clay layers were found to disperse in the composites even at lower percentage of nanoclay. The dispersion was improved when the nanoclay loading was increased to 3 phr. The nanoclay layers became agglomerated with the further increase in the level of clay to 5 phr. Similar findings were reported in the literature [3] during TEM study of organically modified MMT/wood flour/polyvinyl chloride matrix.

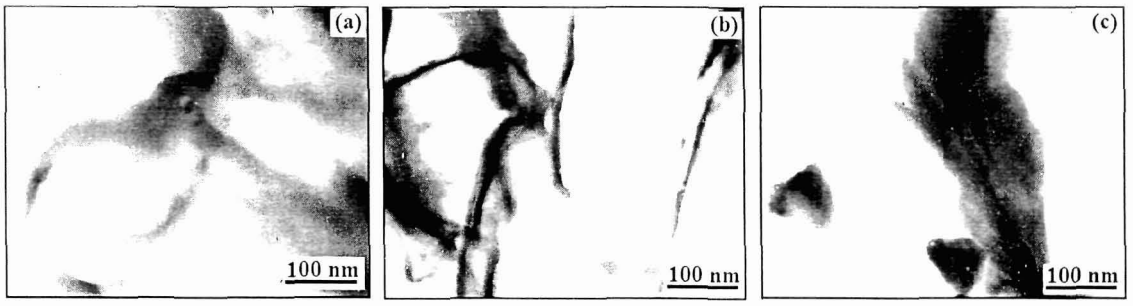


**Figure 3.4.4.** TEM micrographs of (a) PB/G5/W40/N1 (b) PB/G5/W40/N3 (c) PB/G5/W40/N5.

### 3.4.5. Mechanical properties study

Table 3.4.1 shows the flexural and tensile properties of polymer blends and WPC loaded with different percentage of nanoclay content. It was observed that both flexural and tensile properties of the polymer blend increased after the addition of compatibilizer. The compatibilizer enhanced the interfacial adhesion between the polymers and as a result improvement in both tensile and flexural properties were observed [24]. The flexural and tensile properties of the composite were improved further on addition of wood flour (WF). It has been found to improve the mechanical properties of polypropylene after the incorporation of wood flour [42]. The wood flour reinforced the composite and enhanced the mechanical properties. Moreover, the compatibilizer, PE-*co*-GMA, increased the interfacial adhesion between wood and polymer through its glycidyl linkage and long chain of polymer backbone respectively. Both the flexural and tensile properties were further increased after the addition of clay to the composite. The properties were found to improve upto the

addition of 3 phr clay beyond that the properties decreased. The improvement in properties was due to the better dispersion of nanoclay in the wood polymer matrix and restriction in the movement of the polymer chain inside the silicate layers. Nanoclay had some hydrocarbon as well as silane group which favoured the interaction between wood flour and polymer blends. The improvement in mechanical properties of HDPE/wood-flour composites was found due to addition of coupling agent and nanoclay in the composites [2]. The decrease in properties at higher concentration of clay might be ascribed to the transfer of clay to the interface between polymer blend and wood flour. Similar findings was reported [32] the while studying the mechanical properties of HDPE/bamboo fiber/nanoclay composite.

**Table 3.4.1.** Flexural, tensile, hardness and limiting oxygen index (LOI) values of polymer blend and WPC loaded with different percentage of nanoclay.

| Sample | Flexural properties | | Tensile properties | | Hardness | LOI |
|---|---|---|---|---|---|---|
| | Strength (MPa) | Modulus (MPa) | Strength (MPa) | Modulus (MPa) | (Shore D) | (%) |
| PB | 13.93 ± 1.04 | 769.57 ± 1.03 | 6.47 ± 1.61 | 89.26 ± 18.93 | 65.8 (± 0.3) | 21 |
| PB/G5 | 16.01 ± 1.07 | 1082.73 ± 1.09 | 9.98 ± 1.75 | 117.80 ± 17.34 | 67.4 (± 0.5) | 37 |
| PB/G5/N3 | 22.01 ± 0.63 | 4298.58 ± 1.17 | 22.82 ± 1.61 | 344.91 ± 18.59 | 68.4 (± 0.8) | 45 |
| PB/G5/W40 | 16.21 ± 0.86 | 3698.09 ± 1.71 | 17.53 ± 1.74 | 253.53 ± 16.83 | 64.1 (± 0.4) | 40 |
| PB/G5/W40/N1 | 18.94 ± 0.47 | 4066.76 ± 1.83 | 21.72 ± 1.81 | 359.59 ± 19.51 | 70.6 (± 0.2) | 49 |
| PB/G5/W40/N3 | 24.52 ± 1.01 | 4612.55 ± 1.62 | 29.64 ± 1.43 | 575.21 ± 15.11 | 75.0 (± 0.3) | 62 |
| PB/G5/W40/N5 | 22.42 ± 0.91 | 4387.42 ± 1.46 | 26.75 ± 1.09 | 531.91 ± 17.76 | 72.0 (± 0.5) | 64 |

### 3.4.6. Hardness study

Table 3.4.1 also shows the hardness results of polymer blend and WPC with different percentage of clay loading. From the table, it was observed that hardness value of the polymer blend increased as the compatibilizer was added. This was due to the improvement in interfacial adhesion between various polymers by the compatibilizer. Hardness improved a little bit on addition of clay to the polymer blend. The addition of WF to the polymer blend decreased the hardness value. But it increased significantly when nanoclay was incorporated. The value improved upto an addition of 3 phr nanoclay beyond that the value decreased. The

decrease in mobility of the intercalated polymer chains and increase in interaction between wood flour and polymer blend by the silicate layers played an important role in improving the hardness. At higher clay loading, migration of clay to the interface of wood polymer matrix might be responsible for the decrease in the reinforcement effect of clay.

### 3.4.7. Limiting oxygen index (LOI) results

Limiting oxygen index values of polymer blend and nanoclay loaded WPC is shown in Table 3.4.1. It was observed that LOI value increased after the addition of compatibilizer to the blend. The increase in the value was due to the increase in interfacial adhesion among the polymers by the compatibilizer. The value increased by the addition of clay. LOI value decreased a little bit on incorporation of WF to the blend. Wood flour required less percentage of oxygen for burning due to the presence of cellulose, hemicelluloses, lignin and other low molecular weight components. As a result the LOI value of nanoclay untreated WPC decreased. The value was enhanced again after adding nanoclay to the WPC. Nanoclay produced silicate char on the surface of WPC which increased the flame resistance property of the composite. Similar observation was reported in the literature [18]. The silicate rich surface had better barrier property to heat and oxygen transport due to which ignition of the composite delayed. The compatibilizer also played an important role in this case. The compatibilizer improved the adhesion between wood flour and polymer blend. This adhesion might prevent the flame for propagation.

### 3.4.8. Thermal property study

Table 3.4.2 shows the initial decomposition temperature ($T_i$), maximum pyrolysis temperature ($T_m$), decomposition temperature at different weight loss (%) ($T_D$) and residual weight (RW,%) for the polymer blend and WPC. From the table, it was observed that $T_i$ value of WPC was higher than polymer blend. This was due to presence of WF and the compatibilizer. The compatibilizer increased the interfacial adhesion The $T_i$ value increased on addition of clay to the composites. A delay in the thermal degradation was observed after the addition of clay to the composite. The reinforcing effect of inorganic silicate layers enhanced the thermal stability of the composite. The distribution of silicate layers also played an important role. Better distribution of silicate layers delayed the diffusion of decomposed volatile products throughout the composite and improved the thermal stability

[13]. It was found that 3 phr clay loaded WPC showed higher thermal stability followed by 5 and 1 phr clay loaded WPC. The lower value of thermal stability in 5 phr clay loaded WPC was due to the agglomeration of silicate layers in the composite which permits the diffusion of the volatile product easily.

**Table 3.4.2.** Thermal analysis of polymer blend and wood polymer nanocomposite.

| Sample | $T_i$ | $T_m{}^a$ | $T_m{}^b$ | Temperature of decomposition ($T_D$) in °C at different weight loss (%) | | | | RW% at 600°C |
|---|---|---|---|---|---|---|---|---|
| | | | | 20% | 40% | 60% | 80% | |
| PB | 230 | 251 | 406 | 294 | 388 | 438 | 467 | 6.3 |
| PB/G5/W40 | 235 | 255 | 453 | 299 | 396 | 444 | 472 | 7.4 |
| PB/G5/W40/N1 | 242 | 259 | 470 | 311 | 426 | 459 | 480 | 10.3 |
| PB/G5/W40/N3 | 258 | 276 | 481 | 346 | 447 | 473 | 494 | 14.0 |
| PB/G5/W40/N5 | 246 | 268 | 475 | 327 | 437 | 465 | 486 | 12.2 |

$T_i$ value for initial degradation; $^aT_m$ value for 1st step; $^bT_m$ value for 2nd step.

Both polymer blend and WPC showed two decomposition peaks. The first and second decomposition peaks exhibited by the polymer blend were probably due to the dehydrochlorination of PVC [11] and decomposition of HDPE and PP [12,7]. In WPC, the decomposition peak for first stage of pyrolysis was due to the depolymerization of hemicellulose, glycosidic linkage of cellulose, thermal decomposition of cellulose and dehydrochlorination of PVC while the peaks for second stage of pyrolysis was attributed to the decomposition of HDPE and PP. $T_m$ values for WPC was observed more compared to polymer blend. The values increased further after addition of nanoclay. $T_D$ values of clay treated WPC were more compared to clay untreated WPC.

The percentage of weight losses for samples at different temperatures were also presented in the table. RW values for clay treated WPC were more compared to either polymer blend or WPC. All these datas suggested that the addition of nanoclay enhanced the thermal stability of WPC. This improvement in thermal stability may be due to the presence of silicate layers which provided barrier resistance and thereby delayed the diffusion of decomposed volatile products throughout the composites [29].

### 3.4.9. UV test results

The weight loss of polymer blend, normal WPC and WPC loaded with different percentage of nanoclay (1-5 phr) were represented by Figure 3.4.5. The weight losses of the samples were determined as a function of exposure time at room temperature. It was observed almost linear with exposure time. At early stage of exposure time, the samples absorbs moisture due to which a small increase of weight was found and it was greater than the material loss induced by the degradation in the early stage. The rate of weight loss was found minimum for polymer blend followed by PB/G5/W40/N3, PB/G5/W40/N5 and PB/G5/W40/N1. WPC showed the maximum weight losses. After 60 days of exposure, the maximum weight losses in polymer blend, PB/G5/W40, PB/G5/W40/N1, PB/G5/W40/N3 and PB/G5/W40/N5 were 1.24 % ± 0.11 %, 3.25 % ± 0.15 %, 2.38 % ± 0.18 %, 1.59 % ± 0.16 % and 2.14 % ± 0.17 % respectively.

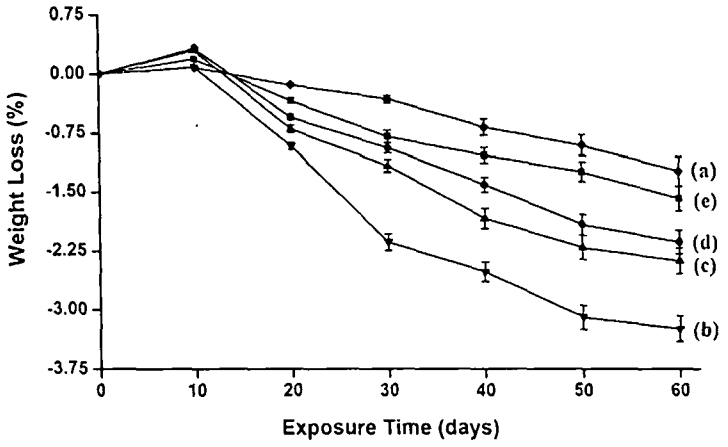


**Figure 3.4.5.** Weight losses vs. exposure time of (a) PB (b) PB/G5/W40 (c) PB/G5/W40/N1 (d) PB/G5/W40/N5 (e) PB/G5/W40/N3.

Figure 3.4.6 shows the carbonyl index values against time. After 60 days of irradiation to UV light, the carbonyl peak intensity of the samples was found to increase (Fig. 3.4.7). This was due to the chain scission of the polymer blend and WPC that leads to decrease in the density of entanglements of polymer chain and decrease in weight of the samples. The polymer blend had lowest carbonyl index value (curve-3.4.6a). Due to higher oxidation of WF, normal wood polymer composite showed highest carbonyl index value (curve-3.4.6b). WPC loaded with 3 phr nanoclay showed lowest carbonyl index values

compared to 1 phr and 5 phr nanoclay loaded WPC. The nanoclay acts as a barrier to UV radiation and stabilizes the WPC by delaying the photo-degradation process. Grigoriadou et al. [43] reported the increased in UV stability of HDPE after incorporating MMT clay.

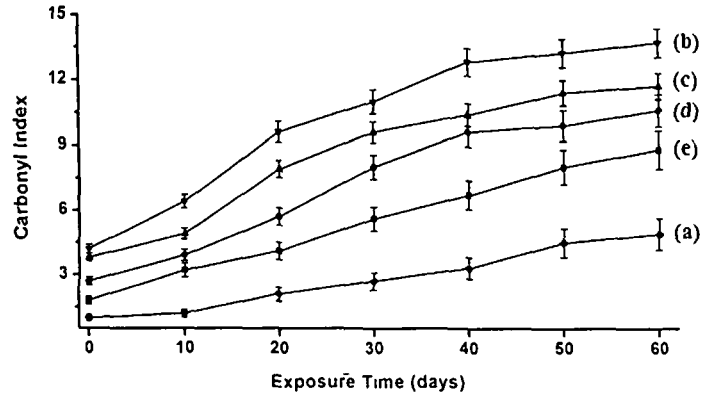


**Figure 3.4.6.** Carbonyl index values of (a) PB (b) PB/G5/W40 (c) PB/G5/W40/N1 (d) PB/G5/W40/N5 (e) PB/G5/W40/N3.

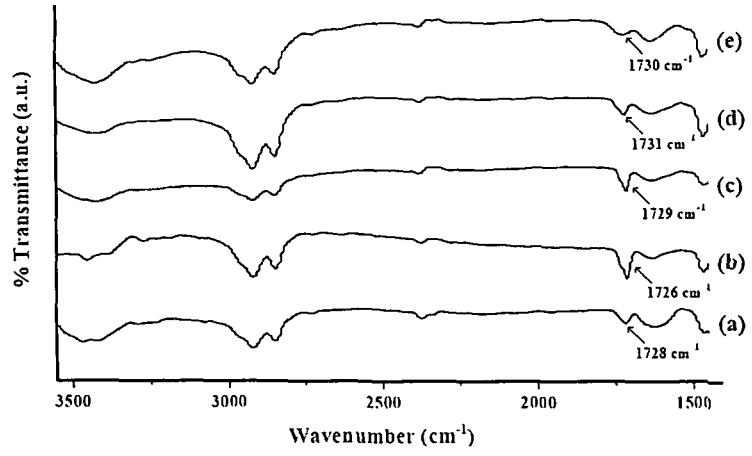


**Figure 3.4.7.** Change in carbonyl peak intensity of (a) PB (b) PB/G5/W40 (c) PB/G5/W40/N1 (d) PB/G5/W40/N5 (e) PB/G5/W40/N3.

Figure 3.4.8 represents the SEM micrographs of the samples after 60 days of UV exposure. In the surface morphologies of the samples showed a drastic change due to exposure to UV radiation. Normal WPC samples were more prone to UV radiation compared to WPC loaded with nanoclay. The change in surface morphology was more irregular in normal WPC compared to nanoclay loaded WPC. WPC containing higher percentage of nanoclay (5 phr)

exhibited lower protection against UV radiation as shown by the decrease in surface smoothness. This might be due to the agglomeration of the silicate layers which provided lower protection against photodegradation.

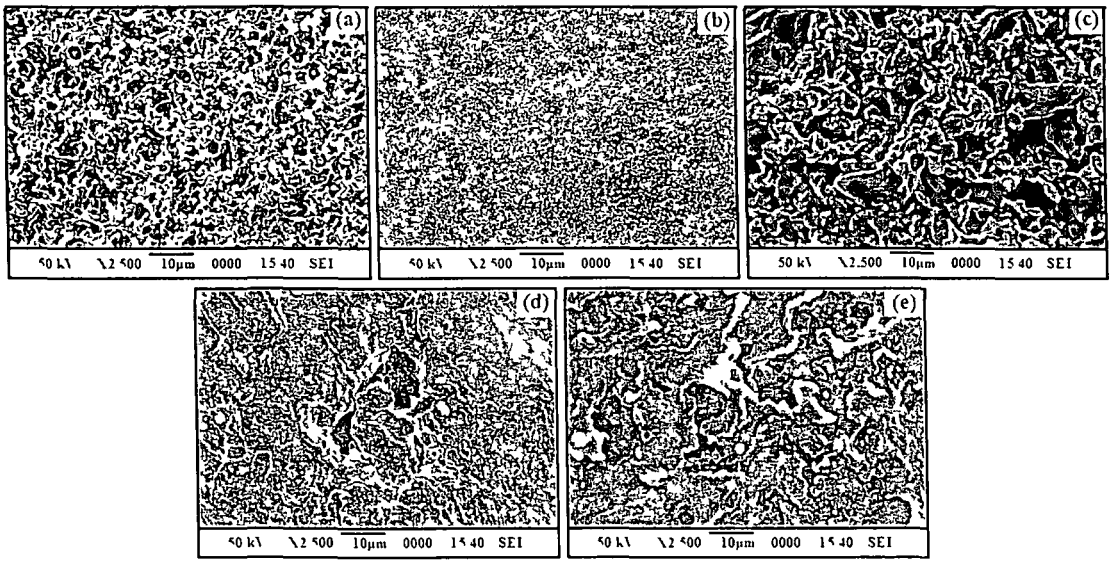


**Figure 3.4.8.** SEM micrographs of UV treated samples after 60 days (a) PB (b) PB/G5/W40 (c) PB/G5/W40/N1 (d) PB/G5/W40/N3 (e) PB/G5/W40/N5.

The changes in the mechanical properties of the composites after the UV treatment are presented in Table 3.4.3. From the table, it was observed that the loss of mechanical properties was more significant in normal WPC compared to the WPC loaded with nanoparticles. WPC was more prone to UV attack and hence it showed maximum loss of mechanical properties. WPC loaded with the nanoparticles offered shielding effect and as a result it showed a less reduction in mechanical properties.

### 3.4.10. Biodegradation study

*3 4 10 1 Decay evaluation and microscopic analysis*

Broth culture technique was employed for the biodegradation of the composite. The wood polymer composites were directly exposed to cellulolytic bacterial strain in broth culture medium. Biodegradation rate and growth of bacteria was distinctly detectable in all the samples after one month of incubation. Figure 3.4.9a shows the bacterial growth of the

**Table 3.4.3.** Flexural and tensile properties of polymer blend and WPC loaded with different percentage of nanoclay after the irradiation to UV light.

| Sample | Flexural Properties | | | | Tensile Properties | | | |
|---|---|---|---|---|---|---|---|---|
| | Before degradation | | After degradation | | Before degradation | | After degradation | |
| | Strength (MPa) | Modulus (MPa) | Strength (MPa) | Modulus (MPa) | Strength (MPa) | Modulus (MPa) | Strength (MPa) | Modulus (MPa) |
| PB | 13.93 ± 1.04 | 769.57 ± 1.03 | 12.31 ± 1.02 | 694.38 ± 1.07 | 6.47 ± 1.61 | 89.26 ± 18.93 | 5.23 ± 1.26 | 43.38 ± 17.49 |
| PB/G5/W40 | 16.21 ± 0.86 | 3698.09 ± 1.71 | 8.61 ± 1.12 | 2776.53 ± 1.06 | 17.53 ± 1.74 | 253.53 ± 16.83 | 8.16 ± 1.52 | 113.42 ± 18.41 |
| PB/G5/W40/N1 | 18.94 ± 0.47 | 4066.76 ± 1.83 | 12.56 ± 0.94 | 3325.19 ± 1.01 | 21.72 ± 1.81 | 359.59 ± 19.51 | 13.75 ± 1.73 | 256.74 ± 17.16 |
| PB/G5/W40/N3 | 24.52 ± 1.01 | 4612.55 ± 1.62 | 20.13 ± 1.07 | 4271.64 ± 1.12 | 29.64 ± 1.43 | 575.21 ± 15.11 | 24.62 ± 1.17 | 498.21 ± 16.35 |
| PB/G5/W40/N5 | 22.42 ± 0.91 | 4387.42 ± 1.46 | 17.36 ± 1.11 | 3729.36 ± 1.09 | 26.75 ± 1.09 | 531.91 ± 17.76 | 20.44 ± 1.31 | 463.63 ± 18.11 |

WPC with respect to time. Presence of wood and clay nanoparticles makes the WPC samples more prone to microbial attack. It was observed that with increasing bacterial exposure time, the growth of the bacterial strains was increased quite steadily, but after three months of incubation the rate of growth decreased. The presence of wood in the composite as carbon source showed higher rate of bacterial growth compared to the polymer blend. This enhancement of bacterial growth might be due to powerful cellulolytic and pectinolytic activity of bacteria [37]. Moreover, lignin present in wood plant stem could be degraded by the *Bacillus sp.* [38]. The decreased rate of microbial growth after three months may be due to the production of toxic metabolites by the microbes. The growth and degradation property of the wood composite by bacteria was also supported by the SEM study (Fig. 3.4.9b-e). It was also observed that with increasing concentration of nanoclay in wood composite the rate of degradation also increased. This may be due to the catalytic role played by nano particles [39]. The mechanical properties of the degraded WPC samples are presented in Table 3.4.4. The decreased in properties might be due to the loss of physical and chemical interaction in the WPC caused by the degradation effect of bacteria.

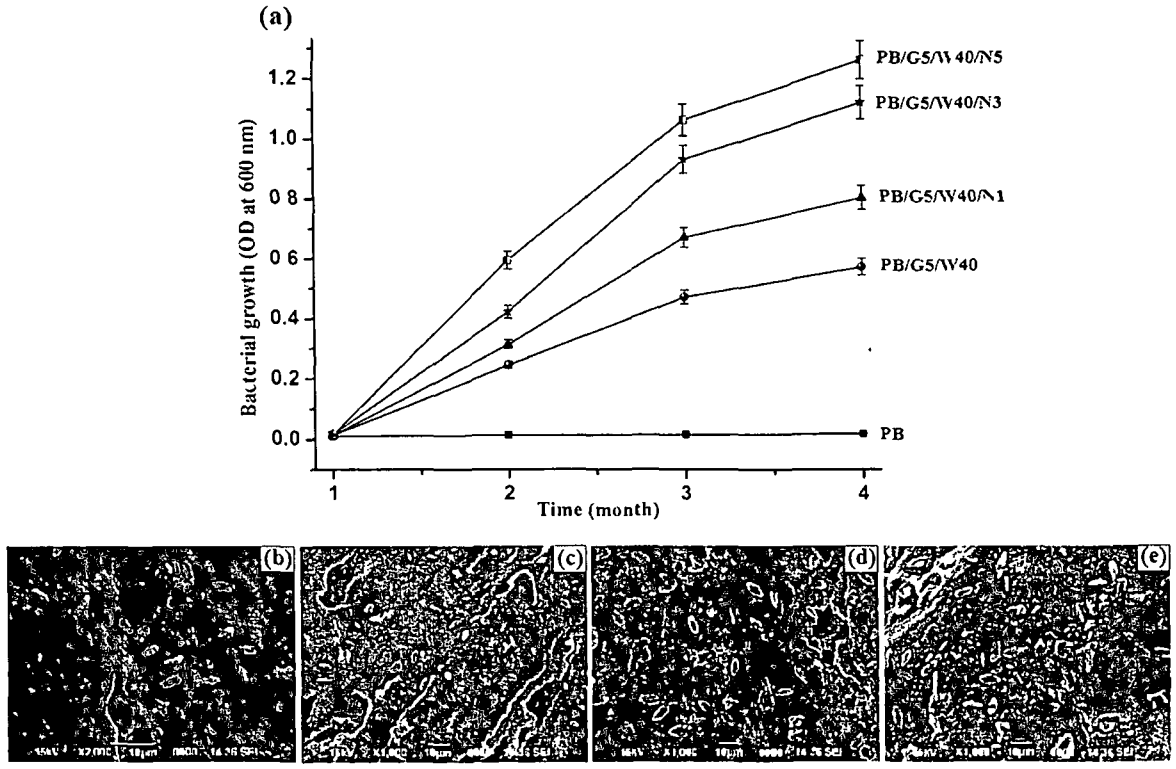


**Figure 3.4.9.** Growth of *Bacillus sp* on (a) Composite samples and SEM micrographs of samples after microbial test (b) PB/G5/W40 (c) PB/G5/W40/N1 (d) PB/G5/W40/N3 (e) PB/G5/W40/N5.

*3.4.10.2. Soil burial test*

The wood composites with different percentage of clay loadings were exposed to natural microbial consortium during in vitro soil experiments for three months. Soil microflora constituted a mixed microbial population (including bacteria, actinomycetes and fungi) which may act synergistically during degradation and reproduce under naturally occurring conditions [44].

**Table 3.4.4.** Flexural, tensile and hardness properties of WPC loaded with different percentage of nanoclay after microbial degradation.

| Sample | Flexural properties | | Tensile properties | | Hardness |
|---|---|---|---|---|---|
| | Strength (MPa) | Modulus (MPa) | Strength (MPa) | Modulus (MPa) | (Shore D) |
| PB | 13.25 ± 1.12 | 743.21 ± 1.24 | 6.03 ± 1.06 | 64.86 ± 16.14 | 63.4 ± 0.2 |
| PB/G5/W40 | 12.05 ± 1.05 | 3412.23 ± 1.07 | 14.97 ± 1.10 | 238.12 ± 14.36 | 51.2 ± 0.7 |
| PB/G5/W40/N1 | 14.76 ± 0.86 | 3587.05 ± 1.04 | 17.58 ± 1.01 | 337.64 ± 18.21 | 59.9 ± 0.3 |
| PB/G5/W40/N3 | 17.74 ± 1.12 | 4253.13 ± 1.05 | 21.65 ± 1.11 | 543.63 ± 16.01 | 61.1 ± 0.5 |
| PB/G5/W40/N5 | 16.97 ± 0.86 | 4187.74 ± 1.09 | 19.63 ± 1.04 | 484.70 ± 14.83 | 60.3 ± 0.9 |

For visualizing the morphological changes and growth of microorganisms due to burial in soil, specimens of wood composite were collected after 90 days and SEM micrographs were taken (Fig. 3.4.10). The SEM micrograph clearly shows the growth of actinomycetes on the surface of wood composite. Extensive growth of bacteria along with penetrated fungal species was also observed. The weight loss and change in mechanical properties of the degraded WPC samples were compared and presented in Table 3.4.5 and 3.5.6. The weights and the mechanical properties of the degraded samples were found to decrease. This might be due to the decrease in physical and chemical interaction of WPC caused by the microorganism present in soil.

**Table 3.4.5.** Weight loss of the wood polymer composite samples after soil burial test.

| Sample | Weight of flexural Specimen (g) | | Weight of tensile Specimen (g) | |
|---|---|---|---|---|
| | Before degradation | After degradation | Before degradation | After degradation |
| PB | 16.39 | 15.89 | 16.56 | 16 02 |
| PB/G5/W40 | 14.27 | 13.22 | 14.95 | 13.73 |
| PB/G5/W40/N1 | 15.31 | 13.13 | 14.64 | 12.26 |
| PB/G5/W40/N3 | 14 79 | 12.05 | 15.43 | 13 57 |
| PB/G5/W40/N5 | 15 14 | 13 05 | 14.75 | 12 92 |

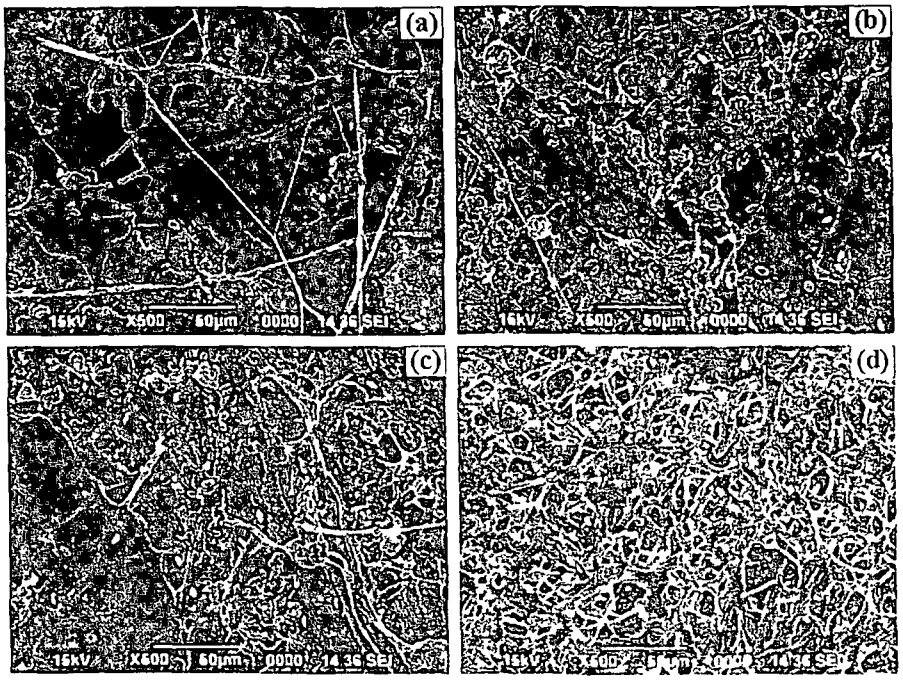


**Figure 3.4.10.** SEM micrographs of samples after soil burial test (a) PB/G5/W40 (b) PB/G5/W40/N1 (c) PB/G5/W40/N3 (d) PB/G5/W40/N5

**Table 3.4.6.** Flexural, tensile and hardness properties of WPC loaded with different percentage of nanoclay after soil burial test.

| Sample | Flexural properties | | Tensile properties | | Hardness |
|---|---|---|---|---|---|
| | Strength (MPa) | Modulus (MPa) | Strength (MPa) | Modulus (MPa) | (Shore D) |
| PB | 13.75 ± 1.04 | 752.52 ± 1.03 | 6.18 ± 1.12 | 72.64 ± 16.07 | 63.1 ± 0.3 |
| PB/G5/W40 | 14.07 ± 1.11 | 3584.41 ± 1.03 | 16.07 ± 1.06 | 238.12 ± 14.36 | 55.6 ± 0.5 |
| PB/G5/W40/N1 | 15.12 ± 1.08 | 3712.92 ± 1.06 | 17.58 ± 1.01 | 337.74 ± 17.93 | 64.1 ± 0.7 |
| PB/G5/W40/N3 | 19.13 ± 1.05 | 4412.81 ± 1.11 | 24.92 ± 1.09 | 551.14 ± 17.13 | 68.4 ± 0.3 |
| PB/G5/W40/N5 | 18.86 ± 1.04 | 4245.34 ± 1.03 | 21.24 ± 1.13 | 501.52 ± 15.17 | 65.3 ± 0.5 |

### 3.4.11. Chemical resistance test result

Chemical resistance test results of WPC and WPC loaded with different percentage of nanoclay is presented in Figure 3.4.11. From the figure, it has been observed that Acetone, $H_2O_2$ and NaOH have a very negligible effect in the weight change of the samples. On the other hand, HCl solution was most effective on all the composite samples. The observed increase in weight after submerging the samples in acetone and NaOH solution might be due to swelling of the composite and absorption of chemical by the voids of the wood flour. Even after drying the samples, the chemical still entrapped by the voids and hence increased the weight of the samples. The maximum decreased in weight percent of the samples after submerging in HCl solution might be due to the degradation of wood fiber by the acid. It has been observed that 3 phr of nanoclay loading WPC shows maximum chemical resistance. This might be due to the proper dispersion of silicate layers of nanoclay that occupies the voids of wood flour uniformally. At 5 phr of nanoclay loaded WPC, due to agglomeration of nanoclay, the chemical resistance property becomes low. So, HCl solution is the most effective chemical for the composite samples, while in case of composite, 3 phr clay based WPC has maximum chemical resistance property. Tajvidi et al. [45] studied the chemical resistance of polypropylene/wood composite and reported the similar findings.

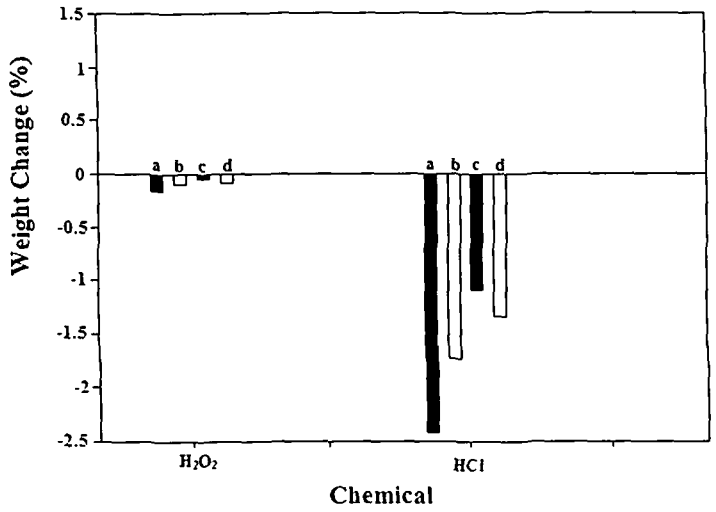


**Figure 3.4.11.** Chemical resistance test for (a) PB/G5/W40 (b) PB/G5/W40/N1 (c) PB/G5/W40/N3 (d) PB/G5/W40/N5.

### 3.4.12. Water absorption and water vapour exclusion study

The water absorption and water vapour uptake results of polymer blend, PE-*co*-GMA treated polymer blend and WPC loaded with different phr clay were presented in Figure 3.4.12. The water uptake capacity of polymer blend was found less. The value decreased after adding PE-*co*-GMA compatibilizer to the polymer blend. PE-*co*-GMA enhanced the interfacial adhesion among polymers and thus a decrease in water vapour absorption was observed. The absorption of water vapour decreased further on addition of nanoclay. The silicate layers of clay provide resistance for transport of water vapour. The incorporation of wood flour in the composite increased the water absorption. This was due to the hydrophilic nature of wood. Water uptake capacity (%) again decreased after addition of nanoclay [46]. The value decreased upto 3 phr clay after that it increased. The exfoliated nature of silicate layers in 3 phr nanoclay loaded WPC provided longer tortuous path for the passage of water. The silicate layers in WPC containing 5 phr clay became agglomerated and hence decreased the tortuous path for diffusion of water. Besides this, the void space in wood was occupied by clay and polymer. As a result, clay treated WPC absorbed less water compared to clay untreated WPC.

The trend of water vapour absorption of samples in the case of 65% relative humidity and 30°C was similar to the samples studied for water absorption.

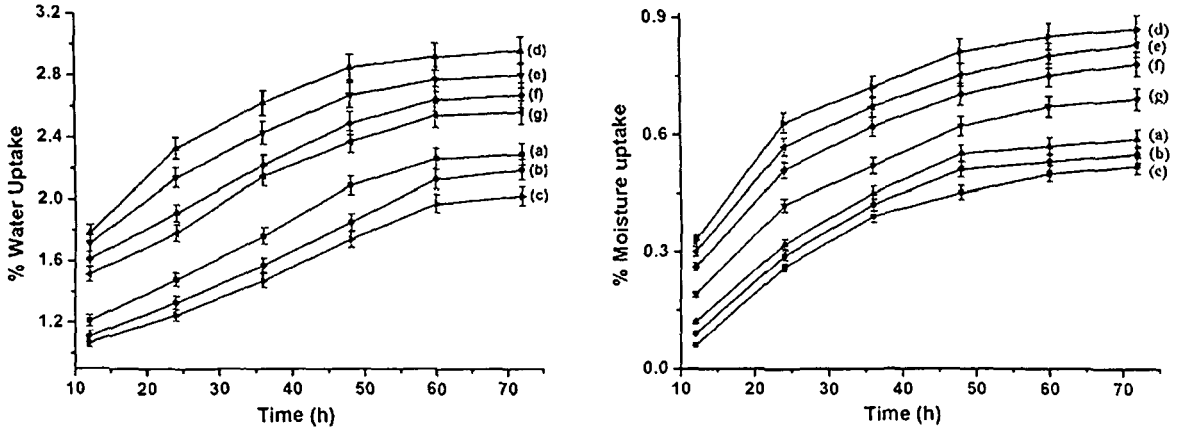


**Figure 3.4.12.** Percent water and water vapour absorption of (a) PB (b) PB/G5 (c) PB/G5/N3 (d) PB/G5/W40 (e) PB/G5/W40/N1 (f) PB/G5/W40/N5 (g) PB/G5/W40/N3.

## REFERENCE

1. Selke, S.E. & Wichman, I. Wood fiber/polyolefin composites, *Composite Part A* **35**(3), 321-326, 2004.

2. Faruk, O. & Matuana, L.M. Nanoclay reinforced HDPE as a matrix for wood-plastic composites, *Compos. Sci. Technol.* **68**(9), 2073-2077, 2008.

3. Zhao, Y., et al. Properties of poly(vinyl chloride)/wood flour/ montmorillonite composites: Effects of coupling agents and layered silicate, *Polym. Degrad. Stab.* **91**(12), 2874-2883, 2006.

4. Awal, A., et al. Thermal properties and spectral characterization of wood pulp reinforced bio-composite fibers, *J. Them. Anal. Calorim.* **99**(2), 695–701, 2010.

5. Lee, S.Y., et al. Thermal, mechanical and morphological properties of polypropylene/ clay/wood flour nanocomposites, *eXPRESS Polym. Lett.* **2**(2), 78-87, 2008.

6. Pracela, M., et al. Recycling of PET and polyolefin based packaging materials by reactive blending, *Polym. Plast. Technol. Eng.* **43**(6), 1711-1722, 2004.

7. Bouza, R., et al. Design of new polypropylene–wood flour composites: Processing and physical characterization, *Polym. Compos.* **30**(7), 880-886, 2009.

8. Lee, H. & Kim, D.S. Preparation and physical properties of wood/polypropylene/clay nanocomposites, *J. Appl. Polym. Sci.* **111**(6), 2769-2776, 2009.

9. Devi, R.R., et al. Studies on dimensional stability and thermal properties of rubber wood chemically modified with styrene and glycidyl methacrylate, *J. Appl. Polym. Sci.* **93**(4), 1938-1945, 2004.

10. Fung, K.L., et al. Interface modification on the properties of sisal fiber- reinforced polypropylene composites, *J. Appl. Polym. Sci.* **85**(1), 169-176, 2002.

11. Meng, Y.Z. & Tjong, S.C. Preparation and properties of injection-moulded blends of poly(vinyl chloride) and liquid crystal copolyester, *Polymer* **40**(10), 2711-2718, 1999.

12. Yemele, M.C.N., et al. Effect of bark fiber content and size on the mechanical properties of bark/HDPE composites, *Composites Part A* **41**(1), 131-137, 2010.

13. Deka, H. & Karak, N. Vegetable oil-based hyperbranched thermosetting polyurethane/ clay nanocomposites, *Nanoscale Res. Lett.* **4**(7), 758-765, 2009.

14. Stevens, M.D. Polymer Chemistry, An Introduction. Oxford: Oxford University Press, 1990.

15. Bledzki, A.K., et al. Physical, chemical and surface properties of wheat husk, rye husk and soft wood and their polypropylene composites, *Composites Part A* **41**(4), 480-488, 2010.

16. Canetti, M., et al. Thermal degradation behaviour of isotactic polypropylene blended with lignin, *Polym. Degrad. Stab.* **91**(3), 494-498, 2006.

17. Tajvidi, M. & Takemura, A. Effect of fiber content and type, compatibilizer, and heating rate on thermogravimetric properties of natural fiber high density polyethylene composites, *Polym. Compos.* **30**(9), 1226-1233, 2009.

18. Camino, G., et al. Thermal and combustion behaviour of layered silicate–epoxy nanocomposite, *Polym. Degrad. Stab.* **90**(2), 354-62, 2005.

19. Rana, H.T., et al. Measurement of moisture diffusivity through layered-silicate nanocomposites, *AIChE J.* **51**(12), 3249-3256, 2005.

20. Shah, A.P., et al. Moisture diffusion through vinyl ester nanocomposites made with montmorillonite clay, *Polym. Eng. Sci.* **42**(9), 1852-1863, 2002.

21. Alexandre, B., et al. Nanocomposite-based polyamide 12/montmorillonite: relationships between structures and transport properties, Desalination **199**(1-3), 164-166, 2006.

22. Lei, Y., et al. Influence of nanoclay on properties of HDPE/wood composites, *J. Appl. Polym. Sci.* **106**(6), 3958-3966, 2007.

23. Sun, Y.J., et al. *In situ* compatibilization of polypropylene and poly(butylene terephthalate) polymer blends by one-step reactive extrusion, *Polymer* **37**(18), 4119-4127, 1996.

24. Sailaja, R.R.N. Mechanical and thermal properties of bleached kraft pulp–LDPE composites: Effect of epoxy functionalized compatibilizer, *Compos. Sci. Technol.* **66**(13), 2039-2048, 2006.

25. Dikobe, D.G. & Luyt, A.S. Effect of poly(ethylene-*co*-glycidyl methacrylate) compatibilizer content on the morphology and physical properties of ethylene vinyl acetate–wood fiber composites, *J. Appl. Polym. Sci.* **104**(5), 3206-3213, 2007.

26. Awal, A., et al. Development and morphological characterization of wood pulp reinforced biocomposite fibers, *J. Mater. Sci.* **44**(11), 2876–2881, 2009.

27. Liu, H., et al. Compatibilizing and toughening bamboo flour-filled HDPE composites: Mechanical properties and morphologies, *Composites Part A* **39**(12), 1891-1900, 2008.

28. Hetzer, M., et al. Influence of compatibilizer blends on mechanical and thermal properties of polymer-clay nanocomposites, *Mater. Sci. Technol.* **27**(1), 53-59, 2011.

29. Qin, H., et al. Thermal stability and flammability of polypropylene/montmorillonite composites, *Polym. Degrad. Stab.* **85**(2), 807-813, 2004.

30. Zhao, Q., et al. Flame retardancy of rice husk-filled high-density polyethylene ecocomposites, *Compos. Sci. Technol.* **69**(15-16), 2675-2681, 2009.

31. Avella, M., et al. Steam-exploded wheat straw fibers as reinforcing material for polypropylene-based composites. Characterization and properties, *Macromol. Mater. Eng.* **233**(1), 149-166, 1995.

32. Han, G., et al. Bamboo-fiber filled high density polyethylene composites: Effect of coupling treatment and nanoclay, *J. Polym. Environ.* **16**(2), 123-30, 2008.

33. Devi, R.R. & Maji, T.K. Chemical modification of rubber wood with styrene and glycidyl methacrylate, *Polym. Compos.* **29**(11), 1258-1262, 2008.

34. Chartoff RP. In: Seyler RJ editor. Assignment of glass transition, ASTM, STP, Philadelphia, PA 1994. 1249, p. 17-31.

35. Idicula, M., et al. Dynamic mechanical analysis of randomly oriented intimately mixed short banana/sisal hybrid fiber reinforced polyester composites, *Compos. Sci. Technol.* **65**(7-8), 1077-1087, 2005.

36. Jiang, H. & Kamdem, D.P. Thermal and dynamic mechanical behavior of poly(vinyl chloride)/wood flour composites, *J. Appl. Polym. Sci.* **107**(2), 951-957, 2008.

37. Clausen, C.A. Bacterial associations with decaying wood: A review, *Int. Biodeter. Biodegr.* **37**(1-2), 101-107, 1996.

38. El-Hanafy, A.A., et al. Molecular characterization of two native egyptian ligninolytic bacterial strains, *J. Appl. Sci. Res.* **4**, 1291–1296, 2008.

39. Karak, N. Polymer (Epoxy) clay nanocomposites, *J. Polym. Mater.* **23**, 1-20, 2006.

40. Lei, Y., et al. Influence of nanoclay on properties of HDPE/wood composites, *J. Appl. Polym. Sci.* **106**(6), 3958-3966, 2007 .

41. Biswal, M., et al. Influence of organically modified nanoclay on the performance of pineapple leaf fiber-reinforced polypropylene nanocomposites, *J. Appl. Polym. Sci.* **114**(6), 4091-4103, 2009.

42. Salemane, M.G. & Luyt, A.S. Thermal and mechanical properties of polypropylene–wood powder composites, *J. Appl. Polym. Sci.* **100**(5), 4173-4180, 2006.

43. Grigoriadou, I., et al. Effect of different nanoparticles on HDPE UV stability, *Polym. Degrad. Stab.* **96**(1), 151-163, 2011.

44. Alvarez, V.A., et al. Degradation of sisal fiber/Mater Bi-Y biocomposites buried in soil, *Polym. Degrad. Stab.* **91**(12), 3156-3162, 2006.

45. Tajvidi, M., et al. Effect of chemical reagents on the mechanical properties of natural fiber polypropylene composites, *Polym. Compos.* **27**(5), 563–569, 2006.

46. Sheshmani, S., et al. Physical properties of polyethylene–wood fiber–clay nanocomposites, *J. Appl. Polym. Sci.* **118**(6), 3255-3259, 2010.

# CHAPTER IV

# RESULTS & DISCUSSION

# CHAPTER IV

# RESULTS & DISCUSSION

## *Section A*: Effect of silica nanopowder on the properties of wood flour/ polymer composite.

In the polymer composites, different types of fillers are used for improving the thermal, mechanical as well as other properties. Among them, nanopowder is widely used as filler. The surface characteristics of nanopowders play a key role in their fundamental properties from phase transformation to reactivity. A dramatic increase in the interfacial area between fillers and polymer can significantly improve the properties of the polymer [1].

In polymer composites, $SiO_2$ nanopowder is one of the widely used fillers [2]. $SiO_2$ can enhance the mechanical as well as thermal properties of the composite. Polymer-$SiO_2$ composites are of technological important due to their potential applications in electrochromic windows, fuel cells, chemical separation, electrochemical sensing and water treatment. $SiO_2$ nanoparticles increase the tensile and impact strength of epoxy nanocomposite [3].

In this communication, we report the modification of $SiO_2$ by treatment with cetyl trimethyl ammonium bromide (CTAB) and study the effect of modified $SiO_2$ on various properties of composites based on wood, PE-*co*-GMA and polymer mixture of HDPE/LDPE/PP/PVC.

### 4.1. RESULTS AND DISCUSSION

#### 4.1.1. X-ray diffraction study

Figure 4.1.1 shows the plots of intensity versus scattering angle, 2θ, for neat polymer blend, the $SiO_2$ nanopowder and 1, 3 and 5 phr $SiO_2$-loaded WPCs. The curve representing neat polymer blends (Fig. 1a) showed some sharp diffraction peaks and diffusion peaks which revealed the presence of crystalline and amorphous region respectively. The most prominent X-ray scattering peaks appeared at 2θ = 14.12 (200) (PP), 17.06 (040) (PP,PVC), 18.64 (211) (PP), 21.62 (110) (PE) and 24.02 (200) (PE,PP,PVC) were for the crystalline portion of different polymers in the polymer blend [4-7].

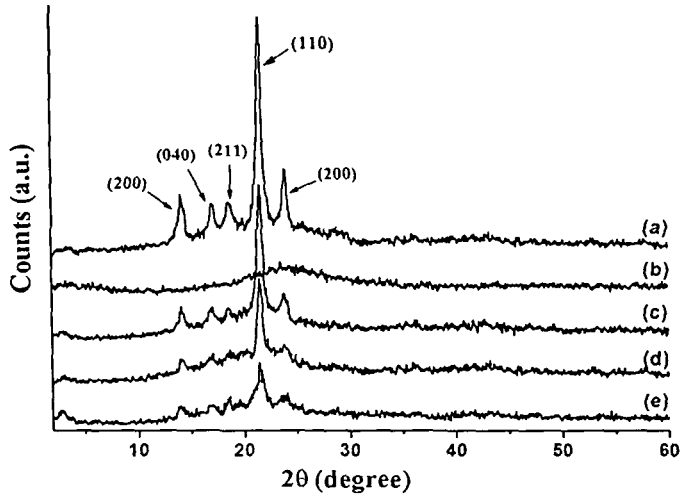


**Figure 4.1.1.** X-ray diffraction of (a) PB (b) modified nano $SiO_2$ (c) PB/G5/W40/S1 (d) PB/G5/W40/S5 (e) PB/G5/W40/S3.

Curve-4.1.1b shows a broad diffraction peak at $2\theta = 23.5$ for the amorphous $SiO_2$ nanoparticles. In WPC loaded with different percentage of $SiO_2$ (curves-4.1.1c-e), a decrease in intensity of the crystalline peak at position 21.62 (110) was observed. The intensity of other crystalline peaks was also found to decrease. The decrease in intensity of the crystalline peaks was due to the enhancement of the amorphous portion in the composites caused by the addition of amorphous $SiO_2$ nanoparticles and wood flour. Mina et al. [4] prepared isotactic polypropylene/$TiO_2$ composite and found that the intensity of the crystalline peaks of PP decreased with increasing the amount of $TiO_2$. This indicated that $SiO_2$ particles were infused into the WPC.

### 4.1.2. Transmission electron microscopy study

Figure 4.1.2 shows the TEM micrographs of WPC loaded with 1, 3 and 5 phr of $SiO_2$ nanopowder. A well dispersion of nanoparticles was observed in WPC loaded with 1 and 3 phr $SiO_2$ nanoparticles. The $SiO_2$ nanoparticles were found to become agglomerated in WPC containing 5 phr $SiO_2$. Higher amount of nanoparticles tend to increase the surface interaction among themselves and thereby enhanced the tendency for agglomeration. Vladimirov et al. [8] studied the morphological properties of isotactic polypropylene/fumed silica nanocomposites and observed that agglomeration of $SiO_2$ nanoparticles occurred at higher $SiO_2$ content.

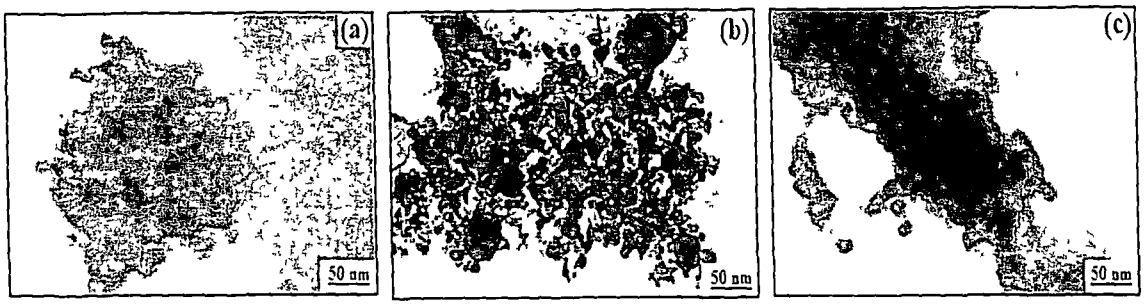


**Figure 4.1.2.** TEM micrographs of (a) PB/G5/W40/S1 (b) PB/G5/W40/S3 (c) PB/G5/W40/S5.

### 4.1.3. Fourier transform infrared spectroscopy study

FTIR spectra of CTAB, unmodified $SiO_2$ and CTAB modified $SiO_2$ are shown in Figure 4.1.3. In the spectrum of CTAB, the absorption peaks at 2918, 2848 and 1475 $cm^{-1}$ were assigned to asymmetric, symmetric stretching and scissor modes of $-CH_2$ in the methylene chains respectively [9]. The spectrum of unmodified $SiO_2$ shows some absorption peaks at 3424 and 1632 $cm^{-1}$ for –OH stretching and hydroxyl group adsorbed on particle surface respectively. The other peaks appeared in the range 1087-465 $cm^{-1}$ were due to Si-O-Si group in the $SiO_2$ [10]. On the spectrum of CTAB modified $SiO_2$, the peaks around 3424,

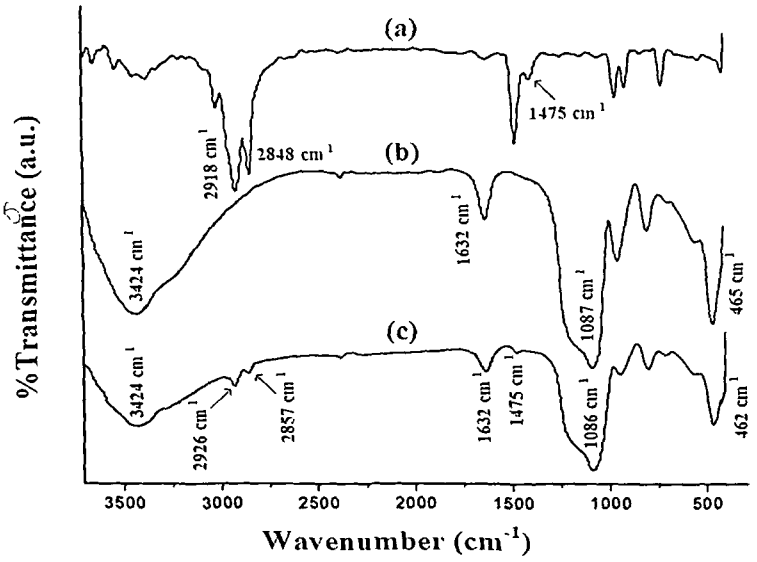


**Figure 4.1.3.** FTIR spectra of (a) CTAB (b) unmodified $SiO_2$ (c) CTAB modified $SiO_2$.

2926, 2857, 1632, 1475 $cm^{-1}$ and 1086-462 $cm^{-1}$ were found. The intensity of –OH stretching in the modified $SiO_2$ was found to decrease, indicating an interaction of the hydroxyl group absorbed on $SiO_2$ surface with CTAB. Qu et al. [11] modified $TiO_2$ with CTAB and reported that the interaction of $TiO_2$ occurred with $Br^-$ of CTAB through hydrogen bond formation or electrostatic attractions. The other notable peaks appeared in the CTAB modified $SiO_2$ spectrum were the characteristic peaks for CTAB and $SiO_2$. These results indicated the incorporation of CTAB on the surface of $SiO_2$ particles.

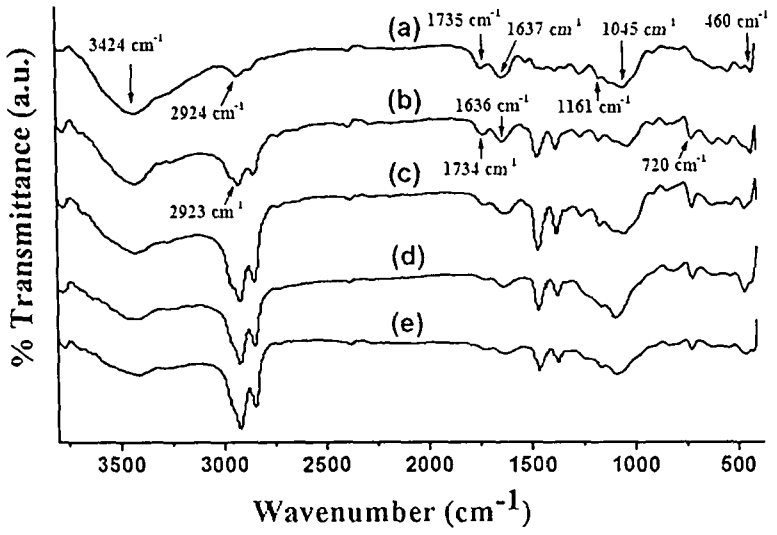


**Figure 4.1.4.** FTIR spectra of (a) Wood (b) PB/G5/W40 (c) PB/G5/W40/S1 (d) PB/G5/W40/S5 (d) PB/G5/W40/S3.

Figure 4.1.4 represents the spectra of wood, PB/G5/W40 and $SiO_2$ loaded WPC. In the spectrum of wood (curve-4.1.4a), the presence of bands corresponding to 3424, 2924, 1735, 1637, 1161, 1045 $cm^{-1}$ and 1000–650 $cm^{-1}$ were attributed to the –OH stretching, -CH stretching, C=O stretching, -OH bending, C-O stretching and C–H bending (out of plane) vibration. PB/G5/W40 (curve-4.1.4b) exhibited peaks at 2923 $cm^{-1}$ (-CH stretching), 1734 $cm^{-1}$ (C=O stretching), 1636 $cm^{-1}$ (-OH bending) and 720 $cm^{-1}$ (-$CH_2$ stretching). Curves-4.1.4c-e represents the FTIR spectra of $SiO_2$ loaded WPC. It was observed that the intensity of hydroxyl as well as the C=O peaks decreased with the increase in the loading of $SiO_2$. The decrease in peak intensity might be due to the increase in interaction of hydroxyl and carbonyl groups of wood fibre with the hydroxyl groups present in $SiO_2$. Motaung and Luyt [12] prepared LDPE/wax/$SiO_2$ nanocomposite and reported that the intensity of carbonyl group of wax decreased due to the formation of hydrogen bonds with the hydroxyl groups on

the silica surface. In the $SiO_2$ loaded composite, the absorption peak at 3424 $cm^{-1}$ (for –OH stretching) was also found to shift little towards lower wave number suggesting the formation of hydrogen bond between wood surface and polymer matrix. Moreover, the intensity of peak in the composites at 2926 $cm^{-1}$ corresponding to –CH stretching increased. The other characteristic peaks for $SiO_2$ appeared in the composites. These results suggested the formation of strong interaction between $SiO_2$, polymer, PE-*co*-GMA and wood.

### 4.1.4. Scanning electron microscopy study

Figure 4.1.5 illustrates the SEM micrographs of polymer blend, WPC and WPC loaded with different percentage of $SiO_2$. The fractured surface of untreated polymer sample is shown in Figure 4.1.5a. The figure shows the immiscibility among different polymers. The immiscibility appeared due to the poor compatibility among the polymers which could be decreased by addition of compatibilizer [13]. Compatibility among the polymer blend was improved by adding wood flour and compatibilizer (Fig. 4.1.5b) to the composite.

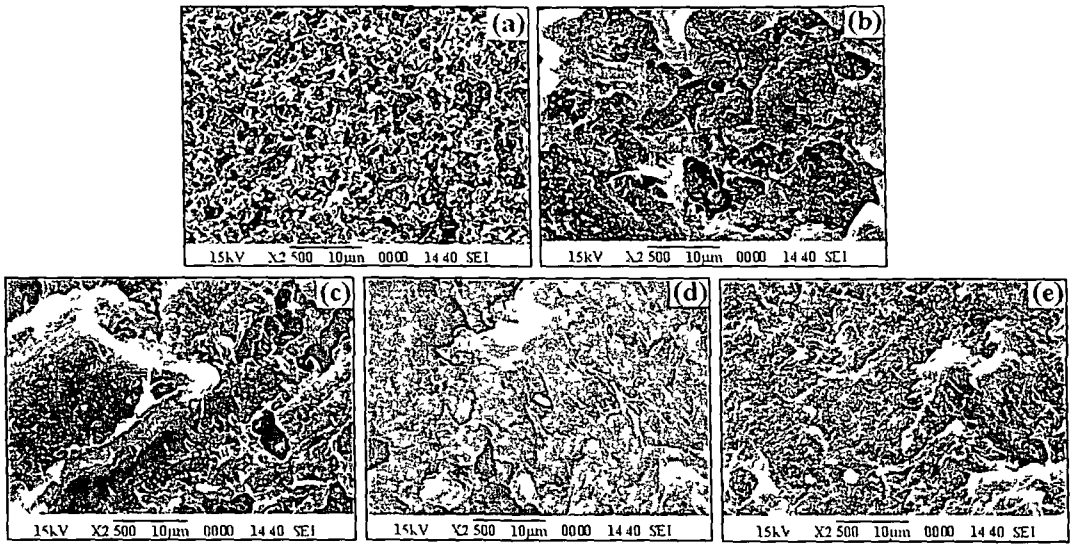


**Figure 4.1.5.** SEM micrographs of (a) PB (b) PB/G5/W40 (c) PB/G5/W40/S1 (d) PB/G5/W40/S5 (e) PB/G5/W40/S3.

Figures 4.1.5c-e show the SEM micrographs of 1, 5 and 3 phr $SiO_2$ loaded WPC. The smoothness of the composites increased upto addition of 3 phr $SiO_2$ into WPC. Beyond that the agglomeration of $SiO_2$ particles occurred and hence the smoothness of the fractured surface decreased. Generally silica particles tend to agglomerate due to formation of

hydrogen bond between the surface hydroxyl groups. Modification of the surface of silica decreased the chance for agglomeration. The agglomeration of silica particles decreased due to addition of PP-*g*-MA as compatibilizer to the PP/$SiO_2$ composites [8]. The less roughness might be attributed to the increase in interaction of the modified silica with the polymer and wood.

### 4.1.5. Mechanical properties study

The flexural and tensile properties of polymer blend and WPC loaded with different percentage of $SiO_2$ loading are shown in the Table 4.1.1. The datas presented in the table are the average of three readings. The addition of PE-*co*-GMA increased the flexural as well as tensile properties of the polymer blend. PE-*co*-GMA enhanced interfacial adhesion among different polymers and hence both flexural and tensile properties improved. The properties were further improved by adding wood flour (WF) to the polymer blend. Natural fillers are generally stiffer than polymer matrix and hence they will increase the properties of WPC [14]. WF acted as load carrier. Therefore, it would reinforce the polymer blend and enhance the flexural and tensile properties. PE-*co*-GMA improved the interfacial adhesion between hydrophilic WF and hydrophobic polymer blend through its glycidyl group and hydrocarbon backbone respectively. The incorporation of $SiO_2$ particles to the WPC further enhanced the flexural and tensile properties. Flexural and tensile properties of the composites increased upto addition of 3 phr $SiO_2$. The flexural and tensile properties decreased at higher loading of $SiO_2$ (5 phr). The interaction between $SiO_2$, polymer, PE-*co*-GMA and wood would restrict the movement of the polymer chains and as a result the flexural and tensile properties would be improved. At lower percentage of $SiO_2$, the nanoparticles were well dispersed and thereby increased the surface area for interaction. Hence improvements in properties were observed. The agglomeration of $SiO_2$ nanoparticles was responsible for lowering in tensile and flexural properties at higher $SiO_2$ loading. Lee et al. [15] prepared polypropylene/polyolefin elastomer blends by the incorporation of nanosilica and found a significant improvement in mechanical properties.

### 4.1.6. Hardness study

Table 4.1.1 shows the hardness results of polymer blend, PE-*co*-GMA treated polymer blend and WPC with different percentage of $SiO_2$ loading. From the table, it was

observed that after the addition of compatibilizer to the polymer blend, hardness value of the blend increased. The increased in value was due to the strong interfacial adhesion between the polymers by the compatibilizer. The incorporation of WF to the polymer blend did not improve the hardness. The hardness values increased to a large extent after addition of $SiO_2$. The value was improved upto addition of 3 phr of $SiO_2$ beyond that it decreased. The increase in hardness values was due to the improvement in interaction between $SiO_2$, polymer matrix and wood. Jinshu et al. [16] has prepared wood/urea formaldehyde composite using nano-$SiO_2$ and found that nano-$SiO_2$ treated composite had higher value of hardness compared to untreated composite.

**Table 4.1.1.** Flexural, tensile and hardness properties of polymer blend and WPC loaded with different percentage of $SiO_2$.

| Sample | Flexural properties | | Tensile properties | | Hardness |
|---|---|---|---|---|---|
| | Strength (MPa) | Modulus (MPa) | Strength (MPa) | Modulus (MPa) | (Shore D) |
| PB | 14.53 ± 1.02 | 771.28 ± 1.05 | 6.51 ± 1.42 | 91.44 ± 19.63 | 66.0 ± 0.4 |
| PB/G5 | 16.42 ± 0.97 | 1104.91 ± 1.12 | 10.72 ± 1.43 | 119.93 ± 18.45 | 68.5 ± 0.3 |
| PB/G5/W40 | 19.27 ± 0.95 | 3915.94 ± 1.12 | 20.28 ± 1.47 | 273.31 ± 16.86 | 67.0 ± 0.6 |
| PB/G5/W40/S1 | 21.56 ± 1.32 | 4337.12 ± 1.32 | 24.74 ± 1.14 | 375.19 ± 17.82 | 71.0 ± 0.5 |
| PB/G5/W40/S3 | 26.46 ± 0.94 | 4812.48 ± 0.86 | 33.74 ± 1.61 | 597.58 ± 19.49 | 78.0 ± 0.3 |
| PB/G5/W40/S5 | 24.52 ± 1.23 | 4616.52 ± 1.09 | 29.56 ± 1.05 | 556.13 ± 21.87 | 75.0 ± 0.4 |

### 4.1.7. Thermal properties analysis

Figure 4.1.6 represents the thermograms for the polymer blend, WPC samples loaded with or without $SiO_2$. Table 4.1.2 shows the initial decomposition temperature ($T_i$), maximum pyrolysis temperature ($T_m$), decomposition temperature at different weight loss (%) ($T_D$) and residual weight (RW,%) for WPC and $SiO_2$ treated WPC. Polymer blend exhibited lowest $T_i$ value. $T_i$ value increased after the addition of WF to the composites. The higher value of $T_i$ was attributed to the presence of WF which delayed the degradation of the polymer matrix. Wood contains cellulose, hemicellulose, lignin, pectin and wax. Besides this, it contains elements mainly carbon, oxygen and small amount of silicon. The lignin

present in the blend could produce a high char. The char was carbon based residue which undergoes slow oxidative degradation. This could form a protective layer and reduce the diffusion of oxygen towards wood polymer composite. The presence of compatibilizer also played a significant role as it improved the adhesion of WF to the polymer matrix. Awal et al. [17] reported that the thermal degradation of the polypropylene composite delayed due to incorporation of wood pulp and maleated polypropylene compatibilizer to the composite.

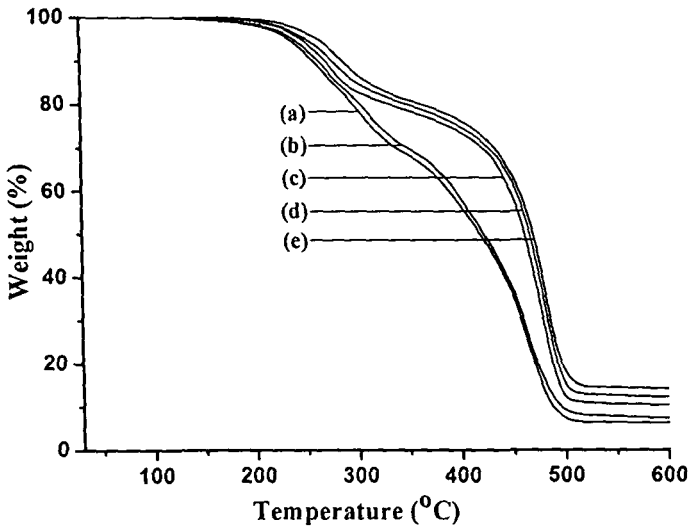


**Figure 4.1.6.** Themogravimetric curves for (a) PB (b) PB/G5/W40 (c) PB/G5/W40/S1 (d) PB/G5/W40/S5 (e) PB/G5/W40/S3.

$T_m$ values for $SiO_2$ treated composites was found more compared to silica untreated composite and polymer blend alone. $T_m$ values for the first stage in polymer blend, WPC and $SiO_2$ treated WPC were due to the decomposition of cellulose [18] and dehydrochlorination of PVC [19,20]. The second stage decomposition peak was due to decomposition of HDPE and PP [21]. $T_m$ value shifted towards higher temperature in both the stages of decomposition when $SiO_2$ was added. The shifting was more for the composites treated with 5 phr $SiO_2$. $T_D$ values were also found to increase with the increase in the percentage of $SiO_2$ upto 3 phr, beyond that it decreased. The well dispersed $SiO_2$ nanoparticles enhanced the interaction and thereby delayed the decomposition of degradable volatile components. At higher $SiO_2$ loading, the agglomeration of $SiO_2$ nanoparticles decreased the interaction and hence decomposition started early. RW value also followed an increasing trend. On the basis of the above observation, it can be concluded that thermal stability of WPC improved due to

addition of $SiO_2$. The increase in thermal stability might be due to the enhancement in interaction between polymer matrix, wood flour and $SiO_2$. Katsikis et al. [22] prepared PMMA/silica nanocomposite and found an improvement in thermal stability of the composite.

**Table 4.1.2.** Thermal analysis and limiting oxygen index (LOI) values of polymer blend and wood polymer nanocomposite.

| Sample | $T_i$ | $^aT_m$ | $^bT_m$ | Temperature of decomposition ($T_D$) in °C at different weight loss (%) | | | | RW% at 600°C | LOI (%) |
|---|---|---|---|---|---|---|---|---|---|
| | | | | 20% | 40% | 60% | 80% | | |
| PB | 232 | 252 | 407 | 295 | 389 | 442 | 470 | 6.2 | 23 ±1.0 |
| PB/G5/W40 | 238 | 257 | 455 | 302 | 395 | 445 | 473 | 7.3 | 46 ±1.0 |
| PB/G5/W40/S1 | 244 | 262 | 475 | 328 | 447 | 470 | 487 | 10.3 | 54 ±3.0 |
| PB/G5/W40/S3 | 260 | 280 | 483 | 360 | 456 | 478 | 496 | 14.3 | 62 ±1.0 |
| PB/G5/W40/S5 | 249 | 270 | 478 | 345 | 453 | 475 | 492 | 12.1 | 68 ±2.0 |

$T_i$ value for initial degradation; $^aT_m$ value for 1st step; $^bT_m$ value for 2nd step.

### 4.1.8. Limiting oxygen index (LOI) study

The LOI values of polymer blend and different percentage of $SiO_2$ loaded WPC are shown in Table 4.1.2. From that table, it was observed that LOI value increased on addition of PE-*co*-GMA to the polymer blend. The increase in interfacial adhesion among polymers by PE-*co*-GMA resulted in higher value of LOI. Surface treatment of $SiO_2$ particles improved the dispersion and enhanced the interfacial adhesion between WF and polymer blend. The higher LOI values observed might be due to the formation of high performance carbonaceous-silica char on the surface. The higher the amount of $SiO_2$, the higher was the amount of char formation.

### 4.1.9. Water uptake study

Figure 4.1.7 shows the percentage of water uptake results for polymer blend and WPC samples. From the figure, it was observed that polymer blend absorbed less water than

the composites, as expected. The addition of compatibilizer decreased the water absorption. The compatibilizer improved the interfacial adhesion between the polymers and thus decreased the water uptake. The addition of GMA as compatibilizer to WPC decreased the water absorption [23]. The water uptake increased significantly when WF was added to the blend. This was due to the hydrophilic nature of wood. But the water uptake capacity decreased on inclusion of modified $SiO_2$ to the WPC. Water uptake was found to decrease with the increase in the percentage of $SiO_2$ in composite. The strong interaction between silica particles, wood and polymer matrix decreased the accessibility of water through WPC. Minelli et al. [24] studied the barrier properties of organic-inorganic hybrid coatings based on polyvinyl alcohol and found an increased in water barrier properties after incorporation of $SiO_2$. Composite loaded with 3 phr $SiO_2$ showed lowest water uptake. The reason was discussed earlier.

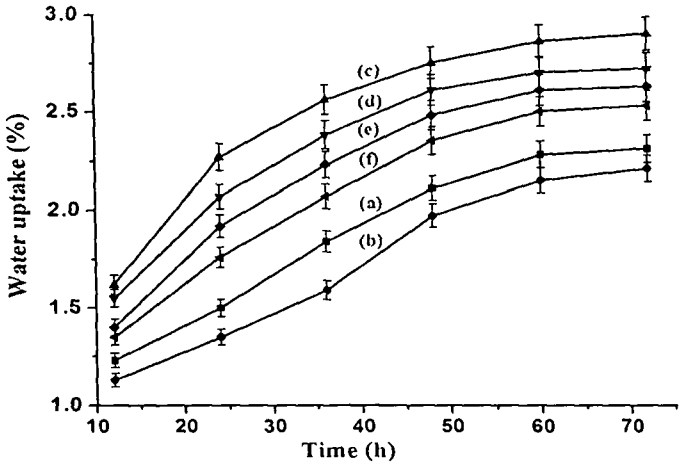


**Figure 4.1.7.** Percent water uptake for (a) PB (b) PB/G5 (c) PB/G5/W40 (d) PB/G5/W40/S1 (e) PB/G5/W40/S5 (f) PB/G5/W40/S3.

## *Section B*: Effect of nanoclay and $SiO_2$ on the properties of wood polymer nanocomposite.

Nanofillers reinforced wood-plastic composite (WPC) have emerged as an important family of composite [25]. They have relatively high strength and stiffness, low cost, low density, low $CO_2$ emission, biodegradability and renewable. Clay based nanocomposites

have evoked a great interest in recent years. Improvements in mechanical, dimensional, thermal, flame retardancy have been the reason for their widespread use [26]. Polymer-$SiO_2$ composites have been explored as technological important due to their potential applications in electrochromic windows, fuel cells, chemical separation, electrochemical sensing and water treatment etc.

In this communication, we report the modification of $SiO_2$ by treatment with cetyl trimethyl ammonium bromide and study the effect of $SiO_2$ nanopowder along with nanoclay on various properties of composites based on wood, PE-*co*-GMA and polymer mixture of HDPE, LDPE, PP and PVC.

## 4.2. RESULTS & DISCUSSION

### 4.2.1. X-ray diffraction results

XRD results of nanoclay, polymer blend, $SiO_2$ and wood polymer composite loaded with clay (3 phr) and different percentage of $SiO_2$ (1-5 phr) is represented by Figure 4.2.1. Organically modified nanoclay (curve-4.2.1a) shows the diffraction peak at $2\theta = 4.11^{\circ}$ with basal spacing of 2.15 nm. In the diffractrogram of polymer blend (Curve-4.2.1b), the most prominent wide-angle X-ray diffraction peaks appeared at $2\theta = 14.12$ (200), 17.06 (040),

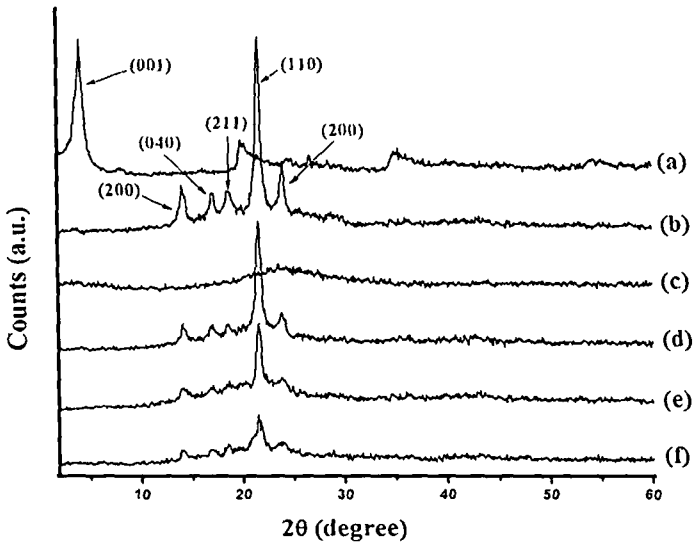


**Figure 4.2.1.** X-ray diffraction of (a) Nanoclay (b) PB (c) nano $SiO_2$ (d) PB/G5/W40/N3/S1 (e) PB/G5/W40/N3/S3 (f) PB/G5/W40/N3/S5.

18.64 (211), 21.62 (110) and 24.02 (200) were for crystalline portion of different polymers present in the blend [4-7]. Curve-4.2.1c shows a broad diffraction peak at $2\theta = 23.5^{\circ}$ for the amorphous $SiO_2$ nanoparticles. Curves-4.2.1d-f represent the diffractograms of WPC loaded with nanoclay (3 phr) and different percentage of $SiO_2$ (1-5 phr). The figures did not exhibit any characteristic peak of nanoclay. The exfoliation of silicate layers in the wood polymer matrix was the cause of disappearance of nanoclay diffraction peak. The crystalline peak intensity of the polymer blend which appeared in the range of $2\theta$ = 14-25°, was found to decrease with the increase in the level of incorporation of $SiO_2$ (1-5 phr). Similar decrease in peak intensities of polymer and increase in peak intensity due to incorporation of $TiO_2$ was observed and reported by Mina et al. [4] while studying the X-ray diffraction profile of polypropylene/titanium dioxide composite. All these suggested that nanoclay layers were exfoliated and $SiO_2$ particles were dispersed in the wood polymer matrix.

### 4.2.2. Transmission electron microscopy results

TEM micrographs of WPC loaded with different percentage of nanoclay and $SiO_2$ (1-5 phr) is represented by Figure 4.2.2. The silicate layers of nanoclay were shown by dark lines and the $SiO_2$ nanoparticles were presented by black spots in the figures. At lower percentage of $SiO_2$ loading (1-3 phr), a well dispersion of clay and $SiO_2$ nanoparticles was observed. Na-MMT layers together with $SiO_2$ nanoparticles was found to disperse well in PMMA matrix as reported by Bao and Ma [2]. At higher percentage of $SiO_2$ (5 phr) loading, an agglomeration of the nanoparticles was observed. The agglomeration occurred due to the surface interaction among the nanoparticles.

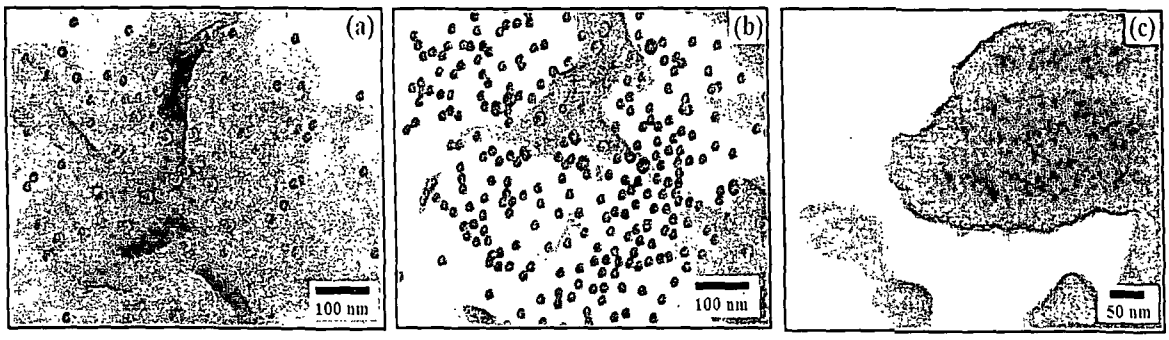


**Figure 4.2.2.** TEM micrographs of (a) PB/G5/W40/N3/S1 (b) PB/G5/W40/N3/S3 (c) PB/G5/W40/N3/S5.

### 4.2.3. Scanning electron microscopy results

Figure 4.2.3 shows the SEM micrographs of different fractured samples of PB, WPC and WPC loaded with nanoclay (3 phr) and different percentage of $SiO_2$ (1-5 phr) nanopowder. The polymers were quite immiscible (Fig. 4.2.3a) at the first stage, but after the incorporation of compatibilizer, the miscibility among the polymers was increased (Fig. 4.2.3b). The compatibilizer increased the interfacial adhesion among the polymers and thereby improved the miscibility among them [27]. The addition of wood flour improved the smoothness of composite (Fig. 4.2.3c). The smoothness of surface was further improved after the incorporation of wood, clay and $SiO_2$. Upto the addition of 3 phr $SiO_2$ and clay (Fig. 4.2.3d-e), the surface smoothness was increased. The surface of WPC loaded with 5 phr $SiO_2$ and clay (Fig. 4.2.3f) appeared less smoother compared to WPC loaded with 3 phr $SiO_2$ and clay. The increase in smoothness might be due to the improvement in interaction among PE-*co*-GMA, hydroxyl groups of wood and clay, along with the organic surfactant present in clay and polymer. Moreover, CTAB modified $SiO_2$ also has long olefinic chain which further improved the interaction among them. The agglomeration occurred at higher percentage of $SiO_2$ loading might be due to the surface interaction between $SiO_2$ nanoparticles. Similar agglomeration of $SiO_2$ nanoparticles at higher percent of loading was observed by Chrissafis et al. [28] during the thermal study of HDPE/fumed silica nanocomposite.

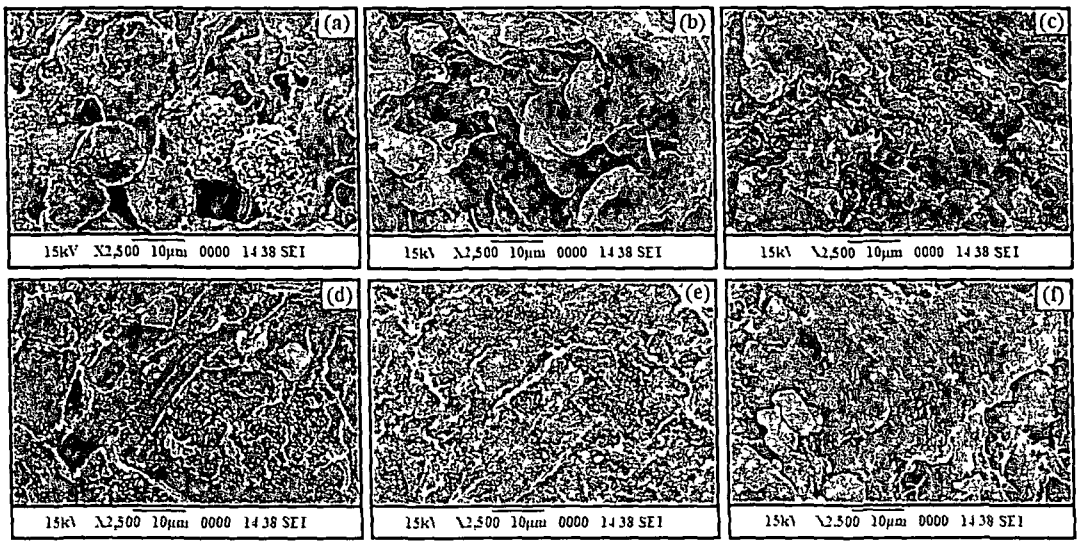


**Figure 4.2.3.** SEM micrographs of (a) PB (b) PB/G5 (c) PB/G5/W40 (d) PB/G5/W40/N3/S1 (e) PB/G5/W40/N3/S3 (f) PB/G5/W40/N3/S5.

### 4.2.4. Fourier transform infrared spectroscopy results

FTIR spectra of CTAB, $SiO_2$ and CTAB modified $SiO_2$ are shown in Figure 4.2.4. Absorption peaks at 2918, 2848 and 1475 $cm^{-1}$ were assigned to asymmetric, symmetric and scissor modes of $-CH_2$ stretching of the CTAB (curve-4.2.4a) respectively [9]. The spectrum of unmodified $SiO_2$ shows some absorption peaks at 3424 $cm^{-1}$ for -OH stretching and 1632 $cm^{-1}$ for –OH bending of hydroxyl group adsorbed on particle surface respectively. The other peaks appeared in the range 1087-465 $cm^{-1}$ were due to Si-O-Si group in the $SiO_2$ [10]. On the spectrum of CTAB modified $SiO_2$, the –OH peak intensity was found to decrease indicating an interaction of the hydroxyl group absorbed on $SiO_2$ surface with CTAB. Two new peaks around 2923 and 2854 $cm^{-1}$ were observed due to the $-CH_2$ stretching of CTAB. The peaks at 1490 and 1398 $cm^{-1}$ were due to the asymmetric and symmetric $CH_3$-$N^+$ deformation mode of CTAB headgroup [9]. Qu et al. [11] modified $TiO_2$ with CTAB and reported that the interaction of $TiO_2$ occurred with $Br^-$ of CTAB through hydrogen bond formation or electrostatic attractions. The other notable peaks appeared in the CTAB modified $SiO_2$ spectrum were the characteristic peaks for CTAB and $SiO_2$. These results indicated the incorporation of CTAB on the surface of $SiO_2$ particles.

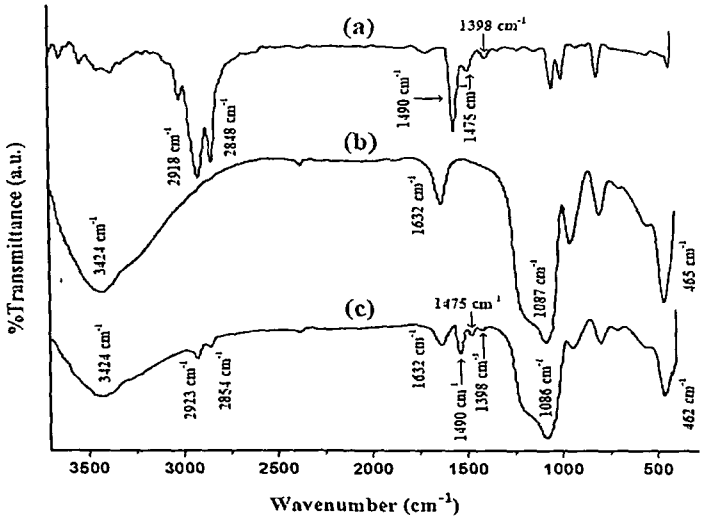


**Figure 4.2.4.** FTIR spectra of (a) CTAB (b) unmodified $SiO_2$ (c) CTAB modified $SiO_2$.

Figure 4.2.5 shows the FTIR spectra of wood, nanoclay, WPC and WPC loaded with nanoclay (3 phr) and $SiO_2$ (1-5 phr). Curve-4.2.5a shows the presence of bands at 3434 $cm^{-1}$ for –OH stretching, 2931 $cm^{-1}$ and 2849 $cm^{-1}$ for –CH stretching, 1730 $cm^{-1}$ for C=O

stretching, 1635 $cm^{-1}$ for –OH bending, 1163 and 1045 $cm^{-1}$ for C–O stretching and 1000-645 $cm^{-1}$ for C-H bending vibration (out of plane) of the wood sample. Organically modified nanoclay (curve-4.2.5b) exhibited the peaks at 3470 $cm^{-1}$ (–OH stretching) 2935 and 2849 $cm^{-1}$ (–CH stretching of modified hydrocarbon), 1620 $cm^{-1}$ (–OH bending) and 1030-460 $cm^{-1}$ (oxide bands of metals like Si, Al, Mg etc.). PB/G5/W40 (curve-4.2.5c) exhibited peaks at 3429 $cm^{-1}$ (-OH stretching), 2921 and 2837 $cm^{-1}$ (-CH stretching), 1731 $cm^{-1}$ (C=O stretching), 1630 $cm^{-1}$ (-OH bending) and 715 $cm^{-1}$ (-$CH_2$ bending).

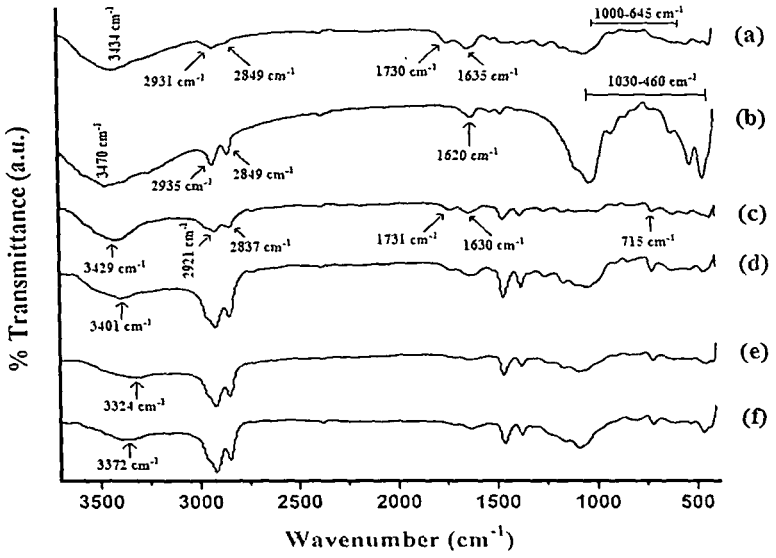


**Figure 4.2.5.** FTIR spectra of (a) Wood (b) Nanoclay (c) PB/G5/W40 (d) PB/G5/W40/N3/S1 (e) PB/G5/W40/N3/S3 (f) PB/G5/W40/N3/S5.

Curves-4.2.5d-f show the FTIR spectra of WPC loaded with 3 phr nanoclay and 1, 3 and 5 phr of $SiO_2$. From the figure, it was observed that the intensity of –OH stretching was decreased and shifted to 3401 $cm^{-1}$ (curve-4.2.5d), 3324 $cm^{-1}$ (curve-4.2.5e) and 3372 $cm^{-1}$ (curve-4.2.5f) compared to wood (3434 $cm^{-1}$), and nanoclay (3470 $cm^{-1}$). The decreased in intensities and shifting to lower wavelength confirmed the bond formation between the hydroxyl groups of wood, nanoclay and $SiO_2$. Moreover, the increase in intensities of –CH stretching at 2921 and 2837 $cm^{-1}$ (curves-4.2.5d-f) compared to those of wood confirmed the interaction between polymer, wood and compatibilizer. Similar type of decrease in intensity of –OH absorption peak, a shifting to lower wave number and increase in –CH peak intensities was reported by Awal et al. [17]. In the spectra of WPC (curves-4.2.5d-f), it was

observed that the intensity of the metal oxides bond in the range 1030-460 $cm^{-1}$ corresponding to nanoclay and $SiO_2$ decreased to a desirable extent which confirmed the formation of bond between wood, clay, $SiO_2$ and polymers.

### 4.2.5. Mechanical properties study

Table 4.2.1 shows the flexural and tensile properties of polymer blends, WPC and WPC loaded with nanoclay and different percentage of $SiO_2$ nanopowder. After incorporation of compatibilizer, both flexural and tensile properties of the polymer blend increased. This was because of improvement in interfacial adhesion between the polymers by the compatibilizer. The values were further improved after the addition of WF. The WF acted as a load carrier that provides reinforcing effect due to which the flexural and tensile properties were improved. Moreover, the compatibilizer, PE-*co*-GMA, increased the interfacial adhesion between wood and polymers by its glycidyl linkage and long olefinic chain and thus improved the strength properties. The properties were further improved after the incorporation of clay and $SiO_2$. The silicate layers of nanoclay act as a reinforcing agent that binds the polymer chain inside the gallery space and thus restricts the mobility of the polymer chains. The increased in mechanical properties of wood-plastic composite after the incorporation of nanoclay was reported by Faruk and Matuana [29]. At a fixed level of nanoclay (3 phr) loading, both flexural and tensile properties were improved upto the addition of 3 phr $SiO_2$, beyond that level of $SiO_2$ loading, these values decreased. The surface hydroxyl groups of CTAB modified $SiO_2$ nanopowder might interact with the hydroxyl groups of wood while the long alkyl chain of CTAB could interact with the polymer blend. Hence, a well distribution of the nanoparticles occurred which increased the flexural and tensile properties of the composite. Yu et al. [30] reported that the mechanical properties of polyacrylonitrile improved due to addition of Na-MMT and $SiO_2$ nanopowder. At higher percentage of $SiO_2$ loading (5 phr), the agglomeration of the nanoparticles resulted in a decrease in mechanical properties.

### 4.2.6. Hardness results

Hardness results of polymer blend and WPC with clay and different percentage of $SiO_2$ loading are also presented in Table 4.2.1. It was observed that after the incorporation of compatibilizer, hardness value of the polymer blend increased. The compatibilizer improved

the interfacial adhesion between the polymers and hence increased the hardness value. After the addition of WF to the polymer blend, the value was found to decrease. But the hardness value was found to increase after the incorporation of nanoclay and $SiO_2$ to the WPC. The improvement was due to the restriction in the mobility of the polymer chains provided by the silicate layers and increase in interaction between clay and $SiO_2$ nanopowder with wood and polymer blend as mentioned earlier. At higher $SiO_2$ (5 phr) loading, hardness value was found to decrease. The decrease in hardness value was due to the agglomeration of $SiO_2$ nanoparticles.

**Table 4.2.1.** Flexural, tensile and hardness properties of polymer blend and WPC loaded with different percentage of nanoclay and $SiO_2$.

| Sample | Flexural properties | | Tensile properties | | Hardness |
|---|---|---|---|---|---|
| | Strength (MPa) | Modulus (MPa) | Strength (MPa) | Modulus (MPa) | (Shore D) |
| PB | 13.47 ± 0.94 | 759.63 ± 1.06 | 5.73 ± 1.04 | 84.72 ± 16.37 | 66.6 ± 0.5 |
| PB/G5 | 16.25 ± 1.13 | 1031.19 ± 1.11 | 8.96 ± 1.26 | 115.51 ± 16.76 | 68.7 ± 0.3 |
| PB/G5/W40 | 18.14 ± 1.21 | 3798.72 ± 1.07 | 17.82 ± 1.15 | 263.42 ± 18.03 | 66.3 ± 0.7 |
| PB/G5/W40/N3/S1 | 30.52 ± 1.03 | 4971.60 ± 1.12 | 35.63 ± 1.17 | 636.41 ± 17.83 | 79.2 ± 0.1 |
| PB/G5/W40/N3/S3 | 37.26 ± 1.09 | 5686.91 ± 1.18 | 40.15 ± 1.26 | 692.75 ± 18.53 | 84.3 ± 0.6 |
| PB/G5/W40/N3/S5 | 32.53 ± 1.12 | 5172.50 ± 1.16 | 36.97 ± 1.12 | 647.53 ± 18.32 | 81.4 ± 0.2 |

### 4.2.7. Thermogravimetric analysis

Table 4.2.2 represents the initial decomposition temperature ($T_i$), maximum pyrolysis temperature ($T_m$), decomposition temperature at different weight loss (%) ($T_D$) and residual weight (RW, %) for the polymer blend and WPCs. From the table, it was observed that after the incorporation of compatibilizer and WF, $T_i$ values of the polymer blend was found to increase. The compatibilizer increased the interfacial adhesion among the polymers and with WF through its long olefinic chain and glycidyl group that leads to an increase in the $T_i$ values. Moreover, the WF also provided reinforcing effect to the polymer blend and that has also an effect on increase in $T_i$ value. $T_i$ value was further improved after the incorporation of clay and $SiO_2$ nanopowder. This was because of the tortuous path provided by the well distributed silicate layers of clay and $SiO_2$ nanopowder that prevent the passage of volatile

decomposed product throughout the composite. The incorporation of nanoclay improved the thermal stability of PP/wood flour nanocomposite [31]. Moreover, better heat dispersion inside the composite takes place due to the higher thermal diffusivity of $SiO_2$ nanoparticles. This would lead to a delay of burning of the surface and of the release of combustible volatile product throughout the composite. The incorporation of silica improved the thermal stability of PMMA [32]. At higher percentage (5 phr) of $SiO_2$ loading, the surface interaction among the oxide nanoparticles occurred and hence it became agglomerated and offered an easy way to the passage of volatile products. Hence, the thermal stability decreased.

**Table 4.2.2.** *Thermal analysis and limiting oxygen index (LOI) values of polymer blend and wood polymer nanocomposite.*

| Sample | $T_i$ | $T_m{}^a$ | $T_m{}^b$ | Temperature of decomposition ($T_D$) in °C at different weight loss (%) | | | | RW% at 600°C | LOI (%) |
|---|---|---|---|---|---|---|---|---|---|
| | | | | 20% | 40% | 60% | 80% | | |
| PB | 248 | 267 | 401 | 287 | 386 | 435 | 467 | 5.7 | 22 |
| PB/G5 | 251 | 270 | 407 | 291 | 389 | 439 | 470 | 6.2 | 35 |
| PB/G5/W40 | 256 | 278 | 448 | 299 | 402 | 447 | 477 | 7.1 | 38 |
| PB/G5/W40/N3/S1 | 272 | 321 | 497 | 324 | 453 | 479 | 495 | 11.1 | 63 |
| PB/G5/W40/N3/S3 | 278 | 329 | 503 | 335 | 461 | 484 | 501 | 14.0 | 66 |
| PB/G5/W40/N3/S5 | 275 | 325 | 501 | 328 | 457 | 481 | 498 | 12.2 | 65 |

$T_i$: value for initial degradation; $^aT_m$: value for 1st step; $^bT_m$: value for 2nd step.

### 4.2.8. Limiting oxygen index (LOI) results

Table 4.2.2 also shows the limiting oxygen index values of polymer blend, WPC and WPC loaded with nanoclay and $SiO_2$. From the table, it was observed that LOI value of the polymer blend increased after the addition of compatibilizer. LOI value was further increased after the incorporation of WF. The compatibilizer improved interfacial adhesion among the polymers through its long olefinic chain and with wood through its glycidyl group respectively. A substantial improvement in LOI value was observed after the addition of clay and $SiO_2$. Upto the addition of 3 phr each of nanoclay and $SiO_2$, the value increased. The dispersion of silicate layers provided a barrier to the transportation of combustion

product through the composite. Moreover, the tortuous path provided by the silicate layers had better barrier property to the oxygen and heat which delayed the burning capacity of the composite. Guo et al. [33] observed that the flame retardancy of wood fiber-plastic composite increased after the incorporation of nanoclay. The addition of CTAB modified $SiO_2$ enhanced the interaction between wood, clay and polymer through its hydroxyl and cetyl groups. $SiO_2$ nanoparticles also provided some thermal barrier to the oxygen and heat leading to an improvement in flame resistant property. The improvement in flame retardancy of PP filament due to the inclusion of nano $SiO_2$ was reported by Erdem et al. [34]. At higher concentration of $SiO_2$ (5 phr), LOI value decreased. This was due to the agglomeration of $SiO_2$ which resulted in decrease of interaction and hence reduction in barrier property as well as LOI value.

### 4.2.9. Water uptake results

The water uptake results of polymer blend, PE-*co*-GMA treated polymer blend and WPC loaded with clay and different percentage of $SiO_2$ are shown in Figure 4.2.6. On addition of PE-*co*-GMA compatibilizer, water uptake capacity of the polymer blend decreased. This was due to the increase in interfacial adhesion between the polymers by the compatibilizer. The value of water uptake capacity was suddenly increased after the addition of WF to the blend. This was because of the hydrophilic nature of wood flour that caused an

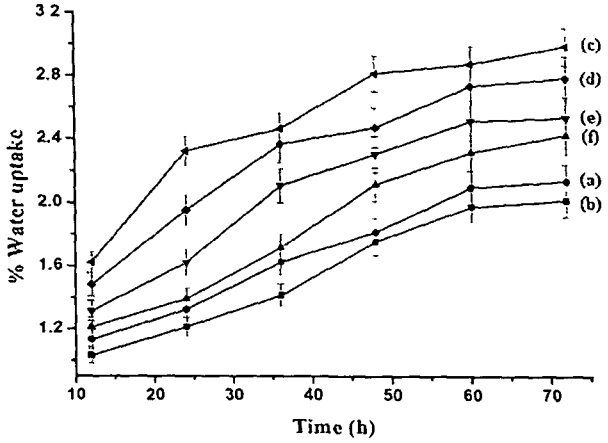


**Figure 4.2.6.** Percent water uptake of (a) PB (b) PB/G5 (c) PB/G5/W40 (d) PB/G5/W40/N3/S1 (e) PB/G5/W40/N3/S5 (f) PB/G5/W40/N3/S3.

increase in the water uptake capacity. But the water uptake capacity was decreased after the addition of clay and $SiO_2$. WPC loaded with 3 phr each of clay and $SiO_2$ showed lowest water uptake capacity followed by WPC with 3 phr clay and 5 phr $SiO_2$, and WPC with 3 phr clay and 1 phr $SiO_2$. The tortuous path provided by the silicate layers of clay increased the barrier property for water transport [35]. The barrier property provided by $SiO_2$ nanopowder also prevents the passage of water. The better the distribution of nanoparticles, the better was the barrier property. Minelli et al. [24] reported that the water uptake of polyvinyl alcohol decreased after the incorporation of $SiO_2$ nanopowder. At higher concentration of $SiO_2$ (5 phr), due to surface interaction of nanoparticles, it became agglomerated in the composite which resulted in an increase in water uptake capacity.

## *Section C*: Effect of nanoclay and $TiO_2$ on the properties of wood polymer nanocomposite.

Now-a-days, nanocomposites provide a new way to overcome the limitations of traditional counterparts [36]. Because of significant increase in interfacial interaction between inorganic and organic phases and size-dependent phenomena of nanoscale particles, polymer nanocomposites are capable of dramatically improving the mechanical and thermal properties including stiffness and heat resistance, gas and solvent barrier property, flame retardance without sacrificing good ductility of polymer (i.e. toughness) as compared with either homopolymer or traditional microcomposites.

Among many nanocomposite precursors, $TiO_2$ nanopowder is increasingly being investigated because it is non-toxic, chemically inert, low cost, corrosion resistant and has a high refractive index, UV filtration capacity and high hardness. Nanoscale $TiO_2$ reinforcement brings new optical, electrical, physiochemical properties attained at very low $TiO_2$ content, which make $TiO_2$ reinforced polymer nanocomposites a promising new class of materials [37].

In the present study, attempt has been made to develop a wood polymer nanocomposite by using polymer blend (HDPE, LDPE, PP, PVC) and wood flour with the co-incorporation of nanoclay/$TiO_2$ nanopowder. Effect of inclusion of nanoclay/$TiO_2$ on different properties of the composite has also been highlighted in the present study.

## 4.3. RESULTS & DISCUSSION

### 4.3.1. X-ray diffraction study

Figure 4.3.1 shows the XRD results of nanoclay, polymer blend, $TiO_2$ and wood polymer composite loaded with clay (3 phr) and different percentage of $TiO_2$ (1-5 phr). Organically modified nanoclay (curve-4.3.1a) shows the diffraction peak at $2\theta = 4.11^{\circ}$ with basal spacing 2.15 nm. In the diffractrogram of polymer blend (Curve-4.3.1b), the most prominent wide-angle X-ray diffraction peaks appeared at $2\theta$ = 14.12 (200), 17.06 (040), 18.64 (211), 21.62 (110) and 24.02 (200) were for crystalline portion of different polymers present in the blend [4-7]. The peaks (curve-4.3.1c) appeared at 2θ = 27.33 (110), 36.11 (200), 37.79 (111), 47.87 (210), 54.32 (211), 56.72 (220) were for the crystalline portion of $TiO_2$ [38,39]. Curves-4.3.1d-f represent the diffractrograms of WPC loaded with nanoclay (3 phr) and different percentage of $TiO_2$ (1-5 phr). The figures did not exhibit any characteristic peak of nanoclay. The exfoliation of silicate layers in the wood polymer matrix was the

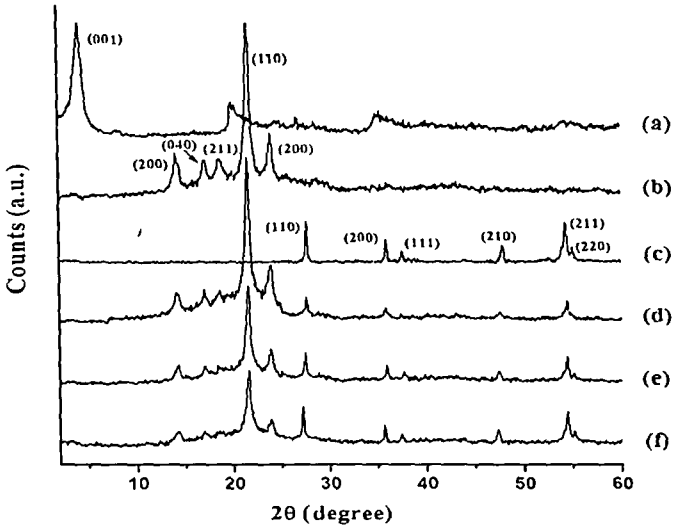


**Figure 4.3.1.** X-ray diffraction of (a) Nanoclay (b) PB (c) nano $TiO_2$ (d) PB/G5/W40/N3/T1 (e) PB/G5/W40/N3/T3 (f) PB/G5/W40/N3/T5.

cause of disappearance of nanoclay diffraction peak. The crystalline peak intensity of the polymer blend appeared in the range of $2\theta$ = 14-25° was found to decrease with the increase in the level of incorporation of $TiO_2$ (1-5 phr). However, the intensities of peak corresponding to $TiO_2$ nanopowder increased with the increase in the concentration of $TiO_2$

in the composite. A similar decrease in peak intensities of polymer and increase in peak intensity of $TiO_2$ was observed and reported by Mina et al. [4] while studying the X-ray diffraction profile of polypropylene/titanium dioxide composite. All these suggested that nanoclay layers were exfoliated and $TiO_2$ particles were dispersed in the wood polymer matrix.

### 4.3.2. Transmission electron microscopy study

Figure 4.3.2 indicates the TEM micrographs of WPC loaded with different percentage of nanoclay and $TiO_2$ (1-5 phr). The dark lines shown in the figures were the silicate layers of nanoclay and the black spots present in the figures were the $TiO_2$ nanoparticles of the composite. A well dispersion of clay and $TiO_2$ nanoparticles was observed at lower percentage of $TiO_2$ loading (1-3 phr) while an agglomeration of the same was observed at higher percentage of $TiO_2$ (5 phr) loading. Yamada et al. [40] incorporated $TiO_2$ nanoparticles into poly(methyl methacrylate) and observed similar increase in aggregation with increasing $TiO_2$ concentration. The agglomeration occurred due to the surface interaction among the nanoparticles.

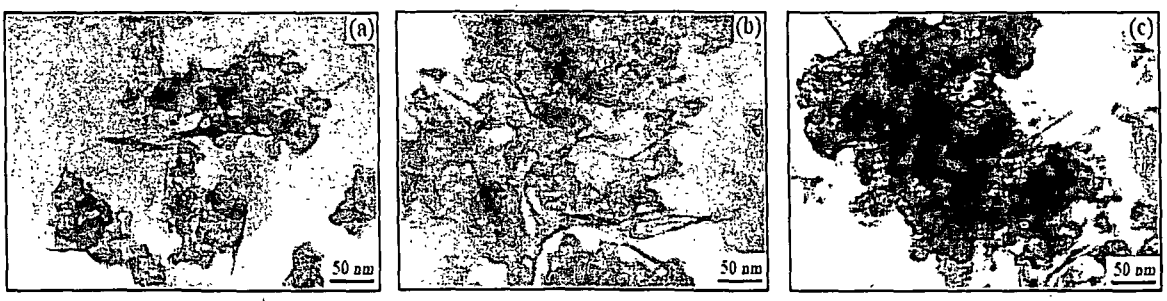


**Figure 4.3.2.** TEM micrographs of (a) PB/G5/W40/N3/T1 (b) PB/G5/W40/N3/T3 (c) PB/G5/W40/N3/T5.

### 4.3.3. Scanning electron microscopy study

SEM micrographs of different fractured samples of PB, WPC and WPC loaded with nanoclay and different percentage of $TiO_2$ nanopowder is represented by Figure 4.3.3. Initially the polymers are quite immiscible (Fig. 4.3.3a). The miscibility among the polymers was increased after the incorporation of compatibilizer (Fig. 4.3.3b). The interfacial adhesion

increased by the compatibilizer improved the miscibility among the polymers [27]. The addition of wood flour improved the smoothness of composite (Fig. 4.3.3c). The smoothness of surface was further improved after the incorporation of wood, clay and $TiO_2$. The surface smoothness was found to enhance upto addition of 3 phr $TiO_2$ and clay (Fig. 4.3.3d-e). The surface of WPC loaded with 5 phr $TiO_2$ and clay appeared less smoother compared to WPC loaded with 3 phr $TiO_2$ and clay (Fig. 4.3.3f). The increase in smoothness might be due to the improvement in interaction among PE-*co*-GMA, hydroxyl groups of wood and clay, along with the organic surfactant present in clay and polymer. Moreover, CTAB modified $TiO_2$ also has long olefinic chain which further improved the interaction among them. The agglomeration occurred at higher percentage of $TiO_2$ loading might be due to the surface interaction among $TiO_2$ nanoparticles. Similar agglomeration of $TiO_2$ nanoparticles at higher percent of loading was observed by Zhu et al. [41] during development of poly(lactic acid)/$TiO_2$ nanocomposite film.

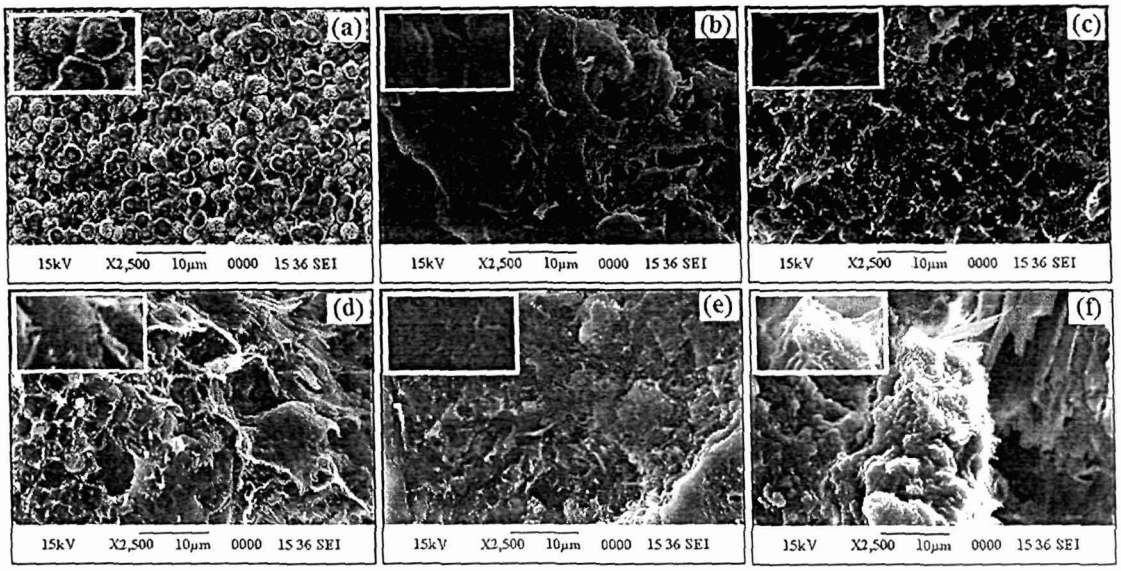


**Figure 4.3.3.** SEM micrographs of (a) PB (b) PB/G5 (c) PB/G5/W40 (d) PB/G5/W40/N3/T1 (e) PB/G5/W40/N3/T3 (f) PB/G5/W40/N3/T5.

### 4.3.4. Furier transform infrared spectroscopy study

FTIR spectra of CTAB, $TiO_2$ and CTAB modified $TiO_2$ are shown in Figure 4.3.4. In the spectrum of CTAB (Fig. 4.3.4a), the absorption peaks at 2918, 2848 and 1475 $cm^{-1}$ were assigned to asymmetric, symmetric, and scissor modes of -$CH_2$ stretching in the methylene

chains respectively [9]. FTIR spectrum of unmodified $TiO_2$ nanoparticles is presented in Figure 4.3.4b. The strong absorbance at 1028-418 $cm^{-1}$ was attributed to the Ti-O-Ti stretching of $TiO_2$. The absorbance at 3431 and 1633 $cm^{-1}$ were assigned to the surface hydroxyl groups of $TiO_2$ [42,43]. The intensity of –OH stretching in the modified $TiO_2$ (Fig. 4.3.4c) was found to decrease, indicating an interaction of the hydroxyl group absorbed on $TiO_2$ surface with CTAB. The frequencies at 2918, 2848 and 1475 $cm^{-1}$ of CTAB were shifted to 2925, 2852 and 1470 $cm^{-1}$ in the modified $TiO_2$ spectrum was due to incorporation of $-CH_2$ group of CTAB. Qu et al. [11] modified $TiO_2$ with CTAB and checked the dispersion of it in toluene as well as in carbon tetrachloride. They observed that modified $TiO_2$ was dispersed evenly in both the system. They suggested that the interaction of $TiO_2$ occurred with $Br^-$ ion of CTAB through hydrogen bond formation or electrostatic attractions. Further, CTAB modified $TiO_2$ was dispersed in a flask containing xylene and kept for checking of any settling of particles. The dispersion of $TiO_2$ was found to be stable. These results indicated the incorporation of CTAB on the surface of $TiO_2$ particles.

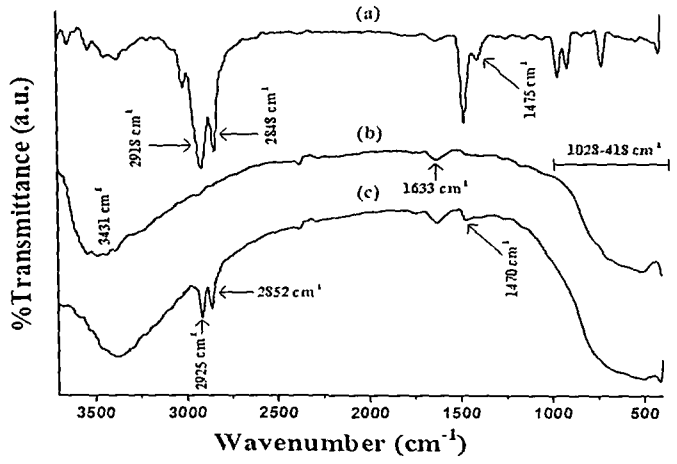


**Figure 4.3.4.** FTIR spectra of (a) CTAB (b) unmodified $TiO_2$ (c) CTAB modified $TiO_2$.

Figure 4.3.5 shows the FTIR spectra of wood, nanoclay, WPC and WPC loaded with nanoclay (3 phr) and $TiO_2$ (1-5 phr). Curve-4.3.5a shows the presence of bands at 3435 $cm^{-1}$ for –OH stretching, 2932 $cm^{-1}$ and 2848 $cm^{-1}$ for –CH stretching, 1731 $cm^{-1}$ for C=O stretching, 1638 $cm^{-1}$ for –OH bending, 1162 and 1046 $cm^{-1}$ for C–O stretching and 1000-650 $cm^{-1}$ for C-H bending (out of plane) vibration of the wood sample. Organically modified nanoclay (curve-4.3.5b) exhibited the peaks at 3471 $cm^{-1}$ (–OH stretching) 2936 and 2851 $cm^{-1}$ (–CH stretching of modified hydrocarbon), 1622 $cm^{-1}$ (–OH bending) and 1031-462

$cm^{-1}$ (oxide bands of metals like Si, Al, Mg etc.) [44]. PB/G5/W40 (curve-4.3.5c) exhibited peaks at 3431 $cm^{-1}$ (-OH stretching), 2925 and 2842 $cm^{-1}$ (-CH stretching), 1732 $cm^{-1}$ (C=O stretching), 1633 $cm^{-1}$ (-OH bending) and 716 $cm^{-1}$ (-$CH_2$ bending).

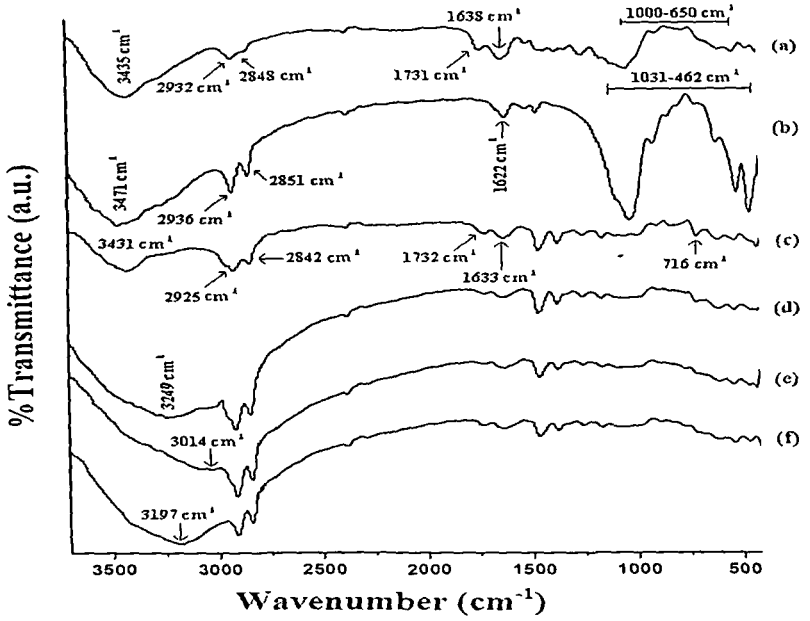


**Figure 4.3.5.** FTIR spectra of (a) Wood (b) Nanoclay (c) PB/G5/W40 (d) PB/G5/W40/N3/T1 (e) PB/G5/W40/N3/T3 (f) PB/G5/W40/N3/T5.

Curves-4.3.5d-f show the FTIR spectra of WPC loaded with 3 phr nanoclay and 1, 3 and 5 phr of $TiO_2$. From the figure, it was observed that the intensity of –OH stretching was decreased and shifted to 3249 $cm^{-1}$ (curve-4.3.5d), 3014 $cm^{-1}$ (curve-4.3.5e) and 3197 $cm^{-1}$ (curve-4.3.5f) compared to wood (3435 $cm^{-1}$), and nanoclay (3471 $cm^{-1}$). The decreased in intensities and shifting to lower wave number confirmed the bond formation between the hydroxyl groups of wood, nanoclay and $TiO_2$. The increase in intensities of –CH stretching at 2932 and 2848 $cm^{-1}$ (curves-4.3.5d-f) compared to those of wood confirmed the interaction between polymer, wood and compatibilizer. Similar increase in –CH peak intensities was observed by Awal et al. [17]. In the spectra of WPC (curves-4.3.5d-f), it was observed that the intensity of the metal oxides bond in the range 1028-414 $cm^{-1}$ corresponding to $TiO_2$ and nanoclay decreased to a desirable extent which confirmed the formation of bond between wood, clay, $TiO_2$ and polymers.

### 4.3.5. Mechanical property study

Table 4.3.1 shows the flexural and tensile properties of polymer blends, WPC and WPC loaded with nanoclay and different percentage of $TiO_2$ nanopowder. From the table, it was observed that both flexural and tensile properties of the polymer blend increased after incorporation of compatibilizer. This was because of improvement in interfacial adhesion between the polymers by the compatibilizer. The values were further improved after the addition of WF. The reinforcing effect provided by WF acted as a load carrier, due to which the flexural and tensile properties were improved. Salemane and Luyt [14] studied the improvement in mechanical properties of wood/polypropylene composite after the incorporation of wood flour. In addition to it, the compatibilizer, PE-*co*-GMA, increased the interfacial adhesion between wood and polymers by its glycidyl linkage and long olefinic chain and thus improved the strength properties. To improve the compatibility of wood pulp-LDPE composite, Sailaja [45] used PE-*co*-GMA as compatibilizer and found a significant improvement in properties of the composite. The properties were further improved after the incorporation of clay and $TiO_2$. The silicate layers of nanoclay act as a reinforcing agent that binds the polymer chain inside the gallery space and restricts the mobility of the polymer chains. Faruk and Matuana [29] observed the increased in mechanical properties of wood-plastic composite after the incorporation of nanoclay. It was also observed that at a fixed level of nanoclay (3 phr), both flexural and tensile properties were improved upto the addition of 3 phr $TiO_2$, beyond that these values decreased. The surface hydroxyl groups of CTAB modified $TiO_2$ nanopowder might interact with the hydroxyl groups of wood while the long alkyl chain of CTAB could interact with the polymer blend. Hence, a well dispersion of the nanoparticles occurred which increased the flexural and tensile properties of the composite. Saeed et al. [46] observed an increase in mechanical properties of electrospun nanofibres after incorporating $TiO_2$ nanopowder. At higher percentage of $TiO_2$ loading (5 phr), the agglomeration of the nanoparticles resulted in a decrease in mechanical properties.

### 4.3.6. Hardness results

Hardness results of polymer blend and WPC with clay and different percentage of $TiO_2$ loading were also presented in Table 4.3.1. It was observed that hardness value of the polymer blend increased after the incorporation of compatibilizer. The compatibilizer

improved the interfacial adhesion between the polymers and increased the hardness value. The value was found to decrease after the addition of WF to the polymer blend. But after the incorporation of nanoclay and $TiO_2$ to the WPC, hardness value was found to increase. At higher $TiO_2$ loading, hardness value was found to decrease. The improvement was due to the restriction in the mobility of the polymer chains provided by the silicate layers and increase in interaction of clay and $TiO_2$ nanopowder with wood and polymer blend as mentioned earlier. The decrease in hardness value was due to the agglomeration of $TiO_2$ nanoparticles.

**Table 4.3.1.** Flexural, tensile and hardness properties of polymer blend and WPC loaded with different percentage of nanoclay and $TiO_2$.

| Sample | Flexural properties | | Tensile properties | | Hardness |
|---|---|---|---|---|---|
| | Strength (MPa) | Modulus (MPa) | Strength (MPa) | Modulus (MPa) | (Shore D) |
| PB | 12.78 ± 0.35 | 755.68 ± 1.12 | 6.06 ± 1.02 | 85.92 ± 17.72 | 67.4 ± 0.6 |
| PB/G5 | 15.51 ± 1.01 | 1014.21 ± 1.09 | 9.05 ± 1.31 | 116.24 ± 16.91 | 68.0 ± 0.5 |
| PB/G5/W40 | 16.86 ± 1.10 | 3770.91 ± 1.14 | 17.14 ± 1.09 | 260.81 ± 17.39 | 66.7 ± 0.3 |
| PB/G5/W40/N3/T1 | 28.62 ± 0.81 | 4842.81 ± 1.08 | 33.52 ± 1.37 | 596.12 ± 18.27 | 77.4 ± 0.3 |
| PB/G5/W40/N3/T3 | 33.85 ± 1.06 | 5072.64 ± 1.25 | 36.03 ± 1.15 | 653.86 ± 17.14 | 80.9 ± 0.5 |
| PB/G5/W40/N3/T5 | 30.38 ± 1.13 | 4903.90 ± 1.72 | 34.72 ± 1.18 | 620.57 ± 17.53 | 78.1 ± 0.3 |

### 4.3.7. Thermal property results

Table 4.3.2 represents the initial decomposition temperature ($T_i$), maximum pyrolysis temperature ($T_m$), decomposition temperature at different weight loss (%) ($T_D$) and residual weight (RW, %) for the polymer blend and WPCs. $T_i$ values of the polymer blend increased after incorporation of compatibilizer and WF. The compatibilizer increased the interfacial adhesion among the polymers and with WF leading to an increase in the $T_i$ values. WF also provided reinforcing effect to the polymer blend. Awal et al. [17] observed an increase in thermal stability of polymer after incorporation of compatibilizer and wood flour. $T_i$ value was further improved after the incorporation of clay and $TiO_2$ nanopowder. The exfoliation of inorganic silicate layers of nanoclay impart long tortuous path to the composite that delayed the diffusion of decomposed volatile products throughout the composite. The improvement in thermal stability of wood polymer composite by the incorporation of clay

was reported in the literature [31]. Moreover, higher thermal diffusivity of $TiO_2$ nanoparticles provided a better dispersion of heat inside the composite. This would lead to a delay of burning of the surface and of the release of combustible volatiles throughout the composite. Laachachi et al. [47] studied the thermal stability of PMMA by using organoclay and $TiO_2$ and found a significant increase in thermal stability of PMMA due to the synergistic effect of clay/$TiO_2$. It should be mentioned that, at higher percentage (5 phr) of $TiO_2$, due to surface interaction, the oxide nanoparticles became agglomerated and offered an easy way to the passage of volatile products. Hence, the thermal stability decreased.

**Table 4.3.2.** Thermal analysis and limiting oxygen index (LOI) values of polymer blend and wood polymer nanocomposite.

| Sample | $T_i$ | $T_m{}^a$ | $T_m{}^b$ | Temperature of decomposition ($T_D$) in °C at different weight loss (%) | | | | RW% at 600°C | LOI (%) |
|---|---|---|---|---|---|---|---|---|---|
| | | | | 20% | 40% | 60% | 80% | | |
| PB | 250 | 271 | 406 | 290 | 390 | 438 | 469 | 6.0 | 21 |
| PB/G5/W40 | 253 | 277 | 450 | 297 | 399 | 448 | 474 | 7.2 | 39 |
| PB/G5/W40/N3/T1 | 274 | 323 | 499 | 326 | 455 | 481 | 497 | 11.4 | 62 |
| PB/G5/W40/N3/T3 | 285 | 334 | 510 | 346 | 475 | 492 | 509 | 14.3 | 67 |
| PB/G5/W40/N3/T5 | 278 | 327 | 506 | 333 | 462 | 486 | 503 | 12.6 | 64 |

$T_i$: value for initial degradation, $^aT_m$: value for 1st step, $^bT_m$: value for 2nd step.

### 4.3.8. Limiting oxygen index (LOI) results

Limiting oxygen index values of polymer blend, WPC and WPC loaded with nanoclay and $TiO_2$ are shown in Table 4.3.2. From the table, it was observed that LOI value of the polymer blend increased after the addition of compatibilizer. The increase in the value was due to the increase in interfacial adhesion among the polymers by the compatibilizer. The addition of WF to the blend further increased the LOI value. The glycidyl and hydrocarbon part of the compatibilizer improved the interaction with the hydroxyl and hydrocarbon part of the wood and polymer. A substantial improvement in LOI value was observed after the addition of clay and $TiO_2$. The value increased upto the addition of 3 phr each of nanoclay and $TiO_2$. LOI value decreased at higher concentration of $TiO_2$ (5 phr). The

nanoclay produced silicate char on the surface of WPC which increased the flame resistance property of the composite [48]. The tortuous path provided by the silicate layers had better barrier property to the oxygen and heat which delayed the burning capacity of the composite. The addition of CTAB modified $TiO_2$ enhanced the interaction among wood, clay and polymer through its hydroxyl and cetyl groups. $TiO_2$ nanoparticles also provided some thermal barrier to the oxygen and heat leading to an improvement in flame resistant property. At higher $TiO_2$ loading, the agglomeration of $TiO_2$ resulted in decrease of interaction and hence reduction in barrier property as well as LOI value.

### 4.3.9. UV test results

Figure 4.3.6 displays the weight loss of polymer blend, normal WPC and WPC loaded with nanoclay and $TiO_2$ (1-3 phr). Weight losses of the samples were determined as a function of exposure time at room temperature. The weight loss in all materials was nearly linear with exposure time. A small increase of weight at early exposure times was due to the moisture uptake, which was greater than the material loss induced by the degradation in the early stage. The rate of weight loss was lowest for polymer blend followed by WPC filled with 3 phr $TiO_2$ and 3 phr clay, 5 phr of $TiO_2$ and 3 phr clay, 1 phr $TiO_2$ and 3 phr clay. Higher weight loss was observed for normal WPC. After 60 days of exposure, the maximum weight losses in polymer blend, normal WPC, 1, 3, 5 phr $TiO_2$ and clay loaded WPCs were 1.31 % ± 0.24 %, 3.37 % ± 0.22 %, 2.81 % ± 0.35 %, 1.76 % ± 0.64 % and 2.21 % ± 0.59 % respectively.

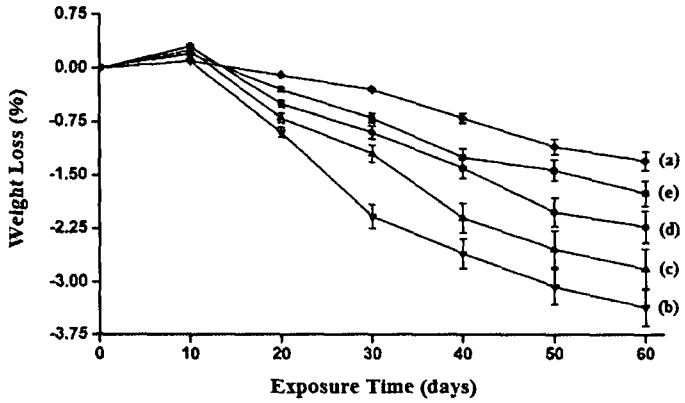


**Figure 4.3.6.** Weight losses vs. exposure time of (a) PB (b) PB/G5/W40 (c) PB/G5/W40/N3/T1 (d) PB/G5/W40/N3/T5 (e) PB/G5/W40/N3/T3.

Figure 4.3.7 shows the carbonyl index values against time. The intensity of the carbonyl peaks was increased after irradiation of the samples for 60 days (Fig. 4.3.8). Upon exposing the samples to UV radiation, chain scission of the polymer blend occurred that increased the carbonyl index value. Further the chain scission decreased the density of entanglements of polymer chain and hence the decrease in weight of the samples. The polymer blend had lowest carbonyl index value while normal WPC had highest carbonyl index value due to higher oxidation of WF. The carbonyl index values decreased upto the addition of 3 phr $TiO_2$ after that it increased. $TiO_2$ nanoparticles played an important role in stabilizing the WPC by acting as screens and delayed the photo-degradation process. $TiO_2$ nanoparticles absorbed the UV radiation and hence reduced the UV intensity required for the oxidation of the WPC. Du et al. [49] observed an increase in UV stability of WF/HDPE composite after the incorporation of $TiO_2$. The presence of nanoclay in the composite also has a screening effect that delayed the photo degradation process. Grigoriadou et al. [50] observed an increase in UV stability of HDPE after incorporating montmorillonite clay. Figure 4.3.9 represents the SEM micrographs of samples after 60 days of irradiation. The micrographs revealed a drastic change in surface morphology of the samples due to exposure to UV radiation. The surface of normal WPC was more irregular compared to clay/$TiO_2$ treated WPC indicating that the normal WPC sample was less effective compared to $TiO_2$/clay containing sample against UV radiation. WPC containing higher percentage of $TiO_2$ (5 phr) exhibited lower protection against UV radiation as shown by the decrease in surface smoothness compared to WPC loaded with 3 phr $TiO_2$ and nanoclay. This might be due to the agglomeration of $TiO_2$ which provided lower protection against photodegradation.

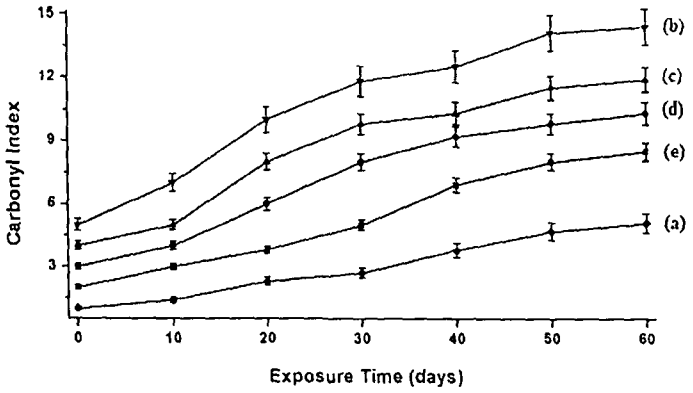


**Figure 4.3.7.** Carbonyl index values of (a) PB (b) PB/G5/W40 (c) PB/G5/W40/N3/T1 (d) PB/G5/W40/N3/T5 (e) PB/G5/W40/N3/T3.

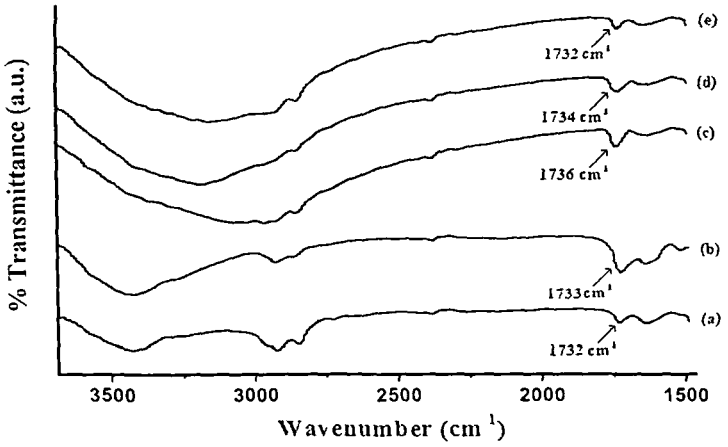


**Figure 4.3.8.** Change in carbonyl peak intensity of (a) PB (b) PB/G5/W40 (c) PB/G5/W40/N3/T1 (d) PB/G5/W40/N3/T5 (e) PB/G5/W40/N3/T3

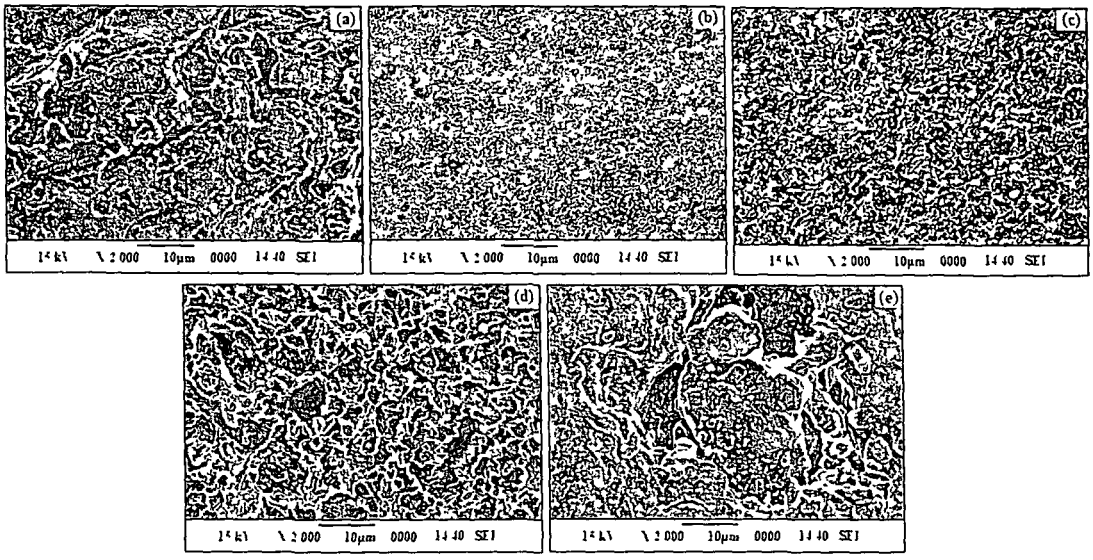


**Figure 4.3.9.** SEM micrographs of UV treated samples after 60 days (a) PB (b) PB/G5/W40 (c) PB/G5/W40/N3/T1 (d) PB/G5/W40/N3/T3 (e) PB/G5/W40/N3/T5.

### 4.3.10. Water uptake and water vapour exclusion results

The water uptake and water vapour uptake results of polymer blend, PE-*co*-GMA treated polymer blend and WPC loaded with clay and different percentage of $TiO_2$ are shown in Figure 4.3.10. The water uptake capacity of polymer blend decreased after the addition of PE-*co*-GMA compatibilizer. The decreased in water uptake capacity of PE-*co*-

GMA treated polymer blend was due to the increase in interfacial adhesion between the polymers by the compatibilizer. The value of water uptake capacity was suddenly increased after the addition of WF to the blend. The hydrophilic nature of wood flour caused an increase in the water uptake capacity. The water uptake capacity was decreased after the addition of clay and $TiO_2$. WPC loaded with 3 phr each of clay and $TiO_2$ showed lowest water uptake capacity followed by WPC with 3 phr clay and 5 phr $TiO_2$, and WPC with 3 phr clay and 1 phr $TiO_2$. The silicate layers of the clay provided tortuous path and increased the barrier property for water transport [51]. $TiO_2$ nanopowder also provided a barrier to the passage of water. Incorporation of nano-$TiO_2$ increased the water absorption and hence it reduced the diffusion coefficient of water. This was because of the strong affinity of water molecules towards nano-$TiO_2$ particles that restricted its free motion. The well distribution nature of modified nanoparticles further improved the resistance and retarded the motion of water molecules through the composite. The diffusion coefficient of water decreased further. Moreover, the water absorption of inorganic particles reduced after the modification of particles by organic surfactant. Zhu et al. [41] reported the increase in barrier property of poly(lactic acid) nanocomposite film after the incorporation of nano-$TiO_2$. The better the distribution of nanoparticles, the better was the barrier property. Chen et al. [52] observed a reduction in water uptake capacity of polyacrylate coating by modified $TiO_2$ due to the even dispersion of nanoparticles. $TiO_2$ nanoparticles at higher concentration were found to become agglomerated in the composite which resulted in an increase in water uptake capacity.

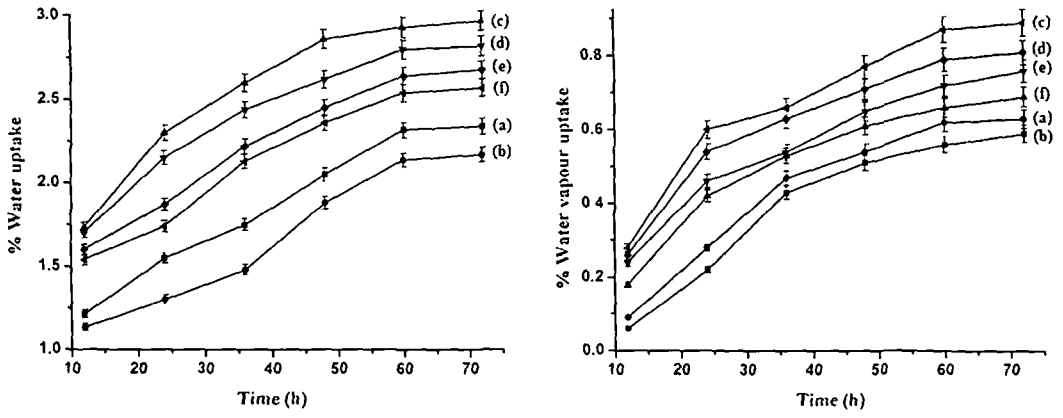


**Figure 4.3.10.** Percent water absorption and water vapour absorption of (a) PB (b) PB/G5 (c) PB/G5/W40 (d) PB/G5/W40/N3/T1 (e) PB/G5/W40/N3/T5 (f) PB/G5/W40/N3/T3.

Water vapor exclusion test for the samples were carried out at 30 °C and 65 % relative humidity. The water vapor uptake was found to increase with time. The trend and explanation for water vapor uptake of different samples were similar to those of samples taken for water uptake study. The optimal loading of $TiO_2$, at which the least water uptake was observed, was 3 phr. The incorporation of $TiO_2$ along with clay decreased the average water uptake by 40%.

## *Section D*: Effect of nanoclay and ZnO on the physical and chemical properties of wood polymer nanocomposite.

Thermal stability is one of the important properties of wood polymer composite (WPC). It has been established that thermostability along with the other properties of the composite can be improved by using clay particles [53]. The addition of nanoclay to the composite enhances the mechanical, thermal and other properties. Besides using clay, different metal oxide nano particles (Si, Zn, Ti etc.) are used to improve the properties like mechanical, thermal, flammability, weathering, etc. of the composites. UV protection, flame retardancy, and weathering resistance are very important for wood based composites used in exterior applications.

ZnO nanopowder is one of the widely used filler. ZnO enhances the thermal, mechanical, UV resistance as well as other relevant properties of the composite [54]. Reports based on wood/ polymer/clay nanocomposite are available in literature. However, far less is known regarding wood polymer nanocomposite by using both clay and metal oxide.

The present study is aimed to discuss the effect of ZnO nanopowder along with nanoclay to the thermal and mechanical properties of HDPE/LDPE/PP/PVC blend/wood/nanoclay composite. The aim is also to study the effect of ZnO to other properties like UV resistance, flame retardancy and water uptake of the composites.

### 4.4. RESULTS & DISCUSSION

#### 4.4.1. X-ray diffraction results

Figure 4.4.1 shows the XRD results of nanoclay, polymer blend, ZnO and wood polymer composite loaded with clay (3 phr) and different percentage of ZnO (1-5 phr).

Organically modified nanoclay (curve-4.4.1a) shows the diffraction peak at $2\theta = 4.11^{\circ}$ with basal spacing 2.15 nm. Curve-4.4.1b represents the diffractrogram of polymer blend. The most prominent wide-angle X-ray diffraction peaks appeared at $2\theta$ = 14.12 (200), 17.06 (040), 18.64 (211), 21.62 (110) and 24.02 (200) were for crystalline portion of different polymers present in the blend [4-7]. The crystalline peaks appeared above $2\theta = 30^{\circ}$ (curve-4.4.1c) were the characteristic peaks of ZnO nanopowder [55]. Curves-4.4.1d-f was for WPC loaded with nanoclay (3 phr) and different percentage of ZnO (1-5 phr). The diffractograms of composites did not exhibit any characteristic peak of nanoclay. It could be said that either an exfoliation or increase in disorder in nanoclay occurred which was not possible to detect by XRD analysis. The crystalline peak intensity of the polymer blend appeared in the range $2\theta = 14\text{-}25^{\circ}$ was found to decrease with the increase in the level of incorporation of ZnO (1-5 phr). However, the intensities of peak corresponding to ZnO nanopowder increased with the increase in the concentration of ZnO in the composite. Similar decreased in peak intensities of polymer and increase of peak intensity of $TiO_2$ was observed and reported by Mina et al. [4] while studying the X-ray diffraction profile of polypropylene/titanium dioxide composite. It could be concluded that nanoclay layers were disordered and ZnO particles were incorporated in the wood polymer matrix.

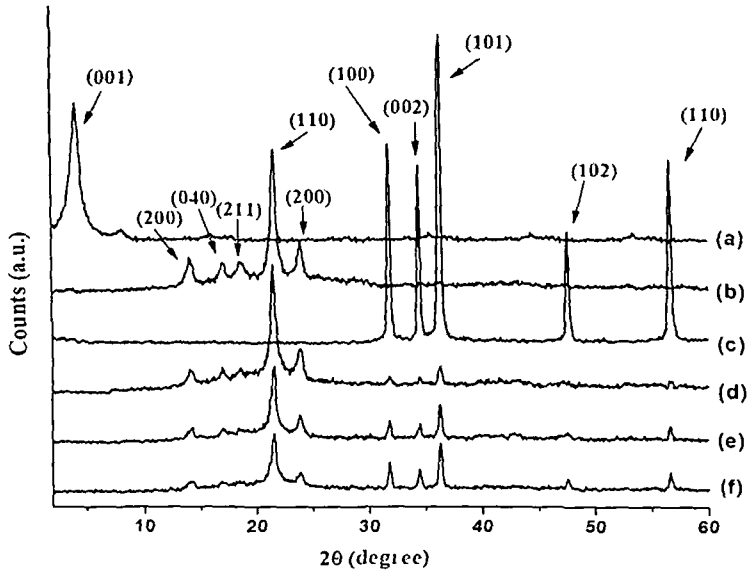


**Figure 4.4.1.** X-ray diffraction of (a) Nanoclay (b) PB (c) nano ZnO (d) PB/G5/W40/N3/Z1 (e) PB/G5/W40/N3/Z3 (f) PB/G5/W40/N3/Z5.

### 4.4.2. Transmission electron microscopy results

Figure 4.4.2 shows the TEM micrographs of WPC loaded with nanoclay (3 phr) and different percentage of ZnO (1-5 phr). The dark slices (arrow marked) represent the layers of nanoclay while the dark spots (arrow marked) are for ZnO nanoparticles. The distribution of ZnO (1-3 phr) was better in the WPC compared to that of composite containing higher proportion (5 phr) of ZnO (Fig. 4.4.2c). Chae and Kim [56] prepared PAN/ZnO nanocomposite and found that ZnO nanoparticles were well dispersed within the composite. At higher concentration of ZnO, the distances between ZnO particles became less and this might have enhanced the tendency for agglomeration.

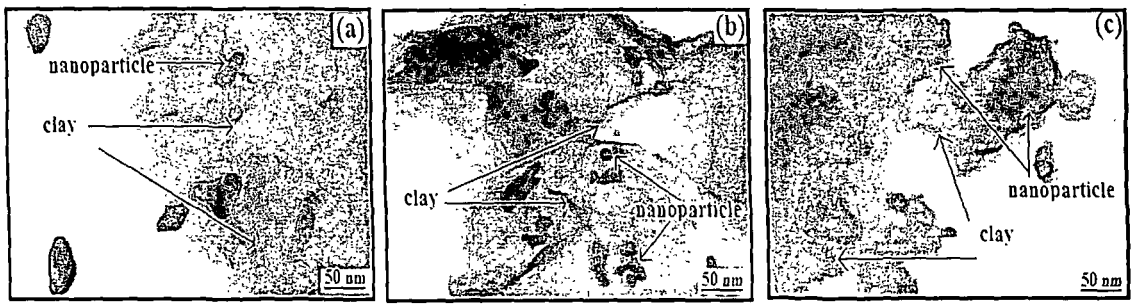


**Figure 4.4.2.** TEM micrographs of (a) PB/G5/W40/N3/Z1 (b) PB/G5/W40/N3/Z3 (c) PB/G5/W40/N3/Z5.

### 4.4.3. Scanning electron microscopy results

Figure 4.4.3 shows the SEM micrographs of polymer blend with and without compatibilizer, WPC and WPC loaded with nanoclay and different percentage of ZnO nanopowder. The fractured surface of some selective samples was considered for this study. The polymer mixtures were immiscible as judged by separation of different phases (Fig. 4.4.3a). The miscibility improved due to addition of PE-*co*-GMA as compatibilizer (Fig. 4.4.3b). The compatibilizer enhanced the interfacial adhesion among the polymers through its long hydrocarbon chain and epoxy group which resulted in an improvement in miscibility. The use of ethylene-glycidyl methacrylate for improving the adhesion between polyolefins and PET was reported in the literature [27]. The addition of wood flour decreased the roughness of fractured surface of the composite (Fig. 4.4.3c). The roughness of the fractured surface decreased further after the incorporation of wood flour, clay and

ZnO to the polymer blend (Fig. 4.4.3d-e). The fractured surface of composite having nanoclay and 3 phr ZnO appeared to be smoother compared to those of composite prepared with either 1 or 5 phr ZnO and nanoclay. This might be due to the improvement in interaction among PE-*co*-GMA, nanoclay, ZnO, polymer and wood. The decrease in smoothness at higher concentration of ZnO was due to the aggregation of ZnO. Similar observation was reported by He et al. [57] during study of the morphology of PET/ZnO nanocomposite.

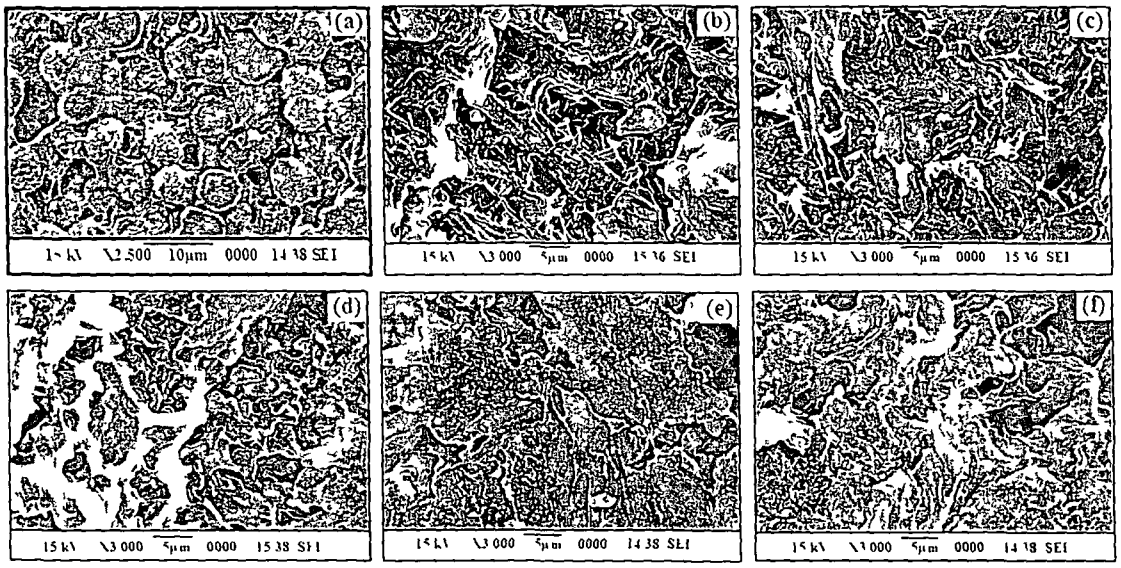


**Figure 4.4.3.** SEM micrographs of (a) PB (b) PB/G5 (c) PB/G5/W40 (d) PB/G5/W40/N3/Z1 (e) PB/G5/W40/N3/Z3 (f) PB/G5/W40/N3/Z5.

### 4.4.4. Fourier transform infrared spectroscopy results

FTIR spectra of CTAB, ZnO and CTAB modified ZnO are shown in Figure 4.4.4. In the spectrum of CTAB (Fig 4.4.4a), the absorption peaks at 2918, 2848 and 1475 $cm^{-1}$ were assigned to asymmetric, symmetric stretching and scissor modes of $-CH_2$ in the methylene chains respectively [9]. FTIR spectrum of unmodified ZnO nanoparticles is presented by the curve-4.4.4b. Absorption peaks at 3438 and 1633 $cm^{-1}$ in the spectra was due to –OH (-stretching) and –OH (-bending) vibrations while the peaks around 420 $cm^{-1}$ was due to the vibration of metal-oxygen (M-O) bond as reported in the literature [58]. The FTIR spectrum of ZnO modified with CTAB is represented by the curve-4.4.4c. It was observed that the intensity of the peak for –OH group decreased to 3342 $cm^{-1}$. Besides this, two new peaks at

2915 and 2849 $cm^{-1}$, which were due to the presence of -$CH_2$ group of CTAB were appeared in the spectrum. The peaks at 1490 $cm^{-1}$ and 1480 $cm^{-1}$ were due to the asymmetric $CH_3$-$N^+$ deformation mode of the CTAB headgroup. Another peak present at 1398 $cm^{-1}$ was due to the symmetric $CH_3$-$N^+$ deformation mode of CTAB headgroup [9]. These results indicated that long chain of CTAB group had been incorporated on the surface of the ZnO nanoparticles. Further, CTAB modified ZnO was dispersed in a flask containing xylene and kept for checking of any settling of particles. The dispersion of ZnO was found to be stable. This indicated that proper modification occurred.

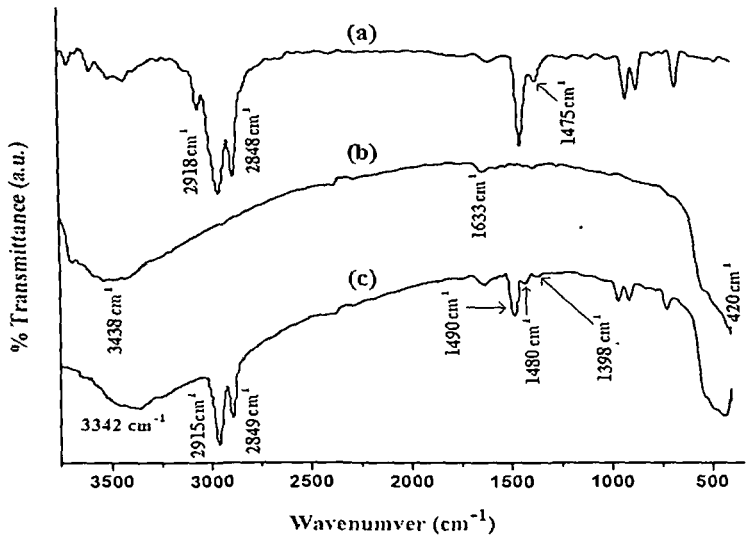


**Figure 4.4.4.** FTIR spectra of (a) CTAB (b) unmodified ZnO (c) CTAB modified ZnO.

Figure 4.4.5 shows the FTIR spectra of wood, nanoclay, WPC excluding nanoclay and ZnO and WPC containing nanoclay with different percentage of ZnO. Curve-4.4.5a representing the wood sample shows the presence of bands at 3436 $cm^{-1}$ for –OH stretching, 2932 and 2849 $cm^{-1}$ for –CH stretching, 1732 $cm^{-1}$ for C=O stretching, 1639 $cm^{-1}$ for –OH bending, 1161 and 1045 $cm^{-1}$ for C–O stretching and 1000 – 650 $cm^{-1}$ for C-H bending(out of plane) vibration. Organically modified nanoclay (curve-4.4.5b) exhibits the peaks at 3470 $cm^{-1}$ (–OH stretching) 2935 and 2852 $cm^{-1}$ (–CH stretching of modified hydrocarbon), 1621 $cm^{-1}$ (–OH bending) and 1032-461 $cm^{-1}$ (oxide bands of metals like Si, Al, Mg etc.) [44]. PB/G5/W40 (curve-4.4.5c) shows peaks at 2923 $cm^{-1}$ (-CH stretching), 1734 $cm^{-1}$ (C=O stretching), 1636 $cm^{-1}$ (-OH bending) and 720 $cm^{-1}$ (-$CH_2$ stretching).

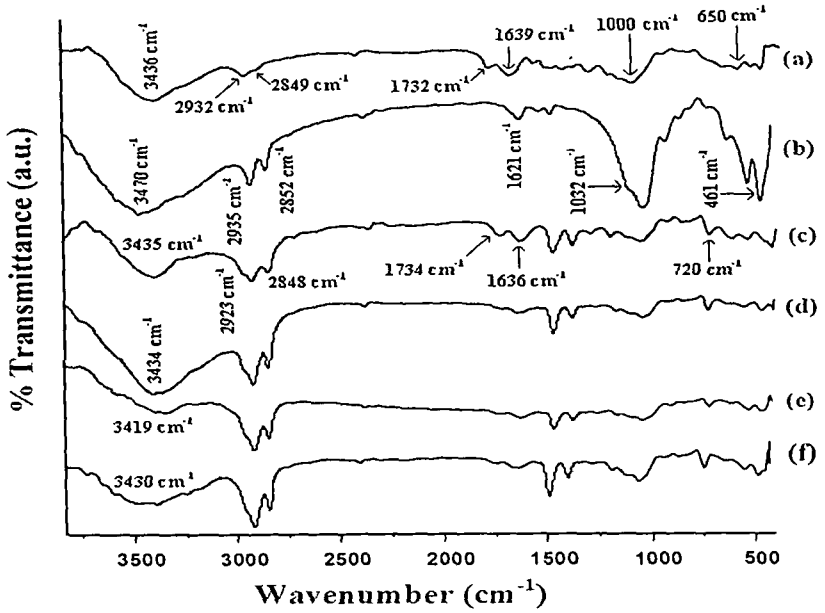


**Figure 4.4.5.** FTIR spectra of (a) Wood (b) Nanoclay (c) PB/G5/W40 (d) PB/G5/W40/N3/Z1 (e) PB/G5/W40/N3/Z3 (f) PB/G5/W40/N3/Z5.

Curves-4.4.5d-f represents the FTIR spectra of WPC loaded with 3 phr nanoclay and 1, 3 and 5 phr of ZnO. From the figure, it was observed that the intensity of –OH stretching was decreased and shifted to 3434 $cm^{-1}$ (curve-4.4.5d), 3419 $cm^{-1}$ (curve-4.4.5e) and 3430 $cm^{-1}$ (curve-4.4.5f) from 3436 $cm^{-1}$ (wood). The decrease in peak intensity of –OH stretching might be ascribed to the participation of hydroxyl group of clay and ZnO in the crosslinking reaction with wood and polymer. The shifting of hydroxyl absorption peak to lower wave number was due to the formation of hydrogen bond between wood flour and polymer. Dhoke et al. [58] studied the interaction between nano-ZnO particles and alkyd resin by FTIR technique. A significant decrease in peak intensity of hydroxyl group of alkyd resin was observed. The intensity of –CH stretching peaks at 2932 $cm^{-1}$ and 2848 $cm^{-1}$ (curves-4.4.5d-f) was found to increase. Similar decrease in intensity of –OH absorption peak and shifting to lower wavelength and increase in –CH peak intensities was observed by Awal et al. [17]. The peak intensities (1032-461 $cm^{-1}$) of metal oxides bond of nanoclay and ZnO (curves-4.4.5d-f) was decreased to a considerable extent. Moreover, the flexural and tensile properties of the composites improved due to incorporation of clay and ZnO as explained later. All these suggested a strong interaction between wood, nanoclay, ZnO and polymer.

### 4.4.5. Mechanical property study

Table 4.4.1 shows the flexural and tensile properties of polymer blends and WPC loaded with nanoclay and different percentage of ZnO nanopowder. From the table, it was observed that both flexural and tensile properties of the polymer blend increased after incorporation of compatibilizer. The compatibilizer improved the interfacial adhesion between the polymers due to which both flexural and tensile properties increased. The flexural and tensile properties of the composite were further improved after the addition of WF. The WF acted as a load carrier, reinforced the composites and increased the flexural and tensile properties. Salemane and Luyt [14] prepared wood/polypropylene composite and found an improvement in mechanical properties due to reinforcement by wood flour. Moreover, the compatibilizer, PE-*co*-GMA, increased the interfacial adhesion between wood and polymers through its glycidyl linkage and long polymeric chain. Sailaja [45] used poly(ethylene-*co*-glycidyl methacrylate) as compatibilizer to improve the compatibility of wood pulp-LDPE composite. The properties were further improved after the incorporation of clay and ZnO nanopowder. At a fixed clay loading (3 phr), both the flexural and tensile properties improved upto addition of 3 phr of ZnO. The properties decreased on addition of higher amount of ZnO (5 phr). The observed higher values might be due to the combined effect of nanoclay and ZnO. The silicate layers of nanoclay acted as a reinforcing agent that binds the polymer chain inside the gallery space and hence restrict the mobility of the polymer chain. It was reported that the incorporation of clay increased the mechanical properties of wood-plastic composite [29]. CTAB modified ZnO improved the interaction between clay, wood and polymer through its surface hydroxyl group and cetyl group respectively. The higher the dispersion of ZnO, the higher would be the interaction. At higher level of ZnO loading (5 phr), the agglomeration occurred and hence the interaction of ZnO with the clay, polymer and wood decreased. The interaction of ZnO nanoparticles increased the tensile modulus of polyacrylonitrile was reported in the literature [56].

### 4.4.6. Hardness study

Table 4.4.1 shows the hardness results of polymer blend and WPC loaded with clay and different percentage of ZnO. Hardness value of the polymer blend increased after the addition of compatibilizer due to enhancement of interfacial adhesion between polymers. On addition of WF to the polymer blend, the hardness value was found to decrease. But after the

incorporation of nanoclay and ZnO to the WPC, hardness value was found to increase again. The improvement was due to combined effect of increase in interaction of clay and ZnO with wood flour and polymer. Hardness value was found maximum at 3 phr of clay/ZnO loading, after that it decreased. At higher loading of ZnO, the reinforcing action of ZnO might decrease due to agglomeration.

**Table 4.4.1.** Flexural, tensile and hardness properties of polymer blend and WPC loaded with nanoclay and different percentage of ZnO.

| Sample | Flexural properties | | Tensile properties | | Hardness (Shore D) |
|---|---|---|---|---|---|
| | Strength (MPa) | Modulus (MPa) | Strength (MPa) | Modulus (MPa) | |
| PB | 12.34 ± 0.36 | 756.41 ± 1.28 | 5.87 ± 1.21 | 85.42 ± 16.23 | 66.7 ± 0.3 |
| PB/G5 | 15.34 ± 1.08 | 1026.32 ± 1.07 | 9.04 ± 1.16 | 113.54 ± 17.23 | 68.4 ± 0.5 |
| PB/G5/W40 | 17.13 ± 1.11 | 3756.18 ± 1.15 | 17.82 ± 1.21 | 254.84 ± 18.26 | 66.8 ± 0.7 |
| PB/G5/W40/N3/Z1 | 28.14 ± 0.72 | 4843.81 ± 1.31 | 32.28 ± 1.47 | 603.45 ± 17.25 | 74.3 ± 0.2 |
| PB/G5/W40/N3/Z3 | 31.79 ± 1.12 | 5052.58 ± 1.36 | 35.65 ± 1.56 | 657.32 ± 17.16 | 79.4 ± 0.2 |
| PB/G5/W40/N3/Z5 | 29.25 ± 1.71 | 4927.41 ± 1.29 | 30.24 ± 1.14 | 629.87 ± 18.74 | 77.1 ± 0.3 |

### 4.4.7. Thermogravimetric analysis

Figure 4.4.6 and Table 4.4.2 shows the initial decomposition temperature ($T_i$), maximum pyrolysis temperature ($T_m$), decomposition temperature at different weight loss (%) ($T_D$) and residual weight (RW, %) for polymer blend and WPCs. It was observed that $T_i$ value increased after the incorporation of compatibilizer and WF to polymer blend. The value increased further after the addition of nanoclay and ZnO. $T_i$ value was found maximum when the concentration of ZnO was 3 phr. At higher concentration of ZnO, the $T_i$ value decreased again.

Both the polymer blend and composite showed two decomposition peaks. The $T_m$ value for the first step in both WPC and WPC loaded with clay and ZnO were due to the depolymerization of hemicellulose, glycosidic linkage of cellulose, thermal decomposition of cellulose [18] and dehydrochlorination of PVC [19,20] while the peak for second step was due to decomposition of HDPE and PP [21]. $T_m$ values of the composites for both the steps were found to follow the similar trend as those of $T_i$ values.

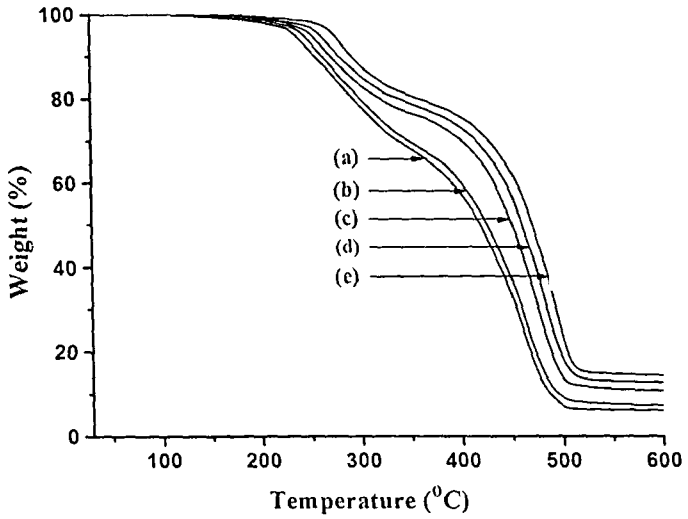


**Figure 4.4.6.** TGA thermographs of (a) PB (b) PB/G5/W40 (c) PB/G5/W40/N3/Z1 (d) PB/G5/W40/N3/Z5 (e) PB/G5/W40/N3/Z3.

The percentage weight losses of sample at different temperature are also listed in the table. WPC containing 3 phr nanoclay and 3 phr ZnO exhibited similar weight losses at higher temperatures compared to polymer blend, WPC and WPC containing 1 or 5 phr ZnO.

The incorporation of compatibilizer enhanced the interaction between the polymer blend and wood flour. The improvement of thermal stability after inclusion of compatibilizer and wood flour to polymer blend was reported by Awal et al. [17]. The silicate layers of nanoclay in nanocomposites provided a long tortuous path which delayed the diffusion of the decomposed volatile product through the composite. Nourbakhsh et al. [31] reported that thermal stability of wood polymer composite enhanced due to addition of clay. Moreover, the incorporation of modified ZnO nanopowder might play a role in enhancing the thermal stability by interacting with clay, wood and polymer through its surface hydroxyl group and cetyl groups respectively. At higher concentration of ZnO, the agglomeration (as evident by TEM study) probably decreased the interaction and could give rise to reduce the thermal stability. Laachachi et al. [59] studied the thermal degradation of PMMA by incorporation of ZnO and organo-modified MMT and found an increased in thermal stability of PMMA after the incorporation of ZnO and OMMT.

**Table 4.4.2.** Thermal analysis and limiting oxygen index (LOI) values of polymer blend and WPC loaded with nanoclay and different percentage of ZnO.

| Sample | $T_i$ | $T_m^a$ | $T_m^b$ | Temperature of decomposition ($T_D$) in °C at different weight loss (%) | | | | RW% at 600°C | LOI (%) |
|---|---|---|---|---|---|---|---|---|---|
| | | | | 20% | 40% | 60% | 80% | | |
| PB | 249 | 270 | 407 | 291 | 388 | 439 | 468 | 6.1 | 20 |
| PB/G5/W40 | 255 | 276 | 451 | 299 | 397 | 446 | 473 | 7.2 | 38 |
| PB/G5/W40/N3/Z1 | 277 | 326 | 503 | 330 | 459 | 484 | 501 | 10.8 | 53 |
| PB/G5/W40/N3/Z3 | 289 | 337 | 517 | 350 | 478 | 497 | 513 | 14.5 | 68 |
| PB/G5/W40/N3/Z5 | 281 | 330 | 510 | 336 | 465 | 490 | 508 | 12.7 | 66 |

$T_i$: value for initial degradation; $^aT_m$: value for 1st step; $^bT_m$: value for 2nd step.

### 4.4.8. Limiting oxygen index (LOI) results

Limiting oxygen index values of polymer blend, WPC and WPC loaded with nanoclay and ZnO are shown in Table 4.4.2. From the table, it was observed that with the addition of compatibilizer, LOI value of the polymer blend increased. The increase in the value was due to the increase in interfacial adhesion among the polymers by the compatibilizer. LOI value increased further after the addition of WF to the blend. The glycidyl and hydrocarbon part of the compatibilizer improved the interaction with the hydroxyl and hydrocarbon part of the wood and polymer. A substantial improvement in LOI value was observed after the addition of clay and ZnO. The value increased upto the addition of 3 phr each of nanoclay and ZnO. LOI value decreased at higher concentration of ZnO (5 phr). The nanoclay produced silicate char on the surface of WPC which increased the flame resistance property of the composite [48]. The tortuous path provided by the silicate layers had better barrier property to the oxygen and heat which delayed the burning capacity of the composite. The incorporation of CTAB modified ZnO enhanced the interaction between clay, wood and polymer through its hydroxyl and cetyl groups. ZnO nanoparticles also provided some thermal barrier to the oxygen and heat leading to an improvement in flame resistant property. At higher ZnO loading, the agglomeration of ZnO resulted in decrease of interaction and hence barrier property as well as LOI value.

### 4.4.9. UV test results

Figure 4.4.7 displays the weight loss of polymer blend, normal WPC and WPC loaded with nanoclay and ZnO (1-5 phr). Weight losses of the samples were determined as a function of exposure time at room temperature and were found nearly linear with exposure time. At early stage of exposure time, due to moisture uptake, a small increase of weight was found, which was greater than the material loss induced by the degradation in the early stage. The rate of weight loss was lowest for polymer blend followed by WPC filled with 3 phr ZnO and 3 phr clay, 5 phr ZnO and 3 phr clay, 1 phr ZnO and 3 phr clay. WPC showed the maximum weight losses. After 60 days of exposure, the maximum weight losses in polymer blend, normal WPC and clay loaded 1, 3, 5 phr ZnO containing WPCs were 1.27 % ± 0.19 %, 3.34 % ± 0.15 %, 2.71 % ± 0.23 %, 1.54 % ± 0.32 % and 2.19 % ± 0.47 % respectively.

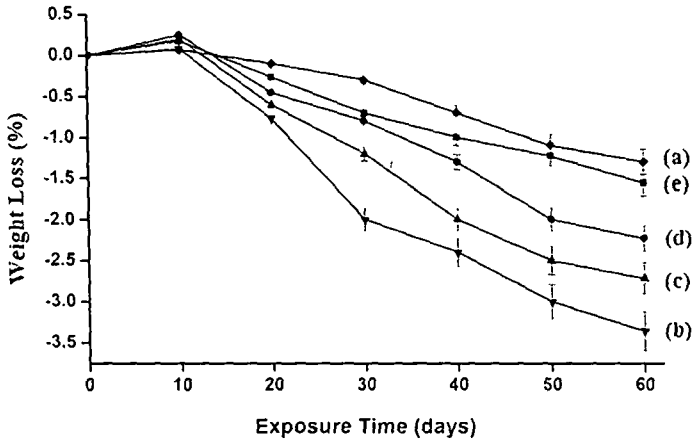


**Figure 4.4.7.** Weight losses vs. exposure time of (a) PB (b) PB/G5/W40 (c) PB/G5/W40/N3/Z1 (d) PB/G5/W40/N3/Z5 (e) PB/G5/W40/N3/Z3.

Figure 4.4.8 shows the carbonyl index values against time. After irradiation of the samples for 60 days, carbonyl peak intensity was found to increase (Fig. 4.4.9). Upon exposing the samples to UV radiation, chain scission of the polymer blend occurred that increased the carbonyl index value. The chain scission followed by decrease in the density of entanglements of polymer chain resulted in the decrease in weight of the samples. The polymer blend had lowest carbonyl index value (curve-4.4.8a). Due to higher oxidation of WF, normal wood polymer composite had highest carbonyl index value (curve-4.4.8b). The

carbonyl index values decreased upto the addition of 3 phr clay and ZnO after that it increased. ZnO nanoparticles played an important role in stabilizing the WPC by acting as screen and delayed the photo-degradation process. ZnO nanoparticles absorbed the UV

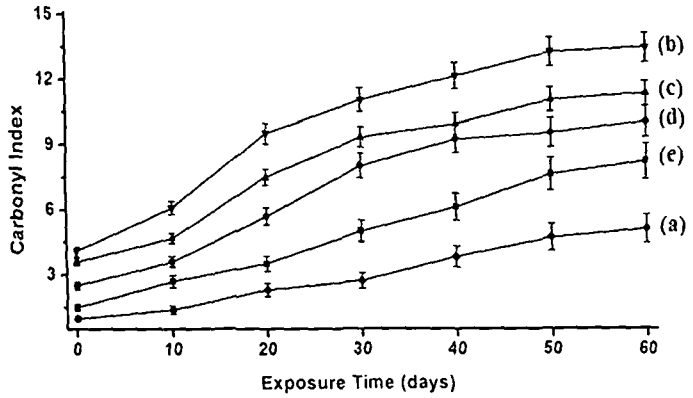


**Figure 4.4.8.** Carbonyl index values of (a) PB (b) PB/G5/W40 (c) PB/G5/W40/N3/Z1 (d) PB/G5/W40/N3/Z5 (e) PB/G5/W40/N3/Z3.

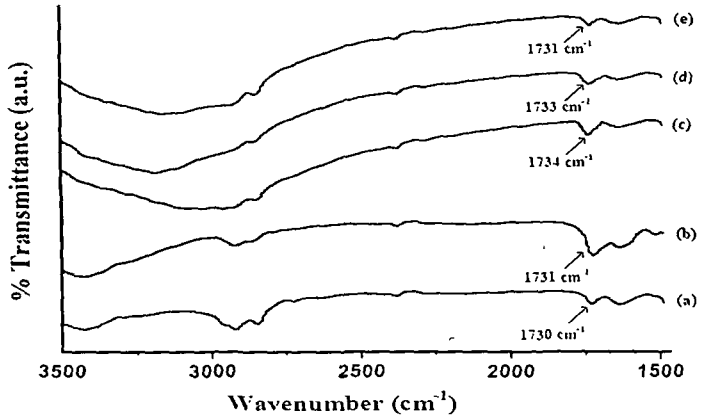


**Figure 4.4.9.** Change in carbonyl peak intensity of (a) PB (b) PB/G5/W40 (c) PB/G5/W40/N3/Z1 (d) PB/G5/W40/N3/Z5 (e) PB/G5/W40/N3/Z3.

radiation and observed an improvement in UV stability of polypropylene nanocomposite due to the incorporation of ZnO. The presence of nanoclay in the composite also had a screening effect that delayed the photo degradation process. Grigoriadou et al. [50] observed an increase in UV stability of HDPE after incorporating montmorillonite clay. Figure 4.4.10 represents the SEM micrographs of samples after 60 days of irradiation. The surface

morphology of the samples showed a drastic change due to exposure to UV radiation. The surface of normal WPC was more irregular compared to clay/ZnO treated WPC indicating that the normal WPC sample was less effective compared to ZnO/clay containing sample against UV radiation. WPC containing nanoclay and higher percentage of ZnO (5 phr) exhibited lower protection against UV radiation as shown by the decrease in surface smoothness compared to WPC loaded with 3 phr ZnO and nanoclay. This might be due to the agglomeration of ZnO which provided lower protection against photodegradation.

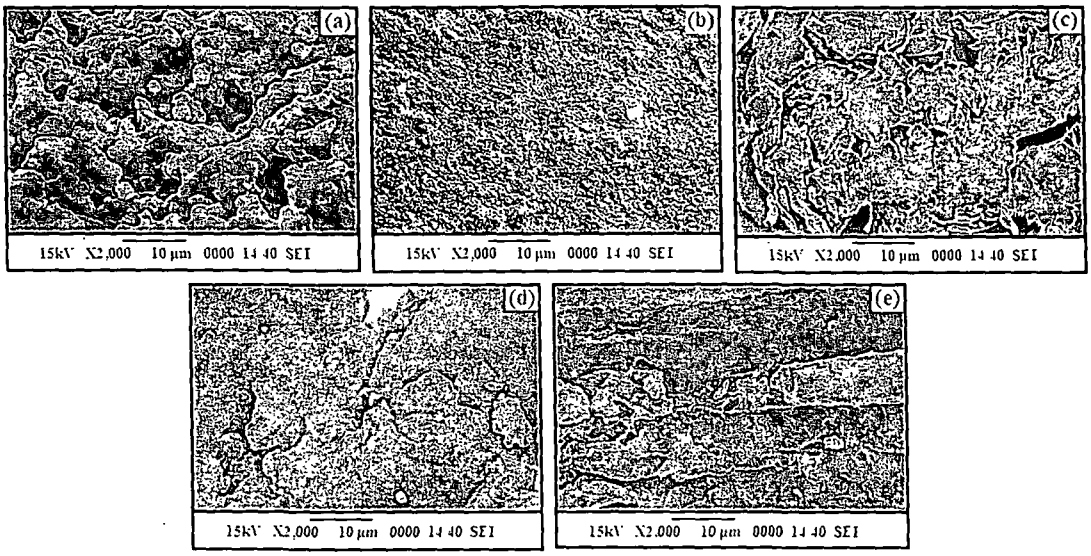


**Figure 4.4.10.** SEM micrographs of UV treated samples after 60 days (a) PB (b) PB/G5/W40 (c) PB/G5/W40/N3/Z1 (d) PB/G5/W40/N3/Z3 (e) PB/G5/W40/N3/Z5.

### 4.4.10. Water uptake and water vapour exclusion results

The water uptake and water vapour uptake results of polymer blend, PE-*co*-GMA treated polymer blend and WPC loaded with clay and different percentage of ZnO are shown in Figure 4.4.11. The water uptake capacity of polymer blend decreased after the addition of PE-*co*-GMA compatibilizer. The decreased in water uptake capacity of PE-*co*-GMA treated polymer blend was due to the increase in interfacial adhesion between the polymers by the compatibilizer. The value of water uptake capacity was suddenly increased after the addition of WF to the blend. The hydrophilic nature of wood flour caused an increase in the water uptake capacity. The water uptake capacity was decreased after the addition of clay/ZnO.

WPC loaded with 3 phr each of clay and ZnO showed lowest water uptake capacity followed by WPC with 3 phr clay and 1 phr ZnO, and WPC with 3 phr clay and 5 phr ZnO. The silicate layers of the clay provided tortuous path and increased the barrier property for water transport [51]. ZnO nanopowder also provided a barrier to the passage of water. Better the distribution of nanoparticles, the higher was the barrier property. ZnO nanoparticles at higher concentration were found to become agglomerated in the composite which resulted in an increase in water uptake capacity.

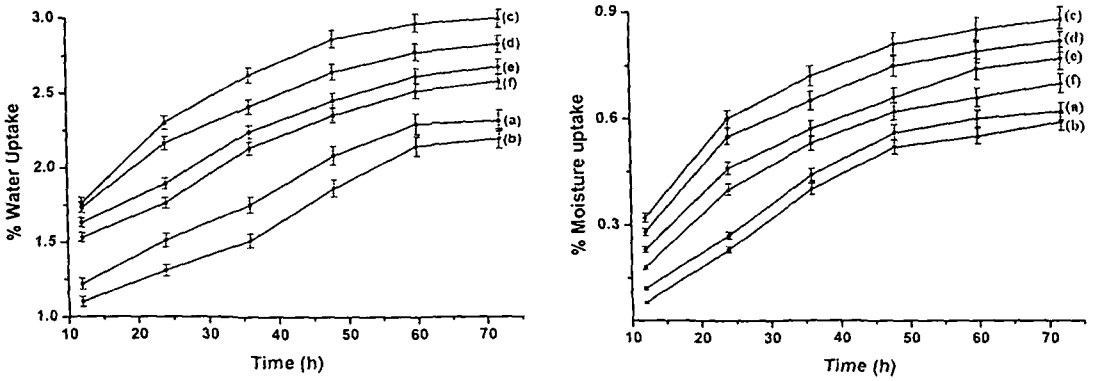


**Figure 4.4.11.** Percent water absorption and water vapour absorption of (a) PB (b) PB/G5 (c) PB/G5/W40 (d) PB/G5/W40/N3/Z1 (e) PB/G5/W40/N3/Z5 (f) PB/G5/W40/N3/Z3.

Water vapor exclusion test for the samples were carried out at 30 °C and 65 % relative humidity. The water vapour uptake was found to increase with time. The trend and explanation for water vapour absorption of different samples were similar to those of samples taken for water uptake study.

## *Section E*: Synergistic effect of $SiO_2$, ZnO and nanoclay on the physical and chemical properties of wood polymer nanocomposite.

Nanocomposite technology with layered silicate as reinforcing phase has been the subject matter of many discussions in recent years. Due to the high aspect ratio of silicate nanolayers, it is ideal for reinforcement and enhancing the properties. The performance of wood/polypropylene composite has been found to improve by the addition of nanoclay [60].

In the polymer composites, different types of fillers are used for improving the thermal, mechanical as well as other properties. Among them, different types of metal oxide nanoparticles such as $SiO_2$, $TiO_2$, ZnO etc. are widely used for these purposes. These are non toxic, stable and highly thermostable inorganic filler. An increase in the interfacial area between fillers and polymer can significantly improve the properties of the polymer. Polymer-$SiO_2$ composites have been explored as technological important due to their potential applications in electrochromic windows, fuel cells, chemical separation, electrochemical sensing, water treatment and in paint industries. Polymer-ZnO composites have also been used in solar cells, electrochromic windows, optical device, gas sensing and in antimicrobial application of food preservation [61].

The present study is aimed to discuss the effect of $SiO_2$ and ZnO nanopowder along with nanoclay to the thermal and mechanical properties of HDPE/LDPE/PP/PVC blend/wood/nanoclay composite. The aim is also to study the effect of nanoclay, $SiO_2$ and ZnO to other physical properties like water uptake, hardness and flame retardancy of the composites.

## 4.5. RESULTS & DISCUSSION

### 4.5.1. X-ray diffraction study

Figure 4.5.1 shows the XRD results of nanoclay, polymer blend, $SiO_2$, ZnO and wood polymer composite loaded with clay (3 phr) and different percentage of $SiO_2$ and ZnO (1-5 phr). The diffraction peak present at $2\theta = 4.11^{\circ}$ with basal spacing 2.15 nm is for the organically modified nanoclay (curve-4.5.1a). Curve-4.5.1b represents the diffractrogram of polymer blend. The most prominent wide-angle X-ray diffraction peaks appeared at $2\theta$ = 14.12 (200), 17.06 (040), 18.64 (211), 21.62 (110) and 24.02 (200) were for crystalline portion of different polymers present in the blend [4-7]. Curve-4.5.1c shows a broad diffraction peak at $2\theta = 23.5$ for the amorphous $SiO_2$ nanoparticles. The crystalline peaks appear above $2\theta = 30^{\circ}$ (shown in curve-4.5.1d) were the characteristic peaks of ZnO nanopowder [55]. Curves-4.5.1e-g was for WPC loaded with nanoclay (3 phr) and different percentage of $SiO_2$ and ZnO (1-5 phr). The diffractograms of composites did not exhibit any characteristic peak of nanoclay. This might be due to the exfoliation of silicate layers that leads to disappearance of the diffraction peak. With the increase in the level of incorporation of $SiO_2$ and ZnO (1-5 phr), the crystalline peak intensity of the polymer blend appeared in

the range $2\theta$ = 14-25° was found to decrease. Though the presence of amorphous portion of $SiO_2$ reduces the intensities of ZnO nanopowder but still the intensities of peak corresponding to ZnO nanopowder increased with the increase in the concentration of ZnO in the composite. Similar effect of $SiO_2$ on peak intensity was observed by Bao and Ma [2] while studying the X-ray diffraction profile of Na-MMT and $SiO_2$ on polymethacrylic acid composite. All these suggested that nanoclay layers were exfoliated and $SiO_2$ and ZnO particles were dispersed in the wood polymer matrix.

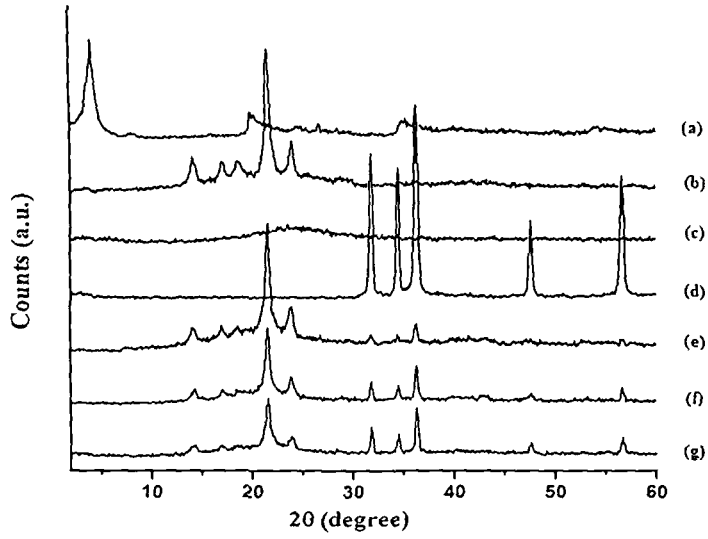


**Figure 4.5.1.** X-ray diffraction of (a) Nanoclay (b) PB (c) nano $SiO_2$ (d) nano ZnO (e) PB/G5/W40/N3/S1/Z1 (f) PB/G5/W40/N3/S3/Z3 (g) PB/G5/W40/N3/S5/Z5.

### 4.5.2. Transmission electron microscopy study

Figure 4.5.2 shows the TEM micrographs of WPC loaded with nanoclay (3 phr) and different percentage of $SiO_2$ and ZnO (1-5 phr). The dark lines correspond to the layers of nanoclay while the dark spots are for $SiO_2$ and ZnO nanoparticles. The $SiO_2$ and ZnO were well distributed in the WPC upto a concentration of 3 phr, beyond that a tendency to agglomeration (5 phr) was observed as shown in Figure 4.5.2c. Lee et al. [62] prepared nanosilica incorporated polypropylene/polypropylene elastomer blend and found that silica nanoparticles were well dispersed within the blend. At higher concentration of $SiO_2$ and ZnO, the distances between the particles became less and this might have enhanced the tendency for agglomeration.

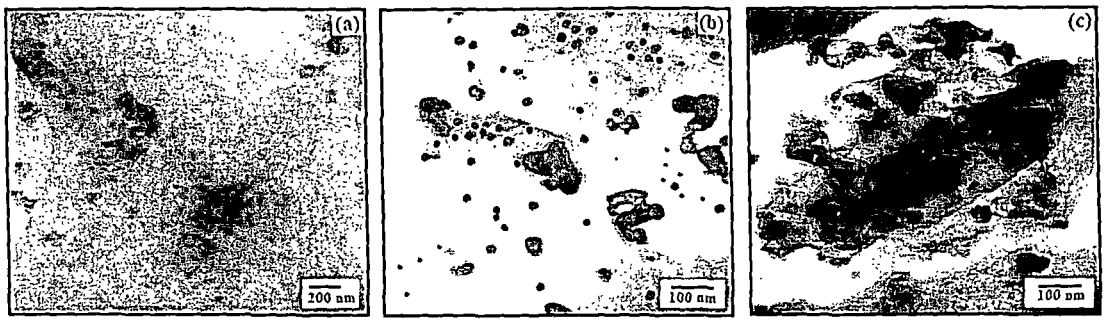


**Figure 4.5.2.** TEM micrographs of (a) PB/G5/W40/N3/S1/Z1 (b) PB/G5/W40/N3/S3/Z3 (c) PB/G5/W40/N3/S5/Z5.

### 4.5.3. Scanning electron microscopy study

SEM micrographs of polymer blend with and without compatibilizer, WPC and WPC loaded with nanoclay and different percentage of $SiO_2$ and ZnO nanopowder are represented in Figure 4.5.3. Figure 4.5.3a and 4.5.3b shows the miscibility among different polymers before and after addition of compatibilizer. The improved miscibility among polymers was due to the improved in interfacial adhesion among polymers by the compatibilizer [27]. The addition of wood flour improved the smoothness of composite (Fig. 4.5.3c). It was increased

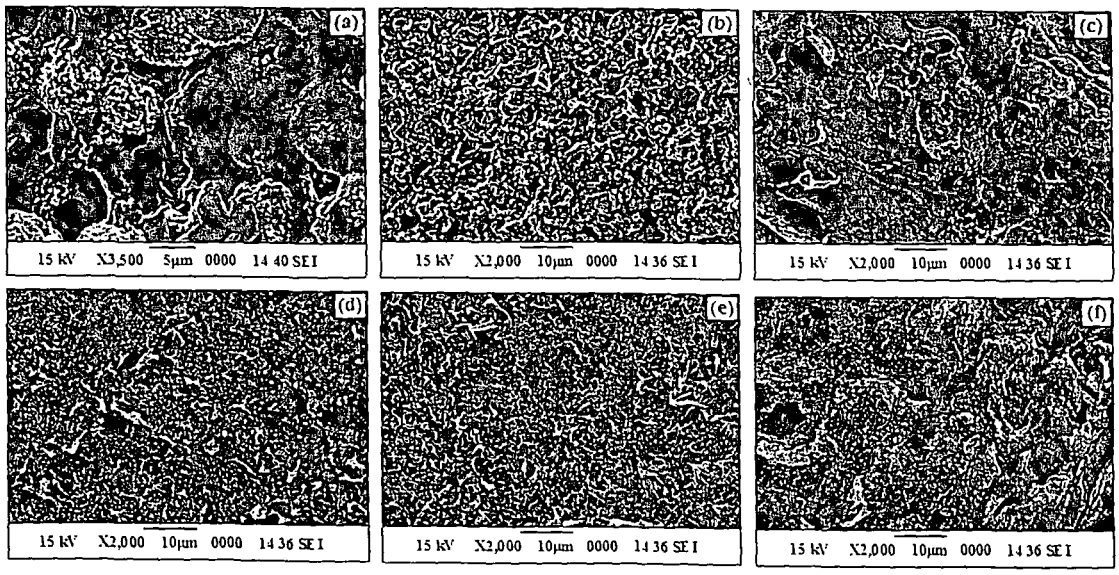


**Figure 4.5.3.** SEM micrographs of (a) PB (b) PB/G5 (c) PB/G5/W40 (d) PB/G5/W40/N3/S1/Z1 (e) PB/G5/W40/N3/S3/Z3 (f) PB/G5/W40/N3/S5/Z5.

further after the incorporation of wood flour, clay, $SiO_2$ and ZnO to the polymer blend (Fig. 4.5.3d-e). The surface smoothness of composite having 3 phr $SiO_2$ and ZnO and nanoclay appeared to be better compared to those of composite prepared with either 1 or 5 phr $SiO_2$/ZnO and nanoclay. This might be due to the improvement in interaction among PE-*co*-GMA, nanoclay, $SiO_2$, ZnO, wood and polymer. The decrease in smoothness at higher concentration of $SiO_2$ and ZnO was due to the aggregation of $SiO_2$ and ZnO. Wang et al. [63] observed the agglomeration of $SiO_2$ nanoparticles at higher loading while developing poly (methyl methacrylate)-$SiO_2$ nanocomposite film.

### 4.5.4. Fourier transform infrared spectroscopy study

FTIR spectra of CTAB, $SiO_2$, CTAB modified $SiO_2$, ZnO and CTAB modified ZnO are shown in Figure 4.5.4. In the spectrum of CTAB (Curve-4.5.4a), the absorption peaks at 2917 and 2847 are assigned to asymmetric and symmetric stretching modes of $-CH_2$ in the methylene chains. Presence of peaks at 1491, 1475 and 1396 $cm^{-1}$ are for the asymmetric and symmetric $CH_3$-$N^+$ deformation modes of the CTAB headgroup respectively [9]. The spectrum of unmodified $SiO_2$ shows absorption peaks at 3472 and 1633 $cm^{-1}$ for –OH stretching and –OH bending of hydroxyl group adsorbed on particle surface. The other peaks appeared in the range 1088-464 $cm^{-1}$ were due to Si-O-Si group in the $SiO_2$ [10]. On the spectrum of CTAB modified $SiO_2$, the peaks around 3424, 2931, 2852, 1633, 1481 $cm^{-1}$ and 1088-464 $cm^{-1}$ were found. The intensity of –OH stretching in the modified $SiO_2$ was found to decrease, indicating an interaction of the hydroxyl group absorbed on $SiO_2$ surface with CTAB. The other characteristic peaks for CTAB are also present in the curve. FTIR spectrum of unmodified ZnO nanoparticles is presented in Curve-4.5.4c. Absorption peaks at 3497 and 1635 $cm^{-1}$ in the spectra were due to –OH (-stretching) and –OH (-bending) vibrations while the peaks around 422 $cm^{-1}$ was due to the vibration of metal-oxygen (M-O) bond [58]. The FTIR spectrum of ZnO modified with CTAB is represented by the curve-4.5.4d. It was observed that the intensity of the peak for –OH group decreased to a desired extent. Besides this, two new peaks at 2918 and 2848 $cm^{-1}$, which were due to the presence of $-CH_2$ group of CTAB were appeared in the spectrum. The peaks at 1496 $cm^{-1}$ and 1476 $cm^{-1}$ were due to the asymmetric $CH_3$-$N^+$ deformation mode of the CTAB headgroup. Another peak present at 1397 $cm^{-1}$ was due to the symmetric $CH_3$-$N^+$ deformation mode of CTAB headgroup [9]. These results indicated that long chain of CTAB group had been incorporated on the surface of the ZnO nanoparticles. Further, CTAB modified $SiO_2$ and

ZnO was dispersed in a flask containing xylene and kept for checking of any settling of particles. The dispersion of ZnO was found to be stable. This indicated that proper modification occurred.

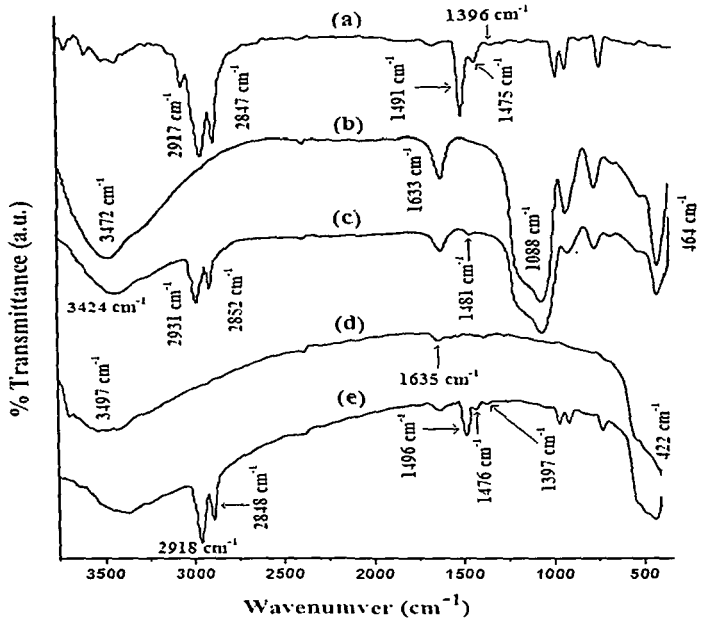


**Figure 4.5.4.** FTIR spectra of (a) CTAB (b) unmodified $SiO_2$ (c) CTAB modified $SiO_2$ (d) unmodified ZnO (e) CTAB modified ZnO.

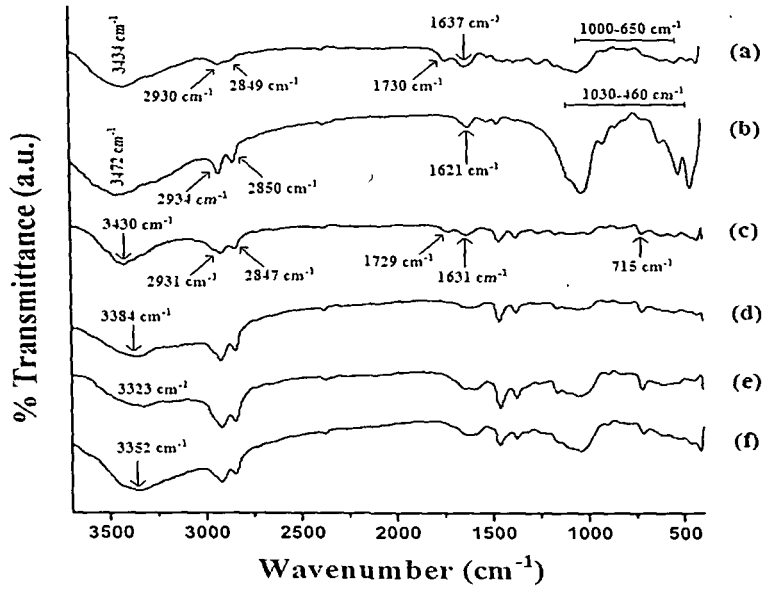


**Figure 4.5.5.** FTIR spectra of (a) Wood (b) Nanoclay (c) PB/G5/W40 (d) PB/G5/W40/N3/S1/Z1 (e) PB/G5/W40/N3/S3/Z3 (f) PB/G5/W40/N3/S5/Z5.

Figure 4.5.5 shows the FTIR spectra of wood, nanoclay, WPC and WPC loaded with nanoclay with different percentage of $SiO_2$ and ZnO. Curve-4.5.5a representing the wood sample shows the presence of bands at 3433 $cm^{-1}$ for –OH stretching, 2930 and 2849 $cm^{-1}$ for –CH stretching, 1730 $cm^{-1}$ for C=O stretching, 1637 $cm^{-1}$ for –OH bending, 1161 and 1045 $cm^{-1}$ for C–O stretching and 1000–650 $cm^{-1}$ for C-H bending (out of plane) vibration. Organically modified nanoclay (curve-4.5.5b) exhibits the peaks at 3472 $cm^{-1}$ (–OH stretching), 2934 and 2850 $cm^{-1}$ (–CH stretching of modified hydrocarbon), 1621 $cm^{-1}$ (–OH bending) and 1030-460 $cm^{-1}$ (oxide bands of metals like Si, Al, Mg etc.). PB/G5/W40 (curve-4.5.5c) shows peaks at 3430 $cm^{-1}$ (-OH stretching), 2931 and 2847 $cm^{-1}$ (-CH stretching), 1729 $cm^{-1}$ (C=O stretching), 1631 $cm^{-1}$ (-OH bending) and 715 $cm^{-1}$ (-$CH_2$ stretching).

Curves-4.5.5d-f represents the FTIR spectra of WPC loaded with 3 phr nanoclay and 1, 3 and 5 phr of $SiO_2$ and ZnO. From the figure, it was observed that the intensity of –OH stretching was decreased and shifted to 3384 $cm^{-1}$ (curve-4.5.5d), 3323 $cm^{-1}$ (curve-4.5.5e) and 3352 $cm^{-1}$ (curve-4.5.5f) from 3434 $cm^{-1}$ (wood). The decrease in intensity and shifting to lower wavelength confirmed the bond formation between polymer and the hydroxyl groups of wood, nanoclay, $SiO_2$ and ZnO. Moreover, the intensity of –CH stretching peaks at 2930 $cm^{-1}$ and 2849 $cm^{-1}$ (curves-4.5.5d-f) was found to increase. Similar decrease in intensity of –OH absorption peak and shifting to lower wave number along with increase in –CH peak intensities was observed by Awal et al. [17]. The peak intensities (1088-464 $cm^{-1}$) of metal oxides bond of $SiO_2$, ZnO and nanoclay (curves-4.5.5d-f) was decreased to a considerable extent. All these suggested a strong interaction between wood, nanoclay, $SiO_2$, ZnO and polymer.

### 4.5.5. Mechanical property study

Table 4.5.1 shows the flexural and tensile properties of polymer blends and WPC loaded with nanoclay and different percentage of $SiO_2$ and ZnO nanopowder. After incorporation of compatibilizer, both flexural and tensile properties of the polymer blend increased. This is because of the increased in interfacial adhesion between the polymers due to which both flexural and tensile properties increased. The flexural and tensile properties of the composite were improved further after the addition of WF. WF acted as a load carrier, reinforced the composites and increased the flexural and tensile properties. Nourbakhsh et al. [31] developed wood flour/polypropylene composite and found an improvement in

mechanical properties due to reinforcement by wood flour. Moreover, the compatibilizer, PE-*co*-GMA, provided strong interfacial adhesion between wood and polymers through its glycidyl linkage and long olefinic chain. Sailaja [45] used poly(ethylene-*co*-glycidyl methacrylate) as compatibilizer to improve the compatibility of wood pulp-LDPE composite. The properties of the WPCs were further improved after the incorporation of clay, $SiO_2$ and ZnO nanopowder. At a fixed clay loading (3 phr), both flexural and tensile properties improved upto addition of 3 phr of $SiO_2$ and ZnO. At higher amount of $SiO_2$ and ZnO (5 phr) loading, the properties were found to be decreased. The observed higher values might be due to the combined effect of nanoclay, $SiO_2$ and ZnO. The silicate layers of nanoclay acted as a reinforcing agent and the long polymer chains inserted inside its gallery space and restricted the mobility of the polymer chain. Lei et al. [51] found an increase in mechanical properties of wood/HDPE composite after incorporation of nanoclay. CTAB modified $SiO_2$ and ZnO improved the interaction between clay, wood and polymer through its surface hydroxyl group and cetyl group respectively. Higher the dispersion of nanoparticles, higher would be the interaction. At higher level of $SiO_2$ and ZnO loading (5 phr), the agglomeration occurred and hence the interaction of ZnO with the clay, polymer and wood decreased. Liu and Kontopoulou [64] observed an increase in mechanical properties of thermoplastic olefin/nanosilica composite at lower loading of nanosilica. The increase in tensile modulus of polyacrylonitrile due to the interaction of ZnO nanoparticles was reported in the literature [56].

**Table 4.5.1.** Flexural, tensile and hardness properties of polymer blend and WPC loaded with nanoclay and different percentage of $SiO_2$ and ZnO.

| Sample | Flexural properties | | Tensile properties | | Hardness |
|---|---|---|---|---|---|
| | Strength (MPa) | Modulus (MPa) | Strength (MPa) | Modulus (MPa) | (Shore D) |
| PB | 13.97 ± 1.01 | 762.72 ± 1.03 | 6.35 ± 1.21 | 93.51 ± 17.49 | 66.3 ± 0.6 |
| PB/G5 | 17.31 ± 0.85 | 1052.76 ± 1.07 | 9.87 ± 1.29 | 125.54 ± 16.71 | 67.9 ± 0.4 |
| PB/G5/W40 | 20.14 ± 1.02 | 3887.63 ± 1.06 | 20.02 ± 1.31 | 267.15 ± 17.64 | 67.2 ± 0.5 |
| PB/G5/W40/N3/S1/Z1 | 29.12 ± 1.63 | 4934.75 ± 1.19 | 34.37 ± 1.21 | 598.43 ± 16.62 | 78.4 ± 0.7 |
| PB/G5/W40/N3/S3/Z3 | 34.19 ± 0.87 | 5184.27 ± 0.83 | 37.88 ± 1.07 | 684.32 ± 18.34 | 81.0 ± 0.2 |
| PB/G5/W40/N3/S5/Z5 | 31.26 ± 1.14 | 5047.24 ± 1.11 | 35.36 ± 1.23 | 632.73 ± 20.63 | 79.1 ± 0.2 |

### 4.5.6. Hardness results

Table 4.5.1 shows the hardness results of polymer blend and WPC loaded with clay and different percentage of $SiO_2$ and ZnO. Addition of compatibilizer increased the hardness value of the polymer blend. The hardness value was found to decrease on addition of WF to the polymer blend. But after the incorporation of nanoclay, $SiO_2$ and ZnO, hardness value of the WPC was found to increase again. The improvement was due to combined effect of decrease in mobility of intercalated polymer chain and increase in reinforcing action of $SiO_2$ and ZnO. Hardness value was found maximum at 3 phr of clay/$SiO_2$/ZnO loading, after that it decreased. The reason was explained earlier.

### 4.5.7. Thermogravimetric analysis

Initial decomposition temperature ($T_i$), maximum pyrolysis temperature ($T_m$), decomposition temperature at different weight loss (%) ($T_D$) and residual weight (RW, %) for polymer blend and WPCs are shown in Table 4.5.2. $T_i$ value of the polymer blend increased after the incorporation of compatibilizer and WF. The addition of nanoclay, $SiO_2$ and ZnO nanoparticle further increased the $T_i$ value. It was found maximum at 3 phr $SiO_2$ and ZnO loading. At higher concentration of $SiO_2$ and ZnO, the $T_i$ value decreased again.

Both the polymer blend and composite showed two decomposition peaks. The $T_m$ value for the first step in both WPC and WPC loaded with clay, $SiO_2$ and ZnO were due to the depolymerization of hemicellulose, glycosidic linkage of cellulose, thermal decomposition of cellulose [18] and dehydrochlorination of PVC [19,20] while the peak for second step was due to decomposition of HDPE and PP [21]. $T_m$ values of the composites for both the steps were found to follow the similar trend as those of $T_i$ values.

The percentage weight losses of sample at different temperature are listed in Table 4.5.2. $T_D$ values of composite containing nanoclay, $SiO_2$, ZnO were more compared to either polymer blend or polymer/wood composites. The higher the percentage of ZnO and $SiO_2$, the higher was the decomposition temperature.

The compatibilizer enhanced the interaction between the polymer blend and wood flour and as a result thermal stability improved. Araujo et al. [65] reported the improvement of thermal stability after inclusion of compatibilizer to high density polyethylene and natural fiber composite. The silicate layers present in nanoclay of the composites provided a long

tortuous path which delayed the diffusion of the decomposed volatile products through the composite. The improvement in thermal stability of wood flour and polypropylene

**Table 4.5.2.** Thermal analysis and limiting oxygen index (LOI) values of polymer blend and WPC loaded with nanoclay, $SiO_2$ and ZnO.

| Sample | $T_i$ | $T_m{}^a$ | $T_m{}^b$ | Temperature of decomposition ($T_D$) in °C at different weight loss (%) | | | | RW% at 600°C | LOI (%) |
|---|---|---|---|---|---|---|---|---|---|
| | | | | 20% | 40% | 60% | 80% | | |
| PB | 248 | 266 | 403 | 288 | 389 | 439 | 468 | 6.2 | 21 |
| PB/G5 | 251 | 271 | 409 | 292 | 393 | 443 | 471 | 6.7 | 34 |
| PB/G5/W40 | 256 | 279 | 453 | 297 | 399 | 448 | 475 | 9.7 | 37 |
| PB/G5/W40/N3/S1/Z1 | 281 | 330 | 508 | 336 | 464 | 488 | 507 | 10.6 | 64 |
| PB/G5/W40/N3/S3/Z3 | 294 | 339 | 521 | 356 | 482 | 504 | 519 | 14.7 | 70 |
| PB/G5/W40/N3/S5/Z5 | 287 | 335 | 516 | 341 | 471 | 495 | 513 | 12.6 | 67 |

$T_i$: value for initial degradation; $^aT_m$: value for 1st step; $^bT_m$: value for 2nd step.

composite after addition of nanoclay was reported by Tabari et al. [66]. Moreover, the incorporation of CTAB modified $SiO_2$ and ZnO nanopowder might play a role in enhancing the thermal stability by interacting with clay, wood and polymer through its surface hydroxyl group and cetyl groups respectively. At higher loading of $SiO_2$ and ZnO, the interaction of $SiO_2$, ZnO and clay with wood and polymer might decrease due to agglomeration and hence a reduction in thermal stability was observed. Bailly and Kontopoulou [67] developed thermoplastic olefin/nanosilica composite and found an increase in thermal properties due to the incorporation of nanosilica. The increase in thermal stability was also reported by He et al. [68] while studying the thermal behavior of PET-ZnO nanocomposite.

### 4.5.8. Limiting oxygen index (LOI) results

Limiting oxygen index values of polymer blend, WPC and WPC loaded with nanoclay, $SiO_2$ and ZnO are shown in Table 4.5.2. LOI value of the polymer blend increased after the incorporation of compatibilizer. The compatibilizer increased the interfacial adhesion among the polymers and thus increased the LOI value. The value was further

increased after the addition of WF to the blend. The glycidyl and hydrocarbon part of the compatibilizer improved the interaction with the hydroxyl and hydrocarbon part of the wood and polymer respectively. A substantial improvement in LOI value was observed after the addition of clay, $SiO_2$ and ZnO. At a fixed nanoclay loading (3 phr), the LOI value increased upto the addition of 3 phr each of $SiO_2$ and ZnO. Beyond that LOI value decreased with the increase in the loading of both $SiO_2$ and ZnO. The nanoclay produced silicate char on the surface of WPC which increased the flame resistance property of the composite [48]. The tortuous path provided by the silicate layers had better barrier property to the oxygen and heat which delayed the burning capacity of the composite. The incorporation of CTAB modified $SiO_2$ and ZnO enhanced the interaction between clay, wood and polymer through their hydroxyl and cetyl groups. The nanoparticles also provided a thermal barrier to oxygen and heat leading to an improvement in flame resistant property. The improvement in flame resistance property of polymer composites after the incorporation of $SiO_2$ and ZnO was observed in the literature [34,69]. At higher $SiO_2$ and ZnO loading, the agglomeration of nanoparticles resulted in the decrease of interaction and hence exhibited reduction in barrier property as well as LOI values.

### 4.5.9. UV test results

The weight loss of polymer blend, normal WPC and WPC loaded with nanoclay, $SiO_2$ and ZnO (1-5 phr) are shown in Figure 4.5.6. Weight losses of the samples were determined at room temperature as a function of exposure time and were observed almost linear with exposure time. At early stage of exposure time, a small increase of weight was found due to moisture uptake by the samples, which was greater than the material loss induced by the degradation in the early stage. The rate of weight loss was lowest for polymer blend followed by PB/G5/W40/N3/S3/Z3, PB/G5/W40/N3/S5/Z5 and PB/G5/W40/N3/S1/Z1. WPC showed the maximum weight losses. After 60 days of exposure, the weight losses in polymer blend, PB/G5/W40, PB/G5/W40/N3/S1/Z1, PB/G5/W40/N3/S3/Z3 and PB/G5/W40/N3/S5/Z5 were 1.22 % ± 0.14 %, 3.27 % ± 0.18 %, 2.24 % ± 0.12 %, 1.43 % ± 0.14 % and 2.03 % ± 0.21 % respectively.

Figure 4.5.7 shows the carbonyl index values against time. It was observed that the carbonyl peak intensity was increased after the irradiation of the samples to UV light for 60 days (Fig. 4.5.8). The increase in carbonyl index value was due to the chain scission of the polymer blend and WPNC. This resulted in decrease in the density of entanglements of

polymer chain and decrease in weight of the samples. The polymer blend had lowest carbonyl index value (curve-4.5.7a). Normal wood polymer composite showed highest

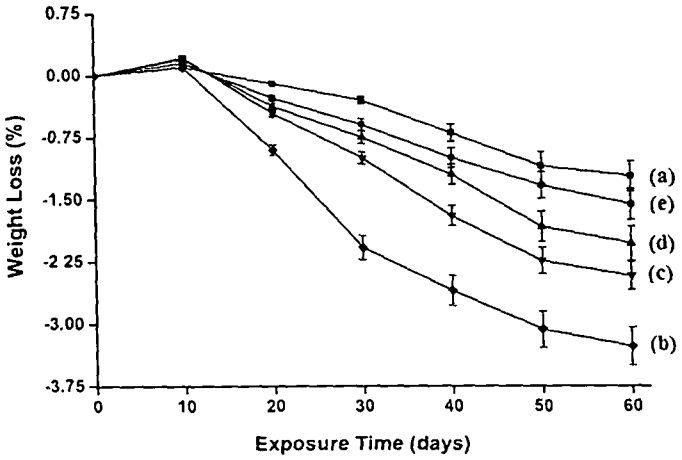


**Figure 4.5.6.** Weight losses vs. exposure time of (a) PB (b) PB/G5/W40 (c) PB/G5/W40/N3/S1/Z1 (d) PB/G5/W40/N3/S5/Z5 (e) PB/G5/W40/N3/S3/Z3.

carbonyl index value due to higher oxidation of WF (curve-4.5.7b). The addition of clay, $SiO_2$ and ZnO decreased the carbonyl index value. Maximum decrease in carbonyl index value was observed on addition of 3 phr each of clay, $SiO_2$ and ZnO. The value increased again on addition of 3 phr clay and 5 phr each of $SiO_2$ and ZnO. Nanoclay alongwith $SiO_2$ and ZnO played an important role in stabilizing the WPC by acting as a barrier to UV radiation that delayed the photo-degradation process. An increase in UV stability of HDPE after incorporating of MMT clay was reported by Grigoriadou et al. [50]. $SiO_2$ and ZnO nanoparticles present in the composites absorbed the UV radiation and hence reduced the UV intensity required for the oxidation of the WPC. Cao et al. [70] studied the UV shielding properties of ZnO nanoparticles modified with $SiO_2$ and trimethyl siloxane and observed an improvement in UV stability compared to unmodified ZnO. The change in the surface morphology of the samples after 60 days of UV exposure was shown in Figure 4.5.9. The surface morphology of the samples showed a drastic change due to exposure to UV radiation. Normal WPC samples were more susceptible to attack by UV radiation compared to WPC loaded with nanoclay/$SiO_2$/ZnO. The surface was more irregular in normal WPC compared to that of WPC containing nanoclay/$SiO_2$/ZnO. $SiO_2$ and ZnO nanoparticles were well distributed in WPC loaded with 3 phr each of nanoclay/$SiO_2$ and ZnO and exhibited

lowest degradation when exposed to UV irradiation. WPC containing nanoclay (3 phr) and higher percentage of $SiO_2$ and ZnO (5 phr) exhibited lower protection against UV radiation as shown by the decrease in surface smoothness. This might be due to the agglomeration of the nanoparticles which provided lower protection against photodegradation.

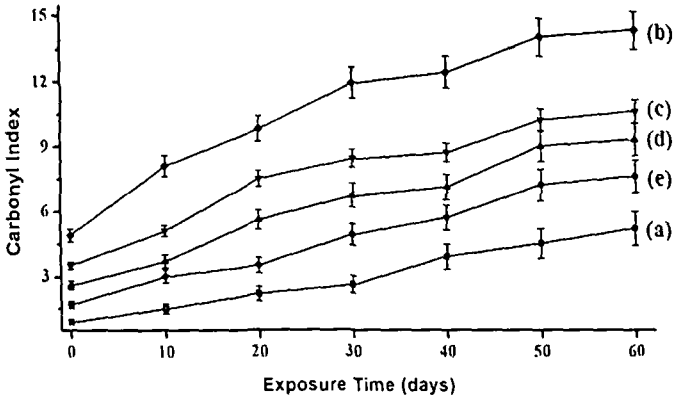


**Figure 4.5.7.** Carbonyl index values of (a) PB (b) PB/G5/W40 (c) PB/G5/W40/N3/S1/Z1 (d) PB/G5/W40/N3/S5/Z5 (e) PB/G5/W40/N3/S3/Z3.

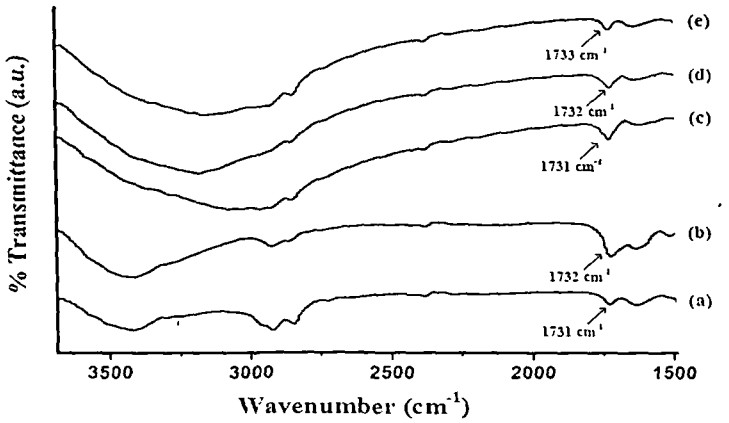


**Figure 4.5.8.** Change in carbonyl peak intensity of (a) PB (b) PB/G5/W40 (c) PB/G5/W40/N3/S1/Z1 (d) PB/G5/W40/N3/S5/Z5 (e) PB/G5/W40/N3/S3/Z3.

The changes in the hardness, flexural and tensile properties of the composites before and after the UV treatment are presented in Table 4.5.3 and 4.5.4. From the table, it was observed that the loss of mechanical properties was more significant in normal WPC

compared to the WPC loaded with nanoparticles. WPC was more prone to UV attack and hence it showed maximum loss of mechanical properties. WPC loaded with the nanoparticles offered shielding effect and as a result it showed a less reduction in mechanical properties.

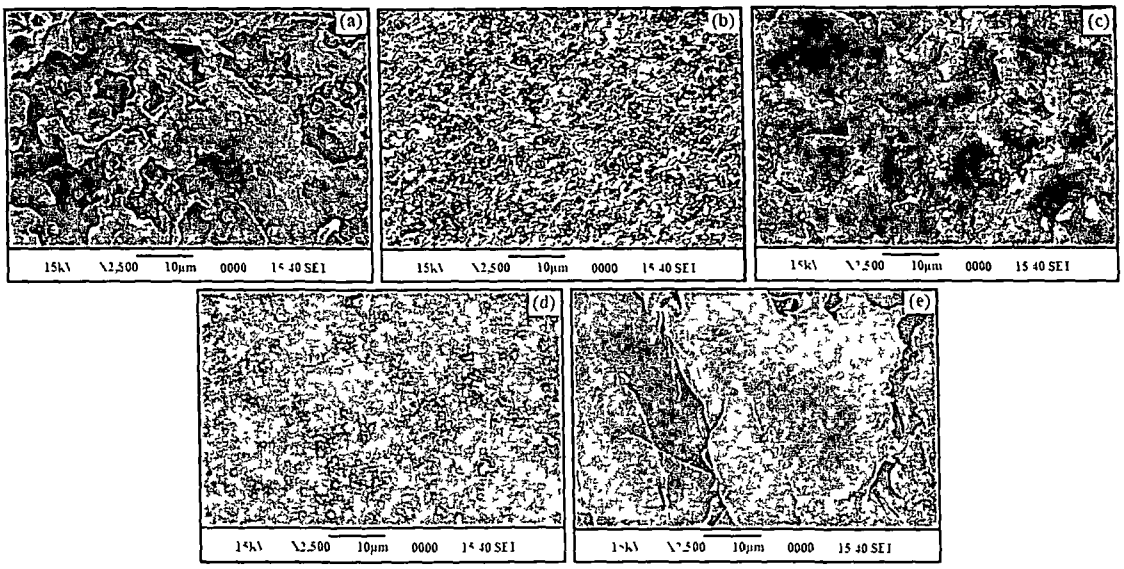


**Figure 4.5.9.** SEM micrographs of UV treated samples after 60 days (a) PB (b) PB/G5/W40 (c) PB/G5/W40/N3/S1/Z1 (d) PB/G5/W40/N3/S3/Z3 (e) PB/G5/W40/N3/S5/Z5.

**Table 4.5.3.** Hardness properties of WPC loaded with nanoclay and different percentage of $SiO_2$ and ZnO after UV radiation, microbial attack and soil burial test.

| Sample | UV radiation | | Microbial attack | | Soil burial test | |
|---|---|---|---|---|---|---|
| | Before | After | Before | After | Before | After |
| PB/G5/W40 | 67 2 ± 0 5 | 55 4 ± 0 3 | 66 8 ± 0 1 | 59 1 ± 0 6 | 67 7 ± 0 5 | 58 3 ± 0 1 |
| PB/G5/W40/N3/S1/Z1 | 78 4 ± 0 7 | 69 2 ± 0 6 | 77 5 ± 0 2 | 56 3 ± 0 4 | 76 9 ± 0 8 | 57 9 ± 0 2 |
| PB/G5/W40/N3/S3/Z3 | 81 0 ± 0 2 | 74 7 ± 0 4 | 82 2 ± 0 6 | 66 2 ± 0 3 | 80 4 ± 0 4 | 68 1 ± 0 7 |
| PB/G5/W40/N3/S5/Z5 | 79 1 ± 0 2 | 72 6 ± 0 7 | 78 7 ± 0 4 | 60 7 ± 0 2 | 78 2 ± 0 9 | 59 9 ± 0 8 |

**Table 4.5.4.** Flexural and tensile properties of WPC loaded with nanoclay and different percentage of $SiO_2$ and ZnO before and after UV treatment.

| Sample | Flexural Properties | | | | Tensile Properties | | | |
|---|---|---|---|---|---|---|---|---|
| | Before degradation | | After degradation | | Before degradation | | After degradation | |
| | Strength (MPa) | Modulus (MPa) | Strength (MPa) | Modulus (MPa) | Strength (MPa) | Modulus (MPa) | Strength (MPa) | Modulus (MPa) |
| PB/G5/W40 | 21.05 ± 1.11 | 3794.11 ± 1.04 | 14.03 ± 1.12 | 3014.71 ± 1.15 | 22.62 ± 1.05 | 295.86 ± 16.58 | 14.24 ± 1.08 | 206.35 ± 14.75 |
| PB/G5/W40/N3/S1/Z1 | 27.96 ± 1.03 | 4685.31 ± 1.01 | 22.73 ± 1.08 | 4157.28 ± 1.13 | 34.79 ± 1.07 | 647.74 ± 16.75 | 25.53 ± 1.14 | 542.85 ± 16.01 |
| PB/G5/W40/N3/S3/Z3 | 34.87 ± 1.01 | 4971.26 ± 1.09 | 29.25 ± 1.11 | 4361.74 ± 1.06 | 37.85 ± 1.12 | 714.63 ± 17.39 | 30.29 ± 1.06 | 623.47 ± 18.36 |
| PB/G5/W40/N3/S5/Z5 | 30.02 ± 1.05 | 4822.52 ± 1.13 | 27.76 ± 1.07 | 4133.29 ± 1.11 | 33.18 ± 1.02 | 607.71 ± 17.65 | 28.48 ± 1.10 | 526.14 ± 16.72 |

### 4.5.10. Chemical resistance test

Chemical resistance test of WPC and WPC loaded with nanoclay and different percentage of $SiO_2$ and ZnO loading under different environment are presented in Figure 4.5.10. From the figure, it was observed that HCl solution was more effective compared to $H_2O_2$ in decreasing the weight of all composites samples. The decrease in weight percent in HCl solution might be due to the degradation of wood fiber by the acid. It was observed that WPC loaded with 3 phr each of clay, $SiO_2$ and ZnO showed maximum chemical resistance. This might be due to the tortuous path provided by the silicate layers of nanoclay and the barrier property offered by the nanoparticles. The nanoparticles might attract the water molecules and decreased the diffusion coefficient of water. The better the distribution of nanoparticles, the lower is the diffusion of water. The even distribution of nanoparticles in the WPC having 3 phr each of clay and nanoparticles provided maximum chemical resistance. The agglomeration occurred at higher percentage of nanoparticles and hence lower chemical resistance was observed. Tajvidi et al. [71] reported that polypropylene/natural fibre composite was affected more in HCl, NaOCl compared to $H_2O_2$, acetone, soap etc. when immersed in their respective solution.

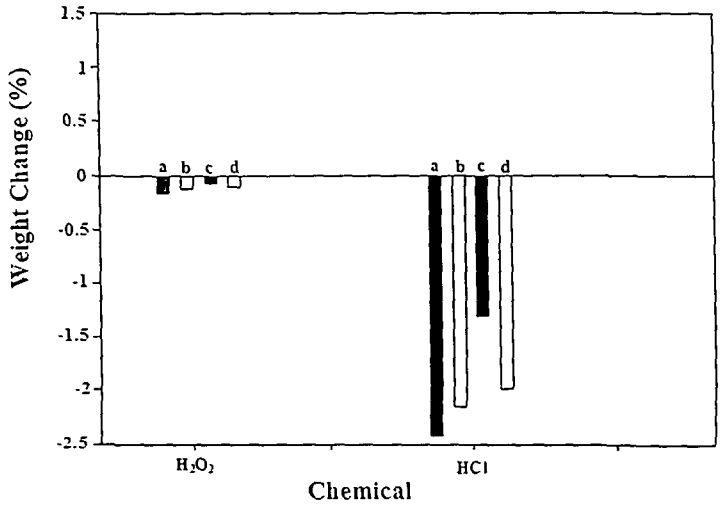


**Figure 4.5.10.** Chemical resistance test for (a) PB/G5/W40 (b) PB/G5/W40/N3/S1/Z1 (c) PB/G5/W40/N3/S3/Z3 (d) PB/G5/W40/N3/S5/Z5.

## 4.5.11. Biodegradation study

### *4.5.11.1. Decay evaluation and microscopic analysis*

WPC and WPNC samples were exposed to cellulolytic bacterial strain directly in broth culture medium for the biodegradation study. After one month of incubation of the samples in broth culture media, the growth of bacteria and biodegradation rate was clearly detectable. The bacterial growth of the samples with respect to time is represented by Figure 4.5.11. The rate of microbial attack was more in WPC loaded with wood and nanoparticles. Initially, the growth of the bacterial strains was increased quite steadily with bacterial exposure time, but the rate of growth decreased after three months of incubation. The higher rate of bacterial growth in the composite compared to the polymer blend was due to the presence of wood which acted as a carbon source for the bacteria. The powerful cellulolytic and pectinolytic activity of bacteria might play an important role in the enhancement of bacterial growth [72]. Furthermore, the *Bacillus sp.* bacteria could degrade the lignin present in wood [73]. After three months, the rate of microbial growth was decreased due to production of toxic metabolites by the microbes. The growth of bacteria and degradation of

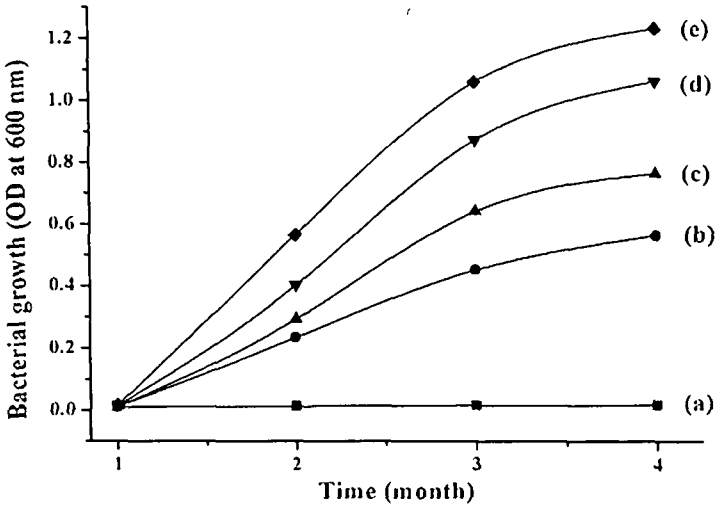


**Figure 4.5.11.** Growth of *Bacillus sp.* on (a) PB (b) PB/G5/W40 (c) PB/G5/W40/N3/S1/Z1 (d) PB/G5/W40/N3/S3/Z3 (e) PB/G5/W40/N3/S5/Z5.

the composites was also supported by the SEM study (Fig. 4.5.12). The rate of degradation of the composites increased with increasing the concentration of nanoparticles in wood

composite. The catalytic role played by the nano particles may be the cause of this degradation pattern [36]. Moreover, the mechanical properties of the degraded WPC samples were also found to decrease after the microbial degradation (Table 4.5.3 and 4.5.5). The bacteria might break the chemical and physical bond within the composite and thereby reduced the mechanical properties.

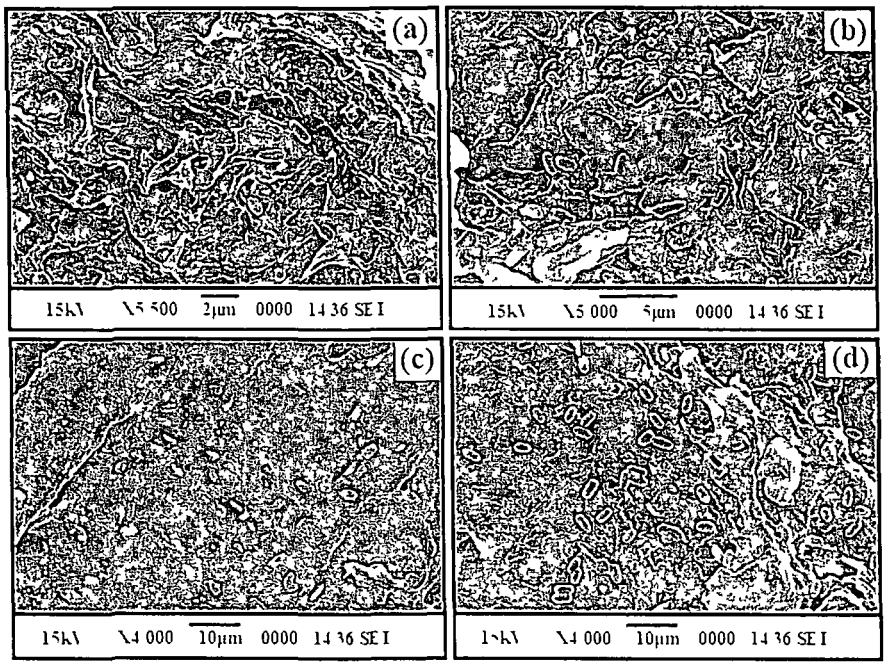


**Figure 4.5.12.** SEM micrographs of samples after microbial test on (a) PB/G5/W40 (b) PB/G5/W40/N3/S1/Z1 (c) PB/G5/W40/N3/S3/Z3 (d) PB/G5/W40/N3/S5/Z5

*4 5 11 2 Soil burial test*

The composite samples loaded with different percentage of nanoparticles were exposed to natural microbial consortium during in vitro soil experiments for three months. Soil microflora constituted a mixed microbial population (including bacteria, actinomycetes and fungi) which may act synergistically during degradation and reproduced under naturally occurring conditions [74].

Wood composites under soil burial experiment were collected after 90 days and the morphological change and growth of microorganism was checked from SEM micrographs (Fig 4.5 13) The growth of actinomycetes on the surface of wood composite was observed

**Table 4.5.5.** Flexural and tensile properties of WPC loaded with nanoclay and different percentage of $SiO_2$ and ZnO after microbial degradation.

| Sample | Flexural Properties | | | | Tensile Properties | | | |
|---|---|---|---|---|---|---|---|---|
| | Before degradation | | After degradation | | Before degradation | | After degradation | |
| | Strength (MPa) | Modulus (MPa) | Strength (MPa) | Modulus (MPa) | Strength (MPa) | Modulus (MPa) | Strength (MPa) | Modulus (MPa) |
| PB/G5/W40 | 21.26 ± 1.04 | 3831.17 ± 1.26 | 16.52 ± 1.05 | 3142.23 ± 1.09 | 20.31 ± 1.07 | 273.63 ± 15.82 | 15.63 ± 1.02 | 219.75 ± 13.91 |
| PB/G5/W40/N3/S1/Z1 | 28.57 ± 1.02 | 4706.34 ± 1.08 | 20.38 ± 1.01 | 3816.46 ± 1.17 | 33.45 ± 1.11 | 612.31 ± 17.13 | 24.15 ± 1.23 | 516.73 ± 15.07 |
| PB/G5/W40/N3/S3/Z3 | 35.06 ± 0.91 | 5046.73 ± 0.91 | 23.93 ± 1.13 | 4187.69 ± 1.05 | 38.71 ± 1.23 | 694.22 ± 16.68 | 26.76 ± 1.04 | 577.37 ± 17.78 |
| PB/G5/W40/N3/S5/Z5 | 30.13 ± 1.08 | 4852.17 ± 1.04 | 20.41 ± 1.14 | 3591.63 ± 1.01 | 34.63 ± 1.09 | 625.14 ± 18.36 | 21.36 ± 1.12 | 496.93 ± 15.84 |

by SEM study. Extensive growth of bacteria along with penetrated fungal species was also observed. The hardness, weight loss of the samples and change in mechanical properties of the degraded WPC samples were compared and presented in Table 4.5.3, 4.5.6 and 4.5.7. The weights and the mechanical properties of the degraded samples were found to decrease. This might be due to the decrease in physical and chemical interaction of WPC caused by the microorganisms present in soil.

**Table 4.5.6.** Weight loss of the wood polymer composite samples after soil burial test.

| Sample | Weight of flexural Specimen (g) | | Weight of tensile Specimen (g) | |
|---|---|---|---|---|
| | Before degradation | After degradation | Before degradation | After degradation |
| PB | 15.26 | 14.81 | 13.45 | 13.11 |
| PB/G5/W40 | 13.72 | 11.37 | 12.57 | 11.04 |
| PB/G5/W40/N3/S1/Z1 | 15.18 | 12.47 | 13.78 | 11.31 |
| PB/G5/W40/N3/S3/Z3 | 16.25 | 12.14 | 14.15 | 11.63 |
| PB/G5/W40/N3/S5/Z5 | 16.36 | 12.01 | 14.39 | 11.26 |

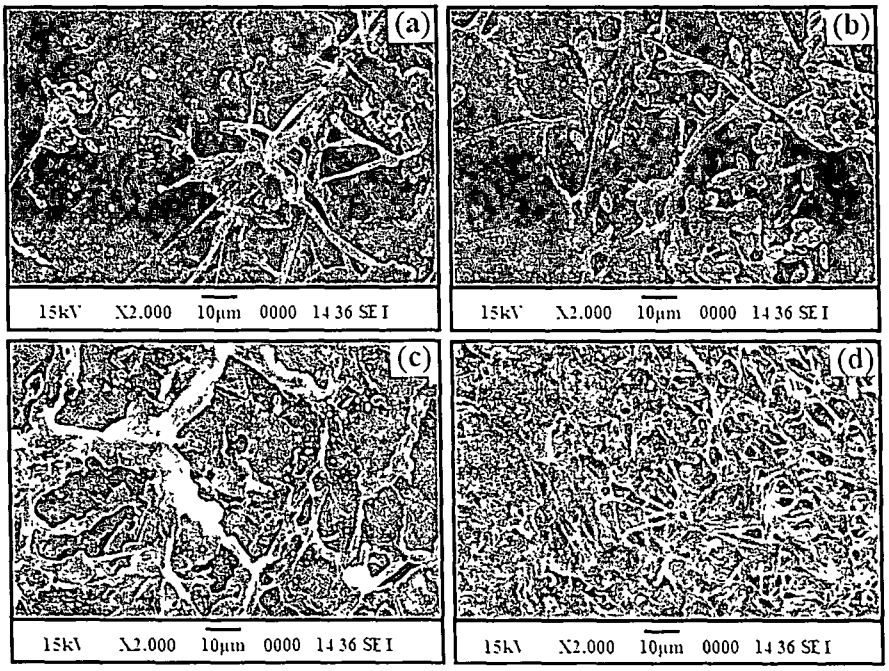


**Figure 4.5.13.** SEM micrographs of samples after soil burial test on (a) PB/G5/W40 (b) PB/G5/W40/N3/S1/Z1 (c) PB/G5/W40/N3/S3/Z3 (d) PB/G5/W40/N3/S5/Z5.

**Table 4.5.7.** Flexural and tensile properties of WPC loaded with nanoclay and different percentage of $SiO_2$ and ZnO after soil burial test.

| Sample | Flexural Properties | | | | Tensile Properties | | | |
|---|---|---|---|---|---|---|---|---|
| | Before degradation | | After degradation | | Before degradation | | After degradation | |
| | Strength (MPa) | Modulus (MPa) | Strength (MPa) | Modulus (MPa) | Strength (MPa) | Modulus (MPa) | Strength (MPa) | Modulus (MPa) |
| PB/G5/W40 | 20.63 ± 1.06 | 3793.12 ± 1.16 | 15.67 ± 1.09 | 3241.52 ± 1.03 | 19.74 ± 1.02 | 254.37 ± 16.17 | 14.20 ± 1.13 | 203.50 ± 14.35 |
| PB/G5/W40/N3/S1/Z1 | 29.14 ± 1.05 | 4727.31 ± 1.02 | 22.12 ± 1.05 | 3962.61 ± 1.09 | 32.73 ± 1.07 | 625.18 ± 15.16 | 25.36 ± 1.09 | 512.61 ± 16.68 |
| PB/G5/W40/N3/S3/Z3 | 36.01 ± 1.11 | 4956.48 ± 1.09 | 24.18 ± 1.15 | 3867.04 ± 1.07 | 37.16 ± 1.14 | 672.91 ± 16.48 | 27.5 ± 1.15 | 535.81 ± 16.27 |
| PB/G5/W40/N3/S5/Z5 | 31.52 ± 1.01 | 4805.14 ± 1.15 | 19.57 ± 1.24 | 36.13 ± 1.08 | 33.38 ± 1.01 | 613.51 ± 17.32 | 20.45 ± 1.01 | 475.81 ± 16.38 |

### 4.5.12. Water uptake and water vapour exclusion results

The water uptake and water vapour uptake results of polymer blend, PE-*co*-GMA treated polymer blend and WPC loaded with clay and different percentage of $SiO_2$ and ZnO are shown in Figure 4.5.14. On addition of PE-*co*-GMA compatibilizer, water uptake capacity of polymer blend decreased. The decreased in water uptake capacity of PE-*co*-GMA treated polymer blend was due to the increase in interfacial adhesion between the polymers by the compatibilizer. After the addition of WF to the blend, the value of water uptake capacity was suddenly increased. The hydrophilic nature of wood flour caused an increase in the water uptake capacity. The water uptake capacity was again decreased after the addition of clay, $SiO_2$ and ZnO nanoparticle. WPC loaded with 3 phr each of clay, $SiO_2$ and ZnO showed lowest water uptake capacity followed by WPC with 3 phr clay and 5 phr $SiO_2$ and ZnO, and WPC with 3 phr clay and 1 phr $SiO_2$ and ZnO. The silicate layers of the clay provided tortuous path and increased the barrier property for water transport. Lei et al. [51] reported a similar increase in barrier properties of wood polymer composite after the incorporation of clay. The presence of $SiO_2$ and ZnO nanopowder also provided a barrier to the passage of water. Better the distribution of nanoparticles, the higher was the barrier property. The incorporation of $SiO_2$ nanoparticles increased the water barrier properties of polyvinyl alcohol based hybrid coatings [24]. At higher concentration $SiO_2$ and ZnO, the nanoparticles became agglomerated in the composite could resulted in an increase in water uptake capacity.

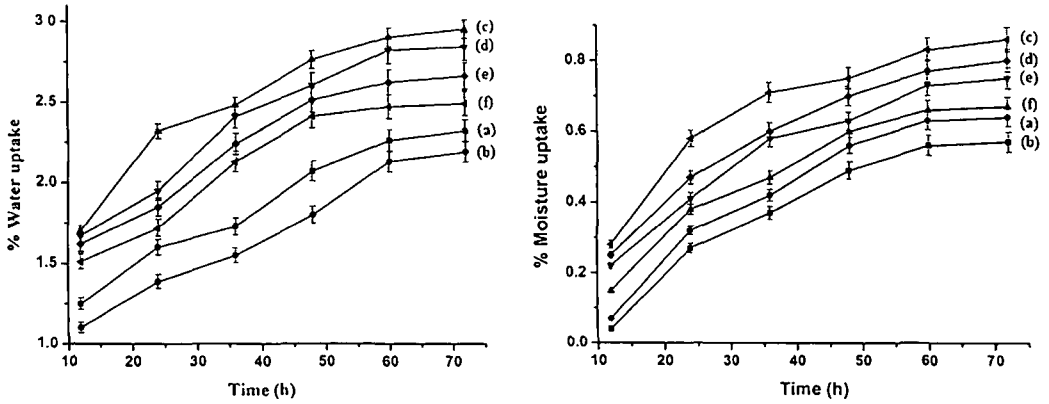


**Figure 4.5.14.** Percent water absorption and water vapour absorption of (a) PB (b) PB/G5 (c) PB/G5/W40 (d) PB/G5/W40/N3/S1/Z1 (e) PB/G5/W40/N3/S5/Z5 (f) PB/G5/W40/N3/S3/Z3.

Water vapour exclusion test for the samples were carried out at 30 °C and 65 % relative humidity. The water vapour uptake was found to increase with time. The trend and explanation for water vapour absorption of different samples were similar to those of samples taken for water uptake study.

## REFERENCE

1. Song, G.J. Polymeric nano-metered composites, *Mater. Rep.* **4**, 57-60, 1996.

2. Bao, Y. & Ma, J.Z. Polymethacrylic acid/Na-montmorillonite/$SiO_2$ nanoparticle composites structures and thermal properties, *Polym. Bull.* **66**(4), 541–549, 2011.

3. Zheng, Y., et al. Effects of nanoparticles $SiO_2$ on the performance of nanocomposites, *Mater. Lett.* **57**(19), 2940-2944, 2003.

4. Mina, F., et al. Improved performance of isotactic polypropylene/titanium dioxide composites: effect of processing conditions and filler content, *Polym. Degrad. Stab.* **94**(2), 183–188, 2009.

5. Han, G., et al. Bamboo–fiber filled high density polyethylene composites: Effect of coupling treatment and nanoclay, *J. Polym. Environ.* **16**(2), 123-130, 2008.

6. Liu, J., et al. Preparation and characterization of poly(vinyl chloride)/layered double hydroxide nanocomposites with enhanced thermal stability, *Polymer* **49**(18), 3923-3927, 2008.

7. De Rosa, C. & Corradini, P. Crystal structure of syndiotactic polypropylene, *Macromolecules* **26**(21), 5711-5718, 1993.

8. Vladimirov, V., et al. Dynamic mechanical and morphological studies of isotactic polypropylene/fumed silica nanocomposites with enhanced gas barrier properties, *Compos. Sci. Technol.* **66**(15), 2935-2944, 2006.

9. Li, H. & Tripp, C.P. Spectroscopic identification and dynamics of adsorbed cetyltrimethyl ammonium bromide structures on $TiO_2$ surfaces, *Langmuir* **18**(24), 9441–9446, 2002.

10. Kang, J.S., et al. Effect of silane modified $sio_2$ particles on poly(mma-hema) soap-free emulsion polymerization, *Iran. Polym. J.* **18**(12), 927-935, 2009.

11. Qu, Y., et al. Surface modification of nanocrystalline anatase with CTAB in the acidic condition and its effects on photocatalytic activity and preferential growth of $TiO_2$. *Appl. Surf. Sci.* **257**(1),151-156, 2010.

12. Motaung, T.E. & Luyt, A.S. Effect of maleic anhydride grafting and the presence of oxidized wax on the thermal and mechanical behaviour of LDPE/silica nanocomposites, *Mater. Sci. Eng. A* **527**(3), 761-768, 2010.

13. Awal, A., et al. Development and morphological characterization of wood pulp reinforced biocomposite fibers, *J. Mater. Sci.* **44**(11), 2876–2881, 2009.

14. Salemane, M.G. & Luyt, A.S. Thermal and mechanical properties of polypropylene–wood powder composites, *J Appl. Polym. Sci.* **100**(5), 4173-4180, 2006.

15. Lee, S.H., et al. Effect of nanosilica on the co-continuous morphology of polypropylene/ polyolefin elastomer blends, *Polymer* **51**(5), 1147-1155, 2010.

16. Jinshu, S., et al. Improvement of wood properties by urea-formaldehyde resin and nano-$SiO_2$, *Front. For. China.* **2**(1), 104-109, 2007.

17. Awal, A., et al. Thermal properties and spectral characterization of wood pulp reinforced bio-composite fibers, *J. Them. Anal. Calorim.* **99**(2), 695–701, 2010.

18. Fung, K.L., et al. Interface modification on the properties of sisal fiber- reinforced polypropylene composites, *J. Appl. Polym. Sci.* **85**(1), 169-176, 2002.

19. Meng, Y.Z. & Tjong, S.C. Preparation and properties of injection-moulded blends of poly(vinyl chloride) and liquid crystal copolyester, *Polymer* **40**(10), 2711-2718, 1999.

20. Yemele, M.C.N., et al. Effect of bark fiber content and size on the mechanical properties of bark/HDPE composites, *Composites Part A* **41**(1), 131-137, 2010.

21. Bouza, R., et al. Design of new polypropylene–wood flour composites: Processing and physical characterization, *Polym. Compos.* **30**(7), 880-886, 2009.

22. Katsikis, N., et al. Thermal stability of poly(methyl methacrylate)/silica nano- and microcomposites as investigated by dynamic-mechanical experiments, *Polym. Degrad. Stab.* **92**(11), 1966-1976, 2007.

23. Devi, R.R., et al. Studies on dimensional stability and thermal properties of rubber wood chemically modified with styrene and glycidyl methacrylate, *J. Appl. Polym. Sci.* **93**(4), 1938-1945, 2004.

24. Minelli, M., et al. Barrier properties of organic–inorganic hybrid coatings based on polyvinyl alcohol with improved water resistance, *Polym. Eng. Sci.* **50**(1), 144-153, 2010.

25. Xu, X., et al. Life cycle assessment of wood-fibre-reinforced polypropylene composites. *J. Mater. Process. Technol.* **198**(1-3), 168-177, 2008.

26. Cho, J.W. & Paul, D.R. Nylon 6 nanocomposites by melt compounding, *Polymer* **42**(3), 1083-1094, 2001.

27. Pracella, M., et al. Recycling of PET and polyolefin based packaging materials by reactive blending, *Polym. Plast. Technol. Eng.* **43**(6), 1711-1722, 2004.

28. Chrissafis, K., et al. Thermal degradation mechanism of HDPE nanocomposites containing fumed silica nanoparticles, *Thermochimica Acta* **485**(1-2), 65–71, 2009.

29. Faruk, O. & Matuana, L.M. Nanoclay reinforced HDPE as a matrix for wood-plastic composites, *Compos. Sci. Technol.* **68**(9), 2073-2077, 2008.

30. Yu, T., et al. Novel polyacrylonitrile/Na-MMT/silica nanocomposite: Co-incorporation of two different form nano materials into polymer matrix, *Compos. Sci. Technol.* **67**(15-16), 3219–3225, 2007.

31. Nourbakhsh, A., et al. Mechanical and thermo-chemical properties of wood flour/ polypropylene blends, *Polym. Bull.* **65**(7), 691–700, 2010.

32. Hu, Y.H., et al. Viscoelastic properties and thermal degradation kinetics of silica/PMMA nanocomposites, *Polym. Degrad. Stab.* **84**(3), 545-553, 2004.

33. Guo, G., et al. Flame retarding effects of nanoclay on wood–fiber composites, *Polym. Eng. Sci.* **47**(3), 330–336, 2007.

34. Erdem, N., et al. Flame retardancy behaviors and structural properties of polypropylene /nano-sio$_2$ composite textile filaments, *J. Appl. Polym. Sci.* **111**(4), 2085–2091, 2009.

35. Yeh, S.K. & Gupta, R.K. Nanoclay-reinforced, polypropylene-based wood–plastic composites, *Polym. Eng. Sci.* **50**(10), 2013–2020, 2010.

36. Karak, N. Polymer (epoxy) clay nanocomposites, *J. Polym. Mater.* **23**, 1-20, 2006.

37. Mirabedini, S.M., et al. Effect of $TiO_2$ on the mechanical and adhesion properties of RTV silicone elastomer coatings, *Colloids Surf., A* **317**(1-3), 80–86, 2008.

38. Sham, E.L., et al. Zirconium titanate from sol–gel synthesis: thermal decomposition and quantitative phase analysis, *J. Solid State Chem.* **139**(2), 225-232, 1998.

39. Wang, H., et al. Effect of surfactants on synthesis of $TiO_2$ nano-particles by homogeneous precipitation method, *Powder Technol.* **188**(1), 52-54, 2008.

40. Yamada, S., et al. Incorporation of titanium dioxide particles into polymer matrix using block copolymer micelles for fabrication of high refractive and transparent organic-inorganic hybrid materials, *J. Polym. Sci. Part A: Polym. Chem.* **49**(3), 712–718, 2011.

41. Zhu, Y., et al. Poly(lactic acid)/titanium dioxide nanocomposite films: influence of processing procedure on dispersion of titanium dioxide and photocatalytic activity, *Polym. Compos.* **32**(4), 519-528, 2011.

42. Zhang, S.L., et al. Morphological structure and physicochemical properties of nanotube $TiO_2$, *Chinese Sci. Bull.* **45**(16), 1533–1536, 2000.

43. Xu, L. & Yang, M. *In Situ* compatibilization between polystyrene-grafted nano-sized $TiO_2$ and polypropylene with friedel-crafts catalyst, *J. Appl. Polym. Sci.* **114**(5), 2755–2763, 2009.

44. Das, G. & Karak, N. Epoxidized *Mesua ferrea* L. seed oil-based reactive diluent for BPA epoxy resin and their green nanocomposites, *Prog. Org. Coat.* **66**(1), 59-64, 2009.

45. Sailaja, R.R.N. Mechanical and thermal properties of bleached kraft pulp–LDPE composites: Effect of epoxy functionalized compatibilizer, *Compos. Sci. Technol.* **66**(13), 2039-2048, 2006.

46. Saeed, K., et al. Characterization of poly(butylene terephthalate) electrspun nanofibres containing titanium oxide, *Iran. Polym. J.* **18**(8), 671-677, 2009.

47. Laachachi, A., et al. Use of oxide nanoparticles and organoclays to improve thermal stability and fire retardancy of poly(methyl methacrylate), *Polym. Degrad. Stab.* **89**(2), 344-352, 2005.

48. Camino, G., et al. Thermal and combustion behaviour of layered silicate–epoxy nanocomposites, *Polym. Degrad. Stab.* **90**(2), 354-362, 2005.

49. Du, H., et al. Effects of pigments on the UV degradation of wood-flour/HDPE composites, *J. Appl. Polym. Sci.* **118**(2), 1068-1076, 2010.

50. Grigoriadou, I., et al. Effect of different nanoparticles on HDPE UV stability, *Polym. Degrad. Stab.* **96**(1), 151-63, 2011.

51. Lei, Y., et al. Influence of nanoclay on properties of HDPE/wood composites, *J. Appl. Polym. Sci.* **106**(6), 3958-3966, 2007 .

52. Chen, Y., et al. Improvement of polyacrylate coating by filling modified nano-$TiO_2$, *Appl. Surf. Sci.* **252**(24), 8635–8640, 2006.

53. Biswal, M., et al. Influence of organically modified nanoclay on the performance of pineapple leaf fiber-reinforced polypropylene nanocomposites, *J. Appl. Polym. Sci.* **114**(6), 4091-4103, 2009.

54. Liufu, S.C., et al. Thermal analysis and degradation mechanism of polyacrylate/ZnO nanocomposites, *Polym. Degrad. Stab.* **87**(1), 103-110, 2005.

55. Leung, Y.H., et al. Zinc oxide ribbon and comb structures: Synthesis and optical properties, *Chem. Phys. Lett.* **394**(4-6), 452-457, 2004.

56. Chae, D.W. & Kim, B.C. Effects of zinc oxide nanoparticles on the physical properties of polyacrylonitrile, *J. Appl. Polym. Sci.* **99**(4), 1854-1858, 2006

57. He, J., et al. Crystallization behavior and UV-protection property of PET-ZnO nanocomposites prepared by *in situ* polymerization, *J. Appl. Polym. Sci.* **114**(2), 1303-1311, 2009.

58. Dhoke, S.K., et al. "Effect of nano-ZnO particles on the corrosion behavior of alkyd-based waterborne coatings", *Prog. Org. Coat.* **64**(4), 371-382, 2009.

59. Laachachi, A., et al. Effect of ZnO and organo-modified montmorillonite on thermal degradation of poly(methyl methacrylate) nanocomposites, *Polym. Degrad. Stab.* **94**(4), 670-678, 2009.

60. Lee, H. & Kim, D.S. Preparation and physical properties of wood/polypropylene/clay nanocomposites, *J. Appl. Polym. Sci.* **111**(6), 2769-2776, 2009.

61. Ji, L.W., et al. Preparation and characteristics of hybrid ZnO-polymer solar cells, *J. Mater. Sci.* **45**(12), 3266-3269, 2010.

62. Lee, S.H., et al. Effect of nanosilica on the co-continuous morphology of polypropylene/ polyolefin elastomer blends, *Polymer* **51**(5), 1147–1155, 2010.

63. Wang, J., et al. Preparation of superhydrophobic poly(methyl methacrylate)-silicon dioxide nanocomposite films, *Appl. Surf. Sci.* **257**(5), 1473-1477, 2010.

64. Liu, Y. & Kontopoulou, M. The structure and physical properties of polypropylene and thermoplastic olefin nanocomposites containing nanosilica, *Polymer* **47**(22), 7731-7739, 2006.

65. Araujo, J.R., et al. Thermal properties of high density polyethylene composites with natural fibres: Coupling agent effect, *Polym. Degrad. Stab.* **93**(10), 1770-1775, 2008.

66. Tabari, H.Z., et al. Effects of nanoclay and coupling agent on the physico-mechanical, morphological, and thermal properties of wood flour/polypropylene composites, *Polym. Eng. Sci.* **51**(2), 272-277, 2011.

67. Bailly, M. & Kontopoulou, M. Preparation and characterization of thermoplastic olefin/ nanosilica composites using a silane-grafted polypropylene matrix, *Polymer* **50**(11), 2472–2480, 2009.

68. He, J., et al. Crystallization behavior and uv-protection property of PET-ZnO nanocomposites prepared by *in situ* polymerization, *J. Appl. Polym. Sci.* **114**(2), 1303-1311, 2009.

69. Zhao, G., et al. Synergistic effect of zinc oxide on the flame retardant and thermal properties of acrylonitrile–butadiene–styrene/poly(ethylene terephthalate)/ammonium polyphosphate systems, *J. Appl. Polym. Sci.* **122**(4), 2338–2344, 2011.

70. Cao, Z., et al. Synthesis and UV shielding properties of zinc oxide ultrafine particles modified with silica and trimethyl siloxane, *Colloids Surf. A* **340**(1-3), 161-167, 2009.

71. Tajvidi, M., et al. Effect of chemical reagents on the mechanical properties of natural fiber polypropylene composites, *Polym. Compos.* **27**(5), 563–569, 2006.

72. Clausen CA. Bacterial associations with decaying wood: a review, *Int. Biodeter. Biodegr.* **37**(1-2), 101–107, 1996.

73. El-Hanafy, A.A., et al. Molecular characterization of two native egyptian ligninolytic bacterial strains, *J. Appl. Sci. Res.* **4**, 1291–1296, 2008.

74. Alvarez, V.A., et al. Degradation of sisal fibre/Mater Bi-Y biocomposites buried in soil, *Polym. Degrad: Stab.* **91**(12), 3156-3162, 2006.

# CHAPTER V

# SUMMARY & CONCLUSIONS

# CHAPTER V

# SUMMARY AND CONCLUSIONS

## 5.1. Summary and conclusions

The salient features that have come out of the present study could be summarized as follows-

In the present investigation, wood polymer composite was developed by solution blending of high density polyethylene (HDPE), low density polyethylene (LDPE), polypropylene (PP), polyvinyl chloride (PVC) and wood flour in combination with different compatibilizers and nanofillers. In order to optimise the solvent ratio, HDPE, LDPE, PP and PVC were mixed in the ratio of 1:1:1:0.5. Preliminary investigations indicated that xylene was a good solvent for HDPE, LDPE and PP. Similarly, tetrahydrofuran (THF) was a good solvent for PVC. Neither xylene nor THF could solubilise the mixture of HDPE, LDPE, PP and PVC (1:1:1:0.5). The solubility of the polymer mixture was checked by varying the ratio of xylene and THF. The optimum ratio of solvent (xylene:THF) and minimum temperature at which a homogeneous solution was obtained, were 70:30 and 120°C respectively.

In the first stage of investigation, wood polymer composite (WPC) was developed by using HDPE, PP, PVC and wood flour (*Phragmites karka*). Glycidyl methacrylate (GMA) was used as compatibilizer and montmorillonite (MMT) clay was used as a nonofiller. MMT was modified by cationic surfactant cetyl trimethyl ammonium bromide (CTAB). The properties of unmodified and modified clay loaded WPC were compared. FTIR study confirmed the modification of MMT by CTAB. Glycidyl methacrylate (GMA) improved the compatibility among the polymers as revealed by SEM study. XRD and TEM study showed a higher increase in interlayer spacing in WPC treated with CTAB modified clay compared to WPC treated with unmodified clay. SEM study showed more roughness on the surface of unmodified clay treated WPC compared to modified clay treated WPC. FTIR study indicated an interaction between wood, GMA treated polymer blend and MMT clay. Significant improvements in mechanical and thermal properties were obtained in WPC treated with CTAB modified clay. Modified clay based WPC showed lower water absorption and highest hardness compared to WPC or unmodified clay treated WPC.

The effect of different compatibilizer on the final properties of wood polymer composite was studied. XRD and TEM study showed an exfoliation of silicate layers in WPC. The improvement in compatibility between the polymer blend and the wood flour by the addition of compatibilizer was examined by SEM study. SEM study also showed that mixed compatibilizer produced maximum compatibility. Mixed compatibilizer

produced highest interaction between wood, polymer and nanoclay as revealed by FTIR study. Flexural, tensile and hardness properties of the nanoclay reinforced WPC compatibilized with 1:1:1 (GMA, PE-*g*-MA, PE-*co*-GMA) mixed compatibilizer were better in comparison with either polymer blend, PE-*co*-GMA, PE-*g*-MA or GMA compatibilized WPC. Maximum improvement in both flexural and tensile properties occurred at 40 phr fiber loading. Thermal stabilities of the WPC enhanced over virgin wood due to incorporation of compatibilizer. Maximum thermal stability and flame resistance property was noticed for nanoclay based WPC compatibilized with (GMA+PE-*g*-MA+PE-*co*-GMA) followed by WPC compatibilized with PE-*co*-GMA, PE-*g*-MA and GMA. Nanoclay reinforced mixed compatibilizer based WPC showed least water absorption in comparison with polymer blend and other compatibilizer based WPC.

The effect of procured nanoclay (MMT modified by 15-35 wt% octadecylamine and 0.5-5 wt% aminopropyltriethoxy silane) on final properties of HDPE, LDPE, PP, PVC blend and wood flour was also investigated. The compatibilizer polyethylene-*co*-glycidyl methacrylate (PE-*co*-GMA) improved the interfacial adhesion between the polymers and wood flour. X-ray diffraction studies of WPC treated with 1 and 3 phr nanoclay showed higher exfoliation compared to WPC treated with 5 phr nanoclay. WPC treated with 3 phr clay showed highest improvement in mechanical and thermal properties. Biodegradability of the WPC improved on addition of clay. SEM study revealed the presence of maximum bacterial growth in clay treated WPC. Both flexural and tensile properties of the WPC decreased due to bacterial degradation of composites. Hardness, flame retardancy and water resistance were improved significantly with the addition of nanoclay to wood/polymer composite.

In this study, nanocomposite was prepared by using a different type of wood flour (*Ipomoea carniva*), PE-*co*-GMA, nanoclay, polymer mixture of HDPE, LDPE, PP and PVC. XRD and TEM studies indicated that WPC treated with 3 phr nanoclay exhibited better dispersion compared to WPC treated with 1 and 5 phr nanoclay. The increase in miscibility among polymers due to addition of PE-*co*-GMA was examined by SEM. WPC treated with 3 phr nanoclay showed highest mechanical, UV and chemical resistance properties. Incorporation of nanoclay had improved flame retardancy and biodegradability of the composite. Water absorption was found to improve in nanoclay loaded WPC.

The influence of nanosilica on the mechanical and thermal properties, flame retardancy and water absorbancy were investigated. In the first step, $SiO_2$ nanoparticles were modified by CTAB. WPC was prepared by employing polymer mixture, PE-*co*-

GMA, wood flour and modified $SiO_2$. X-ray studies showed that $SiO_2$ nanoparticles were infused into the WPC. At lower loading of $SiO_2$ (1-3 phr), the dispersion was found to improve as revealed by TEM study. SEM study showed that the surface of the composite became smooth upto the addition of 3 phr $SiO_2$ nanoparticles. FTIR study indicated the interaction between $SiO_2$, polymer, PE-*co*-GMA and wood. Tensile, flexural and hardness properties of the WPC increased with the increase in $SiO_2$ content upto 3 phr, beyond that it decreased. The incorporation of nanosilica in wood flour/polymer composite significantly improved the thermal stability. Flame retardancy of WPC nanocomposite enhanced due to formation of silica char on the surface of composite. Water absorption of the composite decreased with the incorporation of $SiO_2$ in the composite.

The effect of addition of nanoclay and $SiO_2$ on the properties of the composite was examined. The compatibilizer, PE-*co*-GMA improved the compatibility among the polymers and WF as studied by SEM. XRD and TEM analysis showed the exfoliation of silicate layers of nanoclay and distribution of $SiO_2$ in the composite. Surface modification of $SiO_2$ nanoparticles by cationic surfactant CTAB and the interaction among wood, PE-*co*-GMA, $SiO_2$ and nanoclay were examined by FTIR. WPC loaded with nanoclay and $SiO_2$ showed a remarkable improvement in flame retardancy, mechanical properties and thermal stability. The incorporation of nanoclay and $SiO_2$ nanoparticles decreased the water uptake value of WPC. WPC loaded with 3 phr each of clay and $SiO_2$ exhibited maximum improvement in properties.

The next investigation was carried out to see the effect of incorporation of nanoclay and $TiO_2$ on the final properties of the wood polymer composite. The improvement in miscibility among the polymers was judged by the gradual disappearance of segregated phases as observed by SEM study. The exfoliation of silicate layers and dispersion of $TiO_2$ nanoparticles in the wood polymer composites were investigated by XRD and TEM study. FTIR study showed the shifting of characteristic peaks of $TiO_2$ nanoparticles indicating the surface modification of $TiO_2$ by CTAB. The interactions among wood, PE-*co*-GMA, $TiO_2$ and nanoclay were also studied by FTIR. WPC loaded with nanoclay and $TiO_2$ showed an improvement in mechanical and thermal properties. UV stability of the composite was found to increase by incorporation of $TiO_2$. Nanoclay/$TiO_2$ treated WPC further improved the flame retardancy and decreased the water absorption capacity. WPC loaded with 3 phr each of clay and $TiO_2$ exhibited maximum improvement in properties.

The influence of ZnO nanoparticles on the final properties of the wood/polymer/clay nanocomposite was studied. SEM study revealed the improvement in

compatibility among the polymers and WF after the incorporation of PE-*co*-GMA. The distribution of silicate layers of nanoclay and ZnO in WPCs were examined by XRD and TEM study. The interactions among wood, PE-*co*-GMA, CTAB modified ZnO and nanoclay were studied by FTIR. WPC loaded with nanoclay and ZnO showed an improvement in mechanical and thermal properties. The incorporation of ZnO improved the UV resistance of the composites as judged from the decrease in weight loss, carbonyl index value and SEM study. Nanoclay/ZnO treated WPC further improved the flame retardancy and decreased the water absorption capacity. WPC loaded with 3 phr clay and 3 phr ZnO exhibited maximum improvement in properties.

Finally, the overall effect of nanoclay, $SiO_2$ and ZnO nanoparticles on the properties of the WPC was studied. The compatibility among the polymers and WF was improved by using PE-*co*-GMA compatibilizer as revealed by SEM study. The exfoliation of silicate layers of nanoclay and distribution of $SiO_2$/ZnO in WPCs were examined by XRD and TEM study. Surface modification of $SiO_2$ and ZnO nanoparticles by cationic surfactant CTAB was examined by FTIR studies. The interactions among wood, PE-*co*-GMA, $SiO_2$, ZnO and nanoclay were also studied by FTIR. The shifting of peak corresponding to –OH stretching to lower wave number and decrease of its intensity confirmed the reaction between polymer, wood, $SiO_2$, ZnO and nanoclay. At higher concentration of $SiO_2$ and ZnO loading, the particles became agglomerated. WPC loaded with 3 phr each of nanoclay, $SiO_2$ and ZnO enhanced the mechanical, hardness, thermal properties, flammability, chemical resistance, UV resistance and reduced the water absorption capacity. Bacterial degradation of the WPC increased with the increase in the loading of clay, $SiO_2$ and ZnO.

## 5.2. Future scope

- Although laboratory study indicated a remarkable improvement in various properties by incorporating 3 phr each of nanoclay, ZnO, $TiO_2$ and $SiO_2$ in the wood polymer composites but still a thorough investigation is necessary for commercial utilization of the product.
- Preliminary studies showed that maximum improvements in compatibility as well as properties were achieved by employing equal ratio (1:1:1) of mixed compatibilizer i.e. GMA, PE-*g*-MA and PE-*co*-GMA. Therefore, the future work may include the detailed investigation of the effect of either mixed compatibilizer or any other

suitable new compatibilizer on the compatibility as well as other properties of the composites.

- The study can be tried by using different ratios of polymers.
- Melt blending can be employed for the preparation of composites as it is environmentally safe since no solvents are required.
- The modification of wood flour with compatibilizers prior to compounding with polymer and nanofiller may be investigated as it may enhance the interaction.
- The effect of the nanoparticles used on the crystallization behaviour of the polymer matrix could be explored. The thermal and mechanical properties are suspected to be strong functions of the matrix crystallinity. The relationship between heat deflection temperature (HDT), linear coefficient of thermal expansion (CTE), moduli and the matrix crystallinity need to be improved.
- Besides nanoclay, other nanofillers like carbon nanotube, graphene oxide can be studied for the development of WPC. It may enhance mechanical, thermal and some other important properties of WPC.
- A detailed investigations are necessary for the WPC in the area of biodegradability, fire resistance, pest resistance and emission of volatile organic compounds.
- Future work may also include the use of cellulose nanofibrils as it exhibit a modulus approximately one quarter to one fifth of that of carbon nanotube and above all they are produced naturally without consumption of any further energy.
- One could also explore the possibility of making hybrid construction which combines plastics, wood fiber, steel, concrete etc. together. This could open a new avenue for the generation of value added products.

********

# List of Publication

**In Journals**

1. **B. K. Deka** & T. K. Maji. Effect of coupling agent and nanoclay on properties of HDPE, LDPE, PP, PVC blend and *Phargamites karka* nanocomposite, *Composite Science & Technology* 2010;70(12):1755-1761.

2. **B. K. Deka** & T. K. Maji. Study on the properties of nanocomposite based on high density polyethylene, polypropylene, polyvinyl chloride and wood, *Composites: Part A* 2011;42(6):686-693.

3. **B.K. Deka,** M. Mandal & T.K. Maji, Study on properties of nanocomposites based on HDPE, LDPE, PP, PVC, wood and clay, *Polymer Bulletin* 2011;67(9):1875–1892.

4. **B. K. Deka,** N. Dutta & T. K. Maji. Effect of different compatibilizer and nanoclay on physical properties of wood (*Phragmites karka*) polymer composite, *Polymers from Renewable Resources* 2011;2(3):87-103.

5. **B. K. Deka** & T. K. Maji. Effect of Nanoclay and ZnO on the Physical and Chemical Properties of Wood Polymer Nanocomposite, *Journal of Applied Polymer Science* (In Press).

6. **B. K. Deka** & T. K. Maji. Effect of $TiO_2$ and nanoclay on the properties of wood polymer nanocomposite, *Composites: Part A* 2011;42(12):2117-2125.

7. **B. K. Deka** & T. K. Maji. Effect of silica nanopowder on the properties of wood flour/polymer composite, *Polymer Engineering & Science* (accepted).

8. **B. K. Deka**, M. Mandal & T. K. Maji. Effect Wood Flour Reinforced Polymer/Clay Nanocomposite, (manuscript submitted).

9. **B. K. Deka** & T. K. Maji, Effect of $SiO_2$ and nanoclay on the properties of wood polymer nanocomposite. (manuscript submitted).

10. **B. K. Deka**, P. Baishya, T. K. Maji. Synergistic effect of $SiO_2$, ZnO and nanoclay on mechanical and thermal properties of wood polymer nanocomposite, (manuscript submitted).

11. **B. K. Deka** & T. K. Maji. Study on UV resistance and biodegradation property of wood polymer composite reinforced with $SiO_2$, ZnO and nanoclay, (manuscript submitted).

**In Conferences**

- **B. K. Deka**, P. Baishya & T. K. Maji. Effect of nanoclay and $SiO_2$/ZnO on the properties of HDPE/LDPE/PP/PVC blend and wood nanocomposite, *"National Conference on Chemistry, Chemical Technology and Society"* organized by Tezpur university, Assam, 11-12 November (2011).

- **B. K. Deka** & T. K. Maji. Effect of $SiO_2$ nanopowder on the properties of wood flour/polymer composite, *"National Conference on Smart Nanostructures"* organized by Tezpur University, Assam, 18-20 January (2011).

- **B. K. Deka** & T. K. Maji. Development of polymer nanocomposite based on nanoclay and soft wood (*Ipomoea carniva*), *"National Conference on Frontiers in Chemical Sciences"* organized by Indian Institute of Technology, Guwahati, Assam, 3-4 December (2010).

- **B. K. Deka** & T. K. Maji. Study on properties of nanocomposites based on non-conventional plant materials and waste plastics, *"National Seminar on Emerging Trends in Polymer Science & Technology (POLY-2009)"* organized by Saurastra University, Rajasthan, 8-10 October (2009).

******

Composites: Part A 42 (2011) 686–693

Contents lists available at ScienceDirect

Composites: Part A

journal homepage: www.elsevier.com/locate/compositesa

# Study on the properties of nanocomposite based on high density polyethylene, polypropylene, polyvinyl chloride and wood

B.K. Deka, T.K. Maji *

*Department of Chemical Sciences, Tezpur University, Assam 784 028, India*

ARTICLE INFO

*Article history:*
Received 7 October 2010
Received in revised form 11 February 2011
Accepted 18 February 2011
Available online 22 February 2011

*Keywords:*
A. Polymer–matrix composites (PMCs)
A. Wood
B. Mechanical properties
B. Thermal properties

ABSTRACT

Montmorillonite (MMT) was modified by cetyl trimethyl ammonium bromide (CTAB) and verified by X-ray diffractometer. Wood polymer composite (WPC) was prepared by solution blending of high density polyethylene (HDPE), polypropylene (PP), polyvinyl chloride (PVC), wood flour, modified MMT and glycidyl methacrylate (GMA). The composites were characterized by transmission electron microscopy (TEM), Fourier transform infrared spectroscopy (FTIR) and scanning electron microscopy (SEM). Mechanical properties of modified MMT treated WPC were found better compared to either WPC or unmodified MMT treated WPC. Thermal stability, flammability, hardness and water absorption values of WPCs were improved due to inclusion of modified MMT to WPC.



## 1. Introduction

The north eastern part of India is rich in forest based cellulosic resources. Out of various species available in this region, only a few of them have been explored for economic development of this region. Nal (*Phargamites karka*), a type of nonconventional plant, is abundantly available in the forests of Assam. This plant is not suitable for structural applications due to its poor mechanical, dimensional and other properties. It remains as biowastes. This can be utilized for producing composites to be used for various constructional purposes.

Now-a-days the consumption of plastic materials has increased enormously due to their various advantages. The disposal of post-consumer plastic materials here and there in the form of carry bags, packaging films, boxes, etc. causes environmental pollution. The majority of the waste plastic materials consist of a substantial amount of polyethylene, polypropylene and less amount of poly(vinyl chloride), polystyrene, poly(ethylene terepthalate), etc. Recycling and reusing is one of the processes to reduce the environmental pollution caused by post-consumer plastic materials. The use of recycled plastic materials is restricted due to their poor mechanical properties. The properties can be improved if the waste plastics are combined with cellulosic materials. The nonconventional plant materials can be transformed into value added products by treating with waste plastics.

Solution blending is one of the techniques employed for blending of various types of plastics. Ari and Aydin has used solution blending process to prepare poly(vinyl chloride)/$CaCO_3$ nanocomposite and found an improvement in mechanical properties of the composite [1]. Dana and co-workers [2] has prepared polypropylene–clay composite using xylene as solvent and reported an enhancement in mechanical properties. No single solvent can be able to solubilize completely the mixture of different kind of plastics. The efficiency of blending of different type of plastics can be improved by using a mixture of solvents. The knowledge regarding the proportion of different polymers in the waste plastic is essential in order to optimize the solvent ratio. The situation becomes further critical due to the problems like separation and segregation of different kind of plastics, labels of the container, adhesives in the packaging film, etc. In order to overcome these problems, it has been decided to use virgin polymers such as high density polyethylene, polypropylene, poly(vinyl chloride) of different ratio instead of waste plastics for making composites.

The improvement in adhesion among plastic materials as well as wood fibers is very important for obtaining better composites. The adhesion can be improved by the use of a suitable compatibilizer. The compatibilizer will be such that it can be able to interact with hydrophilic wood fibers and hydrophobic polymers and at the same time will improve the interfacial adhesion among different thermoplastic materials. Glycidyl methacrylate (GMA) has been widely used as a compatibilizer to improve the adhesion between wood and polymer [3]. The use of maleated polypropylene and silane coupling agent have been reported to improve the bonding between cellulose and polypropylene materials [4]. Ethylene–glycidyl methacrylate copolymer, ethylene–propylene copolymer grafted maleic anhydride, isotactic PP-grafted acrylic acid have also been used as compatibilizer for improving the interaction between various polyolefins and poly(ethylene terepthalate) [5].

* Corresponding author. Tel.: +91 3712 267007x5053; fax: +91 3712 267005.
*E-mail address:* tkm@tezu.ernet.in (T.K. Maji).

1359-835X/$ - see front matter © 2011 Elsevier Ltd. All rights reserved.
doi:10.1016/j.compositesa.2011.02.009

Nanocomposite technology with layered silicate nanoclays as an *in situ* reinforcement has been extensively investigated in recent years Nanocomposite improves mechanical, thermal, optical and physiochemical properties remarkably compared to conventional composites [6] Reports on a large number of polymer nanocomposites [7–9] and wood polymer composites [10–13] are available However, far less is known regarding wood polymer nanocomposite The reports available, so far, have addressed the use of single variety of plastics The clay should be modified organically in order to increase its compatibility with polymers The modification of clay can be done in different ways Recently we have prepared and reported the properties of wood polymer nanocomposites by using HDPE/LDPE/PP/PVC, polyethylene-co-glycidyl methacrylate (PE-co-GMA) and nanomer as polymer matrix, compatibilizer and clay [14] It is reported that nanomer contains 15–35% octadecyl amine and 0 5–5% aminopropyl triethoxy silane

In this communication, a mixture of HDPE/PP/PVC and glycidyl methacrylate (GMA) has been used as polymer matrix and compatibilizer respectively Montmorillonite (MMT) has been modified with cetyl trimethyl ammonium bromide (CTAB) and used

The aim of this study is to prepare and evaluate the various properties of the nanocomposite The nanocomposites have been prepared by solution blending using wood flour GMA, CTAB modified MMT, polymer mixture of high density of polyethylene (HDPE), polypropylene (PP) and poly(vinyl chloride) (PVC)

## 2. Experimental

### 2 1 Materials

Nal (*Phargamites karka*), a type of nonconventional wood was collected from a local forest in Assam PP homopolymer (Grade H110MA) was supplied by Reliance Industries Ltd (Mumbai, India) HDPE (Grade PE/20/TK/CN) and PVC (Grade SPVC FS 6701) were collected from Plast Alloys India Ltd (New Delhi, India) and Finolex Industries Ltd (Pune, India) The compatibilizer 2,3-epoxy glycidyl methacrylate (E, Merck, India), N-cetyl-N N,N-trimethyl ammonium bromide (CTAB) (Central Drug house (P) Ltd , Delhi, India) and MMT K10 (Sigma–Aldrich, USA) were used as such received Other reagents used were of analytical grade

### 2 2 Modification of MMT K10

Twenty grams of MMT K10 (CEC = 120 meq/100 g) was dispersed into 400 ml of deionised water and ethanol mixture (1 1) under stirring condition at a temperature of 80 °Ç for 24 h 0 05 mol of CTAB was mixed with 4 8 ml of 1 0 N HCl and 100 ml of (1 1) deionised water and ethanol mixture This solution was poured into MMT dispersed solution and stirred at a temperature of 80 °C for another 24 h The stirring was discontinued when a white precipitate was formed The clay slurry was filtered and washed with deionised water until no chloride ions were detected by using $AgNO_3$ solution [15] The filtered clay was dried in vacuum oven at 45 °C for 3 days, grinded and kept in dark color bottle for subsequent use

### 2 3 Preparation of wood sample

Woods were collected from the local forest It was chopped into small strips The chopped wood strips were initially washed with 1% soap solution, followed by 1% NaOH solution and finally with cold water The washed wood strips were oven dried at 105 ± 5 °C till constant weight was achieved These dried wood strips were grinded in a mixer and sieved The sieved wood flour was kept in a container for further use

### 2 4 Preparation of wood polymer nanocomposite

105 ml of xylene was taken in a flask fitted with a spiral condenser To this, 8 g each of HDPE and PP granules were added slowly at room temperature The temperature of the flask was increased to 130 °C in order to make a clear solution Now, another solution containing 4 g of PVC in 35 ml of THF was prepared In the mean time, the temperature of the flask containing polymer solution was decreased from 130 °C to 120 °C Both these solutions and 50% of the required quantity of GMA (5–15 phr) were mixed at 120 °C (approximately) under stirring condition for 1 h Modified MMT was dispersed in THF solution (10 ml) by sonication This dispersed MMT–THF mixture and rest quantity of GMA was added gradually to the polymer blend Oven dried wood flour (40 phr) was added slowly to this polymer solution and stirring was continued for further 1 h The mixture was transferred in tray and allowed to dry at room temperature The samples were further oven dried, vacuum dried for 24 h to remove the remaining solvent, if any, and finally grinded The composite sheets were obtained by the compression molding press (Santec, New Delhi) at 150 °C under a pressure of 80 MPa

Polymer blend (HDPE + PP + PVC) polymer blend/GMA, polymer blend/GMA/wood were designated as PB, PB/G10, PB/G10/W40 The unmodified and modified MMT treated composites were designated as PB/G10/W40/C3* and PB/G10/W40/C3

## 3. Characterization

### 3 1 X-ray diffraction (XRD)

The modification of nanoclay (MMT) and degree of nanoclay intercalation in nanoclay/polymer composites were evaluated by X-ray diffraction (XRD) analysis XRD measurements were carried out in a Rigaku X-ray diffractometer (Miniflax, UK) using Cu $K_\alpha$ radiation at a scanning rate of 1° $min^{-1}$ with an angle ranging from 2° to 30° of $2\theta$

### 3 2 FTIR studies

FTIR spectra of wood flour, clay and WPCs with or without clay were recorded in FTIR spectrophotometer (Impact-410, Nicolet USA) using KBr pellet

### 3 3 Transmission electron microscopy (TEM)

The study of the dispersion of silicate layers of clay in WPCs was performed by using transmission electron microscope (JEM-100 CX II) at an accelerated voltage of 20–100 kV

### 3 4 Scanning electron microscopy (SEM)

The compatibility among different polymers as well as morphological features of the composites were studied by using scanning electron microscope (JEOL JSM-6390LV) at an accelerated voltage of 5–10 kV Fractured surface of the samples, deposited on a brass holder and sputtered with platinum were used for this study

### 3 5 Mechanical property

The tensile and flexural tests for the polymer blend and WPCs were performed using Universal Testing Machine (Zwick model Z010) at a crosshead speed of 10 mm/min at room temperature according to ASTM D-638 and D-790 respectively The composites were cut into strips of 110 × 10 × 5 $mm^3$ and 100 × 20 × 5 $mm^3$

for tensile and flexural tests Three samples of each category were tested and their average values were reported

### 3 6 Hardness

The hardness of the samples were measured according to ASTM D-2240 using a durameter (model RR12) and expressed as shore D hardness

### 3 7 Thermal property

Thermal properties of wood, polymer blend and WPCs were measured in a thermogravimetric analyser (TGA) (TGA-50, shimadzu) at a heating rate of 10 °C/min up to 600 °C under nitrogen atmosphere at the rate of 30 ml/min

### 3 8 Limiting oxygen index (LOI)

. It was measured by flammability tester (S C Dey Co , Kolkata) according to ASTM D-2863 method The sample was placed vertically in the sample holder of the LOI apparatus The total volume of the gas mixture ($N_2 + O_2$) was kept fixed at 18 cc To begin with experiment, the volume of nitrogen gas and that of oxygen gas were kept initially at a maximum and minimum level Now, the volume of nitrogen gas was decreased and that of oxygen gas was increased gradually However, the total volume of gas mixture was kept fixed at 18 cc during the experiment The ratio of nitrogen and oxygen at which the sample continued to burn for at least 30 s was recorded

$$\text{Limiting oxygen index (LOI)} = \text{Volume of } O_2/\text{Volume of } (O_2 + N_2) \times 100$$

### 3 9 Water uptake test

Percentage water uptake was measured by submerging the samples in distilled water at room temperature (30 °C) for different time periods after conditioning at 65% relative humidity and 30 °C and expressed according to the formulae

$$\text{Water uptake } (\%) = (W_s - W_1)/W_1 \times 100$$

where, $W_s$ is the weight of the specimen after immersion in distilled water for a specified time period and $W_1$ is the weight of the oven dried specimen

### 3 10 Water vapor exclusion test

WPC samples were cut into (2 5 × 0 5 × 2 5) $cm^3$ for the measurement of water vapor uptake test The samples were oven dried and conditioned at room temperature (30 °C) and 30% relative humidity prior to the test The test was carried out by placing the samples at two different relative humidities namely 95% and 65% and maintaining a temperature of 30 °C Weights of the samples were measured after 12, 24 36, 48 60 and 72 h It is expressed as percentage of moisture absorbed based on oven dry weight

## 4. Results and discussion

In order to optimize the solvent ratio, HDPE, PP and PVC were mixed into the ratio of 1 1 0 5 Preliminary studies showed that xylene was a good solvent for HDPE and PP Similarly tetrahydrofuran (THF) was a good solvent for PVC But neither xylene nor THF could solubilize the mixture of HDPE PP and PVC (1 1 0 5) The solubility of the polymer mixture was checked by varying the ratio of xylene and THF The optimum ratio of solvent (xylene THF) and minimum temperature at which a homogenous solution was obtained, were 70 30 and 120 °C respectively

### 4 1 XRD results

The XRD patterns of MMT, organically modified MMT, WPC loaded with unmodified and modified clay are shown in the Fig 1 The interlayer spacing was calculated according to Bragg's law The interlayer spacing for modified clay was found to increase from 0 99 nm to 1 46 nm The higher order peak in modified MMT indicated that MMT had retained its layer structure upon cation exchange with alkyl ammonium cation This increased basal spacing could accommodate the long chains of polymer Composites with unmodified clay showed a diffraction peak at $2\theta = 5\ 55°$ which corresponds to the interlayer spacing of 1 58 nm This diffraction peak shifted towards lower angle ($2\theta = 4\ 11°$) with basal spacing of 2 15 nm when modified clay was used in the composite A shifting of diffraction peak to the lower angle for the clay based HDPE nanocomposite was reported in the literature [16] The results indicated that the modified clay induced a greater increase in interlayer spacing and intercalated more with the polymer mixture than unmodified clay

### 4 2 FTIR analysis

Modification of MMT was further justified by the FTIR spectra Fig 2 shows the FTIR spectra of unmodified and modified clay Unmodified MMT (curve a) exhibited the peaks at 3473 $cm^{-1}$ (—OH stretching), 1639 $cm^{-1}$ (—OH bending) and 1050–460 $cm^{-1}$ for oxide bands of metals (Si, Al, Mg, etc ) MMT modified with CTAB (curve b) showed two new peaks at 2923 and 2854 $cm^{-1}$ which were due to the presence of $-CH_2-$ stretching of long hydrocarbon chain Besides this, another peak which was due to $-CH_2-$ bending appeared at 1476 $cm^{-1}$ [17]

Fig 3 represents the FTIR spectra of MMT, wood flour and wood polymer nanocomposite The FTIR spectra of wood (curve b) showed the presence of peaks at 3423 $cm^{-1}$ (—OH stretching), 2923 $cm^{-1}$ (—CH stretching), 1734 $cm^{-1}$ (C=O stretching), 1636 $cm^{-1}$ (—OH bending), 1160 and 1046 $cm^{-1}$ (C—O stretching) and 1000–650 $cm^{-1}$ (out of plane C—H bending vibration) PB/G10/W40 (curve c) showed characteristics peaks at 2923 $cm^{-1}$ (—CH stretching), 1734 $cm^{-1}$ (C=O stretching) 1636 $cm^{-1}$ (—OH bending) and 720 $cm^{-1}$ ($-CH_2-$ stretching) In the spectrum of PB/G10/W40 (curve c), the intensity of the hydroxyl peak was found to decrease The intensity of the peak was further decreased and

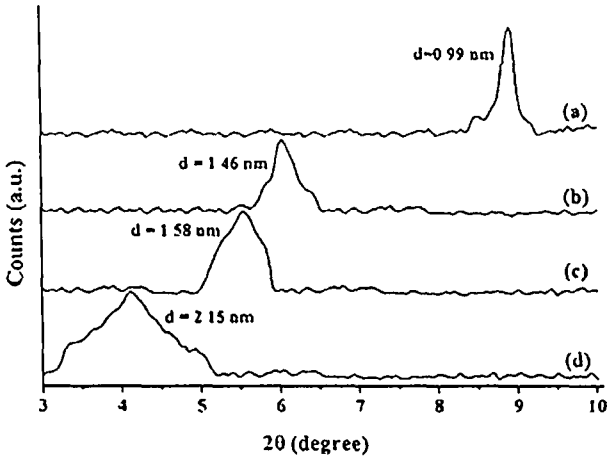


Fig. 1 X ray diffraction of (a) unmodified MMT K10 (b) modified MMT K10 (c) PB/G10/W40/C3• (d) PB/G10/W40/C3

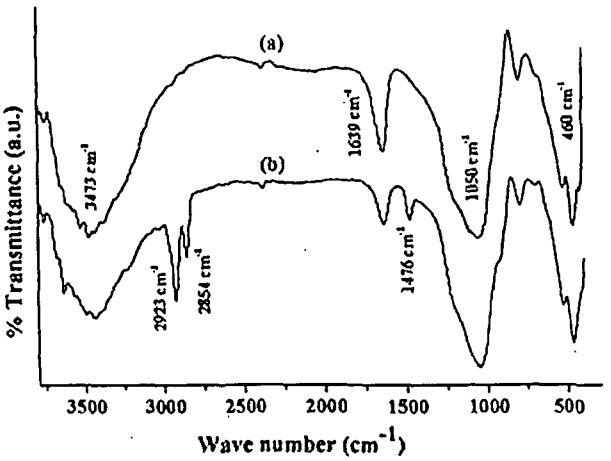


Fig. 2. FTIR spectra of (a) unmodified MMT (b) CTAB modified MMT.

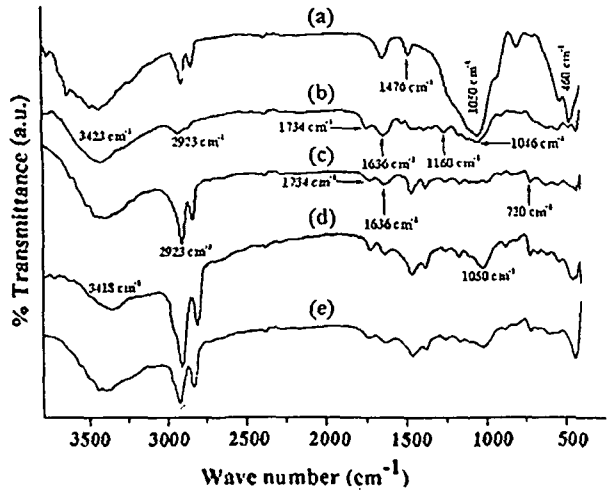


Fig. 3. FTIR spectra of (a) modified MMT (b) wood (c) PB/G10/W40 (d) PB/G10/W40/C3 (e) PB/G10/W40/C3*.

shifted to a lower wave number after the incorporation of modified clay to the WPC (curve d). The decrease in peak intensity in the nanocomposite might be due to the participation of hydroxyl group of clay in the crosslinking reaction with wood and polymer. The shifting of absorption peak, assigned to hydroxyl group, to 3418 $cm^{-1}$ (curve d) from 3423 $cm^{-1}$ (curve b) indicated the formation of hydrogen bond between wood and polymer blend. In the unmodified MMT based WPC (curve e), the shifting and decrease in intensity of the peak assigned for hydroxyl group was not so much significant like those of modified MMT based WPC. Furthermore, the intensity of peak at 2923 $cm^{-1}$ corresponding to —CH stretching was more in wood composites compared to pure wood which indicated the formation of bond between polymers, GMA and wood. The shifting of peak for hydroxyl group to lower wave number and increase in intensity of peak for —C—H stretching was reported by Deka and Maji [14] while studying the FTIR analysis of wood polymer nanocomposite. The other peaks observed in the spectra of wood polymer composites (curves d and e) at 1050 $cm^{-1}$ and 720 $cm^{-1}$ were due to the C—O stretching of wood, oxide bands of silicon and $—CH_2—$ stretching of polymer.

### 4.3. TEM study

Fig. 4 shows the TEM micrographs of WPC loaded with unmodified and modified clay. It was observed that the silicate layers of clay were agglomerated in WPC loaded with unmodified clay. The agglomeration was due to the noncompatibility of inorganic silicate layers to organic polymers. The organophilisation of MMT with CTAB improved the compatibility of silicate layers with the polymers and as a result no such agglomeration was observed in modified clay treated WPC. Rather it was dispersed in the wood polymer matrix which influenced the mechanical, thermal and other properties. Zhao et al. [17] prepared nanocomposite by using organically modified MMT, wood flour and PVC and found a well dispersion of silicate layers in wood polymer matrix. An improvement in properties of the composite as well as exfoliation of clay layers were observed on addition of organically modified clay to the PP and WF mixture [18].

### 4.4. SEM study

Fig. 5 displays the SEM micrographs of different fractured samples. The fractured surface of untreated polymer sample (Fig. 5a) exhibited some segregation among different polymers. The segregation decreased when the polymer blend was treated with glycidyl methacrylate (Fig. 5b–d). Segregation was found to decrease with the increase in the amount of glycidyl methacrylate. This might be due to the improvement in compatibility between HDPE, PP and PVC. The improvement in adhesion between polyolefins and PET by using ethylene-glycidyl methacrylate copolymer as compatibilizer was cited in the literature [5]. In the formulation with WPC, the addition of clay and wood flour altered the fracture modes. The agglomerates of the clay particles were visible in the case of unmodified clay treated composites (Fig. 5e). The organic

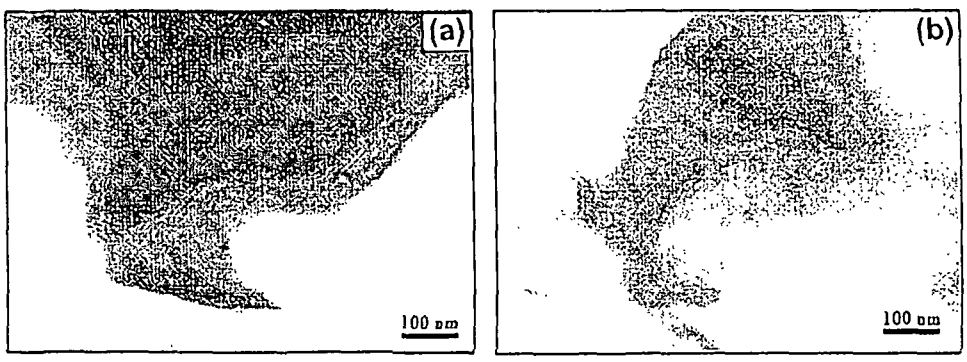


Fig. 4. TEM micrographs of (a) PB/G10/W40/C3* (b) PB/G10/W40/C3.

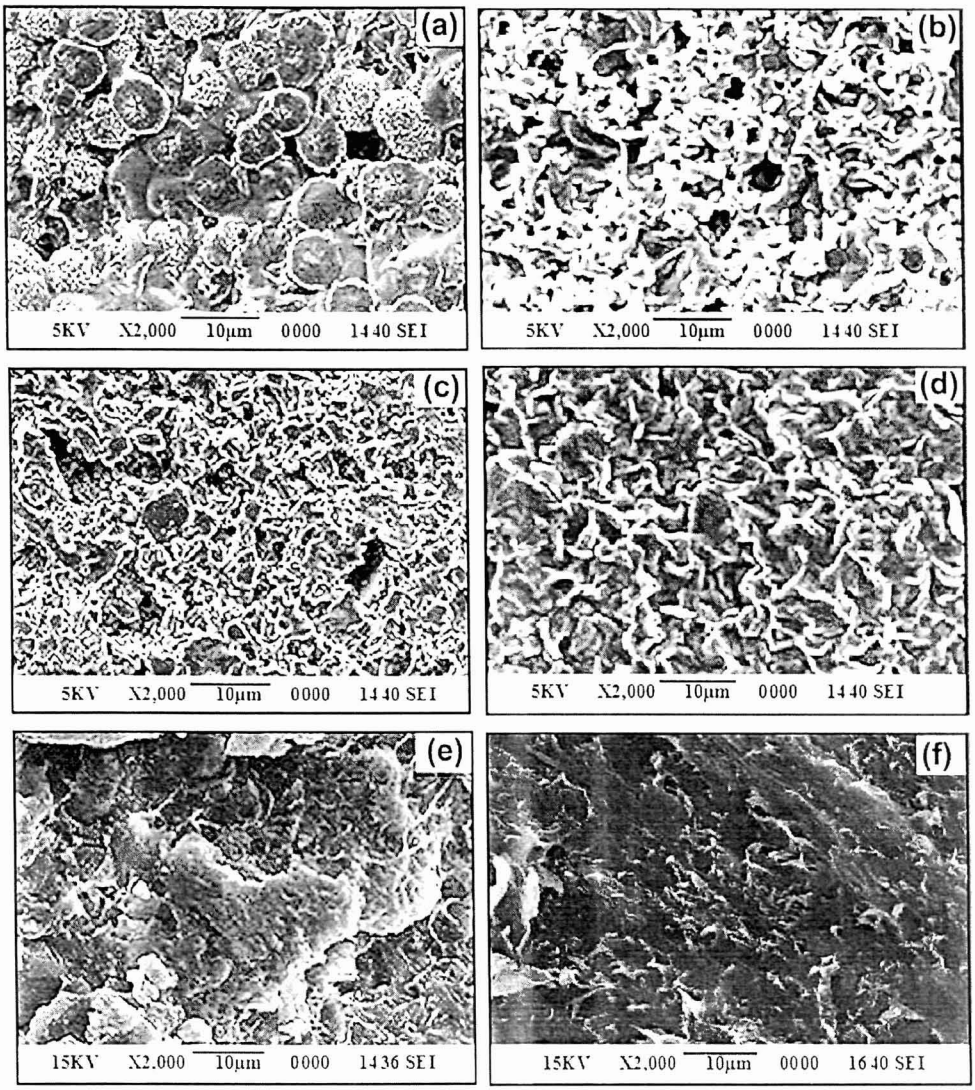


**Fig. 5.** SEM micrographs of (a) PB (b) PB/G5 (c) PB/G10 (d) PB/G15 (e) PB/G10/W40/C3* (f) PB/G10/W40/C3.

modification of the clay resulted in better dispersion of silicate layers in the WPC matrix as seen in Fig. 5f.

### 4.5. Mechanical property study

The flexural and tensile properties of PB, PB/G10, PB/G10/W40, PB/G10/W40/C3* and PB/G10/W40/C3 are shown in Table 1. The data presented in the table were the average of three readings. It was observed that both the flexural and tensile properties increased when GMA as compatibilizer was added to the polymer blend. This was due to the improvement in compatibility between HDPE, PP and PVC by GMA as revealed by SEM study. The incorporation of wood flour to the GMA treated polymer blend further improved the mechanical properties because of the increase in rigidity of the composite caused by the wood flour. Moreover, GMA could improve the adhesion between wood and polymer blend through its glycidyl group and double bond. Bouza et al. [19] reported that the mechanical properties of polypropylene modified with maleated polypropylene enhanced with the addition of wood flour.

**Table 1**
Flexural and tensile properties of polymer blend and WPC loaded with unmodified and modified MMT.

| Sample | Flexural properties | | Tensile properties | |
|---|---|---|---|---|
| | Strength (MPa) | Modulus (MPa) | Strength (MPa) | Modulus (MPa) |
| PB | 13 (±2) | 742 (±1) | 5 (±2) | 84 (±17) |
| PB/G10 | 16 (±2) | 1084 (±2) | 9 (±1) | 172 (±18) |
| PB/G10/W40 | 18 (±1) | 3895 (±1) | 19 (±1) | 315 (±17) |
| PB/G10/W40/C3* | 22 (±2) | 4254 (±1) | 25 (±1) | 444 (±17) |
| PB/G10/W40/C3 | 25 (±1) | 4682 (±1) | 30 (±1) | 513 (±18) |

The addition of unmodified nanoclay had increased the strength and modulus values. A significant increase in the values was observed when organically modified nanoclay was added to the WPC. This enhancement in properties might be attributed to the high stiffness caused by the decreased in mobility of the polymer chains that were intercalated between the nanoclay interlayers. The observed lower values of strength and modulus in unmodified nanoclay loaded composites might be due to the poor dispersion and agglomeration of nanoclay in the system. Similar decrease in flexural properties due to poor dispersion of clay in wood–plastic

**Table 2**
Hardness value of polymer blend and wood/polymer/clay nanocomposite

| Sample code | Hardness (shore D) |
|---|---|
| PB | 65 6 (±1 0) |
| PB/G10 | 68 8 (±0 5) |
| PB/G10/W40 | 67 0 (±1 0) |
| PB/G10/W40/C3* | 72 5 (±0 7) |
| PB/G10/W40/C3 | 76 2 (±0 6) |

**Table 3**
Thermal analysis of wood and wood-polymer nanocomposites

| Sample | $T_i$ | $^aT_m$ | $^bT_m$ | Temperature of decomposition ($T_D$) in °C at different weight loss (%) | | | | RW% at 600 °C |
|---|---|---|---|---|---|---|---|---|
| | | | | 20% | 40% | 60% | 80% | |
| Wood flour | 230 | 315 | - | 283 | 319 | 353 | - | 26 6 |
| PB | 242 | 272 | 407 | 297 | 384 | 441 | 470 | 5 2 |
| PB/G10 | 238 | 296 | 470 | 304 | 390 | 447 | 476 | 5 8 |
| PB/G10/W40 | 245 | 292 | 463 | 299 | 375 | 434 | 469 | 6 2 |
| PB/G10/W40 (phy mix) | 218 | 276 | 455 | 290 | 361 | 422 | 457 | 5 9 |
| MMT K10 | 35 | 50 | - | - | - | - | - | 84 1 |
| PB/G10/W40/C3* | 258 | 302 | 475 | 311 | 394 | 451 | 482 | 12 9 |
| PB/G10/W40/C3 | 265 | 311 | 487 | 321 | 408 | 459 | 490 | 14 9 |

$T_i$ value for initial degradation $^aT_m$ value for 1st step $^bT_m$ value for 2nd step

**Table 4**
Limiting oxygen indices (LOI) and flaming characteristics of polymer blend and wood/polymer/clay nanocomposites

| Samples | LOI (%) | Flame description | Smoke and fumes | Char |
|---|---|---|---|---|
| PB | 23 | Candle like localized | Small and black smoke | Little |
| PB/G10 | 38 | Small localized flame | Small and black smoke | Little |
| PB/G10/W40 | 42 | Small localized flame | Small and black smoke | Medium |
| PB/G10/W40/C3* | 51 | Small localized flame | Small and black smoke | Higher |
| PB/G10/W40/C3 | 59 | Small localized flame | Small and black smoke | Higher |

composites was reported by Faruk and Matuana [16] The inclusion of organoclay resulted in the improvement in mechanical properties was reported by Lee and Kim [20] while studying the physical properties of wood/PP/clay nanocomposites

### 4 6 Hardness

Table 2 shows the hardness results of polymer blend and WPCs The hardness values were found to increase as GMA was added This was due to the improvement in compatibility between various polymers by GMA which increased the interfacial adhesion among the polymers However, incorporation of wood flour to the polymer blend decreased the hardness values Addition of clay further improved the hardness The improvement was more in the case of modified clay treated composite. The improvement was due to the reduction in the mobility of the intercalated polymer chains Deka and Maji [14] reported that incorporation of nanoclay to WPC enhanced the hardness The poor dispersion and agglomeration of clay might be responsible for the observed lower value of hardness exhibited by unmodified clay treated WPC

### 4 7 Thermogravimetric analysis

Table 3 shows the initial decomposition temperature ($T_i$), maximum pyrolysis temperature ($T_m$), decomposition temperature at different weight loss ($T_D$, %) and residual weight (RW, %) for wood flour, polymer blend, MMT and WPCs In both wood flour and WPCs, a decrease in weight loss at 45–50 °C was observed (not shown in Table) due to the removal of moisture Polymer blend showed a higher $T_i$ value than that of wood The addition of GMA to the polymer blend decreased the $T_i$ value. This might be due to the earlier decomposition of GMA polymer [21] The $T_i$ value of WPC was higher than those of either wood flour alone or physical mixture of composite $T_i$ value of WPC increased after the addition of unmodified and modified MMT The improvement was more in the case of modified clay treated WPC The increase in $T_i$ value of clay loaded WPC was due to the intercalated nature of silicate layers which retarded the passage of volatile products The lower value shown by unmodified clay loaded WPC was due to the agglomeration of silicate layers in the WPC

The observed $T_m$ value for wood flour (shown in Table 3) might be attributed to the depolymerisation of hemicellulose, glycosidic linkages of cellulose and thermal decomposition of cellulose The first decomposition peak exhibited by the polymer blend was probably due to the dehydrochlorination of PVC [22] The second decomposition peak was mainly due to the decomposition of HDPE and PP [10,19] $T_m$ values for the first and second stages of pyrolysis of polymer blend were found to shift when GMA was added This may be possibly due to the improvement in interaction among the polymers caused by the addition of GMA $T_m$ values for the first and second stages of pyrolysis of modified MMT loaded WPC were higher than those of composite without MMT, physical mixture or unmodified MMT based composites

The weight losses of various samples at different temperature are also listed in the Table 3 It was observed that wood flour decomposed at lower temperature compared to polymer blend $T_D$ values increased due to addition of wood flour and GMA to the polymer blend This might be due to the increase in interaction between wood flour and polymer blend by GMA through its glycidyl group and double bond respectively Awal et al [23] reported that the incorporation of wood pulp and maleated polypropylene into propylene delayed the thermal degradation of WPC The addition of clay to WPC increased the $T_D$ values The more improvement in $T_D$ values was observed in the case of modified clay treated WPC

RW value for the wood fiber was observed maximum This was due to the carbonization of the wood fiber RW value of polymer blend increased on addition of GMA Modified MMT treated WPC showed higher RW value compared to both unmodified MMT treated WPC or MMT free WPC The maximum improvement in thermal stability was observed by the inclusion of modified clay This might be attributed to the presence of silicate layers which acted as a barrier and delayed the decomposition of volatile products [24] The lowered thermal stability exhibited by unmodified clay treated WPC was due to the poor dispersion and agglomeration of the clay

### 4 8 Limiting oxygen index (LOI)

Limiting oxygen indices value of polymer blend, unmodified and modified clay loaded WPC are shown in Table 4 It was observed that polymer blend without compatibilizer showed lowest LOI value while modified clay treated WPC showed highest LOI value LOI value of the polymer blend increased on incorporation of GMA GMA increased the interfacial adhesion among polymers

which resulted in an increase in LOI value. LOI value enhanced after addition of clay to the WPC. Modified clay treated WPC had higher LOI value compared to clay untreated WPC. Wood contains cellulose, hemicellulose, lignin, pectin and wax [25]. Besides this, it contains elements mainly carbon, oxygen and small amount of silicon [26]. The lignin present in the blend could produce a high char. The char was carbon based residue which undergoes slow oxidative degradation [27]. This could form a protective layer and reduce the diffusion of oxygen towards wood polymer composite. Tajvidi reported that the presence of natural fibers delayed the decomposition of polyethylene in the composites due to formation of protective layer of char on the surface of composites [28]. The small amount of silicon might be capable of producing some char. Further, nanoclay produced silicate char on the surface of WPC which decreased the flame propagation property of the composite [29]. The lower LOI value in unmodified clay treated WPC was due to the poor dispersion and agglomeration of clay in the WPC as discussed earlier.

### 4.9. Water uptake test

The results of water uptake for polymer blends and WPCs are shown in Fig. 6. In all the cases, the water uptake was found to increase with the increase in time of immersion. The water absorption of the polymer blend decreased on addition of GMA. This might be due to the improvement in compatibility among the polymers. GMA increased the interaction between the interfaces of the polymers and thus enhanced water resistance. The water absorption enhanced when wood flour was added. The hydrophilic nature of wood flour was responsible for this. The water absorption of WPC decreased when MMT was added. The decrease in absorption value was more in the case of modified MMT based composite compared to unmodified MMT based composite. The presence of nanoclay in the composite hindered the permeation of water through the composite as reported in the literature [30]. Although the clay on treated with CTAB changed to organophilic in nature, yet it retained its hydrophilic character. The hydrophilic character of unmodified clay surface was more than that of modified clay surface [31]. The surface of modified clay had a tendency to immobilise some of the moisture [20]. Moreover, CTAB modified clay increased the tortuous path for water transport resulting in decrease in water diffusivity [32]. Thus, modified clay treated composite showed lower water absorption compared to unmodified clay.

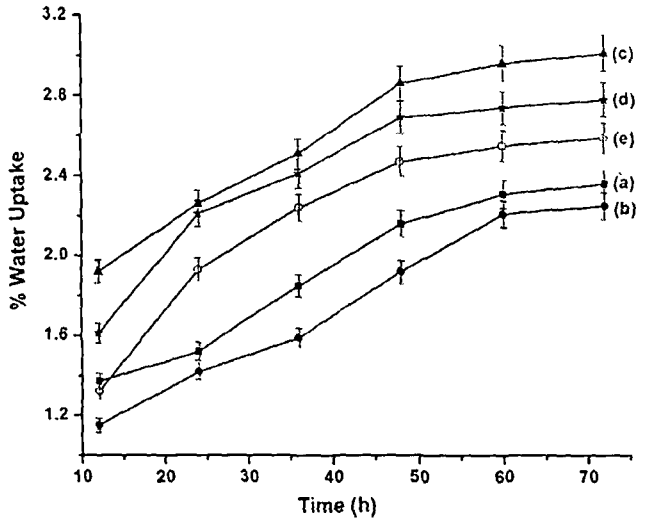


Fig. 6. Percent water uptake capacity of (a) PB (b) PB/G10 (c) PB/G10/W40 (d) PB/G10/W40/C3• (e) PB/G10/W40/C3.

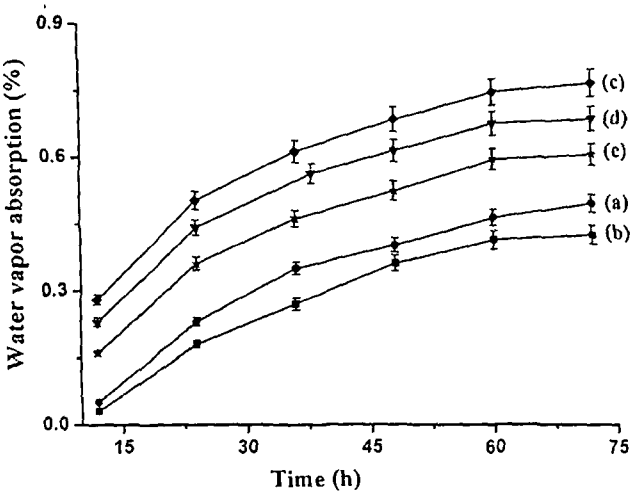


Fig. 7. Percent water vapor absorption of (a) PB (b) PB/G10 (c) PB/G10/W40 (d) PB/G10/W40/C3• (e) PB/G10/W40/C3.

### 4.10. Water vapor exclusion test

Water vapor exclusion test of the samples was carried out at 30 °C and 65% relative humidity as shown in Fig. 7. From the figure, it was observed that water vapor absorption initially occurred at a rapid rate and finally at a slower rate. In all the samples, water vapor absorption rate increased with the increase in time. It was observed that the polymer blend without compatibilizer had a lower rate of water vapor absorption. This was further decreased after addition of compatibilizer to the polymer blend. Maji and co-workers [21] reported that WPC treated with GMA, absorbed less water vapor compared to untreated WPC. The absorption of water vapor was found to enhance when wood flour was added. The incorporation of clay in WPC decreased the rate of water vapor absorption. Similar decrease in water vapor absorption was reported by Lei et al. [33]. The decrease in water vapor absorption was less in modified MMT treated WPC compared to unmodified MMT treated composite. The reason for this was explained as earlier. Therefore, it could concluded that organically modified clay treated composite absorbed less water vapor compared to unmodified clay treated composite.

The water vapor exclusion test was also performed at 30 °C and 95% relative humidity. The results followed similar trends with a little higher rate of water vapor absorption compared to those of samples at 65% relative humidity.

## 5. Conclusions

The solvent ratio of xylene and THF for solution blending of HDPE, PP and PVC (1:1:0.5) was optimized and found to be as 70:30. Glycidyl methacrylate (GMA) improved the compatibility among the polymers as revealed by SEM study. XRD and TEM study showed a higher increase in interlayer spacing in WPC treated with CTAB modified clay compared to WPC treated with unmodified clay. SEM study also showed more roughness on the surface of unmodified clay treated WPC compared to modified clay treated WPC. FTIR study indicated an interaction between wood, GMA treated polymer blend and nanoclay. Significant improvements in mechanical and thermal properties were obtained in WPC treated with CTAB modified clay. Modified clay based WPC showed lower

water absorption and highest hardness compared to WPC or unmodified clay treated WPC.

## Acknowledgment

The authors acknowledge the financial assistance from Council of Scientific and Industrial Research (CSIR), New Delhi.

## References

[1] An GA, Aydın I Nanocomposites prepared by solution blending microstructure and mechanical properties J Macromol Sci Part B Phys 2008,47(2) 260–7
[2] Sarkar M, Dana K, Ghatak S, Banerjee A. Polypropylene-clay composite prepared from Indian bentonite Bull Mater Sci 2008,31(1) 23–8
[3] Devi RR, Maji TK Effect of glycidyl methacrylate on the physical properties of wood-polymer composites Polym Compos 2007,28(1) 1–5
[4] Sain MM, Kotka BV, Imbert C Structure-property relationships of wood fiber-filled polypropylene composite Polym Plast Technol Eng 1994,33(1) 89–104
[5] Pracela M, Chaonna D, Ishak V, Galeski A. Recycling of PET and polyolefin based packaging materials by reactive blending Polym Plast Technol Eng 2004,43(6) 1711–22
[6] Kojima Y, Vsuki A, Kawasumi M, Okada A, Fukushima Y, Karauchi T, et al Mechanical properties of nylon 6-clay hybrid J Mater Res 1993,6 1185–9
[7] Doh JG, Cho I Synthesis and properties of polystyrene-organoammonium montmorillonite hybrid Polym Bull 1998,41(5) 511–8
[8] Ma J Qi Z, Hu Y Synthesis and characterization of polypropylene/clay nanocomposites J Appl Polym Sci 2001,82(14) 3611–7
[9] Zeng C, Lee LJ Poly(methyl methacrylate) and polystyrene/clay nanocomposites prepared by *in-situ* polymerization Macromolecules 2001,34(12) 4098–103
[10] Yemele MCN, Koubaa A, Cloutier A, Soulounganga P, Wolcott M Effect of bark fiber content and size on the mechanical properties of bark/HDPE composites Composites Part A 2010,41(1) 131–7
[11] Bledzki AK, Mamun AA, Volk J Barley husk and coconut shell reinforced polypropylene composites the effect of fibre physical, chemical and surface properties Compos Sci Technol 2010,70(5) 840–6
[12] Tasdemir M, Biltekin H, Caneba GT Preparation and characterization of LDPE and PP-wood fiber composites J Appl Polym Sci 2009,112(5) 3095–102
[13] Megiatto Jr JD, Silva CG, Ramires EC, Frollini E Thermoset matrix reinforced with sisal fibers effect of the cure cycle on the properties of the biobased composite Polym Test 2009,28(8) 793–800
[14] Deka BK, Maji TK. Effect of coupling agent and nanoclay on properties of HDPE, LDPE, PP, PVC blend and *Phargamites karka* nanocomposite Compos Sci Technol 2010,70(12) 1755–61
[15] Zeng QH Wang DZ, Yu AB, Lu GQ. Synthesis of polymer-montmorillonite nanocomposites by in situ intercalative polymerization Nanotechnology 2002 13(5) 549–53
[16] Faruk O, Matuana LM Nanoclay reinforced HDPE as a matrix for wood-plastic composites Compos Sci Technol 2008,68(9) 2073–7
[17] Zhao Y, Wang K, Zhu F, Xue P, Jia M Properties of poly(vinyl chloride)/wood flour/montmorillonite composites effects of coupling agents and layered silicate Polym Degrad Stab 2006,91(12) 2874–83
[18] Lee SY, Kang IA, Doh GH, Kim WJ, Kim JS, Yoon HG, et al Thermal, mechanical and morphological properties of polypropylene/clay/wood flour nanocomposites EXPRESS Polym Lett 2008,2(2) 78–87
[19] Bouza R, Pardo SG, Barral L, Abad MJ Design of new polypropylene-wood flour composites processing and physical characterization Polym Compos 2009,30(7) 880–6
[20] Lee H, Kim DS Preparation and physical properties of wood/polypropylene/clay nanocomposites J Appl Polym Sci 2009,111(6) 2769–76
[21] Devi RR, Maji TK, Banerjee AN Studies on dimensional stability and thermal properties of rubber wood chemically modified with styrene and glycidyl methacrylate J Appl Polym Sci 2004,93(4) 1938–45
[22] Meng YZ, Tjong SC Preparation and properties of injection-moulded blends of poly(vinyl chloride) and liquid crystal copolyester Polymer 1999,40(10) 2711–8
[23] Awal A, Ghosh SB, Sain M Thermal properties and spectral characterization of wood pulp reinforced bio-composite fibers J Therm Anal Calorim 2010,99(2) 695–701
[24] Deka H, Karak N Vegetable oil-based hyperbranched thermosetting polyurethane/clay nanocomposites Nanoscale Res Lett 2009,4(7) 758–65
[25] Stevens MD Polymer chemistry, an introduction Oxford Oxford University Press, 1990
[26] Bledzki AK, Mamun AA, Volk J Physical, chemical and surface properties of wheat husk, rye husk and soft wood and their polypropylene composites Composites Part A 2010,41(4) 480–8
[27] Canetti M Bertini F, De Chirico A, Audisio G Thermal degradation behaviour of isotactic polypropylene blended with lignin Polym Degrad Stab 2006,91(3) 494–8
[28] Tajvidi M, Takemura A. Effect of fiber content and type compatibilizer, and heating rate on thermogravimetric properties of natural fiber high density polyethylene composites Polym Compos 2009,30(9) 1226–33
[29] Camino G, Tartaglione G Frache A, Manferti C, Costa G Thermal and combustion behaviour of layered silicate-epoxy nanocomposite Polym Degrad Stab 2005,90(2) 354–62
[30] Rana HT, Gupta RK, GangaRao HVS, Sridhar LN Measurement of moisture diffusivity through layered-silicate nanocomposites AIChE J 2005,51(12) 3249–56
[31] Shah AP, Gupta RK, Ganga Rao HVS, Pavell CE. Moisture diffusion through vinyl ester nanocomposites made with montmorillonite clay Polym Eng Sci 2002,42(9) 1852–63
[32] Alexandre B Marais S Langevin S, Mederic P Aubry T Nanocomposite-based polyamide 12/montmorillonite relationships between structures and transport properties Desalination 2006,199(1–3) 164–6
[33] Lei Y, Wu Q, Clemons CM, Yao F Xu Y Influence of nanoclay on properties of HDPE/Wood composites J Appl Polym Sci 2007,106(6) 3958–66

# Effect of Different Compatibilisers and Nanoclays on the Physical Properties of Wood (*Phargmites karka*)–Polymer Composites

**Biplab K. Deka, Nipu Dutta, and Tarun K. Maji***

*Department of Chemical Sciences, Tezpur University, Assam 784028, India*

**Received: 25 May 2011, Accepted: 12 August 2011**

## SUMMARY

*Wood–polymer composites (WPCs) were prepared by solution blending of high-density polyethylene (HDPE), polypropylene (PP), polyvinyl chloride (PVC) (1:1:0.5), wood flour, nanoclay, and compatibiliser. Compatibility among different polymers as well as with wood flour was evaluated by using different kinds of compatibiliser, namely glycidyl methacrylate (GMA), polyethylene-grafted maleic anhydride (PE-g-MA) and polyethylene-co-glycidyl methacrylate (PE-co-GMA). The formation of a nanocomposite was confirmed by XRD and TEM studies. An SEM study showed that maximum improvement in compatibility of nanoclay-reinforced WPCs was achieved by using a mixture of compatibilisers (GMA + PE-co-GMA + PE-g-MA). An FTIR study indicated an interaction between the polymer blend, wood flour, nanoclay, and the compatibiliser. WPCs prepared by using blended compatibiliser, nanoclay, and 40 phr wood flour exhibited* maximum hardness, thermal stability, and mechanical and flame-retarding *properties. The water uptake capacity of blended-compatibiliser-based wood–polymer nanocomposites was lower than that of individual-compatibiliser-based nanocomposites.*

**Keywords:** wood; polymer; compatibiliser; composite; characterisation

## INTRODUCTION

During the last decade, wood–plastic composites (WPCs) have emerged as an important family of green composites [1]. They are used in different

*Corresponding author. E-mail address: tkm@tezu.ernet.in

outdoor and indoor applications such as decking, railing, fencing, docks, and landscaping timbers, and in a number of automobile industries [2]. Composites reinforced with wood (WPCs) have shown great growth owing to the many advantages they offer. Their processing is easy, economic, and ecological. They have relatively high strength and stiffness, low cost, low density, low $CO_2$ emission, biodegradability, and renewability. Varieties of non-conventional plant materials such as Nal (*Phargmites karka*), kolomou (*Ipomoea carniva*), kihua (*Saccharum spontaneum*), etc., are available in the forest of Assam, India. These are mostly utilised for fuel purposes or remain as biowastes. Their uses for structural purposes are restricted owing to their poor mechanical properties and dimensional stability. They can be made a value-added material for preparation of structural components by making composites with plastic materials. These composites will not only contribute to economic growth but may also reduce the amount of biowastes. Sui et al. [3] have prepared WPCs by using non-conventional plants such as sunflower hull sanding dust (SHSD) as reinforcing agents and PP as the matrix.

Different types of polyolefin such as high-density polyethylene (HDPE), low-density polyethylene (LDPE), polypropylene (PP), polyvinyl chloride (PVC), polystyrene (PS), etc., are used as the matrix for making wood–plastic composites [4–6]. Wood–plastic composites have several advantages compared with either wood or plastics [7]. Most reports address the use of a single variety of polymer, i.e. polyethylene, polypropylene, polyvinyl chloride, etc., for making WPCs. Therefore, it is assumed that the use of multiple types of polymer in making WPC may provide information to help minimise the environmental pollution caused by post-consumer plastic materials. The majority of waste plastic material consists of substantial amounts of polyethylene and polypropylene and small amounts of polyvinyl chloride, polystyrene, and polyethylene terepthalate. Solution blending is one of the ways to mix different kinds of plastic.

One of the major disadvantages of wood fibres is the poor compatibility between the fibres and polymeric matrices, which results in non-uniform dispersion of fibres within the matrix and poor mechanical properties. Most polymers, especially thermoplastics, are non-polar substances, which are not compatible with polar wood fibres, and therefore poor adhesion between polymer and fibre in WPCs can result. In order to improve the affinity and adhesion between wood fibres and thermoplastic PP matrices, chemical "coupling" or "compatibilising" agents have been employed [8]. Chemical coupling agents are substances, typically polymers, that are used in small quantities to treat a surface so that bonding occurs between it and other surfaces, e.g. wood and thermoplastics. The compatibility between wood and polymer can be improved by using glycidyl methacrylate (GMA) as a compatibiliser [9].

Dikobe and Luyt [10] have used poly(ethylene-*co*-glycidyl methacrylate) as a compatibiliser for the preparation of ethylene vinyl acetate–wood composites with high mechanical properties. The coupling agent forms bonds which include covalent bonds, secondary bonding (such as hydrogen bonding and Van der Waals forces), polymer molecular entanglement, and mechanical interblocking [11]. Therefore, chemical treatments can be considered in modifying the properties of plant fibres. Some other compounds are also used to promote adhesion by chemically coupling to adhesive to the material, such as sodium hydroxide, silane, acetic acid, peroxide, acrylic acid, isocyanates, potassium permanganate, etc. Polymer–clay nanocomposites have emerged as a fascinating field of research owing to their multiple advantages, which include an improvement in mechanical, dimensional, thermal, and flame-retarding properties.

The present investigation has been carried out to study and compare the effect of different compatibilisers on various properties of WPCs prepared by using non-conventional plant materials and a mixture of plastics and nanoclay.

## EXPERIMENTAL

### *Materials*

PP homopolymer (H110MA, MFI 115/10 min) was supplied by Reliance Industries Ltd, India. HDPE (PE/20/TK/CN) and polyvinyl chloride suspension resin (SPVC FS: 6701) were supplied by Plast Alloys India Ltd and Finolex Industries Ltd (Mumbai). Other reagents such as 2,3-epoxy glycidyl methacrylate (GMA), polyethylene-*graft*-maleic anhydride (PE-*g*-MA), poly(ethylene-*co*-glycidyl methacrylate) (PE-*co*-GMA), and nanomer (clay modified with 15–35 wt% octadecylamine and 0.5–5 wt% aminopropyltriethoxy silane) were obtained from E-Merck (Mumbai), Otto Chemicals (Mumbai, India) and Sigma-Aldrich (USA). Nal (*Phargmites karka*), a non-conventional wood, was collected from a local forest of Assam. Other solvents and chemicals used were of analytical grade.

### *Preparation of Wood Samples*

Nals (*Phargmites karka*) were collected from local forests and chopped into small pieces. The chopped wood strips were initially washed with 1% soap solution, followed by 1% NaOH solution, and finally with cold water. These pieces were allowed to dry in an oven at 100 ± 5°C until the attainment of

constant weight. The pieces were then ground and sieved. The sieved wood flour was used for making composites.

### *Preparation of Wood–Polymer Nanocomposites*

PP and HDPE granules (8 g each) were added slowly during stirring at room temperature to a flask containing 105 mL of xylene and fitted with a spiral condenser. The temperature was raised to 130°C, and stirring was continued until the mixture became homogeneous. Once a homogeneous solution had been obtained, the temperature of the flask containing the polymer solution was decreased from 130 to 120°C. Another solution containing 4 g of PVC in 35 mL of tetrahydrofuran (THF) was prepared and added slowly at 120°C to the flask containing the PP and HDPE solutions. Stirring was continued for another hour, followed by the addition of compatibiliser (7 phr). A known quantity of nanoclay (3 phr) was dispersed in 10 mL of THF solution by using a stirrer, followed by sonication. This dispersed mixture was added gradually to the polymer solution while stirring took place. Oven-dried WF (40 phr) was added slowly to this matrix solution. The whole mixture was stirred for another hour. The wood–polymer mixture was transferred in a tray, dried and ground. Composite sheets were prepared by using a compression moulding press at 150°C under a pressure of 80 MPa. The optimum ratio of solvents (xylene:THF) and the minimum temperature at which a homogeneous solution was obtained were 70:30 and 120°C.

The polymer blend (HDPE + PP + PVC), polymer blend/7 phr GMA/40 phr wood, polymer blend/7 phr PE-*co*-MA/40 phr wood, and polymer blend/7 phr PE-*co*-GMA/40 phr wood were designated as PB, PB/G7/W40, PB/PM7/W40, and PB/PG7/W40. Polymer blend/7 phr (GMA + PE-*g*-MA + PE-*co*-GMA)/40 phr wood and polymer blend/7 phr (GMA + PE-*g*-MA + PE-*co*-GMA)/40 phr wood/3 phr nanoclay were designated as PB/(G+PM+PG)7/W40 and PB/(G+PM+PG)7/W40/N3.

## MEASUREMENTS

### *X-ray Diffraction Analysis*

The degree of dispersion of nanoclay in the WPC was evaluated by X-ray diffraction (XRD) analysis. It was carried out in a Rigaku X-ray diffractometer (Miniflax, UK) using Cu$K_\alpha$ ($\lambda = 0.154$ nm) radiation at a scanning rate of 1 deg/min, with an angle ranging from 2 to 70°.

### Transmission Electron Microscopy (TEM)

The dispersion of the silicate layers of nanoclay in composites was studied using transmission electron microscopy (JEM-100 CX II) at an accelerated voltage of 20–100 kV.

### Scanning Electron Microscopy

The morphological features of the fractured surfaces of the composites were observed by scanning electron microscope (SEM) (JEOL JSM-6390 LV) at an accelerated voltage of 5–10 kV. Previously, specimens for each of the samples were coated with platinum.

### FTIR Studies

FTIR spectra of wood flour, polymer blend, and WPCs with GMA, PE-*g*-MA, and PE-*co*-GMA compatibilisers were recorded in a FTIR spectrophotometer (Impact-410; Nicolet, USA) using KBr pellets.

### Mechanical Analysis

Tensile tests and flexural tests were performed according to ASTM D-638 and ASTM D-790 on a universal testing machine (Zwick/Z010) with a crosshead speed of 10 mm/m and at room temperature. The modulus of rupture (MOR) and modulus of elasticity (MOE) of the samples were calculated according to the ASTM D-790 method. Three specimens of each composite were tested, and the average values of the different mechanical parameters were reported.

### Hardness Test

The hardness of samples was measured according to the ASTM D-2240 method using a durometer (model RR12) and expressed as Shore D hardness.

### Thermal Analysis

Thermogravimetric analysis (TGA) was undertaken using a thermogravimetric analyser (TG-60; Simadzu, USA) in a nitrogen atmosphere at a flow rate of 30 mL/min. The samples of 3–5 mg were subjected to a temperature programme from room temperature to 600°C at a heating rate of 10 deg/min.

### Limiting Oxygen Index (LOI)

The LOI was measured by a flammability tester (S.C. Dey Co., Kolkata) according to the ASTM D-2863 method. The sample was placed vertically in the sample holder of the LOI apparatus. The total volume of the gas mixture ($N_2 + O_2$) was kept fixed at 18 $cm^3$. In the experiment, the volumes of nitrogen gas and oxygen gas were kept initially at a maximum and minimum level. The volume of nitrogen gas was then gradually decreased and the volume of oxygen gas was increased, but the total volume was kept constant at 18 $cm^3$. The ratio of nitrogen and oxygen at which the sample continued to burn for at least 30 s was recorded.

$$\text{Limiting oxygen index (LOI)} = \frac{\text{volume of } O_2}{\text{volume of } (O_2 + N_2)} \times 100$$

### Water Uptake Study

WPC samples were dipped in distilled water at room temperature (30°C), and the weights were taken after different time intervals. Water uptake is calculated as:

$$\text{Water uptake (\%)} = \frac{W_2 - W_1}{W_1} \times 100$$

where $W_1$ is oven dry weight of composite blocks before dipping in water, and $W_2$ is the weight of composite blocks after dipping in water.

## RESULTS AND DISCUSSION

### XRD Results

**Figure 1** shows the X-ray diffraction patterns of nanoclay and WPC loaded with 3 phr nanoclay. Organically modified nanoclay (curve *a*) shows a sharp diffraction peak (001) at $2\theta = 4.1°$ with a basal spacing of 2.14 nm, as reported in the literature [12]. The intensity of the peak decreased almost to the baseline after incorporation of nanoclay into the wood–polymer matrix (curve *b*). The silicate layers were completely exfoliated after the incorporation of nanoclay

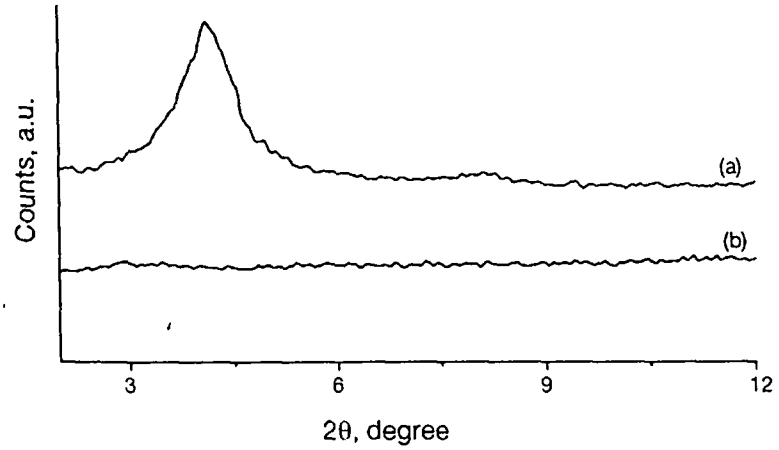


***Figure 1**. X-ray diffraction of (a) nanoclay and (b) PB/(G + PM + PG)7/W40/N3*

into the wood–polymer matrix. The exfoliated nature of the nanoclay was due to the long polymer chains of the polymer matrix that were inserted into the gallery space of the nanoclay, leading to an increase in the interlayer spacing of the silicate layers. Maji and Deka [13] carried out an XRD analysis of nanoclay-loaded WPCs, and found similar exfoliation of silicate layers of WPCs loaded with 3 phr nanoclay.

## *TEM Results*

**Figure 2** shows TEM micrographs of mixed-compatibiliser-based WPCs without nanoclay and loaded with nanoclay. A WPC containing a mixture of compatibilisers (GMA + PE-*g*-MA + PE-*co*-GMA) is represented in **Figure 2a**. The dispersion of nanoclay (dark lines) in the wood–polymer nanocomposite is shown in **Figure 2b**. The silicate layers of nanoclay were found to be distributed well in the wood–polymer matrix. Faruk and Matuana [14] prepared a nanoclay-reinforced wood–HDPE composite and observed a good distribution of silicate layers within it. This result supported the observation of XRD studies.

## *SEM Results*

SEM results for the fractured surface of the polymer blend and WPC samples with different compatibilisers are shown in **Figure 3**. The micrograph of the polymer blend (**Figure 3a**) shows that the polymers are immiscible. The compatibility of the polymer blend was improved on addition of compatibilisers

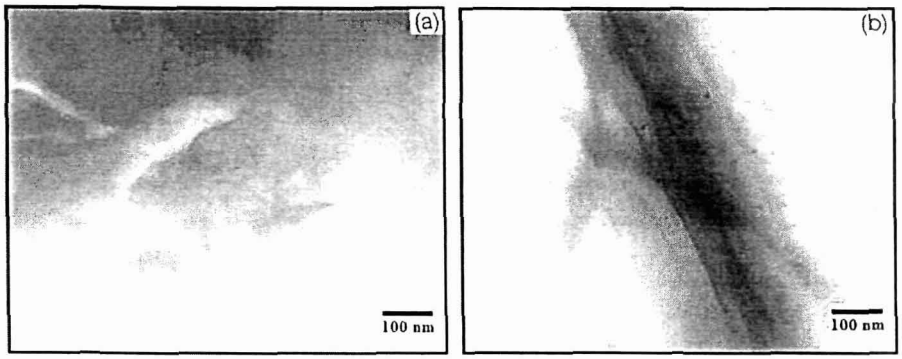


***Figure 2.*** *TEM micrographs of (a) PB/(G + PM + PG)7/W40 and (b) PB/(G + PM + PG)7/W40/N3*

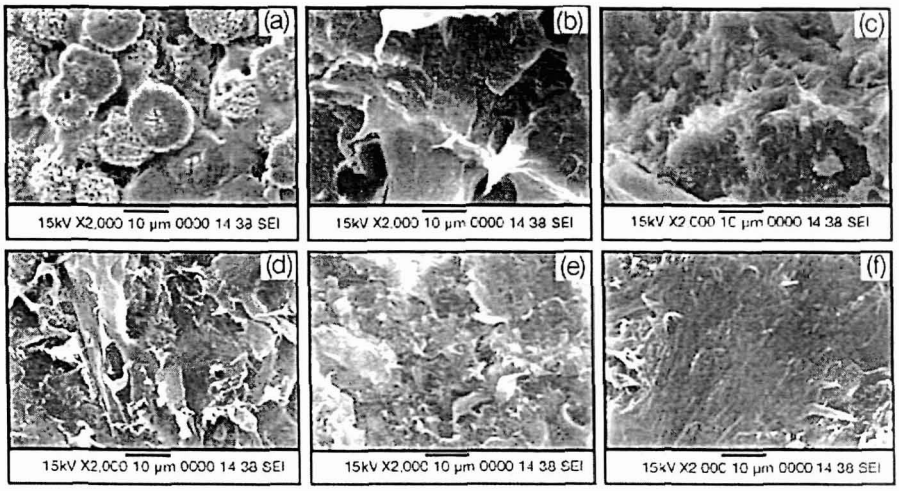


***Figure 3.*** *SEM micrographs of (a) PB, (b) PB/G7/W40, (c) PB/PM7/W40, (d) PB/PG7/W40, (e) PB/(G + PM + PG)7/W40, and (f) PB/(G + PM + PG)7/W40/N3*

(not shown in the figure). An improvement in adhesion between polyolefins and PET obtained by the addition of compatibiliser was reported by Pracella et al. [15]. It was observed that the WPC with a mixture of all three compatibilisers (**Figure 3e**) showed maximum improvement in miscibility compared with WPCs containing GMA (**Figure 3b**), PE-*g*-MA (**Figure 3c**), and PE-*co*-GMA (**Figure 3d**) alone as compatibiliser. The miscibility was judged by the appearance of smoothness. The presence of polar groups in GMA, PE-*g*-MA, and PE-*co*-GMA enhanced the interaction with the hydroxyl group of the wood.

On the other hand, the long polyethylene chain present in PE-*g*-MA and PE-*co*-GMA might interact with the polymer blend. As a result, an improvement in smoothness of the surface would occur. Further, the better compatibility observed in PE-*co*-GMA-added WPC over PE-*g*-MA-added WPC might be attributed to the higher reactivity of the glycidyl group compared with the anhydride group towards the hydroxyl group of wood [16]. Sailaja [17] used poly(ethylene-*co*-glycidyl methacrylate) as a compatibiliser for preparation of a wood pulp–LDPE composite, and found an improvement in interaction between the wood pulp and LDPE owing to the addition of poly(ethylene-*co*-glycidyl methacrylate). The smoothness was further improved after the incorporation of nanoclay (**Figure 3f**). The presence of a long hydrocarbon chain and silane and hydroxyl groups of nanoclay improved the interaction between polymer and wood, resulting in an increase in compatibility.

### *FTIR Results*

FTIR spectra of wood, nanoclay, and wood–polymer composites (WPCs) are shown in **Figure 4**. Curve *a*, representing the spectrum for wood flour, shows the presence of bands at 3435 $cm^{-1}$ for –OH stretching, at 2932 and 2848 $cm^{-1}$ for –CH stretching, at 1731 $cm^{-1}$ for C=O stretching, at 1638 $cm^{-1}$ for –OH bending, at 1161 and 1046 $cm^{-1}$ for C–O stretching, and at 1000–650 $cm^{-1}$ for C–H bending vibration (out of plane). Organically modified nanoclay (curve *b*) exhibits peaks at 3471 $cm^{-1}$ (–OH stretching), 2936 and 2851 $cm^{-1}$ (–CH stretching of modified hydrocarbon), 1622 $cm^{-1}$ (–OH bending), and 1031–462 $cm^{-1}$ (oxide bands of metals such as Si, Al, Mg, etc.) [18]. PB/G7/W40 (curve *c*) exhibits peaks at 3431 $cm^{-1}$ (–OH stretching), 2925 and 2842 $cm^{-1}$ (–CH stretching), 1732 $cm^{-1}$ (C=O stretching), 1633 $cm^{-1}$ (–OH bending) and 716 $cm^{-1}$ ($-CH_2$ bending), and the characteristic peak for the epoxy group at 995 $cm^{-1}$.

**Figure 4** (curves *d* and *e*) shows the spectra for WPCs compatibilised with PE-*g*-MA and PE-*co*-GMA. The peak at 994 $cm^{-1}$, representing the epoxy group, was found to be present in the PE-*co*-GMA-compatibilised WPC system (curve *e*). The intensity of the hydroxyl peak at 3435 $cm^{-1}$ of wood was found to decrease significantly for all the compatibilised WPCs. Moreover, the hydroxyl peak was found to shift to a lower wave number. The reduction in intensity of the hydroxyl group was greater in PE-*co*-GMA- (curve *e*) and PE-*g*-MA-compatibilised WPCs compared with GMA-compatibilised WPC. The shifting of the hydroxyl peak and the decrease in intensity were greater in WPC compatibilised with a 1:1:1 ratio of blended compatibiliser (curve *f*). Both the shifting and the decrease in intensity of the hydroxyl group were further pronounced by the addition of nanoclay (curve *g*). Furthermore, the

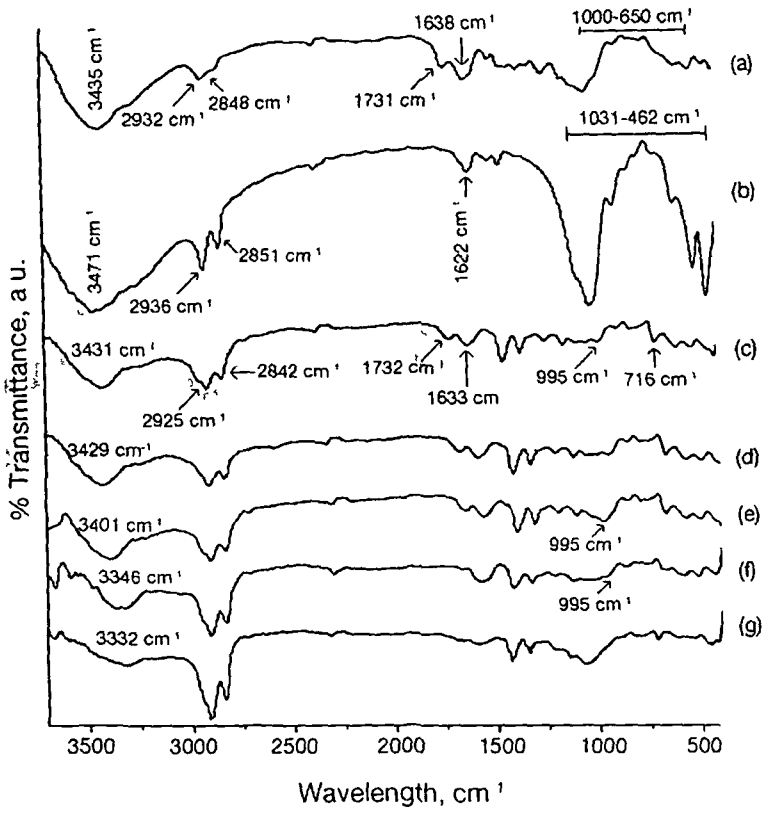


***Figure 4.*** *FTIR spectra of (a) wood flour, (b) nanoclay, (c) PB/G7/W40, (d) PB/PM7/W40, (e) PB/PG7/W40, (f) PB/(G + PM + PG)7/W40, and (g) PB/(G + PM + PG)7/W40/N3*

intensity of the peak at 2925 $cm^{-1}$ corresponding to $-CH_2$ stretching was greater. Dikobe and Luyt [10] reported that the peak intensity of the hydroxyl group decreased owing to interaction between poly(ethylene-*co*-glycidyl methacrylate) and wood flour Awal et al. [19] studied the FTIR spectra of a PP/wood pulp/MAPP composite and reported that the hydroxyl peak shifted to a lower wave number. All this indicated the formation of a strong bond between polymer, compatibiliser, wood and clay.

## *Mechanical Properties*

The flexural and tensile properties of the polymer blend and WPCs containing different compatibilisers and nanoclay are shown in **Table 1**. The data are the average of three values. It was observed that the WPC containing the combined

**Table 1. Mechanical properties of wood–polymer composites with various compatibilisers and nanoclay**

| Sample | Flexural properties | | Tensile properties | | Hardness (Shore D) |
|---|---|---|---|---|---|
| | Strength (MPa) | Modulus (MPa) | Strength (MPa) | Modulus (MPa) | |
| PB | 13.43 ± 1.02 | 758.53 ± 1.05 | 8.27 ± 1.09 | 117.37 ± 11.43 | 66 |
| PB/G7/W40 | 16.19 ± 0.67 | 3221.68 ± 0.93 | 14.56 ± 0.87 | 197.83 ± 17.72 | 65 |
| PB/PM7/W40 | 17.84 ± 0.58 | 3572.37 ± 0.74 | 16.64 ± 0.71 | 231.45 ± 15.86 | 67 |
| PB/PG7/W40 | 19.55 ± 0.74 | 3724.28 ± 0.92 | 19.15 ± 0.54 | 274.09 ± 19.37 | 68 |
| PB/(G+PM+PG)7/W40 | 21.03 ± 0.31 | 4215.64 ± 0.51 | 21.73 ± 0.39 | 325.74 ± 18.68 | 69 |
| PB/(G+PM+PG)7/W20/N3 | 23.69 ± 0.77 | 4319.25 ± 0.05 | 26.48 ± 0.72 | 391.36 ± 19.65 | 71 |
| PB/(G+PM+PG)7/W40/N3 | 27.86 ± 0.56 | 4781.22 ± 0 46 | 32.52 ± 0.16 | 572.96 ± 23 62 | 76 |
| PB/(G+PM+PG)7/W60/N3 | 25.92 ± 0.42 | 4596.79 ± 0.68 | 29.82 ± 0 93 | 458.42 ± 20.27 | 73 |

compatibiliser (GMA + PE-*g*-MA + PE-*co*-GMA) showed higher flexural and tensile properties compared with GMA-, PE-*g*-MA-, and PE-*co*-GMA-based WPCs. GMA and PE-*co*-GMA facilitated interfacial adhesion between polymer blend and wood flour through their double bond or polyethylene chain and epoxy group. The polymer chain and anhydride group of PE-*g*-MA also interacted with the polymer blend and wood flour. The reactivity of the epoxy group towards the hydroxyl group of wood was greater by comparison with the anhydride group of PE-*g*-MA [16]. As a result, both the flexural and tensile properties of PE-*co*-GMA-based WPC were greater than those of either the GMA-based or the PE-*g*-MA-based WPC. The use of poly(ethylene-*co*-glycidyl) methacrylate with wood flour and ethylene–vinyl acetate composite improved the mechanical properties [10]. Liu et al. [20] reported that the mechanical properties of HDPE/bamboo flour were enhanced by the addition of PE-*g*-MA. The combined compatibiliser produced better synergism in improving the flexural and tensile properties of the WPC compared with the individual compatibilisers. The mechanical properties of the WPC prepared by using a mixture of compatibilisers were further improved after the incorporation of nanoclay. The improvement in properties was due to the dispersion of nanoclay in the wood–polymer matrix and to restriction in the movement of the polymer chains inside the silicate layers. The nanomer had some hydrocarbon as well as silane groups, which also favoured the interaction between wood flour and polymer blends. Hence, an improvement in properties was observed. Faruk and Matuana [14] reported that the mechanical properties of HDPE/

wood flour composites were improved by the addition of coupling agent and nanoclay to the composites.

The flexural and tensile properties of WPCs having clay and different percentages of wood fibre loading are also shown in **Table 1**. At a fixed compatibiliser and nanoclay concentration, both flexural and tensile properties increased up to the loading of 40 phr wood flour. Beyond that, the values decreased. The increasing trend was probably due to the improved interaction between wood flour, clay, and polymer blend because of the mixed compatibiliser. The compatibiliser would facilitate the transfer of applied load through the interface between polymer matrix and wood flour. An increase in the mechanical properties of HDPE/bamboo flour composite with increase in bamboo flour loading was reported by Liu et al. [20]. The decrease in the tensile and flexural values at higher loading of wood flour might be due to the reduced interaction caused by the presence of an insufficient amount of compatibiliser for complete reaction with the hydroxyl group of wood flours, nanoclay, and polymers.

### *Hardness Results*

**Table 1** shows the hardness results for the polymer blend and for WPCs with different compatibilisers and nanoclay. From the table it can be seen that the WPC containing the mixed compatibiliser exhibited better hardness than either the polymer blend alone or the other compatibiliser-based WPCs. The increased hardness in the polymer blend was due to the improvement in interfacial adhesion between various polymers and wood by compatibilisers, as explained earlier. The hardness values were further increased after the incorporation of nanoclay. Nanoclay improved the interaction between wood flour and polymer blend and reduced the movement of the polymer chains intercalated inside the silicate layers

### *Thermogravimetric Analysis*

**Table 2** shows the initial decomposition temperature ($T_i$), the maximum pyrolysis temperature ($T_m$), the decomposition temperature at different weight loss (%) ($T_D$), and the residual weight (RW%) for wood flour, the polymer blend, and the WPCs. The $T_i$ and $T_m$ values of the WPCs were found to be higher than those of wood flour and the polymer blend. The maximum improvements in $T_i$, $T_m$, and $T_D$ values were observed in the case of the nanoclay-reinforced (GMA + PE-*g*-MA + PE-*co*-GMA)-compatibilised WPC. The RW(%) values of the WPCs were found to lie in between those of wood flour and the polymer blend.

**Table 2. Thermal analysis of wood–polymer composites with different compatibilisers and nanoclay**

| Sample | $T_i$[a] | $T_m$[b] | $T_m$[c] | Temperature of decomposition $T_D$ (°C) at different percentage weight loss | | | | RW% at 600°C |
|---|---|---|---|---|---|---|---|---|
| | | | | 20% | 40% | 60% | 80% | |
| Wood flour | 232 | 313 | — | 280 | 321 | 349 | — | 26.4 |
| PB | 240 | 271 | 404 | 295 | 386 | 443 | 468 | 5.4 |
| PB/G7/W40 | 247 | 278 | 445 | 302 | 391 | 451 | 474 | 6.3 |
| PB/PM7/W40 | 251 | 285 | 452 | 308 | 397 | 457 | 479 | 6.4 |
| PB/PG7/W40 | 256 | 291 | 460 | 313 | 405 | 463 | 483 | 6.6 |
| PB/(G+PM+PG)7/W40 | 259 | 296 | 465 | 318 | 407 | 468 | 487 | 6.8 |
| PB/(G+PM+PG)7/W40/N3 | 271 | 314 | 477 | 326 | 443 | 480 | 497 | 9.7 |

[a] *$T_i$: value for initial degradation*
[b] *$T_m$: value for first step*
[c] *$T_m$: value for second step*

The thermal stability of WPCs was greater than that of wood flour. The WPC compatibilised with (GMA + PE-*g*-MA + PE-*co*-GMA) was more thermally stable compared with composites compatibilised with GMA, PE-*g*-MA, and PE-*co*-GMA alone. The increase in thermal stability might be attributed to the increased interfacial adhesion caused by the reaction between either the epoxy group of GMA and PE-*co*-GMA or the anhydride group of PE-*co*-GMA with the hydroxyl group of wood flour. The hydrocarbon chains of compatibilisers also enhanced the interaction with the polymer blend. Among the individual compatibilisers, PE-*co*-GMA exhibited maximum interaction. This was due to the higher reactivity of the glycidyl group towards the hydroxyl group of wood. The blend compatibiliser exhibited maximum thermal stability owing to the synergistic effect. Hetzer et al. [21] reported that the thermal properties of a polyethylene/clay composite was improved by adding a blend of low- and high-molecular-weight maleic-anhydride-modified polyethene as a mixed compatibiliser [21]. The increase in $T_D$ values of nanoclay-reinforced WPC was due to the presence of silicate layers of nanoclay, which increased the tortuous path and hence delayed the diffusion of decomposed volatile products throughout the composites [22].

The RW(%) value for clay-treated WPC was greater compared with either the polymer blend or the WPCs. This was due to the formation of char by the inorganic clay.

### Limiting Oxygen Index

**Table 3** shows the limiting oxygen index (LOI) values of the polymer blend and WPCs with different compatibilisers and nanoclay. The LOI values of WPCs were found to be greater than those of the polymer blend. The highest value was observed for the WPC containing the mixed compatibiliser and nanoclay. This was due to improvement in interfacial adhesion by the various functional groups and long-chain hydrocarbon present in the different compatibilisers with hydroxyl groups of wood and the polymer blend. Zhao et al. [23] studied the flame retardancy of a rice hulk–HDPE composite with LLDPE-*g*-MA as a compatibiliser and found that the flame retardancy of the WPC improved over neat HDPE. The silicate char produced by nanoclay on the surface of the WPC also increased the flame resistance of the composite. A similar observation was reported by Camino et al. [24] while studying the combustion behaviour of a silicate–epoxy nanocomposite. The silicate-rich surface had a better barrier property to heat and oxygen transport, on account of which ignition of the composite was delayed.

**Table 3. Limiting oxygen indices (LOIs) and flaming characteristics of the polymer blend and wood–polymer composites**

| Samples | LOI (%) | Flame description | Smoke and fumes | Char |
|---|---|---|---|---|
| PB | 24 | Candle-like localised | — | Little |
| PB/G7/W40 | 40 | Small localised flame | Small and black smoke | Medium |
| PB/PM7/W40 | 43 | Small localised flame | Small and black smoke | Medium |
| PB/PG7/W40 | 45 | Small localised flame | Small and black smoke | Medium |
| PB/(G+PM+PG)7/W40 | 49 | Small localised flame | Small and black smoke | Medium |
| PB/(G+PM+PG)7/W40/N3 | 60 | Small localised flame | Small and black smoke | Higher |

### Water Absorption

The results of water uptake for the polymer blend and wood–plastic composites with and without nanoclay are shown in **Figure 5**. From the figure it can be seen that water uptake increased with increase in immersion time. The WPCs exhibited higher water absorption compared with the polymer blend. Water absorption was found to follow the order: WPC with GMA > WPC with PE-*g*-MA > WPC with PE-*co*-GMA > WPC with (GMA + PE-*g*-MA + PE-*co*-GMA)

> WPC with (GMA + PE-*g*-MA + PE-co-GMA)/nanoclay > polymer blend. The higher water absorption shown by WPCs compared with the polymer blend was due to the hydrophilic nature of wood fibres. The compatibiliser enhanced the interaction between the polymers and wood fibres. The amount of free hydroxyl groups in wood fibres decreased because of the formation of epoxide or ester linkages between the wood fibres and the epoxy part of GMA and PE-*co*-GMA or the anhydride part of PE-*g*-MA. The water absorption of WPCs treated with PE-*g*-MA and with PE-co-GMA decreased owing to these changes. Avella et al. [25] reported that composites made with fibres and treated with maleated polypropylene showed lower water absorption compared with composites made without maleated polypropylene. The blend compatibiliser further increased the interaction between wood and polymer and reduced the water absorption. The absorption of water vapour decreased further on the addition of nanoclay. The silicate layers of clay provided resistance to water transport owing to its longer tortuous path and thus decreased the water transportation.

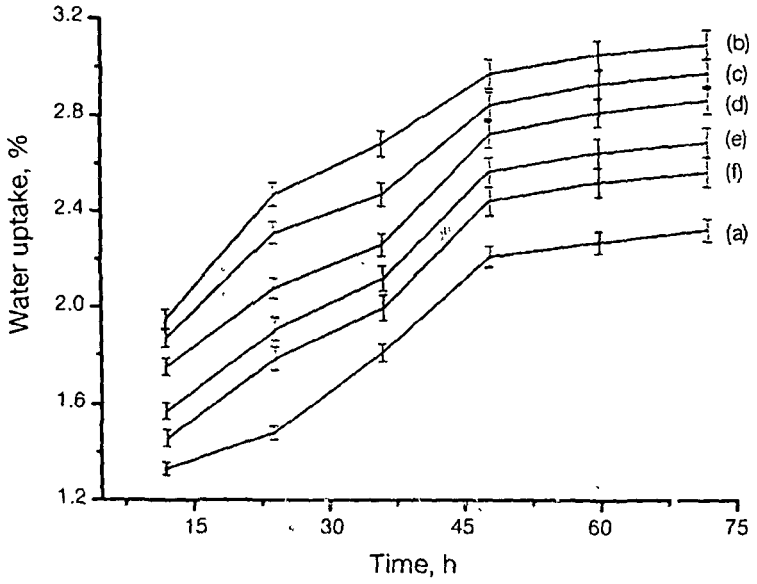


***Figure 5.*** *Water absorption of (a) PB, (b) PB/G7/W40, (c) PB/PM7/W40, (d) PB/PG7/W40, (e) PB/(G + PM + PG)7/W40, and (f) PB/(G + PM + PG)7/W40/N3*

## CONCLUSION

The optimum ratio of xylene and THF for solution blending of HDPE, PP, and PVC (1:1:0.5) was 70:30. XRD and TEM studies showed an exfoliation of silicate layers in WPCs. The improvement in compatibility between the polymer blend and the wood flour by the addition of compatibiliser was revealed by SEM. The SEM study also showed that the mixed compatibiliser produced maximum compatibility. The production of maximum interaction due to the presence of the mixed compatibiliser and nanoclay was reported by the FTIR method. The flexural, tensile, and hardness properties of the nanoclay-reinforced WPC compatibilised with (GMA + PE-*g*-MA + PE-co-GMA) were better in comparison with those of the polymer blend and PE-*co*-GMA-, PE-*g*-MA-, and GMA-compatibilised WPCs. Maximum improvement in properties occurred at 40 phr fibre loading. The thermal stabilities of the WPCs were greater than that of virgin wood owing to incorporation of compatibilisers. Maximum thermal stability and flame resistance were observed for nanoclay-based WPC compatibilised with (GMA + PE-*g*-MA + PE-*co*-GMA), followed by WPC compatibilised with PE-*co*-GMA, PE-*g*-MA, and GMA. The nanoclay-reinforced mixed-compatibiliser-based WPC showed least water absorption in comparison with the polymer blend and other compatibiliser-based WPCs.

## ACKNOWLEDGEMENT

The authors are grateful to the Council for Scientific and Industrial Research (CSIR, New Delhi) for their financial assistance.

## REFERENCES

1. Xu X., Jayaraman K., Morin C., and Pecqueux N , *J. Mater. Process. Technol.*, **198** (2008) 168–177.
2. Ashori A., *Bioresour. Technol.*, **99** (2008) 4661–4667.
3. Sui G., Fuqua M.A., Ulven C.A., and Zhong W.H., *Bioresour. Technol.*, **100** (2009) 1246–1251.
4. Yemele M.C.N., Koubaa A., Cloutier A., Soulounganga P., and Wolcott M., *Compos. Part A: Appl. Sci.*, **41** (2010) 131–137.
5. Bledzki A.K., Mamun A.A. and Volk J., *Compos. Sci. Technol.*, **70** (2010) 840–846.
6. Tasdemir M., Biltekin H., and Caneba G.T., *J. Appl. Polym. Sci.*, **112** (2009) 3095–3102.

7. Zhong Y., Poloso T., Hetzer M., and Kee D.D., *Polym. Eng. Sci.*, **47** (2007) 797–803.

8. Geng Y., Li K., and Simonsen J., *J. Appl. Polym. Sci.*, **91** (2004) 3667–3672.

9. Devi R. and Maji T.K., *Polym. Compos.*, **28** (2007) 1–5.

10. Dikobe D.G. and Luyt A.S., *J. Appl. Polym. Sci.*, **104** (2007) 3206–3213.

11. Lu J.Z., Wu Q., and McNabb H.S., *Wood Fiber Sci.*, **32** (2000) 88–104.

12. Lei Y., Wu Q., Clemons C.M., Yao F., and Xu Y., *J. Appl. Polym. Sci.*, **106** (2007) 3958–3966.

13. Deka B.K. and Maji T.K., *Compos. Sci. Technol.*, **70** (2010) 1755–1761.

14. Faruk O. and Matuana L.M., *Compos. Sci. Technol.*, **68** (2008) 2073–2077.

15. Pracella M., Chionna D., Ishak R., and Galeski A., *Polym. Plast. Technol. Eng.*, **43** (2004) 1711–1722.

16. Sun Y.J., Hu G.H., Lambla M., and Koltar H.K., *Polymer*, **37** (1996) 4119–4127.

17. Sailaja R.R.N., *Compos. Sci. Technol.*, **66** (2006) 2039–2048.

18. Das G. and Karak N., *Prog. Org. Coat.*, **66** (2009) 59–64.

19. Awal A., Ghosh S.B., and Sain M., *J. Mater. Sci.*, **44** (2009) 2876–2881.

20. Liu H., Wu Q., Han G., Yao F., Kojime Y., Suzuki S., *Compos. Part A: Appl. Sci.*, **39** (2008) 1891–1900.

21. Hetzer M., Zhou H.X., Poloso T., and Kee D.D., *Mater. Sci. Technol.*, **27** (2011) 53-59

22. Qin H., Zhang S., Zhao C., Feng M., Yang M., and Shu Z., *Polym. Degrad. Stab.*, **85** (2004) 807–813.

23. Zhao Q., Zhang B., Quan H., Yam R.C.M, Yuen R.K.K., and Li R.K.Y., *Compos. Sci. Technol.*, **69** (2009) 2675–2681.

24. Camino G., Tartagilione G., Frache A., Manferti C., and Costa G , *Polym. Degrad. Stab.*, **90** (2005) 354–362.

25. Avella M., Bozzi C., Erba R.D., Focher B., Marzetti A., and Martuscelli E., *Macromol. Mater. Eng.*, **233** (2003) 149–166.

Composites Science and Technology 70 (2010) 1755–1761

Contents lists available at ScienceDirect

Composites Science and Technology

journal homepage: www.elsevier.com/locate/compscitech

# Effect of coupling agent and nanoclay on properties of HDPE, LDPE, PP, PVC blend and *Phargamites karka* nanocomposite

Biplab K. Deka, T.K. Maji *

*Department of Chemical Sciences, Tezpur University, Assam 784 028, India*

ARTICLE INFO

*Article history:*
Received 11 February 2010
Received in revised form 12 June 2010
Accepted 11 July 2010
Available online 16 July 2010

*Keywords:*
A. Nano composites
A. Wood
A. Polymers
B. Mechanical properties
D. Scanning electron microscopy

ABSTRACT

High density polyethylene (HDPE), low density polyethylene (LDPE), polypropylene (PP) and poly(vinyl chloride) (PVC) were solution blended by using a mixture of xylene and tetrahydrofuran as solvent and polyethylene-co-glycidyl methacrylate (PE-co-GMA) as compatibilizer. The minimum ratio of solvents to obtain a homogenous solution was optimised. Wood polymer composites (WPC) were prepared by using solution blended polymer, wood flour and nanoclay. X-ray diffraction studies of WPC treated with 1 and 3 phr nanoclay showed higher exfoliation compared to WPC treated with 5 phr nanoclay. TEM study also supported the above findings. FTIR studies indicated an interaction between wood, PE-co-GMA and clay. SEM study indicated an increase in miscibility among polymers due to addition of PE-co-GMA as compatibilizer. Thermal stability improved on addition of clay to the WPC. WPC treated with 3 phr clay showed highest mechanical properties. Hardness and water absorption were improved significantly with the addition of nanoclay to wood/polymer composite.



## 1. Introduction

Nal (*Phargamites karka*), a type of nonconventional plant is widely available not only in the forests of Assam but also on both the banks of The Brahmaputra river. These plants are not considered for structural applications due to their poor mechanical, dimensional and other properties. They are mostly used for making temporary shades and domestic fuels. These plants can be made value added products by producing composites with different polymers.

Varieties of waste plastic materials in the form of carry bags, packaging film, container, etc. cause environmental pollution. Recycling is one of the process to reduce the pollution. But the mechanical and other properties of the recycled materials are poor due to poor compatibility among different plastics. The compatibility among different waste plastic material can be improved by the use of a compatibilizer.

Waste plastic materials consist of a higher amount of polyethylene (PE), polypropylene (PP) and a lesser amount of polyvinylchloride (PVC), polystyrene (PS), polyethylene terapthalate (PET). Solution blending is one of the process used for blending of different kind of plastics. The effectivity of the blending process can be improved by the use of a mixture of solvents. The optimum ratio of solvents can be judged properly if the percentage of individual polymer along with their physical characteristics in waste plastics is known. This can be overcome if a mixture of known percentage of virgin HDPE, PP, PVC, etc. is used as starting waste plastic material.

Polymer–clay nanocomposites have evoked a great interest in recent years. Improvements in mechanical, dimensional, thermal, flame retardancy have been the reason for their widespread use [1–3].

In order to make a good composite, the improvement in adhesion among plastics materials as well as with plant material is very important. The adhesion or compatibility can be improved by using a compatibilizer. The compatibilizer should be able to react with hydrophilic plant material and hydrophobic plastic materials. Pracella et al. [4] used ethylene-glycidyl methacrylate copolymer, ethylene-propylene copolymer grafted maleic anhydride, isotactic PP grafted acrylic acid for improvement in interaction between various polyolefins and polyethylene terapthalate.

The use of maleated polypropylene compatibilizer enhances the dimensional stability and mechanical properties of the polypropylene, wood flour and nanoclay composite [5]. Glycidyl methacrylate (GMA) has been used as a compatibilizer to modify the adhesion between wood and polymer [6]. Reports on a large number of polymer nanocomposites [7–9] are available. However, far less is known regarding wood polymer nanocomposite.

The objective of the present study is to prepare the nanocomposites using wood flour, PE-co-GMA, nanoclay, polymer mixture of (HDPE + LDPE + PP + PVC) by solution blending. Efforts have also been made to study the various properties of the nanocomposite.

* Corresponding author. Tel.: +91 3712 267007x5053; fax: +91 3712 267005.
*E-mail address:* tkm@tezu.ernet.in (T.K. Maji).

0266-3538/$ - see front matter © 2010 Elsevier Ltd. All rights reserved.
doi:10.1016/j.compscitech.2010.07.010

## 2. Experimental

### 2.1. Materials

HDPE and LDPE (Grade: PE/20/TK/CN) were obtained by the courtesy of Plast Alloys India Ltd. (Harayana, India). PP homopolymer (Grade: H110MA, MFI 11 g/10 min) and PVC (Grade: SPVC FS: 6701) were supplied by Reliance Industries Ltd. (Mumbai, India) and Finolex Industries Ltd. (Pune, India). The compatibilizer poly(ethylene-co-glycidyl methacrylate)(PE-co-GMA) (Otto, Mumbai, India) and nanomer (clay modified by 15–35 wt.% octadecylamine and 0.5–5 wt.% aminopropyltriethoxy silane, Sigma–Aldrich, USA) were used as such received. A nonconventional wood, Nal, was collected from local forest of Assam. Other reagents used were of analytical grade.

### 2.2. Preparation of wood samples

Nals (*Phargamites karka*) were collected from the local forest and chopped into small strips. The chopped wood strips were initially washed with 1% soap solution, followed by washing with 1% NaOH solution and finally with cold water. The washed wood strips were oven dried at 105 ± 5 °C till attainment of constant weight. These dried wood strips were grinded in a mixer and sieved. The sieved wood flour was kept in a container for subsequent use.

### 2.3. Preparation of wood polymer nanocomposite

A certain amount of xylene was taken in a flask fitted with a condenser. To this, the granules of HDPE, LDPE and PP were added slowly at room temperature. The compatibilizer, PE-co-GMA was also added at the same time. The temperature of the flask was increased to 130 °C in order to make a homogenous solution. The temperature of the flask was then decreased to 120 °C. Now, another solution containing a predetermined quantity of PVC in tetrahydrofuran (THF) was prepared. Both these solutions were mixed at 120 °C (approximately) under stirring condition for 1 h. A known quantity of nanomer was dispersed in tetrahydrofuran (THF) solution by sonication. This dispersed clay-THF mixture was added gradually to the polymer solution under stirring condition. Oven dried wood flour was added slowly to this clay–polymer solution. The mixing was done for another 1 h. The mixture was transferred in tray, dried and grinded. The composite sheets were obtained by the compression molding press (Santec, New Delhi) at 150 °C under a pressure of 80 MPa.

Polymer blend (HDPE + LDPE + PP + PVC), polymer blend/5 phr PE-co-GMA, polymer blend/5 phr PE-co-GMA/3 phr nanomer and polymer blend/5 phr PE-co-GMA/40 phr wood were designated as PB, PB/G5, PB/G5/N3 and PB/G5/W40. WPCs reinforced with 1, 3 and 5 phr clay were designated as PB/G5/W40/N1, PB/G5/W40/N3 and PB/G5/W40/N5.

## 3. Measurements

### 3.1. X-ray diffraction (XRD)

The degrees of clay intercalation in WPCs were evaluated by X-ray diffraction (XRD) analysis. XRD measurements were carried out in a Rigaku X-ray diffractometer (Miniflax, UK) using Cu Kα ($\lambda$ = 0.154 nm) radiation at a scanning rate of 1°/min with an angle ranging from 2° to 30°.

### 3.2. Transmission electron microscopy (TEM)

The study of the dispersion of silicate layers of nanoclay in WPCs were performed by using Transmission Electron Microscope (JEM-100 CX II) at an accelerated voltage of 20–100 kV.

### 3.3. FTIR studies

FTIR spectra of wood flour, nanoclay and WPCs were recorded in FTIR spectrophotometer (Impact-410, Nicolet, USA) using KBr pellet.

### 3.4. Scanning electron microscopy (SEM)

The compatibility among different polymers as well as morphological features of the WPC were studied by using Scanning electron microscope (JEOL JSM – 6390LV) at an accelerated voltage of 5–10 kV. Fractured surface of the samples, deposited on a brass holder and sputtered with platinum, were used for this study.

### 3.5. Thermal property

Thermal properties of WPCs were measured in a thermogravimetric analyser (TGA) (TGA-50, shimadzu) at a heating rate of 10 °C/min up to 600 °C under nitrogen atmosphere.

### 3.6. Mechanical property

The tensile and flexural tests for polymer blend and WPCs were carried out using Universal Testing Machine (Zwick, model Z010) at a crosshead speed of 10 mm/min at room temperature according to ASTM D-638 and D-790 respectively. Three samples of each category were tested and their average values were reported.

### 3.7. Hardness

The hardness of the samples were measured according to ASTM D-2240 using a durameter (model RR12) and expressed as shore D hardness.

### 3.8. Water uptake

Percentage water uptake was measured by submerging the samples in distilled water at room temperature (30 °C) for different time periods after conditioning at 65% relative humidity, according to the formulae below.

$$\text{Water uptake } (\%) = (W_s - W_1)/W_1 \times 100$$

where $W_s$ is the weight of the water saturated specimen and $W_1$ is the weight of the oven dried specimen.

## 4. Results and discussion

In order to optimise the solvent ratio, HDPE, LDPE, PP and PVC were mixed in the ratio of 2:2:2:1. Preliminary investigations indicated that xylene was a good solvent for HDPE, LDPE and PP. Similarly, tetrahydrofuran (THF) was a good solvent for PVC. Neither xylene nor THF could solubilise the mixture of HDPE, LDPE, PP and PVC (2:2:2:1). The solubility of the polymer mixture was checked by varying the ratio of xylene and THF. The optimum ratio of solvent (xylene:THF) and minimum temperature at which a homogeneous solution was obtained, were 70:30 and 120 °C respectively.

### 4.1. XRD results

The XRD patterns of pure nanoclay and WPCs with different percentage of nanoclay loading are shown in Fig. 1. The interlayer spacing was calculated according to Bragg's law,

$$n\lambda = 2d\text{Sin}\theta \quad (1)$$

The organically modified nanoclay (curve a) shows a sharp peak at $2\theta$ = 4.1°. The peak (curve e) shifted to a lower diffraction angle

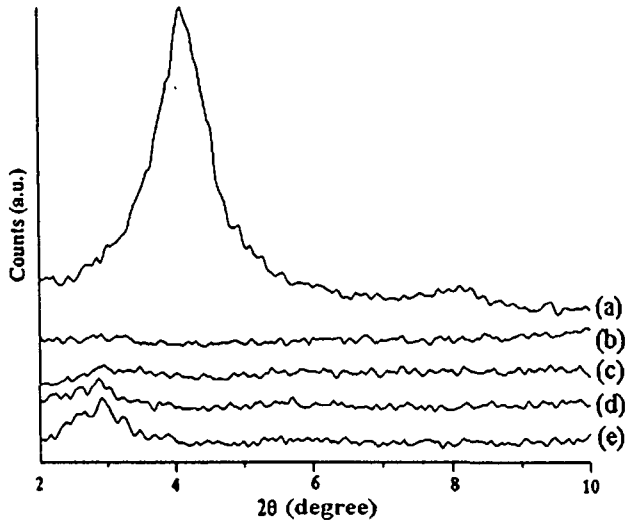


Fig. 1. X-ray diffraction of: (a) nanomer, (b) PB/G5/W40/N1, (c) PB/G5/W40/N3, (d) PB/G5/W40/N5, (e) PB/G5/N3.

($2\theta = 2.9°$) in the case of nanomer and PE-co-GMA containing polymer nanocomposite. The shifting of the peak to lower angle indicated an increase in interlayer spacing of silicate layers. The polymer chains were intercalated into the silicate nanolayers of the polymer composite. A shifting of diffraction peak to the lower angle for the clay based HDPE nanocomposite was reported in the literature [10]. The peak could not be identified in the case of WPC (curves b and c) indicating an exfoliated structure. WPC loaded with 5 phr nanomer (curve d) showed a small peak at $2\theta = 2.8°$. The reduction in peak intensity as well as shifting of peak to lower angle suggested an increased disorder into the nanoclay layers in the nanocomposite. The observed peak at higher loading of nanomer might be due to agglomeration of some clay. The silicates nanolayers might be partially exfoliated and partially intercalated. The shifting of the peak from higher diffraction angle to lower diffraction angle was reported by Lee and Kim [11] while studying the interaction of organoclay with wood/polypropylene composite.

### 4.2. TEM study

Fig. 2 shows the TEM micrographs of WPC with various percentage of nanomer content. The dark line represents the intersection of silicate layers. The dispersion of clay layers in the WPC was observed even at lower level of nanomer (1 phr) loading (Fig. 2a). The nanomer exhibited better dispersion of clay layers in WPC when loading of nanomer increased to 3 phr (Fig. 2b). However, with the increase in the level of nanomer loading to 5 phr (Fig. 2c), the size of nanomer became larger or aggregated. Similar observation was reported by Zhao et al. [12] while studying the dispersion of organically modified montmorillonite into wood flour/polyvinyl chloride matrix. TEM results supported the findings of XRD studies.

### 4.3. FTIR study

FTIR spectra of wood, nanoclay, clay added polymer blend and WPCs are shown in Fig. 3. The FTIR spectra of wood (curve a) showed the presence of bands at 3423 $cm^{-1}$ for -OH stretching, 2923 $cm^{-1}$ for -CH stretching, 1734 $cm^{-1}$ for C=O stretching, 1636 $cm^{-1}$ for -OH bending, 1160 and 1046 $cm^{-1}$ for C-O stretching and 1000–650 $cm^{-1}$ for C-H bending vibration (out of plane). Organically modified nanoclay (curve b) exhibited the peaks at 3467 $cm^{-1}$ (-OH stretching) 2927 and 2852 $cm^{-1}$ (-CH stretching of modified hydrocarbon), 1619 $cm^{-1}$ (-OH bending), 1031–460 $cm^{-1}$ (oxide bands of metals like Si, Al, Mg, etc.). PB/G5/N3 (curve c) exhibited characteristic peaks of -CH stretching at 2927 $cm^{-1}$ and 1460 $cm^{-1}$, C-$CH_3$ stretching at 2850 $cm^{-1}$ along with -$CH_2$- stretching at 720 $cm^{-1}$.

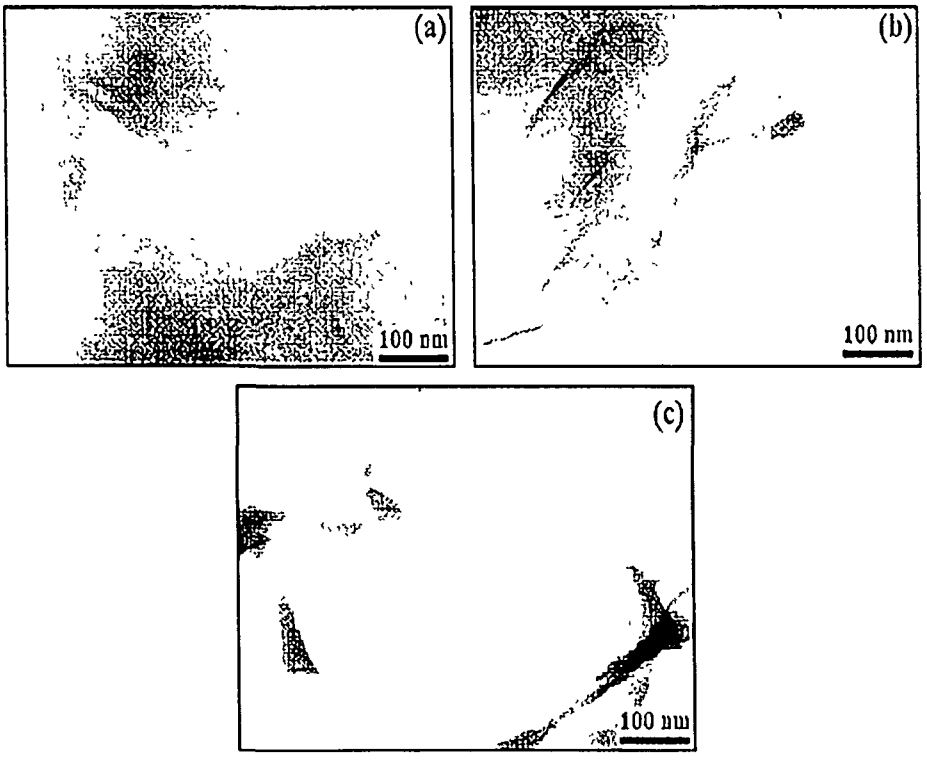


Fig. 2. TEM micrographs of: (a) PB/G5/W40/N1, (b) PB/G5/W40/N3, (c) PB/G5/W40/N5

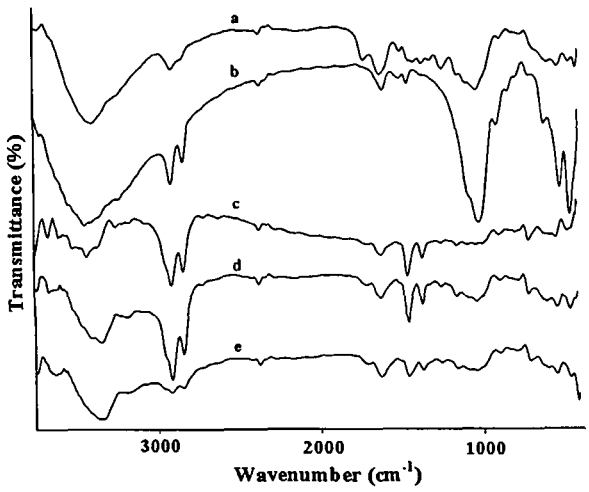


Fig. 3. FTIR spectra of: (a) wood flour, (b) nanomer, (c) PB/G5/N3, (d) PB/G5/W40/N3, (e) PB/G5/W40/N5.

Fig. 3d and e represented the FTIR spectra of wood polymer nanocomposite. It was found that the intensity of the hydroxyl peak decreased as well as shifted to lower wave number in the wood polymer composite. The decrease in peak intensity in the nanocomposite might be attributed to the participation of hydroxyl group of clay in the crosslinking reaction with wood and polymer. The shifting of absorption peak corresponding to hydroxyl group to 3415 $cm^{-1}$ (curve d) and 3411 $cm^{-1}$ (curve e) confirmed the formation of hydrogen bond between wood surfaces and matrix. Furthermore, the intensity of peaks at 2923 $cm^{-1}$ corresponding to -CH stretching was more in wood composites compared to pure wood which indicated the formation of bond between polymers, PE-co-GMA and wood. Similar type of shifting of hydroxyl group to lower wave number and increase in intensity of -C-H stretching was reported by Awal et al. [13] while studying the FTIR analysis of PP/maleated polypropylene/wood composite. The other peaks observed in the spectra of wood polymer composites (curves d and e) at 1050 $cm^{-1}$ and 720 $cm^{-1}$ were due to the C-O stretching of wood, oxide bands of silicon and $-CH_2-$ stretching of polymer. The peaks in the range 450–500 $cm^{-1}$ were due to the oxide bands of metals like aluminium and magnesium respectively.

### 4.4. SEM study

SEM micrographs of different fractured samples are shown in Fig. 4. The fractured surface of untreated polymer sample is shown in Fig. 4a. The figure showed that different polymers were immiscible. The immiscibility decreased drastically when the polymer blend was treated with PE-co-GMA (Fig. 4b). The miscibility among different polymers was found to increase with the increase in the amount of PE-co-GMA (not shown in the figure). This might be due to the improvement in compatibility between HDPE, LDPE, PP and PVC in which PE-co-GMA acted as a compatibilizer among polymers. The improvement in adhesion between polyolefins and PET by using ethylene-glycidyl methacrylate copolymer as compatibilizer was reported in the literature [4]. The surface of the wood/polymer composites became smooth on addition of nanomer (Fig. 4c and d). The presence of octadecyl amine and silane groups on nanomer might have favoured the interaction between polymers and wood. This made both the polymers and wood more compatible with nanoclay. There was no significant difference in the surface characteristics on increasing the amount of nanomer from 1.0 to 3.0 phr. However, the surface appeared little bit rough on addition of 5 phr of clay (Fig. 4e). The partial agglomeration of nanoclay might be responsible for this observation.

### 4.5. Thermal property study

Figs. 5 and 6 show the TG and DTG thermograms of WPC and clay modified WPC. Table 1 shows the initial decomposition temperature ($T_i$), maximum pyrolysis temperature ($T_m$), decomposition temperature at different weight loss (%) ($T_d$) and residual weight (RW, %) for WPC and clay treated WPC. In both the cases, a decrease in weight loss below 100 °C was observed which was due to the removal of moisture. WPC showed a lower $T_i$ value compared to clay treated WPC. Similarly $T_m$ values for WPC were observed less compared to clay treated WPC. The $T_m$ values for the first stage in both WPC and clay treated WPC might be due to the depolymerisation of hemicellulose, glycosidic linkage of cellulose, thermal decomposition of cellulose [14] and dehydrochlorination of PVC [15]. $T_m$ values for the second stage was due to the decomposition of HDPE and PP [16,17]. The $T_m$ values for both the stages of pyrolysis were found to shift towards higher temperature when nanomer (1 phr) was added to the WPC. $T_d$ values of the clay treated WPC were more compared to WPC alone. RW value for nanomer treated WPC was more compared to WPC. Therefore, it could be concluded that thermal stability of WPC improved on addition of nanomer. The increase in thermal stability in clay treated WPC may be attributed to the presence of silicate layers which acted as a barrier and delayed the diffusion of decomposed volatile products throughout the composites [18].

### 4.6. Mechanical property study

The flexural and tensile properties of PB, PB/G5, PB/G5/N3 and WPCs with different percentage of clay loading are shown in Table 2. The datas presented were the average of three readings. It was observed that both flexural and tensile properties of polymer blends increased on addition of PE-co-GMA as compatibilizer. PE-co-GMA acted as a dispersing agent among different polymers resulting in improved interfacial adhesion due to which flexural and tensile properties increased. This was also supported by XRD and SEM study. Pracella et al. [4] studied the effect of various compatibilizers on HDPE, PP and PVC blend and found that ethylene-glycidyl methacrylate copolymer provided better interfacial adhesions among different kinds of polymer. Both flexural and tensile properties were increased on addition of wood flour. Since wood flour acted as load carrier, it reinforced the composite and enhanced the flexural and tensile properties. Moreover, PE-co-GMA improved the adhesion between wood and polymer blend through its glycidyl group and hydrocarbon backbone respectively. The incorporation of nanoclay with wood, polymer blend and PE-co-GMA further enhanced the flexural and tensile properties. Both flexural and tensile values increased with clay loading up to 3 phr, beyond that the values decreased. The observed higher values might be due to the higher dispersion of silicate layers of nanoclay in the wood polymer matrix and the restriction in the mobility of the polymer chains inside the intercalated nanolayers of clay. Besides the nanoclay contained some silane and hydrocarbon portions which facilitated the interaction between wood flour and polymer matrix. All these suggested an improvement in adhesion between polymer blend, wood and clay. The nanocomposites thus exhibited better properties over wood flour/PE-co-GMA treated polymer blend composites. The inclusion of organoclay resulted in the improvement in mechanical properties was reported by Lee and Kim [11] while studying the physical properties of wood/PP/clay nanocomposites. The decreased in mechanical properties of WPC treated with 5 phr clay might be attributed to the migration of clay to the interface between wood flour and polymer blend. The presence of high amount of fibre and its interface with polymer might have reduced the reinforcement effect of clay.

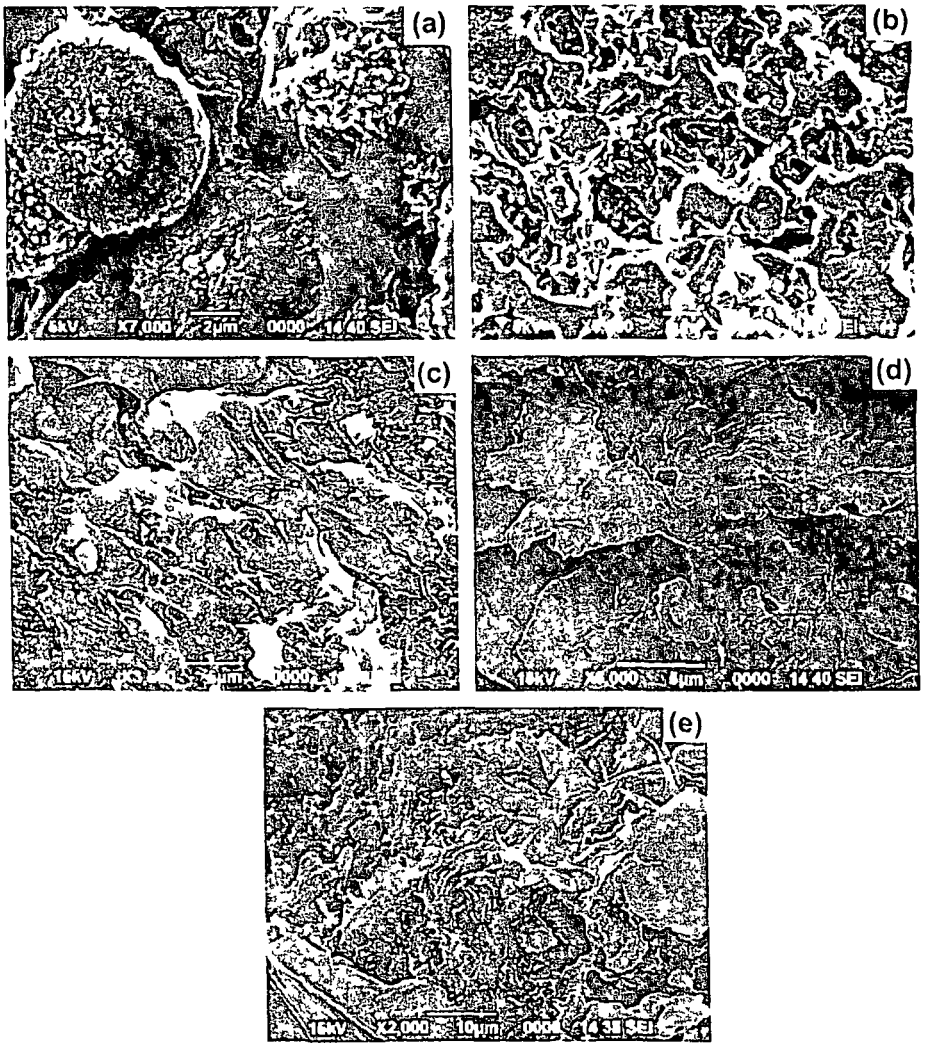


Fig. 4. SEM micrographs of (a) PB (b) PB/G5, (c) PB/G5/W40/N1 (d) PB/G5/W40/N3, (e) PB/G5/W40/N5

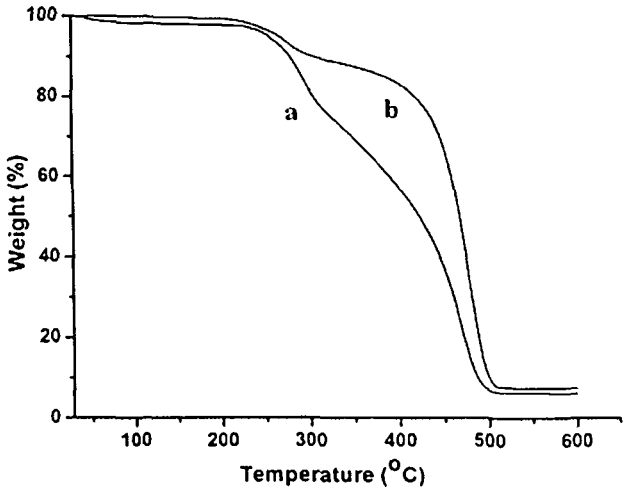


Fig. 5. Themogravimetric curves for (a) PB/G5/W40 (b) PB/G5/W40/N1

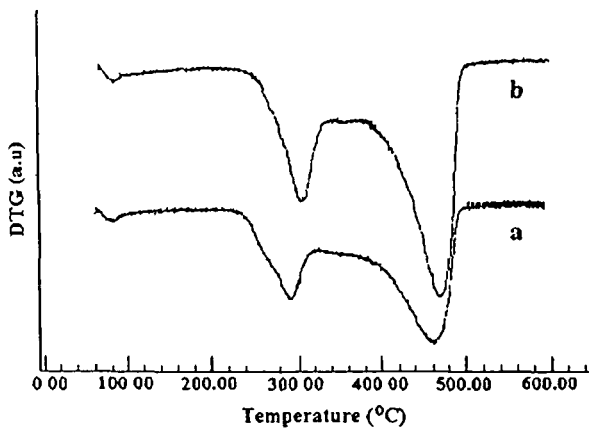


Fig. 6. DTG curves for (a) PB/G5/W40, (b) PB/G5/W40/N1

Similar observation was reported by Han et al [19] during the study of nanoclay reinforced HDPE/bamboo fibre composite

### 4.7. Hardness

Table 3 shows the hardness results of PB and WPCs with different percentage of clay loading From the table, it was observed that hardness increased as PE-co-GMA was added to the polymer blend

**Table 1**
Thermal properties of wood/polymer and wood/polymer/clay nanocomposites.

| Sample | $T_i$ | $T_m$[a] | $T_m$[b] | Temperature of decomposition ($T_D$) in °C at different weight loss (%) | | | | RW% at 600 °C |
|---|---|---|---|---|---|---|---|---|
| | | | | 20% | 40% | 60% | 80% | |
| PB/G5/W40 | 240 | 290 | 460 | 304 | 390 | 443 | 471 | 6.1 |
| PB/G5/W40/N1 | 249 | 302 | 471 | 419 | 458 | 473 | 488 | 7.5 |

[a] $T_m$ value for 1st step.
[b] $T_m$ value for 2nd step.

**Table 2**
Flexural and tensile properties of polymer blend, wood/polymer and wood/polymer/clay nanocomposites.

| Sample | Flexural properties | | Tensile properties | |
|---|---|---|---|---|
| | Strength (MPa) | Modulus (MPa) | Strength (MPa) | Modulus (MPa) |
| PB | 13.24 ± 1.09 | 763.28 ± 1.02 | 5.24 ± 1.13 | 84.38 ± 18.19 |
| PB/G5 | 15.39 ± 1.31 | 1058.36 ± 1.26 | 8.46 ± 1.21 | 113.25 ± 16.19 |
| PB/G5//N3 | 21.42 ± 0.92 | 4375.61 ± 1.43 | 24.47 ± 1.31 | 356.19 ± 19.07 |
| PB/G5/W40 | 17.47 ± 1.06 | 3822.13 ± 1.03 | 18.11 ± 1.20 | 261.71 ± 17.34 |
| PB/G5/W40/N1 | 20.32 ± 0.64 | 4215.34 ± 0.58 | 23.34 ± 1.03 | 368.14 ± 16.25 |
| PB/G5/W40/N3 | 26.17 ± 0.85 | 4749.53 ± 0.72 | 31.57 ± 1.01 | 581.40 ± 18.60 |
| PB/G5/W40/N5 | 23.44 ± 1.02 | 4523.82 ± 1.31 | 28.87 ± 1.27 | 547.82 ± 24.09 |

**Table 3**
Hardness value of polymer blend, wood/polymer and wood/polymer/clay nanocomposites.

| Sample | Hardness (shore D) |
|---|---|
| PB | 66.0 (±1.0) |
| PB/G5 | 68.5 (±0.5) |
| PB/G5/N3 | 68.0 (±1.0) |
| PB/G5/W40 | 66.0 (±0.8) |
| PB/G5/W40/N1 | 72.0 (±0.9) |
| PB/G5/W40/N3 | 77.0 (±0.6) |
| PB/G5/W40/N5 | 75.0 (±0.4) |

The increased in hardness in polymer blend was due to the improvement in interfacial adhesion between various polymers by PE-co-GMA. The hardness did not improve on addition of clay to the polymer blend. However, on addition of wood flour in the PE-co-GMA modified polymer blend, the hardness value decreased. But the hardness was found to increase further as nanoclay was added. The value improved up to an incorporation of certain amount of nanoclay (3 phr) beyond that the value decreased. The improvement was due to the decrease in mobility of the intercalated polymer chains and increase in interaction between wood flour and polymer by the clay as explained earlier. At higher clay loading, migration of clay to the interface of polymer and wood flour surface might decrease the reinforcement effect of clay. As a result the hardness was found to decrease.

### 4.8. Water uptake test

The results of water uptake for PB, PB/G5, PB/G5/N3 and WPCs with different percentage of clay loading are shown in Fig. 7. In all the cases, the water uptake was found to increase with the increase of time of immersion. Water absorption occurred initially at a rapid rate and finally at a slower rate. The water absorption of the neat polymer decreased on addition of PE-co-GMA. It was due to the improvement in compatibility among the polymers. PE-co-GMA increased the interaction between the interfaces of the polymers and thus enhanced water resistance. Water absorption decreased further on addition of nanomer to the PE-co-GMA treated polymer blend. The water absorption was found to enhance when wood flour was added. The hydrophilic nature of wood flour was responsible for this. The water absorption of wood flour/polymer blend composite

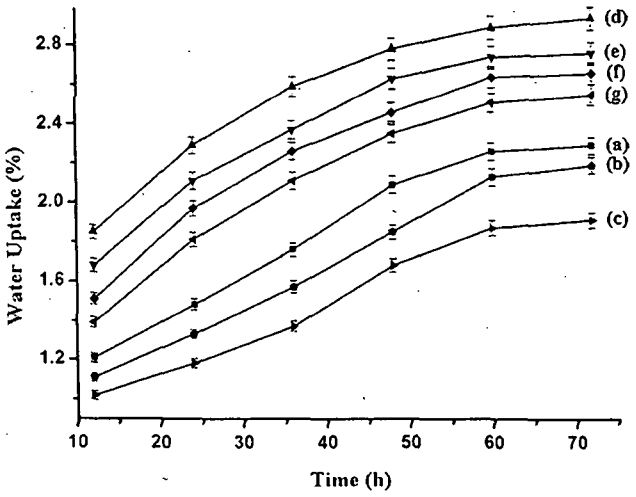


Fig. 7. Water absorption of: (a) PB, (b) PB/G5, (c) PB/G5/N3, (d) PB/G5/W40, (e) PB/G5/W40/N1, (f) PB/G5/W40/N3, (g) PB/G5/W40/N5.

decreased with the incorporation the clay. The higher the amount of clay, the lower was the water absorption. Organically modified clay increased the tortuous path for water transport and as a result water diffusivity decreased [20]. Rana et al. studied the barrier property of nanocomposite where nanoclay hindered the permeation of water through the composite [21]. Moreover, the void spaces in the wood flour were occupied by the polymer and nanoclay. This decreased the available space for water absorption. The higher the nanoclay, the lower was the available space to hold the water. Both the tortuous path and reduction in void space decreased the water absorption capacity of WPC. Hence nanoclay treated composite showed lower water absorption compared to nanoclay untreated composite.

## 5. Conclusions

The solvent ratio of xylene and THF for solution blending of HDPE, LDPE, PP and PVC (2:2:2:1) were optimised and found to be as 70:30. Polyethylene-co-glycidyl methacrylate (PE-co-GMA) improved the compatibility among the polymers as revealed by SEM study. XRD and TEM study indicated a better exfoliation in

WPC loaded with 1 and 3 phr clay compared to that of WPC loaded with 5 phr clay. FTIR studies showed a strong interaction among wood, PE-co-GMA treated polymer blend and nanoclay SEM study exhibited an increase in compatibility in the polymer blend due to the addition of PE-co-GMA. The surface of WPC loaded with 5 phr clay showed more roughness compared to WPC loaded with lower amount of clay. Wood/polymer/clay nanocomposites had shown improved thermal, flexural and tensile properties over wood/polymer composites Nanoclay treated wood/polymer composites showed lower water absorption and highest hardness over nanoclay untreated wood/polymer composites

## Acknowledgement

The authors are thankful to CSIR, New Delhi for their financial assistance

## References

[1] Cho JW, Paul DR. Nylon 6 nanocomposites by melt compounding. Polymer 2001,42 1083–94
[2] Botev M, Betchev H, Bikiaris D, Panayiotou C Mechanical properties and viscoelastic behavior of basalt fiber-reinforced polypropylene J Appl Polym Sci 1999 74(3) 523–31
[3] Vaia RA, Ishii H, Giannelis EP Synthesis and properties of two-dimensional nanostructures by direct intercalation of polymer melts in layered silicates Chem Mater 1993 5 1694–6
[4] Pracella M Chionna D, Ishak R, Galeski A. Recycling of PET and polyolefin based packaging materials by reactive blending Polym Plast Technol Eng 2004 43 1711–22
[5] Ghasemi I, Kord B Long-term water absorption behaviour of polypropylene/wood flour/organoclay hybrid nanocomposite Iran Polym J 2009,18 683–91
[6] Maji TK Devi R. Effect of glycidyl methacrylate on the physical properties of wood–polymer composites Polym Compos 2007 28 1–5
[7] Doh JG, Cho I Synthesis and properties of polystyrene-organoammonium montmorillonite hybrid Polym Bull 1998 41 511–8
[8] Ma J, Qi Z, Hu Y Synthesis and characterization of polypropylene/clay nanocomposites J Appl Polym Sci 2001,82 3611–7
[9] Zeng C, Lee LJ Poly(methyl methacrylate) and polystyrene/clay nanocomposites prepared by in-situ polymerization Macromolecules 2001,34 4098–103
[10] Faruk O, Matuana LM Nanoclay reinforced HDPE as a matrix for wood–plastic composites Compos Sci Technol 2008,68 2073–7
[11] Lee H, Kim DS Preparation and physical properties of wood/polypropylene/clay nanocomposites J Appl Polym Sci 2009 111 2769–76
[12] Zaho Y, Wang K, Zhu F, Xue P, Jia M Properties of poly (vinyl chloride)/wood flour/montmorillonite composites effect of coupling agents and layered silicate Polym Degrad Stab 2006,91 2874–83
[13] Awal A, Ghosh SB, Sain M Thermal properties and spectral characterization of wood pulp reinforced bio-composite fibers J Them Anal Calorim 2010,99 695–701
[14] Fung KL, Li RKY, Tjong SC. Interface modification on the properties of sisal fibre-reinforced polypropylene composites J Appl Polym Sci 2002 85 169–76
[15] Meng YZ, Tjong SC Preparation and properties of injection-moulded blends of poly(vinyl chloride) and liquid crystal copolyester Polymer 1999 40 2711–8
[16] Yemele MCN, Koubaa A, Cloutier A, Soulounganga P Effect of bark fibre content and size on the mechanical properties of bark/HDPE composites Compos Part A 2010,41 131–7
[17] Bouza R, Pardo SG, Barral L, Abad MJ Design of new propylene-wood flour composites processing and physical characterisation Polym Compos 2009,30 880–6
[18] Qin H, Zhang S Zhao C Feng M Yang M Shu Z, et al Thermal stability and flammability of polypropylene/montmorillonite composites Polym Degrade Stab 2004 85 807–13
[19] Han G Lee Y Wu Q, Kozima Y Bamboo-fibre filled high density polyethylene composites effect of coupling treatment and nanoclay J Polym Environ 2008,16 123–30
[20] Alexandre B Marias S Langevin D, Mederic P, Aubry T Nanocomposite-based polyamide 12/montmorillonite relationships between structures and transport property Desalination 2006 199 164–6
[21] Rana HT, Gupta RK, Ganga Rao HVS, Sridhar LN Measurement of moisture diffusivity through layered-silicate nanocomposites AIChE J 2005,51 3249–56

Polym. Bull. (2011) 67:1875–1892
DOI 10.1007/s00289-011-0529-5

ORIGINAL PAPER

# Study on properties of nanocomposites based on HDPE, LDPE, PP, PVC, wood and clay

**Biplab K. Deka · Tarun K. Maji · Manabendra Mandal**

Received: 29 November 2010 / Revised: 6 May 2011 / Accepted: 30 May 2011 /
Published online: 5 June 2011


**Abstract** Wood polymer nanocomposite (WPC) was prepared by solution blending of high density polyethylene, low density polyethylene, polypropylene and polyvinyl chloride (1:1:1:0.5) with wood flour and nanoclay. Xylene and tetrahydrofuran were used as solvent and the ratio was optimized at 70:30. TEM study revealed better dispersion of silicate layers in WPC loaded with 3 wt% of clay. WPC loaded with 3 wt% nanoclay exhibited higher thermal stability compared to WPC loaded with 1 and 5 wt% clay. The storage and loss modulus were found to enhance on incorporation of clay to WPC. The damping peak was found to be lowered by the addition of clay to WPC. Limiting oxygen index value increased due to incorporation of nanoclay. WPCs were subjected to exposure to cellulase producing *Bacillus* sp. and it showed the growth of bacteria as revealed by SEM study. Mechanical properties of WPC decreased due to degradation by bacteria. Water vapour uptake of WPC decreased due to addition of nanoclay.

**Keywords** Nanocomposites · Wood · Polymers · Thermostability · Biodegradability

## Introduction

Polymer is playing an important role in the field of composite. It is used in all class of materials from household items to different exterior products. They are widely

B. K. Deka · T. K. Maji (✉)
Department of Chemical Sciences, Tezpur University, Tezpur, Assam 784028, India
e-mail: tkm@tezu.ernet.in

M. Mandal
Department of Molecular Biology and Biotechnology, Tezpur University, Tezpur, Assam 784028, India
e-mail: mandal@tezu.ernet.in

used because of their versatile properties, light weight, resistance to breakage, low cost, ease of manufacture, fabrication and shaping. Moreover, they can be also used widely with other materials to improve various properties.

Amongst the different types of plastics, high density polyethylene (HDPE), low density polyethylene (LDPE), polypropylene (PP) and polyvinyl chloride (PVC) are mostly used in industries. After use, the throwing of plastic materials here and there in the form of carry bags, boxes, packaging film causes a serious threat to the environment. Recycling and reusing is one of the processes to reduce this environmental pollution problem. One of the fundamental goals of recycling is to improve different properties of the recycled plastics [1]. The properties can be improved substantially if composites are made by combining these waste materials with cellulosic materials.

Solution blending is one of the processes to mix varieties of plastic materials. The efficiency of the solution blending process for mixing different kind of plastics can be enhanced by the use of a mixture of solvents. The percentage of individual polymer in the blend as well as their physical characteristics is needed to optimise the solvent ratio. Waste plastic materials contain substantial amount of HDPE, LDPE, PP and lesser amount of PVC, PET etc. It is difficult to segregate different kinds of plastics. The optimization of solvent ratio can be determined properly if a mixture of known percentage of virgin HDPE, LDPE, PP, PVC etc. is used as starting waste plastic materials.

Solution blending involves the use of solvents which are not eco-friendly. Melt blending suffers from some disadvantages like stress development, temperature etc. [2]. A high level of intercalation with partial exfoliation has been obtained for organoclays/LLDPE composites prepared by solution blending [3] whereas microcomposites have been formed when LLDPE is melt blended with organically modified clay [4]. Chiu et al. [5] observed a well dispersion of silicate layers when they studied PP/clay composite by solution blending method.

Wood is used as a source of natural filler in wood polymer composites. It acts as a reinforcing agent in the polymer matrix. Wood flour (WF) has been treated with HDPE and nylon 6 to prepare composite [6]. Lei et al. [7] has prepared wood plastics composites based on HDPE/PET matrix and noticed a remarkable enhancement of mechanical properties. But most of reports address the use of conventional wood material as a source of cellulosic materials. The nonconventional plant materials like Nal (*Phragmites karka*), Kalmou (*Ipomoea carniva*) etc. are abundantly available in forests of Assam. They remain as bio-wastes. These non conventional plant materials can be made value added by making composites with plastic materials.

In order to make composite, the improvement in miscibility amongst plastic materials as well as with wood fillers is very important. The miscibility can be improved by the use of a suitable compatibilizer. The compatibilizer will be such that it can able to react with the hydrophilic wood fillers and hydrophobic polymers and at the same time will improve the interfacial adhesion amongst different thermoplastic materials. The use of maleated coupling agents to strengthen composites containing filler is reported in the literature [8]. Maji et al. [9] has used glycidyl methacrylate as compatibilizer and found a significant improvement

in properties of wood polymer composites. Luyt et al. [10] has studied the effect of poly(ethylene-*co*-glycidyl methacrylate) content on the morphology and physical properties of ethylene vinyl acetate-wood fibre composite and found an improvement of the properties.

It is well documented that the incorporation of clay as reinforcing filler in polymer matrix improves different physical and chemical properties. Organoclay has been used as nanosized filler [11] to improve the performance of wood/PP composite. PP/clay nanocomposites has been synthesized and found to improve the mechanical and thermal properties [12]. The available reports provide information mostly by making composites with wood and single variety of polymer. Little information regarding the use of more than one variety of polymer for making composite is available. Thus, there is enough scope to do further study in this area.

The object of this investigation is to prepare the nanocomposites using WF, PE-*co*-GMA, nanoclay, polymer mixture (HDPE + LDPE + PP + PVC) by solution blending and study the various properties of the nanocomposites. Waste plastics comprise of higher amount of HDPE, LDPE, PP and lower amount of PS, PVC, PET etc. On the basis of the presence of individual polymers in waste plastics, the ratio of HDPE, LDPE, PP and PVC is chosen as 1:1:1:0.5 for our investigation.

## Experimental

### Materials

The HDPE and LDPE (Grade: PE/20/TK/CN) were supplied by Plast Alloys India Ltd. (Harayana, India). PP homopolymer (Grade: H110MA, MFI 11 g/10 min) and PVC (Grade: SPVC FS: 6701) were procured from Reliance Industries Ltd. (Mumbai, India) and Finolex Industries Ltd. (Pune, India). The compatibilizer, poly(ethylene-*co*-glycidyl methacrylate) (PE-*co*-GMA) was purchased from Otto chemicals (Mumbai, India). Nanomer (clay modified by 15–35 wt% octadecylamine and 0.5–5 wt% aminopropyltriethoxy silane) was obtained from Sigma-Aldrich (USA). These chemicals were used as such received. Nal (*Phragmites karka*), a nonconventional wood was collected from local forest of Assam. Other reagents used were of analytical grade.

### Preparation of wood samples

Nals (*Phragmites karka*) were collected from the forest and chopped into small strips. These were initially washed with 1% soap solution. It was followed by washing with 1% NaOH solution and finally with cold water. The washed wood strips were oven dried at 105 ± 5 °C till attainment of constant weight. These dried wood strips were grinded in a mixer, sieved and kept in a container for subsequent use.

## Preparation of wood polymer nanocomposite (WPC)

Six grams of each HDPE, LDPE and PP (1:1:1) granules were added slowly to 105 mL of xylene taken in a flask fitted with a spiral condenser at room temperature. This was followed by the addition of the PE-*co*-GMA (5 wt%). The temperature of the flask was then increased gradually to 130 °C to make a homogenous solution. Now, another solution containing 3 g of PVC in 35 mL of tetrahydrofuran (THF) was prepared. The temperature of the flask containing polymer solution was decreased from 130 to 120 °C. The PVC solution was then mixed with the polymer solution at 120 °C (approximately) under stirring condition for 1 h. A known quantity of nanomer (1–5 wt%) was dispersed in THF solution (10 mL) by sonication. This dispersed clay–THF mixture was added gradually to the polymer solution under stirring condition. Oven-dried WF (40 wt%) was added slowly to this clay–polymer solution. The whole mixture was stirred for another 1 h. The mixture was then transferred in tray, dried and grinded. The composite sheets were obtained by using grinded WF–polymer powder and employing compression moulding press (Santec, New Delhi) at 150 °C under a pressure of 80 MPa. The abbreviation used for samples are listed in Table 1.

## Bacterial media

Mineral salt medium with the following composition was prepared for bacterial growth. 4.75 g $KH_2PO_4$, 2.0 g $Na_2HPO_4$, 2.0 g $(NH_4)_2SO_4$, 1.2 g $MgSO_4{\cdot}7H_2O$, 100 mg $MnSO_4{\cdot}5H_2O$, 100 mg $CuSO_4{\cdot}7H_2O$, 70 mg $ZnSO_4{\cdot}7H_2O$, 10 mg $H_3BO_3{\cdot}5H_2O$, 10 mg $MoO_3$, 1 mg $FeSO_4{\cdot}7H_2O$ and 0.5 mg $CaCl_2{\cdot}2H_2O$ were dissolved in 1000 mL of demineralised water. 3 mL of this liquid culture medium was poured into 50 mL conical test tube and were sterilized using autoclave at 121 °C and 15 lbf pressure for 15 min. The autoclaved media were then allowed to cool down to room temperature and WPC samples were added into the media under sterile condition inside a laminar air flow hood. Media containing only polymer samples were also cultured as negative control.

**Table 1** Formulation of mixture of samples and their codes

| Samples formulation | Code |
|---|---|
| PB (HDPE + LDPE + PP + PVC) | PB |
| PB/5 wt% PE-*co*-GMA | PB/G5 |
| PB/5 wt% PE-*co*-GMA/3 wt% clay | PB/G5/N3 |
| PB/5 wt% PE-*co*-GMA/40 wt% wood | PB/G5/W40 |
| PB/5 wt% PE-*co*-GMA/40 wt% wood/1 wt% clay | PB/G5/W40/N1 |
| PB/5 wt% PE-*co*-GMA/40 wt% wood/3 wt% clay | PB/G5/W40/N3 |
| PB/5 wt% PE-*co*-GMA/40 wt% wood/5 wt% clay | PB/G5/W40/N5 |

### Bacterial strains

*Bacillus* sp. Cd-3 culture was grown using nutrient broth at 37 °C for 18 h. 1 mL of bacterial cultures were centrifuged at 6000 rpm for 20 min at room temperature and the pellets were washed with 0.9% NaCl and re-suspended in 1 mL of mineral salt medium. Now 0.5 mL of the culture medium containing $1 \times 10^8$/mL microbes was inoculated to the test tube containing 50 mL media for each test. The test tubes were then incubated under sterile condition at 37 °C and 100 rpm for the degradation study.

## Measurements

### Transmission electron microscopy (TEM)

The dispersion of the silicate layers of nanoclay in WPCs were performed by using TEM (JEM-100 CX II) at an accelerated voltage of 20–100 kV.

### Thermal property

Thermal properties of neat polymer and the wood/polymer/clay composites were measured in a thermogravimetric analyser (TGA) (TGA-50, shimadzu) at a heating rate of 10 °C/min up to 600 °C under nitrogen atmosphere.

### Dynamic mechanical analysis (DMA)

The DMA was performed using an Universal 2980 DMA V1.7B TA instrument. The dimensions of specimens were taken as $(5 \times 1.25 \times 0.35)$ cm$^3$. Specimens were scanned over a temperature range of 25–200 °C. Frequency of the oscillation was fixed at 1 Hz ramped at 2 °C/min to 200 °C. Storage modulus, loss modulus and mechanical loss factor (tan $\delta$) were recorded and plotted against temperature.

### Limiting oxygen index (LOI)

The LOI is defined as the minimum concentration of oxygen, expressed in percent volume, in a flowing mixture of oxygen and nitrogen that will support combustion of a material initially at room temperature. It was measured by flammability tester (S.C. Dey Co., Kolkata) according to ASTM D-2863 method. The sample was placed vertically in the sample holder of the LOI apparatus. The total volume of the gas mixture ($N_2 + O_2$) was kept fixed at 18 cc. To begin with experiment, the volume of nitrogen gas and that of oxygen gas were kept initially at a maximum and minimum level. Now, the volume of nitrogen gas was decreased and that of oxygen gas was increased gradually. However, the total volume of gas mixture was kept fixed at 18 cc during the experiment. The ratio of nitrogen and oxygen at which the sample continued to burn for at least 30 s was recorded.

$$\text{Limiting oxygen index} = \text{volume of } O_2 / \text{ volume of } (O_2 + N_2) \times 100.$$

Biodegradation study

The microbial degradation was studied spectrophotometrically by using UV visible spectrophotometer (CECIL CE7400) at 600 nm against blank culture media under sterile condition.

Scanning electron microscopy (SEM)

The morphological features and bacterial growth of the WPCs were studied by using SEM (JEOL JSM-6390LV) at an accelerated voltage of 5–10 kV. Fractured surface of the samples, deposited on a brass holder and sputtered with platinum, were used for this study.

Mechanical property

The tensile and flexural tests for biodegraded WPC samples were carried out using Universal Testing Machine (Zwick, model Z010) at a crosshead speed of 10 mm/min at room temperature according to ASTM D-638 and D-790, respectively. Three samples of each specimen were tested and the average values were reported.

Water vapour uptake test

The WPC samples were cut into (2.5 × 0.5 × 2.5) $cm^3$ for the measurement of water vapour uptake test. The samples were oven dried and conditioned at room temperature (30 °C) and 30% relative humidity before the test. The test was carried out by placing the samples at two different relative humidities namely 95 and 65% and maintaining a temperature of 30 °C. Weights of the sample were measured after 12, 24, 36, 48, 60 and 72 h. The experiment was carried out at different time interval. It is expressed as a percentage of moisture absorbed based on oven dry weight.

$$\text{Water vapour uptake } (\%) = (W_t - W_o)/W_o \times 100$$

where $W_t$ is the weight of the specimen after exposure to humidity and $W_o$ is the weight of oven dried specimen.

## Results and discussion

The HDPE, LDPE, PP and PVC were mixed at the ratio of 1:1:1:0.5 to optimize the solvent ratio. From the investigation, it was observed that xylene was a good solvent for HDPE, LDPE and PP whereas THF was a good solvent for PVC. None of these solvent alone could solubilise the mixture of HDPE, LDPE, PP and PVC (1:1:1:0.5). The solubility of the polymer mixture was checked by varying the ratio of xylene

and THF. The optimum ratio of solvent (xylene:THF) and minimum temperature at which a homogeneous solution was obtained were 70:30 and 120 °C, respectively.

## TEM results

The TEM micrographs of WPC loaded with different percentage of nanomer content are represented in Fig. 1. The dark lines observed in the figure represent the silicate layers present in the composite. At lower level of nanomer (1 wt%) loading (Fig. 1a), a well dispersion of silicate layers in the WPC was observed. The dispersion of clay layers improved up to the addition of 3 wt% of nanomer (Fig. 2b) to the composite. However, at higher level of loading (5 wt%), the silicate layers of clay became to agglomerated (Fig. 2c). Similar dispersion of nanoclay was observed by Faruk and Matuana [13] whilst studying the dispersion of nanoclay in HDPE/wood matrix.

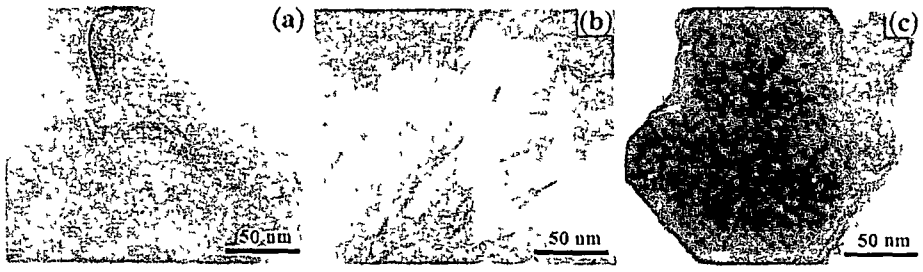


**Fig. 1** TEM micrograph of (a) PB/G5/W40/N1, (b) PB/G5/W40/N3 and (c) PB/G5/W40/N5

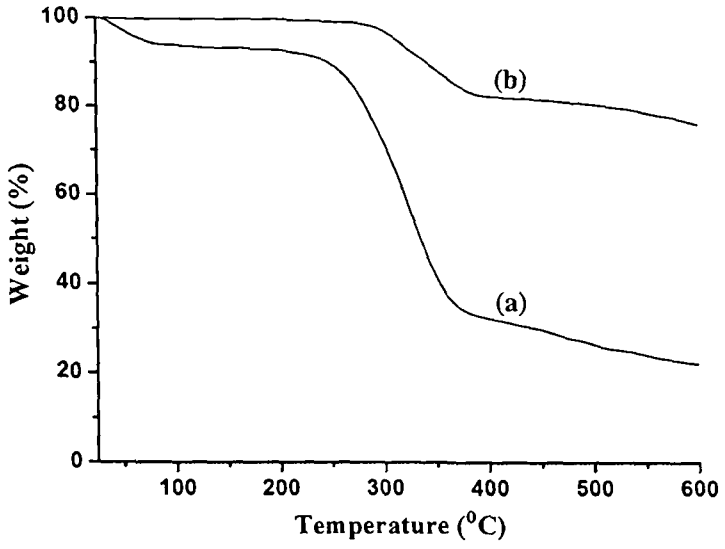


**Fig. 2** Themogravimetric curves of (*a*) WF and (*b*) nanoclay

TGA study

Figures 2 and 3 show the weight losses for WF, nanoclay, polymer blend (PB) and WPC. Table 2 shows the initial decomposition temperature ($T_i$), maximum pyrolysis temperature ($T_m$), weight losses for various samples at different temperature ($T_D$) and residual weight (RW%) for different samples. $T_i$ value of nanomer was found maximum. This was followed by PB and WF. $T_i$ value of PB improved on addition of PE-*co*-GMA and WF. The values were found to enhance further when nanomer was added. $T_i$ value increased up to addition of 3 wt% clay beyond that it decreased. $T_m$ values observed for WF was due to the depolymerisation of hemicelluloses, glycidyl linkage and thermal decomposition of cellulose [14]. The first decomposition peak shown by the PB might be due to the dehydrochlorination of PVC [15], whilst the second decomposition peak was due to the decomposition of LDPE, HDPE and PP [16, 17]. $T_m$ value of PB enhanced due to incorporation of PE-*co*-GMA and WF. $T_m$ value increased further when nanomer was added. The value increased up to addition of 3 wt% nanomer beyond that it decreased. Nanomer showed highest RW values whilst the PB showed lowest RW values. The trend of RW values of clay-treated WPC was similar to those of $T_i$ values. The RW values observed for nanomer and WF were due to the presence of inorganic silicate layer and carbonization of wood, respectively.

Further it was observed from the Table 2 that PB decomposed at higher temperature compared to WF. $T_D$ values increased on addition of WF and PE-*co*-GMA to the PB. This might be due to the enhancement of interaction caused by the increase in interfacial adhesion between WF and PB by PE-*co*-GMA through its glycidyl group and polyethylene chain. A possible reaction mechanism of PE-*co*-GMA with wood and polymer is represented by Scheme 1. Awal et al. [18] reported

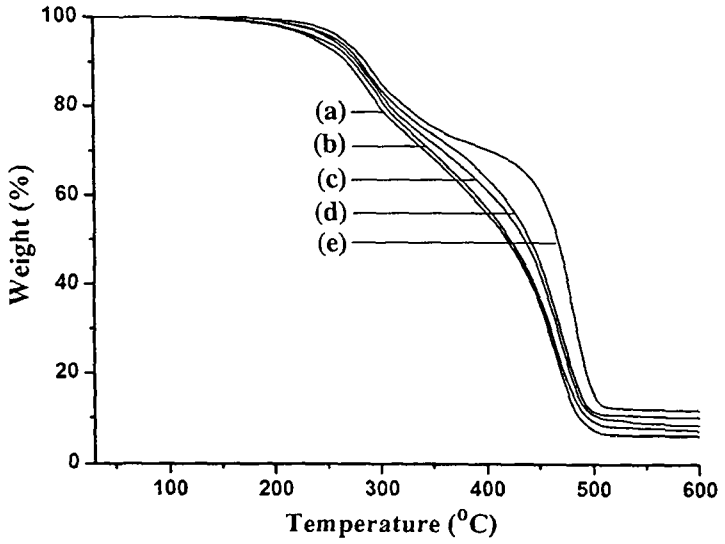


**Fig. 3** Themogravimetric curves of (*a*) PB, (*b*) PB/G5/W40, (*c*) PB/G5/W40/N1, (*d*) PB/G5/W40/N5 and (*e*) PB/G5/W40/N3

**Table 2** Thermal analysis of wood, PB and WPC

| Sample | $T_i$ | $T_m^a$ | $T_m^b$ | Temperature of decomposition ($T_D$) in °C at different weight loss (%) | | | | RW% at 600 °C |
|---|---|---|---|---|---|---|---|---|
| | | | | 20% | 40% | 60% | 80% | |
| WF | 230 | 315 | – | 282 | 320 | 352 | – | 21.9 |
| Nanomer | 294 | 352 | – | 514 | – | – | – | 76.0 |
| PB | 251 | 272 | 407 | 297 | 385 | 441 | 470 | 6.1 |
| PB/G5/W40 | 257 | 277 | 455 | 303 | 390 | 444 | 472 | 7.2 |
| PB/G5/W40/N1 | 260 | 281 | 466 | 309 | 404 | 453 | 478 | 8.4 |
| PB/G5/W40/N3 | 270 | 319 | 496 | 322 | 452 | 476 | 493 | 11.7 |
| PB/G5/W40/N5 | 263 | 309 | 480 | 313 | 414 | 456 | 481 | 10.2 |

$T_i$ value for initial degradation

[a] $T_m$ Value for 1st step

[b] $T_m$ Value for 2nd step

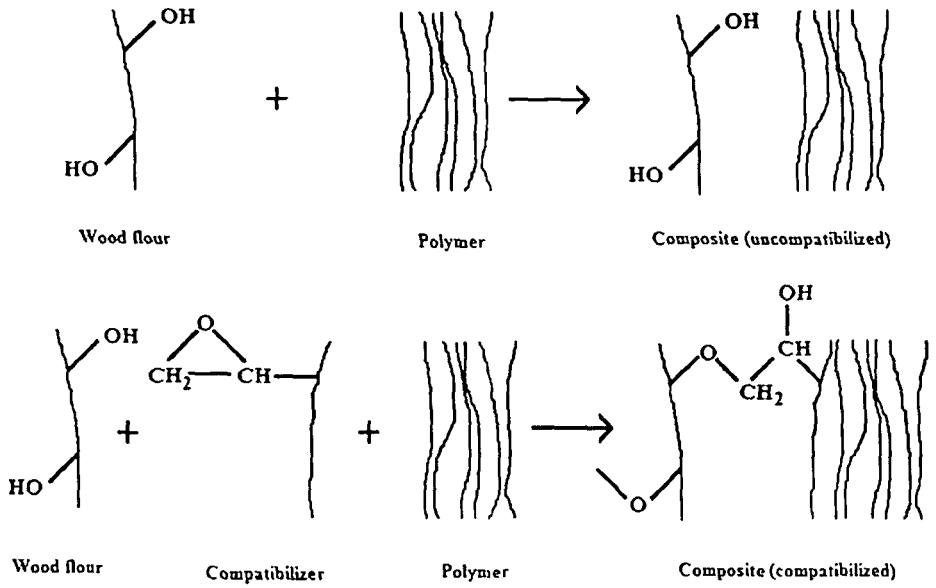


**Scheme 1** A plausible reaction scheme for the compatibilization of WF and polymer by compatibilizer

that the incorporation of wood pulp, maleated PP into PP delayed the thermal degradation of the composite. $T_D$ value increased initially up to addition of 3 wt% clay after that it decreased with the increase in the amount of clay (5 wt%). Therefore, it could be concluded that the inclusion of nanomer improved the thermal stability of WPC. The improvement in thermal stability may be attributed to the presence of silicate layer which acted as a barrier and delayed the diffusion of decomposed volatile products throughout the composites [19]. At higher clay loading, the silicate layer might become agglomerated and decreased the barrier

resistance. As a result, the diffusion of volatile products would be rapid and thermal stability would be less.

## Dynamic mechanical study

Storage modulus and loss modulus of PB, PB/G5/W40 and PB/G5/W40/N3 are presented in the Figs. 4 and 5. PB/G5/W40 exhibited higher storage and loss

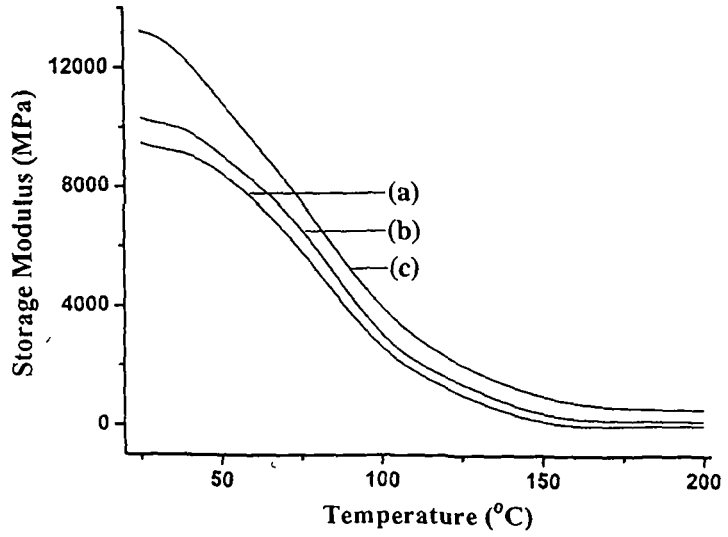


**Fig. 4** Storage modulus of (*a*) PB, (*b*) PB/G5/W40 and (*c*) PB/G5/W40/N3

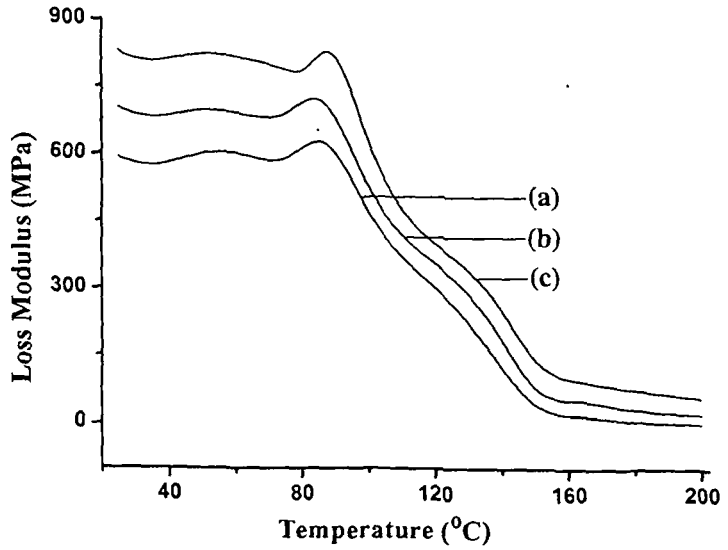


**Fig. 5** Loss modulus of (*a*) PB, (*b*) PB/G5/W40 and (*c*) PB/G5/W40/N3

modulus compared to PB. This enhancement might be due to the development of strong interaction between WF and PB by PE-*co*-GMA. The glycidyl group and long polyethylene chain of PE-*co*-GMA interacted with the hydroxyl group of wood and PB, respectively. Storage and loss modulus were found to increase on addition of glycidyl methacrylate as compatibilizer to the WPC [20]. Both the storage and loss modulus were found maximum in the case of PB/G5/W40/N3. The long chain of polymer molecules intercalated into the interlayer space of the silicate layers and restricted the mobility of the polymer chains. As a result, stiffness of the WPC increased and both storage and loss modulus improved. Matuana et al. [13] studied dynamic mechanical properties of clay/HDPE/wood composite and reported that clay-reinforced HDPE/wood composite showed better storage and loss modulus compared to clay-free HDPE/wood composite. In both the cases, a reduction in modulus with the increase in temperature was observed. This was due to the softening of the matrix at higher temperature [21].

The damping factor or mechanical loss factor (tan $\delta$) is the ratio of loss modulus to storage modulus and is shown in Fig. 6. PB exhibited a tan $\delta$ peak with a peak temperature of 96.8 °C. There was no significant shifting of tan $\delta$ peak in both PB/G5/W40 and PB/G5/W40/N3. However, a lowering of tan $\delta$ peak height was observed with the addition of WF. This was due to the decrease in the volume fraction of the matrix by the incorporation of WF. Similar observation was reported by Thomas and co-workers [22, 23]. The reduction of tan $\delta$ peak height was more pronounced when clay was added to the composite. This might be due to the restricted movement of the polymer chains caused by the silicate layers of clay and rigid WF molecules.

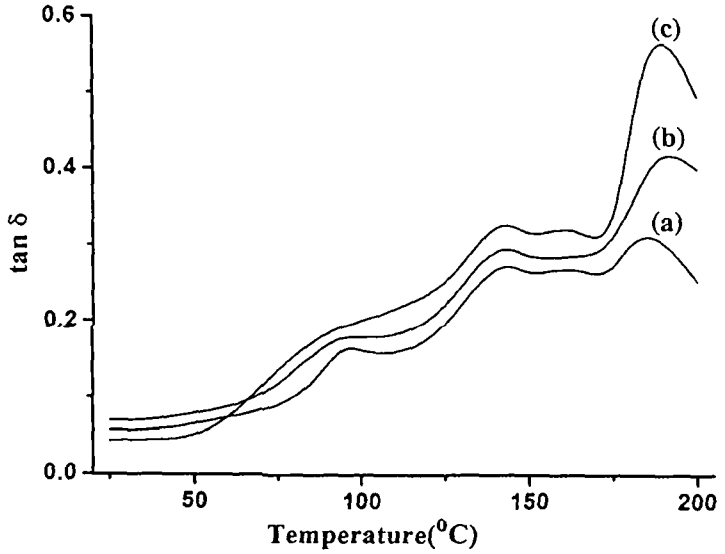


Fig. 6 Tan $\delta$ of (*a*) PB, (*b*) PB/G5/W40 and (*c*) PB/G5/W40/N3

**Table 3** Limiting oxygen indices and flaming characteristics of PB and wood/polymer/clay nanocomposites

| Samples | LOI (%) | Flame description | Smoke and fumes | Char |
|---|---|---|---|---|
| PB | 22 | Candlelike localised | – | Little |
| PB/G5 | 39 | Small localized flame | Small and black smoke | Little |
| PB/G5/N3 | 47 | Small localized flame | Small and black smoke | Higher |
| PB/G5/W40 | 44 | Small localized flame | Small and black smoke | Little |
| PB/G5/W40/N1 | 55 | Small localized flame | Small and black smoke | Higher |
| PB/G5/W40/N3 | 61 | Small localized flame | Small and black smoke | Higher |
| PB/G5/W40/N5 | 66 | Small localized flame | Small and black smoke | Higher |

## Limiting oxygen index (LOI)

Table 3 shows the results of LOI values of PB and WPC with varying percentage of nanoclay. It was observed that the value of LOI increased on addition of PE-*co*-GMA to the PB. The increase in interfacial adhesion amongst polymers by PE-*co*-GMA might be responsible for the observed higher value of LOI. The values were further improved on addition of nanoclay. The LOI values of the nanoclay-treated wood polymer composites were found more compared to nanoclay-untreated wood polymer composite. The higher the percentage of nanoclay, the higher was the LOI. WF contained cellulose, hemicelluloses, lignin and other low molecular weight components which required lower concentration of oxygen for the production of flammable volatiles and propagation of flame. As a result, the LOI of nanoclay-untreated wood polymer composite was found less. On the other hand, nanoclay produced silicate char on the surface of the clay-treated WPC which increased the flame resistance property of the composite [24]. The silicate rich surface had better barrier property to heat and oxygen transport due to which ignition of the composite delayed. Besides this, the nanoclay contains amino propyl triethoxy silane and octadecyl amine groups which could interact and promote adhesion with WF and PB. This adhesion might prevent the flame for propagation. The higher the percentage of clay, the stronger was the adhesion as well as resistance of flame propagation.

## Biodegradation study

The WPC samples were exposed for microbial degradation and after 8 weeks of study, wood polymer composites had shown high rate of degradation. Figure 7 shows the bacterial growth of the WPC with respect to time. From the figure, it was observed that with increasing bacterial exposure time, the growth of bacterial strains increased. Wood composite as sole carbon source showed higher rate of bacterial growth after 3 weeks of incubation and it continued up to eighth week. This enhancement of bacterial growth might be due to powerful cellulolytic and pectinolytic activity of bacteria [25]. Other than cellulose and pectin, lignin was also

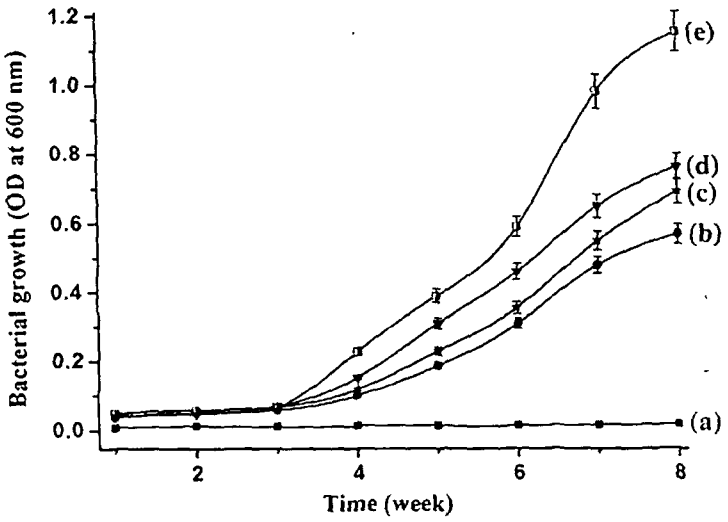


**Fig. 7** Growth of *Bacillus* sp. on (*a*) PB, (*b*) PB/G5/W40, (*c*) PB/G5/W40/N1, (*d*) PB/G5/W40/N3 and (*e*) PB/G5/W40/N5

a constituent of *Phragmites karka* plant stem and it was reported that *Bacillus* sp. could degrade this [26]. The growth and degradation property of the wood composite by bacteria was also supported by the SEM study (Fig. 8). With the increase in the clay content, the rate of bacterial growth enhanced. The improved biodegradability of nanocomposite was due to the catalytic role played by the clay in the biodegradation mechanism [27]. From the study, it was observed that WPC loaded with 5 wt% clay showed maximum bacterial growth. The mechanical properties of the degraded WPC samples were checked, compared with undegraded samples and are presented in Tables 4 and 5. The higher mechanical properties shown by both degraded and undegraded WPC samples loaded with 3 wt% clay was due to the better dispersion of silicate layers of nanoclay and enhanced restriction in the mobility of the polymer chains intercalated inside the silicate layers. The lower mechanical properties exhibited by 5 wt% clay loaded WPC was due to the reduction in reinforcement effect of clay caused by the migration of the same to the interface between WF and PB [28]. It was found that with efficient degradation of WPCs, flexural and tensile properties of the WPCs decreased. This might be due to the loss of physical and chemical interaction in the WPC caused by the degradation effect of bacteria.

## Water vapour uptake test

Water vapour absorption tests of PB, clay treated and untreated WPC were carried out at 30 °C and two different relative humidities namely 95 and 65%, respectively and are shown in Figs. 9 and 10. As expected, all the samples absorbed less water vapour at 65% RH compared to 95% RH. In all the cases, water vapour absorption occurred initially at a faster rate and finally at a slower rate. The rate of water

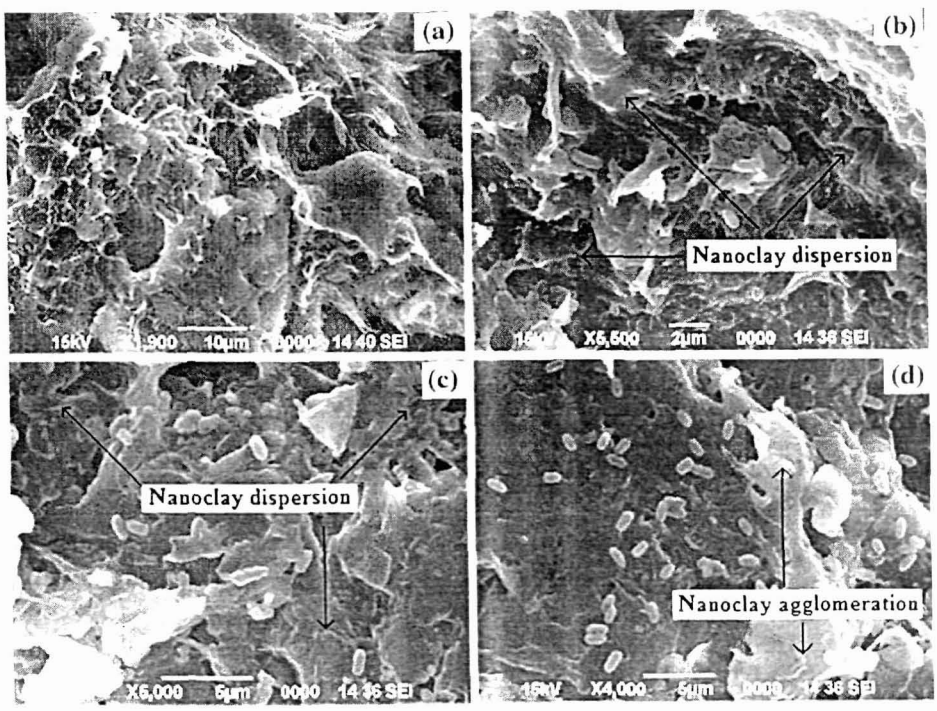


**Fig. 8** SEM micrographs of (**a**) PB/G5/W40, (**b**) PB/G5/W40/N1, (**c**) PB/G5/W40/N3 and (**d**) PB/G5/W40/N5

**Table 4** Flexural properties of WPC loaded with different percentage of nanoclay after the microbial degradation

| Sample | Before degradation | | After degradation | |
|---|---|---|---|---|
| | Strength (MPa) | Modulus (MPa) | Strength (MPa) | Modulus (MPa) |
| PB/G5/W40 | 18.01 ± 1.12 | 3864.24 ± 1.16 | 16.84 ± 1.09 | 3686.49 ± 1.05 |
| PB/G5/W40/N1 | 20.09 ± 0.81 | 4193.27 ± 0.74 | 17.45 ± 1.53 | 3964.75 ± 0.93 |
| PB/G5/W40/N3 | 25.87 ± 0.93 | 4761.36 ± 0.95 | 20.63 ± 0.87 | 4239.72 ± 1.07 |
| PB/G5/W40/N5 | 22.15 ± 1.66 | 4487.65 ± 1.08 | 17.74 ± 1.04 | 3871.84 ± 1.17 |

**Table 5** Tensile properties of WPC loaded with different percentage of nanoclay after microbial degradation

| Sample | Before degradation | | After degradation | |
|---|---|---|---|---|
| | Strength (MPa) | Modulus (MPa) | Strength (MPa) | Modulus (MPa) |
| PB/G5/W40 | 17.93 ± 1.05 | 231.63 ± 18.26 | 15.85 ± 1.21 | 194.52 ± 17.74 |
| PB/G5/W40/N1 | 23.01 ± 1.12 | 312.79 ± 17.16 | 20.91 ± 1.06 | 217.83 ± 17.69 |
| PB/G5/W40/N3 | 30.86 ± 0.93 | 605.48 ± 17.49 | 25.14 ± 0.79 | 496.27 ± 18.92 |
| PB/G5/W40/N5 | 28.12 ± 1.06 | 521.54 ± 23.72 | 22.63 ± 1.13 | 415.86 ± 21.63 |

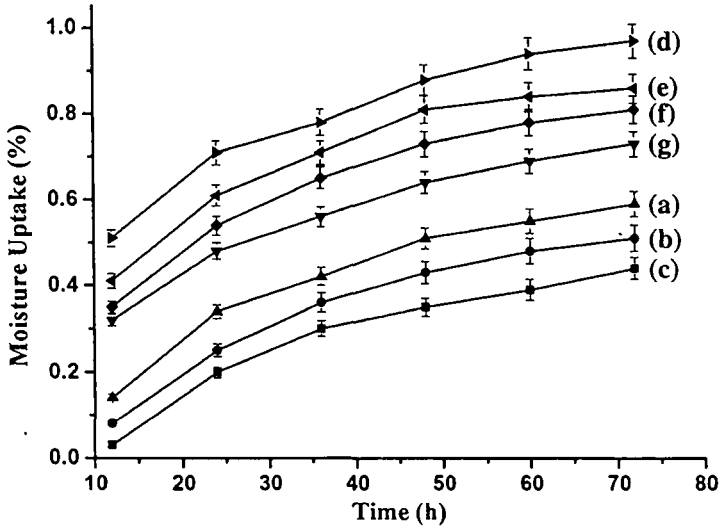


**Fig. 9** Water vapour absorption at room temperature and 95% relative humidity of (*a*) PB, (*b*) PB/G5, (*c*) PB/G5/N3, (*d*) PB/G5/W40, (*e*) PB/G5/W40/N1, (*f*) PB/G5/W40/N5 and (*g*) PB/G5/W40/N3

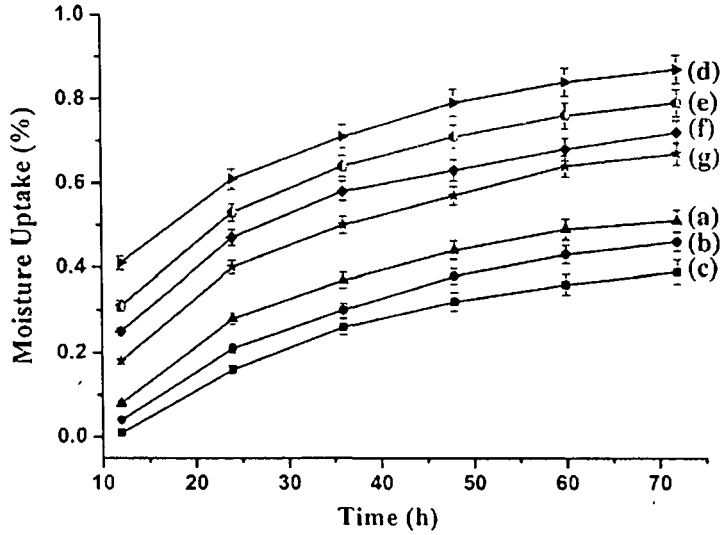


**Fig. 10** Water vapour absorption at room temperature and 65% relative humidity of (*a*) PB, (*b*) PB/G5, (*c*) PB/G5/N3, (*d*) PB/G5/W40, (*e*) PB/G5/W40/N1, (*f*) PB/G5/W40/N5 and (*g*) PB/G5/W40/N3

vapour absorption increased with the increased in time. The water vapour absorption followed the order: PB/G5/W40 > PB/G5/W40/N1 > PB/G5/W40/N5 > PB/G5/W40/N3 > PB > PB/G5 > PB/G5/N3. The water vapour absorption was found to decrease on addition of PE-*co*-GMA to the PB. The compatibiiizer, PE-*co*-GMA increased the interfacial adhesion amongst polymers which led to the decrease in water vapour absorption. Maji and co-workers [29] reported that GMA-treated WPC

absorbed less water vapour compared to untreated WPC. The water vapour absorption was further decreased due to inclusion of clay. The silicate layers of clay acted as a barrier for the moisture which resulted in the decrease of the absorption of water vapour. The value was found to enhance when WF was added. The hydrophilic nature of the WF was responsible for this. Similar results were reported in the literature [30]. The addition of clay to the WPC further decreased the rate of absorption of water vapour. The value decreased up to addition of 3 wt% clay after that it increased. The overall decrease in the moisture absorption was due to the tortuous path imparted by the organically modified silicate layers which prevented the water vapour from transportation and diffusion through the composite [31].

Moreover, there was less void space available in the wood for the absorption of water vapour due to occupation of the same by nanoclay and polymer. As a result, the water vapour absorption of clay-treated WPC would be less due to reduction in void space in wood and the presence of tortuous path imparted by the silicate layers. The higher water vapour absorption exhibited by the WPC containing 5 wt% clay was due to the agglomeration of silicate layers which decreased the tortuous path for transportation and diffusion of water vapour. In general, it can be concluded that nanoclay-treated WPC absorbed less water vapour compared to clay-free WPC. The trend of water vapour absorption of the samples in the case of 65% RH and 30 °C was similar to those of samples tested at 95% RH and 30 °C.

## Conclusions

The solvent ratio of xylene and THF for solution blending of HDPE, LDPE, PP and PVC (1:1:1:0.5) were optimised and found to be as 70:30. Polyethylene-*co*-glycidyl methacrylate (PE-*co*-GMA) acted as an effective compatibilizer for the composite system. The dispersion of silicate layers was found better in WPC loaded with 3 wt% of nanoclay. Thermal stability of the composite was improved due to the incorporation of clay. DMA results indicated an improvement in storage modulus, loss modulus and mechanical loss factor due to incorporation of clay to the WPC. LOI value increased after the incorporation of clay. Biodegradability of the WPC improved on addition of clay. SEM study revealed the presence of maximum bacterial growth in clay-treated WPC. Both flexural and tensile properties of the WPC decreased due to bacterial degradation of composites. Water vapour absorption of the WPC decreased on addition of nanoclay up to 3 wt% beyond that it increased.

**Acknowledgments** Financial assistance from Council of Scientific and Industrial Research (CSIR), New Delhi is gratefully acknowledged. The authors are thankful to Dr. D. Setua, Defence Materials and Stores Research and Development Establishment (DMSRDE), Kanpur for helping to carry out DMA analysis.

## References

1. Cavalieri F, Padella F (2002) Development of composite materials by mechanochemical treatment of post-consumer plastic waste. Waste Manage 22.913–916

2 Filippi S, Marazzato C, Magagnini P, Famulari A, Arosio P, Meille SV (2008) Structure and morphology of HDPE-g-MA/organoclays nanocomposites effects of the preparation procedures Eur Polym J 44 987–1002
3 Qiu L, Chen W, Qu B (2006) Morphology and thermal stabilization mechanism of LLDPE/MMT and LLDPE/LDH nanocomposites Polymer 47 922–930
4 Hotta S, Paul DR (2004) Nanocomposites formed from linear low density polyethylene and organoclays Polymer 45 7639–7654
5 Chiu FC, Chu PH (2006) Characterization of solution-mixed polypropylene/clay nanocomposites without compatibilizers J Polym Res 13 73–78
6 Liu H, Yao F, Xu Y, Wu Q (2010) A novel wood flour-filled composite based on microfibrillar high-density polyethylene (HDPE)/nylon-6 blends Bioresour Technol 101 3295–3297
7 Lei Y, Wu Q (2010) Wood plastic composites based on microfibrillar blends of high density polyethylene/poly(ethylene terephthalate) Bioresour Technol 101 3665–3671
8 Keener TJ, Stuart RK, Brown TK (2004) Maleated coupling agents for natural fibre composites Compos Part A 35 357–562
9 Devi RR, Maji TK (2007) Effect of glycidyl methacrylate on the physical properties of wood–polymer composites Polym Compos 28 1–5
10 Dikobe DG, Luyt AS (2007) Effect of poly(ethylene-*co*-glycidyl methacrylate) compatibilizer content on the morphology and physical properties of ethylene vinyl acetate–wood fiber composites J Appl Polym Sci 104 3206–3213
11 Lee H, Kim DS (2009) Preparation and physical properties of wood/polypropylene/clay nanocomposites J Appl Polym Sci 111 2769–2776
12 Ma J, Qi Z, Hu Y (2001) Synthesis and characterization of polypropylene/clay nanocomposites J Appl Polym Sci 82 3611–3617
13 Faruk O, Matuana L (2008) Nanoclay reinforced HDPE as a matrix for wood–plastic composites Compos Sci Technol 68 2073–2077
14 Fung KL, Li RKY, Tjong SC (2002) Interface modification on the properties of sisal fiber-reinforced polypropylene composites J Appl Polym Sci 85 169–176
15 Meng YZ, Tjong SC (1999) Preparation and properties of injection-moulded blends of poly(vinyl chloride) and liquid crystal copolyester Polymer 40 2711–2718
16 Yemele MCN Koubaa A, Cloutier A, Soulounganga P, Wolcott M (2010) Effect of bark fiber content and size on the mechanical properties of bark/HDPE composites Compos Part A 41 131–137
17 Bouza R, Pardo SG, Barral L, Abad MJ (2009) Design of new polypropylene–woodflour composites processing and physical characterization Polym Compos 30 880–886
18 Awal A, Ghosh SB, Sain M (2010) Thermal properties and spectral characterization of wood pulp reinforced bio-composite fibers J Therm Anal Calorim 99 695–701
19 Qin H, Zhang S, Zhao C, Feng M, Yang M, Shu Z, Yang S (2004) Thermal stability and flammability of polypropylene/montmorillonite composites Polym Degrad Stab 85 807–813
20 Devi RR, Maji TK (2008) Chemical modification of rubber wood with styrene and glycidyl methacrylate Polym Compos 29 1258–1262
21 Wunderlich B (1994) The nature of the glass transition and its determination by thermal analysis In Seyler RJ (ed) Assignment of the glass transition, 1249, ASTM, STP, Philadelphia, pp 17–31
22 Idicula M Malhotra SK, Joseph K, Thomas S (2005) Dynamic mechanical analysis of randomly oriented intimately mixed short banana/sisal hybrid fibre reinforced polyester composites Compos Sci Technol 65 1077–1087
23 Jiang H, Kamdem DP (2008) Thermal and dynamic mechanical behavior of poly(vinyl chloride)/wood flour composites J Appl Polym Sci 107 951–957
24 Camino G, Tartaglione G, Frache A, Manferti C, Costa G (2005) Thermal and combustion behaviour of layered silicate–epoxy nanocomposite Polym Degrad Stab 90 354–362
25 Clausen CA (1996) Bacterial associations with decaying wood a review Int Biodeter Biodegr 37 101–107
26 El-Hanafy AA, Hassan E, Elsalam A, Hafez EE (2008) Molecular characterization of two native egyptian lignınolytic bacterial strains J Appl Sci Res 4 1291–1296
27 Karak N (2006) Polymer (epoxy) clay nanocomposites J Polym Mater 23 1–20
28 Deka BK, Maji TK (2010) Effect of coupling agent and nanoclay on properties of HDPE, LDPE, PP, PVC blend and *Phargamites karka* nanocomposite Compos Sci Technol 70 1755–1761

29. Devi RR, Maji TK, Banerjee AN (2004) Studies on dimensional stability and thermal properties of rubber wood chemically modified with styrene and glycidyl methacrylate. J Appl Polym Sci 93: 1938–1945
30. Lei Y, Wu Q, Clemons CM, Yao F, Xu Y (2007) Influence of nanoclay on properties of HDPE/wood composites. J Appl Polym Sci 106:3958–3966
31. Alexandre B, Marias S, Langevin D, Mederic P, Aubry T (2006) Nanocomposite-based polyamide 12/montmorillonite: relationships between structures and transport property. Desalination 199: 164–166

Composites: Part A 42 (2011) 2117–2125

Contents lists available at SciVerse ScienceDirect

Composites: Part A

journal homepage: www.elsevier.com/locate/compositesa

# Effect of $TiO_2$ and nanoclay on the properties of wood polymer nanocomposite

Biplab K. Deka, Tarun K. Maji *

*Department of Chemical Sciences, Tezpur University, Assam 784 028, India*

ARTICLE INFO

*Article history:*
Received 30 June 2011
Received in revised form 20 August 2011
Accepted 21 September 2011
Available online 25 September 2011

*Keywords:*
A. Polymer-matrix composites (PMCs)
A. Wood
B. Mechanical properties
B. Thermal properties

ABSTRACT

High density polyethylene (HDPE), low density polyethylene (LDPE), polypropylene (PP) and poly(vinyl chloride) (PVC) with *Phragmites karka* wood flour (WF) and polyethylene-*co*-glycidyl methacrylate (PE-*co*-GMA) was used to develop wood polymer composite (WPC) by solution blending method. The effect of addition of nanoclay and $TiO_2$ on the properties of the composite was examined. The exfoliation of silicate layers and dispersion of $TiO_2$ nanopowder was studied by X-ray diffractometry and transmission electron microscopy. The improvement in miscibility among polymers due to addition of compatibilizer was studied by scanning electron microscopy (SEM). WPC treated with 3 phr each of clay and $TiO_2$ showed an improvement in thermal stability. Mechanical, UV resistance and flame retarding properties were also enhanced after the incorporation of clay/$TiO_2$ nanopowder to the composites. Both water and water vapor absorption were found to decrease due to inclusion of nanoclay and $TiO_2$ in WPC.



## 1. Introduction

Now-a-days, the use of wood polymer composite (WPC) has tremendously increased due to their different advantages [1]. The plant fiber used as a reinforcing agent rapidly improves the mechanical, thermal as well as other properties of the composite [2,3]. They are used in different outdoor, indoor applications like decking, railing, fencing, docks, landscaping timbers, and in a number of automobile industries. The composites reinforced with wood (WPC) have shown a great growth due to the many advantages that they present. Their processing is easy, economic, and ecological. They have relatively high strength and stiffness, low cost, low density, low $CO_2$ emission, biodegradability and renewable.

*Phragmites karka* is a type of non conventional plant materials abundantly available in the forest of Assam, India. They do not have any structural application. They remain as bio waste or are used for making temporary shades. These plant materials can be conferred added value by making composites with different kind of polymers.

Blending of different polymers to achieve superior properties is a widely used process [4]. Solution blending is one of the processes that are used for blending varieties of polymers and making polymer composite [5,6]. But the major problems to make composite are the immiscibility among different polymers and decrease in interfacial adhesion between polymers and wood. This results in the formation of inferior composites. In order to improve the miscibility among the polymers as well as with wood, a third component called compatibilizer is used [7]. Compatibilizer is such a compound which can interact with the hydrophobic polymer through their non polar group and with the hydrophilic wood flour (WF) through their polar group. This leads to an improvement in interfacial adhesion that enhances the properties [8]. Different types of compatibilizer like glycidyl methacrylate (GMA), polyethylene grafted glycidyl methacrylate (PE-*g*-GMA), maleic anhydride-grafted polypropylene (MAPP), etc. are widely used to enhance the compatibility among different polymers and WF [9–11].

Now-a-days, nanocomposites provide a new way to overcome the limitations of traditional counterparts. Because of significantly increased interfacial interaction between inorganic and organic phases and size-dependent phenomena of nanoscale particles, polymer nanocomposites are capable of dramatically improving the mechanical and thermal properties including stiffness and heat resistance, gas and solvent barrier property, flame retardance without losing good ductility of polymer (i.e. toughness) as compared with either homopolymer or traditional microcomposites. A number of polymer nanocomposites based on montmorillonite have been reported [12–14].

Among many nanocomposite precursors, $TiO_2$ nanopowder is increasingly being investigated because it is non-toxic, chemically inert, low cost, corrosion resistant and has a high refractive index, UV filtration capacity and high hardness. Literature has also shown that nanoscale $TiO_2$ reinforcement brings new optical, electrical, physiochemical properties attained at very low $TiO_2$ content, which make polymer $TiO_2$ nanocomposites a promising new class of materials [15].

In the present study, we are trying to develop a wood polymer nanocomposite by using polymer blend (HDPE, LDPE, PP, PVC) and

* Corresponding author. Tel.: +91 03712 267007x5053; fax: +91 03712 267005.
*E-mail address:* tkm@tezu.ernet.in (T.K. Maji).

1359-835X/$ - see front matter © 2011 Elsevier Ltd. All rights reserved.
doi:10.1016/j.compositesa.2011.09.023

wood flour with the co-incorporation of nanoclay/$TiO_2$ nanopowder Effect inclusion of nanoclay/$TiO_2$ on different properties of the composite has also been highlighted in the present study The weight ratio of HDPE, LDPE, PP and PVC is chosen as 1 1 1 0 5 for our present investigation

## 2. Experimental

### 2 1 Materials

HDPE, LDPE (Grade PE/20/TK/CN), PP homopolymer (Grade H110MA, MFI 11 g/10 min) and PVC (Grade SPVC FS 6701) were obtained from Plast Alloys India Ltd (Harayana, India), Reliance Industries Ltd (Mumbai, India) and Finolex Industries Ltd (Pune, India) respectively The compatibilizer poly(ethylene-*co*-glycidyl methacrylate) (PE-*co*-GMA) (Otto chemicals, Mumbai, India) N-Cetyl-N,N,N-Trimethyl Ammonium Bromide (CTAB) (Central Drug house (P) Ltd , Delhi, India), nanomer (clay modified by 15–35 wt% octadecylamine and 0 5–5 wt% aminopropyltriethoxy silane) (Sigma–Aldrich, USA) and $TiO_2$ nanopowder (<100 nm) (Aldrich, Germany) were used as such received A nonconventional wood, nals (*P karka*) was collected from local forest of Assam Other reagents used were of analytical grade

### 2 2 Preparation of wood samples

Nals wood was collected and chopped into small strips These were initially washed with 1% soap solution to remove the dust particles It was then washed with 1% NaOH solution and finally with cold water The washed wood strips were oven dried at 100 ± 5 °C till attainment of constant weight These dried wood strips were ground in a mixer and sieved and kept for use

### 2 3 Modification of $TiO_2$

Ten grams of $TiO_2$ were taken in a round bottom flask containing 1 1 ethanol–water mixture It was fitted with spiral condenser and stirred at 80 °C for 12 h 12 g of CTAB was taken in a beaker containing ethanol–water mixture and stirred at 80 °C for 3 h This mixture was poured into the $TiO_2$ solution mixture and stirred for another 6 h, then it was filtered and washed with deionised water for several time It was collected and overnight dried in vacuum oven at 45 °C It was then grinded and stored in desiccator to avoid moisture absorption

### 2 4 Preparation of wood polymer nanocomposite

Six grams each of HDPE, LDPE and PP (1 1 1) were added slowly to 105 ml of xylene taken in a flask fitted with a spiral condenser at room temperature This was followed by the addition of the PE-*co*-GMA (5 phr) The temperature of the flask was increased to 130 °C in order to homogenize the solution Now, another solution containing 3 g of PVC in 35 ml of tetrahydrofuran (THF) was prepared The temperature of the previous polymer solution was decreased to 120 °C The PVC solution is then mixed with the previous polymer solution at 120 °C (approximately) under stirring condition for 1 h A known quantity of CTAB modified $TiO_2$ nanopowder (1–5 phr) and nanoclay (3 phr) was dispersed in 15 ml of tetrahydrofuran (THF) solution using magnetic stirrer and sonication This dispersed mixture was added gradually to the polymer solution while stirring Oven dried WF (40 phr) was added slowly to this matrix solution The whole mixture was stirred for another 1 h The mixture was transferred in tray, dried and grinded By this way, the residual solvent was removed from the wood–polymer mixture The composite sheets were obtained by the compression molding press (Santec, New Delhi) at 150 °C under a pressure of 80 MPa

Polymer blend (HDPE + LDPE + PP + PVC), Polymer blend/5phr PE-*co*-GMA and polymer blend/5phr PE-*co*-GMA/40phr wood were designated as PB, PB/G5 and PB/G5/W40 The 1, 3 and 5 phr $TiO_2$ filled nanoclay based WPC were designated as PB/G5/W40/N3/T1, PB/G5/W40/N3/T3 and PB/G5/W40/N3/T5

## 3. Measurements

### 3 1 X-ray diffraction (XRD)

The degree of dispersion of nanoclay and $TiO_2$ in the WPC was evaluated by X-ray diffraction (XRD) analysis It was carried out in a Rigaku X-ray diffractometer (Miniflax, UK) using Cu Kα ($\lambda$ = 0 154 nm) radiation at a scanning rate of 1°/min with an angle ranging from 2° to 70°

### 3 2 Transmission electron microscopy (TEM)

The dispersion of the silicate layers of nanoclay and $TiO_2$ nanoparticles in WPCs was performed by using transmission electron microscopy (JEM-100 CX II) at an accelerated voltage of 20–100 kV

### 3 3 Scanning electron microscopy (SEM)

The compatibility among different polymers as well as morphological features of the WPC was studied by using scanning electron microscope (JEOL JSM-6390LV) at an accelerated voltage of 5–10 kV Fractured surfaces of the samples, deposited on a brass holder and sputtered with platinum, were used for this study

### 3 4 FTIR studies

FTIR spectra of wood flour, $TiO_2$ nanopowder and WPC loaded with nanoclay and $TiO_2$ nanopowder were recorded in FTIR spectrophotometer (Impact-410, Nicolet, USA) using KBr pellet The samples were prepared by maintaining the sample and KBr ratio as 1 20 approximately Both the powder sample and KBr were homogenously grounded in a mortar 4–10 mg of the sample mixture was taken and pressed in hydraulic press in order to make the pallets The thickness of the pallets was around 4 mm (±0 5)

### 3 5 Mechanical properties

The tensile and flexural tests for polymer blend, PE-*co*-GMA treated polymer blend and WPC loaded with nanoclay and different percentage of $TiO_2$ were carried out using Universal Testing Machine (Zwick, model Z010) at a crosshead speed of 10 mm/min at room temperature according to ASTM D-638 and D-790 respectively Three samples of each category were tested and their average values were reported

### 3 6 Hardness

The hardness of the samples was measured according to ASTM D-2240 using a durometer (model RR12) and expressed as shore D hardness

### 3 7 Thermal properties

Thermal properties of polymer blend and the WPCs were measured in a thermogravimetric analyzer (TGA) (TGA-50, Shimadzu) at a heating rate of 10 °C/min up to 600 °C under nitrogen atmosphere at a flow rate of 30 ml/m

### 3 8 UV resistance test

The degradation study of the WPC samples was done in UV chamber (Model S L W, voltage 230 VAC, Advanced Research Co , India) utilizing a mercury arc lamp system that produces a collimated and highly uniform UV flux in the 254–365 nm range Specimens dimensions of (25 × 25 × 5) $mm^3$ were exposed in the UV chamber at room temperature and characterized at specified time intervals The weight loss was measured and is expressed as [16]

$$\%\ \text{Weight loss} = (W_t - W_o)/W_o \times 100$$

where $W_t$ is the specimen weight at time $t$, $W_o$ is the specimen weight before exposure Surface morphology of UV degraded specimen was characterized by scanning electron microscopy (SEM) Chemical degradation was studied by FTIR. The intensity of the carbonyl (C=O) stretching peaks at 1715 $cm^{-1}$ in cellulose of WF was measured The net peak heights were determined by subtracting the height of the baseline directly from the total peak height The same base line was taken for each peak before and after exposure to UV [17] The carbonyl index was calculated by using the following equation

$$\text{Carbonyl index} = I_{1715}/I_{2912}\,(100)$$

where $I$ represent the intensity of the peak The peak intensities were normalized by using —CH stretching peak of alkane at 2912 $cm^{-1}$ This peak was chosen as reference due to its least change during irradiation

### 3 9 Limiting oxygen index (LOI)

LOI values of the samples were measured by flammability tester (S C Dey Co , Kolkata) according to ASTM D-2863 method The sample was placed vertically in the sample holder of the LOI apparatus The ratio of nitrogen and oxygen at which the sample continued to burn for at least 30 s was recorded

$$\text{Limiting oxygen index (LOI)} = \text{Volume of } O_2/\text{Volume of } (O_2 + N_2) \times 100$$

### 3 10 Water uptake and water vapor absorption test

WPC samples were cut into 2 5 × 0 5 × 2 5 $cm^3$ for the test Percentage water uptake was measured by submerging the samples in distilled water at room temperature (30 °C) for different time periods after conditioning at 65% relative humidity and 30 °C and expressed according to the formulae below,

$$\text{Water uptake}\,(\%) = (W_s - W_1)/W_1 \times 100$$

where $W_s$ is the weight of the water saturated specimen and $W_1$ is the weight of the oven dried specimen

Samples having similar dimension were used for water exclusion test It was carried out at 65% relative humidity at 30 °C Weights of the samples were measured after 12, 24 36, 48, 60 and 72 h The samples were oven dried and conditioned at 30 °C and 30% relative humidity prior to the test It is expressed as a percentage of moisture absorbed based on oven dry weight

## 4. Results and discussion

### 4 1 XRD results

Fig 1 shows the XRD results of nanoclay, polymer blend, $TiO_2$ and wood polymer composite loaded with clay (3 phr) and different percentage of $TiO_2$ (1–5 phr) Organically modified nanoclay (curve-a) shows the diffraction peak at $2\theta = 4\ 11°$ with basal spacing 2 15 nm In the diffractrogram of polymer blend (Curve-b), the most prominent wide-angle X-ray diffraction peaks appeared at $2\theta = 14\ 12$ (200), 17 06 (040), 18 64 (211), 21 62 (110) and 24 02 (200) were for crystalline portion of different polymers present in the blend [18–21] The peaks (curve-c) appeared at $2\theta = 27\ 33$ (110), 36 11 (200), 37 79 (111), 47 87 (210), 54 32 (211), 56 72 (220) were for the crystalline portion of $TiO_2$ [22,23] Curves (d–f) represents the diffractrograms of WPC loaded with nanoclay (3 phr) and different percentage of $TiO_2$ (1–5 phr) The figures did not exhibit any characteristic peak of nanoclay The exfoliation of silicate layers in the wood polymer matrix was supposed to be the cause of disappearance of nanoclay diffraction peak The crystalline peak intensity of the polymer blend appeared in the range of $2\theta = 14–25°$ was found to decrease with the increase in the level of incorporation of $TiO_2$ (1–5 phr) However, the intensities of peak corresponding to $TiO_2$ nanopowder increased with higher concentration of $TiO_2$ in the composite A similar decrease in peak intensities of polymer and increase in peak intensity of $TiO_2$ was observed and reported by Mina et al [18] while studying the X-ray diffraction profile of polypropylene/titanium dioxide composite All these data suggested that nanoclay layers were exfoliated and $TiO_2$ particles were dispersed in the wood polymer matrix

### 4 2 TEM results

Fig 2 indicates the TEM micrographs of WPC loaded with different percentage of nanoclay and $TiO_2$ (1–5 phr) The dark lines shown in the figures were the silicate layers of nanoclay and the black spots present in the figures were the $TiO_2$ nanoparticles of the composite An even dispersion of clay and $TiO_2$ nanoparticles was observed at lower percentage of $TiO_2$ loading (1–3 phr) while an agglomeration of the same was observed at higher percentage of $TiO_2$ (5 phr) loading Yamada et al [24] incorporated $TiO_2$ nanoparticles into poly(methyl methacrylate) and observed similar increase in aggregation with increasing $TiO_2$ concentration The agglomeration occurred due to the surface interaction among the nanoparticles

### 4 3 SEM results

SEM micrographs of different fractured samples of PB, WPC and WPC loaded with nanoclay and different percentage of $TiO_2$

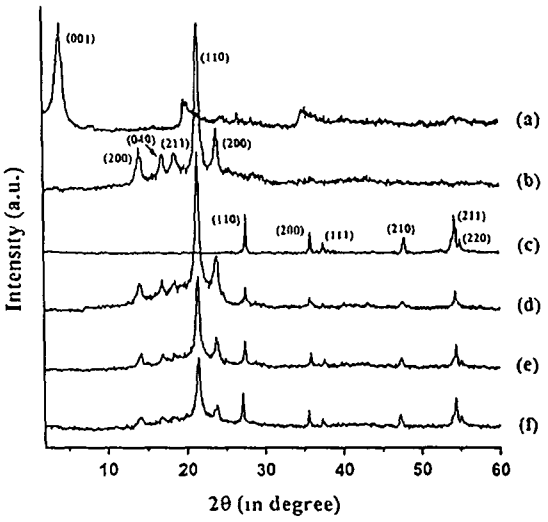


Fig 1 X-ray diffraction of (a) Nanoclay (b) PB (c) nano $TiO_2$ (d) PB/G5/W40/N3/T1 (e) PB/G5/W40/N3/T3 and (f) PB/G5/W40/N3/T5


**Fig. 2.** TEM micrographs of: (a) PB/G5/W40/N3/T1, (b) PB/G5/W40/N3/T3 and (c) PB/G5/W40/N3/T5.

nanopowder are represented by Fig. 3. Initially the polymers are quite immiscible (Fig. 3a) as judged by the separation of different phases. The miscibility among the polymers was increased after the incorporation of compatibilizer (Fig. 3b). The interfacial adhesion increased by the compatibilizer improved the miscibility among the polymers [25]. The addition of wood flour improved the smoothness of composite surface (Fig. 3c). This was further improved after the incorporation of wood, clay and $TiO_2$. This was found to enhance upto addition of 3 phr $TiO_2$ and clay (Fig. 3d,e). The surface of WPC loaded with 5 phr $TiO_2$ and clay appeared rougher compared to WPC loaded with 3 phr $TiO_2$ and clay (Fig. 3f). The increase in smoothness might be due to the improvement in interaction among PE-*co*-GMA, hydroxyl groups of wood and clay, along with the organic surfactant present in clay and polymer. Moreover, CTAB modified $TiO_2$ also has long olefinic chain which further improved the interaction among them. The agglomeration occurred at higher percentage of $TiO_2$ loading might be due to the surface interaction between $TiO_2$ nanoparticles. Similar agglomeration of $TiO_2$ nanoparticles at higher percent of loading was observed by Zhu et al. [26] during development of poly(lactic acid)/$TiO_2$ nanocomposite film.

### 4.4. FTIR results

FTIR spectra of CTAB, $TiO_2$ and CTAB modified $TiO_2$ are shown in Fig. 4. In the spectrum of CTAB (Fig. 4a), the absorption peaks at 2918, 2848 and 1475 $cm^{-1}$ were assigned to asymmetric, symmetric, and scissor modes of $-CH_2$ stretching in the methylene chains respectively [27]. FTIR spectrum of unmodified $TiO_2$ nanoparticles is presented in Fig. 4b. The strong absorbance at 1028–418 $cm^{-1}$ was attributed to the Ti—O—Ti stretching of $TiO_2$. The absorbance at 3431 and 1633 $cm^{-1}$ were assigned to the surface hydroxyl groups of $TiO_2$ [28,29]. The intensity of —OH stretching in the modified $TiO_2$ (Fig. 4c) was found to decrease, indicating an interaction of the hydroxyl group absorbed on $TiO_2$ surface with CTAB. The frequencies at 2918, 2848 and 1475 $cm^{-1}$ of CTAB were shifted to 2925, 2852 and 1470 $cm^{-1}$ in the modified $TiO_2$ spectrum was due to incorporation of $-CH_2$ group of CTAB. Qu et al. [30] modified $TiO_2$ with CTAB and checked the dispersion of it in toluene as well as in carbon tetrachloride. They observed that modified $TiO_2$ was dispersed evenly in both the system. They suggested that the interaction of $TiO_2$ occurred with $Br^-$ ion of CTAB through hydrogen bond formation or electrostatic attractions. Further, CTAB modified $TiO_2$ was dispersed in a flask containing xylene and kept for checking of any settling of particles. The dispersion of $TiO_2$ was found to be stable. These results indicated the incorporation of CTAB on the surface of $TiO_2$ particles.

Fig. 5 shows the FTIR spectra of wood, nanoclay, WPC and WPC loaded with nanoclay (3 phr) and $TiO_2$ (1–5 phr). Curve-a shows the presence of bands at 3435 $cm^{-1}$ for —OH stretching, 2932 $cm^{-1}$ and 2848 $cm^{-1}$ for —CH stretching, 1731 $cm^{-1}$ for C=O stretching, 1638 $cm^{-1}$ for —OH bending, 1162 and 1046 $cm^{-1}$ for C—O stretching and 1000–650 $cm^{-1}$ for C—H bending vibration (out of plane) of the wood sample. Organically modified nanoclay (curve b) exhibited the peaks at 3471 $cm^{-1}$ (—OH stretching) 2936 and 2851 $cm^{-1}$ (—CH stretching of modified hydrocarbon), 1622 $cm^{-1}$ (—OH bending) and 1031–462 $cm^{-1}$ (oxide bands of metals like Si, Al, Mg, etc.) [31]. PB/G5/W40 (curve c) exhibited peaks at 3431 $cm^{-1}$ (—OH stretching), 2925 and 2842 $cm^{-1}$ (—CH stretching), 1732 $cm^{-1}$ (C=O stretching), 1633 $cm^{-1}$ (—OH bending) and 716 $cm^{-1}$ ($-CH_2$ bending).

Fig. 5d–f shows the FTIR spectra of WPC loaded with 3 phr nanoclay and 1, 3 and 5 phr of $TiO_2$. From the figure, it was observed that the intensity of —OH stretching was decreased and shifted to 3249 $cm^{-1}$ (curve-d), 3014 $cm^{-1}$ (curve-e) and 3197 $cm^{-1}$ (curve-f) compared to wood (3435 $cm^{-1}$), and nanoclay (3471 $cm^{-1}$). The decreased in intensities and shifting to lower wavelength confirmed the bond formation between the hydroxyl groups of wood,

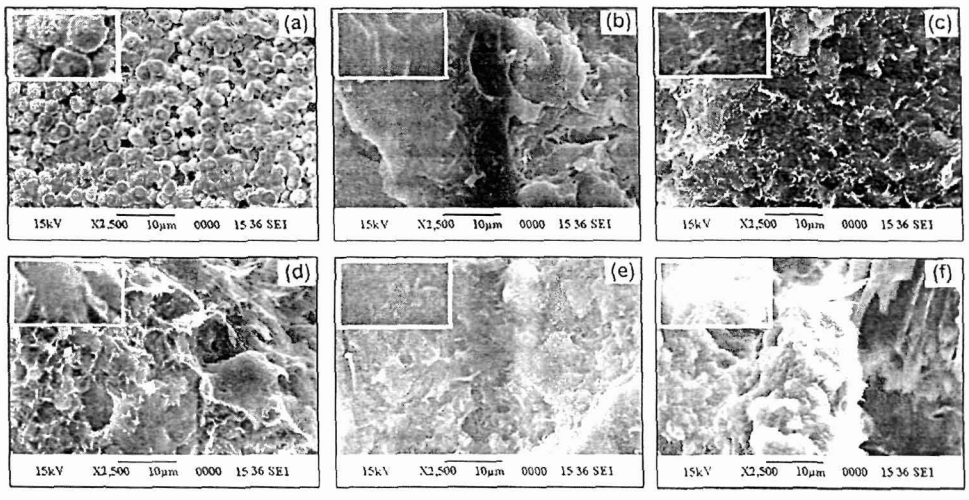


**Fig. 3.** SEM micrographs of: (a) PB, (b) PB/G5, (c) PB/G5/W40, (d) PB/G5/W40/N3/T1, (e) PB/G5/W40/N3/T3 and (f) PB/G5/W40/N3/T5.

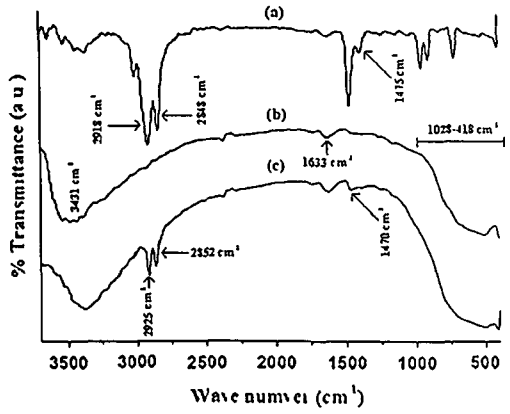


Fig 4 FTIR spectra of (a) CTAB (b) unmodified $TiO_2$ nanopowder and (c) CTAB modified $TiO_2$

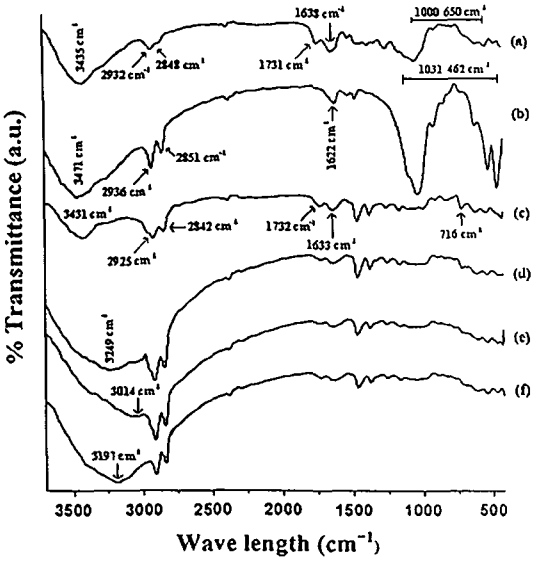


Fig. 5 FTIR spectra of (a) Wood (b) Nanoclay (c) PB/G5/W40 (d) PB/G5/W40/N3/T1 (e) PB/G5/W40/N3/T3 and (f) PB/G5/W40/N3/T5

nanoclay and $TiO_2$ A similar decreased of intensity of —OH absorption peak and shifting to lower wavelength was reported by Maji and Deka [5] The increase in intensities of —CH stretching at 2932 and 2848 $cm^{-1}$ (curves d–f) compared to those of wood confirmed the interaction between polymer, wood and compatibilizer Similar increase in —CH peak intensities was observed by Awal et al [32] In the spectra of WPC (curves d–f), it was observed that the intensity of the metal oxides bond in the range 1028–414 $cm^{-1}$ corresponding to $TiO_2$ and nanoclay decreased to a desirable extent which confirmed the formation of bond between wood clay, $TiO_2$ and polymers

### 4 5 Mechanical properties results

Table 1 shows the flexural and tensile properties of polymer blends, WPC and WPC loaded with nanoclay and different percentage of $TiO_2$ nanopowder From the table, it was observed that both flexural and tensile properties of the polymer blend increased after incorporation of compatibilizer This was because of improvement in interfacial adhesion between the polymers by the compatibilizer The values were further improved after the addition of WF The reinforcing effect provided by WF acted as a load carrier, due to which the flexural and tensile properties were improved Salemane and Luyt [33] studied the improvement in mechanical properties of wood/polypropylene composite after the incorporation of wood flour In addition to it, the compatibilizer, PE-*co*-GMA, increased the interfacial adhesion between wood and polymers by its glycidyl linkage and long olefinic chain and thus improved the strength properties To improve the compatibility of wood pulp-LDPE composite, Sailaja [34] used PE-*co*-GMA as compatibilizer and found a significant improvement in properties of the composite The properties were further improved after the incorporation of clay and $TiO_2$ The silicate layers of nanoclay act as a reinforcing agent that binds the polymer chain inside the gallery space and restricts the mobility of the polymer chains Faruk and Matuana [35] observed the increased in mechanical properties of wood–plastic composite after the incorporation of nanoclay It was also observed that at a fixed level of nanoclay (3 phr), both flexural and tensile properties were improved upto the addition of 3 phr $TiO_2$ beyond that these values decreased The surface hydroxyl groups of CTAB modified $TiO_2$ nanopowder might interact with the hydroxyl groups of wood while the long alkyl chain of CTAB could interact with the polymer blend Hence an even dispersion of the nanoparticles occurred which increased the flexural and tensile properties of the composite Saeed et al [36] observed an increase in mechanical properties of electrospun nanofibers after incorporating $TiO_2$ nanopowder At higher percentage of $TiO_2$ loading (5 phr), the effective agglomeration of the nanoparticles resulted in a decrease in mechanical properties TEM study supported the agglomeration of $TiO_2$ nanoparticles

### 4 6 Hardness results

Hardness results of polymer blend and WPC with clay and different percentage of $TiO_2$ loading were also presented in Table 1 It was observed that hardness value of the polymer blend increased after the incorporation of compatibilizer The compatibilizer improved the interfacial adhesion between the polymers and increased the hardness value The value was found to decrease after the addition of WF to the polymer blend But after the incorporation of nanoclay and $TiO_2$ to the WPC hardness value was found to increase At higher $TiO_2$ loading hardness value was found to decrease The improvement was due to the restriction in the mobility of the polymer chains provided by the silicate layers and increase in interaction between clay and $TiO_2$ nanopowder with wood and polymer blend as mentioned earlier The decrease in hardness value was due to the agglomeration of $TiO_2$ nanoparticles

### 4 7 Thermal properties results

Fig 6 and Table 2 represent the initial decomposition temperature ($T_i$) maximum pyrolysis temperature ($T_m$), decomposition temperature at different weight loss (%) ($T_D$) and residual weight (RW %) for the polymer blend and WPCs $T_i$ values of the polymer blend increased after incorporation of compatibilizer and WF The compatibilizer increased the interfacial adhesion between the polymers and with WF leading to an increase in the $T_i$ values WF also provided reinforcing effect to the polymer blend Awal et al [32] observed an increase in thermal stability of polymer after incorporation of compatibilizer and wood flour $T_i$ value was further improved after the incorporation of clay and $TiO_2$ nanopowder The exfoliation of inorganic silicate layers of nanoclay impart long tortuous path to the composite that delayed the diffusion of decomposed volatile products throughout the composite The improvement in thermal stability of wood polymer composite by the incorporation of clay was reported by Maji and Deka [5]

**Table 1**
Flexural tensile and hardness properties of polymer blend and WPC loaded with different percentage of nanoclay and $TiO_2$

| Sample | Flexural properties | | Tensile properties | | Hardness |
|---|---|---|---|---|---|
| | Strength (MPa) | Modulus (MPa) | Strength (MPa) | Modulus (MPa) | (Shore D) |
| PB | 12 78 ± 0.35 | 755 68 ± 1 12 | 6 06 ± 1 02 | 85 92 ± 17 72 | 67 4 (±0 6) |
| PB/G5 | 15 51 ± 1 01 | 1014 21 ± 1 09 | 9 05 ± 1 31 | 116 24 ± 16 91 | 68 0 (±0 5) |
| PB/G5/W40 | 16 86 ± 1 10 | 3770 91 ± 1 14 | 17 14 ± 1 09 | 260 81 ± 17.39 | 66 7 (±0.3) |
| PB/G5/W40/N3/T1 | 28 62 ± 0 81 | 4842 81 ± 1 08 | 33 52 ± 1 37 | 596 12 ± 18 27 | 77 4 (±0.3) |
| PB/G5/W40/N3/T3 | 33 85 ± 1 06 | 5072 64 ± 1 25 | 36 03 ± 1 15 | 653 86 ± 17 14 | 80 9 (±0 5) |
| PB/G5/W40/N3/T5 | 30 38 ± 1 13 | 4903 90 ± 1 72 | 34 72 ± 1 18 | 620 57 ± 17 53 | 78 1 (±0.3) |

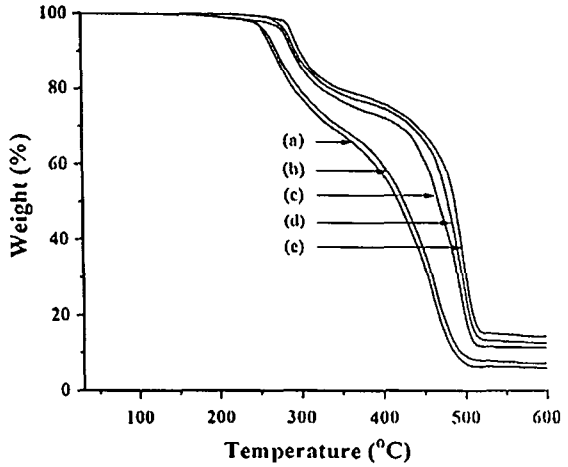


Fig. 6 Themogravimetric curves of (a) PB (b) PB/G5/W40 (c) PB/G5/W40/N3/T1, (d) PB/G5/W40/N3/T5 and (e) PB/G5/W40/N3/T3

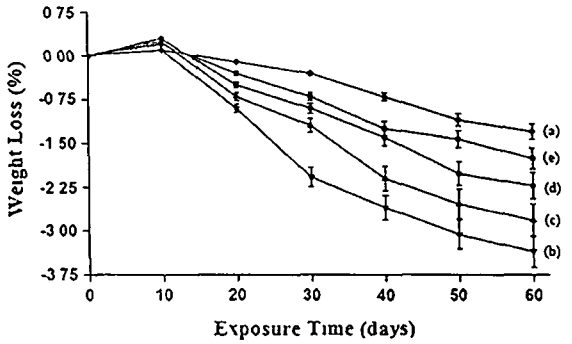


Fig 7 Weight losses vs exposure time of (a) PB (b) PB/G5/W40 (c) PB/G5/W40/N3/T1 (d) PB/G5/W40/N3/T5 and (e) PB/G5/W40/N3/T3

Moreover, higher thermal diffusivity of $TiO_2$ nanoparticles provided a better dispersion of heat inside the composite This would lead to a delay of burning of the surface and of the release of combustible volatiles throughout the composite Laachachi et al [37] studied the thermal stability of PMMA by using organoclay and $TiO_2$ and found a significant increase in thermal stability of PMMA due to the synergistic effect of clay/$TiO_2$ It should be mentioned that, at higher percentage (5 phr) of $TiO_2$, due to surface interaction, the oxide nanoparticles became agglomerated and offered an easy way to the passage of volatile products Hence, the thermal stability decreased

### 4 8 UV test results

Fig 7 displays the weight loss of polymer blend, normal WPC and WPC loaded with nanoclay and $TiO_2$ (1–3 phr) Weight losses of the samples were determined as a function of exposure time at room temperature The weight loss in all materials was nearly linear with exposure time A small increase of weight at early exposure times was due to the moisture uptake, which was greater than the material loss induced by the degradation in the early stage The rate of weight loss was lowest for polymer blend followed by WPC filled with 3 phr $TiO_2$ and 3 phr clay, 5 phr of $TiO_2$ and 3 phr clay 1 phr $TiO_2$ and 3 phr clay Higher weight loss was observed for normal WPC After 60 days of exposure, the maximum weight losses in polymer blend, normal WPC, 1, 3, 5 phr $TiO_2$ and clay loaded WPCs were 1 31 ± 0 24%, 3 37 ± 0 22%, 2 81 ± 0 35%, 1 76 ± 0 64% and 2 21 ± 0 59%, respectively

Fig 8 shows the carbonyl index values against time The intensity of the carbonyl peaks increased after irradiation of the samples for 60 days (Fig 9) Upon exposing the samples to UV radiation, chain scission of the polymer blend occurred that increased the carbonyl index value Further the chain scission decreased the density of entanglements of polymer chain and hence the decrease in weight of the samples The polymer blend had lowest carbonyl index value while normal WPC had highest carbonyl index value due to higher oxidation of WF The carbonyl index values decreased upto the addition of 3 phr $TiO_2$ after that it increased $TiO_2$ nanoparticles played an important role in stabilizing the WPC by acting as screens and delayed the photo-degradation process $TiO_2$ nanoparticles absorbed the UV radiation and hence

**Table 2**
Thermal analysis of polymer blend and wood polymer nanocomposite

| Sample | $T_i$[a] | $T_m$[b] | $T_m$[c] | Temperature of decomposition ($T_D$) in °C at different weight loss (%) | | | | RW% at 600 °C |
|---|---|---|---|---|---|---|---|---|
| | | | | 20% | 40% | 60% | 80% | |
| PB | 250 | 271 | 406 | 290 | 390 | 438 | 469 | 6 0 |
| PB/G5/W40 | 253 | 277 | 450 | 297 | 399 | 448 | 474 | 7 2 |
| PB/G5/W40/N3/T1 | 274 | 323 | 499 | 326 | 455 | 481 | 497 | 11 4 |
| PB/G5/W40/N3/T3 | 285 | 334 | 510 | 346 | 475 | 492 | 509 | 14 3 |
| PB/G5/W40/N3/T5 | 278 | 327 | 506 | 333 | 462 | 486 | 503 | 12 6 |

[a] $T_i$ value for initial degradation
[b] $T_m$ value for 1st step
[c] $T_m$ value for 2nd step

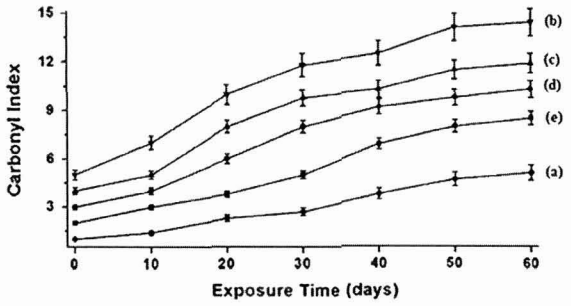


**Fig. 8.** Carbonyl index value of: (a) PB, (b) PB/G5/W40, (c) PB/G5/W40/N3/T1, (d) PB/G5/W40/N3/T5 and (e) PB/G5/W40/N3/T3.

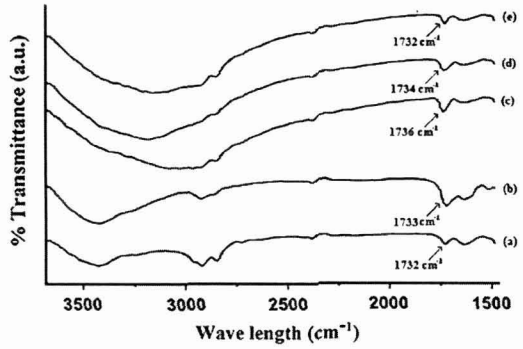


**Fig. 9.** Change in carbonyl peak intensity of: (a) PB, (b) PB/G5/W40, (c) PB/G5/W40/N3/T1, (d) PB/G5/W40/N3/T5 and (e) PB/G5/W40/N3/T3.

reduced the UV intensity required for the oxidation of the WPC. Du et al. [38] observed an increase in UV stability of WF/HDPE composite after the incorporation of $TiO_2$. The presence of nanoclay in the composite also has a screening effect that delayed the photo degradation process. Grigoriadou et al. [39] observed an increase in UV stability of HDPE after incorporating montmorillonite clay. Fig. 10 represents the SEM micrographs of samples after 60 days of irradiation. The micrographs revealed a drastic change in surface morphology of the samples due to exposure to UV radiation. The surface of normal WPC was more irregular compared to clay/$TiO_2$ treated WPC indicating that the normal WPC sample was less effective compared to $TiO_2$/clay containing sample against UV radiation. WPC containing higher percentage of $TiO_2$ (5 phr) exhibited lower protection against UV radiation as shown by the decrease in surface smoothness compared to WPC loaded with 3 phr $TiO_2$ and nanoclay. This might be due to the agglomeration of $TiO_2$ which provided lower protection against photodegradation.

### 4.9. Limiting oxygen index (LOI) results

Limiting oxygen index values of polymer blend, WPC and WPC loaded with nanoclay and $TiO_2$ are shown in Table 3. From the table, it can be observed that LOI value of the polymer blend increased after the addition of compatibilizer. The increase in the value was due to the increase in interfacial adhesion among the polymers by the compatibilizer. The addition of WF to the blend further increased the LOI value. The glycidyl and hydrocarbon part of the compatibilizer improved the interaction with the hydroxyl and hydrocarbon part of the wood and polymer. A substantial improvement in LOI value was observed after the addition of clay and $TiO_2$. The value increased upto the addition of 3 phr each of nanoclay and $TiO_2$. LOI value decreased at higher concentration of $TiO_2$ (5 phr). The nanoclay produced silicate char on the surface of WPC which increased the flame resistance property of the composite [40]. The tortuous path provided by the silicate layers provided better barrier property to the oxygen and heat which delayed the burning capacity of the composite. The addition of CTAB modified $TiO_2$ enhanced the interaction between wood, clay and polymer through its hydroxyl and cetyl groups. $TiO_2$ nanoparticles also provided some thermal barrier to the oxygen and heat leading to an improvement in flame resistant property. At higher $TiO_2$ loading, the agglomeration of $TiO_2$ resulted in decrease of interaction and hence reduction in barrier property as well as LOI value.

### 4.10. Water uptake and water vapor exclusion results

The water uptake and water vapor uptake results of polymer blend, PE-*co*-GMA treated polymer blend and WPC loaded with clay and different percentage of $TiO_2$ are shown in Fig. 11. The water uptake capacity of polymer blend decreased after the addition of PE-*co*-GMA compatibilizer. The decreased in water uptake capacity of PE-*co*-GMA treated polymer blend was due to the increase in interfacial adhesion between the polymers by the compatibilizer. The value of water uptake capacity was suddenly increased after the addition of WF to the blend. The hydrophilic nature of wood flour

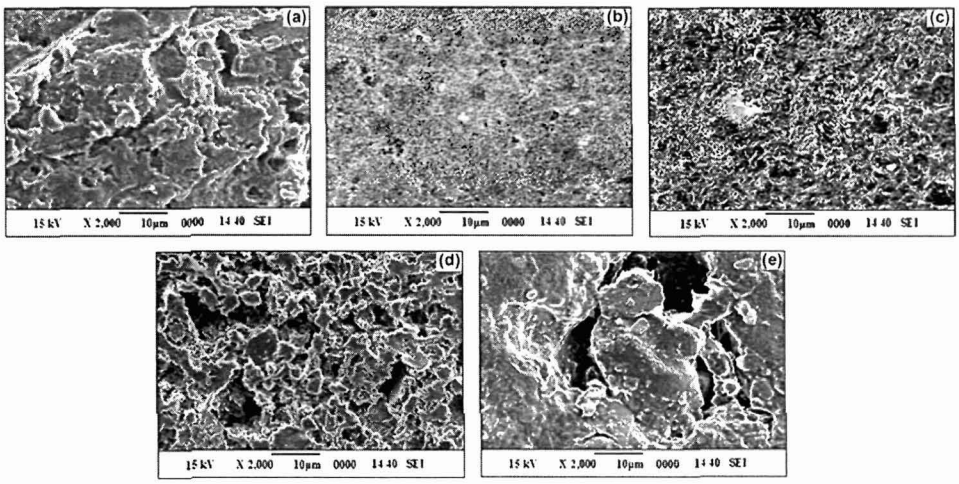


**Fig. 10.** SEM micrographs of UV treated samples after 60 days: (a) PB, (b) PB/G5/W40, (c) PB/G5/W40/N3/T1, (d) PB/G5/W40/N3/T3 and (e) PB/G5/W40/N3/T5.

**Table 3**
Limiting oxygen indices (LOI) and flaming characteristics of polymer blend and wood/polymer/clay/$TiO_2$ nanocomposites.

| Samples | LOI (%) | Flame description | Smoke & fumes | Char |
|---|---|---|---|---|
| PB | 21 (±0.43) | Candle like localized | Small and black smoke | Little |
| PB/G5 | 36 (±0.35) | Small localized flame | Small and black smoke | Little |
| PB/G5/W40 | 39 (±0.52) | Small localized flame | Small and black smoke | Little |
| PB/G5/W40/N3/T1 | 62 (±0.47) | Small localized flame | Small and black smoke | Higher |
| PB/G5/W40/N3/T3 | 67 (±0.32) | Small localized flame | Small and black smoke | Higher |
| PB/G5/W40/N3/T5 | 64 (±0.39) | Small localized flame | Small and black smoke | Higher |

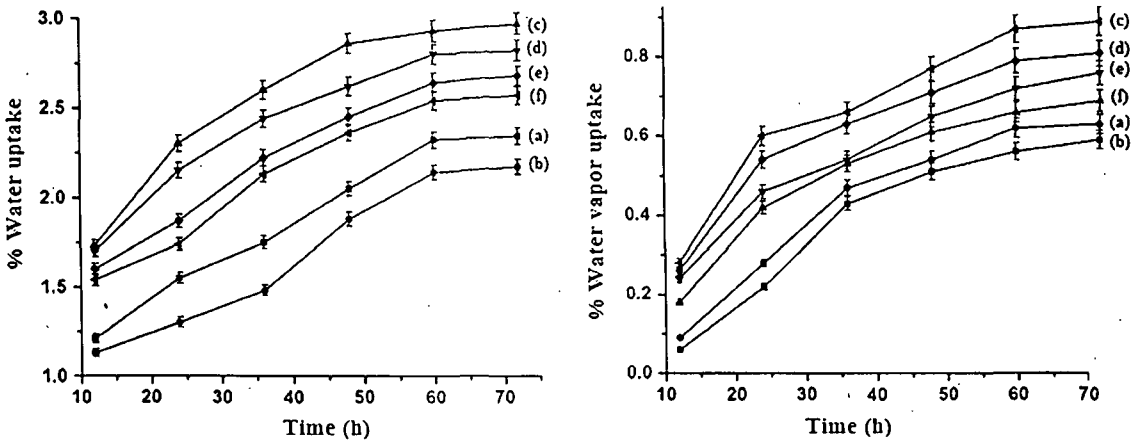


**Fig. 11.** Water uptake and water vapor absorption of: (a) PB, (b) PB/G5, (c) PB/G5/W40, (d) PB/G5/W40/N3/T1, (e) PB/G5/W40/N3/T5 and (f) PB/G5/W40/N3/T3.

caused an increase in the water uptake capacity. The water uptake capacity was decreased after the addition of clay and $TiO_2$. WPC loaded with 3 phr each of clay and $TiO_2$ showed lowest water uptake capacity followed by WPC with 3 phr clay and 5 phr $TiO_2$, and WPC with 3 phr clay and 1 phr $TiO_2$. The silicate layers of the clay provided tortuous path and increased the barrier property for water transport [5]. $TiO_2$ nanopowder also provided a barrier to the passage of water. Incorporation of nano-$TiO_2$ increased the water absorption and hence it reduced the diffusion coefficient of water. This was because of the strong affinity of water molecules towards nano-$TiO_2$ particles that restricted its free motion. The well distribution nature of modified nanoparticles further improved the resistance and retarded the motion of water molecules through the composite. The diffusion coefficient of water decreased further. Moreover, the water absorption of inorganic particles reduced after the modification of particles by organic surfactant. Zhu et al. [26] reported the increase in barrier property of poly(lactic acid) nanocomposite film after the incorporation of nano-$TiO_2$. The better the distribution of nanoparticles, the better was the barrier property. Chen et al. [41] observed a reduction in water uptake capacity of polyacrylate coating by modified $TiO_2$ due to the even dispersion of nanoparticles. $TiO_2$ nanoparticles at higher concentration were found to become agglomerated in the composite which resulted in an increase in water uptake capacity.

Water vapor exclusion test for the samples were carried out at 30 °C and 65% relative humidity. The water vapor uptake was found to increase with time. The trend and explanation for water vapor uptake of different samples were similar to those of samples taken for water uptake study. The optimal loading of $TiO_2$, at which the least water uptake was observed, was 3 phr. The incorporation of $TiO_2$ along with clay decreased the average water uptake by 40%.

## 5. Conclusions

The ratio of xylene and THF for solution blending of HDPE, LDPE, PP and PVC (1:1:1:0.5) was optimized as 70:30. The incorporation of polyethylene-*co*-glycidyl methacrylate (PE-*co*-GMA) improved the miscibility among the polymers as judged by the gradual disappearance of different phases. XRD and TEM study showed that silicate layers were exfoliated and $TiO_2$ nanoparticles were dispersed in the wood polymer composites. The shifting of characteristic peaks of $TiO_2$ nanoparticles indicated the surface modification of $TiO_2$ by CTAB as revealed by FTIR study. The interactions among wood, PE-*co*-GMA, $TiO_2$ and nanoclay were also studied by FTIR. WPC loaded with nanoclay and $TiO_2$ showed an improvement in mechanical and thermal properties. UV stability of the composite was found to increase by incorporation of $TiO_2$. Nanoclay/$TiO_2$ treated WPC further improved the flame retardancy and decreased the water absorption capacity. WPC loaded with 3 phr each of clay and $TiO_2$ exhibited maximum improvement in properties.

## Acknowledgment

The authors thank Council of Scientific and Industrial Research (CSIR)-New Delhi for their financial assistance (Grant number: 01(2287)/08/EMR-II).

## References

[1] Ayrilmis N, Buyuksari U, Dundar T. Waste pine cones as a source of reinforcing fillers for thermoplastic composites. J Appl Polym Sci 2010;117(4):2324–30.
[2] De Rosa IM, Kenny JM, Puglia D, Santulli C, Sarasini F. Morphological, thermal and mechanical characterization of okra (*Abelmoschus esculentus*) fibres as potential reinforcement in polymer composites. Compos Sci Technol 2010;70(1):116–22.
[3] Sui G, Fuqua MA, Ulven CA, Zhong WH. A plant fiber reinforced polymer composite prepared by a twin-screw extruder. Bioresour Technol 2009;100(3):1246–51.
[4] Park ES. Morphology, mechanical and dielectric breakdown properties of PBT/PET/TPE, PBT/PET/PA66, PBT/PET/LMPE and PBT/PET/$TiO_2$ blends. Polym Compos 2008;29(10):1111–8.
[5] Deka BK, Maji TK. Effect of coupling agent and nanoclay on properties of HDPE, LDPE, PP, PVC blend and *Phargamites karka* nanocomposite. Compos Sci Technol 2010;70(12):1755–61.

[6] Deka BK, Mandal M, Maji TK Study on properties of nanocomposites based on HDPE, LDPE, PP, PVC, wood and clay Polym Bull 2011 doi 10.1007/s00289-011-0529-5.
[7] Ashori A. Wood–plastic composites as promising green-composites for automotive industries! Bioresour Technol 2008,99(11) 4661–7
[8] Chiu FC, Yen HZ, Lee CE Characterization of PP/HDPE blend-based nanocomposites using different maleated polyolefins as compatibilizers Polym Testing 2010,29(3) 397–406
[9] Devi RR, Maji TK Effect of glycidyl methacrylate on the physical properties of wood–polymer composites Polym Compos 2007,28(1) 1–5
[10] Dikobe DG, Luyt AS Effect of poly(ethylene-co-glycidyl methacrylate) compatibilizer content on the morphology and physical properties of ethylene vinyl acetate–wood fiber composites J Appl Polym Sci 2007,104(5) 3206–13
[11] Kim HS, Lee BH, Choi SW, Kim S, Kim HJ The effect of types of maleic anhydride-grafted polypropylene (MAPP) on the interfacial adhesion properties of bio-flour-filled polypropylene composites Composites Part A 2007,38(6) 1473–82
[12] Liang G, Xu J, Bao S, Xu W Polyethylene/maleic anhydride grafted polyethylene/organic-montmorillonite nanocomposites I Preparation, microstructure, and mechanical properties J Appl Polym Sci 2004,91(6) 3974–80
[13] Ding C, He H Guo B, Jia D Structure and properties of polypropylene/clay nanocomposites compatibilized by solid-phase grafted polypropylene Polym Compos 2008,29(6) 698–707
[14] Yarahmadi N, Jakubowicz I, Hjertberg T Development of poly(vinyl chloride)/montmorillonite nanocomposites using chelating agents Polym Degrad Stab 2010,95(2) 132–7
[15] Mirabedini SM, Mohseni M, PazokiFard Sh, Esfandeh M Effect of $TiO_2$ on the mechanical and adhesion properties of RTV silicone elastomer coatings Colloids Surf A Physicochem Eng Aspects 2008,317(1–3) 80–6
[16] Fa W Yang C, Gong C, Peng T Zan L Enhanced photodegradation efficiency of polyethylene–$TiO_2$ nanocomposite film with oxidized polyethylene wax J Appl Polym Sci 2010 118(1) 378–84
[17] Stark NM, Matuana LM Surface chemistry changes of weathered HDPE/wood-flour composites studied by XPS and FTIR spectroscopy Polym Degrad Stab 2004,86(1) 1–9
[18] Mina F Seema S, Matin R, Rahaman J, Sarker RB, Gafur A et al Improved performance of isotactic polypropylene/titanium dioxide composites effect of processing conditions and filler content Polym Degrad Stab 2009,94(2) 183–8
[19] Han G, Lei Y, Wu Q, Kojima Y Bamboo-fiber filled high density polyethylene composites effect of coupling treatment and nanoclay J Polym Environ 2008,16(2) 123–30
[20] Liu J, Chen G, Yang J Preparation and characterization of poly(vinyl chloride)/layered double hydroxide nanocomposites with enhanced thermal stability Polymer 2008,49(18) 3923–7
[21] De Rosa C, Corradini P Crystal structure of syndiotactic polypropylene Macromolecules 1993,26(21) 5711–8
[22] Sham EL, Aranda MAG, Torres EMF, Gottifredi JC Lara MM, Bruque S Zirconium titanate from sol-gel synthesis thermal decomposition and quantitative phase analysis J Solid State Chem 1998 139(2) 225–32
[23] Wang H, Liu P, Cheng X, Shui A, Zeng L Effect of surfactants on synthesis of $TiO_2$ nano-particles by homogeneous precipitation method Powder Technol 2008,188(1) 52–4
[24] Yamada S, Mouri E, Yoshinaga K Incorporation of titanium dioxide particles into polymer matrix using block copolymer micelles for fabrication of high refractive and transparent organic–inorganic hybrid materials J Polym Sci Part A Polym Chem 2011,49(3) 712–8
[25] Pracella M, Chionna D, Ishak R, Galeski A. Recycling of PET and polyolefin based packaging materials by reactive blending. Polym Plast Technol Eng 2004,43(6) 1711–22
[26] Zhu Y, Buonocore GG, Lavorgna M Ambrosio L Poly(lactic acid)/titanium dioxide nanocomposite films influence of processing procedure on dispersion of titanium dioxide and photocatalytic activity Polym Compos 2011,32(4) 519–28
[27] Li H, Tripp CP Spectroscopic identification and dynamics of adsorbed cetyltrimethylammonium bromide structures on $TiO_2$ surfaces Langmuir 2002,18(24) 9441–6
[28] Zhang SL, Zhou JF, Zhang ZJ Du ZL, Vorontsov AV, Jin ZS Morphological structure and physicochemical properties of nanotube $TiO_2$ Chinese Sci Bull 2000 45(16) 1533–6
[29] Xu L, Yang M *In Situ* compatibilization between polystyrene-grafted nano-sized $TiO_2$ and polypropylene with friedel–crafts catalyst J Appl Polym Sci 2009 114(5) 2755–63
[30] Qu Y, Wang W, Jing L, Song S, Shi X, Xue L, et al Surface modification of nanocrystalline anatase with CTAB in the acidic condition and its effects on photocatalytic activity and preferential growth of $TiO_2$ Appl Surf Sci 2010,257(1) 151–6
[31] Das G, Karak N Epoxidized Mesua ferrea L Seed oil-based reactive diluent for BPA epoxy resin and their green nanocomposites Prog Org Coat 2009 66(1) 59–64
[32] Awal A Ghosh SB, Sain M Thermal properties and spectral characterization of wood pulp reinforced bio-composite fibers J Therm Anal Calorim 2010 99(2) 695–701
[33] Salemane MG Luyt AS Thermal and mechanical properties of polypropylene–wood powder composites J Appl Polym Sci 2006,100(5) 4173–80
[34] Sailaja RRN Mechanical and thermal properties of bleached kraft pulp–LDPE composites effect of epoxy functionalized compatibilizer Compos Sci Technol 2006 66(13) 2039–48
[35] Faruk O, Matuana LM Nanoclay reinforced HDPE as a matrix for wood–plastic composites Compos Sci Technol 2008 68(9) 2073–7
[36] Saeed K Park SY, Ali N Characterization of poly(butylene terephthalate) electrspun nanofibres containing titanium oxide Iran Polym J 2009,18(8) 671–7
[37] Laachachi A Leroy E, Cochez M, Ferriol M Lopez Cuesta JM Use of oxide nanoparticles and organoclays to improve thermal stability and fire retardancy of poly(methyl methacrylate) Polym Degrad Stab 2005 89(2) 344–52
[38] Du H, Wang W Wang Q, Zhang Z Sui S Zhang Y Effects of pigments on the UV degradation of wood-flour/HDPE composites J Appl Polym Sci 2010,118(2) 1068–76
[39] Grigoriadou I, Paraskevopoulos KM Chrissafis K, Pavlidou E, Stamkopoulos TG, Bikiaris D Effect of different nanoparticles on HDPE UV stability Polym Degrad Stab 2011,96 151–63
[40] Camino G, Tartaglione G Frache A, Manferti C, Costa G Thermal and combustion behaviour of layered silicate-epoxy nanocomposites Polym Degrad Stab 2005,90(2) 354–62
[41] Chen Y, Lin A Gan F Improvement of polyacrylate coating by filling modified nano-$TiO_2$ Appl Surf Sci 2006,252 8635–40

# Effect of Nanoclay and ZnO on the Physical and Chemical Properties of Wood Polymer Nanocomposite

**Biplab K. Deka, Tarun K. Maji**

*Department of Chemical Sciences, Tezpur University, Assam 784028, India*

Received 18 April 2011; accepted 20 July 2011
DOI 10.1002/app.35314
Published online in Wiley Online Library (wileyonlinelibrary.com).

**ABSTRACT:** Wood polymer composite (WPC) was prepared by using solution blended high density polyethylene, low density polyethylene, polypropylene, and poly(vinyl chloride) with *Phragmites karka* wood flour and polyethylene-*co*-glycidyl methacrylate (PE-*co*-GMA). The effect of addition of nanoclay and ZnO on the properties of the composite was examined. The distribution of silicate layers and ZnO nanopowder was studied by X-ray diffractometry and transmission electron microscopy. The improvement in miscibility among polymers due to addition of PE-*co*-GMA as compatibilizer was studied by scanning electron microscopy. WPC treated with 3 phr each of clay and ZnO showed an improvement in thermal stability and UV resistance. Mechanical and flame retarding properties were also enhanced after the incorporation of clay/ZnO nanopowder. Both water and water vapor absorption were found to decrease due to inclusion of nanoclay and ZnO in WPC. © 2011 Wiley Periodicals, Inc. J Appl Polym Sci 000: 000–000, 2011

**Key words:** nanocomposites; wood; organoclay; mechanical properties; thermal properties

## INTRODUCTION

The northeastern part of India is rich in forest based cellulosic resources to a lucrative amount. Only a few of the different species available in this region have been explored. Nal, a type of non conventional plant available in this region, do not have any structural application.

The pollution caused by post consumer plastic materials comprising mostly of polyethylene, polypropylene (PP), polyvinyl chloride, etc. has become a matter of concern. Recycling is one of the processes to minimize the waste pollution. The poor mechanical, thermal, and other properties of recycled waste plastic materials restrict their use in a number of applications. The nonconventional plant material can be made value added material suitable for preparation of structural components by treating with waste plastic materials. Structural components include window, window profiles, table tops, partition walls, etc.

Solution blending is one of the process to mix varieties of waste plastics. No single solvent can alone be able to solubilize different kind of plastics. Moreover, it is difficult to segregate different kind of plastics. The optimization of solvent ratio can be determined properly if a mixture of known percentage of virgin high density polyethylene (HDPE), low density polyethylene (LDPE), PP, poly(vinyl chloride) (PVC), etc. is used as starting waste plastic materials.

Plant fiber reinforced polymer composite is a widespread used branch of composite materials.[1] Wood is ecofriendly, biodegradable, and renewable, but they have poor mechanical properties and dimensional stability. These properties can be improved by making composites with polymer matrix.[2,3] The main disadvantage of using wood flour (WF) to the polymer matrix is its poor compatibility to the polymer. As WFs are hydrophilic and polymers are hydrophobic in nature, there always remain an interfacial phase separation between the wood and the polymers. These results in poor compatibility among the constituents, and hence, decrease the properties of the composites. To improve the miscibility between polymers and WF, compatibilizers are used. They act as a bridging agent between the two interfaces. Compatibilizers like glycidyl methacrylate and maleated PP have significantly improved the properties of the wood polymer composite (WPC).[4,5]

Thermal stability is one of the important properties of WPC. It has been established that thermostability along with the other properties of the composite can be improved by using clay particles.[6] Research on nanometer-sized materials has increased remarkably during the past few years due to their unique characteristics of large fraction of surface atoms and a higher surface area. The addition of

*Correspondence to:* T. K. Maji (tkm@tezu.ernet.in).

nanoclay to the composite enhances the mechanical, thermal, and other properties. Besides using clay, different metal oxide nano particles (Si, Zn, Ti, etc.) are used to improve the properties like mechanical, thermal, flammability, weathering, etc. of the composites. The surface characteristics of nanopowders play a key role in their fundamental properties from phase transformation to reactivity. A dramatic increase in the interfacial area between fillers and polymer can significantly improve the properties of the polymer.[7] These nanoparticles are non toxic, stable, and highly themostable inorganic filler. Owing to all these properties, these are widely used in all types of materials like plastics, rubbers, etc. UV protection, flame retardancy, and weathering resistance are very important for wood based composites used in exterior applications.

In polymer composite, ZnO nanopowder is one of the widely used filler. ZnO enhances the thermal, mechanical, UV resistance, as well as other relevant properties of the composite.[8–10] Polymer-ZnO composites have been explored as technological important due to their potential applications in solar cells, electrochromic windows, optical device, gas sensing, and in antimicrobial application of food preservation.[11–14] Reports based on wood/polymer/clay nanocomposite are available in literature. However, far less is known regarding wood polymer nanocomposite by using both clay and metal oxide. It is envisaged that a thorough study may provide some valuable information for the development of WPC in future.

This study is aimed to discuss the effect of ZnO nanopowder along with nanoclay to the thermal and mechanical properties of HDPE/LDPE/PP/PVC blend/wood/nanoclay composite. The aim is also to study the effect of ZnO to other properties like UV resistance, flame retardancy, and water uptake of the composites.

## EXPERIMENTAL

### Materials

HDPE and LDPE (Grade: PE/20/TK/CN) were collected from Plast Alloys India Ltd. (Harayana, India). PP homopolymer (Grade: H110MA, MFI 11g/10 min) was collected from Reliance Industries Ltd. (Mumbai, India). PVC (Grade: SPVC FS: 6701) was collected from Finolex Industries Ltd. (Pune, India). The compatibilizer, polyethylene-*co*-glycidyl methacrylate (PE-*co*-GMA; Otto chemicals, Mumbai, India), *N*-Cetyl-N,N,*N*-trimethyl ammonium bromide (CTAB; Central Drug house (P) Ltd., Delhi, India), nanomer (clay modified by 15–35 wt % octadecylamine and 0.5–5 wt % aminopropyltriethoxy silane, ζ-Aldrich, USA), and ZnO nanopowder (<100 nm; Aldrich, Germany) were used as received. A nonconventional wood, nal (*Phragmites karka*) was collected from local forest of Assam. Other reagents used were of analytical grade.

### Preparation of wood samples

Nal (*P. karka*) is a kind of softwood available in the forest of Assam. It was collected and chopped into small strips. These strips were initially washed with 1% soap solution. It was followed by washing with 1% NaOH solution and finally washed with cold water. The washed wood strips were oven dried at 100 ± 5°C till attainment of constant weight. These dried wood strips were grinded in a mixer, sieved at about 60 mesh size, and kept for subsequent use.

### Modification of ZnO

The surface of ZnO nanoparticles was modified with cationic surfactant CTAB to improve its miscibility with the hydrophobic polymers. Approximately 10 g of ZnO was taken in a round bottom flask containing 1:1 ethanol–water mixture. It was fitted with spiral condenser and stirred at 80°C for 24 h. Then 12 g of CTAB was taken in a beaker containing ethanol–water mixture and stirred at 80°C for 6 h. This mixture was added to ZnO mixture and finally stirred for another 24 h. The mixture was then filtered and washed with deionized water for several times. It was collected and dried overnight in vacuum oven at 45°C. After completion of drying, the mixture was grinded and stored in desiccator to avoid moisture absorption. The presence of long organic chain of cetyl group and the surface hydroxyl group of modified ZnO would enhance the interaction between ZnO, polymers, wood, and clay.

### Preparation of wood polymer nanocomposite

Approximately 6 gram each of HDPE, LDPE, and PP (1 : 1 : 1) were added slowly to 105 mL of xylene taken in a flask fitted with a spiral condenser at room temperature. This was followed by the addition of the PE-*co*-GMA (5 phr). The temperature of the flask was increased to 130°C to make a homogenous solution. Now, another solution containing 3 g of PVC in 35 mL of tetrahydrofuran (THF) was prepared. The temperature of the previous polymer solution was decreased to 120°C. The PVC solution was then mixed with the other polymer solution at 120°C (approximately) under stirring condition for 1 h. A known quantity of nanoclay (3 phr) and CTAB modified ZnO nanopowder (1–5 phr) was dispersed in 15 mL of THF solution using stirrer and sonication. This dispersed mixture was added gradually to the polymer solution under stirring condition. Oven

dried WF (40 phr) was added slowly to this mixture and stirred for another 1 h. It was transferred in tray, dried, and grinded. The composite sheets were obtained by the compression molding press (Santec, New Delhi) at 150°C under a pressure of 80 MPa.

Polymer blend (HDPE + LDPE + PP + PVC), Polymer blend/5phr PE-*co*-GMA, and polymer blend/5 phr PE-*co*-GMA/40 phr wood were designated as PB, PB/G5, and PB/G5/W40. The 1, 3, and 5 phr ZnO filled WPC containing 3 phr nanoclay were designated as PB/G5/W40/N3/Z1, PB/G5/W40/N3/Z3, and PB/G5/W40/N3/Z5.

### Measurements

#### XRD study

The degree of intercalation of nanoclay and distribution of ZnO in WPC was examined by X-ray diffractometry. It was carried out in a Rigaku X-ray diffractometer (Miniflax, UK) using CuKα ($\lambda$ = 0.154 nm) radiation at a scanning rate of 1° per minute with an angle ranging from 2° to 70°.

#### TEM study

The dispersion of the silicate layers of nanoclay and ZnO nanoparticles in WPCs was performed by using transmission electron microscopy (TEM; JEM-100 CX II) at an accelerated voltage of 20–100 kV.

#### SEM study

The compatibility among different polymers as well as morphological features of the WPC was studied by using scanning electron microscope (JEOL JSM - 6390LV) at an accelerated voltage of 5–10 kV. Fractured surface of the samples, deposited on a brass holder and sputtered with platinum, were used for this study.

#### FTIR Studies

FTIR spectra of WF, ZnO nanopowder, and WPC loaded with nanoclay and ZnO nanopowder were recorded in Fourier Transform Infrared spectrophotometer (Impact-410, Nicolet, USA) using KBr pellet.

#### Mechanical property study

The tensile and flexural tests for polymer blend, PE-*co*-GMA treated polymer blend, and WPC loaded with different percentage of ZnO were carried out using Universal Testing Machine (Zwick, model Z010) at a crosshead speed of 10 mm $min^{-1}$ at room temperature according to ASTM D-638 and D-790, respectively. A total of 10 samples of each category were tested and their average values were reported.

#### Hardness study

The hardness of the samples was measured according to ASTM D-2240 using a durameter (model RR12) and expressed as shore D hardness.

#### Thermal property study

Thermal properties of polymer blend and the WPCs were measured in a thermogravimetric analyzer (TGA-50, shimadzu) at a heating rate of 10°C $min^{-1}$ up to 600°C under nitrogen atmosphere.

#### UV resistance test

The degradation study of the WPC samples was done in UV chamber (Model: S.L.W, voltage: 230 V; Advanced Research Co., India) using a mercury arc lamp system that produces a collimated and highly uniform UV flux in the 254–365 nm range. Specimen's dimensions of 25 × 25 × 5 $mm^3$ were exposed in the UV chamber at room temperature and characterized at specified time intervals. The weight loss was measured and is expressed as follows[15]:

$$\%\text{weightloss} = (W_t - W_o/W_o) \times 100$$

where, $W_t$ is the specimen weight at time $t$ and $W_o$ is the specimen weight before exposure. Surface morphology of UV degraded specimen was characterized by scanning electron microscopy (SEM). Chemical degradation was studied by FTIR. The intensity of the carbonyl (C=O) stretching peaks at 1715 $cm^{-1}$ in cellulose of WF was measured. The net peak heights were determined by subtracting the height of the baseline directly from the total peak height. The same base line was taken for each peak before and after exposure to UV.[16] The carbonyl index was calculated by using the following equation:

$$\text{Carbonyl index} = I_{1715}/I_{2912}(100)$$

where, $I$ represent the intensity of the peak. The peak intensities were normalized by using —CH stretching peak of alkane at 2912 $cm^{-1}$. This peak was chosen as reference due to its least change during irradiation.

#### LOI study

WPC samples were cut into the dimensions of 100 × 10 × 5 $mm^3$ for limiting oxygen index (LOI) test by using flammability tester (S.C. Dey Co., Kolkata) according to ASTM D-2863 method.[17] The total volume of the gas mixture ($N_2$ + $O_2$) was kept fixed at 18 cc. The volume of nitrogen gas and that of oxygen gas were kept initially at a maximum and minimum level. Now, the volume of nitrogen gas was decreased and

that of oxygen gas was increased gradually. However, the total volume of gas mixture was kept fixed at 18 cc during the experiment. The sample was placed vertically in the sample holder of the LOI apparatus. The ratio of nitrogen and oxygen at which the sample continued to burn for at least 30 s was recorded.

$$\text{Limiting oxygen index (LOI)} = \text{Volume of } O_2/\text{Volume of } (O_2 + N_2)100.$$

### Water uptake and water vapor exclusion study

WPC samples were cut into 2.5 × 0.5 × 2.5 $cm^3$ for water uptake and water vapor exclusion study. Percentage water uptake was measured by submerging the samples in distilled water at room temperature (30°C) for different time periods after conditioning at 65% relative humidity and 30°C and expressed according to the formulae,

$$\text{Water uptake}\,(\%) = (W_s - W_1)/W_1 \times 100$$

where, $W_s$ is the weight of the water saturated sample and $W_1$ is the weight of the oven dried sample.

The water vapor exclusion test was carried out at 65% relative humidity and 30°C. Weights of the samples were measured after 12, 24, 36, 48, 60, and 72 h. The samples were oven dried and conditioned at 30°C and 30% relative humidity before the test. It is expressed as a percentage of moisture absorbed based on oven dry weight.

## RESULTS AND DISCUSSION

### XRD results

Figure 1 shows the X-ray diffraction (XRD) results of nanoclay, polymer blend, ZnO, and WPC loaded with clay (3 phr) and different percentage of ZnO (1–5 phr). Organically modified nanoclay (curve-a) shows the diffraction peak at 2θ = 4.11° with basal spacing 2.15 nm. Curve-b represents the diffractrogram of polymer blend. The most prominent wide-angle XRD peaks appeared at 2θ = 14.12, (200) 17.06, (040) 18.64, (211) 21.62 (110), and 24.02 (200) were for crystalline portion of different polymers present in the blend.[18–21] The crystalline peaks appear above 2θ = 30° (shown in curve-c) were the characteristic peaks of ZnO nanopowder.[22] Curve (d–f) was for WPC loaded with nanoclay (3 phr) and different percentage of ZnO (1–5 phr). The diffractograms of composites did not exhibit any characteristic peak of nanoclay. It could be said that either an exfoliation or increase in disorder in nanoclay occurred which was not possible to detect by XRD analysis. The crystalline peak intensity of the polymer blend appeared in the range 2θ = 14–25° was found to decrease with the increase in the level of incorporation of ZnO (1–5 phr). However, the intensities of peak corresponding to ZnO nanopowder increased with the increase in the concentration of ZnO in the composite. Similar decreased in peak intensities of polymer and increase of peak intensity of $TiO_2$ was observed and reported by Mina et al.[18] while studying the XRD profile of PP /titanium dioxide composite. It could be concluded that nanoclay layers were disordered and ZnO particles were incorporated in the wood polymer matrix.

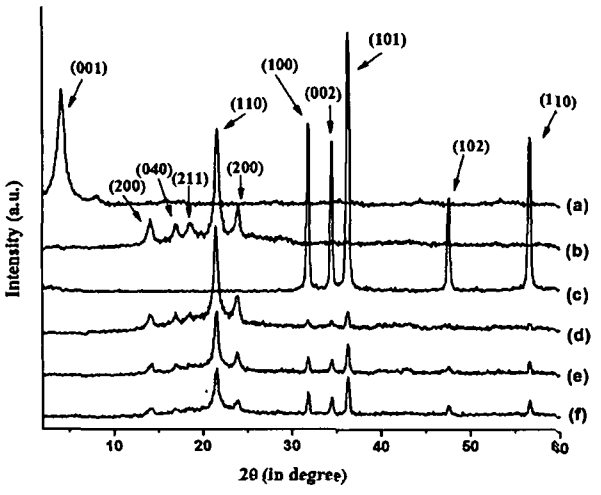


**Figure 1** XRD of (a) Nanoclay, (b) PB, (c) nano ZnO, (d) PB/G5/W40/N3/Z1, (e) PB/G5/W40/N3/Z3, and (f) PB/G5/W40/N3/Z5.

### TEM results

Figure 2 shows the TEM micrographs of WPC loaded with nanoclay (3 phr) and different percentage of ZnO (1–5 phr). The dark slices (arrow marked) represent the layers of nanoclay while the dark spots (arrow marked) are for ZnO nanoparticles. The distribution of ZnO (1–3 phr) was better in the WPC compared with that of composite containing higher proportion (5 phr) of ZnO [ig. 2(c)]. Kim et al.[23] prepared PAN/ZnO nanocomposite and found that ZnO nanoparticles were well dispersed within the composite. At higher concentration of ZnO, the distances between ZnO particles became less and this might have enhanced the tendency for agglomeration.

### SEM Study

Figure 3 shows the SEM micrographs of polymer blend with and without compatibilizer, WPC and WPC loaded with nanoclay, and different percentage of ZnO nanopowder. The fractured surface of some selective samples was considered for this study. The polymer mixtures were immiscible as judged by separation of different phases [Fig. 3(a)]. The miscibility

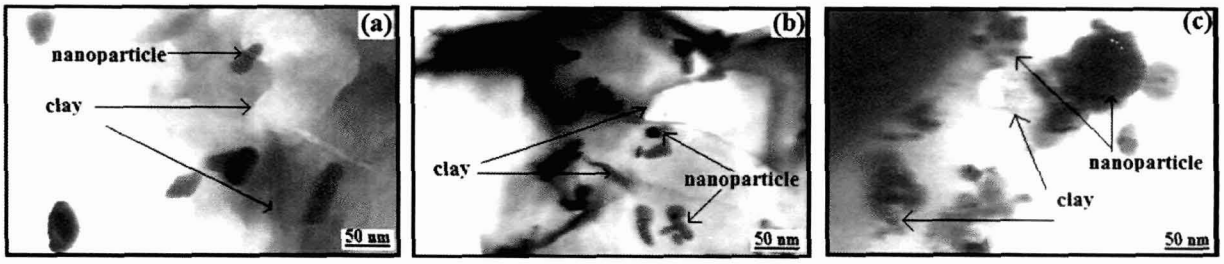


**Figure 2** TEM micrographs of (a) PB/G5/W40/N3/Z1, (b) PB/G5/W40/N3/Z3, and (c) PB/G5/W40/N3/Z5.

improved due to addition of PE-*co*-GMA as compatibilizer [Fig. 3(b)]. The compatibilizer enhanced the interfacial adhesion among the polymers through its long hydrocarbon chain and epoxy group which resulted in an improvement in miscibility. The use of ethylene–glycidyl methacrylate for improving the adhesion between polyolefins and PET was reported in the literature.[24] The addition of WF decreased the roughness of fractured surface of the composite [Fig. 3(c)]. The roughness of the fractured surface decreased further after the incorporation of WF, clay, and ZnO to the polymer blend [Fig. 3(d–e)]. The fractured surface of composite having nanoclay and 3 phr ZnO appeared to be smoother compared with those of composite prepared with either 1 or 5 phr ZnO and nanoclay. This might be due to the improvement in interaction among PE-*co*-GMA, nanoclay, ZnO, polymer, and wood. The decrease in smoothness at higher concentration of ZnO was due to the aggregation of ZnO. Similar observation was reported by He et al.[25] during study of the morphology of PET/ZnO nanocomposite.

## FTIR study

FTIR spectra of CTAB, ZnO, and CTAB modified ZnO are shown in Figure 4. In the spectrum of CTAB [Fig. 4(a)], the absorption peaks at 2918, 2848, and 1475 $cm^{-1}$ were assigned to asymmetric, symmetric stretching, and scissor modes of $-CH_2$ in the methylene chains, respectively.[26] FTIR spectrum of unmodified ZnO nanoparticles is presented in Figure 4(b). Absorption peaks at 3438 and 1633 $cm^{-1}$ in the spectra was due to —OH (-stretching) and —OH (-bending) vibrations while the peaks around 420 $cm^{-1}$ was due to the vibration of metal–oxygen (M–O) bond as reported in the literature.[27] The FTIR spectrum of ZnO modified with CTAB is represented by the curve 4c. It was observed that the intensity of the peak for —OH group decreased to

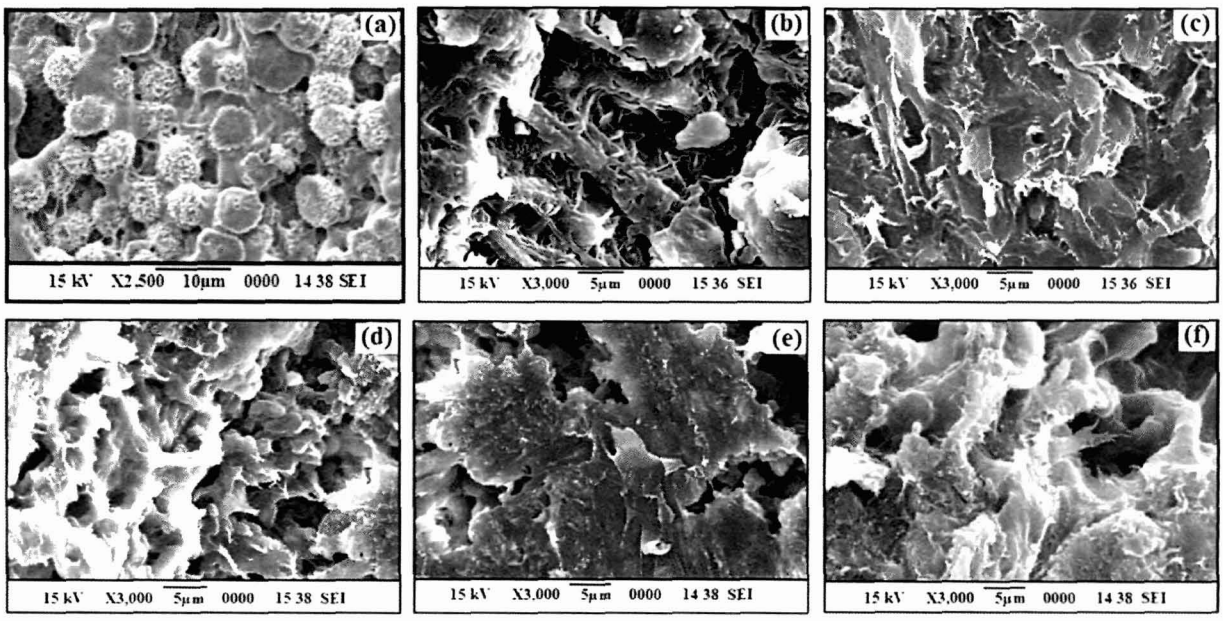


**Figure 3** SEM micrographs of (a) PB, (b) PB/G5, (c) PB/G5/W40, (d) PB/G5/W40/N3/Z1, (e) PB/G5/W40/N3/Z3, and (f) PB/G5/W40/N3/Z5.

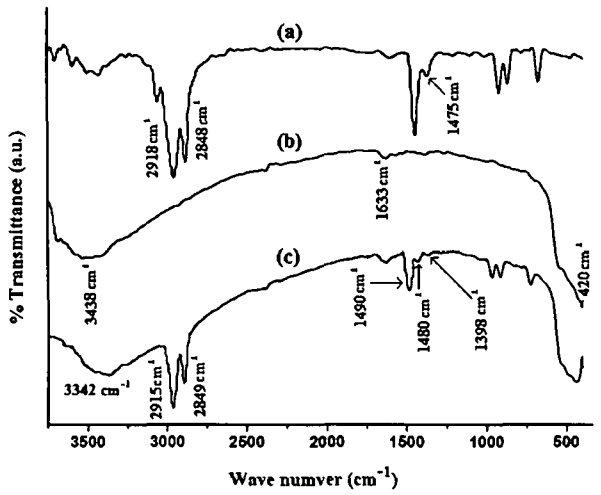


Figure 4 FTIR spectra of (a) CTAB, (b) unmodified ZnO nanopowder, and (c) CTAB modified ZnO.

wave number 3342 $cm^{-1}$. Besides this, two new peaks at 2915 and 2849 $cm^{-1}$, which were due to the presence of $-CH_2$ group of CTAB were appeared in the spectrum. The peaks at 1490 and 1480 $cm^{-1}$ were due to the asymmetric $CH_3$-$N^+$ deformation mode of the CTAB head group. Another peak present at 1398 $cm^{-1}$ was due to the symmetric $CH_3$—$N^+$ deformation mode of CTAB head group.[26] These results indicated that long chain of CTAB group had been incorporated on the surface of the ZnO nanoparticles. Furthermore, CTAB modified ZnO was dispersed in a flask containing xylene and kept for checking of any settling of particles. The dispersion of ZnO was found to be stable. This indicated that proper modification occurred.

Figure 5 shows the FTIR spectra of wood, nanoclay, WPC excluding nanoclay and ZnO, and WPC containing nanoclay with different percentage of ZnO. Curve-a representing the wood sample shows the presence of bands at 3436 $cm^{-1}$ for —OH stretching, 2932 and 2849 $cm^{-1}$ for —CH stretching, 1732 $cm^{-1}$ for C=O stretching, 1639 $cm^{-1}$ for —OH bending, 1161 and 1045 $cm^{-1}$ for C—O stretching, and 1000–650 $cm^{-1}$ for C—H bending vibration (out of plane). Organically modified nanoclay (curve b) exhibits the peaks at 3470 $cm^{-1}$ (—OH stretching) 2935 and 2852 $cm^{-1}$ (—CH stretching of modified hydrocarbon), 1621 $cm^{-1}$ (—OH bending), and 1032–461 $cm^{-1}$ (oxide bands of metals like Si, Al, Mg, etc.).[28] PB/G5/W40 (curve c) shows peaks at 2923 $cm^{-1}$ (—CH stretching), 1734 $cm^{-1}$ (C=O stretching), 1636 $cm^{-1}$ (—OH bending), and 720 $cm^{-1}$ ($-CH_2$ stretching).

Figure 5(d–f) represents the FTIR spectra of WPC loaded with 3 phr nanoclay and 1, 3, and 5 phr of ZnO. From the figure, it was observed that the intensity of —OH stretching was decreased and shifted to 3434 $cm^{-1}$ (curve-d), 3419 $cm^{-1}$ (curve-e), and 3430 $cm^{-1}$ (curve-f) from 3436 $cm^{-1}$ (wood). The decrease in peak intensity of —OH stretching might be ascribed to the participation of hydroxyl group of clay and ZnO in the crosslinking reaction with wood and polymer. The shifting of hydroxyl absorption peak to lower wave number was due to the formation of hydrogen bond between WF and polymer. A similar decrease in intensity of —OH absorption peak and shifting to lower wavelength was reported by Deka and Maji [29] while studying the FTIR spectra of nanoclay treated WPC. Dhoke et al.[27] studied the interaction between nano-ZnO particles and alkyd resin by FTIR technique. A significant decrease in peak intensity of hydroxyl group of alkyd resin was observed. The intensity of —CH stretching peaks at 2932 $cm^{-1}$ and 2848 $cm^{-1}$ (curve *d*–f) was found to increase. Similar increase in —CH peak intensities was observed by Awal et al.[30] The peak intensities (1032–461 $cm^{-1}$) of metal oxides bond of nanoclay and ZnO (curve *d*–f) was decreased to a considerable extent. Moreover, the flexural and tensile properties of the composites improved due to incorporation of clay and ZnO as explained later. All these suggested a strong interaction between wood, nanoclay, ZnO, and polymer.

## Mechanical Property

Table I shows the flexural and tensile properties of polymer blends and WPC loaded with nanoclay and different percentage of ZnO nanopowder. From the table, it was observed that both flexural and tensile properties of the polymer blend increased after incorporation of compatibilizer. The compatibilizer

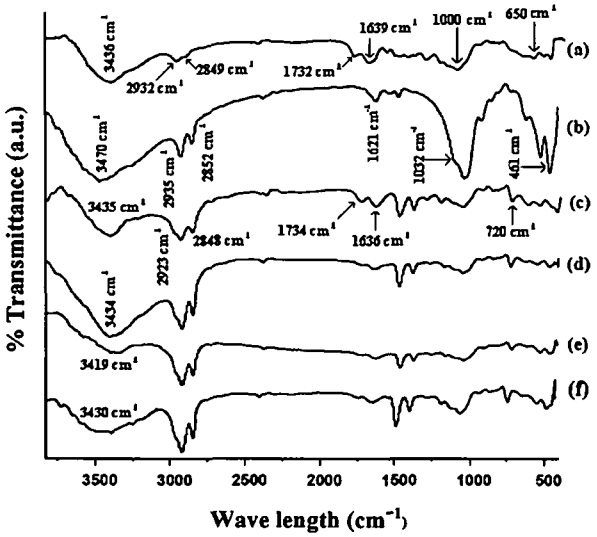


Figure 5 FTIR spectra of (a) wood, (b) nanoclay, (c) PB/G5/W40, (d) PB/G5/W40/N3/Z1, (e) PB/G5/W40/N3/Z3, and (f) PB/G5/W40/N3/Z5.

**TABLE I**
**Flexural, Tensile and Hardness Properties of Polymer Blend and WPC Loaded with Nanoclay and Different Percentage of ZnO**

| | Flexural properties | | Tensile properties | | Hardness |
|---|---|---|---|---|---|
| Sample | Strength (MPa) | Modulus (MPa) | Strength (MPa) | Modulus (MPa) | (Shore D) |
| PB | 12.34 ± 0.36 | 756.41 ± 1.28 | 5.87 ± 1.21 | 85.42 ± 16.23 | 66.7 (± 0.3) |
| PB/G5 | 15.34 ± 1.08 | 1026.32 ± 1.07 | 9.04 ± 1.16 | 113.54 ± 17.23 | 68.4 (± 0.5) |
| PB/G5/W40 | 17.13 ± 1.11 | 3756.18 ± 1.15 | 17.82 ± 1.21 | 254.84 ± 18.26 | 66.8 (± 0.7) |
| PB/G5/W40/N3/Z1 | 28.14 ± 0.72 | 4843.81 ± 1.31 | 32.28 ± 1.47 | 603.45 ± 17.25 | 74.3 (± 0.2) |
| PB/G5/W40/N3/Z3 | 31.79 ± 1.12 | 5052.58 ± 1.36 | 35.65 ± 1.56 | 657.32 ± 17.16 | 79.4 (± 0.2) |
| PB/G5/W40/N3/Z5 | 29.25 ± 1.71 | 4927.41 ± 1.29 | 30.24 ± 1.14 | 629.87 ± 18.74 | 77.1 (± 0.3) |

improved the interfacial adhesion between the polymers due to which both flexural and tensile properties increased. The flexural and tensile properties of the composite were further improved after the addition of WF. The WF acted as a load carrier, reinforced the composites, and increased the flexural and tensile properties. Salemane and Luyt[31] prepared wood/PP composite and found an improvement in mechanical properties due to reinforcement by WF. Moreover, the compatibilizer, PE-*co*-GMA, increased the interfacial adhesion between wood and polymers through its glycidyl linkage and long polymeric chain. Sailaja[32] used poly(ethylene-*co*-glycidyl methacrylate) as compatibilizer to improve the compatibility of wood pulp-LDPE composite. The properties were further improved after the incorporation of clay and ZnO nanopowder. At a fixed clay loading (3 phr), both the flexural and tensile properties improved upto addition of 3 phr of ZnO. The properties decreased on addition of higher amount of ZnO (5 phr). The observed higher values might be due to the combined effect of nanoclay and ZnO. The silicate layers of nanoclay acted as a reinforcing agent that binds the polymer chain inside the gallery space and hence restrict the mobility of the polymer chain. The incorporation of clay increased the mechanical properties of wood-plastic composite was reported.[33] CTAB modified ZnO improved the interaction between clay, wood, and polymer through its surface hydroxyl group and cetyl group, respectively. The higher the dispersion of ZnO, the higher would be the interaction. At higher level of ZnO loading (5 phr), the agglomeration occurred, and hence the interaction of ZnO with the clay, polymer, and wood decreased. The interaction of ZnO nanoparticles increased the tensile modulus of polyacrylonitrile was reported in the literature.[23]

### Hardness results

Table I shows the hardness results of polymer blend and WPC loaded with clay and different percentage of ZnO. Hardness value of the polymer blend increased after the addition of compatibilizer due to enhancement of interfacial adhesion between polymers. On addition of WF to the polymer blend, the hardness value was found to decrease. But after the incorporation of nanoclay and ZnO to the WPC, hardness value was found to increase again. The improvement was due to combined effect of increase in interaction of clay and ZnO with WF and polymer. Hardness value was found maximum at 3 phr of clay/ZnO loading, after that it decreased. At higher loading of ZnO, the reinforcing action of ZnO might decrease due to agglomeration.

### Thermogravimetric analysis

Table II shows the initial decomposition temperature ($T_i$), maximum pyrolysis temperature ($T_m$),

**TABLE II**
**Thermal Analysis of Polymer Blend and Wood Polymer Nanocomposite Loaded with Clay and Different Percentage of ZnO**

| | | | | Temperature of decomposition ($T_D$) in °C at different weight loss (%) | | | | |
|---|---|---|---|---|---|---|---|---|
| Sample | $T_i$ | $T_m$[a] | $T_m$[b] | 20% | 40% | 60% | 80% | RW% at 600°C |
| PB | 249 | 270 | 407 | 291 | 388 | 439 | 468 | 6.1 |
| PB/G5/W40 | 255 | 276 | 451 | 299 | 397 | 446 | 473 | 7.2 |
| PB/G5/W40/N3/Z1 | 277 | 326 | 503 | 330 | 459 | 484 | 501 | 10.8 |
| PB/G5/W40/N3/Z3 | 289 | 337 | 517 | 350 | 478 | 497 | 513 | 14.5 |
| PB/G5/W40/N3/Z5 | 281 | 330 | 510 | 336 | 465 | 490 | 508 | 12.7 |

$T_i$, value for initial degradation.
[a] $T_m$, value for first step
[b] $T_m$, value for second step.

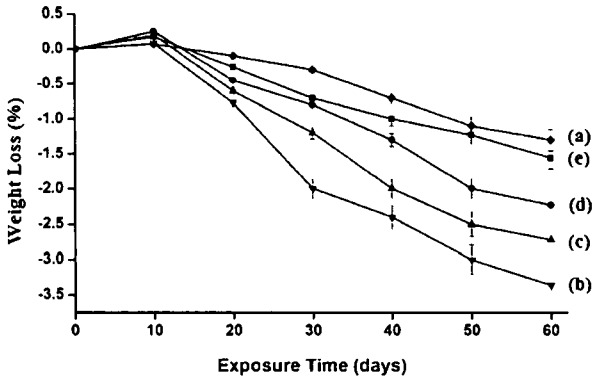


**Figure 6** Weight losses versus exposure time of (a) PB, (b) PB/G5/W40, (c) PB/G5/W40/N3/Z1, (d) PB/G5/W40/N3/Z5, and (e) PB/G5/W40/N3/Z3.

decomposition temperature at different weight loss (%; $T_D$), and residual weight (RW, %) for polymer blend and WPCs. It was observed that $T_i$ value increased after the incorporation of compatibilizer and WF to polymer blend. The value increased further after the addition of nanoclay and ZnO. $T_i$ value was found maximum when the concentration of ZnO was 3 phr. At higher concentration of ZnO, the $T_i$ value decreased again.

Both the polymer blend and composite showed two decomposition peaks. The $T_m$ value for the first step in both WPC and WPC loaded with clay and ZnO were due to the depolymerization of hemicellulose, glycosidic linkage of cellulose, thermal decomposition of cellulose,[34] and dehydrochlorination of PVC while the peak for second step was due to decomposition of HDPE and PP.[35–37] $T_m$ values of the composites for both the steps were found to follow the similar trend as those of $T_i$ values.

The percentage weight losses of sample at different temperature are listed in Table II. WPC containing 3 phr nanoclay and 3 phr ZnO exhibited similar weight losses at higher temperatures compared to polymer blend, WPC, and WPC containing 1 or 5 phr ZnO.

The incorporation of compatibilizer enhanced the interaction between the polymer blend and WF. The improvement of thermal stability after inclusion of compatibilizer and WF to polymer blend was reported by Awal et al.[30] The silicate layers of nanoclay in nanocomposites provided a long tortuous path which delayed the diffusion of the decomposed volatile product through the composite. Deka and Maji [29] reported that thermal stability of WPC enhanced due to addition of clay. Moreover, the incorporation of modified ZnO nanopowder might play a role in enhancing the thermal stability by interacting with clay, wood and polymer through its surface hydroxyl group and cetyl groups, respectively. At higher concentration of ZnO, the agglomeration (as evident by TEM study) probably decreased the interaction and could give rise to reduce the thermal stability. Laachachi et al.[38] studied the thermal degradation of PMMA by incorporation of ZnO and organo-modified montmorillonite and found an increased in thermal stability of polymethyl methacrylate after the incorporation of ZnO and organo-montmorillonite.

## UV test results

Figure 6 displays the weight loss of polymer blend, normal WPC and WPC loaded with nanoclay and ZnO (1–5 phr). Weight losses of the samples were determined as a function of exposure time at room temperature and were found nearly linear with exposure time. At early stage of exposure time, due to moisture uptake, a small increase of weight was found, which was greater than the material loss induced by the degradation in the early stage. The rate of weight loss was lowest for polymer blend followed by WPC filled with 3 phr ZnO and 3 phr clay, 5 phr ZnO and 3 phr clay, as well as 1 phr ZnO and 3 phr clay. WPC showed the maximum weight losses. After 60 days of exposure, the maximum weight losses in polymer blend, normal WPC and clay loaded 1, 3, and 5 phr ZnO containing WPCs were 1.3% ± 0.2%, 3.3% ± 0.2%, 2.7% ± 0.2%, 1.5% ± 0.3%, and 2.2% ± 0.5%, respectively. On exposure to UV radiation, the chain scission followed by decrease in the density of the entanglements of the polymer chains occurred. This resulted in the decrease in the weight of the samples.

Figure 7 shows the carbonyl index values against time. After irradiation of the samples for 60 days, carbonyl peak intensity was found to increase (Fig. 8). On exposing the samples to UV radiation, chain scission of the polymer blend occurred that increased the carbonyl index value. The polymer blend had lowest carbonyl index value (curve-7a).

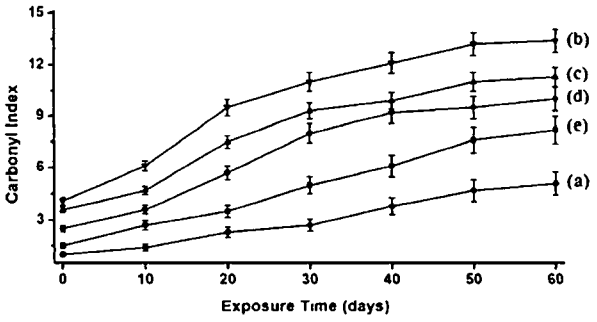


**Figure 7** Carbonyl index value of (a) PB, (b) PB/G5/W40, (c) PB/G5/W40/N3/Z1, (d) PB/G5/W40/N3/Z5, and (e) PB/G5/W40/N3/Z3.

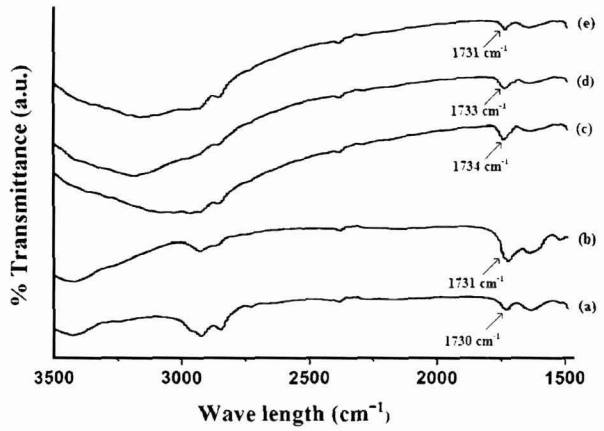


**Figure 8** Change in carbonyl peak intensity of (a) PB, (b) PB/G5/W40, (c) PB/G5/W40/N3/Z1, (d) PB/G5/W40/N3/Z5, and (e) PB/G5/W40/N3/Z3.

Due to higher oxidation of WF, normal WPC had highest carbonyl index value (curve-7b). The carbonyl index values decreased upto the addition of 3 phr clay and ZnO after that it increased. ZnO nanoparticles played an important role in stabilizing the WPC by acting as screen and delayed the photodegradation process. ZnO nanoparticles absorbed the UV radiation and hence reduced the UV intensity required for the oxidation of the WPC. Zhao and Li[39] observed an improvement in UV stability of PP nanocomposite due to the incorporation of ZnO. The presence of nanoclay in the composite also had a screening effect that delayed the photo degradation process. Grigoriadou et al.[40] observed an increase in UV stability of HDPE after incorporating montmorillonite clay. Figure 9 represents the SEM micrographs of samples after 60 days of irradiation. The surface morphology of the samples showed a drastic change due to exposure to UV radiation. The surface of normal WPC was more irregular compared with clay/ZnO treated WPC indicating that the normal WPC sample was less effective compared with ZnO/clay containing sample against UV radiation. WPC containing nanoclay and higher percentage of ZnO (5 phr) exhibited lower protection against UV radiation as shown by the decrease in surface smoothness compared to WPC loaded with 3 phr ZnO and nanoclay. This might be due to the agglomeration of ZnO which provided lower protection against photodegradation.

## LOI results

LOI values of polymer blend, WPC, and WPC loaded with nanoclay and ZnO are shown in Table III. From the table, it was observed that with the addition of compatibilizer, LOI value of the polymer blend increased. The increase in the value was due to the increase in interfacial adhesion among the polymers by the compatibilizer. LOI value increased further after the addition of WF to the blend. The glycidyl and hydrocarbon part of the compatibilizer improved the interaction with the hydroxyl and hydrocarbon part of the wood and polymer. A

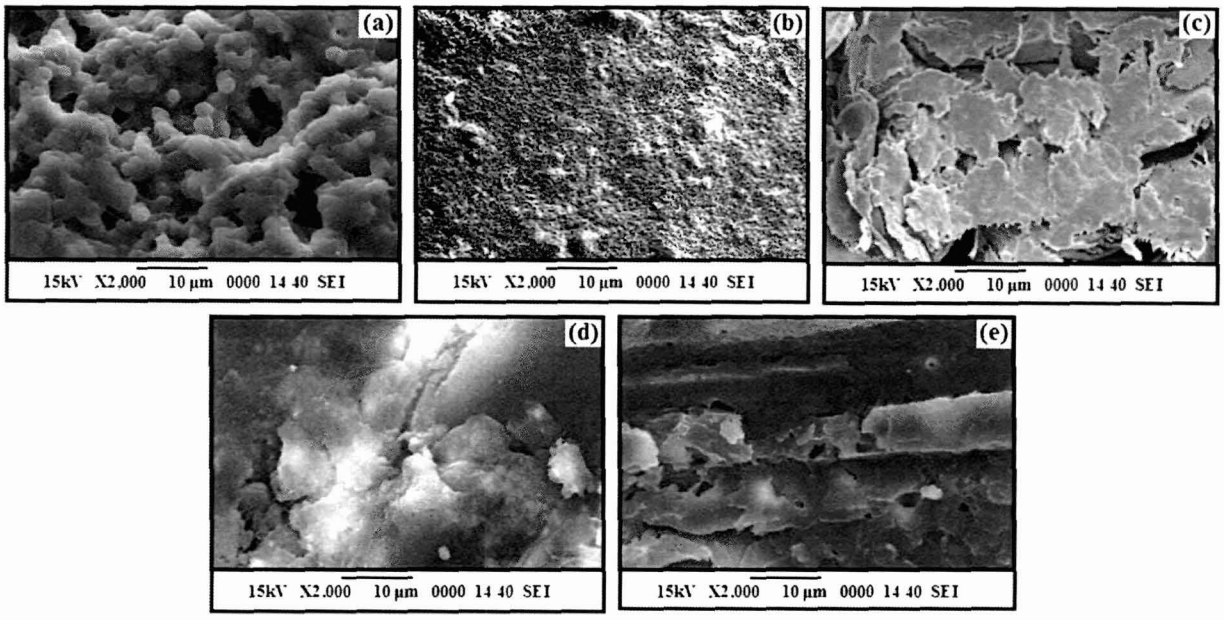


**Figure 9** SEM micrographs of UV treated samples after 60 days: (a) PB, (b) PB/G5/W40, (c) PB/G5/W40/N3/Z1, (d) PB/G5/W40/N3/Z3, and (e) PB/G5/W40/N3/Z5.

TABLE III
LOIs and Flaming Characteristics of Polymer Blend and Wood/Polymer/Clay/ZnO Nanocomposites

| Samples | LOI (%) | Flame description | Smoke and Fumes | Char |
|---|---|---|---|---|
| PB | 20 | Candle-like localized flame | Small and black smoke | little |
| PB/G5 | 35 | Small localized flame | Small and black smoke | little |
| PB/G5/W40 | 38 | Small localized flame | Small and black smoke | little |
| PB/G5/W40/N3/Z1 | 53 | Small localized flame | Small and black smoke | higher |
| PB/G5/W40/N3/Z3 | 68 | Small localized flame | Small and black smoke | higher |
| PB/G5/W40/N3/Z5 | 66 | Small localized flame | Small and black smoke | higher |

substantial improvement in LOI value was observed after the addition of clay and ZnO. The value increased upto the addition of 3 phr each of nanoclay and ZnO. LOI value decreased at higher concentration of ZnO (5 phr). The nanoclay produced silicate char on the surface of WPC which increased the flame resistance property of the composite.[41] The tortuous path provided by the silicate layers had better barrier property to the oxygen and heat which delayed the burning capacity of the composite. The incorporation of CTAB modified ZnO enhanced the interaction between clay, wood, and polymer through its hydroxyl and cetyl groups. ZnO nanoparticles also provided some thermal barrier to the oxygen and heat leading to an improvement in flame resistant property. At higher ZnO loading, the agglomeration of ZnO resulted in decrease of interaction and hence barrier property as well as LOI value.

### Water uptake and water vapor exclusion results

The water uptake and water vapor uptake results of polymer blend, PE-*co*-GMA treated polymer blend, and WPC loaded with clay and different percentage of ZnO are shown in Figure 10. The water uptake capacity of polymer blend decreased after the addition of PE-*co*-GMA compatibilizer. The decreased in water uptake capacity of PE-*co*-GMA treated polymer blend was due to the increase in interfacial adhesion between the polymers by the compatibilizer. The value of water uptake capacity was suddenly increased after the addition of WF to the blend. The hydrophilic nature of WF caused an increase in the water uptake capacity. The water uptake capacity was decreased after the addition of clay/ZnO. WPC loaded with 3 phr each of clay and ZnO showed lowest water uptake capacity followed by WPC with 3 phr clay and 1 phr ZnO, and WPC with 3 phr clay and 5 phr ZnO. The silicate layers of the clay provided tortuous path and increased the barrier property for water transport.[29] ZnO nanopowder also provided a barrier to the passage of water. Better the distribution of nanoparticles, the higher was the barrier property. ZnO nanoparticles at higher concentration were found to become agglomerated in the composite which resulted in an increase in water uptake capacity.

Water vapor exclusion test for the samples were carried out at 30°C and 65% relative humidity. The water vapor uptake was found to increase with time. The trend and explanation for water vapor absorption of different samples were similar to those of samples taken for water uptake study.

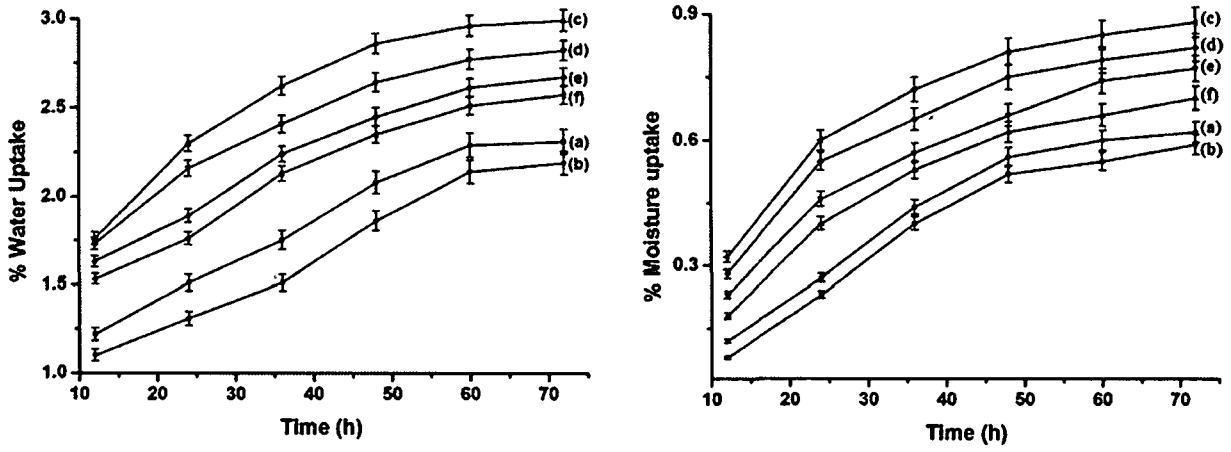


Figure 10 Water absorption and Water vapor absorption of (a) PB, (b) PB/G5, (c) PB/G5/W40, (d) PB/G5/W40/N3/Z1, (e) PB/G5/W40/N3/Z5, and (f) PB/G5/W40/N3/Z3.

## CONCLUSIONS

The optimized ratio of xylene and THF for solution blending of HDPE, LDPE, PP, and PVC (1 . 1 : 1: 0.5) was 70 : 30. The compatibility among the polymers and WF was improved by using PE-*co*-GMA compatibilizer as revealed by SEM study. The distribution of silicate layers of nanoclay and ZnO in WPCs were examined by XRD and TEM study. Surface modification of ZnO nanoparticles by cationic surfactant CTAB was examined by FTIR studies The interactions among wood, PE-*co*-GMA, ZnO, and nanoclay were also studied by FTIR. WPC loaded with nanoclay and ZnO showed an improvement in mechanical and thermal properties. The incorporation of ZnO improved the UV resistance of the composites as judged from the decrease in weight loss, carbonyl index value and SEM study. Nanoclay/ZnO treated WPC further improved the flame retardancy and decreased the water absorption capacity. WPC loaded with 3 phr clay and 3 phr ZnO exhibited maximum improvement in properties.

The authors thank Council of Scientific and Industrial Research (CSIR), New Delhi, for their financial assistance (grant number 01(2287)/08/EMR-II)

## References


1 Selke, S E, Wichman, I Compos Part A Appl Sci 2004, 35, 321
2 Ashori A Bioresour Technol 2008, 99, 4661
3 Ashori, A, Nourbakhsh, A Bioresour Technol 2010, 101, 2515
4 Qiu, W, Zhang, F, Endo, T, Hirotsu, T Polym Compos 2005, 26, 448
5 Devi, R R, Maji, T K Polym Compos 2007, 28, 1
6 Biswal, M, Mohanty, S, Nayak, S K J Appl Polym Sci 2009, 114, 4091
7 Song, G J Mater Rep 1996, 4, 57
8 Liufu, S C, Xiao, H N, Li, Y P Polym Degrad Stab 2005, 87, 103
9 Demir, M M, Memesa, M, Castignolles, P, Wegner, G Macromol Rapid Commun 2006, 27, 763
10 Lu, N, Lu, X, Jin, X, Lu, C Polym Int 2007, 56, 138
11 Ji, L W, Shih, W S, Fang, T H, Wu, C Z, Peng, S M, Meen, T H J Mater Sci 2010, 45, 3266
12 Zhang, H, Wu, J, Zhai, C, Du, N, Ma, X, Yang, D Nanotechnology 18 455604 2007
13 Jin, T, Sun, D, Su, J Y, Zhang, H, Sue, H J J Food Sci 2009, 74, M46
14 Yang, H, Xiao, Y, Liu, K, Feng, Q J Am Ceram Soc 2008, 91, 1591
15 Fa, W, Yang, C, Gong, C, Peng, T, Zan, L J Appl Polym Sci 2010, 118, 378
16 Stark, N M, Matuana, L M Polym Degrad Stab 2004, 86, 1
17 Standard Test Method for Measuring the Minimum Oxygen Concentration to support Candle-Like Combustion of Plastics (Oxygen Index), ASTM D2863, ASTM International, West Conshohocken, PA, 1997
18 Mina, F, Seema, S, Matin, R, Rahaman, J, Sarker, R B, Gafur, A, Bhuiyan, A H Polym Degrad Stab 2009, 94, 183
19 Han, G, Lei, Y, Wu, Q, Kojima, Y J Polym Environ 2008, 16, 123
20 Liu, J, Chen, G, Yang, J Polymer 2008, 49, 3923
21 De Rosa, C, Corradini, P Macromolecules 1993, 26, 5711
22 Leung, Y H, Djurisic, A B, Gao, J, Xie, M H, Wei, Z F, Xu, S J, Chan, W K Chem Phys Lett 2004, 394, 452
23 Chae, D W, Kim, B C J Appl Polym Sci 2006, 99, 1854
24 Pracella, M, Chionna, D, Ishak, R, Galeski, A Polym Plast Technol Eng 2004, 43, 1711
25 He, J, Shao, W, Zhang, L, Deng, C, Li, C J Appl Polym Sci 2009, 114, 1303
26 Li, H, Tripp, C P Langmuir 2002, 18, 9441
27 Dhoke, S K, Khanna, A S, Sinha, T J M Prog Org Coat 2009, 64, 371
28 Das, G, Karak, N Prog Org Coat 2009, 66, 59
29 Deka, B K, Maji, T K Compos Sci Technol 2010, 70, 1755
30 Awal, A, Ghosh, S B, Sain, M J Therm Anal Calorim 2010, 99, 695
31 Salemane, M G, Luyt, A S J Appl Polym Sci 2006, 100, 4173
32 Sailaja, R R N Compos Sci Technol 2039 2006, 66
33 Faruk, O, Matuana, L M Compos Sci Technol 2073 2008, 68
34 Fung, K L, Li, R K Y, Tjong, S C J Appl Polym Sci 2002, 85, 169
35 Meng, Y Z, Tjong, S C Polymer 1999, 40, 2711
36 Yemele, M C N, Koubaa, A, Cloutier, A, Soulounganga, P, Wolcott, M Compos Part A Appl Sci 2010, 41, 131
37 Bouza, R, Pardo, S G, Barral, L, Abad, M J Polym Compos 2009, 30, 880
38 Laachachi, A, Ruch, D, Addiego, F, Ferriol, M, Cochez, M, Lopez Cuesta, J M Polym Degrad Stab 2009, 94, 670
49 Zhao, H, Li, R K Y Polymer 2006, 47, 3207
40 Grigoriadou, I, Paraskevopoulos, K M, Chrissafis, K, Pavlidou, E, Stamkopoulos, T G, Bikiaris, D Polym Degrad Stab 2011, 96, 151
41 Camino, G, Tartaglione, G, Frache, A, Manferti, C, Costa, G Polym Degrad Stab 2005, 90, 354